



**Syntheses and Characterization of Ruthenium(II) Complexes  
with 5-Chloro-2-(phenylazo)pyridine Ligands**

**Luksamee Sahavisit**

**A Thesis Submitted in Fulfillment of the Requirements  
for the Degree of Doctor of Philosophy in Chemistry**

**Prince of Songkla University**

**2008**

**Copyright of Prince of Songkla University**

**Thesis Title**            Syntheses and Characterization of Ruthenium(II) Complexes  
with 5-Chloro-2-(phenylazo)pyridine Ligands  
**Author**                    Miss Luksamee Sahavisit  
**Major Program**        Chemistry

---

**Major Advisor**

.....  
(Asst. Prof. Dr. Kanidtha Hansongnern)

**Examining Committee :**

.....Chairperson  
(Assoc. Prof. Dr. Sutatip Siripaisarnpipat)

.....Committee  
(Asst. Prof. Dr. Kanidtha Hansongnern)

.....Committee  
(Asst. Prof. Dr. Chaveng Pakawatchai)

.....Committee  
(Asst. Prof. Dr. Adisorn Ratanaphan)

.....Committee  
(Dr. Nararak Leesakul)

The Graduate School, Prince of Songkla University, has approved this thesis as fulfillment of the requirements for the Doctor of Philosophy Degree in Chemistry

.....  
(Assoc. Prof. Dr. Krerckchai Thongnoo)  
Dean of Graduate School

ชื่อวิทยานิพนธ์	ศึกษาการสังเคราะห์และ โครงสร้างสารประกอบเชิงซ้อนของโลหะ รูทีเนียมกับลิแกนด์ 5-Chloro-2-(phenylazo)pyridine
ผู้เขียน	นางสาวลักขมี สหวิศิษฐ์
สาขาวิชา	เคมี
ปีการศึกษา	2550

### บทคัดย่อ

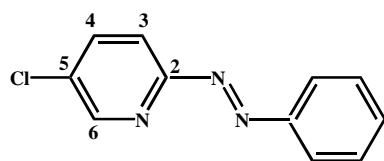
5-Chloro-2-(phenylazo)pyridine (Clazpy) เป็นลิแกนด์ไบเดนเตดชนิดใหม่ จัดเป็นอนุพันธ์ของลิแกนด์ 2-(phenylazo)pyridine (azpy) สารประกอบเชิงซ้อน  $[Ru(Clazpy)_2Cl_2]$  เตรียมจากปฏิกิริยาระหว่าง  $RuCl_3 \cdot 3H_2O$  กับลิแกนด์ Clazpy โครงสร้างของสารประกอบเชิงซ้อนที่สังเคราะห์ได้ศึกษาด้วยเทคนิคการเลี้ยวเบนของรังสีเอ็กซ์บนผลึกเดี่ยว (X-ray Crystallography) พบว่าการจัดเรียงโครงสร้างเป็นแบบ *tcc-*, *ctc-* และ *ccc-*  $[Ru(Clazpy)_2Cl_2]$  ผลจากเทคนิคทางสเปกโทรสโกปีและเทคนิคทางไฟฟ้าเคมีพบว่าลิแกนด์ Clazpy มีความสามารถในการเป็นตัวรับไพออิเล็กทรอนิกส์ ( $\pi$ -acceptor) ได้ดีเช่นเดียวกับลิแกนด์ azpy แต่มีความสามารถในการเป็นตัวให้ซิกมาอิเล็กทรอนิกส์ ( $\sigma$ -donor) ที่ดีกว่าลิแกนด์ azpy สารประกอบเชิงซ้อน  $[Ru(Clazpy)(5dmazpy)Cl_2]$  เตรียมจากปฏิกิริยา addition-elimination ของสารประกอบ *ctc-*  $[Ru(Clazpy)_2Cl_2]$  ศึกษาโครงสร้างและเทคนิคทางไฟฟ้าเคมีพบว่าลิแกนด์ Clazpy มีคุณสมบัติในการเป็นตัวรับไพออิเล็กทรอนิกส์ที่ดีกว่าลิแกนด์ 5dmazpy แต่มีคุณสมบัติในการเป็นตัวให้ซิกมาอิเล็กทรอนิกส์น้อยกว่าลิแกนด์ 5dmazpy

*ctc-*  $[Ru(Clazpy)_2Cl_2]$  เป็นสารตั้งต้นเพื่อสังเคราะห์สารประกอบเชิงซ้อน  $[Ru(Clazpy)_2(L)](X)_2$  ( $L = bpy, phen, azpy, Clazpy$ ;  $X = PF_6^-, NO_3^-, Cl^-$ ) ยิ่งไปกว่านั้นสังเคราะห์สารประกอบเชิงซ้อน  $[Ru(bpy)_2(Clazpy)](X)_2$  และ  $[Ru(phen)_2(Clazpy)](X)_2$  ( $X = PF_6^-, Cl^-$ ) จากสารตั้งต้น  $[Ru(bpy)_2Cl_2]$  และ  $[Ru(phen)_2Cl_2]$  สมบัติทางเคมีของสารประกอบเชิงซ้อนที่สังเคราะห์ได้ศึกษาด้วยเทคนิคทางสเปกโทรสโกปีและเทคนิคทางไฟฟ้าเคมี ได้ศึกษาผลึกเดี่ยวของสารประกอบเชิงซ้อน  $[Ru(Clazpy)_2(phen)](PF_6)_2$ ,  $[Ru(Clazpy)_2(azpy)](PF_6)_2$  และ  $[Ru(Clazpy)_2(phen)](NO_3)_2 \cdot 3.5 H_2O$

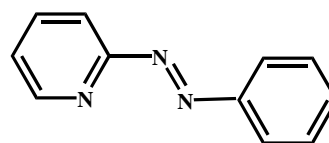
การออกฤทธิ์ทางชีวภาพเบื้องต้นของสารประกอบที่สังเคราะห์กับเซลล์มะเร็ง 3 ชนิด (Anti-NCI-H187, BC, KB) ผลที่ได้พบว่าลิแกนด์ Clazpy ออกฤทธิ์ต่อเซลล์มะเร็งชนิด Anti-NCI-H187 ในระดับปานกลาง แต่สารประกอบเชิงซ้อน  $[Ru(Clazpy)_2Cl_2]$  พบความเป็น

พิษของสารต่อเซลล์มะเร็งทั้งสามชนิดในระดับปานกลางถึงสูง อย่างไรก็ตาม  $[\text{Ru}(\text{Clazpy})(5\text{dmazpy})\text{Cl}_2]$  ไม่แสดงความเป็นพิษของสารต่อเซลล์มะเร็ง นอกจากนี้แทนที่ลิแกนด์คลอโรในสารประกอบ  $\text{cis-}[\text{Ru}(\text{Clazpy})_2\text{Cl}_2]$  ได้สารประกอบเชิงซ้อนที่เป็นไอออนิก  $[\text{Ru}(\text{Clazpy})_2(\text{L})](\text{X})_2$  ( $\text{L} = \text{bpy}, \text{phen}, \text{azpy}, \text{Clazpy}; \text{X} = \text{PF}_6^-, \text{NO}_3^-, \text{Cl}^-$ ) ซึ่งพบว่ามีการออกฤทธิ์ต่อเซลล์มะเร็งที่ดีกว่า  $\text{cis-}[\text{Ru}(\text{Clazpy})_2\text{Cl}_2]$  แต่สารประกอบเชิงซ้อน  $[\text{Ru}(\text{bpy})_2(\text{Clazpy})]\text{Cl}_2 \cdot 7\text{H}_2\text{O}$  และ  $[\text{Ru}(\text{phen})_2(\text{Clazpy})]\text{Cl}_2 \cdot 8\text{H}_2\text{O}$  ไม่พบการออกฤทธิ์ต่อเซลล์มะเร็ง

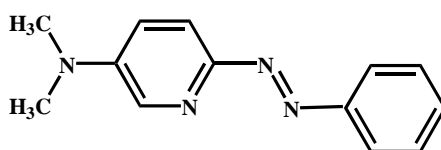
การจับดีเอ็นเอ (DNA-binding) ของสารประกอบเชิงซ้อนชนิดละลายน้ำได้ ศึกษาด้วยเทคนิคทางสเปกโทรสโกปี การหาค่าความหนืด (viscosity measurement) และเทคนิคทางไฟฟ้าเคมีพบว่าอันตรกิริยาของสารประกอบเชิงซ้อน  $[\text{Ru}(\text{Clazpy})_2(\text{L})]^{2+}$  ( $\text{L} = \text{azpy}, \text{Clazpy}$ ) กับดีเอ็นเอ ดีกว่าสารประกอบเชิงซ้อน  $[\text{Ru}(\text{Clazpy})_2(\text{L})]^{2+}$  ( $\text{L} = \text{bpy}, \text{phen}$ ) ยิ่งไปกว่านั้นลิแกนด์ bpy และ phen ในสารประกอบเชิงซ้อน  $[\text{Ru}(\text{bpy})_2(\text{Clazpy})]\text{Cl}_2 \cdot 7\text{H}_2\text{O}$  และ  $[\text{Ru}(\text{phen})_2(\text{Clazpy})]\text{Cl}_2 \cdot 8\text{H}_2\text{O}$  แสดงพฤติกรรมการจับกับดีเอ็นเอ ที่ต่างออกไปซึ่งให้ผลที่สอดคล้องกับผลการออกฤทธิ์ทางชีวภาพต่อเซลล์มะเร็ง



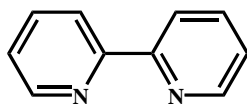
Clazpy



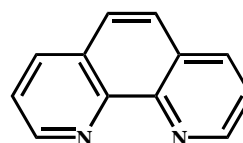
azpy



5dmazpy



bpy



phen

**Thesis Title**                Syntheses and Characterization of Ruthenium(II) Complexes  
with 5-Choloro-2-(phenylazo)pyridine Ligands

**Author**                        Miss Luksamee Sahavisit

**Major Program**            Chemistry

**Academic Year**            2007

### ABSTRACT

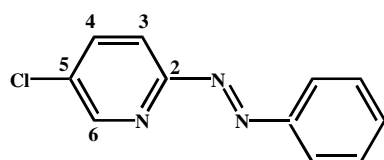
The new bidentate ligand, 5-Choloro-2-(phenylazo)pyridine (Clazpy) is a derivative of a known azo compound like 2-(phenylazo)pyridine (azpy). Three isomeric complexes of  $[\text{Ru}(\text{Clazpy})_2\text{Cl}_2]$  were prepared by the reaction of  $\text{RuCl}_3 \cdot 3\text{H}_2\text{O}$  with corresponding Clazpy ligand. The molecular structures were confirmed by X-ray diffraction analyses as found to be *tcc*-, *ctc*- and *ccc*- $[\text{Ru}(\text{Clazpy})_2\text{Cl}_2]$ . Results from spectroscopic data and cyclic voltammetry (CV) showed that the Clazpy ligand is a strong  $\pi$ -acceptor ligand like azpy but stronger  $\sigma$ -donor. The addition-elimination reaction of *ctc*- $[\text{Ru}(\text{Clazpy})_2\text{Cl}_2]$  gives rise to a  $[\text{Ru}(\text{Clazpy})(5\text{dmazpy})\text{Cl}_2]$  complex (5dmazpy = *N,N*-dimethyl-2-(phenylazo)pyridine) which is also achieved and fully characterized. The X-ray crystallographic and CV data of this molecule supported that the Clazpy ligand is a better  $\pi$ -acceptor property than 5dmazpy but less  $\sigma$ -donor.

The *ctc*- $[\text{Ru}(\text{Clazpy})_2\text{Cl}_2]$  was used as a precursor to synthesize the complexes of  $[\text{Ru}(\text{Clazpy})_2(\text{L})](\text{X})_2$  ( $\text{L} = 2,2'$ -bipyridine (bpy), 1,10-phenanthroline (phen), azpy, Clazpy;  $\text{X} = \text{PF}_6^-$ ,  $\text{NO}_3^-$ ,  $\text{Cl}^-$ ). Moreover,  $[\text{Ru}(\text{bpy})_2(\text{Clazpy})](\text{X})_2$  and  $[\text{Ru}(\text{phen})_2(\text{Clazpy})](\text{X})_2$  ( $\text{X} = \text{PF}_6^-$ ,  $\text{Cl}^-$ ) were also synthesized via precursors  $[\text{Ru}(\text{bpy})_2\text{Cl}_2]$  and  $[\text{Ru}(\text{phen})_2\text{Cl}_2]$ , respectively. All compounds were fully characterized by spectroscopic and electrochemical techniques. Single crystals of  $[\text{Ru}(\text{Clazpy})_2\text{phen}](\text{PF}_6)_2$ ,  $[\text{Ru}(\text{Clazpy})_2(\text{azpy})](\text{PF}_6)_2$  and  $[\text{Ru}(\text{Clazpy})_2(\text{phen})](\text{NO}_3)_2 \cdot 3.5\text{H}_2\text{O}$  were obtained.

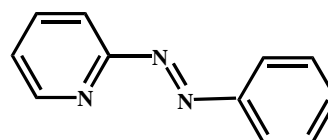
Preliminary study of synthesized compounds with three cancer cell lines (Anti-NCl-H187, BC, KB,) revealed that the Clazpy ligand shows only active for Anti-NCl-H187 but the isomeric complexes,  $[\text{Ru}(\text{Clazpy})_2\text{Cl}_2]$ , show a moderate

to strongly active in all cell lines. However,  $[\text{Ru}(\text{Clazpy})(5\text{dmazpy})\text{Cl}_2]$  displays no effect to cancer cell lines. It is concluded that the Clazpy ligand in  $[\text{Ru}(\text{Clazpy})_2\text{Cl}_2]$  shows an effect to cytotoxic activity. In addition, replacing two chloro ligands in *ctc*- $[\text{Ru}(\text{Clazpy})_2\text{Cl}_2]$  give rise the ionic complexes,  $[\text{Ru}(\text{Clazpy})_2(\text{L})]^{2+}$  (L = bpy, phen, azpy, Clazpy; X =  $\text{PF}_6^-$ ,  $\text{NO}_3^-$ ,  $\text{Cl}^-$ ) which show higher cytotoxic activity than *ctc*- $[\text{Ru}(\text{Clazpy})_2\text{Cl}_2]$ . On the other hand, there is no observation of cytotoxic activity in  $[\text{Ru}(\text{bpy})_2(\text{Clazpy})]^{2+}$  and  $[\text{Ru}(\text{phen})_2(\text{Clazpy})]^{2+}$ .

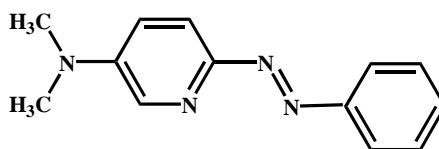
The DNA-binding study of water-soluble compounds by spectrophotometric methods, viscosity measurements and electrochemical study demonstrate that the interaction of CT-DNA with  $[\text{Ru}(\text{Clazpy})_2(\text{L})]^{2+}$  (L = azpy, Clazpy) is greater than that of  $[\text{Ru}(\text{Clazpy})_2(\text{L})]^{2+}$  (L = bpy, phen). Moreover, bpy and phen in  $[\text{Ru}(\text{bpy})_2(\text{Clazpy})]\text{Cl}_2 \cdot 7\text{H}_2\text{O}$  and  $[\text{Ru}(\text{phen})_2(\text{Clazpy})]\text{Cl}_2 \cdot 8\text{H}_2\text{O}$  show different binding modes corresponding to their biological cytotoxic activities to cancer cell lines.



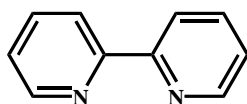
Clazpy



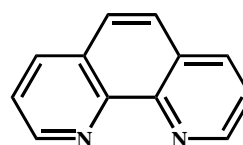
azpy



5dmazpy



bpy



phen

## ACKNOWLEDGEMENTS

I would like to thank my advisor, Asst. Prof. Dr. Kanidtha Hansongnern who gave knowledge, useful discussion and kindness during the laboratory work and the preparation of this thesis. Everything will be always kept in my mind.

My sincere thanks are expressed to Assoc. Prof. Dr. Suthatip Siripaisanpipat, Asst. Prof. Dr. Adisorn Ratanaphan and Dr. Nararak Leesakul for their kindness, valuable suggestions and improvements throughout this report. I would like to thank Asst. Prof. Dr. Chaveng Pakawatchai for X-ray data and helpful advice.

I am grateful to Prof. S.A.R. Knox and Prof. Neil Connelly for results of the elemental analysis and FAB mass spectrometric data. Special thank is addressed to Prof. G. Pyne who gave me chance to do research at Wollongong University in order to obtain ES-MS data, NMR data and also X-ray structure of  $[\text{Ru}(\text{Clazpy})_2(\text{phen})](\text{NO}_3)_2 \cdot 3.5\text{H}_2\text{O}$ .

I would like to thank Miss Saowanit Saithong for measuring X-ray structure and preparing crystallographic data, Miss Thunwadee Ritthiwigrom for helpful suggestion of mechanism in organic chemistry. Special thank is addressed to Mr. Peerajit Vittaya for his meaningful advice.

I would like to extend my appreciation to the staff of the Department of Chemistry, Faculty of Science, Prince of Songkla University and all member of CH 439. Their friendship, kindness, and help have been valuable to me.

I am very grateful to the Postgraduate Education and Research Program in Chemistry (PERCH), Prince of Songkla University Graduate Studies Grant and Graduate School, Prince of Songkla University for financial supports.

Finally, I would like to thank Mr. Anan and Mrs. Ladda Sahavisit, my parents for love, care and encouragement. None of these would have been possible without them.

Luksamee Sahavisit

## THE RELEVANCE OF THIS RESEARCH WORK

In this work the three isomeric complexes of  $[\text{Ru}(\text{Clazpy})_2\text{Cl}_2]$  (Clazpy = 5-Chloro-(2-phenylazo)pyridine) were synthesized. Their chemical and structural properties were determined by spectroscopic techniques and X-ray diffraction analysis. Redox properties were studied by cyclic voltammetry. Preliminary cytotoxicity study of all isomers with three cancer cell lines result in moderately to strongly cytotoxic activity with  $\text{IC}_{50}$  values in range of 0.2-35  $\mu\text{M}$ . In addition, to further synthesize the ionic compounds by replacing two chloro ligands in  $[\text{Ru}(\text{Clazpy})_2\text{Cl}_2]$  with others bidentate ligands are useful in cytotoxicity testing.

This research work is useful to us for understanding in syntheses and characterization of compounds. Moreover, the new compounds may be developed into more effective medicinal drug i.e. anticancer agents in the future.

## CONTENTS

	Page
ABSTRACT (Thai)	iii
ABSTRACT (English)	v
ACKNOWLEDGEMENT	vii
THE RELEVANCE OF THE RESEARCH WORK	viii
CONTENTS	ix
LIST OF TABLES	xi
LIST OF FIGURES	xvii
LIST OF ABBREVIATIONS AND SYMBOLS	xxxviii
CHAPTER 1: INTRODUCTION	1
1.1 Introduction	1
1.2 Background	3
1.3 Review of Literatures	10
1.4 Objectives	28
CHAPTER 2: MATERIALS AND METHODS	29
2.1 Materials	29
2.2 Instruments and apparatus	30
2.3 Syntheses of ligands	32
2.4 Syntheses of complexes	33
2.5 Techniques for structural determination	40
2.6 DNA-binding experiments	44
CHAPTER 3: RESULTS AND DISCUSSION	47
3.1 Syntheses and characterization of ligands	48
3.2 Syntheses and characterization of the isomeric [Ru(Clazpy) <sub>2</sub> Cl <sub>2</sub> ] complexes	63
3.3 Synthesis and characterization of [Ru(Clazpy)(5dmazpy)Cl <sub>2</sub> ]	105
3.4 Syntheses and characterization of [Ru(Clazpy) <sub>2</sub> (L)](PF <sub>6</sub> ) <sub>2</sub> (L = bpy, phen, azpy, Clazpy)	124

## CONTENTS (continued)

	Page
3.5 Syntheses and characterization of [Ru(Clazpy) <sub>2</sub> (L)](NO <sub>3</sub> ) <sub>2</sub> .xH <sub>2</sub> O (L = bpy, phen, azpy, Clazpy)	168
3.6 Syntheses and characterization of [Ru(Clazpy) <sub>2</sub> (L)]Cl <sub>2</sub> .xH <sub>2</sub> O (L = bpy, phen, azpy, Clazpy)	209
3.7 Syntheses and characterization of [Ru(bpy) <sub>2</sub> (Clazpy)]X <sub>2</sub> and [Ru(phen) <sub>2</sub> (Clazpy)]X <sub>2</sub> (X = PF <sub>6</sub> <sup>-</sup> , Cl <sup>-</sup> )	247
3.8 DNA-binding experiments	285
3.8.1 Absorption spectroscopic studies	285
3.8.2 Viscosity measurements	303
3.8.3 Fluorescence quenching studies	309
3.8.4 Electrochemical studies	316
3.9 Cytotoxicity test	324
CHAPTER 4: CONCLUSION	328
BIBLIOGRAPHY	331
APPENDIX	346
A Cut off solvents	347
B Bond length (Å) and bond angle (°)	348
C Cyclic voltammograms	378
VITAE	398

## LIST OF TABLES

Table	Page
1.1 Some common buffer systems employed for biochemical studies	10
3.1 The physical properties of azpy and the Clazpy ligands	49
3.2 Elemental analysis data of the Clazpy ligand	50
3.3 FAB mass spectrometric data of the Clazpy ligand	51
3.4 IR data of the Clazpy ligand	52
3.5 UV-Visible absorption spectroscopic data of the Clazpy ligand	54
3.6 $^1\text{H}$ - $^{13}\text{C}$ NMR spectroscopic data of the Clazpy ligand	56
3.7 Cyclic voltammetric data of the Clazpy ligand in 0.1 M TBAH CH <sub>2</sub> Cl <sub>2</sub> at scan rate 50 mV/s (ferrocene as an internal standard)	61
3.8 The physical properties of the isomeric [Ru(Clazpy) <sub>2</sub> Cl <sub>2</sub> ] complexes	65
3.9 Elemental analysis data of the isomeric [Ru(Clazpy) <sub>2</sub> Cl <sub>2</sub> ] complexes	66
3.10 Crystal data and structure refinement for <i>tcc</i> -[Ru(Clazpy) <sub>2</sub> Cl <sub>2</sub> ]	67
3.11 Selected bond lengths (Å) and angles (°) and estimated standard deviations for <i>tcc</i> -[Ru(Clazpy) <sub>2</sub> Cl <sub>2</sub> ]	68
3.12 Crystal data and structure refinement for <i>ctc</i> -[Ru(Clazpy) <sub>2</sub> Cl <sub>2</sub> ]	70
3.13 Selected bond lengths (Å) and angles (°) and estimated standard deviations for <i>ctc</i> -[Ru(Clazpy) <sub>2</sub> Cl <sub>2</sub> ]	71
3.14 Crystal data and structure refinement for <i>ccc</i> -[Ru(Clazpy) <sub>2</sub> Cl <sub>2</sub> ]	73
3.15 Selected bond lengths (Å) and angles (°) and estimated standard deviations for <i>ccc</i> -[Ru(Clazpy) <sub>2</sub> Cl <sub>2</sub> ]	74
3.16 FAB mass spectrometric data of the isomeric [Ru(Clazpy) <sub>2</sub> Cl <sub>2</sub> ] complexes	76
3.17 IR data of the isomeric [Ru(Clazpy) <sub>2</sub> Cl <sub>2</sub> ] complexes	79
3.18 UV-Visible absorption spectroscopic data of the isomeric [Ru(Clazpy) <sub>2</sub> Cl <sub>2</sub> ] complexes	82
3.19 $^1\text{H}$ - $^{13}\text{C}$ NMR spectroscopic data of <i>tcc</i> -[Ru(Clazpy) <sub>2</sub> Cl <sub>2</sub> ] in CDCl <sub>3</sub>	86
3.20 $^1\text{H}$ - $^{13}\text{C}$ NMR spectroscopic data of <i>ctc</i> -[Ru(Clazpy) <sub>2</sub> Cl <sub>2</sub> ] in CDCl <sub>3</sub>	90

## LIST OF TABLES (continued)

Table	Page
3.21 $^1\text{H}$ - $^{13}\text{C}$ NMR spectroscopic data of <i>ccc</i> -[Ru(Clazpy) $_2$ Cl $_2$ ] in CDCl $_3$	94
3.22 Cyclic voltammetric data of the isomeric [Ru(Clazpy) $_2$ Cl $_2$ ] complexes in 0.1 TBAH CH $_2$ Cl $_2$ at scan rate 50 mV/s (ferrocene as an internal standard)	100
3.23 Cyclic voltammetric data of ruthenium(II) complexes in 0.1 M TBAH CH $_2$ Cl $_2$ at scan rate 50 mV/s (ferrocene as an internal standard)	102
3.24 The physical properties of the [Ru(Clazpy)(5dmazpy)Cl $_2$ ] complex	105
3.25 Elemental analysis data of the [Ru(Clazpy)(5dmazpy)Cl $_2$ ] complex	107
3.26 Crystal data and structure refinement for [Ru(Clazpy)(5dmazpy)Cl $_2$ ]	108
3.27 Selected bond lengths (Å) and angles (°) and estimated standard deviations for [Ru(Clazpy)(5dmazpy)Cl $_2$ ]	109
3.28 FAB mass spectrometric data of the [Ru(Clazpy)(5dmazpy)Cl $_2$ ] complex	110
3.29 IR data of the [Ru(Clazpy)(5dmazpy)Cl $_2$ ] complex	113
3.30 The IR data and X-ray data of N=N in [Ru(Clazpy)(5dmazpy)Cl $_2$ ] compared to free Clazpy ligand	114
3.31 UV-Visible absorption spectroscopic data of the [Ru(Clazpy)(5dmazpy)Cl $_2$ ] complex	115
3.32 $^1\text{H}$ - $^{13}\text{C}$ NMR spectroscopic data of [Ru(Clazpy)(5dmazpy)Cl $_2$ ] in CDCl $_3$	117
3.33 Cyclic voltammetric data of [Ru(Clazpy)(5dmazpy)Cl $_2$ ] in 0.1 M TBAH CH $_2$ Cl $_2$ at scan rate 50 mV/s (ferrocene as an internal standard)	121
3.34 Comparisons of CV and X-ray data in ruthenium azoimine complexes	123
3.35 The physical properties of [Ru(Clazpy) $_2$ (L)](PF $_6$ ) $_2$ (L = bpy, phen, azpy, Clazpy)	125
3.36 Elemental analysis data of [Ru(Clazpy) $_2$ (L)](PF $_6$ ) $_2$ (L = bpy, phen, azpy, Clazpy)	126

## LIST OF TABLES (continued)

Table	Page
3.37 Crystal data and structure refinement for [Ru(Clazpy) <sub>2</sub> (phen)](PF <sub>6</sub> ) <sub>2</sub>	127
3.38 Selected bond lengths (Å) and angles (°) and estimated standard deviations for [Ru(Clazpy) <sub>2</sub> (phen)](PF <sub>6</sub> ) <sub>2</sub>	128
3.39 Crystal data and structure refinement for [Ru(Clazpy) <sub>2</sub> (azpy)](PF <sub>6</sub> ) <sub>2</sub>	130
3.40 Selected bond lengths (Å) and angles (°) and estimated standard deviations for [Ru(Clazpy) <sub>2</sub> (azpy)](PF <sub>6</sub> ) <sub>2</sub>	131
3.41 ES mass spectrometric data of [Ru(Clazpy) <sub>2</sub> (L)](PF <sub>6</sub> ) <sub>2</sub> (L = bpy, phen, azpy, Clazpy)	133
3.42 IR data of [Ru(Clazpy) <sub>2</sub> (L)](PF <sub>6</sub> ) <sub>2</sub> (L = bpy, phen, azpy, Clazpy)	136
3.43 UV-Visible absorption spectroscopic data of [Ru(Clazpy) <sub>2</sub> (L)](PF <sub>6</sub> ) <sub>2</sub> (L = bpy, phen)	139
3.44 UV-Visible absorption spectroscopic data of Ru(Clazpy) <sub>2</sub> (L)](PF <sub>6</sub> ) <sub>2</sub> (L = azpy, Clazpy)	140
3.45 <sup>1</sup> H- <sup>13</sup> C NMR spectroscopic data of [Ru(Clazpy) <sub>2</sub> (bpy)](PF <sub>6</sub> ) <sub>2</sub>	144
3.46 <sup>1</sup> H- <sup>13</sup> C NMR spectroscopic data of [Ru(Clazpy) <sub>2</sub> (phen)](PF <sub>6</sub> ) <sub>2</sub>	149
3.47 <sup>1</sup> H- <sup>13</sup> C NMR spectroscopic data of [Ru(Clazpy) <sub>2</sub> (azpy)](PF <sub>6</sub> ) <sub>2</sub>	154
3.48 <sup>1</sup> H- <sup>13</sup> C NMR spectroscopic data of [Ru(Clazpy) <sub>3</sub> ](PF <sub>6</sub> ) <sub>2</sub>	158
3.49 Cyclic voltammetric data of [Ru(Clazpy) <sub>2</sub> (L)](PF <sub>6</sub> ) <sub>2</sub> (L = bpy, phen, azpy, Clazpy) in 0.1 M TBAH CH <sub>3</sub> CN at scan rate 50 mV/s (ferrocene as an internal standard)	162
3.50 Comparison of electronic and redox properties of the [Ru(Clazpy) <sub>2</sub> (L)](PF <sub>6</sub> ) <sub>2</sub> and <i>ctc</i> -[Ru(Clazpy) <sub>2</sub> Cl <sub>2</sub> ]	163
3.51 The physical properties of [Ru(Clazpy) <sub>2</sub> (L)](NO <sub>3</sub> ) <sub>2</sub> .xH <sub>2</sub> O (L = bpy, phen, azpy, Clazpy)	169
3.52 Elemental analysis data of [Ru(Clazpy) <sub>2</sub> (L)](NO <sub>3</sub> ) <sub>2</sub> .xH <sub>2</sub> O (L = bpy, phen, azpy, Clazpy)	170

## LIST OF TABLES (continued)

Table	Page
3.53 Crystal data and structure refinement for [Ru(Clazpy) <sub>2</sub> (phen)](NO <sub>3</sub> ) <sub>2</sub> .3.5H <sub>2</sub> O	171
3.54 Selected bond lengths (Å) and angles (°) and estimated standard deviations for [Ru(Clazpy) <sub>2</sub> (phen)](NO <sub>3</sub> ) <sub>2</sub> .3.5H <sub>2</sub> O	172
3.55 ES mass spectrometric data of [Ru(Clazpy) <sub>2</sub> (L)](NO <sub>3</sub> ) <sub>2</sub> .xH <sub>2</sub> O (L = bpy, phen, azpy, Clazpy)	173
3.56 IR data of [Ru(Clazpy) <sub>2</sub> (L)](NO <sub>3</sub> ) <sub>2</sub> .xH <sub>2</sub> O (L = bpy, phen, azpy, Clazpy)	177
3.57 UV-Visible absorption spectroscopic data of [Ru(Clazpy) <sub>2</sub> (L)](NO <sub>3</sub> ) <sub>2</sub> .xH <sub>2</sub> O (L = bpy, phen)	180
3.58 UV-Visible absorption spectroscopic data of [Ru(Clazpy) <sub>2</sub> (L)](NO <sub>3</sub> ) <sub>2</sub> .xH <sub>2</sub> O (L = azpy, Clazpy)	181
3.59 <sup>1</sup> H- <sup>13</sup> C NMR spectroscopic data of [Ru(Clazpy) <sub>2</sub> (bpy)](NO <sub>3</sub> ) <sub>2</sub> .5H <sub>2</sub> O	185
3.60 <sup>1</sup> H- <sup>13</sup> C NMR spectroscopic data of [Ru(Clazpy) <sub>2</sub> (phen)](NO <sub>3</sub> ) <sub>2</sub> .3H <sub>2</sub> O	189
3.61 <sup>1</sup> H- <sup>13</sup> C NMR spectroscopic data of [Ru(Clazpy) <sub>2</sub> (azpy)](NO <sub>3</sub> ) <sub>2</sub> .H <sub>2</sub> O	196
3.62 <sup>1</sup> H- <sup>13</sup> C NMR spectroscopic data of [Ru(Clazpy) <sub>3</sub> ](NO <sub>3</sub> ) <sub>2</sub> .5H <sub>2</sub> O	200
3.63 Cyclic voltammetric data of [Ru(Clazpy) <sub>2</sub> (L)](NO <sub>3</sub> ) <sub>2</sub> .xH <sub>2</sub> O (L = bpy, phen, azpy, Clazpy) in 0.1 TBAH CH <sub>3</sub> CN at scan rate 50 mV/s (ferrocene as an internal standard)	205
3.64 The physical properties of [Ru(Clazpy) <sub>2</sub> (L)]Cl <sub>2</sub> .xH <sub>2</sub> O (L = bpy, phen, azpy, Clazpy)	210
3.65 Elemental analysis data of [Ru(Clazpy) <sub>2</sub> (L)]Cl <sub>2</sub> .xH <sub>2</sub> O (L = bpy, phen, azpy, Clazpy)	211
3.66 ES mass spectrometric data of [Ru(Clazpy) <sub>2</sub> (L)]Cl <sub>2</sub> .xH <sub>2</sub> O (L = bpy, phen, azpy, Clazpy)	212
3.67 IR data of [Ru(Clazpy) <sub>2</sub> (L)]Cl <sub>2</sub> .xH <sub>2</sub> O (L = bpy, phen, azpy, Clazpy)	215

## LIST OF TABLES (continued)

Table	Page
3.68 UV-Visible absorption spectroscopic data of [Ru(Clazpy) <sub>2</sub> (L)]Cl <sub>2</sub> .xH <sub>2</sub> O (L = bpy, phen)	219
3.69 UV-Visible absorption spectroscopic data of [Ru(Clazpy) <sub>2</sub> (L)]Cl <sub>2</sub> .xH <sub>2</sub> O (L = azpy, Clazpy)	220
3.70 <sup>1</sup> H- <sup>13</sup> C NMR spectroscopic data of [Ru(Clazpy) <sub>2</sub> (bpy)]Cl <sub>2</sub> .7H <sub>2</sub> O	224
3.71 <sup>1</sup> H- <sup>13</sup> C NMR spectroscopic data of [Ru(Clazpy) <sub>2</sub> (phen)]Cl <sub>2</sub> .8H <sub>2</sub> O	228
3.72 <sup>1</sup> H- <sup>13</sup> C NMR spectroscopic data of [Ru(Clazpy) <sub>2</sub> (azpy)]Cl <sub>2</sub> .4H <sub>2</sub> O	234
3.73 <sup>1</sup> H- <sup>13</sup> C NMR spectroscopic data of [Ru(Clazpy) <sub>3</sub> ]Cl <sub>2</sub> .3H <sub>2</sub> O	239
3.74 Cyclic voltammetric data of [Ru(Clazpy) <sub>2</sub> (L)]Cl <sub>2</sub> .x H <sub>2</sub> O (L = bpy, phen, azpy, Clazpy) in 0.1 M TBAH CH <sub>3</sub> CN at scan rate 50 mV/s (ferrocene as an internal standard)	243
3.75 The physical properties of [Ru(bpy) <sub>2</sub> (Clazpy)](X) <sub>2</sub> and [Ru(phen) <sub>2</sub> (Clazpy)](X) <sub>2</sub> (X = PF <sub>6</sub> <sup>-</sup> , Cl <sup>-</sup> )	248
3.76 Elemental analysis data of [Ru(bpy) <sub>2</sub> (Clazpy)](X) <sub>2</sub> and [Ru(phen) <sub>2</sub> (Clazpy)](X) <sub>2</sub> (X = PF <sub>6</sub> <sup>-</sup> , Cl <sup>-</sup> )	249
3.77 ES mass spectrometric data of [Ru(bpy) <sub>2</sub> (Clazpy)](X) <sub>2</sub> and [Ru(phen) <sub>2</sub> (Clazpy)](X) <sub>2</sub> (X = PF <sub>6</sub> <sup>-</sup> , Cl <sup>-</sup> )	250
3.78 IR data of [Ru(bpy) <sub>2</sub> (Clazpy)](X) <sub>2</sub> and [Ru(phen) <sub>2</sub> (Clazpy)](X) <sub>2</sub> (X = PF <sub>6</sub> <sup>-</sup> , Cl <sup>-</sup> )	254
3.79 UV-Visible absorption spectroscopic data of [Ru(bpy) <sub>2</sub> (Clazpy)](PF <sub>6</sub> ) <sub>2</sub> and [Ru(phen) <sub>2</sub> (Clazpy)](PF <sub>6</sub> ) <sub>2</sub>	257
3.80 UV-Visible absorption spectroscopic data of [Ru(bpy) <sub>2</sub> (Clazpy)]Cl <sub>2</sub> .7H <sub>2</sub> O and [Ru(phen) <sub>2</sub> (Clazpy)]Cl <sub>2</sub> .8H <sub>2</sub> O	258
3.81 <sup>1</sup> H- <sup>13</sup> C NMR spectroscopic data of [Ru(bpy) <sub>2</sub> (Clazpy)](PF <sub>6</sub> ) <sub>2</sub>	262
3.82 <sup>1</sup> H- <sup>13</sup> C NMR spectroscopic data of [Ru(phen) <sub>2</sub> (Clazpy)](PF <sub>6</sub> ) <sub>2</sub>	267
3.83 <sup>1</sup> H- <sup>13</sup> C NMR spectroscopic data of [Ru(bpy) <sub>2</sub> (Clazpy)]Cl <sub>2</sub> .7H <sub>2</sub> O	271
3.84 <sup>1</sup> H- <sup>13</sup> C NMR spectroscopic data of [Ru(phen) <sub>2</sub> (Clazpy)]Cl <sub>2</sub> .8H <sub>2</sub> O	276

## LIST OF TABLES (continued)

Table	Page
3.85 Cyclic voltammetric data of [Ru(bpy) <sub>2</sub> (Clazpy)](X) <sub>2</sub> and [Ru(phen) <sub>2</sub> (Clazpy)](X) <sub>2</sub> (X = PF <sub>6</sub> <sup>-</sup> , Cl <sup>-</sup> ) in 0.1 M TBAH CH <sub>3</sub> CN at scan rate 50 mV/s (ferrocene as an internal standard)	280
3.86 UV-Visible absorption spectroscopic data of Ru(II) complexes upon addition of CT-DNA in 5 mM Tris/ 50 mM NaCl pH 7.1	287
3.87 Electronic absorption spectral data upon addition of CT-DNA	290
3.88 Different ancillary ligand effect to interaction with CT-DNA	292
3.89 Fluorescence quenching values of complexes	310
3.90 Cyclic voltammetric behavior for the Ru(II) complexes on interaction with CT-DNA	317
3.91 IC <sub>50</sub> values in μg/mL (μM) of Clazpy and its complexes against a series of tumor cell lines	324
3.92 IC <sub>50</sub> values in μg/mL (μM) of some ruthenium(II) complexes against a vero cell	326
A.1 UV-Visible spectra of solvents and the minimal values for measurement in 1 mm of quartz cell	347
B.1 Bond length (Å) and angle (°) of <i>tcc</i> -[Ru(Clazpy) <sub>2</sub> Cl <sub>2</sub> ]	348
B.2 Bond length (Å) and angle (°) of <i>ctc</i> -[Ru(Clazpy) <sub>2</sub> Cl <sub>2</sub> ]	351
B.3 Bond length (Å) and angle (°) of <i>ccc</i> -[Ru(Clazpy) <sub>2</sub> Cl <sub>2</sub> ]	353
B.4 Bond length (Å) and angle (°) of [Ru(Clazpy)(5dmazpy)Cl <sub>2</sub> ]	359
B.5 Bond length (Å) and angle (°) of [Ru(Clazpy) <sub>2</sub> (phen)](PF <sub>6</sub> ) <sub>2</sub>	363
B.6 Bond length (Å) and angle (°) of [Ru(Clazpy) <sub>2</sub> (azpy)](PF <sub>6</sub> ) <sub>2</sub>	368
B.7 Bond length (Å) and angle (°) of [Ru(Clazpy) <sub>2</sub> (phen)](NO <sub>3</sub> ) <sub>2</sub> .3.5H <sub>2</sub> O	373

## LIST OF FIGURES

Figure	Page
1.1 The structure of cisplatin	3
1.2 The structure of carboplatin (1) and nedaplatin (2)	4
1.3 Five possible isomers of [Ru(Clazpy) <sub>2</sub> Cl <sub>2</sub> ] complexes	6
1.4 The structure of Ethidium Bromide (EB)	8
1.5 The structure of 2-(phenylazo)pyridine (azpy)	10
1.6 The structure of 2-( <i>m</i> -tolylazo)pyridine (left) and 2,2'-bipyridine (bpy) (right)	11
1.7 The structure of 2-((4-nitrophenyl)azo)pyridine (NAz)	11
1.8 The structure of L (L = NC <sub>5</sub> H <sub>4</sub> -N=N-C <sub>6</sub> H <sub>5</sub> (R); R = H, <i>o</i> -Me/Cl, <i>m</i> -Me/Cl, <i>p</i> -Me/Cl)	12
1.9 The structure of L (L = 1-methyl-2-(arylazo)imidazole; L <sub>1</sub> and 1-benzyl-2-(arylazo)imidazole; L <sub>2</sub> )	13
1.10 The structure of 2-(arylazo)pyrimidine (aapm)	13
1.11 The structures of $\alpha$ -[Ru(azpy) <sub>2</sub> (9-MeAde)](PF <sub>6</sub> ) <sub>2</sub> (1) and <i>cis</i> -[Ru(bpy) <sub>2</sub> (9-MeAde)](PF <sub>6</sub> ) <sub>2</sub> (2)	15
1.12 The structure of $\alpha$ -[Ru(azpy) <sub>2</sub> (cbdca- <i>O,O'</i> )] (1); $\alpha$ -[Ru(azpy) <sub>2</sub> (ox)] (2); $\alpha$ -[Ru(azpy) <sub>2</sub> (mal)] (3)	16
1.13 The structure of 2-phenylazopyridine-5-sulfonic acid (Hsazpy)	17
1.14 The structures of <i>o</i> -tolylazopyridine (tazpy) 4-methyl-2-(phenylazo)pyridine (mazpy)	18
1.15 $\alpha$ -(trans Nazo 9-EtGua) and $\alpha'$ -(trans Nbpy 9-EtGua) of [Ru(azpy)(bpy)(9-EtGua)(H <sub>2</sub> O)] <sup>2+</sup>	18
1.16 The structure of 2-phenylazo-4,6-dimethylpyridine (dazpy)	19
1.17 The structure of 9-alkylated quinine derivatives	21
1.18 2,9-dimethyl-1,10-phenanthroline (dmp) 4,4'-dimethyl-2,2'-bipyridine (dmb)	22
1.19 The structure of 2,6-bis(benzimidazol-2-yl) (bzimpy)	22

## LIST OF FIGURES (continued)

Figure	Page
1.20 The structures of phen = 1,10-phenanthroline, bpy = 2,2'-bipyridine, dpq = dipyrido[3,2-d:2',3'-f]quinoxaline, dppz = dipyrido[3,2-a:2',3'-c]phenazine, tpphz = tetrapyrido[3,2-a:2',3'-c:3'',2''-h:2''',3'''-f]phenazine, phi = 9,10-phenanthrene quinonediimine	23
1.21 2'-(2''-nitro-3'',4''-methylenedioxyphenyl)imidazo-[4',5'-f][1,10]phenanthroline (NMIP)	25
1.22 2-(3'-phenoxyphenyl)imidazo[4,5-f]-[1,10]phenanthroline (MPPIP)	26
1.23 2-(4'-benzyloxyphenyl)imidazo[4,5-f]-[1,10]phenanthroline (BPIP)	26
1.24 2-(4'-biphenyl)imidazo[4,5-f][1,10]phenanthroline (BPIP)	27
1.25 2,9-dimethyl-1,10-phenanthroline (dmp); MIP = 2-(2,3-methylene dioxypheyl)imidazo[4,5-f]1,10-phenanthroline	27
3.1 Synthetic routes for the preparation of the azpy and the Clazpy ligands	48
3.2 The structure of the Clazpy ligand	49
3.3 FAB mass spectrum of the Clazpy ligand	51
3.4 IR spectrum of the Clazpy ligand	53
3.5 UV-Visible absorption spectrum of the Clazpy ligand in CH <sub>2</sub> Cl <sub>2</sub>	55
3.6 <sup>1</sup> H NMR spectrum of the Clazpy ligand in CDCl <sub>3</sub>	58
3.7 <sup>1</sup> H- <sup>1</sup> H COSY NMR spectrum of the Clazpy ligand in CDCl <sub>3</sub>	58
3.8 <sup>13</sup> C NMR spectrum of the Clazpy ligand in CDCl <sub>3</sub>	59
3.9 DEPT NMR spectrum of the Clazpy ligand in CDCl <sub>3</sub>	59
3.10 <sup>1</sup> H- <sup>13</sup> C HMQC NMR spectrum of the Clazpy ligand in CDCl <sub>3</sub>	60
3.11 Cyclic voltammogram of the Clazpy ligand in 0.1 M TBAH CH <sub>2</sub> Cl <sub>2</sub> at scan rate 50 mV/s (ferrocene as an internal standard)	62
3.12 Synthetic route for preparation of the isomeric [Ru(Clazpy) <sub>2</sub> Cl <sub>2</sub> ] complexes (method I)	63

## LIST OF FIGURES (continued)

Figure	Page
3.13 Synthetic route for preparation of isomeric [Ru(Clazpy) <sub>2</sub> Cl <sub>2</sub> ] complexes (method II)	64
3.14 The structure of <i>tcc</i> -[Ru(Clazpy) <sub>2</sub> Cl <sub>2</sub> ] (H-atom omitted)	69
3.15 The structure of <i>ctc</i> -[Ru(Clazpy) <sub>2</sub> Cl <sub>2</sub> ] (H-atom omitted)	72
3.16 The structure of <i>ccc</i> -[Ru(Clazpy) <sub>2</sub> Cl <sub>2</sub> ] (H-atom omitted)	75
3.17 FAB mass spectrum of <i>tcc</i> -[Ru(Clazpy)Cl <sub>2</sub> ]	77
3.18 FAB mass spectrum of <i>ctc</i> -[Ru(Clazpy)Cl <sub>2</sub> ]	77
3.19 FAB mass spectrum of <i>ccc</i> -[Ru(Clazpy)Cl <sub>2</sub> ]	78
3.20 IR spectrum of <i>tcc</i> -[Ru(Clazpy) <sub>2</sub> Cl <sub>2</sub> ]	80
3.21 IR spectrum of <i>ctc</i> -[Ru(Clazpy) <sub>2</sub> Cl <sub>2</sub> ]	80
3.22 IR spectrum of <i>ccc</i> -[Ru(Clazpy) <sub>2</sub> Cl <sub>2</sub> ]	81
3.23 UV-Visible absorption spectrum of <i>tcc</i> -[Ru(Clazpy) <sub>2</sub> Cl <sub>2</sub> ]	83
3.24 UV-Visible absorption spectrum of <i>ctc</i> -[Ru(Clazpy) <sub>2</sub> Cl <sub>2</sub> ]	84
3.25 UV-Visible absorption spectrum of <i>ccc</i> -[Ru(Clazpy) <sub>2</sub> Cl <sub>2</sub> ]	84
3.26 UV-Visible absorption spectra of <i>tcc</i> -, <i>ctc</i> - and <i>ccc</i> - [Ru(Clazpy) <sub>2</sub> Cl <sub>2</sub> ] in CH <sub>2</sub> Cl <sub>2</sub>	85
3.27 <sup>1</sup> H NMR spectrum of <i>tcc</i> -[Ru(Clazpy) <sub>2</sub> Cl <sub>2</sub> ] in CDCl <sub>3</sub>	87
3.28 <sup>1</sup> H- <sup>1</sup> H COSY NMR spectrum of <i>tcc</i> -[Ru(Clazpy) <sub>2</sub> Cl <sub>2</sub> ] in CDCl <sub>3</sub>	87
3.29 <sup>13</sup> C NMR spectrum of <i>tcc</i> -[Ru(Clazpy) <sub>2</sub> Cl <sub>2</sub> ] in CDCl <sub>3</sub>	88
3.30 DEPT NMR spectrum of <i>tcc</i> -[Ru(Clazpy) <sub>2</sub> Cl <sub>2</sub> ] in CDCl <sub>3</sub>	88
3.31 <sup>1</sup> H- <sup>13</sup> C HMQC NMR spectrum of <i>tcc</i> -[Ru(Clazpy) <sub>2</sub> Cl <sub>2</sub> ] in CDCl <sub>3</sub>	89
3.32 <sup>1</sup> H NMR spectrum of <i>ctc</i> -[Ru(Clazpy) <sub>2</sub> Cl <sub>2</sub> ] in CDCl <sub>3</sub>	91
3.33 <sup>1</sup> H- <sup>1</sup> H COSY NMR spectrum of <i>ctc</i> -[Ru(Clazpy) <sub>2</sub> Cl <sub>2</sub> ] in CDCl <sub>3</sub>	92
3.34 <sup>13</sup> C NMR spectrum of <i>ctc</i> -[Ru(Clazpy) <sub>2</sub> Cl <sub>2</sub> ] in CDCl <sub>3</sub>	92
3.35 DEPT NMR spectrum of <i>ctc</i> -[Ru(Clazpy) <sub>2</sub> Cl <sub>2</sub> ] in CDCl <sub>3</sub>	93
3.36 <sup>1</sup> H- <sup>13</sup> C HMQC NMR spectrum of <i>ctc</i> -[Ru(Clazpy) <sub>2</sub> Cl <sub>2</sub> ] in CDCl <sub>3</sub>	93
3.37 <sup>1</sup> H NMR spectrum of <i>ccc</i> -[Ru(Clazpy) <sub>2</sub> Cl <sub>2</sub> ] in CDCl <sub>3</sub>	95

## LIST OF FIGURES (continued)

Figure	Page
3.38 $^1\text{H}$ - $^1\text{H}$ COSY NMR spectrum of <i>ccc</i> -[Ru(Clazpy) <sub>2</sub> Cl <sub>2</sub> ] in CDCl <sub>3</sub>	96
3.39 $^{13}\text{C}$ NMR spectrum of <i>ccc</i> -[Ru(Clazpy) <sub>2</sub> Cl <sub>2</sub> ] in CDCl <sub>3</sub>	96
3.40 DEPT NMR spectrum of <i>ccc</i> -[Ru(Clazpy) <sub>2</sub> Cl <sub>2</sub> ] in CDCl <sub>3</sub>	97
3.41 $^1\text{H}$ - $^{13}\text{C}$ HMQC NMR spectrum of <i>ccc</i> -[Ru(Clazpy) <sub>2</sub> Cl <sub>2</sub> ] in CDCl <sub>3</sub>	97
3.42 $^1\text{H}$ NMR spectra of (a) Clazpy; (b) <i>tcc</i> ; (c) <i>ctc</i> ; (d) <i>ccc</i> in CDCl <sub>3</sub>	99
3.43 Cyclic voltammogram of <i>tcc</i> -[Ru(Clazpy) <sub>2</sub> Cl <sub>2</sub> ] in 0.1 M TBAH CH <sub>2</sub> Cl <sub>2</sub> at scan rate 50 mV/s (ferrocene as an internal standard)	103
3.44 Cyclic voltammogram of <i>ctc</i> -[Ru(Clazpy) <sub>2</sub> Cl <sub>2</sub> ] in 0.1 M TBAH CH <sub>2</sub> Cl <sub>2</sub> at scan rate 50 mV/s (ferrocene as an internal standard)	103
3.45 Cyclic voltammogram of <i>ccc</i> -[Ru(Clazpy) <sub>2</sub> Cl <sub>2</sub> ] in 0.1 M TBAH CH <sub>2</sub> Cl <sub>2</sub> at scan rate 50 mV/s (ferrocene as an internal standard)	104
3.46 The proposed mechanism of [Ru(Clazpy)(5dmazpy)Cl <sub>2</sub> ]	106
3.47 The structure of [Ru(Clazpy)(5dmazpy)Cl <sub>2</sub> ] (H-atom omitted)	110
3.48 FAB mass spectrum of [Ru(Clazpy)(5dmazpy)Cl <sub>2</sub> ]	111
3.49 Fragmentation of [Ru(Clazpy)(5dmazpy)Cl <sub>2</sub> ]	112
3.50 IR spectrum of [Ru(Clazpy)(5dmazpy)Cl <sub>2</sub> ]	113
3.51 UV-Visible absorption spectrum of [Ru(Clazpy)(5dmazpy)Cl <sub>2</sub> ] in CH <sub>2</sub> Cl <sub>2</sub>	116
3.52 $^1\text{H}$ NMR spectrum of [Ru(Clazpy)(5dmazpy)Cl <sub>2</sub> ] in CDCl <sub>3</sub>	118
3.53 $^1\text{H}$ - $^1\text{H}$ COSY NMR spectrum of [Ru(Clazpy)(5dmazpy)Cl <sub>2</sub> ] in CDCl <sub>3</sub>	119
3.54 $^{13}\text{C}$ NMR spectrum of [Ru(Clazpy)(5dmazpy)Cl <sub>2</sub> ] in CDCl <sub>3</sub>	119
3.55 DEPT NMR spectrum of [Ru(Clazpy)(5dmazpy)Cl <sub>2</sub> ] in CDCl <sub>3</sub>	120
3.56 $^1\text{H}$ - $^{13}\text{C}$ HMQC NMR spectrum of [Ru(Clazpy)(5dmazpy)Cl <sub>2</sub> ] in CDCl <sub>3</sub>	120
3.57 Cyclic voltammogram of [Ru(Clazpy)(5dmazpy)Cl <sub>2</sub> ] in 0.1 M TBAH CH <sub>2</sub> Cl <sub>2</sub> at scan rate 50 mV/s (ferrocene as an internal standard)	123

## LIST OF FIGURES (continued)

Figure	Page
3.58 Synthetic routes for the preparation of $[\text{Ru}(\text{Clazpy})_2(\text{L})](\text{PF}_6)_2$ (L = bpy, phen, azpy, Clazpy)	124
3.59 The structure of $[\text{Ru}(\text{Clazpy})_2(\text{phen})](\text{PF}_6)_2$ (H-atom omitted)	129
3.60 The structure of $[\text{Ru}(\text{Clazpy})_2(\text{azpy})](\text{PF}_6)_2$ (H-atom omitted)	132
3.61 ES mass spectrum of $[\text{Ru}(\text{Clazpy})_2(\text{bpy})](\text{PF}_6)_2$	134
3.62 ES mass spectrum of $[\text{Ru}(\text{Clazpy})_2(\text{phen})](\text{PF}_6)_2$	134
3.63 ES mass spectrum of $[\text{Ru}(\text{Clazpy})_2(\text{azpy})](\text{PF}_6)_2$	135
3.64 ES mass spectrum of $[\text{Ru}(\text{Clazpy})_3](\text{PF}_6)_2$	135
3.65 IR spectrum of $[\text{Ru}(\text{Clazpy})_2(\text{bpy})](\text{PF}_6)_2$	137
3.66 IR spectrum of $[\text{Ru}(\text{Clazpy})_2(\text{phen})](\text{PF}_6)_2$	137
3.67 IR spectrum of $[\text{Ru}(\text{Clazpy})_2(\text{azpy})](\text{PF}_6)_2$	138
3.68 IR spectrum of $[\text{Ru}(\text{Clazpy})_3](\text{PF}_6)_2$	138
3.69 UV-Visible absorption spectrum of $[\text{Ru}(\text{Clazpy})_2(\text{bpy})](\text{PF}_6)_2$ in $\text{CH}_3\text{CN}$	141
3.70 UV-Visible absorption spectrum of $[\text{Ru}(\text{Clazpy})_2(\text{phen})](\text{PF}_6)_2$ in $\text{CH}_3\text{CN}$	141
3.71 UV-Visible absorption spectrum of $[\text{Ru}(\text{Clazpy})_2(\text{azpy})](\text{PF}_6)_2$ in $\text{CH}_3\text{CN}$	142
3.72 UV-Visible absorption spectrum of $[\text{Ru}(\text{Clazpy})_3](\text{PF}_6)_2$ in $\text{CH}_3\text{CN}$	142
3.73 $^1\text{H}$ NMR spectrum of $[\text{Ru}(\text{Clazpy})_2(\text{bpy})](\text{PF}_6)_2$ in acetone- $d_6$	145
3.74 $^1\text{H}$ - $^1\text{H}$ COSY NMR spectrum of $[\text{Ru}(\text{Clazpy})_2(\text{bpy})](\text{PF}_6)_2$ in acetone- $d_6$	146
3.75 $^{13}\text{C}$ NMR spectrum of $[\text{Ru}(\text{Clazpy})_2(\text{bpy})](\text{PF}_6)_2$ in acetone- $d_6$	146
3.76 DEPT NMR spectrum of $[\text{Ru}(\text{Clazpy})_2(\text{bpy})](\text{PF}_6)_2$ acetone- $d_6$	147
3.77 $^1\text{H}$ - $^{13}\text{C}$ HMQC NMR spectrum of $[\text{Ru}(\text{Clazpy})_2(\text{bpy})](\text{PF}_6)_2$ in acetone- $d_6$	147
3.78 $^1\text{H}$ NMR spectrum of $[\text{Ru}(\text{Clazpy})_2(\text{phen})](\text{PF}_6)_2$ in acetone- $d_6$	150

## LIST OF FIGURS (continued)

Figure	Page
3.79 <sup>1</sup> H NMR spectrum of [Ru(Clazpy) <sub>2</sub> (phen)](PF <sub>6</sub> ) <sub>2</sub> in acetone- <i>d</i> <sub>6</sub> (Cont.)	150
3.80 <sup>1</sup> H- <sup>1</sup> H COSY NMR spectrum of [Ru(Clazpy) <sub>2</sub> (phen)](PF <sub>6</sub> ) <sub>2</sub> in acetone- <i>d</i> <sub>6</sub>	151
3.81 <sup>13</sup> C NMR spectrum of [Ru(Clazpy) <sub>2</sub> (phen)](PF <sub>6</sub> ) <sub>2</sub> in acetone- <i>d</i> <sub>6</sub>	151
3.82 DEPT NMR spectrum of [Ru(Clazpy) <sub>2</sub> (phen)](PF <sub>6</sub> ) <sub>2</sub> in acetone- <i>d</i> <sub>6</sub>	152
3.83 <sup>1</sup> H- <sup>13</sup> C HMQC NMR spectrum of [Ru(Clazpy) <sub>2</sub> (bpy)](PF <sub>6</sub> ) <sub>2</sub> in acetone- <i>d</i> <sub>6</sub>	152
3.84 <sup>1</sup> H NMR spectrum of [Ru(Clazpy) <sub>2</sub> (azpy)](PF <sub>6</sub> ) <sub>2</sub> in acetone- <i>d</i> <sub>6</sub>	155
3.85 <sup>1</sup> H- <sup>1</sup> H COSY NMR spectrum of [Ru(Clazpy) <sub>2</sub> (azpy)](PF <sub>6</sub> ) <sub>2</sub> in acetone- <i>d</i> <sub>6</sub>	155
3.86 <sup>13</sup> C NMR spectrum of [Ru(Clazpy) <sub>2</sub> (azpy)](PF <sub>6</sub> ) <sub>2</sub> in acetone- <i>d</i> <sub>6</sub>	156
3.87 DEPT NMR spectrum of [Ru(Clazpy) <sub>2</sub> (azpy)](PF <sub>6</sub> ) <sub>2</sub> acetone- <i>d</i> <sub>6</sub>	156
3.88 <sup>1</sup> H- <sup>13</sup> C HMQC NMR spectrum of [Ru(Clazpy) <sub>2</sub> (azpy)](PF <sub>6</sub> ) <sub>2</sub> in acetone- <i>d</i> <sub>6</sub>	157
3.89 <sup>1</sup> H NMR spectrum of [Ru(Clazpy) <sub>3</sub> ](PF <sub>6</sub> ) <sub>2</sub> in acetone- <i>d</i> <sub>6</sub>	159
3.90 <sup>1</sup> H- <sup>1</sup> H COSY NMR spectrum of [Ru(Clazpy) <sub>3</sub> ](PF <sub>6</sub> ) <sub>2</sub> in acetone- <i>d</i> <sub>6</sub>	160
3.91 <sup>13</sup> C NMR spectrum of [Ru(Clazpy) <sub>3</sub> ](PF <sub>6</sub> ) <sub>2</sub> in acetone- <i>d</i> <sub>6</sub>	160
3.92 DEPT NMR spectrum of [Ru(Clazpy) <sub>3</sub> ](PF <sub>6</sub> ) <sub>2</sub> acetone- <i>d</i> <sub>6</sub>	161
3.93 <sup>1</sup> H- <sup>13</sup> C HMQC NMR spectrum of [Ru(Clazpy) <sub>3</sub> ](PF <sub>6</sub> ) <sub>2</sub> in acetone- <i>d</i> <sub>6</sub>	161
3.94 Cyclic voltammogram of [Ru(Clazpy) <sub>2</sub> (bpy)](PF <sub>6</sub> ) <sub>2</sub> in 0.1 M TBAH CH <sub>3</sub> CN at scan rate 50 mV/s (ferrocene as an internal standard)	165
3.95 Cyclic voltammogram of [Ru(Clazpy) <sub>2</sub> (phen)](PF <sub>6</sub> ) <sub>2</sub> in 0.1 M TBAH CH <sub>3</sub> CN at scan rate 50 mV/s (ferrocene as an internal standard)	166
3.96 Cyclic voltammogram of [Ru(Clazpy) <sub>2</sub> (azpy)](PF <sub>6</sub> ) <sub>2</sub> in 0.1 M TBAH CH <sub>3</sub> CN at scan rate 50 mV/s (ferrocene as an internal standard)	166

## LIST OF FIGURES (continued)

Figure	Page
3.97 Cyclic voltammogram of $[\text{Ru}(\text{Clazpy})_3](\text{PF}_6)_2$ in 0.1 M TBAH $\text{CH}_3\text{CN}$ at scan rate 50 mV/s (ferrocene as an internal standard)	167
3.98 Synthetic routes for the preparation of $[\text{Ru}(\text{Clazpy})_2(\text{L})](\text{NO}_3)_2 \cdot x\text{H}_2\text{O}$ (L = bpy, phen, azpy, Clazpy)	168
3.99 The structure of $[\text{Ru}(\text{Clazpy})_2(\text{phen})](\text{NO}_3)_2 \cdot 3.5\text{H}_2\text{O}$ (H-atom omitted)	173
3.100 ES mass spectrum of $[\text{Ru}(\text{Clazpy})_2(\text{bpy})](\text{NO}_3)_2 \cdot 5\text{H}_2\text{O}$	175
3.101 ES mass spectrum of $[\text{Ru}(\text{Clazpy})_2(\text{phen})](\text{NO}_3)_2 \cdot 3\text{H}_2\text{O}$	175
3.102 ES mass spectrum of $[\text{Ru}(\text{Clazpy})_2(\text{azpy})](\text{NO}_3)_2 \cdot \text{H}_2\text{O}$	176
3.103 ES mass spectrum of $[\text{Ru}(\text{Clazpy})_3](\text{NO}_3)_2 \cdot 5\text{H}_2\text{O}$	176
3.104 IR spectrum of $[\text{Ru}(\text{Clazpy})_2(\text{bpy})](\text{NO}_3)_2 \cdot 5\text{H}_2\text{O}$	178
3.105 IR spectrum of $[\text{Ru}(\text{Clazpy})_2(\text{phen})](\text{NO}_3)_2 \cdot 3\text{H}_2\text{O}$	178
3.106 IR spectrum of $[\text{Ru}(\text{Clazpy})_2(\text{azpy})](\text{NO}_3)_2 \cdot \text{H}_2\text{O}$	179
3.107 IR spectrum of $[\text{Ru}(\text{Clazpy})_3](\text{NO}_3)_2 \cdot 5\text{H}_2\text{O}$	179
3.108 UV-Visible absorption spectrum of $[\text{Ru}(\text{Clazpy})_2(\text{bpy})](\text{NO}_3)_2 \cdot 5\text{H}_2\text{O}$ in $\text{CH}_3\text{CN}$	182
3.109 UV-Visible absorption spectrum of $[\text{Ru}(\text{Clazpy})_2(\text{phen})](\text{NO}_3)_2 \cdot 3\text{H}_2\text{O}$ in $\text{CH}_3\text{CN}$	183
3.110 UV-Visible absorption spectrum of $[\text{Ru}(\text{Clazpy})_2(\text{azpy})](\text{NO}_3)_2 \cdot \text{H}_2\text{O}$ in $\text{CH}_3\text{CN}$	183
3.111 UV-Visible absorption spectrum of $[\text{Ru}(\text{Clazpy})_3](\text{NO}_3)_2 \cdot 5\text{H}_2\text{O}$ in $\text{CH}_3\text{CN}$	184
3.112 $^1\text{H}$ NMR spectrum of $[\text{Ru}(\text{Clazpy})_2(\text{bpy})](\text{NO}_3)_2 \cdot 5\text{H}_2\text{O}$ in methanol- $d_4$	186
3.113 $^1\text{H}$ - $^1\text{H}$ COSY NMR spectrum of $[\text{Ru}(\text{Clazpy})_2(\text{bpy})](\text{NO}_3)_2 \cdot 5\text{H}_2\text{O}$ in methanol- $d_4$	187

## LIST OF FIGURES (continued)

Figure	Page
3.114 $^{13}\text{C}$ NMR spectrum of $[\text{Ru}(\text{Clazpy})_2(\text{bpy})](\text{NO}_3)_2 \cdot 5\text{H}_2\text{O}$ in methanol- $d_4$	187
3.115 DEPT NMR spectrum of $[\text{Ru}(\text{Clazpy})_2(\text{bpy})](\text{NO}_3)_2 \cdot 5\text{H}_2\text{O}$ in methanol- $d_4$	188
3.116 $^1\text{H}$ - $^{13}\text{C}$ HMQC NMR spectrum of $[\text{Ru}(\text{Clazpy})_2(\text{bpy})](\text{NO}_3)_2 \cdot 5\text{H}_2\text{O}$ in methanol- $d_4$	188
3.117 $^1\text{H}$ NMR spectrum of $[\text{Ru}(\text{Clazpy})_2(\text{phen})](\text{NO}_3)_2 \cdot 3\text{H}_2\text{O}$ in methanol- $d_4$	191
3.118 $^1\text{H}$ - $^1\text{H}$ COSY NMR spectrum of $[\text{Ru}(\text{Clazpy})_2(\text{phen})](\text{NO}_3)_2 \cdot 3\text{H}_2\text{O}$ in methanol- $d_4$	191
3.119 $^1\text{H}$ - $^1\text{H}$ TOCSY NMR spectrum of $[\text{Ru}(\text{Clazpy})_2(\text{phen})](\text{NO}_3)_2 \cdot 3\text{H}_2\text{O}$ in methanol- $d_4$	192
3.120 $^1\text{H}$ - $^1\text{H}$ ROESY NMR spectrum of $[\text{Ru}(\text{Clazpy})_2(\text{phen})](\text{NO}_3)_2 \cdot 3\text{H}_2\text{O}$ in methanol- $d_4$	192
3.121 $^{13}\text{C}$ NMR spectrum of $[\text{Ru}(\text{Clazpy})_2(\text{phen})](\text{NO}_3)_2 \cdot 3\text{H}_2\text{O}$ in methanol- $d_4$	193
3.122 DEPT NMR spectrum of $[\text{Ru}(\text{Clazpy})_2(\text{phen})](\text{NO}_3)_2 \cdot 3\text{H}_2\text{O}$ in methanol- $d_4$	193
3.123 $^1\text{H}$ - $^{13}\text{C}$ HSQC NMR spectrum of $[\text{Ru}(\text{Clazpy})_2(\text{phen})](\text{NO}_3)_2 \cdot 3\text{H}_2\text{O}$ in methanol- $d_4$	194
3.124 $^1\text{H}$ - $^{13}\text{C}$ HMBC NMR spectrum of $[\text{Ru}(\text{Clazpy})_2(\text{phen})](\text{NO}_3)_2 \cdot 3\text{H}_2\text{O}$ in methanol- $d_4$	194
3.125 $^1\text{H}$ NMR spectrum of $[\text{Ru}(\text{Clazpy})_2(\text{azpy})](\text{NO}_3)_2 \cdot \text{H}_2\text{O}$ in methanol- $d_4$	197
3.126 $^1\text{H}$ - $^1\text{H}$ COSY NMR spectrum of $[\text{Ru}(\text{Clazpy})_2(\text{azpy})](\text{NO}_3)_2 \cdot \text{H}_2\text{O}$ in methanol- $d_4$	197

## LIST OF FIGURES (continued)

Figure	Page
3.127 $^{13}\text{C}$ NMR spectrum of $[\text{Ru}(\text{Clazpy})_2(\text{azpy})](\text{NO}_3)_2 \cdot \text{H}_2\text{O}$ in methanol- $d_4$	198
3.128 DEPT NMR spectrum of $[\text{Ru}(\text{Clazpy})_2(\text{azpy})](\text{NO}_3)_2 \cdot \text{H}_2\text{O}$ in methanol- $d_4$	198
3.129 $^1\text{H}$ - $^{13}\text{C}$ HMQC NMR spectrum of $[\text{Ru}(\text{Clazpy})_2(\text{azpy})](\text{NO}_3)_2 \cdot \text{H}_2\text{O}$ in methanol- $d_4$	199
3.130 $^1\text{H}$ NMR spectrum of $[\text{Ru}(\text{Clazpy})_3](\text{NO}_3)_2 \cdot 5\text{H}_2\text{O}$ in methanol- $d_4$	202
3.131 $^1\text{H}$ - $^1\text{H}$ COSY NMR spectrum of $[\text{Ru}(\text{Clazpy})_3](\text{NO}_3)_2 \cdot 5\text{H}_2\text{O}$ in methanol- $d_4$	202
3.132 $^{13}\text{C}$ NMR spectrum of $[\text{Ru}(\text{Clazpy})_3](\text{NO}_3)_2 \cdot 5\text{H}_2\text{O}$ in methanol- $d_4$	203
3.133 DEPT NMR spectrum of $[\text{Ru}(\text{Clazpy})_3](\text{NO}_3)_2 \cdot 5\text{H}_2\text{O}$ in methanol- $d_4$	203
3.134 $^1\text{H}$ - $^{13}\text{C}$ HMQC NMR spectrum of $[\text{Ru}(\text{Clazpy})_3](\text{NO}_3)_2 \cdot 5\text{H}_2\text{O}$ in methanol- $d_4$	204
3.135 Cyclic voltammogram of $[\text{Ru}(\text{Clazpy})_2(\text{bpy})](\text{NO}_3)_2 \cdot 5\text{H}_2\text{O}$ in 0.1 M TBAH $\text{CH}_3\text{CN}$ at scan rate 50 mV/s (ferrocene as an internal standard)	206
3.136 Cyclic voltammogram of $[\text{Ru}(\text{Clazpy})_2(\text{phen})](\text{NO}_3)_2 \cdot 3\text{H}_2\text{O}$ in 0.1 M TBAH $\text{CH}_3\text{CN}$ at scan rate 50 mV/s (ferrocene as an internal standard)	207
3.137 Cyclic voltammogram of $[\text{Ru}(\text{Clazpy})_2(\text{azpy})](\text{NO}_3)_2 \cdot \text{H}_2\text{O}$ in 0.1 M TBAH $\text{CH}_3\text{CN}$ at scan rate 50 mV/s (ferrocene as an internal standard)	207
3.138 Cyclic voltammogram of $[\text{Ru}(\text{Clazpy})_3](\text{NO}_3)_2 \cdot 5\text{H}_2\text{O}$ in 0.1 M TBAH $\text{CH}_3\text{CN}$ at scan rate 50 mV/s (ferrocene as an internal standard)	208
3.139 Synthetic routes for the preparation of $[\text{Ru}(\text{Clazpy})_2(\text{L})]\text{Cl}_2 \cdot x\text{H}_2\text{O}$	209
3.140 ES mass spectrum of $[\text{Ru}(\text{Clazpy})_2(\text{bpy})]\text{Cl}_2 \cdot 7\text{H}_2\text{O}$	213

## LIST OF FIGURES (continued)

Figure	Page
3.141 ES mass spectrum of [Ru(Clazpy) <sub>2</sub> (phen)]Cl <sub>2</sub> .8H <sub>2</sub> O	213
3.142 ES mass spectrum of [Ru(Clazpy) <sub>2</sub> (azpy)]Cl <sub>2</sub> .4H <sub>2</sub> O	214
3.143 ES mass spectrum of [Ru(Clazpy) <sub>3</sub> ]Cl <sub>2</sub> .3H <sub>2</sub> O	214
3.144 IR spectrum of [Ru(Clazpy) <sub>2</sub> (bpy)]Cl <sub>2</sub> .7H <sub>2</sub> O	216
3.145 IR spectrum of [Ru(Clazpy) <sub>2</sub> (phen)]Cl <sub>2</sub> .8H <sub>2</sub> O	217
3.146 IR spectrum of [Ru(Clazpy) <sub>2</sub> (azpy)]Cl <sub>2</sub> .4H <sub>2</sub> O	218
3.147 IR spectrum of [Ru(Clazpy) <sub>3</sub> ]Cl <sub>2</sub> .3H <sub>2</sub> O	219
3.148 UV-Visible absorption spectrum of [Ru(Clazpy) <sub>2</sub> (bpy)]Cl <sub>2</sub> .7H <sub>2</sub> O in CH <sub>3</sub> CN	221
3.149 UV-Visible absorption spectrum of [Ru(Clazpy) <sub>2</sub> (phen)]Cl <sub>2</sub> .8H <sub>2</sub> O in CH <sub>3</sub> CN	222
3.150 UV-Visible absorption spectrum of [Ru(Clazpy) <sub>2</sub> (azpy)]Cl <sub>2</sub> .4H <sub>2</sub> O in CH <sub>3</sub> CN	222
3.151 UV-Visible absorption spectrum of [Ru(Clazpy) <sub>3</sub> ]Cl <sub>2</sub> .3H <sub>2</sub> O in CH <sub>3</sub> CN	223
3.152 <sup>1</sup> H NMR spectrum of [Ru(Clazpy) <sub>2</sub> (bpy)]Cl <sub>2</sub> .7H <sub>2</sub> O in methanol- <i>d</i> <sub>4</sub>	225
3.153 <sup>1</sup> H- <sup>1</sup> H COSY NMR spectrum of [Ru(Clazpy) <sub>2</sub> (bpy)]Cl <sub>2</sub> .7H <sub>2</sub> O in methanol- <i>d</i> <sub>4</sub>	226
3.154 <sup>13</sup> C NMR spectrum of [Ru(Clazpy) <sub>2</sub> (bpy)]Cl <sub>2</sub> .7H <sub>2</sub> O in methanol- <i>d</i> <sub>4</sub>	226
3.155 DEPT NMR spectrum of [Ru(Clazpy) <sub>2</sub> (bpy)]Cl <sub>2</sub> .7H <sub>2</sub> O in methanol- <i>d</i> <sub>4</sub>	227
3.156 <sup>1</sup> H- <sup>13</sup> C HMQC NMR spectrum of [Ru(Clazpy) <sub>2</sub> (bpy)]Cl <sub>2</sub> .7H <sub>2</sub> O in methanol- <i>d</i> <sub>4</sub>	227
3.157 <sup>1</sup> H NMR spectrum of [Ru(Clazpy) <sub>2</sub> (phen)]Cl <sub>2</sub> .8H <sub>2</sub> O in methanol- <i>d</i> <sub>4</sub>	229
3.158 <sup>1</sup> H- <sup>1</sup> H COSY NMR spectrum of [Ru(Clazpy) <sub>2</sub> (phen)]Cl <sub>2</sub> .8H <sub>2</sub> O in methanol- <i>d</i> <sub>4</sub>	230

## LIST OF FIGURES (continued)

Figure	Page
3.159 $^1\text{H}$ - $^1\text{H}$ TOCSY NMR spectrum of $[\text{Ru}(\text{Clazpy})_2(\text{phen})]\text{Cl}_2 \cdot 8\text{H}_2\text{O}$ in methanol- $d_4$	230
3.160 $^1\text{H}$ - $^1\text{H}$ ROESY NMR spectrum of $[\text{Ru}(\text{Clazpy})_2(\text{phen})]\text{Cl}_2 \cdot 8\text{H}_2\text{O}$ in methanol- $d_4$	231
3.161 $^{13}\text{C}$ NMR spectrum of $[\text{Ru}(\text{Clazpy})_2(\text{phen})]\text{Cl}_2 \cdot 8\text{H}_2\text{O}$ in methanol- $d_4$	231
3.162 DEPT NMR spectrum of $[\text{Ru}(\text{Clazpy})_2(\text{phen})]\text{Cl}_2 \cdot 8\text{H}_2\text{O}$ in methanol- $d_4$	232
3.163 $^1\text{H}$ - $^{13}\text{C}$ HSQC NMR spectrum of $[\text{Ru}(\text{Clazpy})_2(\text{phen})]\text{Cl}_2 \cdot 8\text{H}_2\text{O}$ in methanol- $d_4$	232
3.164 $^1\text{H}$ - $^{13}\text{C}$ HMBC NMR spectrum of $[\text{Ru}(\text{Clazpy})_2(\text{phen})]\text{Cl}_2 \cdot 8\text{H}_2\text{O}$ in methanol- $d_4$	233
3.165 $^1\text{H}$ NMR spectrum of $[\text{Ru}(\text{Clazpy})_2(\text{azpy})]\text{Cl}_2 \cdot 4\text{H}_2\text{O}$ in methanol- $d_4$	235
3.166 $^1\text{H}$ - $^1\text{H}$ COSY NMR spectrum of $[\text{Ru}(\text{Clazpy})_2(\text{azpy})]\text{Cl}_2 \cdot 4\text{H}_2\text{O}$ in methanol- $d_4$	236
3.167 $^{13}\text{C}$ NMR spectrum of $[\text{Ru}(\text{Clazpy})_2(\text{azpy})]\text{Cl}_2 \cdot 4\text{H}_2\text{O}$ in methanol- $d_4$	236
3.168 DEPT NMR spectrum of $[\text{Ru}(\text{Clazpy})_2(\text{azpy})]\text{Cl}_2 \cdot 4\text{H}_2\text{O}$ methanol- $d_4$	237
3.169 $^1\text{H}$ - $^{13}\text{C}$ HMQC NMR spectrum of $[\text{Ru}(\text{Clazpy})_2(\text{azpy})]\text{Cl}_2 \cdot 4\text{H}_2\text{O}$ in methanol- $d_4$	237
3.170 $^1\text{H}$ NMR spectrum of $[\text{Ru}(\text{Clazpy})_3]\text{Cl}_2 \cdot 3\text{H}_2\text{O}$ in methanol- $d_4$	240
3.171 $^1\text{H}$ - $^1\text{H}$ COSY NMR spectrum of $[\text{Ru}(\text{Clazpy})_3]\text{Cl}_2 \cdot 3\text{H}_2\text{O}$ in methanol- $d_4$	240
3.172 $^{13}\text{C}$ NMR spectrum of $[\text{Ru}(\text{Clazpy})_3]\text{Cl}_2 \cdot 3\text{H}_2\text{O}$ in methanol- $d_4$	241
3.173 DEPT NMR spectrum of $[\text{Ru}(\text{Clazpy})_3]\text{Cl}_2 \cdot 4\text{H}_2\text{O}$ in methanol- $d_4$	241
3.174 $^1\text{H}$ - $^{13}\text{C}$ HMQC NMR spectrum of $[\text{Ru}(\text{Clazpy})_3]\text{Cl}_2 \cdot 3\text{H}_2\text{O}$ in methanol- $d_4$	242

## LIST OF FIGURES (continued)

Figure	Page
3.175 Cyclic voltammogram of [Ru(Clazpy) <sub>2</sub> (bpy)]Cl <sub>2</sub> ·5H <sub>2</sub> O in 0.1 M TBAH CH <sub>3</sub> CN at scan rate 50 mV/s (ferrocene as an internal standard)	245
3.176 Cyclic voltammogram of [Ru(Clazpy) <sub>2</sub> (phen)]Cl <sub>2</sub> ·4H <sub>2</sub> O in 0.1 M TBAH CH <sub>3</sub> CN at scan rate 50 mV/s (ferrocene as an internal standard)	245
3.177 Cyclic voltammogram of [Ru(Clazpy) <sub>2</sub> (azpy)]Cl <sub>2</sub> ·3H <sub>2</sub> O in 0.1 M TBAH CH <sub>3</sub> CN at scan rate 50 mV/s (ferrocene as an internal standard)	246
3.178 Cyclic voltammogram of [Ru(Clazpy) <sub>3</sub> ]Cl <sub>2</sub> ·5H <sub>2</sub> O in 0.1 M TBAH CH <sub>3</sub> CN at scan rate 50 mV/s (ferrocene as an internal standard)	246
3.179 Synthetic routes for the preparation of <i>cis</i> -[Ru(bpy) <sub>2</sub> Cl <sub>2</sub> ] and <i>cis</i> -[Ru(phen) <sub>2</sub> Cl <sub>2</sub> ]	247
3.180 Synthetic routes for the preparation of [Ru(bpy) <sub>2</sub> (Clazpy)](PF <sub>6</sub> ) and [Ru(phen) <sub>2</sub> Clazpy](PF <sub>6</sub> )	248
3.181 ES mass spectrum of [Ru(bpy) <sub>2</sub> (Clazpy)](PF <sub>6</sub> ) <sub>2</sub>	251
3.182 ES mass spectrum of [Ru(phen) <sub>2</sub> (Clazpy)](PF <sub>6</sub> ) <sub>2</sub>	252
3.183 ES mass spectrum of [Ru(bpy) <sub>2</sub> (Clazpy)]Cl <sub>2</sub> ·7H <sub>2</sub> O	252
3.184 ES mass spectrum of [Ru(phen) <sub>2</sub> (Clazpy)]Cl <sub>2</sub> ·8H <sub>2</sub> O	253
3.185 IR spectrum of [Ru(bpy) <sub>2</sub> (Clazpy)](PF <sub>6</sub> ) <sub>2</sub>	255
3.186 IR spectrum of [Ru(phen) <sub>2</sub> (Clazpy)](PF <sub>6</sub> ) <sub>2</sub>	255
3.187 IR spectrum of [Ru(bpy) <sub>2</sub> (Clazpy)]Cl <sub>2</sub> ·7H <sub>2</sub> O	256
3.188 IR spectrum of [Ru(phen) <sub>2</sub> (Clazpy)]Cl <sub>2</sub> ·8H <sub>2</sub> O	256
3.189 UV-Visible absorption spectrum of [Ru(bpy) <sub>2</sub> (Clazpy)](PF <sub>6</sub> ) <sub>2</sub> in CH <sub>3</sub> CN	259
3.190 UV-Visible absorption spectrum of [Ru(phen) <sub>2</sub> (Clazpy)](PF <sub>6</sub> ) <sub>2</sub> in CH <sub>3</sub> CN	260

## LIST OF FIGURES (continued)

Figure	Page
3.191 UV-Visible absorption spectrum of [Ru(bpy) <sub>2</sub> (Clazpy)]Cl <sub>2</sub> ·7H <sub>2</sub> O in CH <sub>3</sub> CN	260
3.192 UV-Visible absorption spectrum of [Ru(phen) <sub>2</sub> (Clazpy)]Cl <sub>2</sub> ·8H <sub>2</sub> O in CH <sub>3</sub> CN	261
3.193 <sup>1</sup> H NMR spectrum of [Ru(bpy) <sub>2</sub> (Clazpy)](PF <sub>6</sub> ) <sub>2</sub> in acetone- <i>d</i> <sub>6</sub>	263
3.194 <sup>1</sup> H- <sup>1</sup> H COSY NMR spectrum of [Ru(bpy) <sub>2</sub> (Clazpy)](PF <sub>6</sub> ) <sub>2</sub> in acetone- <i>d</i> <sub>6</sub>	264
3.195 <sup>13</sup> C NMR spectrum of [Ru(bpy) <sub>2</sub> (Clazpy)](PF <sub>6</sub> ) <sub>2</sub> in acetone- <i>d</i> <sub>6</sub>	264
3.196 DEPT NMR spectrum of [Ru(bpy) <sub>2</sub> (Clazpy)](PF <sub>6</sub> ) <sub>2</sub> in acetone- <i>d</i> <sub>6</sub>	265
3.197 <sup>1</sup> H- <sup>13</sup> C HMQC NMR spectrum of [Ru(bpy) <sub>2</sub> (Clazpy)](PF <sub>6</sub> ) <sub>2</sub> in acetone- <i>d</i> <sub>6</sub>	265
3.198 <sup>1</sup> H NMR spectrum of [Ru(phen) <sub>2</sub> (Clazpy)](PF <sub>6</sub> ) <sub>2</sub> in acetone- <i>d</i> <sub>6</sub>	268
3.199 <sup>1</sup> H- <sup>1</sup> H COSY NMR spectrum of [Ru(phen) <sub>2</sub> (Clazpy)](PF <sub>6</sub> ) <sub>2</sub> in acetone- <i>d</i> <sub>6</sub>	268
3.200 <sup>13</sup> C NMR spectrum of [Ru(phen) <sub>2</sub> (Clazpy)](PF <sub>6</sub> ) <sub>2</sub> in acetone- <i>d</i> <sub>6</sub>	269
3.201 DEPT NMR spectrum of [Ru(phen) <sub>2</sub> (Clazpy)](PF <sub>6</sub> ) <sub>2</sub> in acetone- <i>d</i> <sub>6</sub>	269
3.202 <sup>1</sup> H- <sup>13</sup> C HMQC NMR spectrum of [Ru(phen) <sub>2</sub> (Clazpy)](PF <sub>6</sub> ) <sub>2</sub> in acetone- <i>d</i> <sub>6</sub>	270
3.203 <sup>1</sup> H NMR spectrum of [Ru(bpy) <sub>2</sub> (Clazpy)]Cl <sub>2</sub> ·7H <sub>2</sub> O in methanol- <i>d</i> <sub>4</sub>	272
3.204 <sup>1</sup> H- <sup>1</sup> H COSY NMR spectrum of [Ru(bpy) <sub>2</sub> (Clazpy)]Cl <sub>2</sub> ·7H <sub>2</sub> O in methanol- <i>d</i> <sub>4</sub>	273
3.205 <sup>13</sup> C NMR spectrum of [Ru(bpy) <sub>2</sub> (Clazpy)]Cl <sub>2</sub> ·7H <sub>2</sub> O in methanol- <i>d</i> <sub>4</sub>	273
3.206 DEPT NMR spectrum of [Ru(bpy) <sub>2</sub> (Clazpy)]Cl <sub>2</sub> ·7H <sub>2</sub> O methanol- <i>d</i> <sub>4</sub>	274
3.207 <sup>1</sup> H- <sup>13</sup> C HMQC NMR spectrum of [Ru(bpy) <sub>2</sub> (Clazpy)]Cl <sub>2</sub> ·7H <sub>2</sub> O in methanol- <i>d</i> <sub>4</sub>	274
3.208 <sup>1</sup> H NMR spectrum of [Ru(phen) <sub>2</sub> (Clazpy)]Cl <sub>2</sub> ·8H <sub>2</sub> O in methanol- <i>d</i> <sub>4</sub>	277

## LIST OF FIGURES (continued)

Figure	Page
3.209 $^1\text{H}$ - $^1\text{H}$ COSY NMR spectrum of $[\text{Ru}(\text{phen})_2(\text{Clazpy})]\text{Cl}_2 \cdot 8\text{H}_2\text{O}$ in methanol- $d_4$	277
3.210 $^{13}\text{C}$ NMR spectrum of $[\text{Ru}(\text{phen})_2(\text{Clazpy})]\text{Cl}_2 \cdot 8\text{H}_2\text{O}$ in methanol- $d_4$	278
3.211 DEPT NMR spectrum of $[\text{Ru}(\text{phen})_2(\text{Clazpy})]\text{Cl}_2 \cdot 8\text{H}_2\text{O}$ in methanol- $d_4$	278
3.212 $^1\text{H}$ - $^{13}\text{C}$ HMQC NMR spectrum of $[\text{Ru}(\text{phen})_2(\text{Clazpy})]\text{Cl}_2 \cdot 8\text{H}_2\text{O}$ in methanol- $d_4$	279
3.213 Cyclic voltammogram of $[\text{Ru}(\text{bpy})_2(\text{Clazpy})](\text{PF}_6)_2$ in 0.1 M TBAH $\text{CH}_3\text{CN}$ at scan rate 50 mV/s (ferrocene as an internal standard)	282
3.214 Cyclic voltammogram of $[\text{Ru}(\text{phen})_2(\text{Clazpy})](\text{PF}_6)_2$ in 0.1 M TBAH $\text{CH}_3\text{CN}$ at scan rate 50 mV/s (ferrocene as an internal standard)	283
3.215 Cyclic voltammogram of $[\text{Ru}(\text{bpy})_2(\text{Clazpy})]\text{Cl}_2 \cdot 7\text{H}_2\text{O}$ in 0.1 M TBAH $\text{CH}_3\text{CN}$ at scan rate 50 mV/s (ferrocene as an internal standard)	283
3.216 Cyclic voltammogram of $[\text{Ru}(\text{phen})_2(\text{Clazpy})]\text{Cl}_2 \cdot 8\text{H}_2\text{O}$ in 0.1 M TBAH $\text{CH}_3\text{CN}$ at scan rate 50 mV/s (ferrocene as an internal standard)	284
3.217 Absorption spectra of $[\text{Ru}(\text{Clazpy})_2(\text{bpy})]\text{Cl}_2 \cdot 7\text{H}_2\text{O}$ in 5 mM Tris/50 mM NaCl buffer pH 7.1 upon addition of calf thymus DNA. $[\text{Ru}] = 4 \times 10^{-4}$ M, $[\text{DNA}] = (0-30) \times 10^{-5}$ M. Arrow show the absorbance changing upon increasing DNA concentrations. Inset plots of $[\text{DNA}]/(\epsilon_a - \epsilon_f)$ versus $[\text{DNA}]$ for the titration of DNA with the complex.	293

## LIST OF FIGURES (continued)

Figure	Page
3.218 Absorption spectra of $[\text{Ru}(\text{Clazpy})_2(\text{phen})]\text{Cl}_2 \cdot 8\text{H}_2\text{O}$ in 5 mM Tris/50 mM NaCl buffer pH 7.1 upon addition of calf thymus DNA. $[\text{Ru}] = 4 \times 10^{-4} \text{ M}$ , $[\text{DNA}] = (0-30) \times 10^{-5} \text{ M}$ . Arrow show the absorbance changing upon increasing DNA concentrations. Inset plots of $[\text{DNA}]/(\epsilon_a - \epsilon_f)$ versus $[\text{DNA}]$ for the titration of DNA with the complex.	294
3.219 Absorption spectra of $[\text{Ru}(\text{Clazpy})_2(\text{azpy})]\text{Cl}_2 \cdot 4\text{H}_2\text{O}$ in 5 mM Tris/50 mM NaCl buffer pH 7.1 upon addition of calf thymus DNA. $[\text{Ru}] = 4 \times 10^{-4} \text{ M}$ , $[\text{DNA}] = (0-30) \times 10^{-5} \text{ M}$ . Arrow show the absorbance changing upon increasing DNA concentrations. Inset plots of $[\text{DNA}]/(\epsilon_a - \epsilon_f)$ versus $[\text{DNA}]$ for the titration of DNA with the complex.	295
3.220 Absorption spectra of $[\text{Ru}(\text{Clazpy})_3]\text{Cl}_2 \cdot 3\text{H}_2\text{O}$ in 5 mM Tris/50 mM NaCl buffer pH 7.1 upon addition of calf thymus DNA. $[\text{Ru}] = 4 \times 10^{-4} \text{ M}$ , $[\text{DNA}] = (0-30) \times 10^{-5} \text{ M}$ . Arrow show the absorbance changing upon increasing DNA concentrations. Inset plots of $[\text{DNA}]/(\epsilon_a - \epsilon_f)$ versus $[\text{DNA}]$ for the titration of DNA with the complex.	296
3.221 Absorption spectra of $[\text{Ru}(\text{Clazpy})_2(\text{bpy})](\text{NO}_3) \cdot 5\text{H}_2\text{O}$ in 5 mM Tris/50 mM NaCl buffer pH 7.1 upon addition of calf thymus DNA. $[\text{Ru}] = 4 \times 10^{-4} \text{ M}$ , $[\text{DNA}] = (0-30) \times 10^{-5} \text{ M}$ . Arrow show the absorbance changing upon increasing DNA concentrations. Inset plots of $[\text{DNA}]/(\epsilon_a - \epsilon_f)$ versus $[\text{DNA}]$ for the titration of DNA with the complex.	297

## LIST OF FIGURES (continued)

Figure	Page
3.222 Absorption spectra of $[\text{Ru}(\text{Clazpy})_2(\text{phen})](\text{NO}_3)\cdot 3\text{H}_2\text{O}$ in 5 mM Tris/50 mM NaCl buffer pH 7.1 upon addition of calf thymus DNA. $[\text{Ru}] = 4 \times 10^{-4}$ M, $[\text{DNA}] = (0-30) \times 10^{-5}$ M. Arrow show the absorbance changing upon increasing DNA concentrations. Inset plots of $[\text{DNA}]/(\epsilon_a - \epsilon_f)$ versus $[\text{DNA}]$ for the titration of DNA with the complex	298
3.223 Absorption spectra of $[\text{Ru}(\text{Clazpy})_2(\text{azpy})](\text{NO}_3)\cdot \text{H}_2\text{O}$ in 5 mM Tris/50 mM NaCl buffer pH 7.1 upon addition of calf thymus DNA. $[\text{Ru}] = 4 \times 10^{-4}$ M, $[\text{DNA}] = (0-30) \times 10^{-5}$ M. Arrow show the absorbance changing upon increasing DNA concentrations. Inset plots of $[\text{DNA}]/(\epsilon_a - \epsilon_f)$ versus $[\text{DNA}]$ for the titration of DNA with the complex.	299
3.224 Absorption spectra of $[\text{Ru}(\text{Clazpy})_3](\text{NO}_3)\cdot 5\text{H}_2\text{O}$ in 5 mM Tris/50 mM NaCl buffer pH 7.1 upon addition of calf thymus DNA. $[\text{Ru}] = 4 \times 10^{-4}$ M, $[\text{DNA}] = (0-30) \times 10^{-5}$ M. Arrow show the absorbance changing upon increasing DNA concentrations. Inset plots of $[\text{DNA}]/(\epsilon_a - \epsilon_f)$ versus $[\text{DNA}]$ for the titration of DNA with the complex.	300
3.225 Absorption spectra of $[\text{Ru}(\text{bpy})_2(\text{Clazpy})]\text{Cl}_2\cdot 7\text{H}_2\text{O}$ in 5 mM Tris/50 mM NaCl buffer pH 7.1 upon addition of calf thymus DNA. $[\text{Ru}] = 4 \times 10^{-4}$ M, $[\text{DNA}] = (0-30) \times 10^{-5}$ M. Arrow show the absorbance changing upon increasing DNA concentrations. Inset plots of $[\text{DNA}]/(\epsilon_a - \epsilon_f)$ versus $[\text{DNA}]$ for the titration of DNA with the complex.	301

## LIST OF FIGURES (continued)

Figure	Page
<p>3.226 Absorption spectra of <math>[\text{Ru}(\text{phen})_2(\text{Clazpy})]\text{Cl}_2 \cdot 8\text{H}_2\text{O}</math> in 5 mM Tris/50 mM NaCl buffer pH 7.1 upon addition of calf thymus DNA. <math>[\text{Ru}] = 4 \times 10^{-4}</math> M, <math>[\text{DNA}] = (0-30) \times 10^{-5}</math> M. Arrow show the absorbance changing upon increasing DNA concentrations. Inset plots of <math>[\text{DNA}]/(\varepsilon_a - \varepsilon_f)</math> versus <math>[\text{DNA}]</math> for the titration of DNA with the complex.</p>	302
<p>3.227 Effect of increasing amounts of <math>[\text{Ru}(\text{Clazpy})_2(\text{bpy})]\text{Cl}_2 \cdot 7\text{H}_2\text{O}</math> and <math>[\text{Ru}(\text{Clazpy})_2(\text{phen})]\text{Cl}_2 \cdot 8\text{H}_2\text{O}</math> compared with EB and <math>[\text{Ru}(\text{phen})_3]\text{Cl}_2 \cdot 7\text{H}_2\text{O}</math> on the relative viscosity of calf thymus at <math>29(\pm 0.5)</math> °C. The total concentration is 0.3 mM</p>	304
<p>3.228 Effect of increasing amounts of <math>[\text{Ru}(\text{Clazpy})_2(\text{azpy})]\text{Cl}_2 \cdot 4\text{H}_2\text{O}</math> and <math>[\text{Ru}(\text{Clazpy})_3]\text{Cl}_2 \cdot 3\text{H}_2\text{O}</math> compared with EB and <math>[\text{Ru}(\text{phen})_3]\text{Cl}_2 \cdot 7\text{H}_2\text{O}</math> on the relative viscosity of calf thymus at <math>29(\pm 0.5)</math> °C. The total concentration is 0.3 mM</p>	305
<p>3.229 Effect of increasing amounts of <math>[\text{Ru}(\text{Clazpy})_2(\text{bpy})](\text{NO}_3)_2 \cdot 5\text{H}_2\text{O}</math> and <math>[\text{Ru}(\text{Clazpy})_2(\text{phen})](\text{NO}_3)_2 \cdot 3\text{H}_2\text{O}</math> compared with EB and <math>[\text{Ru}(\text{phen})_3]\text{Cl}_2 \cdot 7\text{H}_2\text{O}</math> on the relative viscosity of calf thymus at <math>29(\pm 0.5)</math> °C. The total concentration is 0.3 mM</p>	306
<p>3.230 Effect of increasing amounts of <math>[\text{Ru}(\text{Clazpy})_2(\text{azpy})](\text{NO}_3)_2 \cdot \text{H}_2\text{O}</math> and <math>[\text{Ru}(\text{Clazpy})_3](\text{NO}_3)_2 \cdot 5\text{H}_2\text{O}</math> compared with EB and <math>[\text{Ru}(\text{phen})_3]\text{Cl}_2 \cdot 7\text{H}_2\text{O}</math> on the relative viscosity of calf thymus at <math>29(\pm 0.5)</math> °C. The total concentration is 0.3 mM</p>	307
<p>3.231 Effect of increasing amounts of <math>[\text{Ru}(\text{bpy})_2(\text{Clazpy})]\text{Cl}_2 \cdot 7\text{H}_2\text{O}</math> and <math>[\text{Ru}(\text{phen})_2(\text{Clazpy})]\text{Cl}_2 \cdot 8\text{H}_2\text{O}</math> compared with EB and <math>[\text{Ru}(\text{phen})_3]\text{Cl}_2 \cdot 7\text{H}_2\text{O}</math> on the relative viscosity of calf thymus at <math>29(\pm 0.5)</math> °C. The total concentration is 0.3 mM</p>	308

## LIST OF FIGURES (continued)

Figure	Page
<p>3.232 (a) Fluorescence quenching curve of EB bound to DNA in the absence and the presence of <math>[\text{Ru}(\text{Clazpy})_2(\text{bpy})]\text{Cl}_2 \cdot 7\text{H}_2\text{O}</math> and <math>[\text{Ru}(\text{Clazpy})_2(\text{phen})]\text{Cl}_2 \cdot 8\text{H}_2\text{O}</math>. <math>[\text{EB}] = 2 \mu\text{M}</math>, <math>[\text{DNA}] = 40 \mu\text{M}</math>, <math>[\text{Ru}] = 0, 0.1, 0.3, 0.6 \mu\text{M}</math>. (b) in the plot of <math>[\text{Ru}(\text{Clazpy})_2(\text{bpy})]\text{Cl}_2 \cdot 7\text{H}_2\text{O}</math> and <math>[\text{Ru}(\text{Clazpy})_2(\text{phen})]\text{Cl}_2 \cdot 8\text{H}_2\text{O}</math> of <math>I_0/I</math> versus <math>[\text{Ru}]/[\text{DNA}] = 0-0.02</math></p>	311
<p>3.233 (a) Fluorescence quenching curve of EB bound to DNA in the absence and the presence of <math>[\text{Ru}(\text{Clazpy})_2(\text{azpy})]\text{Cl}_2 \cdot 4\text{H}_2\text{O}</math> and <math>[\text{Ru}(\text{Clazpy})_3]\text{Cl}_2 \cdot 3\text{H}_2\text{O}</math>. <math>[\text{EB}] = 2 \mu\text{M}</math>, <math>[\text{DNA}] = 40 \mu\text{M}</math>, <math>[\text{Ru}] = 0, 0.1, 0.3, 0.6 \mu\text{M}</math>. (b) in the plot of <math>[\text{Ru}(\text{Clazpy})_2(\text{azpy})]\text{Cl}_2 \cdot 4\text{H}_2\text{O}</math> and <math>[\text{Ru}(\text{Clazpy})_3]\text{Cl}_2 \cdot 3\text{H}_2\text{O}</math> of <math>I_0/I</math> versus <math>[\text{Ru}]/[\text{DNA}] = 0-0.02</math>.</p>	312
<p>3.234 (a) Fluorescence quenching curve of EB bound to DNA in the absence and the presence of <math>[\text{Ru}(\text{Clazpy})_2(\text{bpy})](\text{NO}_3)_2 \cdot 5\text{H}_2\text{O}</math> and <math>[\text{Ru}(\text{Clazpy})_2(\text{phen})](\text{NO}_3)_2 \cdot 3\text{H}_2\text{O}</math> <math>[\text{EB}] = 2 \mu\text{M}</math>, <math>[\text{DNA}] = 40 \mu\text{M}</math>, <math>[\text{Ru}] = 0, 0.1, 0.3, 0.6 \mu\text{M}</math>. (b) in the plot of <math>[\text{Ru}(\text{Clazpy})_2(\text{bpy})](\text{NO}_3)_2 \cdot 5\text{H}_2\text{O}</math> and <math>[\text{Ru}(\text{Clazpy})_2(\text{phen})](\text{NO}_3)_2 \cdot 3\text{H}_2\text{O}</math> of <math>I_0/I</math> versus <math>[\text{Ru}]/[\text{DNA}] = 0-0.02</math>.</p>	313
<p>3.235 (a) Fluorescence quenching curve of EB bound to DNA in the absence and the presence of <math>[\text{Ru}(\text{Clazpy})_2(\text{azpy})](\text{NO}_3)_2 \cdot \text{H}_2\text{O}</math> and <math>[\text{Ru}(\text{Clazpy})_3](\text{NO}_3)_2 \cdot 3\text{H}_2\text{O}</math> <math>[\text{EB}] = 2 \mu\text{M}</math>, <math>[\text{DNA}] = 40 \mu\text{M}</math>, <math>[\text{Ru}] = 0, 0.1, 0.3, 0.6 \mu\text{M}</math>. (b) in the plot of <math>[\text{Ru}(\text{Clazpy})_2(\text{azpy})](\text{NO}_3)_2 \cdot \text{H}_2\text{O}</math> and <math>[\text{Ru}(\text{Clazpy})_3](\text{NO}_3)_2</math> of <math>I_0/I</math> versus <math>[\text{Ru}]/[\text{DNA}] = 0-0.02</math>.</p>	314

## LIST OF FIGURES (continued)

Figure	Page
<p>3.236 (a) Fluorescence quenching curve of EB bound to DNA in the absence and the presence of <math>[\text{Ru}(\text{bpy})_2(\text{Clazpy})]\text{Cl}_2 \cdot 7\text{H}_2\text{O}</math> and <math>[\text{Ru}(\text{phen})_2(\text{Clazpy})]\text{Cl}_2 \cdot 7\text{H}_2\text{O}</math>. <math>[\text{EB}] = 2 \mu\text{M}</math>, <math>[\text{DNA}] = 40 \mu\text{M}</math>, <math>[\text{Ru}] = 0, 0.1, 0.3, 0.6 \mu\text{M}</math>. (b) in the plot of <math>[\text{Ru}(\text{bpy})_2(\text{Clazpy})]\text{Cl}_2 \cdot 7\text{H}_2\text{O}</math> and <math>[\text{Ru}(\text{phen})_2(\text{Clazpy})]\text{Cl}_2 \cdot 7\text{H}_2\text{O}</math> of <math>I_0/I</math> versus <math>[\text{Ru}]/[\text{DNA}] = 0-0.02</math>.</p>	315
<p>3.237 Cyclic voltammograms of 0.5 mM <math>[\text{Ru}(\text{Clazpy})_2(\text{bpy})]\text{Cl}_2 \cdot 7\text{H}_2\text{O}</math> and <math>[\text{Ru}(\text{Clazpy})_2(\text{phen})]\text{Cl}_2 \cdot 8\text{H}_2\text{O}</math> in the absence and presence of 2.5 mM DNA. Supporting electrolyte, 5 mM Tris base/50 mM NaCl, pH 7.2 (<math>\text{H}_2\text{O}:\text{DMSO}</math> 100:5), <math>[\text{DNA}]/[\text{Ru}] = 5</math>, scan rate <math>50 \text{ mV} \cdot \text{s}^{-1}</math></p>	319
<p>3.238 Cyclic voltammograms of 0.5 mM <math>[\text{Ru}(\text{Clazpy})_2(\text{azpy})]\text{Cl}_2 \cdot 4\text{H}_2\text{O}</math> and <math>[\text{Ru}(\text{Clazpy})_3]\text{Cl}_2 \cdot 3\text{H}_2\text{O}</math> in the absence and presence of 2.5 mM DNA. Supporting electrolyte, 5 mM Tris base/50 mM NaCl, pH 7.2 (<math>\text{H}_2\text{O}:\text{DMSO}</math> 100:5), <math>[\text{DNA}]/[\text{Ru}] = 5</math>, scan rate <math>50 \text{ mV} \cdot \text{s}^{-1}</math></p>	320
<p>3.239 Cyclic voltammograms of 0.5 mM <math>[\text{Ru}(\text{bpy})_2(\text{Clazpy})]\text{Cl}_2 \cdot 7\text{H}_2\text{O}</math> and <math>[\text{Ru}(\text{phen})_2(\text{Clazpy})]\text{Cl}_2 \cdot 8\text{H}_2\text{O}</math> in the absence and presence of DNA 2.5 mM DNA. Supporting electrolyte, 5 mM Tris base/50 mM NaCl, pH 7.2 (<math>\text{H}_2\text{O}:\text{DMSO}</math> 100:5), <math>[\text{DNA}]/[\text{Ru}] = 5</math>, scan rate <math>50 \text{ mV} \cdot \text{s}^{-1}</math></p>	321
<p>3.240 Cyclic voltammograms of 0.5 mM <math>[\text{Ru}(\text{Clazpy})_2(\text{bpy})](\text{NO}_3)_2 \cdot 5\text{H}_2\text{O}</math> and <math>[\text{Ru}(\text{Clazpy})_2(\text{phen})](\text{NO}_3)_2 \cdot 3\text{H}_2\text{O}</math> in the absence and presence of 2.5 mM DNA. Supporting electrolyte, 5 mM Tris base/50 mM NaCl, pH 7.2 (<math>\text{H}_2\text{O}:\text{DMSO}</math> 100:5), <math>[\text{DNA}]/[\text{Ru}] = 5</math>, scan rate <math>50 \text{ mV} \cdot \text{s}^{-1}</math></p>	322
<p>3.241 Cyclic voltammograms of 0.5 mM <math>[\text{Ru}(\text{Clazpy})_2(\text{azpy})](\text{NO}_3)_2 \cdot \text{H}_2\text{O}</math> and <math>[\text{Ru}(\text{Clazpy})_3](\text{NO}_3)_2 \cdot 3\text{H}_2\text{O}</math> in the absence and presence of 2.5 mM DNA. Supporting electrolyte, 5 mM Tris base/50 mM NaCl, pH 7.2 (<math>\text{H}_2\text{O}:\text{DMSO}</math> 100:5), <math>[\text{DNA}]/[\text{Ru}] = 5</math>, scan rate <math>50 \text{ mV} \cdot \text{s}^{-1}</math></p>	323

## LIST OF FIGURES (continued)

Figure	Page
C.1 Cyclic voltammograms of couple I, II and Ru(II)/(III) in <i>tcc</i> -[Ru(Clazpy) <sub>2</sub> Cl <sub>2</sub> ] by varying scan rate 50-500 mV.s <sup>-1</sup>	378
C.2 Cyclic voltammograms of couple I, II and Ru(II)/(III) in <i>ctc</i> -[Ru(Clazpy) <sub>2</sub> Cl <sub>2</sub> ] by varying scan rate 50-500 mV.s <sup>-1</sup>	379
C.3 Cyclic voltammograms of couple I, II and Ru(II)/(III) in <i>ccc</i> -[Ru(Clazpy) <sub>2</sub> Cl <sub>2</sub> ] by varying scan rate 50-500 mV.s <sup>-1</sup>	380
C.4 Cyclic voltammogram of couple I, II and Ru(II)/(III) in [Ru(Clazpy)(5dmazpy)Cl <sub>2</sub> ] by varying scan rate 50-500 mV.s <sup>-1</sup>	381
C.5 Cyclic voltammograms of couple I, II, III, IV, V and Ru(II)/(III) in [Ru(Clazpy) <sub>2</sub> (bpy)](PF <sub>6</sub> ) <sub>2</sub> by varying scan rate 50-500 mV.s <sup>-1</sup>	382
C.6 Cyclic voltammograms of couple I, II, III, IV, V and Ru(II)/(III) in [Ru(Clazpy) <sub>2</sub> (phen)](PF <sub>6</sub> ) <sub>2</sub> by varying scan rate 50-500 mV.s <sup>-1</sup>	383
C.7 Cyclic voltammograms of couple I, II, III, IV, V and VI in [Ru(Clazpy) <sub>2</sub> (azpy)](PF <sub>6</sub> ) <sub>2</sub> by varying scan rate 50-500 mV.s <sup>-1</sup>	384
C.8 Cyclic voltammograms of couple I, II, III, IV, V and VI in [Ru(Clazpy) <sub>3</sub> ](PF <sub>6</sub> ) <sub>2</sub> by varying scan rate 50-500 mV.s <sup>-1</sup>	385
C.9 Cyclic voltammograms of couple I, II, III, IV and V in [Ru(Clazpy) <sub>2</sub> (bpy)](NO <sub>3</sub> ) <sub>2</sub> .5H <sub>2</sub> O by varying scan rate 50-500 mV.s <sup>-1</sup>	386
C.10 Cyclic voltammograms of couple I, II, III, IV and V in [Ru(Clazpy) <sub>2</sub> (phen)](NO <sub>3</sub> ) <sub>2</sub> .3H <sub>2</sub> O by varying scan rate 50-500 mV.s <sup>-1</sup>	387
C.11 Cyclic voltammograms of couple I, II, III, IV, V and VI in [Ru(Clazpy) <sub>2</sub> (azpy)](NO <sub>3</sub> ) <sub>2</sub> .H <sub>2</sub> O by varying scan rate 50-500 mV.s <sup>-1</sup>	388
C.12 Cyclic voltammograms of couple I, II, III, IV and V in [Ru(Clazpy) <sub>3</sub> ](NO <sub>3</sub> ) <sub>2</sub> .5H <sub>2</sub> O by varying scan rate 50-500 mV.s <sup>-1</sup>	389
C.13 Cyclic voltammograms of couple I, II, III, IV, V and Ru(II)/(III) in [Ru(Clazpy) <sub>2</sub> (bpy)]Cl <sub>2</sub> .7H <sub>2</sub> O by varying scan rate 50-500 mV.s <sup>-1</sup>	390

## LIST OF FIGURES (continued)

Figure	Page
C.14 Cyclic voltammograms of couple I, II, III, IV, V and Ru(II)/(III) in [Ru(Clazpy) <sub>2</sub> phen]Cl <sub>2</sub> .8H <sub>2</sub> O by varying scan rate 50-500 mV.s <sup>-1</sup>	391
C.15 Cyclic voltammograms of couple I, II, III, IV, V and Ru(II)/(III) in [Ru(Clazpy) <sub>2</sub> azpy]Cl <sub>2</sub> .4H <sub>2</sub> O by varying scan rate 50-500 mV.s <sup>-1</sup>	392
C.16 Cyclic voltammograms of couple I, II, III, IV, V and Ru(II)/(III) in [Ru(Clazpy) <sub>3</sub> ]Cl <sub>2</sub> .3H <sub>2</sub> O by varying scan rate 50-500 mV.s <sup>-1</sup>	393
C.17 Cyclic voltammograms of couple I, II, III and IV in [Ru(bpy) <sub>2</sub> Clazpy](PF <sub>6</sub> ) <sub>2</sub> by varying scan rate 50-500 mV.s <sup>-1</sup>	394
C.18 Cyclic voltammograms of couple I, II, III and IV in [Ru(phen) <sub>2</sub> Clazpy](PF <sub>6</sub> ) <sub>2</sub> by varying scan rate 50-500 mV.s <sup>-1</sup>	395
C.19 Cyclic voltammograms of couple I, II, III, IV and Ru(II)/(III) in [Ru(bpy) <sub>2</sub> Clazpy]Cl <sub>2</sub> .7H <sub>2</sub> O by varying scan rate 50-500 mV.s <sup>-1</sup>	396
C.20 Cyclic voltammograms of couple I, II, III IV and Ru(II)/(III) in [Ru(phen) <sub>2</sub> Clazpy]Cl <sub>2</sub> .8H <sub>2</sub> O by varying scan rate 50-500 mV.s <sup>-1</sup>	397

## LIST OF ABBREVIATIONS AND SYMBOLS

aapm	= 2-(phenylazo)pyrimidine
AgCl	= silver chloride
AgNO <sub>3</sub>	= silver nitrate
Anti-NCI-H187	= oral human epidermal carcinoma
A.R. grade	= Analytical reagent grade
azpy	= 2-(phenylazo)pyridine
Å	= Angstrom unit (1 Å = 10 <sup>-10</sup> m)
A2780	= human ovarian carcinoma
A2780cis	= human ovarian carcinoma resistance
A498	= renal cancer
b	= broad
BC	= breast cancer
BPIP	= 2-(4'-benzyloxyphenyl)imidazo[4,5-f]- [1,10]phenanthroline
BPIP	= 2-(4'-biphenyl)imidazo[4,5-f][1,10] phenanthroline
bpy	= 2,2'-bipyridine
bs	= broad of singlet
bzimp	= 2,6-bis(benzimidazol-2-yl)
Cbdca- <i>O, O'</i>	= 1,1-cyclobutanedicarboxylate
CD	= circular dichroism
CHCl <sub>3</sub>	= chloroform
CH <sub>2</sub> Cl <sub>2</sub>	= dichloromethane
CH <sub>3</sub> CN	= acetonitrile
CH <sub>3</sub> OCH <sub>3</sub>	= acetone
Clazpy	= 5-Chloro-2-(phenylazo)pyridine
cm <sup>-1</sup>	= wave number
COSY	= COrrrelation SpectroscopY

## LIST OF ABBREVIATIONS AND SYMBOLS (continued)

CT-DNA	= calf-thymus deoxyribonucleic acid
CV	= cyclic voltammetry
°C	= degree Celsius
d	= doublet
1D	= one dimension
2D	= two dimension
dcb	= 4,4'-(COOH) <sub>2</sub> -2,2'-bipyridine
dd	= doublet of doublet
ddd	= doublet of doublet of doublet
DFT	= the density functional theory
5dmazpy	= 5-dimethyl-2-(phenylazo)pyridine
dmb	= 4,4'-dimethyl-2,2'-bipyridine
DMF	= <i>N, N</i> -dimethylformamide
dmp	= 2,9-dimethyl-1,10-phenanthroline
DMSO	= <i>N, N</i> -dimethylsulfoxide
DNA	= deoxyribonucleic acid
dppz	= dipyrrophenazine
dpq	= dipyrro[3,2-d:2',3'-f]quinoxaline
dt	= doublet of triplet
E <sub>1/2</sub>	= peak potential
EB	= ethidium bromide
E <sub>pa</sub>	= anodic peak potential
E <sub>pc</sub>	= cathodic peak potential
ES	= electrospray
9-EtGua	= 9-ethylguanine
EtOAc	= ethylacetate
EtOH	= ethanol
EVSA-T	= breast cancer

## LIST OF ABBREVIATIONS AND SYMBOLS (continued)

$F_c^{+/c}$	= ferrocene/ferricinium
FAB	= fast-atom bombardment
g	= gram
gly	= glycine
h	= hour
HaaiMe	= 1-methyl-2-(phenylazo)imidazole
HCl	= hydrochloric acid
HMBC	= Hetrnuclear Multiple Bond Correlation
HMQC	= Hetrnuclear Multiple Quantum Correlation
Hsazpy	= 2-phenylazopyridine-5-sulfonic acid
H <sub>2</sub> O	= water
H266	= nonsmall cell lung cancer
Hz	= hertz
$i_{pa}$	= anodic peak current
$i_{pc}$	= cathodic peak current
IGROV	= ovarian cancer
IR	= Infrared
$J$	= coupling constant
K	= Kelvin
$K_b$	= intrinsic binding constant
KB	= small cell lung cancer
KH <sub>2</sub> PO <sub>4</sub>	= potassium dihydrogenphosphate
K <sub>2</sub> HPO <sub>4</sub>	= potassium hydrogenphosphate
L-ala	= alanine
L-arg	= argenine
LiCl	= lithium chloride
m	= multiplet

## LIST OF ABBREVIATIONS AND SYMBOLS (continued)

M	= molar
mal	= malonate
mazpy	= 4-methyl-2-(phenylazo)pyridine
MCF-7	= breast cancer
9-MeAde	= 9-methyladenine
Me <sub>4</sub> phen	= 3,7,4,8-tetramethyl-1,10-phenanthroline
MeOH	= methanol
<i>mer</i>	= meridional
min	= minute
MIP	= 2-(2,3-methylenedioxyphenyl)imidazo [4,5- <i>f</i> ]1,10-phenanthroline
mg	= milligram
mg/mL	= milligram per milliliter
mL	= milliliter
MLCT	= metal-to-ligand charge transfer
mmol	= millimol
MPPIP	= 2-(3'-phenoxyphenyl)imidazo[4,5- <i>f</i> ]- [1,10]phenanthroline)
mV.s <sup>-1</sup> , mV/s	= millivolt per second
m/z	= a value of mass divided by charge
MW.	= molecular weight
M19	= melanoma
NaCl	= sodium chloride
NaOH	= sodium hydroxide
NAz	= 2-((4-nitrophenyl)azo)pyridine
Na <sub>2</sub> HPO <sub>4</sub>	= sodium hydrogenphosphate
NH <sub>4</sub> PF <sub>6</sub>	= ammonium hexafluorophosphate
nm	= nanometer

## LIST OF ABBREVIATIONS AND SYMBOLS (continued)

NMIP	= 2-(3'-phenoxyphenyl)imidazo[4,5- <i>f</i> ]- [1,10]phenanthroline)
NMR	= Nuclear Magnetic Resonance
ox	= oxalate
phen	= 1,10-phenanthroline
phi	= 9,10-phenanthrenequinonediimine
ppm	= part per million
Rel. Abun.	= relative abundance
ROESY	= ROtational nuclear overhauser Effect SpectroscopY
RSD	= standard deviation
Ru	= ruthenium
s	= singlet
Si(CH <sub>3</sub> ) <sub>4</sub> , TMS	= tetramethyl silane
t	= triplet
taptp	= 4,5,9,18-tetraazaphenanthreno[9,10- <i>b</i> ] triphenylene
tazpy	= <i>o</i> -tolylazopyridine
TBACl	= tetra- <i>n</i> -butylammonium chloride
TBAH	= tetra- <i>n</i> -butylammonium hexafluorophosphate
Tris base	= Tris(hydroxymethyl)aminomethane
TLC	= thin layer chromatography
TOCSY	= TOtal Correlation SpectroscopY
tpphz	= tetrapyrido[3,2- <i>a</i> :2',3'- <i>c</i> :3'',2''- <i>h</i> :2''',3'''- <i>f</i> ]phenazine
tt	= triplet of triplet
UV-Vis	= Ultraviolet-Visible

## LIST OF ABBREVIATIONS AND SYMBOLS (continued)

WIDR	= colon cancer
$\gamma$	= gamma
$\alpha$	= alpha
$\beta$	= beta
$\delta$	= delta
$\varepsilon$	= eta
$\Delta$	= heat
$^{\circ}$	= degree
$\lambda$	= wavelength
$\varepsilon$	= molar extinction coefficient

# CHAPTER 1

## INTRODUCTION

### 1.1 Introduction

Since the first discovery of the antitumor activity of cisplatin (*cis*-diamminedichloroplatinium(II), *cis*-[Pt(NH<sub>3</sub>)<sub>2</sub>Cl<sub>2</sub>]) by Rosenberg *et al.*, in 1969, many other metal complexes have been investigated for their possible applications as antitumor agents (Zhang and Lippard, 2003). Complexes based on ruthenium, one of the platinum group metals, have been proposed as potential antitumor substances (Vilaplana *et al.*, 2006).

Stable, inert and water-soluble octahedral complexes containing spectroscopically active metal centers are valuable as probes of biological system (Erkkila *et al.*, 1999). For example, the isomers of [Ru(azpy)<sub>2</sub>Cl<sub>2</sub>], where azpy is 2-(phenylazo)pyridine, were found to be reactive as antitumor agents especially the *ctc*-[Ru(azpy)<sub>2</sub>Cl<sub>2</sub>] complex (*ctc*-indicating the coordinating atoms Cl, N(pyridine), and N(azo) in mutual *cis*, *trans*, and *cis*-positions, respectively or  $\alpha$ -[Ru(azpy)<sub>2</sub>Cl<sub>2</sub>]). This isomer has been reported to exhibit a remarkably high cytotoxicity, even higher than that of cisplatin in many of the tested cell lines (e.g. MCF-7, IGROV, and H266) (Velder *et al.*, 2000). So far, a few azoimine compounds having substituent on the pyridine ring have been extensively studied (Hotze *et al.*, 2004). On the other hand, only a few studies on ruthenium complexes containing mixed-azoimine ligands have been reported. Such complex is *cis*-[Ru(azpy)(bpy)Cl<sub>2</sub>], where bpy is 2,2'-bipyridine, showed its cytotoxicity mostly a low to moderate (Hotze *et al.*, 2004).

In addition, replacing the chloro ligands of  $\alpha$ -[Ru(azpy)<sub>2</sub>Cl<sub>2</sub>] by other bidentate ligands resulted in [Ru(azpy)<sub>2</sub>(L)](PF<sub>6</sub>)<sub>2</sub> (L = azpy and bpy) which displayed less cytotoxic than the parent dichloro complex (Hotze *et al.*, 2005). Although no *cis*-chloro ligands are presented in [Ru(azpy)<sub>2</sub>(L)](PF<sub>6</sub>)<sub>2</sub> molecule like cisplatin, the cytotoxic activity have been observed. At this point, one should also consider the fact that ruthenium is octahedrally coordinated in the two most common oxidation states, +2 and +3, whereas platinum is square planar. This difference might

have important consequences for the interaction with biomolecules and thus biological activity (Hotze *et al.*, 2004).

In order to investigate structure-activity relationships, this work has been focused on the syntheses of related complexes by variation of the active azpy complex,  $[\text{Ru}(\text{azpy})_2\text{Cl}_2]$  and replacing the chloro ligands by other bidentate ligands to give new tris ruthenium complexes,  $[\text{Ru}(\text{L})_3]^{2+}$  and mixed-ligand complexes  $[\text{Ru}(\text{L})_2\text{L}']^{2+}$ . We have also determined how variation of the active azpy and changing chloro ligand influence the electronic, structural, and cytotoxic properties of such complexes.

In previous work, binding studies of small molecule to DNA are very important in the development of new therapeutic reagents and DNA molecular probes (Liu *et al.*, 2006). Metal complexes have been investigated for their DNA binding affinities. The binding modes are dependent on their size, functions and stereochemical properties. Generally, the interaction with DNA has occurred as non-covalent interaction fashion such as electrostatic binding for cation with DNA (Jiang *et al.*, 2003), groove binding for large molecule (Yang *et al.*, 1997) and intercalative binding or partial interactive binding for the planar molecules or compounds containing planar ring systems (Tan *et al.*, 2007). For the past research, the useful application of such complexes generally requires that they bind to DNA by intercalation of the main ligands. Thus, the vast majority of studies have been focused on modifying the intercalative ligands (Tan *et al.*, 2007; Liu *et al.*, 2006). In contrast, investigations on the influence of the ancillary ligands of ruthenium(II) complexes have been relative few. Since the octahedral Ru(II) complexes bind to DNA in three dimensions, the ancillary ligands can also play an important role in governing the DNA-binding of these complexes. It is interesting to study the effects of the ancillary ligands on the interaction and the binding mode of these complexes to DNA. Therefore, bpy and phen were selected as ligands for ruthenium to give  $[\text{Ru}(\text{bpy})_2(\text{L})]^{2+}$  and  $[\text{Ru}(\text{phen})_2(\text{L})]^{2+}$  (L = Clazpy) and compared the results with  $[\text{Ru}(\text{Clazpy})_3]^{2+}$ . These data may also helpful to explain how the small differences of ancillary ligands influence on DNA binding properties.

Herein, we report the synthesis a new azoimine ligand, 5-Chloro-2-(phenylazo)pyridine (Clazpy) and preparing of  $[\text{Ru}(\text{Clazpy})_2\text{Cl}_2]$  used as a precursor

for syntheses a mixed-azoimine complex  $[\text{Ru}(\text{Clazpy})(5\text{dmazpy})\text{Cl}_2]$  and  $[\text{Ru}(\text{Clazpy})_2(\text{L})](\text{X})_2$  ( $\text{L} = \text{bpy}, \text{phen}, \text{azpy}, \text{Clazpy}$ ;  $\text{X} = \text{PF}_6^-, \text{NO}_3^-, \text{Cl}^-$ ). Characterization of these complexes was also successfully by spectroscopic techniques and electrochemical method. The DNA-binding properties of water-soluble complexes toward CT-DNA were explored by various physico-chemical and biochemical techniques including UV/Visible, fluorescence, viscometric titration, and cyclic voltammetry. Moreover,  $[\text{Ru}(\text{L})_2(\text{Clazpy})](\text{X})_2$  ( $\text{L} = \text{bpy}$  and  $\text{phen}$ ;  $\text{X} = \text{PF}_6^-, \text{Cl}^-$ ) were synthesized and compared the effect of ancillary ligand on DNA interaction. We hope that our results will aid in the understanding DNA binding by Ru(II) complexes, as well as using the foundation for the rational design of new potent anticancer agent.

## 1.2 Background

### 1.2.1 Cisplatin

Cisplatin is very simply inorganic molecule having a platinum as metal located in center and surrounded with ammine and chloro ligands,  $[\text{Pt}(\text{NH}_3)_2\text{Cl}_2]$ , shown in Figure 1.1. It is reported that cisplatin can covalently bind to DNA primarily through the N donors of guanine (Reedijk, 2003; Clark, 2002).

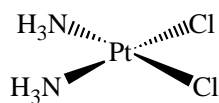


**Figure 1.1** The structure of cisplatin

It is highly effective for the treatment of testicular and ovarian cancer and is used in combination regimens for a variety of other carcinomas, including bladder, small cell lung and head and neck cancers (Brabec and Nováková., 2006). However, its application is still limited to a relatively narrow range of tumors. Some tumors have natural resistance to cisplatin, while others develop resistance after the initial treatment. Moreover, cisplatin is administered intravenously due to its limited solubility in water and has severe side effects (Wong and Giandomenico, 1999).

These limitations have encouraged a search for more effective and less toxic other metal based-anticancer agents, for example carboplatin (1) closed analogues to cisplatin and nedaplatin (2) (Wong and Giandomenico, 1999). However, very few active of these complexes were found. Thus, the search for new anticancer agents with other metal has been studied.

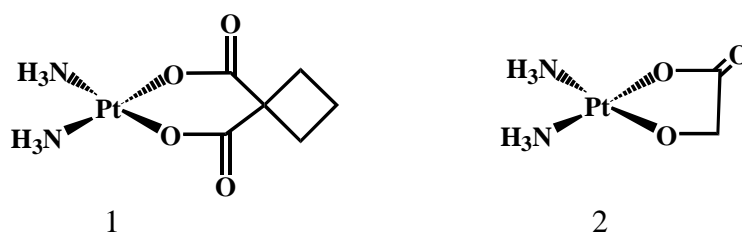


**Figure 1.2** The structures of carboplatin (1) and nedaplatin (2)

### 1.2.2 Ruthenium(II) complexes

Ruthenium is one of the second transition series elements and has electronic configuration  $[\text{Kr}]4d^75s^1$ . The common oxidation state is 2+ and 3+. Generally, trichlororuthenium(III) hydrate,  $\text{RuCl}_3 \cdot 3\text{H}_2\text{O}$  has been used as starting material for syntheses of new ruthenium compounds. Recently, majority of ruthenium(II) complexes have been chosen because of (i) the kinetically inert character of the low-spin  $d^6$  species, (ii) their intense metal-to-ligand charge transfer (MLCT) bands in the visible spectrum and (iii) many chemical and spectroscopic properties of these complexes have been established (Barton *et al.*, 1984). The complexes with polypyridine and azoimine have been extensively studied (Santra, *et al.*, 1999).

The coordination chemistry of polypyridyl ligand having  $\alpha$ -diimine **1**, is widely studied as it includes bidentate ligands i.e. 2,2'-bipyridine (bpy) and 1,10-phenanthroline (phen). These ligands are  $\pi$ -acceptor and when they bound to Ru(II), characteristic metal-to-ligand charge transfer (MLCT) bands arise in the visible region of the electronic absorption spectra.



Several ruthenium(II) complexes containing such ligands is that  $[\text{Ru}(\text{bpy})_3]^{2+}$  and  $[\text{Ru}(\text{dcb})_2(\text{X})_2]$  (dcb = 4,4'-(COOH)<sub>2</sub>-2,2'-bipyridine and X = Cl<sup>-</sup>, Br<sup>-</sup>, I<sup>-</sup>, SCN<sup>-</sup>, H<sub>2</sub>O) used as the most efficient and stable redox sensitizer on nanocrystalline TiO<sub>2</sub> solar cell for conversion light-to-electrical energy (Meyer, 1997). The other useful complexes are  $[\text{Ru}(\text{phen})_2(\text{L})]^{2+}$  where L is 2-(3'-phenoxyphenyl)imidazo[4,5-f]-[1,10]phenanthroline (MPPIP); 2-(4'-biphenyl)imidazo[4,5-f][1,10]phenanthroline (BPIP) used as probe in DNA conformation (Tan *et al.*, 2007). Besides, the complex of  $[\text{Ru}(\text{phen})_2(\text{tapt})]^{2+}$  (tapt = 4, 5, 9, 18-tetraazaphenanthreno[9,10-b]triphenylene) acts as luminescent probes in DNA conformation (Zhen, *et al.*, 2000). However, these several applications could be due to the different chemical properties of the ligands.

Besides polypyridyl, the azoimine functionality **2** is isoelectronic with **1** but is expected to be a significant better  $\pi$ -acceptor ligand because of greater electronegativity of nitrogen compared to carbon (Al-Noaimi *et al.*, 2006). The chelating ligand of this type is able to stabilize metals in their lower oxidation state which have been reported previously (Dougan *et al.*, 2006). One of these ligands is 2-(phenylazo)pyridine (azpy). The cytotoxic properties of isomers and derivative of  $[\text{Ru}(\text{azpy})_2\text{Cl}_2]$  (azpy = 2-(phenylazo)pyridine) have been investigated in several cancer cell lines. In particular,  $\alpha$ - $[\text{Ru}(\text{azpy})_2\text{Cl}_2]$  was found to be highly active against a range of cancer cell lines, with cytotoxicity comparable to cisplatin (Velder *et al.*, 2000). Additionally, they have been used as catalyst for epoxidation reactions of olefin to give epoxide (Barf and sheldon, 1995).

In the present work, it is interesting in octahedrally ruthenium(II) complexes due to their proposed application as antitumor agents and other advantage reasons, (i) the stable complexes with predictable structures can be prepared through reliable methods; (ii) the shape selectivity of the complexes can be improved by functionalization of the ligands; (iii) the knowledge of the biological effects of ruthenium complexes can be greatly developed (Liu *et al.*, 2007).

### 1.2.3 The isomeric complexes of $[\text{Ru}(\text{L})_2\text{Cl}_2]$

The chemistry of ruthenium(II) with arylazopyridine have been special interest in the coordination chemistry. In theoretically, the pseudo-octahedral complexes of the formula,  $[\text{Ru}(\widehat{\text{N}}\text{N})_2\text{Cl}_2]$  with unsymmetric chelating ligands may exist in five geometrically isomeric forms as shown in Figure 1.3 (Misra *et al.*, 1998). The isomers are assigned in terms of sequences of coordinating pairs Cl; N(pyridine) and N(azo). Two isomers *trans-trans-trans* and *trans-cis-cis* belong to *trans-RuCl<sub>2</sub>* configuration whereas three isomers; *cis-trans-cis*, *cis-cis-trans* and *cis-cis-cis* belong to *cis-RuCl<sub>2</sub>* configuration (Mathur *et al.*, 2006). In this work, only three compounds; green, blue and purple in color are isolated and confirmed their structures as *trans-cis-cis* (*tcc*), *cis-trans-cis* (*ctc*) and *cis-cis-cis* (*ccc*) configurations. Since the structure of Clazpy is an asymmetric bidentate ligand, then in principle, the six coordinations of  $[\text{Ru}(\text{Clazpy})_2\text{Cl}_2]$  gives five possible geometrical isomers (Figure 1.3) similar to  $[\text{Ru}(\text{azpy})_2\text{Cl}_2]$  complexes.

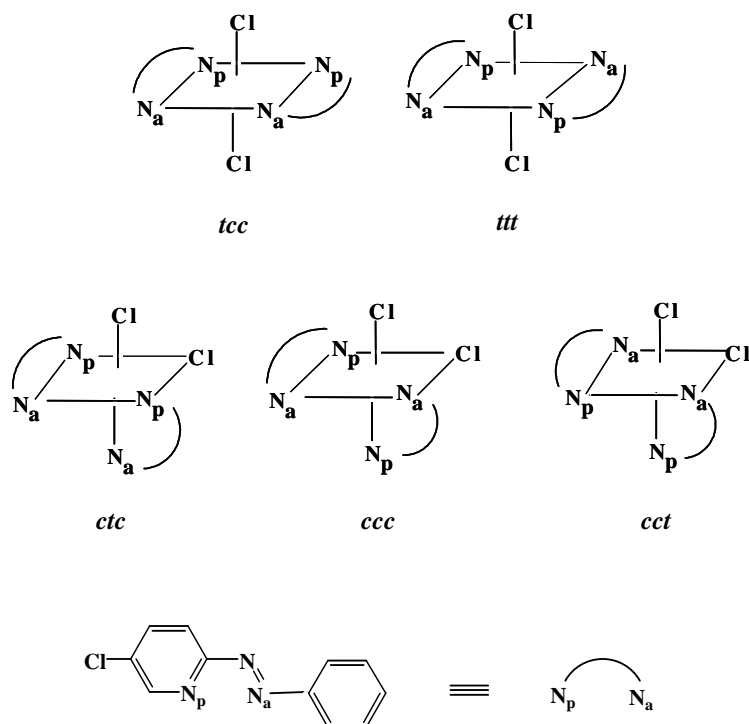


**Figure 1.3** Five possible isomers of  $[\text{Ru}(\text{Clazpy})_2\text{Cl}_2]$  complexes

## 1.2.4 DNA-binding experiments

### 1.2.4.1 DNA

Double helical DNA has many conformations, such as A, B, C, D and Z forms, but the B form is regarded as the most common right-handed duplex. Each conformation has a characteristic of width and depth, which together results in the distinctive shape associated with this helical form. The Z form is left-handed helix which is long and slender. The major groove is in fact a shallow, almost convex surface, and the minor groove is a narrow crevice, zigzagging in a left-handed fashion along the side of the major groove. As such they are quite amenable to probing with transition metal complexes (Ji *et al.*, 1999).

In this work, Calf-Thymus DNA was chosen to study the interaction with synthesized water-soluble complexes. In Watson-Crick double helical DNA, N3 of thymine bases would not be expected to be available for binding to ruthenium(II) because N3 is involved in hydrogen-bonding in base-pairs. Only N7 coordinated to ruthenium as evidenced by both the increase in absorption peak intensities and hypochromism shifts (Nakabayashi *et al.*, 2006). The major noncovalent interactions that determine the structure and function of biomolecules are electrostatic and hydrophobic interactions. Electrostatic interaction includes hydrogen bonding, and van der Waals forces (Horton *et al.*, 1996). Thus the nature of interaction is determined by the characteristic of the metal complex because all cationic metal complexes exhibit electrostatic interactions with polyanionic DNA molecule.

### 1.2.4.2 Type of DNA-binding modes

Generally, metal complexes bind to DNA by electrostatic interactions, classical intercalation, or a combination of both. The different binding modes come from various types of forces or processes responsible for a decrease of the free energy of the system (electrostatic interactions, hydrogen bonding, London dispersion forces, an entropy increase for the hydrophobic interaction (Jing *et al.*, 2004). For the previous report, there are mainly three possible binding modes between DNA and

complexes: (i) an electrostatic interaction that extends the negatively charge phosphate outside the DNA double helix; (ii) the interaction with groove of DNA involved direct interaction of the bound molecule with the edges of base-pairs in grooves of DNA strands (Yau *et al.*, 2002); (iii) an intercalation model in which the base pairs of DNA unwind to accommodate the  $\pi$ -stacking of a ligand and intercalating agent (Aslanoglu, M., 2006). This  $\pi$ -stacking interaction requires the intercalating ligand to be a flat, extended aromatic system, which is annulated with heterocyclic rings, e.g. pyridine and pyrazine (Jing *et al.*, 2004). The former mode causes a slight change in the DNA structure, whilst the later lead to lengthening and unwinding of the DNA helix (Yau *et al.*, 2002). However, the DNA-binding affinity depends on the conformation of DNA, the size, shape, chirality, and hydrophobic character of the complex as determined by the chemical structure of the ligands of the complex.

#### 1.2.4.3 Ethidium Bromide (EB)

Ethidium bromide, the common name for 3,8-diamino-5-ethyl-6-phenylphenanthridinium bromide (Figure 1.4), is used to study viscosity measurement and fluorescence quenching experiment in DNA experiment parts (<http://www.purdne.edu/REM/nmm/ethidbr.htm>).

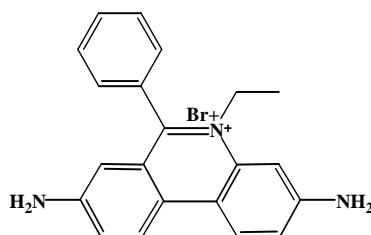


**Figure 1.4** The structure of Ethidium bromide (EB)

It is aromatic having the main portion of the molecule is a tricyclic structure with aniline (aminobenzene) groups on either side of a pyridine. The dibenzopyridine structure is known as a phenanthridine. The reason for intense fluorescence of ethidium bromide after binding with DNA is probably not due to rigid stabilization of the phenyl moiety, because the phenyl ring has been shown to project outside the intercalated bases. It is in fact that the phenyl group is almost

perpendicular to the plane of the ring system, it rotates about its single bond to find a position where it will about the ring system minimally. Consequently, the hydrophobic environment between the base pairs allow EB in place to DNA. By moving into this hydrophobic environment and away from the solvent, the ethidium cation is forced to shine any water molecules that were associated with it. As water is a highly efficient fluorescent quencher, the removal of these water molecules allows the ethidium to fluoresce. Therefore, EB is the common stain for double-stranded DNA and RNA (From [http://en.wikipedia.org/wiki/Ethidium\\_bromide](http://en.wikipedia.org/wiki/Ethidium_bromide)).

#### **1.2.4.4 Buffer**

Since it is desirable to study many biochemical reactions near physiological pH, there is a particular need for mixtures that buffer the pH in the pH range 6.5-8.0 (Mathews and Holde, 1996). In this work, the buffer of Tris (hydroxymethyl)aminomethane was chosen because of chemically stable, readily soluble in water and not be readily extracted by organic solvent (Perrin and Dempsey, 1979). Indeed, it is to mention that in biochemical investigation, a good buffer remains nearly constant when small amounts of strong acidic or basic materials was added. The ability of a solution to resist changes in pH is known as its buffer capacity (Horton *et al.*, 1996). In addition the effects of ionic interactions on the behavior of biological macromolecules are necessary to be considered by biochemist who must pay attention to both ionic strength and pH. Experimenters usually use a neutral salt (like NaCl and KCl) to control the ionic strength of a solution, as well as a buffer to control pH (Mathews and Holde, 1996). Some varieties of buffer systems were used to study the interaction in physiological range (Table 1.1).

**Table 1.1** Some common buffer systems employed for biochemical studies

Composition	pH range
Glycine and HCl	1.0-3.7
Acetate and acetic acid	3.7-5.6
KH <sub>2</sub> PO <sub>4</sub> and K <sub>2</sub> HPO <sub>4</sub>	6.1-7.5
Tris (hydroxymethyl)aminomethane and HCl	7.2-9.0
Carbonate and hydrogen carbonate	9.2-11.1
Na <sub>2</sub> HPO <sub>4</sub> and NaOH	11.0-12.0

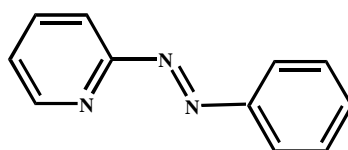
(Source: คณาจารย์ภาควิชาเคมี คณะวิทยาศาสตร์ จุฬาลงกรณ์มหาวิทยาลัย, 2541)

### 1.3 Review of Literatures

For the past decade, the chemistry of ruthenium(II) complexes has received attention since 1980 to present according to their interesting properties in many areas.

#### 1.3.1 Chemistry of ruthenium(II) complexes

Krause and Krause, (1980) initially reported ruthenium(II) complexes with azoimine ligand. [Ru(azpy)<sub>2</sub>Cl<sub>2</sub>] (azpy = 2-(phenylazo)pyridine) was synthesized and isolated as three isomeric forms. One of these is *trans*-isomer that referred to a pair of chloride atoms. Others were *cis*-isomer; *cis-trans-cis* and *cis-cis-cis*. Characterization was carried out by IR, UV-Visible absorption spectroscopy. The results from cyclic voltammetric data revealed that azpy acts as a better  $\pi$ -acceptor than bpy in [Ru(bpy)<sub>2</sub>Cl<sub>2</sub>] complex to stabilize Ru(II) center.



azpy

**Figure 1.5** The structure of 2-(phenylazo)pyridine (azpy)

Goswami and co-workers, (1981) were interested in the syntheses of  $\text{RuX}_2\text{Cl}_2$  and  $[\text{Ru}(\text{bpy})_2\text{L}](\text{ClO}_4)_2 \cdot \text{H}_2\text{O}$  where X were Cl, Br, I and L is 2-(phenylazo)pyridine (azpy) or 2-(*m*-tolylazo)pyridine (tap), bpy = 2,2'-bipyridine. These complexes were characterized by spectroscopic techniques. Their electrochemical behavior showed that complex having azoimine moiety of azpy is a better potential  $\pi$ -acceptor ligand than imine ligand of bpy to stabilize lower oxidation state of ruthenium. These results were compared with those of  $[\text{Ru}(\text{bpy})_3]^{2+}$  and *cis*- $[\text{Ru}(\text{bpy})_2\text{Cl}_2]$ .

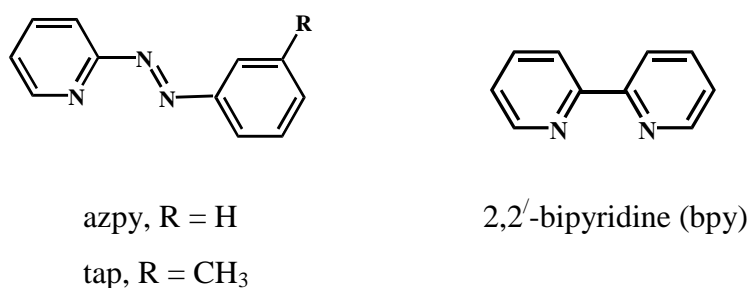


**Figure 1.6** The structure of 2-(*m*-tolylazo)pyridine (left) and 2,2'-bipyridine (bpy) (right)

Krause and Krause, (1984) attempted to demonstrate the effect of a substituent on the phenyl ring of 2-(phenylazo)pyridine (azpy) by preparing ruthenium(II) complexes of 2-((4-nitrophenyl)azo)pyridine (NAz),  $[\text{Ru}(\text{NAz})_2\text{Cl}_2]$ . The chemistry and electrochemistry behaviors of the isomeric  $[\text{Ru}(\text{NAz})_2\text{Cl}_2]$  complexes showed interesting properties. The redox behavior of  $[\text{Ru}(\text{NAz})_2\text{Cl}_2]$  showed Ru(II)/(III) couple greater than that of  $[\text{Ru}(\text{azpy})_2\text{Cl}_2]$ . This result implies that the NAz ligand having the inductive nitro group is strong  $\pi$ -acceptor to stabilize the lower oxidation state of Ru(II).

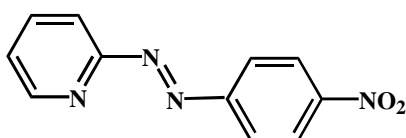
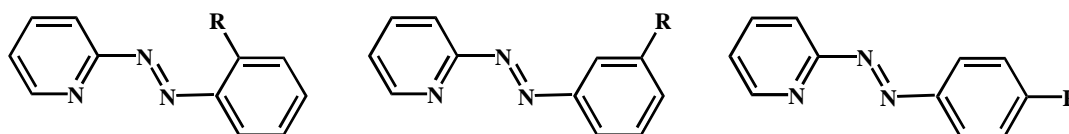


**Figure 1.7** The structure of 2-((4-nitrophenyl)azo)pyridine (NAz)

Seal and Ray, (1984) presented the molecular structure of two isomeric forms of  $[\text{Ru}(\text{azpy})_2\text{Cl}_2]$  as *ctc*- and *ccc*- configuration which two coordinated chloride ions in the *cis* position and differ in the mutual orientation of the bidentate ligand. The *ctc*-isomer indicates the coordinating pairs Cl, N(pyridine), and N(azo) in mutual *cis*, *trans*, and *cis*-positions, respectively or  $\alpha$ - $[\text{Ru}(\text{azpy})_2\text{Cl}_2]$ ; *ccc*-isomer mean coordinating atoms Cl, N(pyridine), and N(azo) as *cis*, *cis*, *cis*-positions.

Barf and Sheldon, (1995) studied the useful application of isomeric complexes of  $[\text{Ru}(\text{azpy})_2\text{Cl}_2]$ . They were two *cis*-isomers ( $\alpha$ ,  $\beta$ ) and one *trans*-isomer ( $\gamma$ ) and used them as catalysts for epoxidation reactions of olefin to give epoxide. Results from study indicated that the both of  $\beta$ - $[\text{Ru}(\text{azpy})_2\text{Cl}_2]$  and  $\gamma$ - $[\text{Ru}(\text{azpy})_2\text{Cl}_2]$  complexes gave good selectivity however,  $\alpha$ - $[\text{Ru}(\text{azpy})_2\text{Cl}_2]$  gave both lower conversion and selectivity.

Munshi *et al.*, (1998) developed the direct and convenient procedure for the synthesis of important *ctc*- $[\text{Ru}(\text{L})_2\text{Cl}_2]$  isomer (*ctc* = *cis-trans-cis* with respect to chlorides, pyridine and azo nitrogens, respectively;  $\text{L} = \text{NC}_5\text{H}_4\text{-N=N-C}_6\text{H}_5(\text{R})$ ,  $\text{R} = \text{H}$ , *o*-Me/Cl, *m*-Me/Cl, *p*-Me/Cl). The chemistry of these complexes was studied by spectroscopic and electrochemical techniques. The results from cyclic voltammetric data showed that the stability of complexes depended on nature and specific location of the substituents present in the phenyl ring of the ligand. The presence of electron donating group decreased the metal oxidation potential.



$\text{R} = \text{H}, \text{Me}, \text{Cl}$

**Figure 1.8** The structure of L ( $\text{L} = \text{NC}_5\text{H}_4\text{-N=N-C}_6\text{H}_5(\text{R})$ ;  $\text{R} = \text{H}$ , *o*-Me/Cl, *m*-Me/Cl, *p*-Me/Cl)

Misra *et al.*, (1998) showed two isomeric complexes of each  $[\text{Ru}(\text{L})_2\text{Cl}_2]$  complex ( $\text{L} = 1\text{-methyl-2-(arylazo)imidazole}$ ;  $\text{L}_1$  and  $1\text{-benzyl-2-(arylazo)imidazole}$ ;  $\text{L}_2$ ). Single crystal X-ray diffraction analysis supported the *trans-cis-cis* and *cis-trans-cis* isomers of bis-compounds. The spectroscopy, i.e. IR, UV-Vis, NMR was used to determine the chemistry and stereochemistry of these complexes. The results from electrochemical behavior showed that these azoimidazole ligands were better  $\pi$ -acceptor ligands than imine like bpy and phen but were weaker than that of azpy. Furthermore, the ruthenium-imidazole complexes were of interest for their antitumor activities.

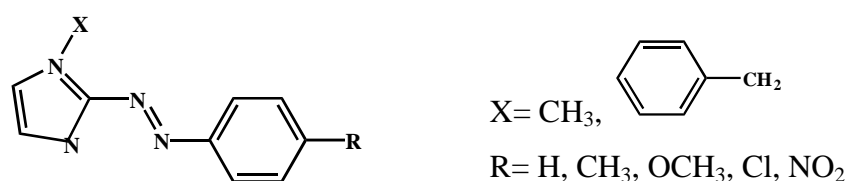


**Figure 1.9** The structure of L ( $\text{L} = 1\text{-methyl-2-(arylazo)imidazole}$ ;  $\text{L}_1$  and  $1\text{-benzyl-2-(arylazo)imidazole}$ ;  $\text{L}_2$ )

Santra *et al.*, (1999) synthesized the neutral complex of  $[\text{Ru}(\text{aapm})_2\text{Cl}_2]$  ( $\text{aapm} = 2\text{-(arylazo)pyrimidine}$ ). After isolation, three compounds were obtained as *trans-cis-cis*, *cis-trans-cis* and *cis-cis-cis* (indicating as a pair of Cl; N(pyrimidine); N(azo), respectively). Two of the three isomers, *ctc* and *ccc*, were studied the structures by X-ray Crystallography. The spectroscopic techniques and electrochemical study were also used to investigate the chemistry of these complexes.

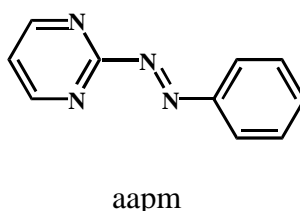


**Figure 1.10** The structure of 2-(arylazo)pyrimidine (aapm)

Panneerselvam *et al.*, (2000) reported the crystal structure of the [protonated 2-(phenylazo)pyridine and protonated 2-(hydroxylazo)pyridine (3:1)] tetrafluoroborate compound. The results from X-ray data indicated that the protonation occurred at N(azo) atom which was more basicity than N(pyridine). The azpy compound was normally liquid at ambient temperature but this crystal structure was stabilized by intramolecular H-bonding, N-H-N and Van der Waals force.

Velder *et al.*, (2000) presented the isomeric complexes of  $\gamma$ ,  $\alpha$ ,  $\beta$ -[Ru(azpy)<sub>2</sub>Cl<sub>2</sub>] which  $\alpha$ ,  $\beta$ ,  $\gamma$  referred to *ctc*, *ccc*, *tcc* configurations. All complexes were tested with several tumor cell lines i.e. breast cancer, ovarian cancer, non small cell lung cancer and colon cancer. The result showed that  $\alpha$ -[Ru(azpy)<sub>2</sub>Cl<sub>2</sub>] isomer as a potent complex inhibited more proliferate of cancer cells than the other forms. In addition, the structure of *tcc* isomer was confirmed by a single crystal X-ray diffraction and it was found that the *tcc* had two chloride atoms in *trans* position, but the N(pyridine) and N(azo) groups were in *cis* geometry. Furthermore, the binding of DNA bases to the *ctc*-[Ru(azpy)<sub>2</sub>Cl<sub>2</sub>] was studied and compared with the similar complexes such as *cis*-[Ru(bpy)<sub>2</sub>Cl<sub>2</sub>]. The binding of the *ctc* isomer with guanine and purine base was sterically less hindered than that in *cis*-[Ru(bpy)<sub>2</sub>Cl<sub>2</sub>] complex. Therefore the *ctc*-isomer was found to show high cytotoxicity against a series of tumor-cell lines.

Hotze *et al.*, (2000) reported the synthesis and characterization of  $\alpha$ -[Ru(azpy)<sub>2</sub>(NO<sub>3</sub>)<sub>2</sub>] which prepared via the precursor of  $\alpha$ -[Ru(azpy)<sub>2</sub>Cl<sub>2</sub>] having as a potential substance for cytotoxicity against a series of tumor cell lines. X-ray diffraction analysis and nuclear magnetic resonance spectroscopic techniques have been used to determine the accuracy structure of the title compound. Binding study of  $\alpha$ -[Ru(azpy)<sub>2</sub>(NO<sub>3</sub>)<sub>2</sub>] with guanines derivative revealed that this complex exactly bound guanine via the N7 atom. Interestingly, the guanine derivatives of 9-EtGua coordinated to the  $\alpha$ -[Ru(azpy)<sub>2</sub>] moiety could have two orientations, whereas 9-EtGua coordinated to the *cis*-[Ru(bpy)<sub>2</sub>] moiety was fixed in one orientation.

Byabartta *et al.*, (2001) prepared ruthenium(II) with 1-alkyl-2-(naphthyl-( $\alpha/\beta$ -azo)imidazoles or abbreviated as  $\alpha/\beta$ -NaiR where R is Me, Et, and Bz. Two isomeric forms,  $[\text{Ru}(\text{NaiR})_2\text{Cl}_2]$  were obtained as greenish-blue and blue in color of complexes. The synthesized complexes were characterized by spectroscopic techniques i.e. infrared (IR), ultraviolet-visible absorption (UV-Visible), nuclear magnetic resonance (NMR). The structural geometry was investigated by X-ray diffraction analysis. The electrochemical behavior of compound was studied by cyclic voltammetry.

Hotze *et al.*, 2002 investigated the interaction of  $\alpha$ - $[\text{Ru}(\text{azpy})_2\text{Cl}_2]$  and *cis*- $[\text{Ru}(\text{bpy})_2\text{Cl}_2]$  with the DNA model base, 9-methyladenine (9-MeAde) to give  $\alpha$ - $[\text{Ru}(\text{azpy})_2(9\text{-MeAde})](\text{PF}_6)_2$  (1) and *cis*- $[\text{Ru}(\text{bpy})_2(9\text{-MeAde})](\text{PF}_6)_2$  (2). Characterization was carried out by 2D NMR (COSY and NOESY) and variable temperature NMR studies. It was found that in both compounds 9-MeAde is present in its rare neutral imine tautomeric form, apparently stabilized by the chelating coordination via its N7 and exocyclic N6 atoms. Thus the difference in cytotoxicity of the parent chloride complexes could not be explained by differences in the coordination of 9-MeAde around the ruthenium center.

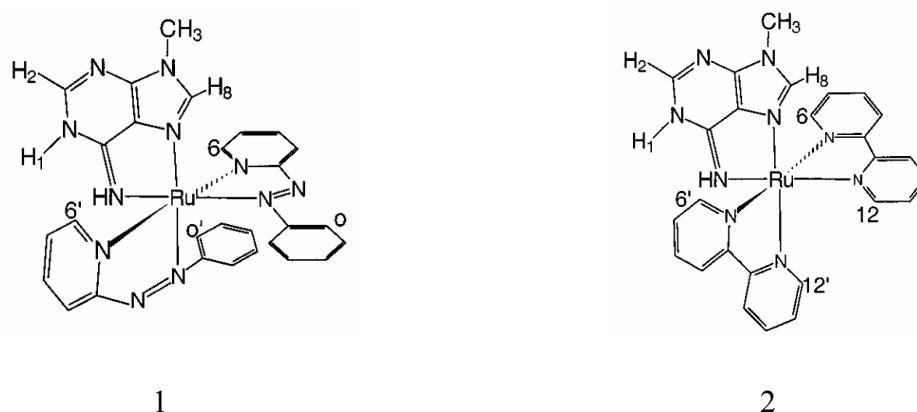


**Figure 1.11** The structures of  $\alpha$ - $[\text{Ru}(\text{azpy})_2(9\text{-MeAde})](\text{PF}_6)_2$  (1) and *cis*- $[\text{Ru}(\text{bpy})_2(9\text{-MeAde})](\text{PF}_6)_2$  (2)

Hotze *et al.*, (2003) presented a new series of water-soluble complexes;  $\alpha$ -[Ru(azpy)<sub>2</sub>(cbdca-*O,O'*)] (1);  $\alpha$ -[Ru(azpy)<sub>2</sub>(ox)] (2);  $\alpha$ -[Ru(azpy)<sub>2</sub>(mal)] (3) (where cbdca-*O,O'* = 1,1-cyclobutanedicarboxylate; ox = oxalate; mal = malonate). The single crystal X-ray diffraction studies of both 1 and 2 were reported. Their original  $\alpha$  configuration was retained during the reaction correspond to the coordination pairs O, N(pyridine) and N(azo) in order to *cis-trans-cis* (*ctc*). The cytotoxicity of these new water-soluble bis(2-(phenylazo)pyridine)ruthenium(II) carboxylato complexes was described and compared to the cytotoxicity of the parent compounds, [Ru(azpy)<sub>2</sub>Cl<sub>2</sub>]. It was shown that the cytotoxicity data of 1, 2, 3 compared to the parent complex results in a decrease of activity but a parallel increase in water solubility when these compound has been tested in A2780 (human ovarian carcinoma) and A2780cis (cisplatin-resistant cell lines).

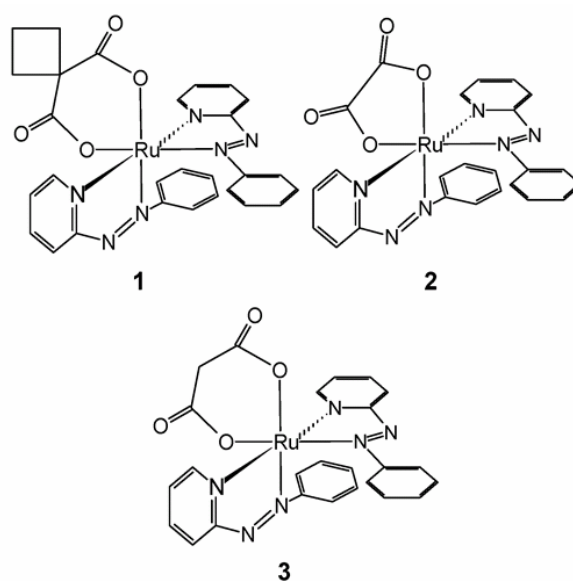
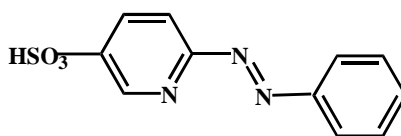


**Figure 1.12** The structures of  $\alpha$ -[Ru(azpy)<sub>2</sub>(cbdca-*O,O'*)] (1);  $\alpha$ -[Ru(azpy)<sub>2</sub>(ox)] (2);  $\alpha$ -[Ru(azpy)<sub>2</sub>(mal)] (3)

Hotze *et al.*, (2004) synthesized a water-soluble derivative of azpy, 2-phenylazopyridine-5-sulfonic acid (Hsazpy). It was used for the synthesis of the corresponding dichlorobis(Hsazpy)ruthenium(II) complexes,  $[\text{Ru}(\text{Hsazpy})_2\text{Cl}_2]$ . Its structure was confirmed as *cis-trans-cis* configuration considered in order to the coordination pairs of Cl, N(pyridine) and N(azo), respectively. The cytotoxicity of *ctc*- $[\text{Ru}(\text{Hsazpy})_2\text{Cl}_2]$  has been determined by mean of  $\text{IC}_{50}$  value and compared with the activity of the related and highly cytotoxic *ctc*- $[\text{Ru}(\text{azpy})_2\text{Cl}_2]$ . The results showed that the  $\text{IC}_{50}$  value of *ctc*- $[\text{Ru}(\text{Hsazpy})_2\text{Cl}_2]$  against the human ovarium carcinoma cell lines A2780 is exceed  $100 \mu\text{M}$ , which identified the compound as non-cytotoxic.



Hsazpy

**Figure 1.13** The structure of 2-phenylazopyridine-5-sulfonic acid (Hsazpy)

Hotze *et al.*, (2004) presented the synthesis and characterization of the three isomers,  $\gamma, \alpha, \beta$ - $[\text{RuL}_2\text{Cl}_2]$  with L = *o*-tolylazopyridine (tazpy) and 4-methyl-2-phenylazo)pyridine (mazpy) by NMR spectroscopy. In addition, the molecular structures of  $\gamma$ - $[\text{Ru}(\text{tazpy})_2\text{Cl}_2]$  and  $\alpha$ - $[\text{Ru}(\text{mazpy})_2\text{Cl}_2]$  were determined by X-ray diffraction analysis. The  $\text{IC}_{50}$  values of geometrically isomer  $[\text{Ru}(\text{tazpy})_2\text{Cl}_2]$  and  $[\text{Ru}(\text{mazpy})_2\text{Cl}_2]$  complexes compared with those of the parent  $[\text{Ru}(\text{azpy})_2\text{Cl}_2]$  complexes were determined in a series of human tumor cell lines such as breast cancer, ovarian cancer and colon cancer. The result showed that the  $\alpha$ -isomer showed a very cytotoxicity, whereas the  $\beta$ -isomer was a factor 10 less cytotoxic. However, the  $\gamma$ -isomers of  $[\text{Ru}(\text{tazpy})_2\text{Cl}_2]$  and  $[\text{Ru}(\text{mazpy})_2\text{Cl}_2]$  displayed a very high cytotoxicity comparable to that of the  $\gamma$ -isomer of the parent compound  $[\text{Ru}(\text{azpy})_2\text{Cl}_2]$  and to that of the  $\alpha$ -isomer.

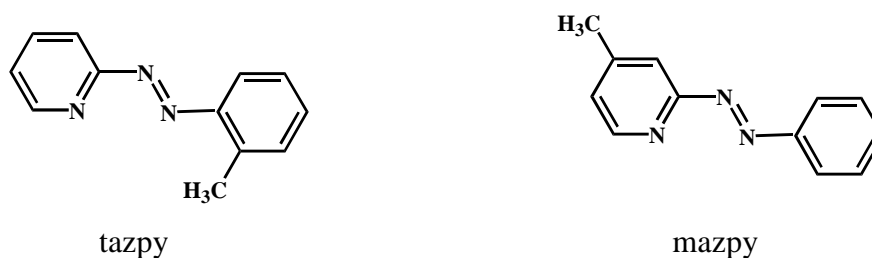


**Figure 1.14** The structures of *o*-tolylazopyridine (tazpy) 4-methyl-2-(phenylazo)pyridine (mazpy)

Hotze *et al.*, (2004) studied the synthesis of a mixed-ligand complex,  $\alpha$ -[Ru(azpy)(bpy)Cl<sub>2</sub>] and its structure has been determined by X-ray structure analysis. Although the  $\alpha$ -[Ru(azpy)(bpy)Cl<sub>2</sub>] showed a low to moderate cytotoxicity in several cell lines (A498, H226, M19, MCF-7), it was an interesting compound to compare the cytotoxicity of  $\alpha$ -[Ru(azpy)(bpy)Cl<sub>2</sub>] with those of the highly cytotoxic  $\alpha$ -[Ru(azpy)<sub>2</sub>Cl<sub>2</sub>] and inactive *cis*-[Ru(bpy)<sub>2</sub>Cl<sub>2</sub>] described previously. The isomerization of  $\alpha$ -[Ru(azpy)(bpy)Cl<sub>2</sub>] with DNA model base 9-ethylguanine (9-EtGua) was studied and compared its result with its cytotoxicity to both  $\alpha$ -[Ru(azpy)<sub>2</sub>Cl<sub>2</sub>] and *cis*-[Ru(bpy)<sub>2</sub>Cl<sub>2</sub>]. The results indicated that the isomerization process of coordinated 9-EtGua to  $\alpha$ -[Ru(azpy)(bpy)Cl<sub>2</sub>] influenced its cytotoxic activity by the fact that only part of the “active *trans*-Nazo 9-EtGua adduct” was converted to the inactive *trans*-Nbpy adduct.

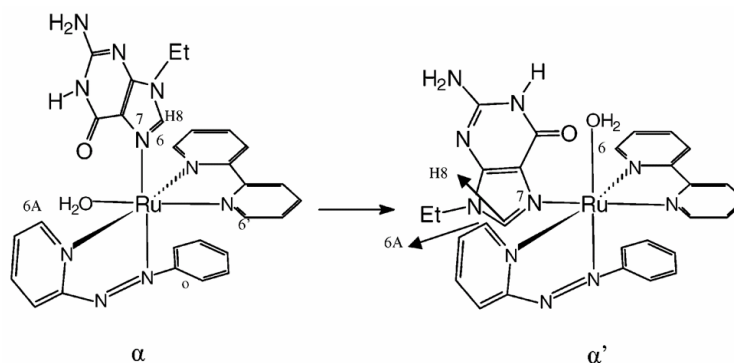


**Figure 1.15**  $\alpha$ -(*trans* Nazo 9-EtGua) and  $\alpha'$ -(*trans* Nbpy 9-EtGua) of [Ru(azpy)(bpy)(9-EtGua)(H<sub>2</sub>O)]<sup>2+</sup>

Velder *et al.*, (2004) presented the new isomeric  $\delta$ -[Ru(azpy)<sub>2</sub>Cl<sub>2</sub>] complex. This structure has been determined by <sup>1</sup>H NMR spectroscopy and single-crystal X-ray diffraction analysis, and was all *trans*-isomer (two chlorides, two nitrogen from pyridine and two nitrogen from azo). In this work,  $\delta$ -[Ru(azpy)<sub>2</sub>Cl<sub>2</sub>] was compared and discussed with other forms of [Ru(azpy)<sub>2</sub>Cl<sub>2</sub>] with 1D and 2D NMR.

Kooijman *et al.*, (2004) described crystal structure of [Ru(dazpy)<sub>2</sub>Cl<sub>2</sub>] (dazpy = 2-phenylazo-4,6-dimethylpyridine) which recrystallize from CHCl<sub>3</sub> and diethyl ether. The results showed that the dazpy is coordinated to ruthenium in distorted octahedral geometry in the so-called  $\alpha$  configuration (*cis-trans-cis* of two Cl, two N(py) and two N(azo), respectively). The distortion was due to the small bite angle of the dazpy ligand.

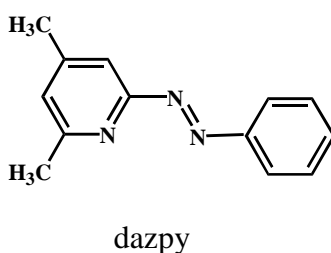


**Figure 1.16** The structure of 2-phenylazo-4,6-dimethylpyridine (dazpy)

Chen *et al.*, (2006) studied the electronic and geometric structures of a series of isomeric complexes  $\gamma$ -,  $\alpha$ -,  $\beta$ -,  $\delta$ -,  $\varepsilon$ -[Ru(azpy)<sub>2</sub>Cl<sub>2</sub>] using the density functional theory (DFT) method and compared their structure relationship to antitumor agent properties. The results showed that the structure of  $\gamma$ -[Ru(azpy)<sub>2</sub>Cl<sub>2</sub>] was more advantageous to the DNA-binding affinity than  $\alpha$ - and  $\beta$ -form. In addition, the antimetastatic activity of  $\delta$ -,  $\varepsilon$ -[Ru(azpy)<sub>2</sub>Cl<sub>2</sub>] complexes have been predicted and summarized that the anticancer activity of  $\delta$ -[Ru(azpy)<sub>2</sub>Cl<sub>2</sub>] was higher than that of  $\gamma$ -[Ru(azpy)<sub>2</sub>Cl<sub>2</sub>] but  $\delta$ -[Ru(azpy)<sub>2</sub>Cl<sub>2</sub>] was thermodynamically labile, whereas the activity of  $\varepsilon$ -[Ru(azpy)<sub>2</sub>Cl<sub>2</sub>] lied between those of  $\alpha$ - and  $\beta$ - form.

Ye *et al.*, (1995) studied the complexes of  $[\text{Ru}(\text{bpy})_2(\text{phen})](\text{ClO}_4)_2 \cdot \text{H}_2\text{O}$  and  $[\text{Ru}(\text{bpy})_2(\text{Me-phen})](\text{ClO}_4)_2$ . They reported the synthesis, spectral characterization and single crystal structures of both complexes. The results from X-ray data indicated that the Ru-N(bpy) and Ru-N(phen) bond distances were comparable and as expected of  $\pi$ -backbonding interaction which involved of each ligand in the coordination sphere.

Byabartta *et al.*, 2003 studied the synthesis and characterization of hetero-tris-chelates complex,  $[\text{Ru}(\text{HaaiMe})_2(\text{phen})](\text{ClO}_4)_2$  (HaaiMe = 1-methyl-2-(phenylazo)imidazole, phen = 1,10-phenanthroline). The stereochemistry about Ru center was compared with the parent complex, *ctc*- $[\text{Ru}(\text{HaaiMe})_2\text{Cl}_2]$  and stereochemistry about Ru was retained. The X-ray structure determination suggested formation of a *trans-cis* isomer with reference to coordination pairs of N(imidazole) and N(azo).

Hotze and co-worker (2005) reported the synthesis of  $[\text{Ru}(\text{L})_3](\text{PF}_6)_2$  (L = 2-phenylazopyridine or *o*-tolylazopyridine) and  $[\text{Ru}(\text{L}')_2(\text{L}'')](\text{PF}_6)_2$  (L', L'' = 2-phenylazopyridine, 2,2'-bipyridine) and characterization was carried out by NMR spectroscopy. Only two compounds, *mer*- $[\text{Ru}(\text{azpy})_3](\text{PF}_6)_2$  and *mer*- $[\text{Ru}(\text{tazpy})_3](\text{PF}_6)_2$  (tazpy = *o*-tolylazopyridine) have been determined by X-ray diffraction. Interestingly, the cytotoxicity data of these tris(chelated) complexes with a series of human tumor cell lines (A498, EVSA-T, H226, IGROV, M19, MCF-7 and WIDR) showed a moderate cytotoxic activity eventhrough no *cis* chloride ligand such in the parent complex,  $[\text{Ru}(\text{azpy})_2\text{Cl}_2]$ . This would imply that the 2-(phenylazo)pyridine ruthenium(II) complexes acted via a different mechanism from the well-known cisplatin. This different mechanism was important to study how their structural complexes effected to cytotoxic activity and to give information to design a new anticancer drugs later on.

Hansongnern *et al.*, (2007) reported the X-ray structure of  $[\text{Ru}(\text{azpy})_2(\text{bpy})](\text{PF}_6)_2$  which was synthesized from the precursor  $\alpha\text{-}[\text{Ru}(\text{azpy})_2\text{Cl}_2]$  corresponding to mole ratio of bpy in ethanolic solution. The X-ray result showed that the configuration of the title compound is retained with two coordinated azpy and one bpy ligand. In addition, this data confirmed that azpy was a better  $\pi$ -acceptor than bpy to stabilize metal center.

### 1.3.2 Interaction between ruthenium(II) complexes with DNA base pair

Vliet *et al.*, (1994) reported the interaction of *cis*- $[\text{Ru}(\text{bpy})_2\text{Cl}_2]$  with model compounds for guanine. This study proved that *cis*- $[\text{Ru}(\text{bpy})_2\text{Cl}_2]$  bound only one 9-alkylated guanine derivative at the N7 site. Since the N7 sites of adenine and guanine had a nucleophilic character, it was available for a metal complex when located in the major groove.

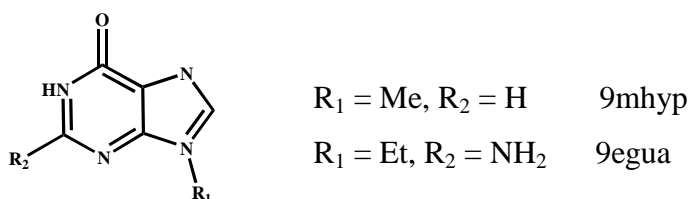


**Figure 1.17** The structure of 9-alkylated guanine derivatives

Naing and co-worker (1995) reported the spectroscopic titrations, emission measurements, circular dichroism (CD) and photoactivated reactions which have been used to study the interaction of the enantiomers of  $[\text{Ru}(\text{bpy})_2\text{phi}]\text{Cl}_2$  and  $\text{Ru}(\text{phen})_2\text{phi}]\text{Cl}_2$  (phi = 9,10-phenanthrenequinonediimine) with different compositions of polynucleotides. From data showed that the phi ligands intercalates between the base pairs of polynucleotides. In addition, there were no emission and photoactivated cleavage activities between enantiomers and polynucleotides.

Liu *et al.*, (2001) investigated the synthesis and characterization of  $[\text{Ru}(\text{dmp})_2(\text{dppz})]^{2+}$  and  $[\text{Ru}(\text{dmb})_2(\text{dppz})]^{2+}$  (dmp = 2,9-dimethyl-1,10-phenanthroline; dmb = 4,4'-dimethyl-2,2'-bipyridine). Interaction of both compounds with DNA has been studied and compared the effect of ancillary ligands, dmp and dmb, on the DNA-binding behaviors. The X-ray structure of  $[\text{Ru}(\text{dmp})_2(\text{dppz})]^{2+}$  was useful data to explain how substitution on the 2- and 9-positions of the ancillary phen ligand may cause strict steric constrains near the core of Ru(II) when the complex intercalates into the DNA base pairs. This steric prevented this complex from intercalating effectively. The results from spectroscopic techniques and viscosity measurement showed that the  $[\text{Ru}(\text{dmp})_2(\text{dppz})]^{2+}$  complex was less efficient intercalator than  $[\text{Ru}(\text{dmb})_2(\text{dppz})]^{2+}$ .

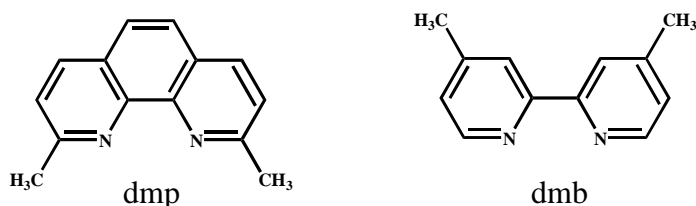


**Figure 1.18** 2,9-dimethyl-1,10-phenanthroline (dmp) 4,4'-dimethyl-2,2'-bipyridine (dmb)

Vaidyanathan and Nair, (2002) introduced the  $[\text{Ru}(\text{bzimpy})_2]\text{Cl}_2$  complex where bzimpy was 2,6-bis(benzimidazol-2-yl). Characterization was carried out by spectroscopic techniques. The DNA-binding affinity was studied by absorption titration, viscosity, fluorescence and photophysical properties. These results showed that the title complex bind to DNA via surface binding. In addition, photoexcitation of the complex in the MLCT region in the presence of plasmid DNA have been found to give rise to nicking of DNA.

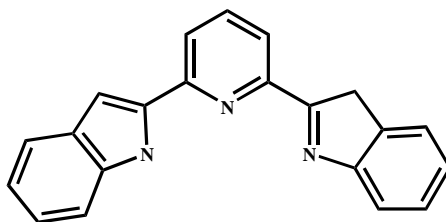


**Figure 1.19** The structure of 2,6-bis(benzimidazol-2-yl) (bzimpy)

Zhang and Lippard., (2003) reported the development of metal-based therapeutics. Since the discovery of cisplatin, other metal-based chemotherapeutic compounds have been studied for potential medicinal application i.e. ruthenium and gold. These complexes have investigated for medicinal applications i.e. antitumor agents.

Han *et al.*, (2004) introduced the molecular modeling method which has been applied to study the structural characterization of the interaction of transition metal complexes containing the ligands such as bpy, phen, dpq, dppz, tpphz and phi with B-DNA. The optimum binding position of each complex to DNA was found by exploring the shape of complexes which fitted best with the intercalation site and these data could be used to consider compared with the previous experimental data. Thus, the modeling results should extend the knowledge of the nature of binding of these complexes to B-DNA.

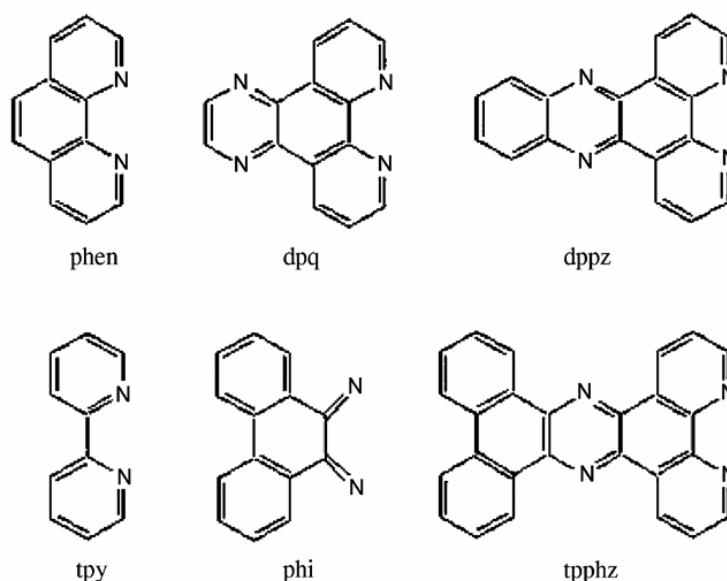


**Figure 1.20** The structure of phen = 1,10-phenanthroline, bpy = 2,2'-bipyridine, dpq = dipyrido[3,2-d:2',3'-f]quinoxaline, dppz = dipyrido[3,2-a:2',3'-c]phenazine, tpphz = tetrapyrrodo[3,2-a:2',3'-c:3'',2''-h:2''',3'''-f]phenazine, phi = 9,10-phenanthrene quinediimine

Maheswari and Palaniandavar, (2004) described the interaction of a series of mixed ligand complexes of the type  $[\text{Ru}(\text{NH}_3)_4(\text{diimine})]\text{Cl}_2$ , (where diimine = 2,2'-bipyridine (bpy), 1,10-phenanthroline (phen), 5,6-dimethyl-1,10-phenanthroline (5,6-dmp), 4,7-dimethyl-1,10-phenanthroline (4,7-dmp) 2,9-dimethyl-1,10-phenanthroline (2,9-dmp), 3,7,4,8-tetramethyl-1,10-phenanthroline ( $\text{Me}_4\text{phen}$ )) with calf thymus DNA. Their interaction has been studied by using absorption, emission and circular dichroism spectral measurements, viscometry and electrochemical techniques showed that the  $[\text{Ru}(\text{NH}_3)_4(\text{diimine})]^{2+}$  complexes bound to CT-DNA through their diimine rather than  $\text{NH}_3$  'face'.

Nakabayashi *et al.*, (2004) reported the synthesis and characterization of ruthenium(II) complexes,  $[\text{Ru}(\text{phen})_2(\text{AA})]^{n+}$  ( $n = 1,2$ ; AA = gly, L-ala, L-arg) and  $[\text{Ru}(\text{phen})_3]^{2+}$ . The interaction of these compounds and  $[\text{Ru}(\text{phen})_3]^{2+}$  with DNA have been examined by absorption, luminescence and circular dichroism spectroscopic methods. The results showed that all the MLCT bands of the ruthenium(II) complexes exhibited hypochromism and red shifts in the presence of CT-DNA.

Jing *et al.*, (2004) presented three ruthenium(II) complexes of a  $[\text{Ru}(\text{II})(\text{bpy})_2(\text{L})]^{2+}$  where L are 1,10-phenanthroline derivatives of imidazole (1), having at position 2  $\alpha$ -naphthyl (2), 3-methoxy-4-hydroxy-phenyl (3). The DNA-binding with these complexes was studied by using spectroscopic techniques such as electronic absorption and circular dichroism spectra. These result indicated that these compounds showed strong affinity with DNA by hypochromism, red-shifted absorption spectra and stereoselective binding. Moreover, the DNA binding affinity was sensitive to the nature of ligands, such as planarity,  $\pi$ -electron extension and hydrophobicity. From data suggested that complex 3 exhibited the strongest binding with DNA, which could be attributed to hydrogen bonding.

Hong *et al.*, 2005 reported the new complex of  $[\text{Ru}(\text{bpy})_2(\text{S},\text{O}-\text{H}_2\text{L})] \cdot 1,5\text{CH}_3\text{CN}$  where  $\text{H}_4\text{L}$  is a *p-tert*-butyltetrahydrocalix[4]arene. The characterization was carried out by mass spectrometric and X-ray diffraction analysis. In addition, fluorescence quenching of EB-DNA complex by the ruthenium(II) complex agreed with linear Stern-Volmer equation and the quenching was realized via the DNA-mediated electron transfer from the excited EB to the Ru(II) complex.

Tan *et al.*, (2005) investigated the synthesis of a novel ligand 2'-(2''-nitro-3'',4''-methylenedioxyphenyl)imidazo-[4',5'-f][1,10]-phenanthroline (NMIP) and its complex  $[\text{Ru}(\text{phen})_2(\text{NMIP})]^{2+}$ . Characterization was achieved by mass spectroscopy,  $^1\text{H}$  NMR and cyclic voltammetry. Binding of the complex with calf thymus DNA (CT-DNA) has been investigated by spectroscopic methods, viscosity and electrophoresis measurements. The experimental results indicated that  $[\text{Ru}(\text{phen})_2(\text{NMIP})]^{2+}$  bound to DNA via partial intercalative mode via the extended methylenedioxyphenyl ring into the base pairs of DNA. This might be related to the molecular structure of the complex. In  $[\text{Ru}(\text{phen})_2(\text{NMPIP})]^{2+}$ , due to the large substituent group  $\text{NO}_2$ , the NMIP ligand was somewhat sterically hindered from planarity and did not completely intercalate DNA.

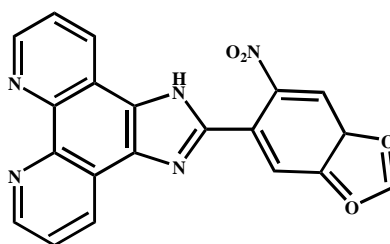


**Figure 1.21** 2'-(2''-nitro-3'',4''-methylenedioxyphenyl)imidazo-[4',5'-f][1,10]-phenanthroline (NMIP)

Tan *et al.*, (2007) reported the new polypyridine ligand, MPPIP (MPPIP = 2-(3'-phenoxyphenyl)imidazo[4,5-f]-[1,10]phenanthroline) and its ruthenium(II) complexes,  $[\text{Ru}(\text{bpy})_2(\text{MPPIP})]^{2+}$  (1) and  $[\text{Ru}(\text{phen})_2(\text{MPPIP})]^{2+}$  (2). The binding of the two complexes with calf thymus DNA (CT-DNA) has been investigated with spectroscopic method and viscosity measurement. The results suggested that both complexes bound to DNA through intercalation. In addition, when irradiated at 365 nm, both complexes were efficient photocleavers of the plasmid. Thus these complexes might be useful as tool for probing DNA.

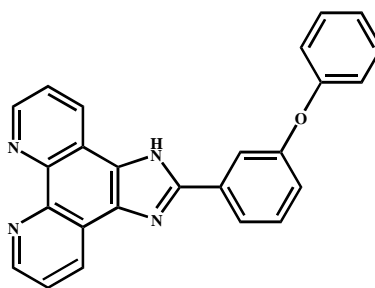


**Figure 1.22** 2-(3'-phenoxyphenyl)imidazo[4,5-f]-[1,10]phenanthroline (MPPIP)

Tan *et al.*, (2007) introduced a novel of  $[\text{Ru}(\text{L})_2(\text{BPIP})]^{2+}$  (L = bpy, phen) which synthesized and characterized by elemental analysis, electrospray mass spectrometry and NMR. The DNA binding properties of the both complexes were investigated by spectroscopic and viscosity measurement. The results suggest that both complexes bound to DNA via intercalative mode.

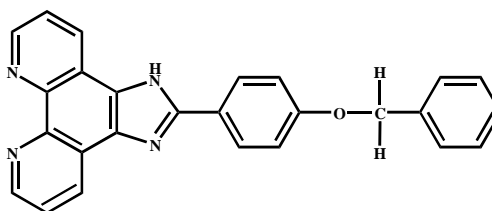


**Figure 1.23** 2-(4'-benzyloxyphenyl)imidazo[4,5-f]-[1,10]phenanthroline (BPIP)

Tan *et al.*, (2007) presented the synthesis and characterization of  $[\text{Ru}(\text{bpy})_2(\text{BPIP})]^{2+}$  (1) and  $[\text{Ru}(\text{phen})_2(\text{BPIP})]^{2+}$  (2) (BPIP = 2-(4'-biphenyl)imidazo[4,5-f][1,10]phenanthroline). Mass spectrometry and cyclic voltammetry were used to study these compounds. The interaction of two Ru(II) complexes with calf thymus DNA was intercalative mode. Additionally, the DNA-binding affinity of complex 2 was much greater than that of complex 1.

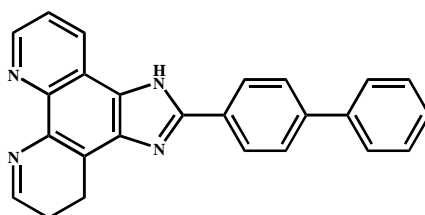


**Figure 1.24** 2-(4'-biphenyl)imidazo[4,5-f][1,10]phenanthroline (BPIP)

Tan *et al.*, (2007) investigated the effect of ancillary ligand (phen, dmp) of  $[\text{Ru}(\text{phen})_2(\text{MIP})]^{2+}$  (1) and  $[\text{Ru}(\text{dmp})_2(\text{MIP})]^{2+}$  (2) (dmp = 2,9-dimethyl-1,10-phenanthroline; MIP = 2-(2,3-methylenedioxyphenyl)imidazo[4,5-f]1,10-phenanthroline) to DNA-binding properties by different spectrophotometric methods and viscosity measurements, as well as equilibrium dialysis and circular dichroism spectroscopy. The results suggested that complex 1 bound to DNA through intercalation, and complex 2 bound to CT-DNA via a partial intercalative mode. It was concluded that the different ancillary ligands probably influenced the binding mode to DNA.

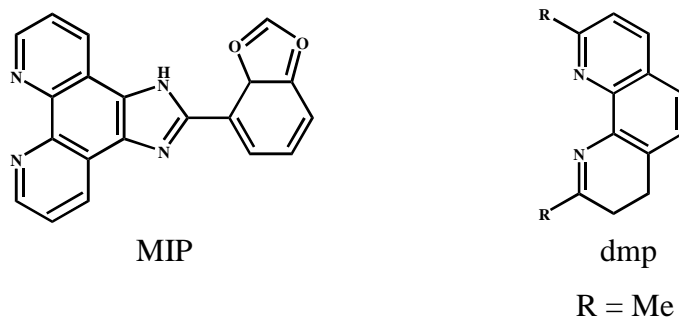


**Figure 1.25** 2,9-dimethyl-1,10-phenanthroline (dmp); MIP = 2-(2,3-methylenedioxyphenyl)imidazo[4,5-f]1,10-phenanthroline

Tan and Chao (2007) reported new mixed polypyridyl complexes,  $[\text{Ru}(\text{dmb})_2(\text{NMIP})]^{2+}$  (1) and  $[\text{Ru}(\text{bpy})_2(\text{NMIP})]^{2+}$  (2) (dmb = 4,4'-dimethyl-2,2'-bipyridine, NMIP = 2'-(2''-nitro-3'',4''-methylenedioxyphenyl)imidazo-[4',5'-f][1,10]-phenanthroline). Characterization of these complexes has been investigated by spectroscopic methods and viscosity measurement was used to study DNA-binding properties of these compounds. The results showed that both complexes bound to DNA via partial intercalation with stronger DNA binding in complex 2 than that of 1. The methyl groups substituted at 4 and 4' -positions of bpy had a profound effect on the DNA-binding, as revealed by the decreased binding affinity.

#### 1.4 Objectives

- to synthesize and to characterize the 5-chloro-2-(phenylazo)pyridine (Clazpy) ligand
- to synthesize and to characterize the isomeric complexes of  $[\text{Ru}(\text{Clazpy})_2\text{Cl}_2]$
- to synthesize and to characterize the  $[\text{Ru}(\text{Clazpy})(5\text{dmazpy})\text{Cl}_2]$  complex
- to synthesize and to characterize the  $[\text{Ru}(\text{Clazpy})_2(\text{L})](\text{PF}_6)_2$  (L = bpy, phen, azpy, Clazpy) complexes
- to synthesize and to characterize the  $[\text{Ru}(\text{Clazpy})_2(\text{L})](\text{NO}_3)_2 \cdot x\text{H}_2\text{O}$  (L = bpy, phen, azpy, Clazpy) complexes
- to synthesize and to characterize the  $[\text{Ru}(\text{Clazpy})_2(\text{L})]\text{Cl}_2 \cdot x\text{H}_2\text{O}$  (L = bpy, phen, azpy, Clazpy) complexes
- to synthesize and to characterize the  $[\text{Ru}(\text{bpy})_2(\text{Clazpy})](\text{X})_2$  and  $[\text{Ru}(\text{bpy})_2(\text{Clazpy})](\text{X})_2$  (X =  $\text{PF}_6^-$ ,  $\text{Cl}^-$ ) complexes
- to study the interaction between these complexes with CT-DNA by spectroscopic techniques such as absorption titration, emission, viscosity and electrochemical study
- to test the cytotoxicity

## CHAPTER 2

### MATERIALS AND METHODS

#### 2.1 Materials

##### 2.1.1 Chemical substances

###### Materials from Aldrich Chemical Company, Inc.

- Ruthenium(III) chloride hydrate,  $C_{12}H_8N_2 \cdot H_2O$ , A.R. grade
- Ferrocenemethanol,  $C_{11}H_{12}FeO$ , A.R. grade

###### Materials from BDH Laboratory Supplies, Poole

- Silver nitrate,  $AgNO_3$ , A.R. grade

###### Materials from Fluka

- 2-Aminopyridine,  $C_5H_5N$ , A.R. grade
- 2-Amino-5-chloropyridine,  $C_5H_5N_2Cl$ , A.R. grade
- Nitrosobenzene,  $C_6H_5NO$ , A.R. grade
- Ammonium hexafluorophosphate,  $NH_4PF_6$ , A.R. grade
- Tetrabutylammonium hexafluorophosphate,  $[NBu_4]PF_6$ , A.R. grade
- Tetra-*n*-butylammonium chloride hydrate 98%,  
[ $CH_3(CH_2)_3$ ]<sub>4</sub>NCl.XH<sub>2</sub>O]; TBACl, A.R. grade

###### Materials from Merck

- Silica gel 60 (0.040-0.063 nm) GF<sub>254</sub>
- Sodium hydroxide, NaOH, A.R. grade
- Sodium Chloride, NaCl, A.R. grade
- 2,2'-Bipyridine,  $C_{10}H_8N_2$ , A.R. grade
- 1, 10-Phenanthroline,  $C_{12}H_8N_2$ , A.R. grade

###### Materials from Sigma

- Deoxyribonucleic acid (DNA)
- Tris(hydroxymethyl)aminomethane (Tris-base)

### 2.1.2 Solvents

#### Solvents from Lab. Scan analytical science

- Acetone, CH<sub>3</sub>OCH<sub>3</sub>, A.R.grade
- Acetonitrile, CH<sub>3</sub>CN, A.R. grade
- Chloroform, CHCl<sub>3</sub>, A.R. grade
- Dichloromethane, CH<sub>2</sub>Cl<sub>2</sub>, A.R. grade
- Dimethyl sulphoxide, DMSO, A.R. grade
- Ethanol, EtOH, A.R.grade
- Ether, A.R.grade
- Hexane, C<sub>6</sub>H<sub>14</sub>, A.R. grade
- Methanol, MeOH, A.R.grade
- Toluene, C<sub>7</sub>H<sub>8</sub>, A.R. grade
- Ethyl acetate, EtOAc

#### Solvent from Merck

- Hydrochloric acid, HCl, A.R. grade

#### Solvent from M&B Laboratory Chemical

- Dimethylformamide, DMF, HCON(CH<sub>3</sub>)<sub>2</sub>, A.R. grade

The solvents, dichloromethane; hexane; ethyl acetate; toluene; and acetonitrile were used for purification compounds by column chromatographic technique.

## 2.2 Instruments and apparatus

**2.2.1** Melting points of all compounds were measured on an Electrothermal melting point apparatus (Electrothermal 9100)

**2.2.2** Elemental analysis data were obtained by using Carlo Erbra 1108 Elemental Analyser (University of Bristol, U.K.) and CE instruments Flash 1112 Series EA CHNS-O Analyzer (Prince of Songkla University).

- 2.2.3** Fast-atom bombardment (FAB) mass spectra were recorded on a VG Autospec instrument (University of Britol, U.K.).
- Electrospray (ES) mass spectrometric experiments were measured on a VG Quattro triple quaudrupole system mass spectrometer for HRMS and Micromass platform LCZ single quadrupole LC/MS using 50% CH<sub>3</sub>CN as mobile phase (University of Wollongong, Australia).
- 2.2.4** The Fourier-transform IR spectra were collected by using KBr pellets on a Perkin Elmer Spectrum GX FT-IR Spectrophotometer from 4,000-400 cm<sup>-1</sup>. KBr has no infrared absorption in the range 4000-650 cm<sup>-1</sup>.
- 2.2.5** The Ultraviolet Visible absorption spectra were monitored in the range 200-800 nm by S100 specord spectrophotometer.
- 2.2.6** 1D and 2D NMR spectra were performed with a Varian UNITY SNOVA500MHz FT-NMR spectrometer, and a Varian Inova 500MHz NMR spectrometer. All chemical shifts were given relative to tetramethylsilane (Si(CH<sub>3</sub>)<sub>4</sub>) used as an internal standard.
- 2.2.7** Electrochemical experiments were performed using cyclic voltammetric technique coupled with Echem1.5.1 program. The supporting electrolyte was 0.1 M tetrabutylammonium hexafluorophosphate and all potentials were quoted *versus* the ferrocene/ ferricenium couple. All sample were purged with argon prior to measurement. A standard three electrodes system comprising of a glassy carbon working electrode, platinum-wire auxiliary electrode and platinum disk reference electrode was used and all immersed in a liquid and connected to a potentiostat. The scan rate was varying from 50 to 500 mV/s.
- 2.2.8** X-ray diffraction data were collected on a Smart APEX CCD diffractometer using monochromated Mo K $\alpha$  radiation ( $\lambda = 0.71073\text{\AA}$ ). The structures were solved and refined using the SHELXTL NT (version 6.12) and SHELXTL-97 programs.
- 2.2.9** A pH Denver pH meter was used to read the pH values directly.

**2.2.10** Steady state emission experiments were using a Perkin-Elmer LS 55 luminescence spectrometer. All experiment were done at room temperature.

## **2.3 Syntheses of ligands**

### **2.3.1 2-(phenylazo)pyridine (azpy)**

The 2-(phenylazo)pyridine (azpy) ligand was prepared by modified procedure reported in literature (Krause and Krause, 1980).

2-aminopyridine (950 mg, 0.01 mol) reacted with nitrobenzene (1080 mg, 0.01 mol) in a presence of 20 M NaOH and 10 mL of benzene solution. The reaction mixture was warmed on the water bath for 45 min. The mixture was then extracted with 3x5 mL of benzene. The solvent was removed and the residue was purified by column chromatography. A mixture of hexane and ethyl acetate was used as an eluent to elute the orange band of the desired product. The solvent was removed to give 640 mg (35 %) of azpy ligand.

### **2.3.2 5-Chloro-(2-phenylazo)pyridine (Clazpy)**

The 5-Chloro-2-(phenylazo)pyridine (Clazpy) ligand was synthesized via modification of the method reported by Krause and Krause in 1980.

A 2-amino-5-chloropyridine (378 mg, 2.94 mmol) was condensed with nitrosobenzene (318 mg, 2.97 mmol) in the presence of sodium hydroxide in benzene solution. The mixture was refluxed with stirring continued for 12 h. The light-green solution gradually turned to reddish brown. The product was extracted with benzene and purified by column chromatography on a silica gel. The orange band was collected after elution with dichloromethane (CH<sub>2</sub>Cl<sub>2</sub>) and hexane (1:9 by volume). The solution was evaporated to dryness. The yield was 354 mg (54%).

## 2.4 Syntheses of complexes

### 2.4.1 Isomeric complexes of dichlorobis(5-chloro-(2-phenylazo)pyridine)ruthenium(II), [Ru(Clazpy)<sub>2</sub>Cl<sub>2</sub>]

There are two methods for preparation isomeric complexes of [Ru(Clazpy)<sub>2</sub>Cl<sub>2</sub>].

**Method I**, A mixture of RuCl<sub>3</sub>.3H<sub>2</sub>O 105 mg (0.506 mmol) and Clazpy 237 mg (1.088 mmol) were refluxed in 50 mL of ethanol for 6 h. The solution gradually turned from dark brown to dark purple. After the solution was filtered, the filtrate was evaporated to dryness. The residue was purified by column chromatography. Three bands of green, blue and purple were isolated from the mixture of toluene and acetonitrile (CH<sub>3</sub>CN) (9:1 by volume), respectively and then evaporated to dryness. The yield was 110 mg (36%) for green, 39 mg (13%) for blue and 47 mg (15%) for purple solids.

**Method II**, [Ru(Clazpy)<sub>2</sub>Cl<sub>2</sub>] was synthesized by reaction of RuCl<sub>3</sub>.3H<sub>2</sub>O (22 mg, 0.106 mmol) and Clazpy (46 mg, 0.212 mmol). The solution was refluxed in 25 mL of *N,N*-dimethylformamide (DMF) for 40 min. The solution mixture was filtered and solvent was removed. The crude product was purified by column chromatography on a silica gel with toluene:CH<sub>3</sub>CN (9:1 by volume) as eluent. The blue was separated and the purple and the dark green bands were collected. The solvent was removed and a blue, purple and dark green solids were obtained. The yield was 32 mg (50%) for blue, 5 mg (8%) for purple, and 4 mg (7%) for dark green.

### 2.4.2 Isomer conversion, *trans* → *cis*

The isomer conversion was prepared by modified literature method (Misra *et al.*, 1998)

Isomer conversion was carried out thermally as detailed below. The green-[Ru(Clazpy)<sub>2</sub>Cl<sub>2</sub>] (15 mg, 0.025 mmol) was suspended in 10 mL of DMF and heated to reflux for 30 min (conversion was tested by TLC). The solution was evaporated to dryness on water bath. Then, it was dissolved in a minimal volume of CH<sub>2</sub>Cl<sub>2</sub> and subjected to chromatography as before. The blue band was eluted slowly using 9:1 by volume of toluene and CH<sub>3</sub>CN along with a purple and dark green bands. Three bands in color was evaporated to dryness. The yield was 11 mg (74%) for blue, 1 mg (7%) for purple and 1 mg (7%) for dark green.

### 2.4.3 Dichloro(5-chloro-(2-phenylazo)pyridine)(*N,N*-dimethyl)-(2-phenylazo)pyridine ruthenium(II), [Ru(Clazpy)(5dmazpy)Cl<sub>2</sub>]

There are two methods for synthesis a mixed-ligand, [Ru(Clazpy)(5dmazpy)Cl<sub>2</sub>] complex.

**Method I;** The [Ru(Clazpy)(5dmazpy)Cl<sub>2</sub>] complex was prepared by the similar procedure of [Ru(Clazpy)<sub>2</sub>Cl<sub>2</sub>] (method II). However, the reaction was refluxed for 3 h afforded an increasing amount of the complex [Ru(Clazpy)(5dmazpy)Cl<sub>2</sub>] and then evaporated to dryness. The product was purified by column chromatography on silica gel, using CH<sub>2</sub>Cl<sub>2</sub>:EtOAc as eluents. A small portion of blue and purple bands with a major dark green band was collected. The last band was evaporated to give dark green in high yield (40 mg, 61%). Recrystallization of this complex was done in CH<sub>2</sub>Cl<sub>2</sub> and toluene.

**Method II;** The 17 mg (0.026 mmol) of blue solid was dissolved in 3 mL of DMF. This solution was heated to reflux for 10 h. After filtered, the solvent was removed to dryness by water bath. The dark green residue was purified by column chromatography. Initially, a small amount of blue and purple compounds corresponding to  $[\text{Ru}(\text{Clazpy})_2\text{Cl}_2]$  was eluted slowly by  $\text{CH}_2\text{Cl}_2$  and EtOAc (9:1 by volume), a mainly dark green compound corresponding to  $[\text{Ru}(\text{Clazpy})(5\text{dmazpy})\text{Cl}_2]$  was separated later. Evaporation of solvent under reduced pressure yielded complex  $[\text{Ru}(\text{Clazpy})_2\text{Cl}_2]$  2 mg (12%) for blue, 1 mg (6%) for purple and 13 mg (76%) for dark green- $[\text{Ru}(\text{Clazpy})(5\text{dmazpy})\text{Cl}_2]$ .

#### 2.4.4 $[\text{Ru}(\text{Clazpy})_2(\text{bpy})](\text{PF}_6)_2$

The  $[\text{Ru}(\text{Clazpy})_2\text{Cl}_2]$  complex 25 mg (0.04 mmol),  $\text{AgNO}_3$  15 mg (0.08 mmol) and bpy 13 mg (0.08 mmol) were suspended in methanol 50 mL. The reaction mixture was heated to reflux for 12 h. The initial colored solution slowly changed to a dark-red at the end of reaction, which was verified by TLC on silica plates. The solvent was then removed using a rotary evaporator and the resulting red-brown product was dissolved by water and then the ligand excess was extracted by  $\text{CH}_2\text{Cl}_2$ . After reducing the solvent volume to 5 mL, the product was precipitated by adding 15 g (0.09 mmol) of ammonium hexafluorophosphate ( $\text{NH}_4\text{PF}_6$ ) to the filtrate with mixing of 5 mL ethanol, and the mixture was heated further for 1 h. After 2 days, the product was collected as dark-brown solid in 27 mg (68%). Recrystallization was done by the mixture of acetone and ethanol.

#### 2.4.5 $[\text{Ru}(\text{Clazpy})_2(\text{phen})](\text{PF}_6)$

The complex was synthesized in the same way as that had been described for  $[\text{Ru}(\text{Clazpy})_2(\text{bpy})](\text{PF}_6)_2$  complex with 1,10-phenatroline (phen) (15 mg, 0.08 mmol) in place of bpy. The yield was 36 mg (88%).

#### 2.4.6 [Ru(Clazpy)<sub>2</sub>(azpy)](PF<sub>6</sub>)

The synthesis was similar to that of [Ru(Clazpy)<sub>2</sub>(bpy)](PF<sub>6</sub>)<sub>2</sub> complex. Only bpy was replaced by an equivalent amount of 2-(phenylazo)pyridine (azpy) (16 mg, 0.08 mmol). The yield was 37 mg (88%).

#### 2.4.7 [Ru(Clazpy)<sub>3</sub>](PF<sub>6</sub>)

The synthesis was similar to that of [Ru(Clazpy)<sub>2</sub>(bpy)](PF<sub>6</sub>)<sub>2</sub> complex. Only bpy was replaced by an equivalent amount of 5-Chloro-2-(phenylazo)pyridine (Clazpy) (17 mg, 0.08 mmol). The yield was 29 mg (68%).

#### 2.4.8 [Ru(Clazpy)<sub>2</sub>(bpy)](NO<sub>3</sub>)<sub>2</sub>.5H<sub>2</sub>O

The starting complex [Ru(Clazpy)<sub>2</sub>Cl<sub>2</sub>] 25 mg (0.04 mmol), AgNO<sub>3</sub> 15 mg (0.091 mmol) and bpy 13 mg (0.082 mmol) was dissolved in 50 mL of methanol, and the mixture was heated under reflux for 12 h. The initially purple solution gradually changed to orangish-brown. After the completed reaction was monitored by TLC, the white solid of AgCl was filtered. The solvent was evaporated to dryness under reduced pressure and the solid mass obtained was purified by extraction process using H<sub>2</sub>O and CH<sub>2</sub>Cl<sub>2</sub> to get rid off the residue starting material. The desired product was evaporated and then dissolved in ethanol and the resulting solid was obtained by slow diffusion of hexane into the solvated ruthenium(II). The yield was 28 mg (77%).

#### 2.4.9 [Ru(Clazpy)<sub>2</sub>(phen)](NO<sub>3</sub>)<sub>2</sub>.3H<sub>2</sub>O

The synthesis was similar to that of [Ru(Clazpy)<sub>2</sub>(bpy)](NO<sub>3</sub>)<sub>2</sub>.5H<sub>2</sub>O complex. Only bpy was replaced by an equivalent amount of 1,10-phenatroline (phen) (15 mg, 0.08 mmol). The yield was 30 mg (84 %).

#### 2.4.10 [Ru(Clazpy)<sub>2</sub>(azpy)](NO<sub>3</sub>).H<sub>2</sub>O

The synthesis was similar to that of [Ru(Clazpy)<sub>2</sub>(bpy)](NO<sub>3</sub>)<sub>2</sub>.5H<sub>2</sub>O complex. Only bpy was replaced by an equivalent amount of 2-(phenylazo)pyridine (azpy) (16 mg, 0.08 mmol). The yield was 27 g (77%).

#### 2.4.11 [Ru(Clazpy)<sub>3</sub>](NO<sub>3</sub>).3H<sub>2</sub>O

The synthesis was similar to that of [Ru(Clazpy)<sub>2</sub>bpy](NO<sub>3</sub>)<sub>2</sub>.5H<sub>2</sub>O complex. Only bpy was replaced by an equivalent amount of 5-Chloro-2-(phenyl azo)pyridine (Clazpy) (17 mg, 0.08 mmol). The yield was 31 g (80%).

#### 2.4.12 Ru(Clazpy)<sub>2</sub>(bpy)]Cl<sub>2</sub>.7H<sub>2</sub>O

The chloride salts of [Ru(Clazpy)<sub>2</sub>bpy]Cl<sub>2</sub>.7H<sub>2</sub>O was prepared by dissolving [Ru(Clazpy)<sub>2</sub>bpy](PF<sub>6</sub>)<sub>2</sub> 50 mg (0.051 mmol) in a small amount of acetone and added a saturated solution of tetra-*n*-butylammonium chloride hydrate (TBACl) in acetone until the precipitation was completed. The obtained chloride salts thus were filtered, washed thoroughly with acetone, ether and vacuum dried. The yield was 37 mg (82% ).

#### 2.4.13 [Ru(Clazpy)<sub>2</sub>(phen)]Cl<sub>2</sub>.8H<sub>2</sub>O

The preparation was similar to that of [Ru(Clazpy)<sub>2</sub>(bpy)]Cl<sub>2</sub>.7H<sub>2</sub>O complex using the [Ru(Clazpy)<sub>2</sub>(phen)](PF<sub>6</sub>)<sub>2</sub> 50 mg (0.049 mmol). The yield was 18 mg (40%).

#### 2.4.14 [Ru(Clazpy)<sub>2</sub>(azpy)]Cl<sub>2</sub>.H<sub>2</sub>O

The preparing was similar to that of [Ru(Clazpy)<sub>2</sub>(bpy)]Cl<sub>2</sub>.7H<sub>2</sub>O complex using the [Ru(Clazpy)<sub>2</sub>(azpy)](PF<sub>6</sub>)<sub>2</sub> 59 mg (0.058 mmol). The yield was 37 mg (74%).

#### 2.4.15 [Ru(Clazpy)<sub>3</sub>]Cl<sub>2</sub>·3H<sub>2</sub>O

The preparing was similar to that of [Ru(Clazpy)<sub>2</sub>(bpy)]Cl<sub>2</sub>·7H<sub>2</sub>O complex using the [Ru(Clazpy)<sub>3</sub>](PF<sub>6</sub>)<sub>2</sub> 60 mg (0.058 mmol). The yield was 47 mg (92%).

#### 2.4.16 *cis*-[Ru(bpy)<sub>2</sub>Cl<sub>2</sub>]

The *cis*-[Ru(bpy)<sub>2</sub>Cl<sub>2</sub>] complex was prepared by the published method (Sullivan *et al.*, 1978) with a modified purification procedure (Ji *et al.*, 2000).

The 273 mg (1.32 mmol) of RuCl<sub>3</sub>·3H<sub>2</sub>O, 409 mg (2.6 mmol) of 2,2'-bipyridine (bpy), and 559 mg (1.32 mmol) of LiCl were heated by refluxing in 15 mL of DMF for 6 h. The reaction was stirred magnetically throughout this period. The reaction mixture was cooled to room temperature and 80 mL of acetone was added. Black crystals were obtained by filtration and washed several times of water and ether, respectively. The yield was 315 mg (50%).

#### 2.4.17 *cis*-[Ru(phen)<sub>2</sub>Cl<sub>2</sub>]

The *cis*-[Ru(phen)<sub>2</sub>Cl<sub>2</sub>] complex was prepared by using literature method (Sullivan *et al.*, 1978) with the modified purification procedure (Ji *et al.*, 2000).

The 250 mg (1.2 mmol) of RuCl<sub>3</sub>·3H<sub>2</sub>O, 495 mg (2.5 mmol) of 1,10-phenanthroline(phen), and 495 mg (12 mmol) of LiCl were heated by refluxing in 15 mL of DMF for 8 h. The reaction was stirred magnetically throughout this period. After reaction mixture was cooled to room temperature, 50 mL of acetone was added. The dark solution was filtered and the dark solid was washed several time with water and 20 mL of ether, respectively. The yield was 263 mg (41%).

#### 2.4.18 [Ru(bpy)<sub>2</sub>(Clazpy)](PF<sub>6</sub>)<sub>2</sub>

A mixture of *cis*-[Ru(bpy)<sub>2</sub>Cl<sub>2</sub>] 50 g (0.094 mmol) and AgNO<sub>3</sub> 38 g (0.22 mmol) in 50 mL methanol was heated with constant stirring for 2 h. The precipitate AgCl was removed by using a sintered-glass funnel resulting in a clear solution containing [Ru(bpy)<sub>2</sub>MeOH](NO<sub>3</sub>)<sub>2</sub>. The Clazpy 27 g (0.12 mmol) was added to the filtrate and the mixture was heated under reflux for 3 h. The completed reaction was monitored by TLC by changing color from red-violet to brownish-red. The solvent was then removed to dryness under reduced pressure. The resulting red-brown mass was dissolved in water and impurity was extracted by CH<sub>2</sub>Cl<sub>2</sub>. After reducing the volume of the solution about 5 mL, 32 mg (0.19 mmol) of ammonium hexafluorophosphate was added. A dark precipitate was obtained. The desired product was collected as dark-brown solid with 75 mg (79%) after 2 days and ready for recrystallization by the mixture of acetone and methanol.

#### 2.4.19 [Ru(phen)<sub>2</sub>(Clazpy)](PF<sub>6</sub>)<sub>2</sub>

The synthesis was similar to that of [Ru(bpy)<sub>2</sub>(Clazpy)](PF<sub>6</sub>)<sub>2</sub> complex. Only *cis*-[Ru(bpy)<sub>2</sub>Cl<sub>2</sub>] was replaced by an equivalent amount of *cis*-[Ru(phen)<sub>2</sub>Cl<sub>2</sub>]. The yield was 76 mg (84%).

#### 2.4.20 [Ru(bpy)<sub>2</sub>(Clazpy)]Cl<sub>2</sub>·7H<sub>2</sub>O

The hexafluorophosphate salt obtained above [Ru(bpy)<sub>2</sub>(Clazpy)](PF<sub>6</sub>)<sub>2</sub> was dissolved in a minimum amount of acetone, and a saturated solution of tetra-*n*-butylammonium chloride hydrate (TBACl) in acetone was added dropwise until precipitation was completed. The water-soluble chloride salt was filtered off, washed thoroughly with acetone, ether and vacuum dried. Recovery was about 90% of the theoretical yield.

#### 2.4.21 [Ru(phen)<sub>2</sub>(Clazpy)]Cl<sub>2</sub>.8H<sub>2</sub>O

The chloride salt of [Ru(phen)<sub>2</sub>(Clazpy)]Cl<sub>2</sub>.7H<sub>2</sub>O 70 mg (0.072 mmol) was prepared by dissolving [Ru(phen)<sub>2</sub>Clazpy](PF<sub>6</sub>)<sub>2</sub> in a small amount of acetone and adding a saturated solution of tetra-*n*-butylammonium chloride hydrate (TBACl) in acetone until the precipitation was completed. The solid was then washed with acetone, ether and vacuum dried. The yield was 55 mg (86%).

### 2.5 Techniques for structural determination

#### 2.5.1 Elemental analysis

Elemental analysis is a principle which is important method for studying composition of element in compound such as C, H and N.

#### 2.5.2 Mass spectrometry

Fast-atom bombardment (FAB) mass spectrometry is a basic technique used to determine molecular mass of compound or to establish characterization of individual compound. This method is very efficient for producing ions from polar compounds with high molecular weights. An essential feature of FAB is that the sample must be dissolved in a non-volatile liquid matrix.

Electrospray mass spectrometry (ES-MS) is a powerful, but still relative new technique for the characterization of inorganic or organometallic compounds, which may be thermally unstable and involatile compounds (Jiang, 2004) like nitrate complexes and chloride complexes. The ES-MS mass spectra normally correspond to a statistical distribution of consecutive peaks characteristic of multiply charged molecular ions obtained through protonation  $(M+zH)^{z+}$  which avoiding the contributions from dissociations or from fragmentations. Indeed, the technical characteristic of mass spectrometers is such that the value being measured is not the mass, but rather the mass to charge ratio (Hoffmann *et al.*, 1996).

### 2.5.3 Infrared spectroscopy

Infrared (IR) spectroscopy is one of the most common spectroscopic techniques used by organic and inorganic chemists. The main goal of IR spectroscopic analysis is to determine the chemical functional groups and involved some data in the sample. Different functional groups absorb characteristic frequencies of IR radiation. Using various sampling accessories, IR spectrometers can accept a wide range of sample types such as gases, liquids, and solids. Thus, IR spectroscopy is an important and popular tool for structural elucidation and compound identification. The IR region is commonly divided into three smaller area: near IR, mid IR and far IR.

	near IR	mid IR	far IR
wave number (cm <sup>-1</sup> )	13,000-4,000	4,000-200	200-10

This work focus on the most frequently used mid IR region, between 4,000-400 cm<sup>-1</sup> (Settle, F. 1997).

### 2.5.4 UV-Visible absorption spectroscopy

UV-Visible absorption spectroscopy is the technique to characterize complexes roughly but it is useful for describing colored. The chromophoric group or  $\pi$ -conjugated system in compounds give rise the absorption in ultra-violet region (200-800 nm). The colors of transition metal compounds are usually attributed to electronic transition involved d orbitals. These transitions are of two main types that are d-d transition which gives pale colors and charge transfer transition which gives intense colors.

### 2.5.5 Nuclear magnetic resonances spectroscopy

Nuclear magnetic resonance spectroscopy is an important technique for determining molecular structure or stereochemistry of compounds. 1D and 2D were suitable to investigate a large molecule which has complicated structure i.e. COSY, HMQC, ROESY. The  $\text{CDCl}_3$ ,  $\text{CD}_3\text{OCD}_3$  and  $\text{CD}_3\text{OD}$  were used as solvent to dissolve tested compounds and tetramethylsilane as an internal standard. The chemical shift ( $\delta$ ) and coupling constant ( $J$ ) values are given in parts per million and hertz, respectively.

### 2.5.6 Cyclic voltammetry

The cyclic voltammetry is an electrochemical method which leads to the knowledge of redox phenomena. It shows current-potential curve, which is called cyclic voltammogram. This voltammogram displayed metal oxidations on the positive side and ligand reductions at the negative side with corresponding half-wave potentials. The one-electron stoichiometry of the couple is established by comparing the current height of the main couple with that of the standard ferrocene-ferricenium couple under identical experimental conditions. The  $i_{\text{pa}} / i_{\text{pc}}$  ratio ( $i_{\text{pa}}$  = anodic peak current and  $i_{\text{pc}}$  = cathodic peak current) is closed to 1.0, as expected for reversible couples. In general, a typical voltammetric experiment utilizes three types of electrodes;

- (i) reference electrode: commonly used are aqueous Ag/AgCl or calomel half cells which can be obtained commercially or easily prepared in the laboratory. Sometimes when a suitable conventional reference electrode is not available (e.g. for some organic solvents) or introduce problems with salt leakage or junction potentials, pseudo-reference electrodes such as a sample silver or platinum wire are used in conjunction with an internal potential reference such as ferrocene. Experimentally, ferrocene is added into the cell at the end of a series of measurements, and the reversible voltammetric response for the  $\text{Fc}^{+/0}$  couple is taken as reference point on the potential scale ( $E_{1/2} = 0.0 \text{ V}$ )

- (ii) counter electrode (auxiliary): is used in the three-electrode system only. In this system, the current flows between the working and the counter electrode. Either a piece of platinum foil or a platinum wire is usually employed as a counter electrode. It is recommended that the area of the counter electrode is substantially largely than that of the working electrode. If this condition is met the counter electrode should not affect the current measurement due to, e.g., passivation, deactivation and blocking (Stojek, Z. 2002).
- (iii) working electrode is the electrode at which the investigated process occurs. Usually, in the range of positive potentials, platinum, gold, carbon (graphite, glassy carbon) electrode are used. The surface of these materials is partially oxidized in aqueous solution at this potential range. In the negative range of potential, in aqueous solution and other protic solvents, mercury electrodes are superior due to high over potential of the reduction of hydrogen. On the other hand, many organic compounds strongly adsorb on mercury which may complicate the analysis of voltammograms. In aprotic solvent, Pt, Au and C electrode can be used in both positive and negative ranges of potential (Stojek, Z., 2002). Therefore, in this work glassy carbon was used to study

### 2.5.7 X-ray structure determination

The molecular structure of isomeric  $\gamma$ -,  $\alpha$ -,  $\beta$ -[Ru(Clazpy)<sub>2</sub>Cl<sub>2</sub>], [Ru(Clazpy)(5dmazpy)Cl<sub>2</sub>], [Ru(Clazpy)<sub>2</sub>phen](PF<sub>6</sub>)<sub>2</sub>, [Ru(Clazpy)<sub>2</sub>azpy](PF<sub>6</sub>)<sub>2</sub> and [Ru(Clazpy)<sub>2</sub>phen](NO<sub>3</sub>)<sub>2</sub>·3.5H<sub>2</sub>O were determined. This technique is importance which provides highly accurate stereochemical information including absolute configurations. In this work, the CCD is used as detector. The SHELXTL NT (version 6.12), SHELXTL-97 programs and the Xtal program are used to study the crystal structures.

## 2.6 DNA-binding experiments

### 2.6.1 Preparation of DNA sample

The DNA-binding of water-soluble complexes was investigated. The stock solution was made by dissolving CT-DNA in appropriate buffers which prepared in Ultra-pure Milli Q water (18.2 mΩ) and kept overnight at 4°C to ensure complete dissociation as well as use within 4 days after their preparation. The concentration of DNA (nucleotide phosphate) was measured by using its known extinction coefficient at 260 nm ( $6600 \text{ M}^{-1} \text{ cm}^{-1}$ ) (Murali *et al.*, 2002).

### 2.6.2 Absorption titration experiments

The absorption titration with DNA was carried out as follow: A solution of metal complex  $40 \mu\text{M}$  in aqueous 50 mM NaCl/5 mM Tris base buffer at pH 7.1 was placed in the sample cell of the spectrophotometer (Selvi *et al.*, 2005). The spectrum of free complex was obtained. Then an aliquot of DNA solution (DNA concentration  $4 \times 10^{-4}$  -  $1 \times 10^{-2}$  M) was added to the sample. After the addition of DNA to metal complex, the solution was agitated and allowed to equilibrate for 15 min, the spectrum was then recorded by S100 specord. This process was repeated until no changes were observed in the spectrum. The data were then fitted to the following equation to obtain the intrinsic binding constant,  $K_b$ .

$$[\text{DNA}]/(\varepsilon_a - \varepsilon_f) = [\text{DNA}]/(\varepsilon_b - \varepsilon_f) + 1/K_b(\varepsilon_b - \varepsilon_f)$$

where  $\varepsilon_a$ ,  $\varepsilon_f$  and  $\varepsilon_b$  are the apparent, free and bound metal complex extinction coefficients respectively. In plot of  $[\text{DNA}]/(\varepsilon_a - \varepsilon_f)$  vs  $[\text{DNA}]$  gave a slope of  $1/(\varepsilon_b - \varepsilon_f)$  and a y intercept;  $K_b$  is the ratio of slope to y intercept (Murali *et al.*, 2002). From these spectra the red shift and percentage of hypochromicity upon binding to DNA were determined. Each measured point was the average value of at least three spectra

measurements with the relative standard deviation (RSD) of less than 15% (Mudasir *et al.*, 2003).

### 2.6.3 Viscosity measurements

Viscosity measurements were carried out using simple technique in buffer pH 7.2 and the temperature was controlled at  $29\pm 0.5$  °C in prior to experiments. CT-DNA samples were prepared by sonicating in order to minimize complexities arising from DNA flexibility. Flow time was measured with a digital stop watch, at least three times and were accepted if successive values within 0.1 s. Flow time was calculated. Data were presented as  $(\eta/\eta_0)^{1/3}$  versus binding ratio ( $r$ ) = [DNA]/[complex], where  $\eta$  is the viscosity of CT-DNA in the presence of complex and  $\eta_0$  is the viscosity of CT-DNA alone. Viscosity values is calculated as  $\eta = t - t_0$  where  $t$  is the time for the sample to flow through the viscometer and  $t_0$  is the time measured for the buffer only (Luedtke *et al.*, 2003).

### 2.6.4 Fluorescence quenching experiments

The DNA-binding properties of complexes were studied by fluorescence spectral method using ethidium bromide (EB) bound CT-DNA solution in Tris base/NaCl buffer (pH 7.1). EB was non-emissive in Tris-buffer medium due to fluorescence quenching by the solvent molecules (Patra *et al.*, 2006). In the presence of CT-DNA, EB showed enhancing emission intensity due to its intercalative binding to DNA. A competitive binding of ruthenium complexes to CT-DNA resulted in the displacement of bound EB and/or quenching of the fluorescence of EB and as a consequence the emission intensity of EB decreased. In the typical experiment, a 40  $\mu$ M of CT-DNA solution was added to a 2  $\mu$ M of EB buffer solution pH 7.1 (5 mM Tris-base/ 50 mM NaCl) and the fluorescence intensity was measured using excitation wavelength of 340 nm resulting an emission at 600 nm at room temperature. Aliquots of a 10  $\mu$ M ruthenium(II) complex solutions were then added to the DNA-EB solution and the fluorescence was measured after incubating 5 minute. Each samples were

excited at 340 nm and the emission spectra were recorded between 500-700 nm. (Wang *et al.*, 2004; Chao *et al.*, 2002; Mei *et al.*, 2003; Vaidyanathan *et al.*, 2003).

### **2.6.5 Electrochemical studies**

The electrochemical properties of ruthenium(II) complexes in the presence of DNA were investigated using cyclic voltammetry using Echem1.5.1 program. A three electrode, a glassy carbon working electrode, a platinum wire reference electrode and a platinum disc auxiliary electrode was used. The voltammetric experiments were carried out using a solvent of 5 mM Tris-base/ 50 mM NaCl buffer (pH 7.2). The experiments were performed in 0.50 mM complex solutions in the absence and presence of CT-DNA. After solutions were deoxygenated by purging with Argon gas for 30 min prior in each measurement, different scan rates were recorded. During measurements Argon gas was passed over the solution.

### **2.6.6 Cytotoxicity**

The cytotoxic activity of synthesized compounds were tested by National Center of Genetic Engineering and Biotechnology (BIOTECH). Three cancer cell lines i.e. small cell lung cancer (Anti-NCl-H187), breast cancer (BC), oral epidermal carcinoma (KB) were used. The results were recorded as IC<sub>50</sub> values (IC<sub>50</sub> is a concentration of drug that is required 50% reduction of cellular growth).

## CHAPTER 3

### RESULTS AND DISCUSSION

The preparation of ruthenium(II) complexes with azoimine and imine ligands was investigated and characterization of synthesized compound was studied by using a basic techniques such as Elemental analysis, mass spectrometry and spectroscopic techniques. The molecular structures of compounds were measured by using X-ray diffraction analysis. In addition, the electrochemical behavior was studied electron transfer properties. To further study the interaction between complexes with CT-DNA by mean of DNA-binding experiments, water-soluble ruthenium(II) complexes were chosen. The results are reported in this chapter and could be separated into nine sections as following:

- 3.1 syntheses and characterization of ligands
- 3.2 syntheses and characterization of the isomeric  $[\text{Ru}(\text{Clazpy})_2\text{Cl}_2]$  complexes
- 3.3 synthesis and characterization of  $[\text{Ru}(\text{Clazpy})(5\text{dmazpy})\text{Cl}_2]$  complex
- 3.4 syntheses and characterization of  $[\text{Ru}(\text{Clazpy})_2\text{L}](\text{PF}_6)_2$  (L = bpy, phen, azpy, Clazpy)
- 3.5 syntheses and characterization of  $[\text{Ru}(\text{Clazpy})_2\text{L}](\text{NO}_3)_2 \cdot x\text{H}_2\text{O}$  (L = bpy, phen, azpy, Clazpy)
- 3.6 syntheses and characterization of  $[\text{Ru}(\text{Clazpy})_2\text{L}]\text{Cl}_2 \cdot x\text{H}_2\text{O}$  (L = bpy, phen, azpy, Clazpy)
- 3.7 syntheses and characterization of  $[\text{Ru}(\text{bpy})_2\text{Clazpy}](\text{X})_2$  (X =  $\text{PF}_6^-$ ,  $\text{Cl}^-$ )
- 3.8 DNA-binding experiments
  - 3.8.1 Absorption spectroscopic studies
  - 3.8.2 Viscosity measurements
  - 3.8.3 Fluorescence quenching studies
  - 3.8.4 Electrochemical studies
- 3.9 Cytotoxicity test

### 3.1 Syntheses and characterization of ligands

#### 3.1.1 Syntheses of ligands

In the present work, there are two ligands to be synthesized, 2-(phenylazo)pyridine (azpy) and 5-Chloro-(2-phenylazo)pyridine (Clazpy). These ligands were prepared by the similar method to that described previously (Krause and Krause, 1980).

A coupling reaction of 2-aminopyridine or 2-amino-5-chloropyridine with nitrosobenzene in 1:1 molar ratio in basic solution produced the azpy and Clazpy, respectively. Both compounds isolated from the reaction mixture by column chromatographic technique described in Chapter 2. An outline of the synthesis of ligands is presented in Figure 3.1.

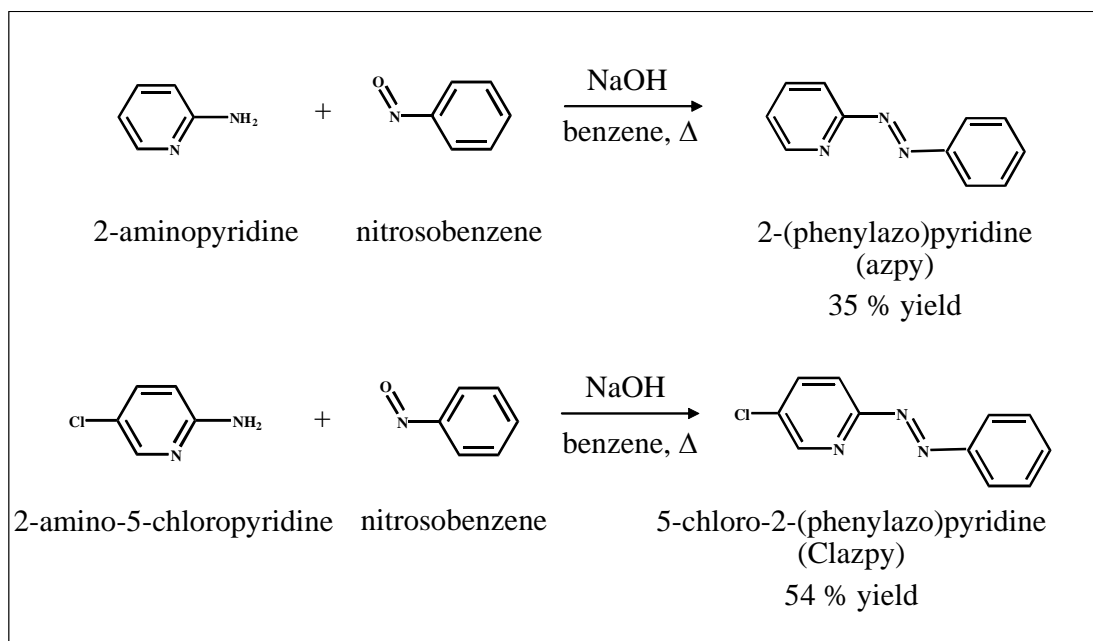


**Figure 3.1** Synthetic routes for the preparation of the azpy and the Clazpy ligands

Clazpy is unsymmetric bidentate ligand having azoimine functional moiety,  $-N=N-C=N-$ . Its structure is similar to azpy which is a good  $\pi$ -acceptor ligand (Krause and Krause, 1980) but the hydrogen at the fifth position on pyridine ring is

replaced by a high electronegative chlorine atom. It used nitrogen atoms from pyridine and from azo donate electron to metal center. This is an evidence to support a  $\pi$ -accepting ability of Clazpy like azpy to stabilize a lower oxidation state of metal center. The atom numbering scheme of Clazpy is shown in Figure 3.2.

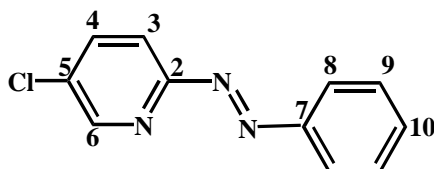


**Figure 3.2** The structure of the Clazpy ligand

The physical properties of azpy and Clazpy ligands are shown in Table 3.1.

**Table 3.1** The physical properties of azpy and the Clazpy ligands

Ligands	Physical properties		
	Appearance	Color	Melting point ( $^{\circ}\text{C}$ )
azpy	liquid	orange	32-34 <sup>a</sup>
Clazpy	solid	orange	98-99

<sup>a</sup>Results from Krause and Kruse (1980)

From Table 3.1, the melting point of both compounds indicated that the azpy ligand was a liquid state, whereas the Clazpy ligand was a solid state at room temperature. The solubility of 0.010 g of Clazpy was tested in 5 mL of hexane, benzene, toluene, chloroform ( $\text{CHCl}_3$ ), dichloromethane ( $\text{CH}_2\text{Cl}_2$ ), ethyl acetate (EtOAc), acetone ( $\text{CH}_3\text{OCH}_3$ ), *N,N*-dimethylformamide (DMF), *N,N*-dimethyl sulfoxide (DMSO), acetonitrile ( $\text{CH}_3\text{CN}$ ), ethanol (EtOH), methanol (MeOH) and water. The ligand was very soluble in most of solvents, but insoluble in water.

### 3.1.2 Characterization of ligand

The chemistry of Clazpy was characterized by following these techniques:

- 3.1.2.1 Elemental analysis
- 3.1.2.2 Fast-atom bombardment mass spectrometry
- 3.1.2.3 Infrared spectroscopy
- 3.1.2.4 UV-Visible absorption spectroscopy
- 3.1.2.5 Nuclear Magnetic Resonance spectroscopy (1D and 2D)
- 3.1.2.6 Cyclic voltammetry

#### 3.1.2.1 Elemental analysis

Elemental analysis is an important principle method to study composition of elements in the ligand. From Table 3.2, the analytical values corresponded to the calculated values. Therefore, the composition of the Clazpy ligand was confirmed by this method

**Table 3.2** Elemental analysis data of the Clazpy ligand

Ligand	% C		% H		% N	
	Calc.	Found	Calc.	Found	Calc.	Found
Clazpy	60.70	60.06	3.70	3.49	19.30	19.31

#### 3.1.2.2 Fast-atom bombardment mass spectrometry

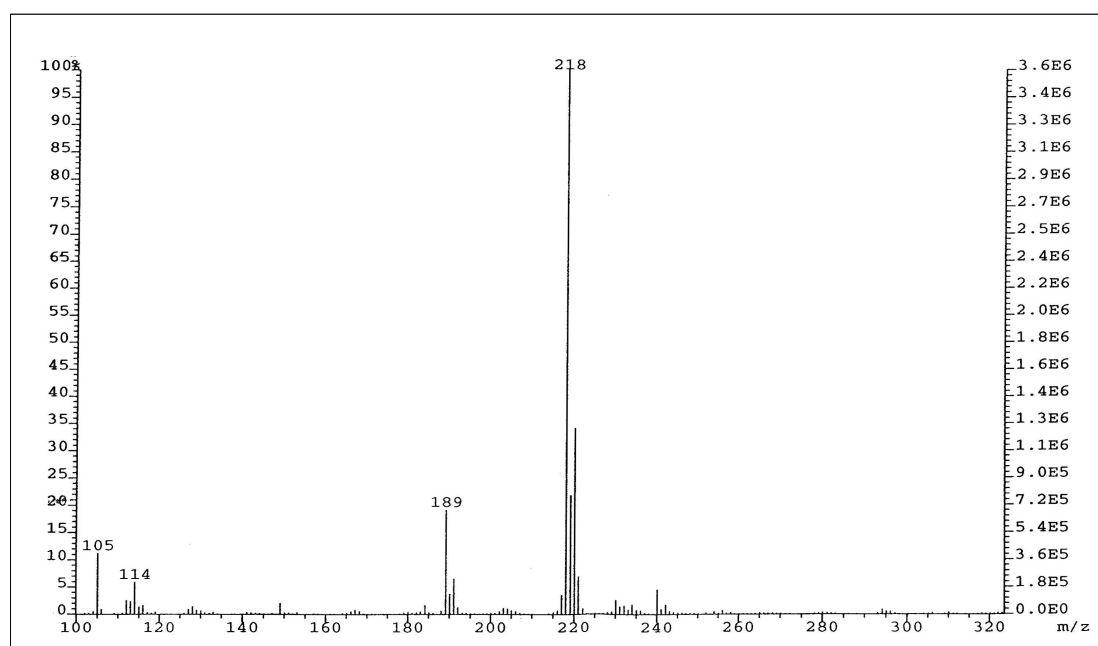
The Fast-atom bombardment (FAB) mass spectrometry is a basic technique to determine molecular mass of compound. The important FAB mass spectroscopic data of Clazpy with corresponding relative abundance is listed in Table 3.3 and the FAB mass spectrum of the Clazpy ligand is shown in Figure 3.3.

**Table 3.3** FAB mass spectrometric data of the Clazpy ligand

m/z	Stoichiometry	Equivalent species	Rel. Abun. (%)
218	[Clazpy + H] <sup>+</sup>	[M + H] <sup>+</sup>	100

M = Molecular weight of Clazpy = 217.66 g/mol

The maximum peak in an isotropic mass distribution which gave 100% relative abundance at m/z 218 is very closed to the molecular weight of Clazpy with one protonation. Thus, the measured molecular weight was consistent with expected value.

**Figure 3.3** FAB mass spectrum of the Clazpy ligand

### 3.1.2.3 Infrared spectroscopy

Infrared spectroscopy is an useful technique to identify the functional group in compound. The IR spectrum of Clazpy ligand was recorded in the range 4000-400  $\text{cm}^{-1}$  using KBr pellets and shown in Figure 3.4. The selected spectral data are collected in Table 3.4.

**Table 3.4** IR data of the Clazpy ligand

Vibrational frequencies	Wave numbers ( $\text{cm}^{-1}$ )
C=N, C=C stretching	1565(m), 1441(s)
N=N stretching	1364(s)
C-H out of plane bending in monosubstituted benzene	776(s) 685(s) 638(m)
C-Cl stretching	547(s)

s = strong, m = medium

The characteristic peaks for determining structures of Clazpy ligand were observed. There are several stretching modes in different intensities below 1800  $\text{cm}^{-1}$  such as C=C, C=N stretching modes, C-H bending modes of monosubstituted benzene and C-Cl stretching mode belonged to pyridine and phenyl rings. Those modes showed strong to medium absorption at the frequencies similar to azpy which appeared at 1584, 1578, 1498 and 1495  $\text{cm}^{-1}$  for C=C, C=N (Krause and Krause, 1980).

The free Clazpy shows the N=N stretching vibration at 1364  $\text{cm}^{-1}$ , meanwhile the N=N stretching mode of the free azpy ligand appeared at 1420  $\text{cm}^{-1}$  (Krause and Krause, 1980). The results indicated that the electron delocalized into the  $\pi^*$  orbital of the azo function in Clazpy is greater than that in azpy. It is due to the effect of substituted chlorine at the fifth position on pyridine ring which decreases the

electron density on benzene ring. Thus, stabilization of the ring is occurred from resonances of electron from N=N functional group.

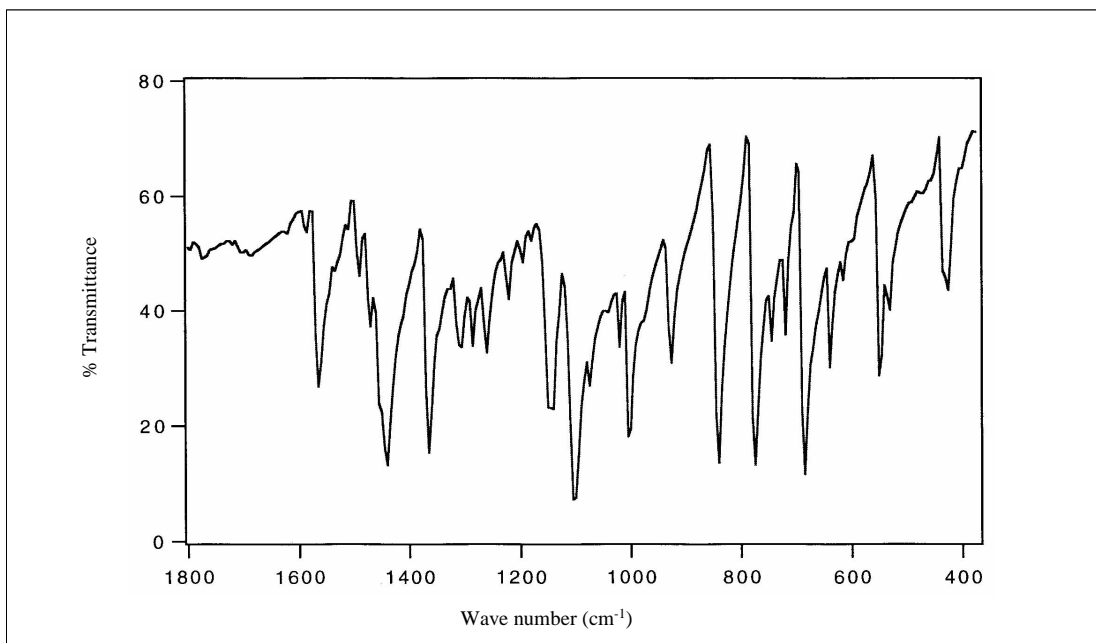


**Figure 3.4** IR spectrum of the Clazpy ligand

#### 3.1.2.4 UV-Visible absorption spectroscopy

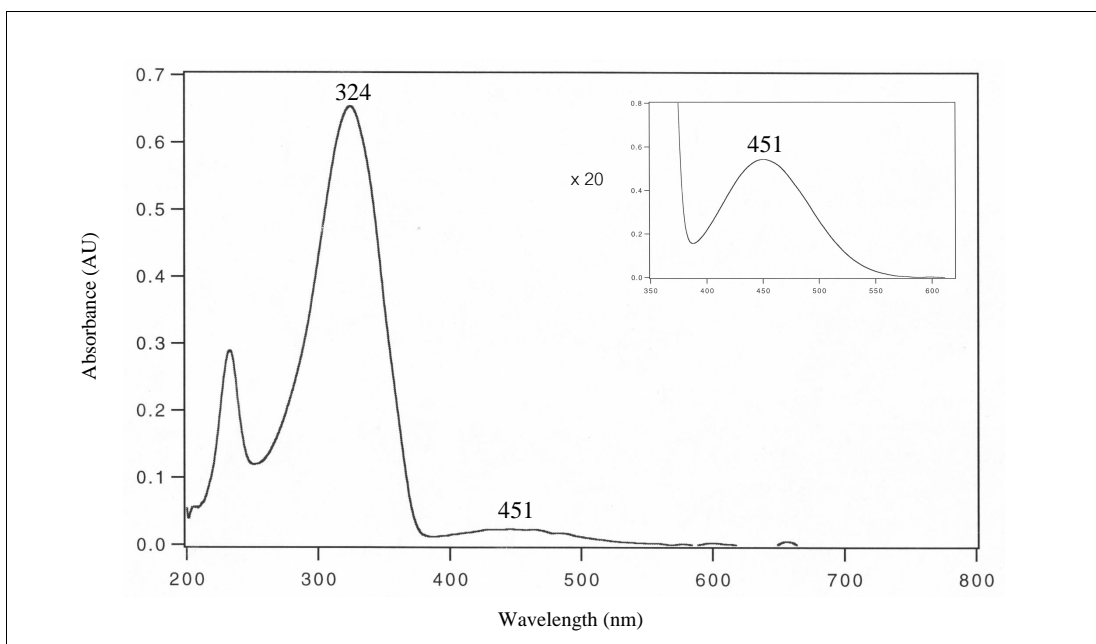
UV-Visible absorption spectroscopy is a technique used to study electronic transitions of compounds having chromophore and  $\pi$ -conjugated system. The electronic absorption spectra were measured in the range 200-800 nm in various solvents: hexane,  $\text{CHCl}_3$ ,  $\text{CH}_2\text{Cl}_2$ , EtOAc,  $\text{CH}_3\text{OCH}_3$ , DMF, DMSO,  $\text{CH}_3\text{CN}$ , EtOH and MeOH solvents. In addition, the absorption spectrum of Clazpy in  $\text{CH}_2\text{Cl}_2$  is shown in Figure 3.5. The summarized data are listed in Table 3.5.

**Table 3.5** UV-Visible absorption spectroscopic data of the Clazpy ligand

Solvent	$\lambda_{\max}$ , nm ( $\epsilon^a \times 10^{-4} \text{ M}^{-1} \text{ cm}^{-1}$ )
Hexane	319 (2.4), 454 (0.1)
$\text{CHCl}_3$	327 (2.8), 449 (0.1)
$\text{CH}_2\text{Cl}_2$	324 (2.3), 451 (0.1)
EtOAc	321 (2.2), 452 (0.1)
$\text{CH}_3\text{OCH}_3$	332 (1.7), 450 (0.1)
DMF	324 (1.6), 449 (0.1)
DMSO	327 (2.0), 449 (0.1)
$\text{CH}_3\text{CN}$	230 (0.8), 320 (2.1), 446 (0.1)
EtOH	226 (1.3), 325 (2.5), 449 (0.1)
MeOH	224 (1.1), 324 (2.2), 446 (0.1)

<sup>a</sup> Molar extinction coefficient

The absorption spectra of the Clazpy ligand displayed two intense bands in the range 220-460 nm except  $\text{CH}_3\text{CN}$ , EtOH and MeOH showed three bands correspond to cut off solvent ranges. They are assigned to  $\pi \rightarrow \pi^*$  with high molar extinction coefficient ( $\epsilon \sim 28000 - 8500 \text{ M}^{-1} \text{ cm}^{-1}$ ) in UV region and  $n \rightarrow \pi^*$  transitions with lower molar extinction coefficient ( $\epsilon \sim 6000 - 4000 \text{ M}^{-1} \text{ cm}^{-1}$ ) in visible region.

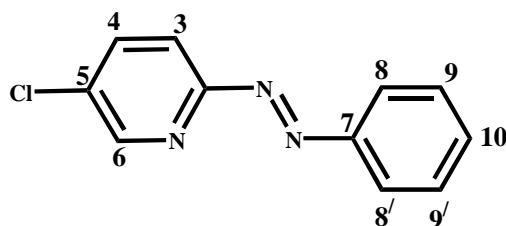


**Figure 3.5** UV-Visible absorption spectrum of the Clazpy ligand in  $\text{CHCl}_2$

### 3.1.2.5 Nuclear Magnetic Resonance spectroscopy (1D and 2D)

Nuclear Magnetic resonance spectroscopy is an important technique for determination molecular structure of compound. The NMR spectra of Clazpy was recorded in  $\text{CDCl}_3$  and the tetramethylsilane was used as an internal reference. The structure of Clazpy was determined by using 1D and 2D NMR spectroscopic techniques;  $^1\text{H}$  NMR,  $^{13}\text{C}$  NMR,  $^1\text{H}$ - $^1\text{H}$  COSY NMR, DEPT NMR,  $^1\text{H}$ - $^{13}\text{C}$  HMQC NMR. The chemical shift and  $J$ -coupling constant data of Clazpy are listed in Table 3.6 and NMR spectra are shown in Figure 3.6 to Figure 3.10.

## Nuclear Magnetic Resonance spectroscopy of the Clazpy ligand

**Table 3.6**  $^1\text{H}$ - $^{13}\text{C}$  NMR spectroscopic data of the Clazpy ligand

positions	$^1\text{H}$ NMR			$^{13}\text{C}$ NMR (CH-type)
	$\delta$ (ppm)	$J$ (Hz)	number of H	
6	8.69 (dd)	2.5, 0.5	1	148.33
8, 8'	8.04 (m)	-	2	123.63
4	7.87 (dd)	8.5, 2.5	1	138.00
3	7.81 (dd)	8.5, 0.5	1	115.86
9, 9'	7.54 (m)	-	3	132.43 (C9)
10				129.18 (C10)
Quaternary carbon (C)				160.96 (C2)
				152.21 (C5)
				133.57 (C7)

d = doublet, dd = doublet of doublet, tt = triplet of triplet

The  $^1\text{H}$  NMR spectrum of Clazpy (Figure 3.6) displayed 5 resonance signals for 8 protons which belonged to pyridine and phenyl rings. The detail of each signal could be explained below.

The proton 3 resonance appeared at 7.81 ppm as doublet of doublet (dd) due to the coupling with proton H4 ( $J = 8.5$  Hz) and long range coupling with proton H6 ( $J = 0.5$  Hz).

The proton 4 resonance appeared at 7.87 ppm as doublet of doublet (dd) due to the coupling with proton H3 ( $J = 8.5$  Hz) and long range coupling with proton H6 ( $J = 2.5$  Hz).

The proton 6 resonance appeared at 8.69 ppm as doublet of doublet (dd) due to the coupling with proton H4 ( $J = 2.5$  Hz) and proton H3 ( $J = 0.5$  Hz). The effect of chlorine and nitrogen atom on pyridine ring to proton H6 was to decrease electron density. So, this proton appeared at the most downfield.

The proton 8, 8' positions was equivalent. They gave multiple (m) peak at 8.04 ppm because the located next to the azo nitrogen.

The proton 9, 9' were equivalent which located next to proton 8. The resonance showed multiplet (m) peak at 7.54 ppm.

The proton 10 was located next to proton 9. The splitting pattern was multiplet (m) at the same position of proton 9 (7.54 ppm).

Moreover, the peak assignments were confirmed by using  $^1\text{H}$ - $^1\text{H}$  COSY NMR spectrum (Figure 3.7). They showed the correlation of  $^1\text{H}$ - $^1\text{H}$  coupling.

The results from  $^{13}\text{C}$  NMR spectrum (Figure 3.8) corresponded to the result of DEPT NMR spectrum (Figure 3.9), which showed only methane carbon signals. The  $^{13}\text{C}$  NMR spectrum of Clazpy ligand showed 9 signals for 11 carbons. The signal of quaternary carbon C2 which located between nitrogen of azo functional group and nitrogen of pyridine ring appeared at the most downfield (160.96 ppm). The signals at 152.21 and 133.57 ppm belonged to quaternary carbon C5 bonded directly to chlorine atom on pyridine ring and C7 which located near only nitrogen azo, respectively. The carbon C6, C4, C3 signals on pyridine ring occurred at 148.33 ppm, 138.00, 115.86, respectively. The carbon C10 signal on phenyl ring occurred at 129.18 ppm. The signal at 123.63 and 132.43 ppm were assigned to two equivalent carbon of carbon C8 and C9, respectively.

Moreover, the  $^{13}\text{C}$  assignments were supported by the HMQC NMR spectrum (Figure 3.10), which showed the correlation between  $^1\text{H}$  and  $^{13}\text{C}$  NMR spectra.

Therefore, the results of 1D and 2D NMR spectra were helpful to us to assign all signals corresponded to the correctly expected structure of Clazpy ligand.

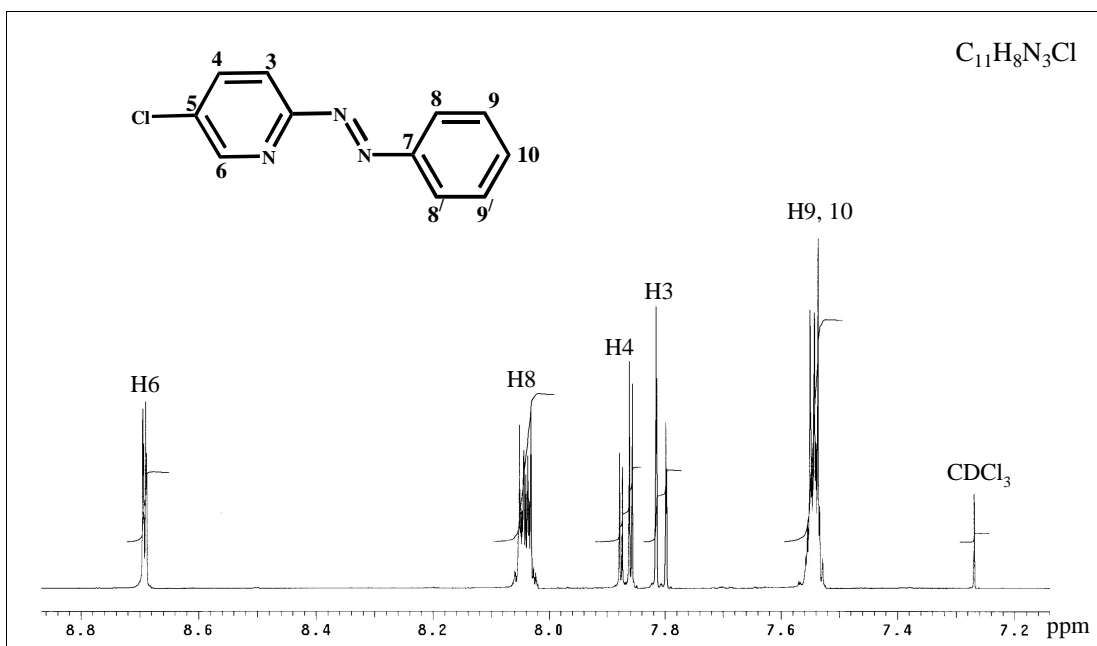


**Figure 3.6**  $^1H$  NMR spectrum of the Clazpy ligand in  $CDCl_3$

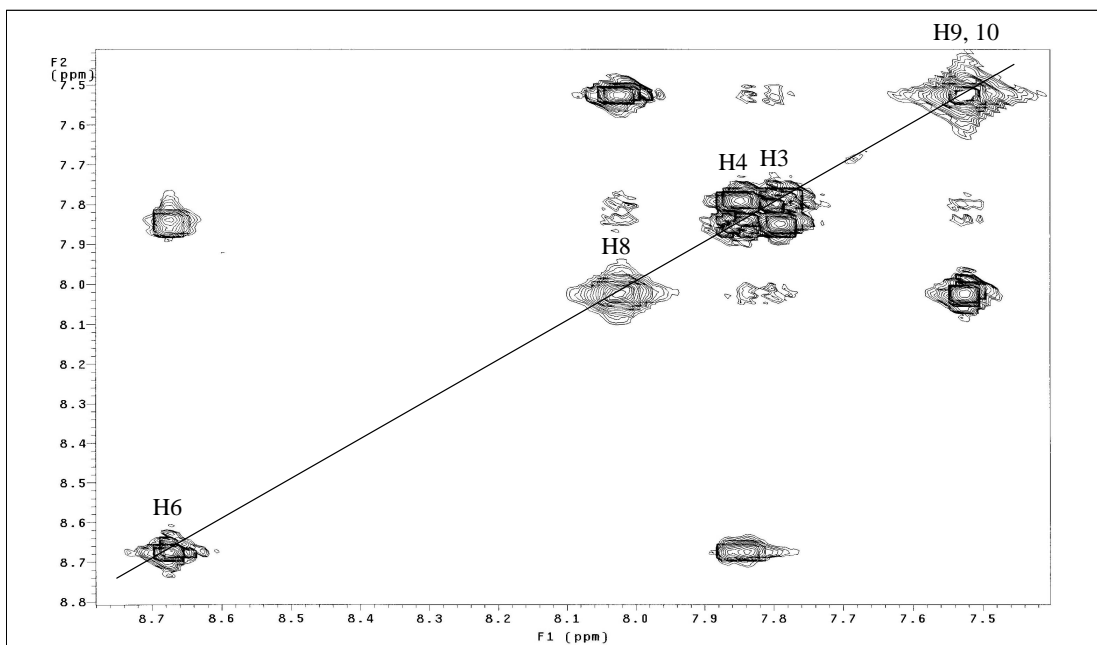


**Figure 3.7**  $^1H$ - $^1H$  COSY NMR spectrum of the Clazpy ligand in  $CDCl_3$

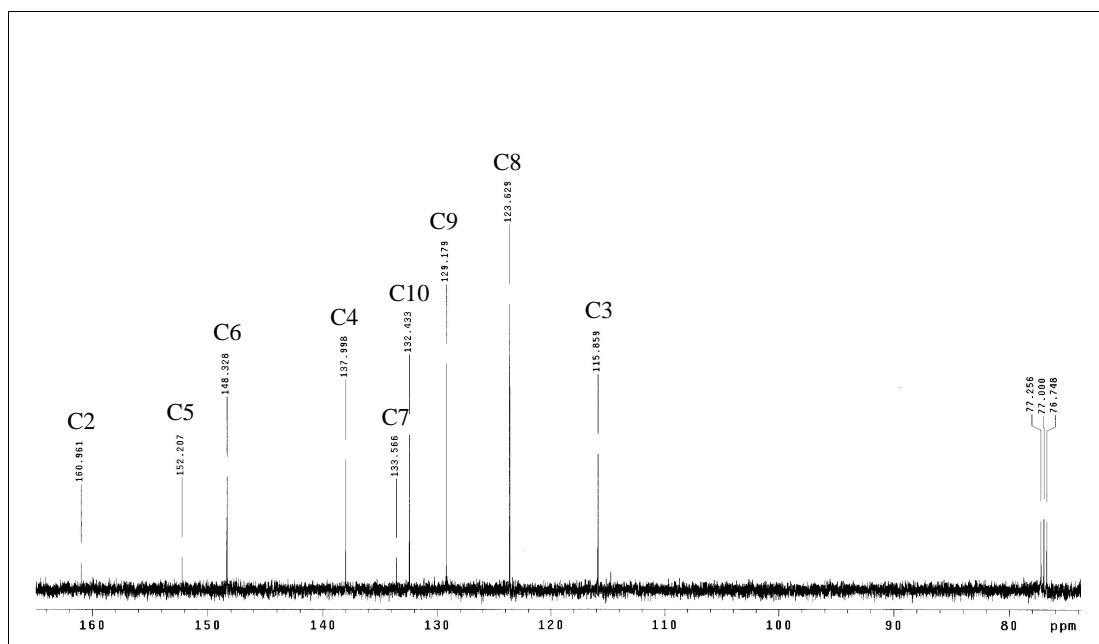


**Figure 3.8**  $^{13}\text{C}$  NMR spectrum of the Clazpy ligand in  $\text{CDCl}_3$

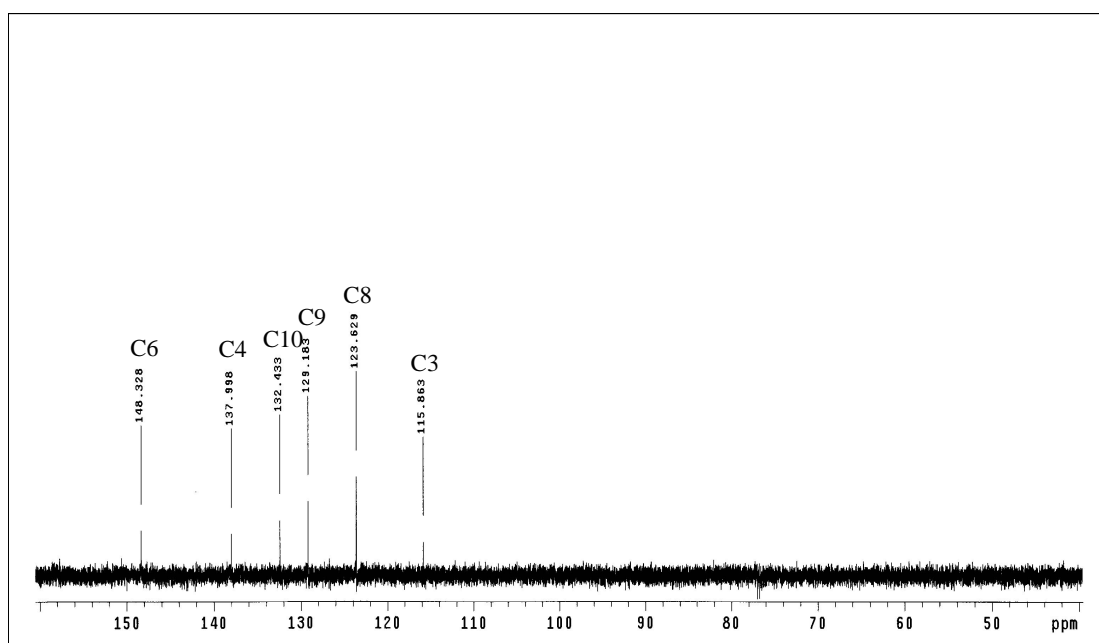


**Figure 3.9** DEPT NMR spectrum of the Clazpy ligand in  $\text{CDCl}_3$

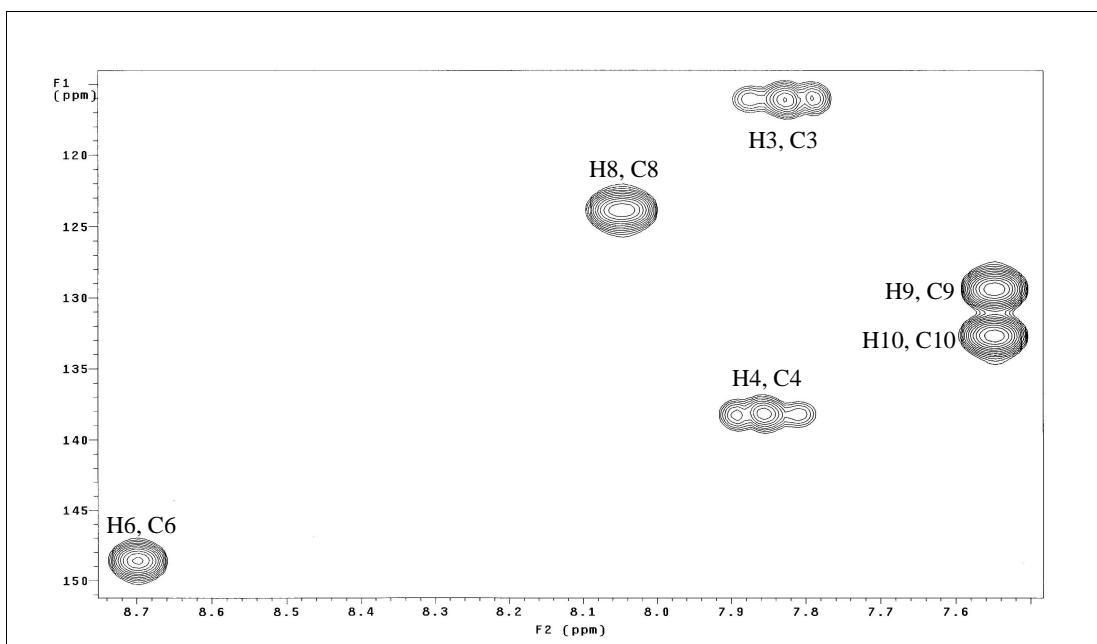


**Figure 3.10**  $^1\text{H}$ - $^{13}\text{C}$  HMQC NMR spectrum of the Clazpy ligand in  $\text{CDCl}_3$

### 3.1.2.6 Cyclic voltammetry

The redox behavior of Clazpy ligand in  $\text{CH}_2\text{Cl}_2$  solution was examined by cyclic voltammetric technique using a glassy carbon as working electrode, platinum wire as a reference electrode and a platinum disk as auxiliary electrode. All potentials were reported with reference to the ferrocene/ ferricinium couple.

In this experiment, the different scan rates were used to check the couple or the redox reaction. The couple having almost equal anodic and cathodic current was referred to reversible couple. On the other hand, the unequal currents were referred to the unequally transfer of the electron in reduction and oxidation leading to irreversible couple. The cyclic voltammogram in dichloromethane solution of Clazpy ligand is shown in Figure 3.11. The cyclic voltammetric data is listed in Table 3.7.

**Table 3.7** Cyclic voltammetric data of the Clazpy ligand in 0.1 M TBAH CH<sub>2</sub>Cl<sub>2</sub> at scan rate 50 mV/s (ferrocene as an internal standard)

Compounds	<sup>a</sup> E <sub>1/2</sub> , V (ΔE <sub>p</sub> , mV)	
	Oxidation	Reduction
azpy	-	-1.96 <sup>b</sup>
Clazpy	-	-1.57 (125)

<sup>a</sup>E<sub>1/2</sub> = (E<sub>pa</sub> + E<sub>pc</sub>)/2, where E<sub>pa</sub> and E<sub>pc</sub> are anodic and cathodic peak potentials, respectively; ΔE<sub>p</sub> = E<sub>pa</sub> – E<sub>pc</sub>

<sup>b</sup> cathodic peak potential, V (Jullapun, T., 2004).

### Oxidation range

The cyclic voltammograms of the azpy and Clazpy ligands showed no signal in potential range 0.00 to +1.50 V.

### Reduction range

The ligand reduction was studied in the range 0.00 to -2.00 V. The Clazpy ligand showed a quasi-reversible couple with two electrons transfer process at -1.57 V with peak-to-peak separation 125 mV, corresponding to the electron acceptor of the azo function as equation 3.1.



The electrochemistry behavior of Clazpy was different from that of azpy. The one quasi-reversible was observed. While, azpy showed only one irreversible peak in this range. The negative potential values of Clazpy and azpy were compared and showed that Clazpy could accept electron better than azpy. In addition, CV data correspond to IR data which showed the N=N stretching mode at lower

frequency of Clazpy ( $1364\text{ cm}^{-1}$ ) than that of azpy ( $1420\text{ cm}^{-1}$ ) (Krause and Krause, 1980).

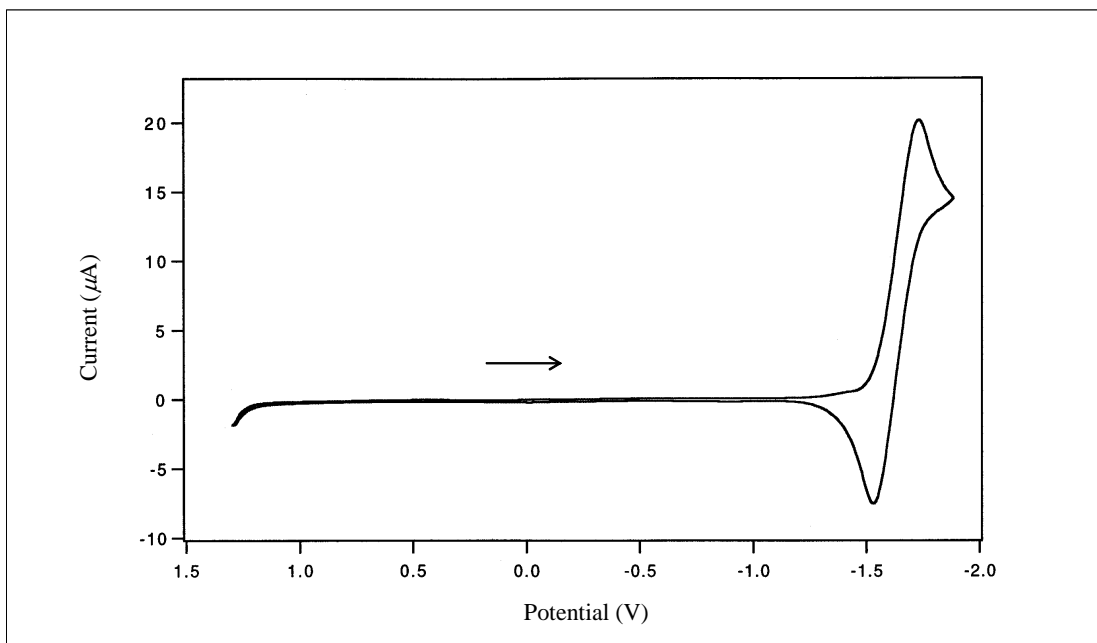


**Figure 3.11** Cyclic voltammogram of the Clazpy ligand in 0.1 M TBAH  $\text{CH}_2\text{Cl}_2$  at scan rate 50 mV/s (ferrocene as an internal standard)

## 3.2 Syntheses and characterization of the isomeric $[\text{Ru}(\text{Clazpy})_2\text{Cl}_2]$ complexes

### 3.2.1 Syntheses of the isomeric $[\text{Ru}(\text{Clazpy})_2\text{Cl}_2]$ complexes

The isomeric  $[\text{Ru}(\text{Clazpy})_2\text{Cl}_2]$  complexes were prepared by direct reaction of Clazpy with an appropriate mole ratio of hydrated ruthenium(III) chloride in refluxing ethanol as outline in Figure 3.12 (Method I). Three isomers as green, blue and purple have been separated from the mixture by chromatographic separation. Their structural determinations were investigated by X-ray diffraction analysis corresponding to color bands as *tcc* (green), *ctc* (blue), and *ccc* (purple) isomers,  $[\text{Ru}(\text{Clazpy})_2\text{Cl}_2]$  complexes, respectively.

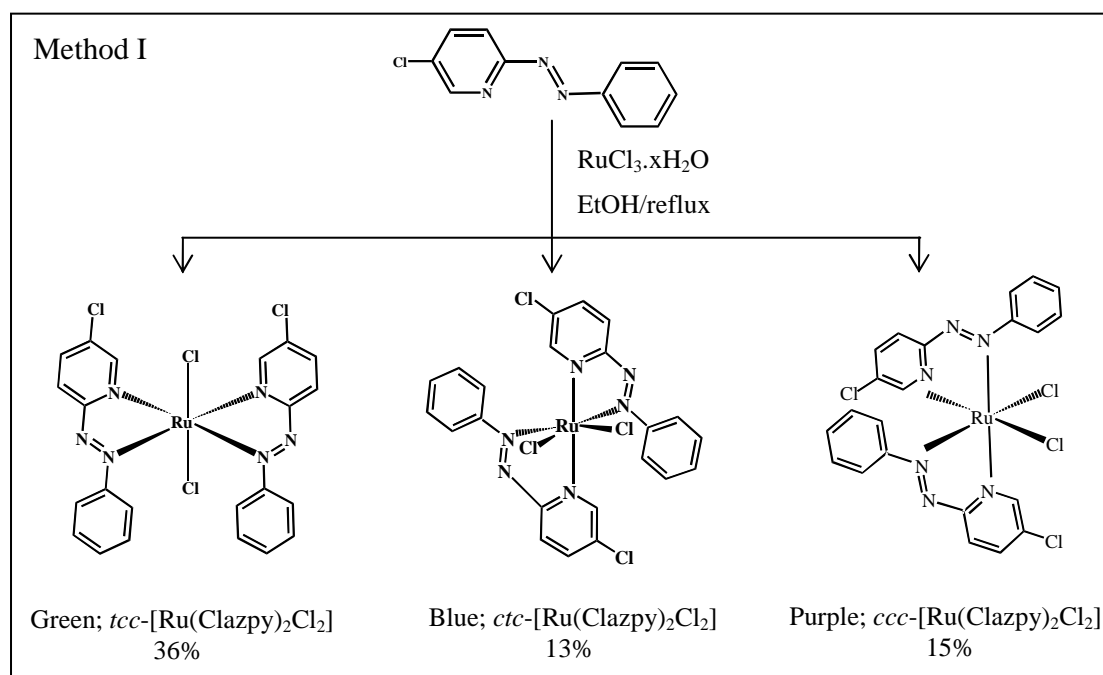


**Figure 3.12** Synthetic route for preparation of the isomeric  $[\text{Ru}(\text{Clazpy})_2\text{Cl}_2]$  complexes (method I)

Interestingly, in method I, the green-isomer was the most favored isomer kinetically during reaction and was found as a major product, while the blue and the purple isomers are minor. On the other hand, the blue isomer is found as a

main product in method II (Figure 3.13) with two minor products as the purple and dark green-[Ru(Clazpy)(5dmazpy)Cl<sub>2</sub>] that will be described later. It is noting that only stable compounds occur in solvent with high-boiling point. So, blue and purple isomers are thermodynamically stable. In addition, isomerization from the green to the blue and the purple isomers has also been observed.

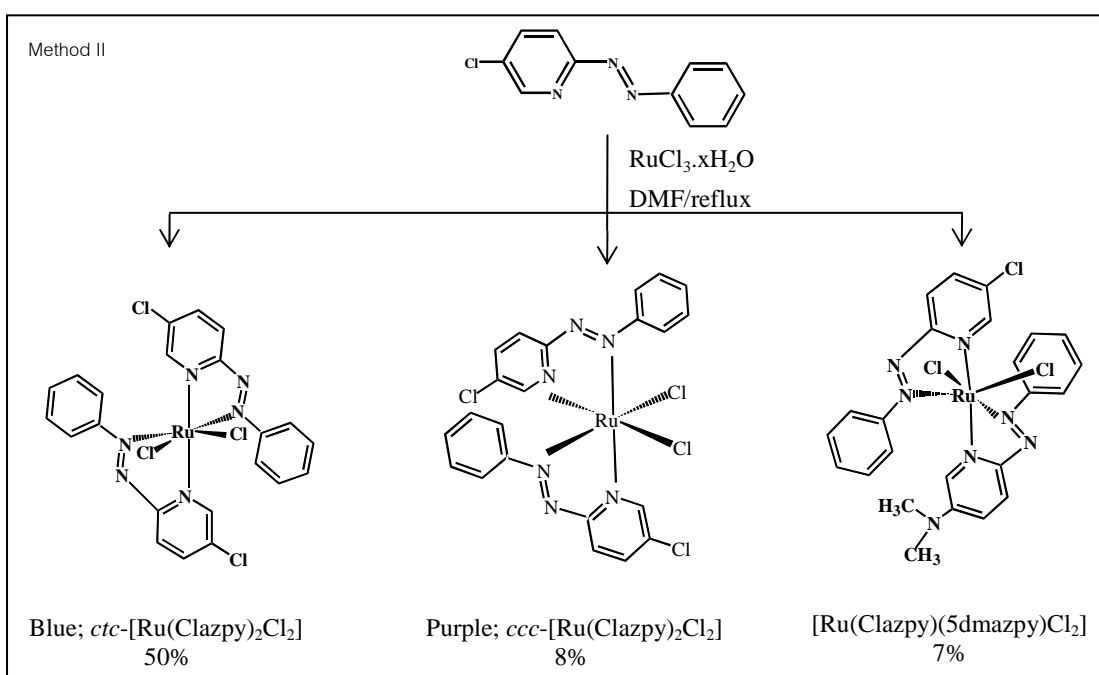


**Figure 3.13** Synthetic route for preparation of the isomeric [Ru(Clazpy)<sub>2</sub>Cl<sub>2</sub>] complexes (method II)

The physical properties of isomeric complexes, [Ru(Clazpy)<sub>2</sub>Cl<sub>2</sub>] are summarized in Table 3.8.

**Table 3.8** The physical properties of the isomeric [Ru(Clazpy)<sub>2</sub>Cl<sub>2</sub>] complexes

Complexes	Physical properties			
	Appearance	Color		Melting point (°C)
		solid	Solution	
<i>tcc</i> -[Ru(Clazpy) <sub>2</sub> Cl <sub>2</sub> ]	solid	dark green	green	319-320
<i>ctc</i> -[Ru(Clazpy) <sub>2</sub> Cl <sub>2</sub> ]	solid	dark blue	blue	330-331
<i>ccc</i> -[Ru(Clazpy) <sub>2</sub> Cl <sub>2</sub> ]	solid	dark purple	purple	329-330

The solubility of 0.0012 g of [Ru(Clazpy)<sub>2</sub>Cl<sub>2</sub>] complexes was tested in 10 mL of various organic solvents such as hexane, toluene, CHCl<sub>3</sub>, CH<sub>2</sub>Cl<sub>2</sub>, EtOAc, CH<sub>3</sub>OCH<sub>3</sub>, DMF, DMSO, CH<sub>3</sub>CN, EtOH, MeOH and H<sub>2</sub>O. These compounds were slightly soluble in EtOAc, toluene and MeOH and they were more soluble in CH<sub>3</sub>CN and CH<sub>3</sub>OCH<sub>3</sub>. They were very soluble in CHCl<sub>3</sub>, CH<sub>2</sub>Cl<sub>2</sub>, DMF, DMSO but insoluble in hexane, EtOH and H<sub>2</sub>O.

### 3.2.2 Characterization of the isomeric [Ru(Clazpy)<sub>2</sub>Cl<sub>2</sub>] complexes

The chemistry of isomeric [Ru(Clazpy)<sub>2</sub>Cl<sub>2</sub>] complexes were characterized by Elemental analysis, Mass spectrometry, Infrared spectroscopy, UV-Visible absorption spectroscopy, Nuclear Magnetic Resonance spectroscopy (1D and 2D NMR). The electrochemical properties of all complexes were studied by using cyclic voltammetric technique. The structure of these complexes was confirmed by X-ray crystallography.

#### 3.2.2.1 Elemental analysis

Elemental analysis was used to confirm composition of C, H, N in complexes. The analytical and the calculated values of isomeric [Ru(Clazpy)<sub>2</sub>Cl<sub>2</sub>] complexes are slightly different. Therefore, the composition of complexes was confirmed by this method. The results are given in Table 3.9.

**Table 3.9** Elemental analysis data of the isomeric [Ru(Clazpy)<sub>2</sub>Cl<sub>2</sub>] complexes

Complexes	% C		% H		% N	
	Calc.	Found	Calc.	Found	Calc.	Found
<i>tcc</i> -[Ru(Clazpy) <sub>2</sub> Cl <sub>2</sub> ]	43.51	43.99	2.65	2.55	13.84	13.93
<i>ctc</i> -[Ru(Clazpy) <sub>2</sub> Cl <sub>2</sub> ]	43.51	44.14	2.65	2.58	13.84	13.88
<i>ccc</i> -[Ru(Clazpy) <sub>2</sub> Cl <sub>2</sub> ]	43.51	44.15	2.65	2.68	13.84	13.78

### 3.2.2.2 X-ray crystallography

The X-ray crystallography is the most important technique to confirm the geometry of compounds. In this work, three isomers, *tcc*-[Ru(Clazpy)<sub>2</sub>Cl<sub>2</sub>], *ctc*-[Ru(Clazpy)<sub>2</sub>Cl<sub>2</sub>] and *ccc*-[Ru(Clazpy)<sub>2</sub>Cl<sub>2</sub>] were determined. It is noting that the arrangement of ligands around ruthenium center was similar to those obtained by others (Velder *et al.*, 2000; Seal and Ray, 1984).

#### X-ray structure of *tcc*-[Ru(Clazpy)<sub>2</sub>Cl<sub>2</sub>]

Crystals suitable for X-ray analysis were grown by slow diffusion of acetonitrile into a chloroform solution at room temperature. The crystal structure of *tcc*-[Ru(Clazpy)<sub>2</sub>Cl<sub>2</sub>] is shown in Figure 3.14. The crystallographic data are shown in Table 3.10. Selected bond parameters associated with the metal ions are listed in Table 3.11.

**Table 3.10** Crystal data and structure refinement for *tcc*-[Ru(Clazpy)<sub>2</sub>Cl<sub>2</sub>]

Empirical formula	C <sub>22</sub> H <sub>16</sub> Cl <sub>4</sub> N <sub>6</sub> Ru	
Formula weight	607.28	
Temperature	293(2) K	
Wavelength	0.71073 Å	
Crystal system	Monoclinic	
Space group	C2/c	
Unit cell dimensions	$a = 16.6777(8) \text{ \AA}$	$\alpha = 90^\circ$
	$b = 15.2136(8) \text{ \AA}$	$\beta = 7.8600(10)^\circ$
	$c = 18.3256(9) \text{ \AA}$	$\gamma = 90^\circ$
Volume	4606.0(4) Å <sup>3</sup>	
Z	8	
Density (calculated)	1.751 Mg/m <sup>3</sup>	
Absorption coefficient	1.169 mm <sup>-1</sup>	
F(000)	2416	
Crystal size	0.398 x 0.18 x 0.127 mm <sup>3</sup>	
Refinement method	Full-matrix least-squares on $F^2$	
Goodness-of-fit on $F^2$	1.093	
Final R indices [ $I > 2\sigma(I)$ ]	$R1 = 0.0268$ , $wR2 = 0.0635$	
R indices (all data)	$R1 = 0.0296$ , $wR2 = 0.0647$	

**Table 3.11** Selected bond lengths (Å) and angles (°) and estimated standard deviations for *tcc*-[Ru(Clazpy)<sub>2</sub>Cl<sub>2</sub>]

Distances			
Ru(1)-N(1)	2.000(2)	Ru(1)-N(4)	2.088(2)
Ru(1)-N(3)	1.991(2)	Ru(1)-N(6)	1.996(2)
Ru(1)-Cl(2)	2.381(1)	Ru(1)-Cl(1)	2.365(1)
N(2)-N(3)	1.292(3)	N(2)-N(3)	1.284(3)
Angles			
Cl(1)-Ru(1)-Cl(2)	171.32(2)	Cl(2)-Ru(1)-N(3)	96.03(6)
Cl(1)-Ru(1)-N(4)	87.89(5)	N(6)-Ru(1)-N(4)	75.22(8)
Cl(1)-Ru(1)-N(6)	94.91(5)	N(4)-Ru(1)-N(1)	103.95(7)
Cl(1)-Ru(1)-N(1)	85.25(5)	N(4)-Ru(1)-N(3)	177.73(7)
Cl(1)-Ru(1)-N(3)	89.85(6)	N(6)-Ru(1)-N(1)	179.14(7)
Cl(2)-Ru(1)-N(4)	86.20(5)	N(3)-Ru(1)-N(6)	105.14(8)
Cl(2)-Ru(1)-N(6)	89.73(5)	N(3)-Ru(1)-N(1)	75.70(7)
Cl(2)-Ru(1)-N(1)	90.01(5)		

In *tcc*-[Ru(Clazpy)<sub>2</sub>Cl<sub>2</sub>], the molecule consists of a central Ru atom surrounded by six coordination centers. The atomic arrangement around ruthenium involves sequentially two *trans*-chlorides, *cis*-N<sub>py</sub> and *cis*-N<sub>azo</sub> corresponding to *trans-cis-cis* configuration. The Ru-N(azo), Ru(1)-N(3) and Ru(1)-N(6) distances (1.991(2), 1.996(2)Å) are shorter than the Ru-N(pyridine), the Ru(1)-N(1) and Ru(1)-N(4) (2.000(2), 2.088(2)Å). This situation is similar to the corresponding distances in [Ru(azpy)<sub>2</sub>Cl<sub>2</sub>] and other azoimine complexes (Velder *et al.*, 2000; Hotze *et al.*, 2004). This is due to greater  $\pi$ -backbonding from  $d\pi(\text{Ru}) \rightarrow \pi^*(\text{azo})$ . Moreover, the average Ru-N(azo) distances in the title complex (1.993(2)Å) is longer than those in [Ru(azpy)<sub>2</sub>Cl<sub>2</sub>] (1.987(5)Å) (Velder *et al.*, 2000) and [Ru(tazpy)<sub>2</sub>Cl<sub>2</sub>] (1.967(3)Å) (Hotze *et al.*, 2004). However, the N=N bond distances (1.292(3), 1.284(3)Å) of the title complex are shorter than those in [Ru(azpy)<sub>2</sub>Cl<sub>2</sub>] (1.302(8), 1.306(7)Å) (Velder *et al.*, 2000) and in [Ru(tazpy)<sub>2</sub>Cl<sub>2</sub>] (1.300(4), 1.294(4)Å) (Hotze *et al.*, 2004). It is

interesting to note that the Ru(1)-N(1) and Ru(1)-N(4) distances in *tcc*-[Ru(Clazpy)<sub>2</sub>Cl<sub>2</sub>] (2.000(18), 2.088(2)Å) is shorter than those in [Ru(azpy)<sub>2</sub>Cl<sub>2</sub>] (2.116(6), 2.099(5)Å) (Velder *et al.*, 2000) and in [Ru(tazpy)<sub>2</sub>Cl<sub>2</sub>] (2.085(3), 2.103(3)Å) (Hotze *et al.*, 2004). This could be due to the effect of chloride substituent at the fifth position on the pyridine ring. This accounts for stronger  $\sigma$ -donor property of Clazpy than the azpy and the tazpy ligands. Furthermore, the Ru(1)-Cl(1), and Ru(1)-Cl(2) bond lengths in the *tcc*-[Ru(Clazpy)<sub>2</sub>Cl<sub>2</sub>] (2.381(1), 2.365(1)Å) are comparable to those observed in the [Ru(azpy)<sub>2</sub>Cl<sub>2</sub>] complex (2.377(2), 2.368(2)Å) (Velder *et al.*, 2000) and [Ru(tazpy)<sub>2</sub>Cl<sub>2</sub>] (2.377(2), 2.368(2)Å) (Hotze *et al.*, 2004). In addition, the bite angles N(1)-Ru(1)-N(3), and N(4)-Ru(1)-N(6) are 75.70(7)<sup>o</sup> and 75.22(8)<sup>o</sup>, respectively around Ru(II) center reveal a greater considerable distortion of the octahedral than that in [Ru(azpy)<sub>2</sub>Cl<sub>2</sub>] (75.80(19), 75.4(2)<sup>o</sup>) (Velder *et al.*, 2000).

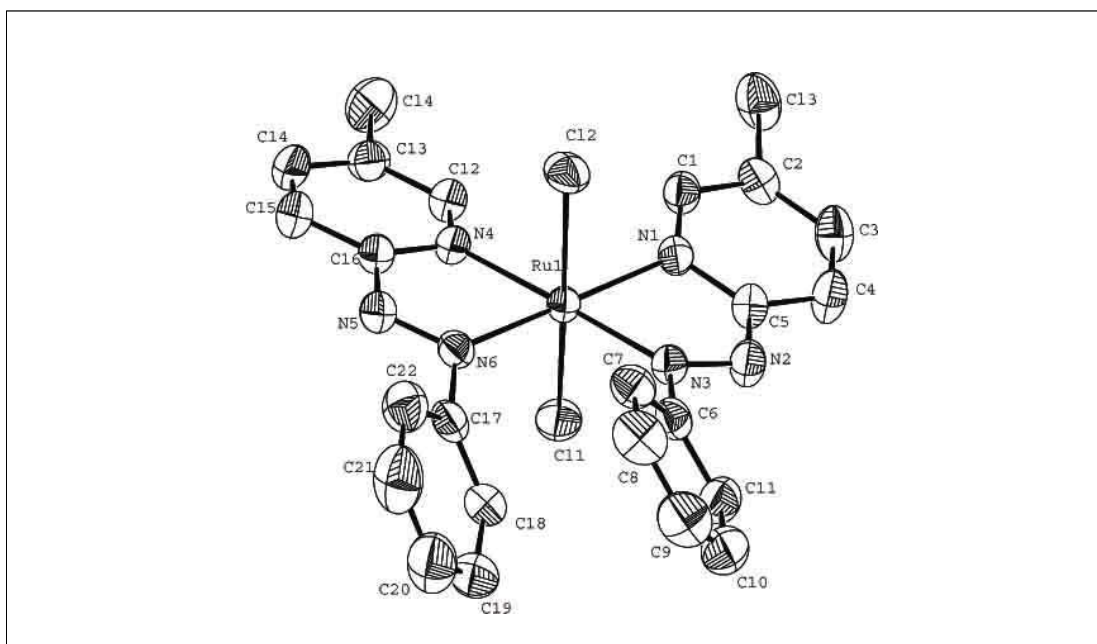


**Figure 3.14** The structure of *tcc*-[Ru(Clazpy)<sub>2</sub>Cl<sub>2</sub>] (H-atom omitted)

X-ray structure of *ctc*[Ru(Clazpy)<sub>2</sub>Cl<sub>2</sub>]

Crystals suitable for X-ray analysis were grown by slow diffusion of toluene into a dichloromethane solution at room temperature. The crystal structure of *ctc*-[Ru(Clazpy)<sub>2</sub>Cl<sub>2</sub>] is shown in Figure 3.15. The crystallographic data are shown in Table 3.12. Selected bond parameters associated with the metal ions are listed in Table 3.13.

**Table 3.12** Crystal data and structure refinement for *ctc*-[Ru(Clazpy)<sub>2</sub>Cl<sub>2</sub>]

Empirical formula	C <sub>22</sub> H <sub>16</sub> Cl <sub>4</sub> N <sub>6</sub> Ru	
Formula weight	607.28	
Temperature	293(2) K	
Wavelength	0.71073 Å	
Crystal system	Monoclinic	
Space group	C2/c	
Unit cell dimensions	$a = 10.8904(10)$ Å	$\alpha = 90^\circ$
	$b = 15.3931(13)$ Å	$\beta = 91.320(2)^\circ$
	$c = 14.5846(13)$ Å	$\gamma = 90^\circ$
Volume	2444.3(4) Å <sup>3</sup>	
Z	4	
Density (calculated)	1.650 Mg/m <sup>3</sup>	
Absorption coefficient	1.102 mm <sup>-1</sup>	
$F(000)$	1208	
Crystal size	0.35 x 0.3 x 0.2 mm <sup>3</sup>	
Refinement method	Full-matrix least-squares on $F^2$	
Goodness-of-fit on $F^2$	1.040	
Final R indices [ $I > 2\sigma(I)$ ]	$RI = 0.0274$ , $wR2 = 0.0662$	
R indices (all data)	$RI = 0.0304$ , $wR2 = 0.0676$	
Extinction coefficient	0.00306(19)	

**Table 3.13** Selected bond lengths (Å) and angles (°) and estimated standard deviations for *ctc*-[Ru(Clazpy)Cl<sub>2</sub>]

Distances			
Ru(1)-N(1)	2.037(2)	Ru(1)-N(1)#1	2.037(2)
Ru(1)-N(3)	1.973(2)	Ru(1)-N(3)#1	1.973(2)
Ru(1)-Cl(1)	2.403(1)	Ru(1)-Cl(1)#1	2.403(1)
N(2)-N(3)	1.283(2)		
Angles			
Cl(1)-Ru(1)-N(1)	88.61(5)	N(1)#1-Ru(1)-N(3)#1	76.73(7)
Cl(1)-Ru(1)-N(3)#1	171.05(5)	N(3)-Ru(1)-Cl(1)	85.27(5)
Cl(1)-Ru(1)-Cl(1)#1	90.69(3)	N(3)-Ru(1)-N(1)	76.73(7)
Cl(1)-Ru(1)-N(1)#1	95.22(5)	N(3)-Ru(1)-N(3)#1	99.82(1)
Cl(1)#1-Ru(1)-N(3)#1	85.27(5)	Cl(1)#1-Ru(1)-N(1)#1	88.60(5)
N(1)-Ru(1)-N(3)#1	99.70(7)	Cl(1)#1-Ru(1)-N(3)	171.05(5)
N(1)-Ru(1)-Cl(1)#1	95.22(5)	N(1)#1-Ru(1)-N(3)	99.70(7)
N(1)-Ru(1)-N(1)#1	174.57(7)		

Symmetry transformation used to generate equivalent atoms: #1,  $-x+1, y, -z+1/2$ .

In *ctc*-[Ru(Clazpy)<sub>2</sub>Cl<sub>2</sub>] complex, the ruthenium complex is sequentially a distorted octahedral with atomic arrangement around ruthenium involves sequentially two *cis*-chlorides, *trans*-N(pyridine) and *cis*-N(azo). The Ru-N(azo) distance (1.973(2) Å) is shorter than the Ru-N(py) (2.037(2) Å) which is similar to the corresponding distances in [Ru(azpy)<sub>2</sub>Cl<sub>2</sub>] (Seal and Ray, 1984) and  $\square$ -[Ru(Hsazpy)<sub>2</sub>Cl<sub>2</sub>] (Hotze *et al.*, 2004). The average Ru-N(azo) distance in [Ru(Clazpy)<sub>2</sub>Cl<sub>2</sub>] (1.973(2) Å) is comparable to those in [Ru(azpy)<sub>2</sub>Cl<sub>2</sub>] (1.9805(4) Å). In addition, the N=N(azo) 1.284(2) Å distance in [Ru(Clazpy)<sub>2</sub>Cl<sub>2</sub>] is comparable to those in [Ru(azpy)<sub>2</sub>Cl<sub>2</sub>] (1.281(6) Å) and  $\alpha$ -[Ru(Hsazpy)<sub>2</sub>Cl<sub>2</sub>] (1.287(10) Å). Furthermore, the Ru-Cl bond lengths in this compound (2.403(1) Å) slightly longer than those observed in the [Ru(azpy)<sub>2</sub>Cl<sub>2</sub>] complex (2.401(1) Å, 2.397(1) Å) (Seal and

Ray, 1984). In addition, the bite angle, N(1)-Ru(1)-N(3) is  $76.73(7)^\circ$ , similar to those observed in the  $[\text{Ru}(\text{azpy})_2\text{Cl}_2]$  complex. However, two angles around ruthenium(II) center, Cl(1)-Ru-N(1) ( $88.61(5)^\circ$ ) and Cl(1)-Ru-N(3)  $85.27(5)^\circ$ , reveal a greater distortion of the title molecule than that in  $[\text{Ru}(\text{azpy})_2\text{Cl}_2]$  (Seal and Ray, 1984) and  $\alpha$ - $[\text{Ru}(\text{Hszapy})_2\text{Cl}_2]$  (Hotze *et al.*, 2004) complexes. It is worth to note that the Ru-N(py) distance in  $[\text{Ru}(\text{Clazpy})_2\text{Cl}_2]$  ( $2.037(2)\text{\AA}$ ) is shorter than that of  $[\text{Ru}(\text{azpy})_2\text{Cl}_2]$  ( $2.045(4)\text{\AA}$  and  $2.051(4)\text{\AA}$ ). This could be due to the effect of chloride atom at the fifth position increasing electron density on pyridine ring and  $\sigma$ -donor property of the N(pyridine) of Clazpy becomes stronger than that in the azpy ligand.

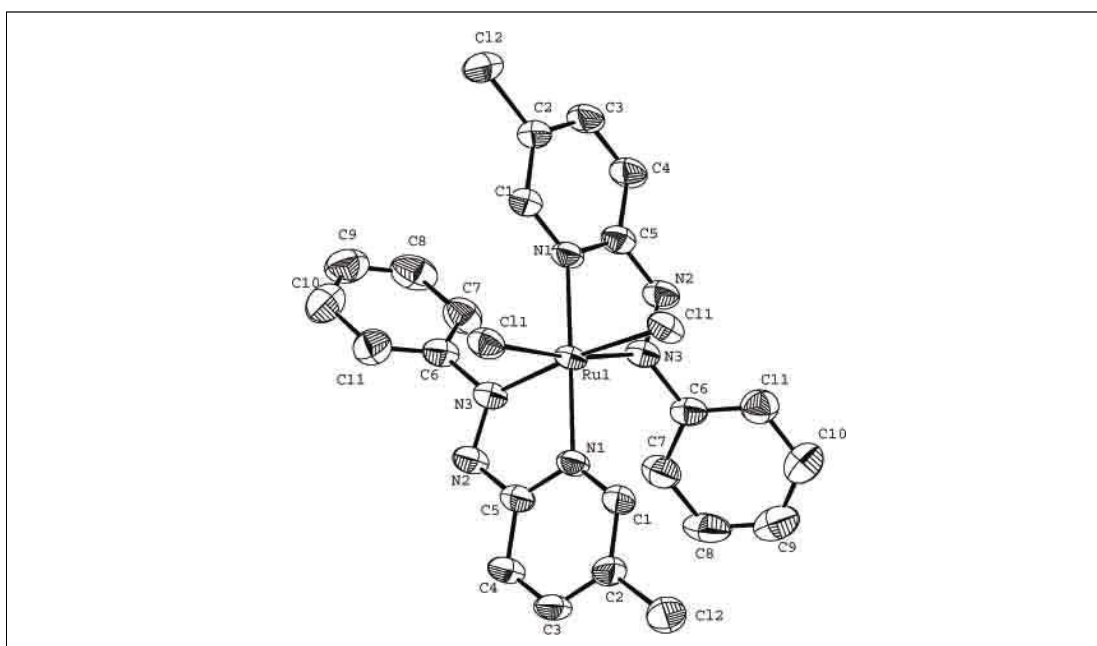


**Figure 3.15** The structure of *ctc*- $[\text{Ru}(\text{Clazpy})_2\text{Cl}_2]$  (H-atom omitted)

X-ray structure of *ccc*[Ru(Clazpy)<sub>2</sub>Cl<sub>2</sub>]

Crystals suitable for X-ray analysis were grown by slow diffusion of toluene into a dichloromethane solution at room temperature. The crystal structure of *ccc*-[Ru(Clazpy)<sub>2</sub>Cl<sub>2</sub>] is shown in Figure 3.16. The crystallographic data are shown in Table 3.14. Selected bond parameters associated with the metal ions are listed in Table 3.15.

**Table 3.14** Crystal data and structure refinement for *ccc*-[Ru(Clazpy)<sub>2</sub>Cl<sub>2</sub>]

Empirical formula	C <sub>51</sub> H <sub>40</sub> C <sub>18</sub> N <sub>12</sub> Ru <sub>2</sub>
Formula weight	1306.69
Temperature	293(2) K
Wavelength	0.71073 Å
Crystal system	Triclinic
Space group	<i>P</i> 1
Unit cell dimensions	$a = 9.1099(6)$ Å $\alpha = 74.7050(10)^\circ$ $b = 10.2403(7)$ Å $\beta = 74.3050(10)^\circ$ $c = 15.7105(10)$ Å $\gamma = 85.1320(10)^\circ$
Volume	1360.84(16) Å <sup>3</sup>
<i>Z</i>	1
Density (calculated)	1.594 Mg/m <sup>3</sup>
Absorption coefficient	0.996 mm <sup>-1</sup>
<i>F</i> (000)	654
Crystal size	0.238 x 0.219 x 0.154 mm <sup>3</sup>
Refinement method	Full-matrix least-squares on <i>F</i> <sup>2</sup>
Goodness-of-fit on <i>F</i> <sup>2</sup>	1.011
Final R indices [ <i>I</i> > 2σ( <i>I</i> )]	<i>R</i> 1 = 0.0258, <i>wR</i> 2 = 0.0623
R indices (all data)	<i>R</i> 1 = 0.0292, <i>wR</i> 2 = 0.0649

**Table 3.15** Selected bond lengths (Å) and angles (°) and estimated standard deviations for *ccc*-[Ru(Clazpy)Cl<sub>2</sub>]

Distances			
Ru(1)-N(3)	1.967(6)	Ru(2)-N(10)	2.053(8)
Ru(1)-N(6)	1.977(7)	Ru(2)-N(7)	2.063(7)
Ru(1)-N(4)	2.026(8)	Ru(2)-Cl(6)	2.390(2)
Ru(1)-N(1)	2.075(6)	Ru(2)-Cl(5)	2.392(2)
Ru(1)-Cl(2)	2.376(2)	N(2)-N(3)	1.236(9)
Ru(1)-Cl(1)	2.395(2)	N(5)-N(6)	1.304(10)
Ru(2)-N(9)	1.924(7)	N(8)-N(9)	1.344(9)
Ru(2)-N(12)	2.010(6)	N(11)-N(12)	1.271(10)
Angles			
N(3)-Ru(1)-N(6)	96.5(3)	N(9)-Ru(2)-N(12)	97.8(3)
N(3)-Ru(1)-N(4)	92.9(3)	N(9)-Ru(2)-N(10)	93.1(3)
N(6)-Ru(1)-N(4)	76.1(3)	N(12)-Ru(2)-N(10)	76.9(3)
N(3)-Ru(1)-N(1)	76.2(3)	N(9)-Ru(2)-N(7)	76.7(3)
N(6)-Ru(1)-N(1)	171.2(3)	N(12)-Ru(2)-N(7)	172.8(3)
N(4)-Ru(1)-N(1)	99.3(3)	N(10)-Ru(2)-N(7)	98.6(3)
N(3)-Ru(1)-Cl(2)	88.6(2)	N(9)-Ru(2)-Cl(6)	88.5(2)
N(6)-Ru(1)-Cl(2)	99.2(2)	N(12)-Ru(2)-Cl(6)	97.9(2)
N(4)-Ru(1)-Cl(2)	175.1(2)	N(10)-Ru(2)-Cl(6)	174.7(2)
N(1)-Ru(1)-Cl(2)	85.5(2)	N(7)-Ru(2)-Cl(6)	86.7(2)
N(3)-Ru(1)-Cl(1)	169.9(2)	N(9)-Ru(2)-Cl(5)	170.1(2)
N(6)-Ru(1)-Cl(1)	93.6(2)	N(12)-Ru(2)-Cl(5)	92.0(2)
N(4)-Ru(1)-Cl(1)	88.5(2)	N(10)-Ru(2)-Cl(5)	88.6(2)
N(1)-Ru(1)-Cl(1)	93.7(2)	N(7)-Ru(2)-Cl(5)	93.5(2)
Cl(2)-Ru(1)-Cl(1)	90.91(9)	Cl(6)-Ru(2)-Cl(5)	90.62(9)

In *ccc*-[Ru(Clazpy)<sub>2</sub>Cl<sub>2</sub>] complex, the molecular structure (Figure 3.45) are all-*cis* geometries with the atomic arrangement around ruthenium involving sequentially two *cis*-chlorides, *cis*-N<sub>py</sub> and *cis*-N<sub>azo</sub>. The majority bond distances of Ru-N<sub>azo</sub> (N3, N6, N9, N12: 1.967(6), 1.977(7), 1.924(7) and 2.010(6) Å) are shorter than that of Ru-N<sub>py</sub> (N1, N4, N7, N11: 2.075(6), 2.026(8), 2.053(8) and 2.063(7) Å). Again, this situation is similar to the corresponding distances in [Ru(azpy)<sub>2</sub>Cl<sub>2</sub>] and other azoimine complexes which described previously (Seal and Ray, 1984). The average Ru-N<sub>azo</sub> distances in the title complex, *ccc*-[Ru(Clazpy)<sub>2</sub>Cl<sub>2</sub>] (1.969(6) Å) is slightly shorter than those in [Ru(azpy)<sub>2</sub>Cl<sub>2</sub>] (1.981(1) Å) (Seal and Ray, 1984). Consequently, the average bond N=N 1.289(9) Å distance in [Ru(Clazpy)<sub>2</sub>Cl<sub>2</sub>] is longer than those in [Ru(azpy)<sub>2</sub>Cl<sub>2</sub>] (1.281(6) Å). Furthermore, the average bond distance of Ru-Cl is comparable to those observed in the [Ru(azpy)<sub>2</sub>Cl<sub>2</sub>] complexes. The *cis*-chloro angle of 90.91° and 90.62° is nearly octahedral. In addition, the bite angle (76.1(3), 76.2(3), 76.9(3), 76.7(3)) around Ru(II) center play an important role to its structurally distortion.

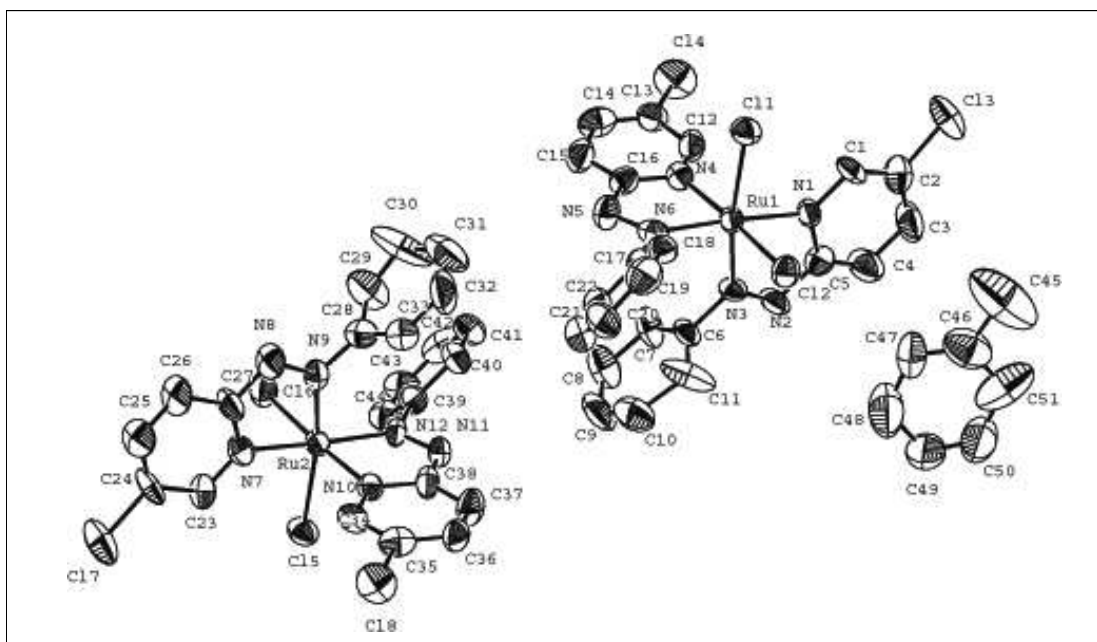


**Figure 3.16** The structure of *ccc*-[Ru(Clazpy)<sub>2</sub>Cl<sub>2</sub>] (H-atom omitted)

### 3.2.2.3 Fast-atom bombardment (FAB) mass spectrometry

The FAB mass spectrum of the isomeric  $[\text{Ru}(\text{Clazpy})_2\text{Cl}_2]$  complexes are shown in Figure 3.17 to 3.19. The results are given in Table 3.16.

**Table 3.16** FAB mass spectrometric data of the isomeric  $[\text{Ru}(\text{Clazpy})_2\text{Cl}_2]$  complexes

m/z	Stoichiometry	Equivalent species	Rel. Abun. (%)
<i>tcc</i> - $[\text{Ru}(\text{Clazpy})_2\text{Cl}_2]$			
391	$[\text{Ru}(\text{Clazpy})\text{Cl}_2 + \text{H}]^+$	$[\text{M}-\text{Clazpy}+\text{H}]^+$	100
413	$[\text{Ru}(\text{Clazpy})\text{Cl}_2 + \text{Na}]^+$	$[\text{M}-\text{Clazpy}+\text{Na}]^+$	72
<i>ctc</i> - $[\text{Ru}(\text{Clazpy})_2\text{Cl}_2]$			
573	$[\text{Ru}(\text{Clazpy})_2\text{Cl}]^+$	$[\text{M}-\text{Cl}]^+$	100
608	$[\text{Ru}(\text{Clazpy})_2\text{Cl}_2 + \text{H}]^+$	$[\text{M}+\text{H}]^+$	82
631	$[\text{Ru}(\text{Clazpy})_2\text{Cl}_2 + \text{Na}]^+$	$[\text{M}+\text{Na}]^+$	40
<i>ccc</i> - $[\text{Ru}(\text{Clazpy})_2\text{Cl}_2]$			
573	$[\text{Ru}(\text{Clazpy})_2\text{Cl}]^+$	$[\text{M}-\text{Cl}]^+$	100
608	$[\text{Ru}(\text{Clazpy})_2\text{Cl}_2 + \text{H}]^+$	$[\text{M}+\text{H}]^+$	84
631	$[\text{Ru}(\text{Clazpy})_2\text{Cl}_2 + \text{Na}]^+$	$[\text{M}+\text{Na}]^+$	50

M = molecular weight (MW) of each compounds

MW of  $[\text{Ru}(\text{Clazpy})_2\text{Cl}_2] = 607.29$  g/mol; MW of Clazpy = 217.66 g/mol

In *tcc*- $[\text{Ru}(\text{Clazpy})_2\text{Cl}_2]$ , the parent peak gave 100% relative abundance at m/z 391 corresponding to the loss of a Clazpy ligand from the unstable molecular ion at m/z 608. On the other hand, in *ctc* and *ccc*-isomers, the parent peak gave 100% relative abundance at m/z 573 corresponding to the lossing of a chloro atom from the molecular ion at m/z 608. It was concluded that the structure of complexes could be confirmed to be the *trans*- or *cis*-isomers based on results of FAB pattern. In addition,  $[\text{M}+\text{H}]^+$  and a cationized  $[\text{M}+\text{Na}]^+$  complex are also detected.

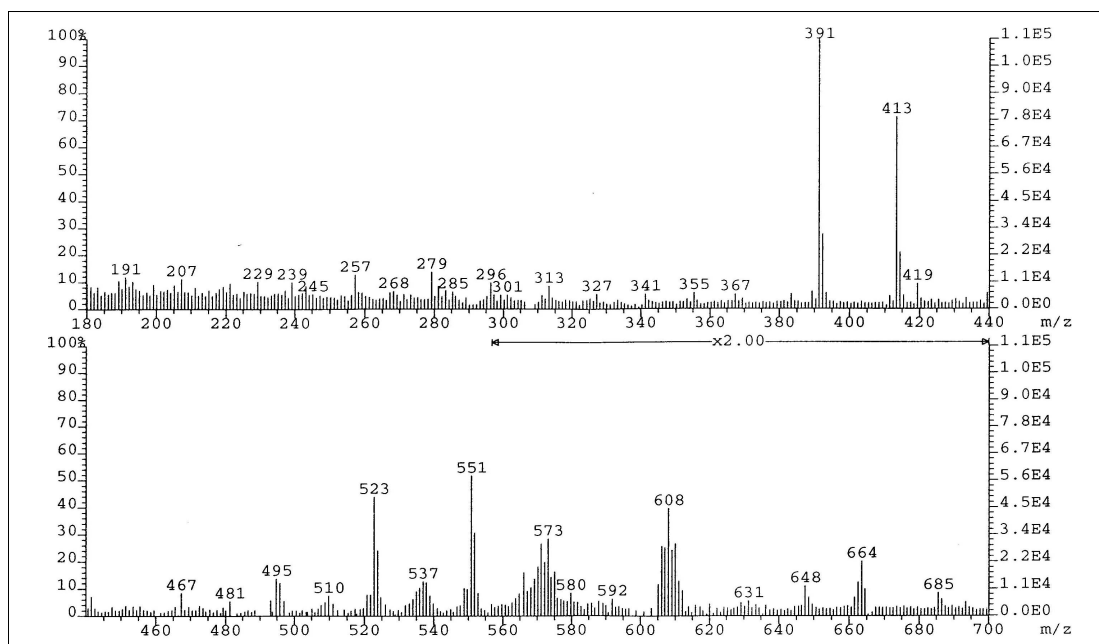


**Figure 3.17** FAB mass spectrum of  $tcc\text{-}[\text{Ru}(\text{Clazpy})_2\text{Cl}_2]$

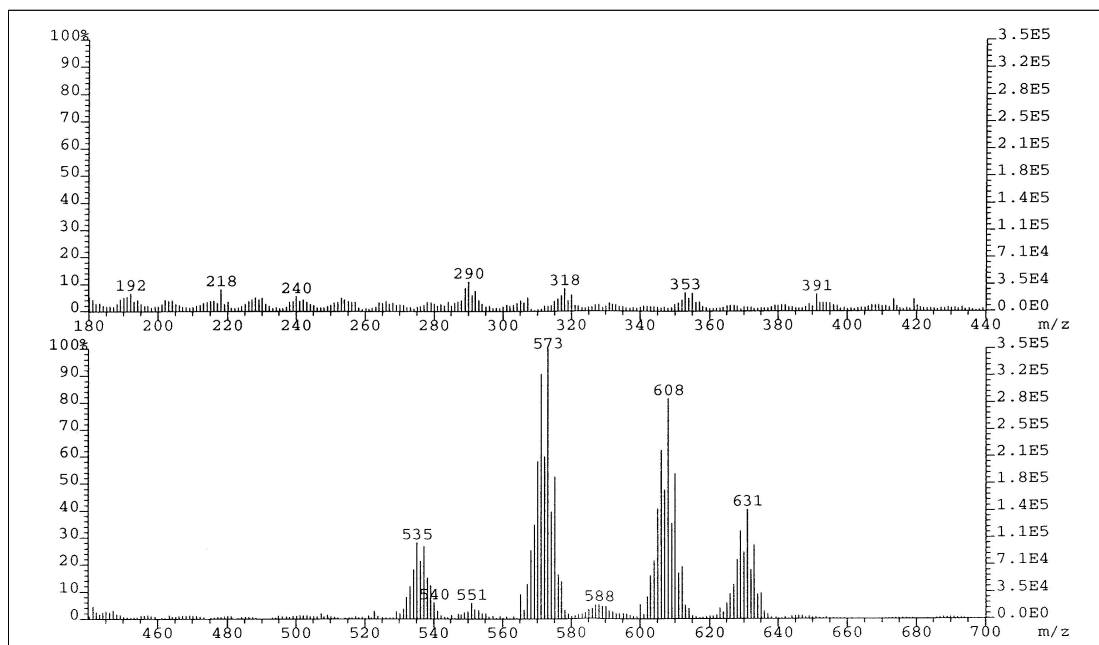


**Figure 3.18** FAB mass spectrum of  $ctc\text{-}[\text{Ru}(\text{Clazpy})_2\text{Cl}_2]$

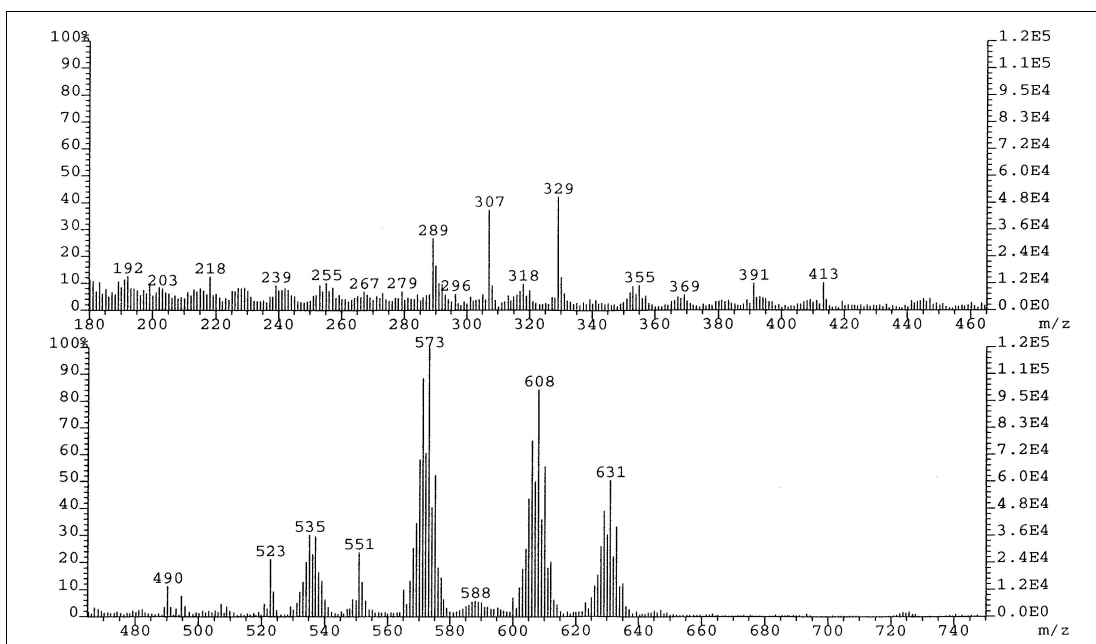


**Figure 3.19** FAB mass spectrum of *ccc*-[Ru(Clazpy)<sub>2</sub>Cl<sub>2</sub>]

### 3.2.2.4 Infrared spectroscopy

The vibrational spectra of isomeric [Ru(Clazpy)<sub>2</sub>Cl<sub>2</sub>] complexes are significant in the range 1600-400 cm<sup>-1</sup>. They showed many vibration frequencies such as C=C, C=N, N=N (azo), C-H bending of monosubstituted benzene and C-Cl. The infrared spectroscopic data of these complexes are given in Table 3.17 and these spectra are shown in Figure 3.20 to 3.22.

**Table 3.17** IR data of the isomeric [Ru(Clazpy)<sub>2</sub>Cl<sub>2</sub>] complexes

Vibrational frequencies	Wave numbers (cm <sup>-1</sup> )		
	<i>tcc</i> - [Ru(Clazpy) <sub>2</sub> Cl <sub>2</sub> ]	<i>ctc</i> - [Ru(Clazpy) <sub>2</sub> Cl <sub>2</sub> ]	<i>ccc</i> - [Ru(Clazpy) <sub>2</sub> Cl <sub>2</sub> ]
C=N stretching	1592(m)	1588(m)	1587(m)
C=C stretching	1551(m)	1541(m)	1543(m)
	1459(m)	1454(m)	1444(s)
		1443(s)	
N=N stretching	1299(s)	1336(s)	1308(s)
	1283(s)		1284(s)
C-H out of plane bend in monosub.benzene	766(m)	770(m)	775(m)
	738(m)	732(m)	733(m)
	691(s)	694(m)	689(s)
C-Cl	596(s)	601(m)	596(m)

s = strong, m = medium

From data, they showed many vibrations with different intensities below 1600 cm<sup>-1</sup> which were used to give information about ligand coordinated to the ruthenium center. Among of these modes, N=N stretching is an important peak used to be considered the  $\pi$ -acid property in azo complexes. This mode exhibited at 1364 cm<sup>-1</sup> in the free Clazpy ligand and was shifted to lower frequencies in the isomeric [Ru(Clazpy)<sub>2</sub>Cl<sub>2</sub>] complexes around 1283-1336 cm<sup>-1</sup>. This evidence confirmed the coordination of the Clazpy ligand to ruthenium center as well as characteristic of azo function to stabilize the lower oxidation state of ruthenium. Moreover, the N=N stretching mode of *trans*-orientation of two chelated azoimine groups in *tcc*-[Ru(Clazpy)<sub>2</sub>Cl<sub>2</sub>] occurred lower frequency than that of *cis*-orientation that in *ctc*- and *ccc*-[Ru(Clazpy)<sub>2</sub>Cl<sub>2</sub>]. It was due to the competition for the same metal d-orbital and may not perturb N=N stretching frequency significantly. This results is similar to the previous work (Misra *et al.*, 1998).

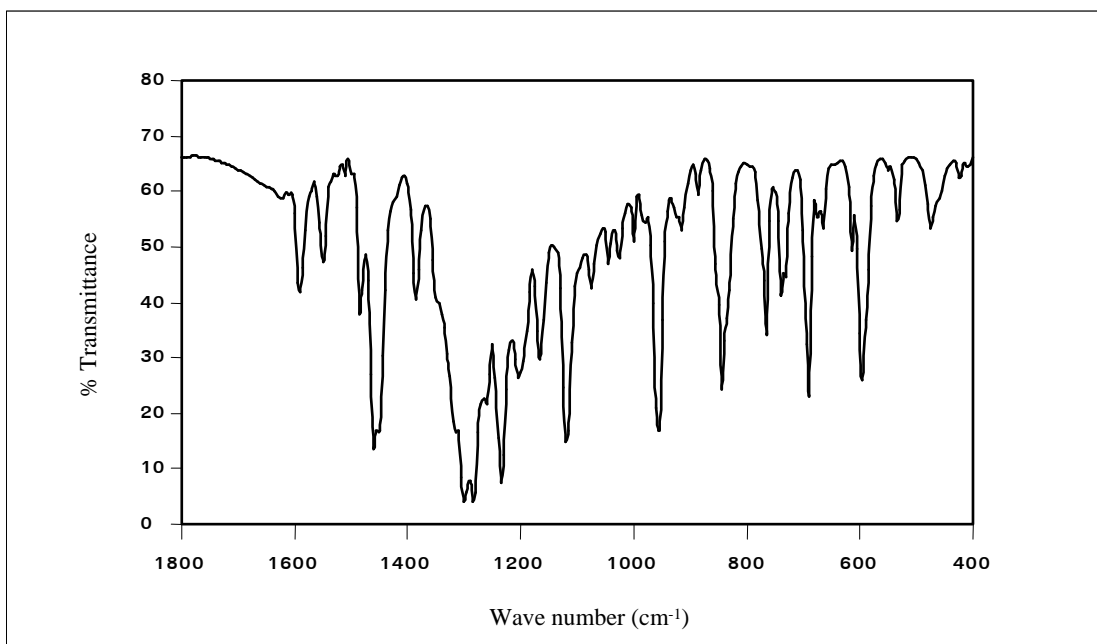


**Figure 3.20** IR spectrum of *tcc*-[Ru(Clazpy)<sub>2</sub>Cl<sub>2</sub>]

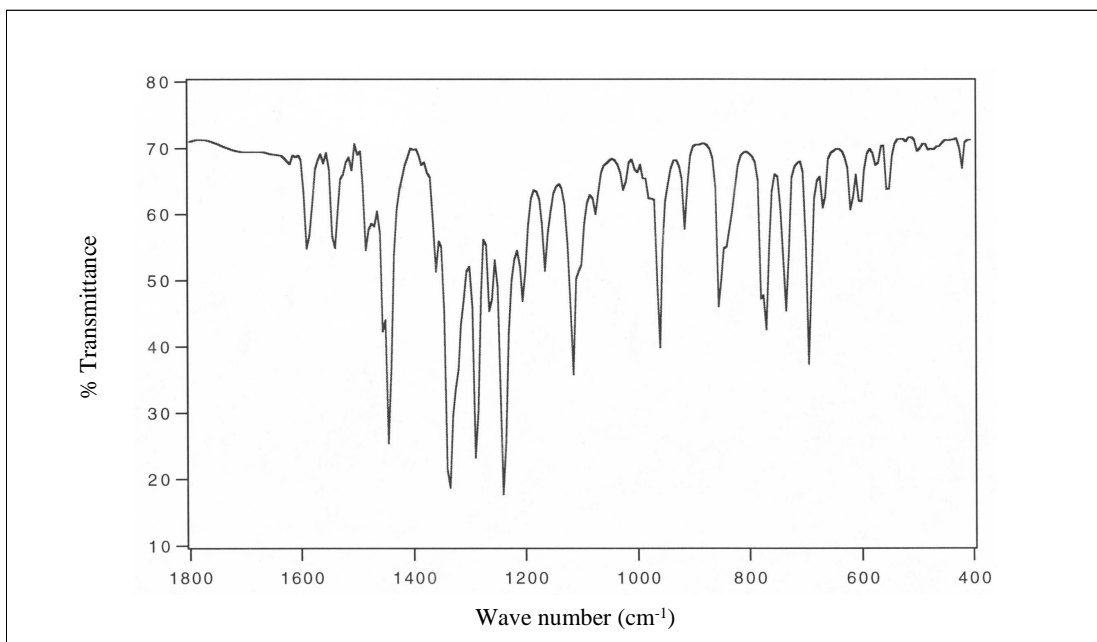


**Figure 3.21** IR spectrum of *ctc*-[Ru(Clazpy)<sub>2</sub>Cl<sub>2</sub>]

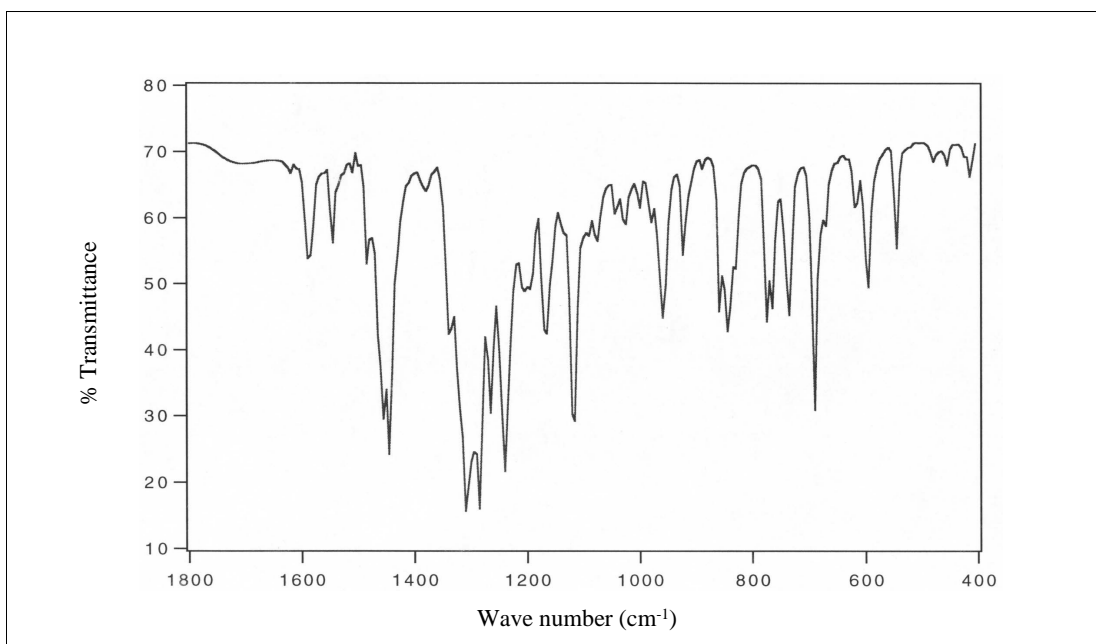


**Figure 3.22** IR spectrum of *ccc*-[Ru(Clazpy)<sub>2</sub>Cl<sub>2</sub>]

### 3.2.2.5 UV-Visible absorption spectroscopy

The UV-Visible absorption spectra of the isomeric [Ru(Clazpy)<sub>2</sub>Cl<sub>2</sub>] complexes were recorded in five solvents; CHCl<sub>3</sub>, CH<sub>2</sub>Cl<sub>2</sub>, DMF, DMSO and CH<sub>3</sub>CN in 200-800 nm range. Electronic spectra of these complexes in CH<sub>2</sub>Cl<sub>2</sub> solution are shown in Figure 3.23 to 3.25 and absorption spectroscopic data are listed in Table 3.18.

**Table 3.18** UV-Visible absorption spectroscopic data of the isomeric [Ru(Clazpy)<sub>2</sub>Cl<sub>2</sub>] complexes

Compounds	$\lambda_{\max}$ ( $\epsilon^a \times 10^4 \text{ M}^{-1}\text{cm}^{-1}$ )				
	CHCl <sub>3</sub>	CH <sub>2</sub> Cl <sub>2</sub>	DMF	DMSO	CH <sub>3</sub> CN
<i>tcc</i> - [Ru(Clazpy) <sub>2</sub> Cl <sub>2</sub> ]	247 (2.4)	237 (2.4)	272 (2.4)	247 (2.1)	205 (4.2)
	305 (1.9)	305 (1.7)	307 (2.7)	308 (1.7)	305 (2.1)
	422 (1.3)	419 (1.1)	413 (1.7)	421 (1.2)	410 (1.3)
	638 (1.4)	639 (1.1)	644 (1.8)	638 (1.2)	639 (1.5)
<i>ctc</i> - [Ru(Clazpy) <sub>2</sub> Cl <sub>2</sub> ]	246 (2.0)	236 (3.0)			205 (4.1)
	329 (3.0)	329 (3.8)	329 (3.2)	329 (3.2)	326 (3.3)
	590 (1.4)	591 (1.4)	589 (1.4)	588 (1.4)	584 (1.5)
<i>ccc</i> - [Ru(Clazpy) <sub>2</sub> Cl <sub>2</sub> ]	246 (2.1)	234 (2.5)			220 (3.4)
	359 (2.4)	356 (2.2)	348 (2.3)	349 (2.2)	346 (2.3)
	580 (1.2)	580 (1.1)	578 (1.2)	575 (1.2)	572 (1.2)

<sup>a</sup> Molar extinction coefficient

The spectral data of complexes show absorption within 200-800 nm (Table 3.12). The previous results of Clazpy ligand exhibit transition at 325±8 nm ( $\epsilon \sim 20000 \text{ M}^{-1}\text{cm}^{-1}$ ) and 450±4 nm ( $\epsilon \sim 550 \text{ M}^{-1}\text{cm}^{-1}$ ) which are due to intraligand charge transfer transitions,  $\pi \rightarrow \pi^*$  and  $n \rightarrow \pi^*$  transition, respectively. Thus, the transition in the complexes around 300-400 nm (in UV region) are probably the ligand origin. While, transition around 572-640 nm (in visible region) are charge-transfer transitions from metal-to-ligand charge transfer (MLCT) which are almost observed in complexes with ligands having low-lying  $\pi^*$  orbitals (Misra, et. al., 1998).

In addition to *tcc*-[Ru(Clazpy)<sub>2</sub>Cl<sub>2</sub>] complex, a high intense transitions ( $\epsilon \sim 10^4 \text{ M}^{-1}\text{cm}^{-1}$ ) in the region 641±3 nm was observed. Whereas, the *ctc* and *ccc*-[Ru(Clazpy)<sub>2</sub>Cl<sub>2</sub>] exhibit highly intense transition ( $\epsilon \sim 10^4 \text{ M}^{-1}\text{cm}^{-1}$ ) around 587±4

and  $576 \pm 4$  nm. The energy of the MLCT transition is symmetry-dependent (Santra *et al.*, 1999).

The less symmetric *ccc*-isomer ( $C_1$  symmetry) exhibit a stronger interaction compared to the other isomers (*ctc* and *ccc*-isomers;  $C_2$  symmetry) (Santra *et al.*, 1999). Thus, the *ccc*-isomer exhibits a transition at the higher energy than those of *ctc* and *tcc*-isomers which can be arranged in order as follows in  $\text{CH}_2\text{Cl}_2$ :

Complexes;  $ccc\text{-[Ru(Clazpy)Cl}_2\text{]} < ctc\text{-[Ru(Clazpy)Cl}_2\text{]} < tcc\text{-[Ru(Clazpy)Cl}_2\text{]}$   
 $\lambda_{\text{max}}(\text{nm}); \quad 580 \qquad \qquad 591 \qquad \qquad 639$

The overlay spectra were shown in Figure 3.23. In addition, the lowest energy absorption bands of  $[\text{Ru}(\text{Clazpy})_2\text{Cl}_2]$  were not shifted when the polarity of solvents was increased.

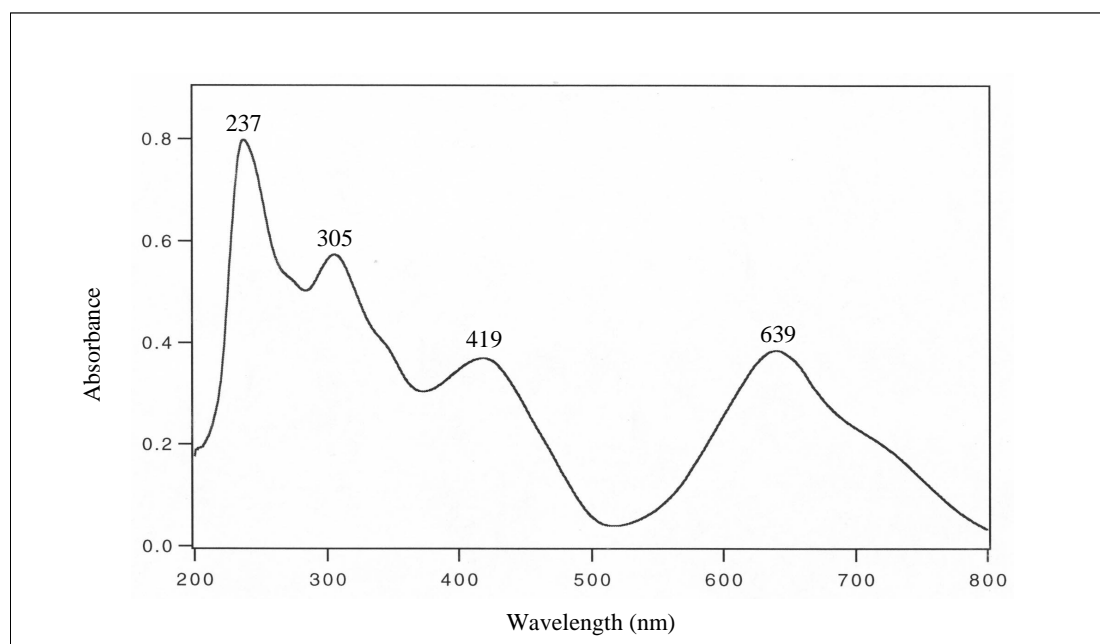


**Figure 3.23** UV-Visible absorption spectrum of *tcc*- $[\text{Ru}(\text{Clazpy})_2\text{Cl}_2]$  in  $\text{CH}_2\text{Cl}_2$

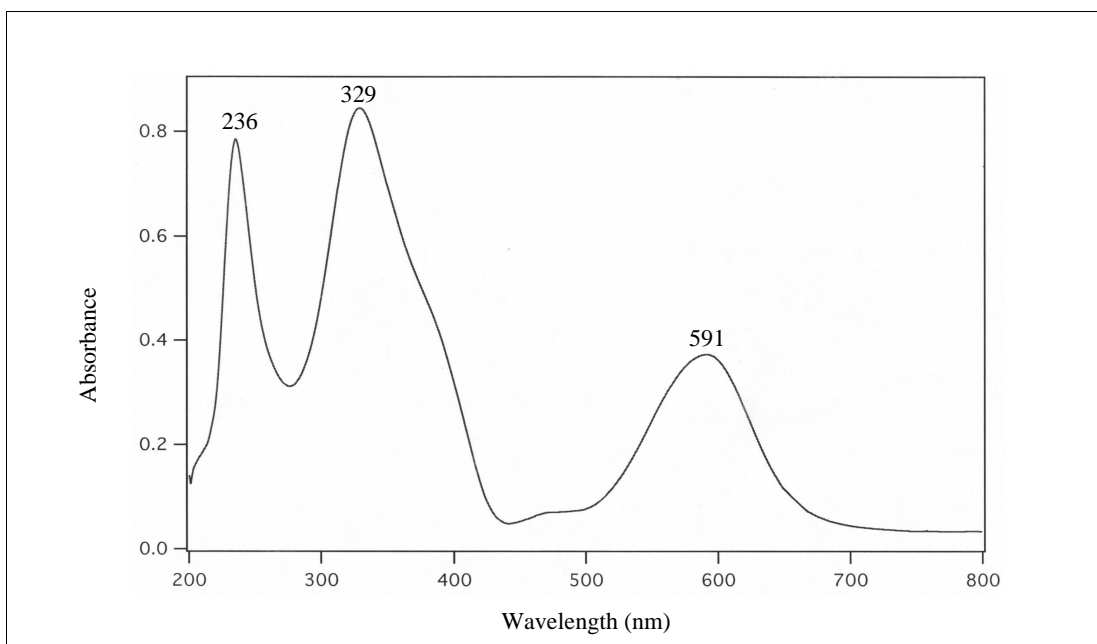


**Figure 3.24** UV-Visible absorption spectrum of *ctc*-[Ru(Clazpy)<sub>2</sub>Cl<sub>2</sub>] in CH<sub>2</sub>Cl<sub>2</sub>

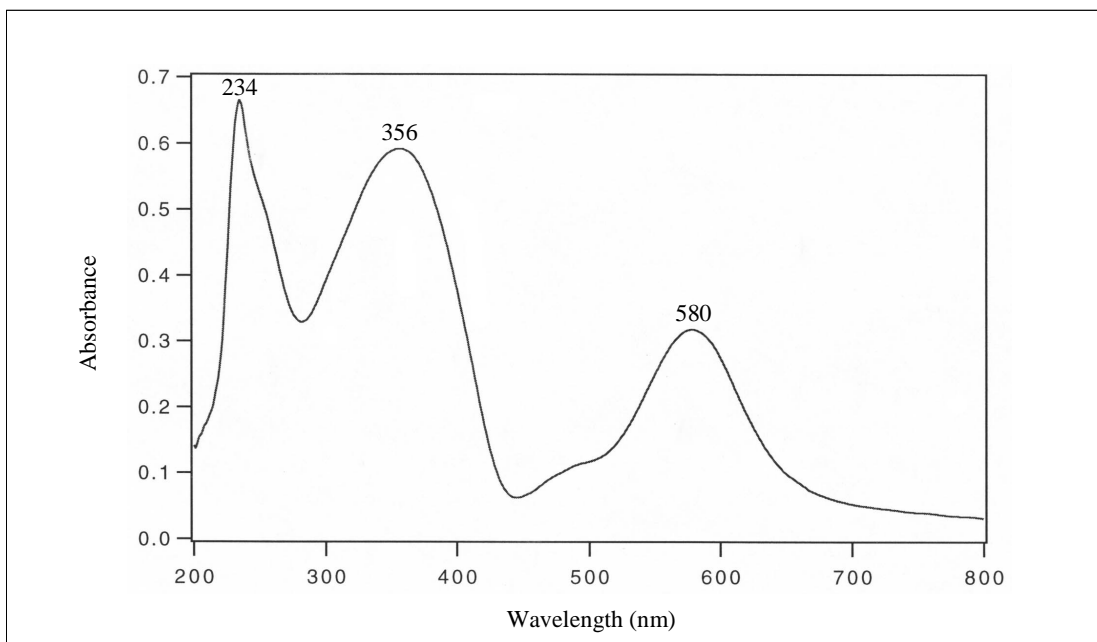


**Figure 3.25** UV-Visible absorption spectrum of *ccc*-[Ru(Clazpy)<sub>2</sub>Cl<sub>2</sub>] in CH<sub>2</sub>Cl<sub>2</sub>

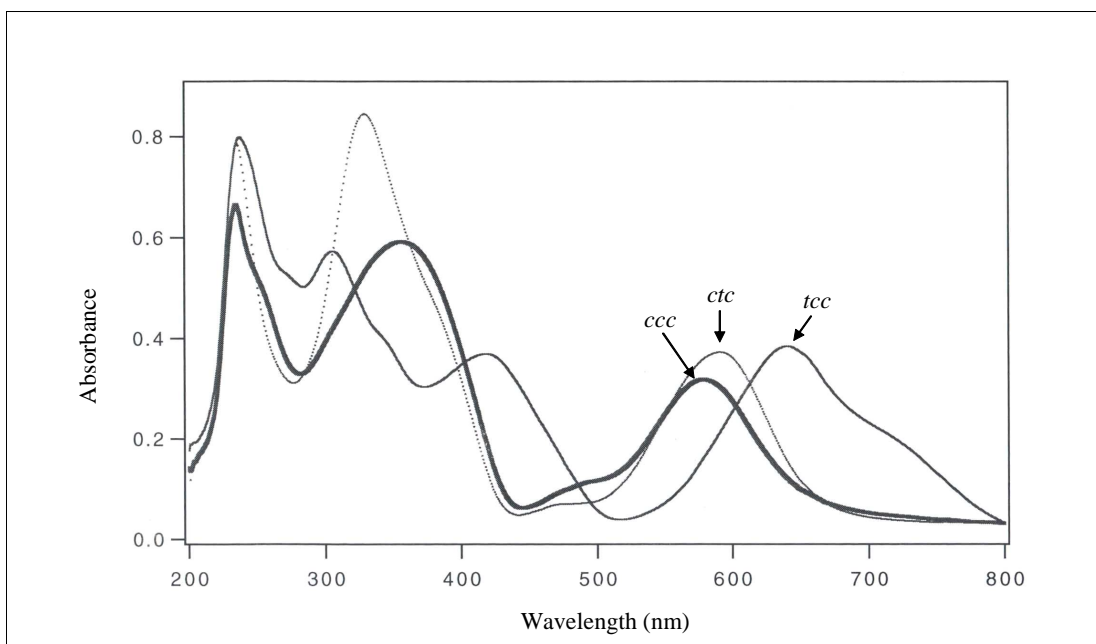


**Figure 3.26** UV-Visible absorption spectra of *tcc*-, *ctc*- and *ccc*-[Ru(Clazpy)<sub>2</sub>Cl<sub>2</sub>] in CH<sub>2</sub>Cl<sub>2</sub>

### 3.2.2.6 Nuclear Magnetic Resonance spectroscopy (1D and 2D NMR)

The isomeric [Ru(Clazpy)<sub>2</sub>Cl<sub>2</sub>] complexes were prepared in CDCl<sub>3</sub> using tetramethylsilane (Si(CH<sub>3</sub>)<sub>4</sub>) as an internal reference. Their structures were assigned by using 1D and 2D NMR (500 MHz) and the NMR spectroscopic data of isomeric [Ru(Clazpy)<sub>2</sub>Cl<sub>2</sub>] are presented in Table 3.19 to 3.21.

Nuclear magnetic resonance spectroscopy of *tcc*-[Ru(Clazpy)<sub>2</sub>Cl<sub>2</sub>]

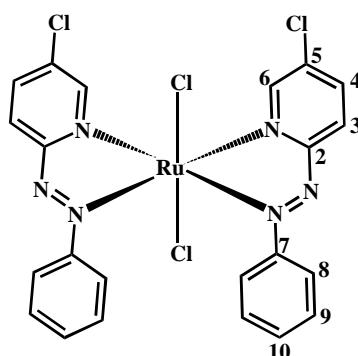


**Table 3.19**  $^1\text{H}$ - $^{13}\text{C}$  NMR spectroscopic data of *tcc*-[Ru(Clazpy) $_2$ Cl $_2$ ] in CDCl $_3$ 

H-position	$^1\text{H}$ NMR			$^{13}\text{C}$ NMR (CH-type)
	$\delta$ (ppm)	$J$ (Hz)	Amount of H	
6	8.80 (d)	2.5	1	147.72
3	8.53 (d)	8.5	1	125.01
4	8.15 (dd)	8.5, 2.5	1	140.67
8	7.52 (dd)	8.0, 1.0	2	122.91
10	7.19 (tt)	8.0, 1.0	1	130.94
9	6.98 (tt)	8.0, 1.0	2	128.24
Quaternary carbon (C)				164.06 (C2) 157.73 (C5) 130.03 (C7)

d = doublet, dd = doublet of doublet, tt = triplet of triplet

The  $^1\text{H}$  NMR spectrum (Figure 3.27) of *tcc*-[Ru(Clazpy) $_2$ Cl $_2$ ] complex showed a symmetric complex with six signals of sixteenth protons. The chemical shifts of the pyridine protons appeared at lower field than the phenyl protons, especially proton H6 (8.80 ppm) due to its position located between the coordinated nitrogen atom and inductive effect of chloride atom. The proton H3 and H4 occurred in higher field than H6 at 8.53 and 8.15 ppm, respectively. The chemical shift of phenyl protons (H8, H9 and H10) appeared at the higher field than those of proton on pyridine ring, especially proton H9 (6.98 ppm). Moreover, all protons were also confirmed their positions using simple correlation  $^1\text{H}$ - $^1\text{H}$  COSY NMR experiment (Figure 3.28).

The  $^{13}\text{C}$  NMR (Figure 3.29) results corresponded to the DEPT NMR (Figure 3.30) which showed only methane carbon. The downfield signals at 164.06, 157.73 ppm were assigned to two quaternary carbons C2 and C5, respectively. While, the high field signal at 130.03 ppm was assigned to C7. Moreover, the  $^{13}\text{C}$  NMR signals assignments were based on  $^1\text{H}$ - $^{13}\text{C}$  HMQC NMR spectrum (Figure 3.31).

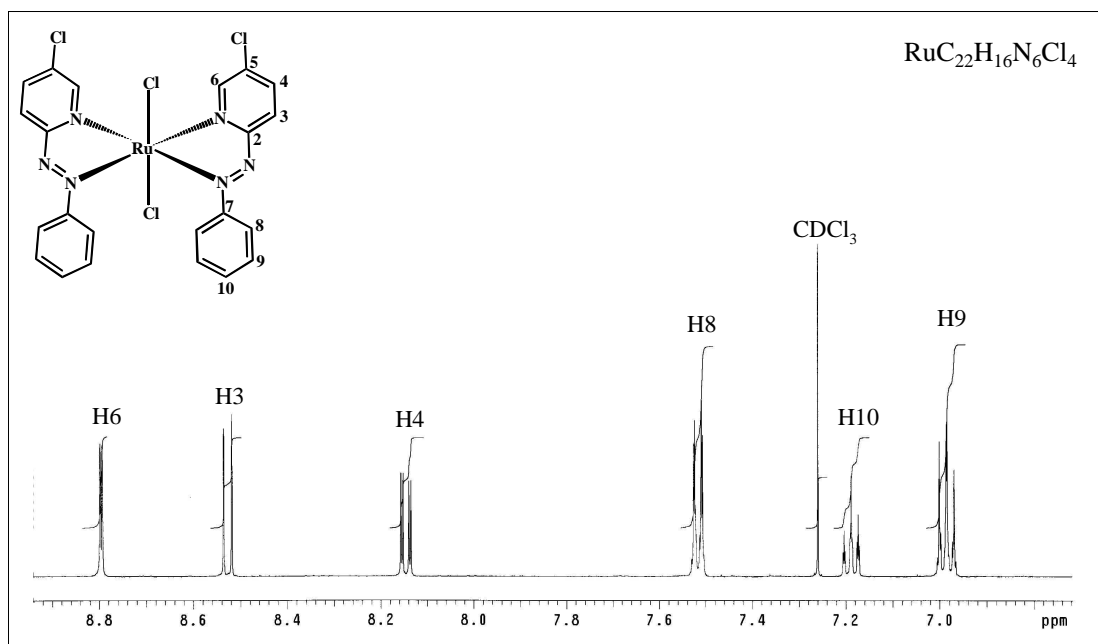


**Figure 3.27**  $^1\text{H}$  NMR spectrum of *tcc*-[Ru(Clazpy)<sub>2</sub>Cl<sub>2</sub>] in CDCl<sub>3</sub>

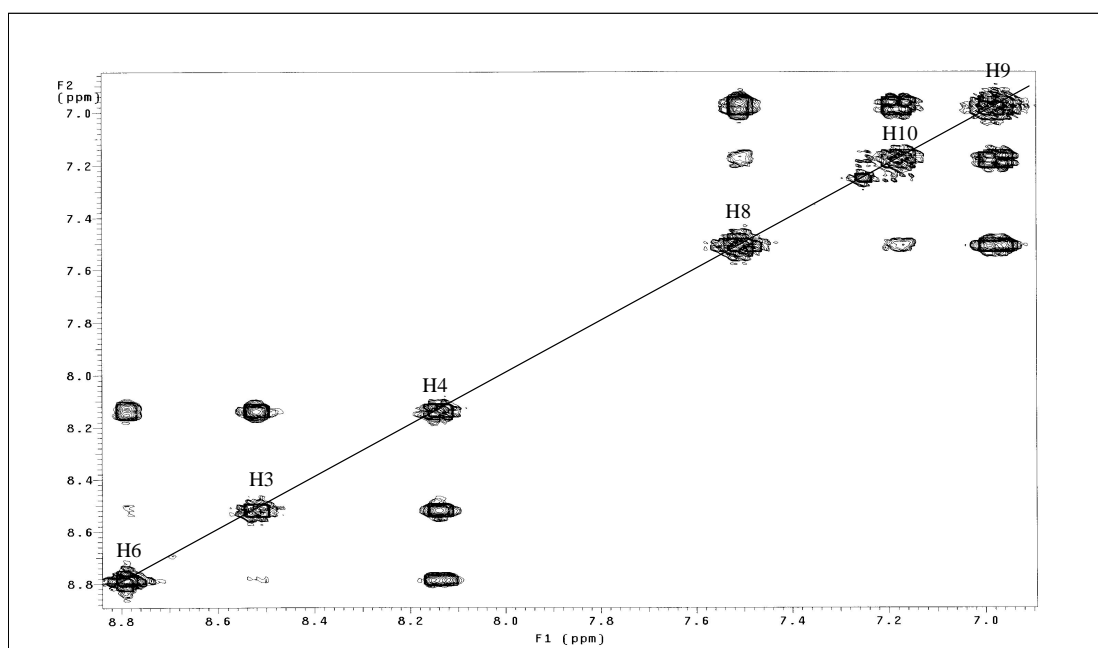


**Figure 3.28**  $^1\text{H}$ - $^1\text{H}$  COSY NMR spectrum of *tcc*-[Ru(Clazpy)<sub>2</sub>Cl<sub>2</sub>] in CDCl<sub>3</sub>

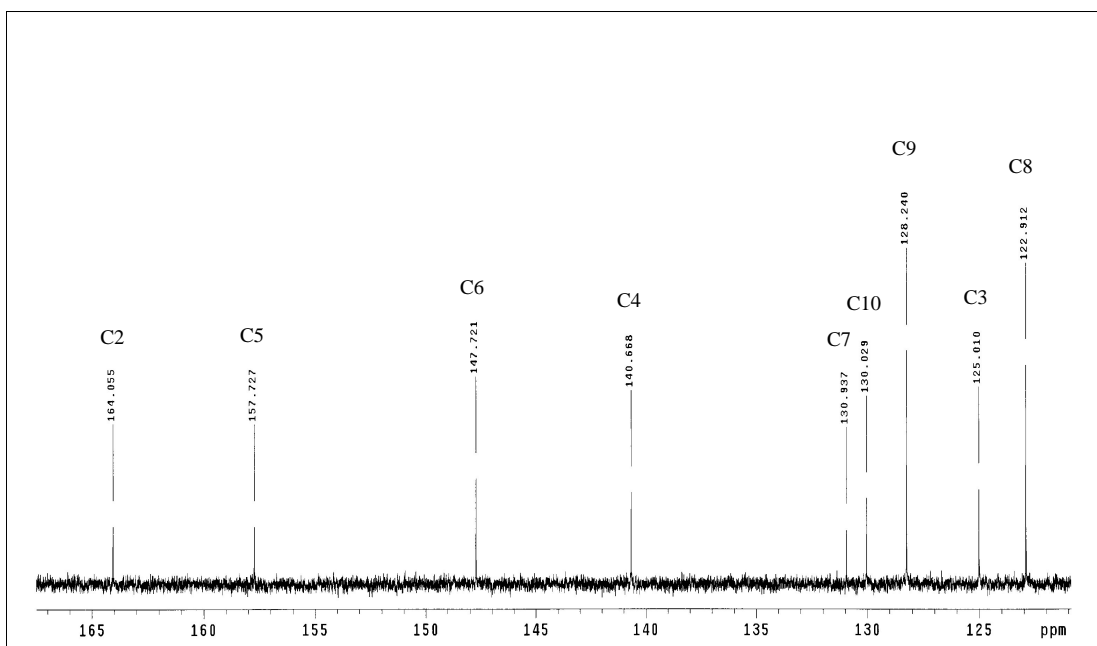


**Figure 3.29**  $^{13}\text{C}$  NMR spectrum of *tcc*-[Ru(Clazpy)<sub>2</sub>Cl<sub>2</sub>] in CDCl<sub>3</sub>

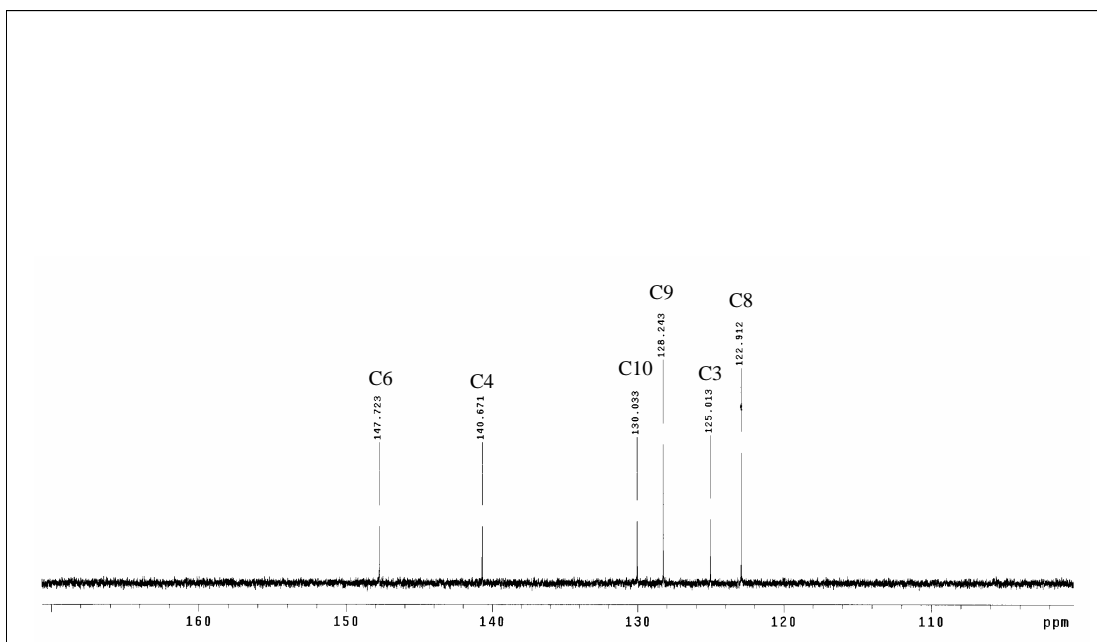


**Figure 3.30** DEPT NMR spectrum of *tcc*-[Ru(Clazpy)<sub>2</sub>Cl<sub>2</sub>] in CDCl<sub>3</sub>

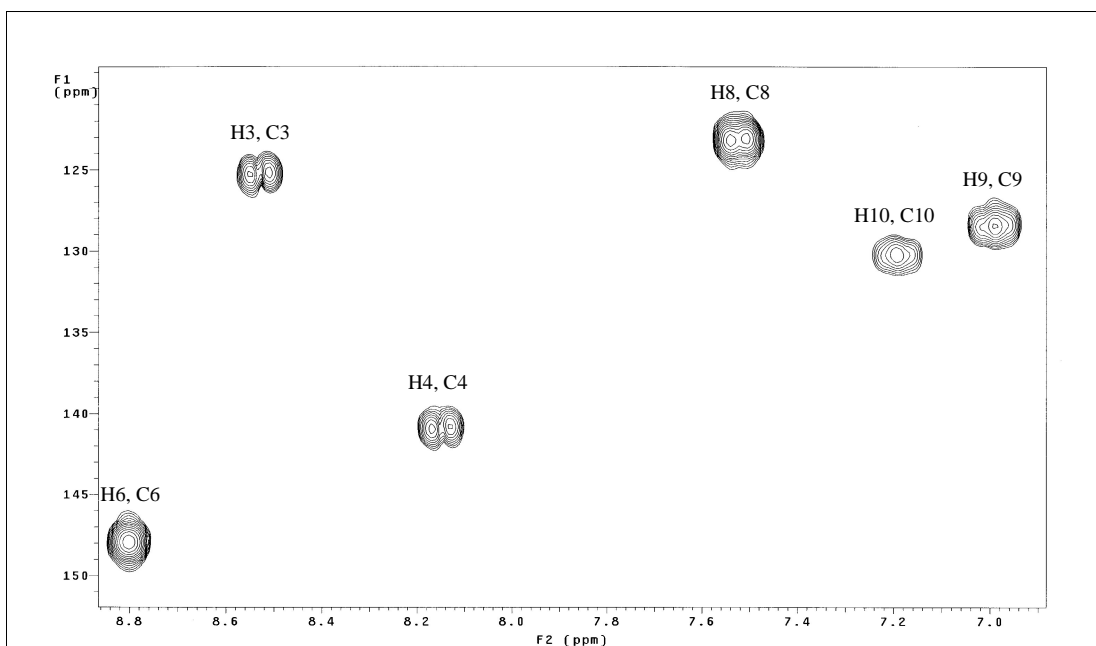


**Figure 3.31**  $^1\text{H}$ - $^{13}\text{C}$  HMQC NMR spectrum of *tcc*-[Ru(Clazpy) $_2$ Cl $_2$ ] in CDCl $_3$

Nuclear magnetic resonance spectroscopy of *ctc*-[Ru(Clazpy) $_2$ Cl $_2$ ]

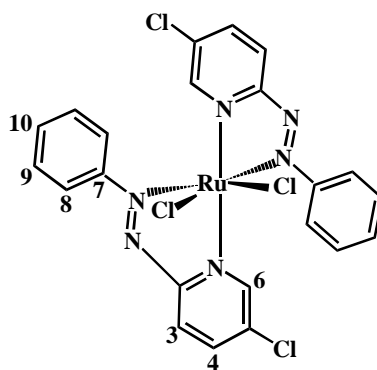


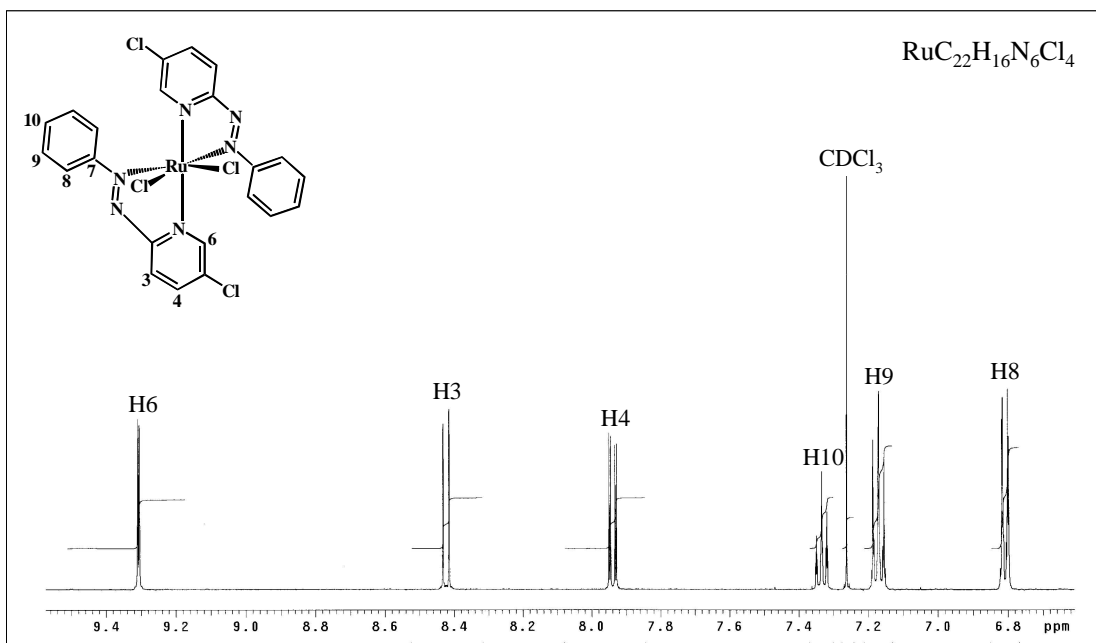
**Table 3.20**  $^1\text{H}$ - $^{13}\text{C}$  NMR spectroscopic data of *ctc*-[Ru(Clazpy) $_2$ Cl $_2$ ] in CDCl $_3$ 

H-position	$^1\text{H}$ NMR			$^{13}\text{C}$ NMR (CH-type)
	$\delta$ (ppm)	$J$ (Hz)	Amount of H	
6	9.31 (dd)	3.0, 1.0	1	150.00
3	8.42 (dd)	9.0, 1.0	1	126.82
4	7.94 (dd)	9.0, 3.0	1	137.38
10	7.33 (tt)	8.0, 1.5	1	130.51
9	7.17 (t)	8.0	2	128.67
8	6.81 (dd)	8.0, 1.5	2	121.85
Quaternary carbon (C)				164.76 (C2) 155.20 (C5) 133.14 (C7)

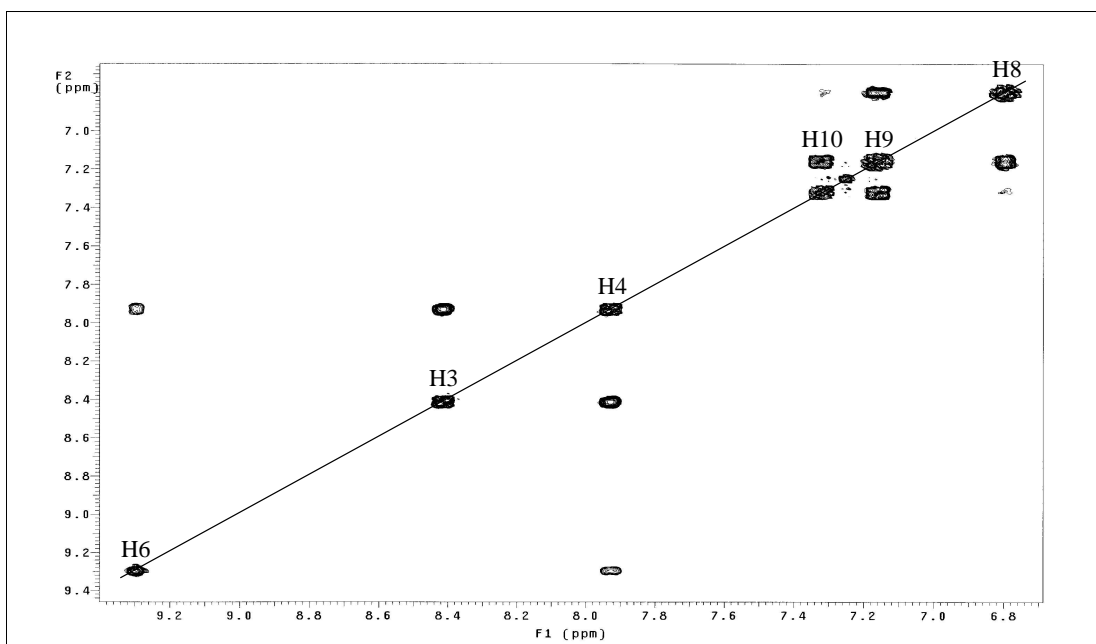
dd = doublet of doublet, t = triplet, tt = triplet of triplet

The  $^1\text{H}$  NMR spectrum (Figure 3.32) and the chemical shift values of the *ctc*-[Ru(Clazpy) $_2$ Cl $_2$ ] complex are listed in Table 3.20. Again, one set of signal was observed which similar to the results of *tcc*-[Ru(Clazpy) $_2$ Cl $_2$ ]. However, each signal in the former slightly shifted to lower field or higher field than the later. So, it suggested that it basically represents half of the molecule. The spectrum of the *ctc*-isomer is clearly divided into two parts. The downfield protons (H3, H4, H6) were due to the pyridine ring and the upfield signals referred to the phenyl protons (H8, H9, H10). The signal of proton H6 occurred at the lowest field (9.31 ppm) due to the affectiveness of both of the coordinated nitrogen and chloride atom. The proton H3 and H4 occurred at 8.42 and 7.94 ppm, respectively. The proton H8 appeared at the most high field (6.81 ppm). It was splitted by proton H9 and H10 ( $J = 8.0, 1.5$  Hz). A triplet and doublet of doublet at 7.17 and 7.33 ppm was due to proton H9 and H10, respectively. In addition, this complex was also studied by using simple correlation  $^1\text{H}$ - $^1\text{H}$  COSY NMR spectroscopy (Figure 3.33).

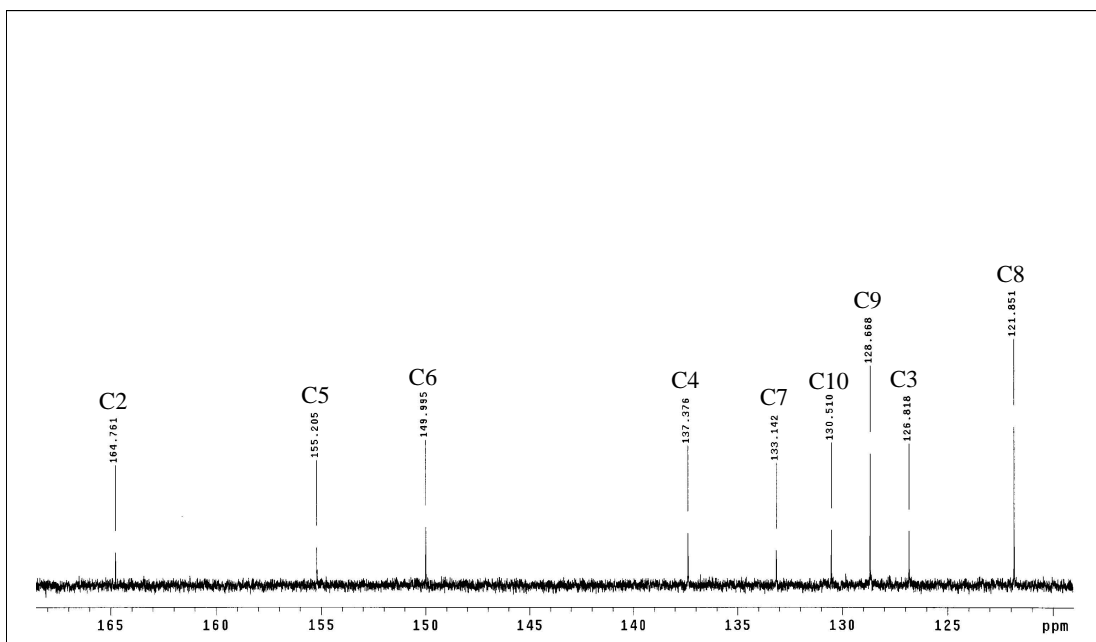
The  $^{13}\text{C}$  NMR (Figure 3.34) results corresponded to the DEPT NMR (Figure 3.35) which showed only methine carbon. The downfield signals at 164.76, 155.20 ppm were assigned to two quaternary carbons C2 and C5, respectively. While, the high field signal at 133.14 ppm was assigned to C7. Moreover, the  $^{13}\text{C}$  NMR signals assignments were based on  $^1\text{H}$ - $^{13}\text{C}$  HMQC NMR spectrum (Figure 3.36).



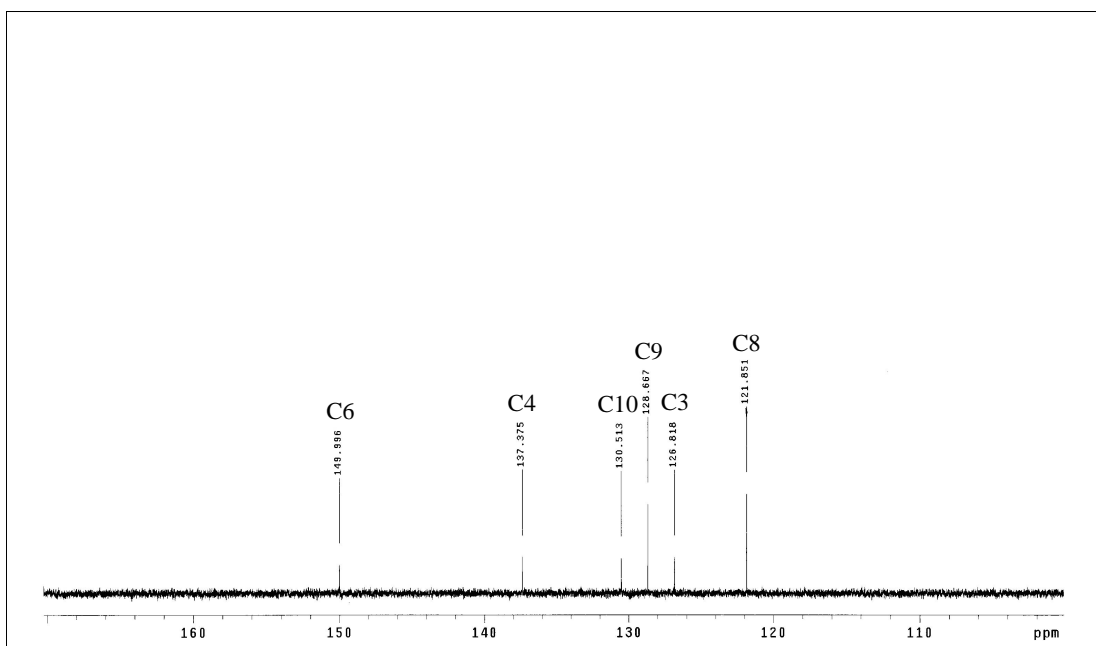
**Figure 3.32**  $^1\text{H}$  NMR spectrum of *cis*- $[\text{Ru}(\text{Clazpy})_2\text{Cl}_2]$  in  $\text{CDCl}_3$



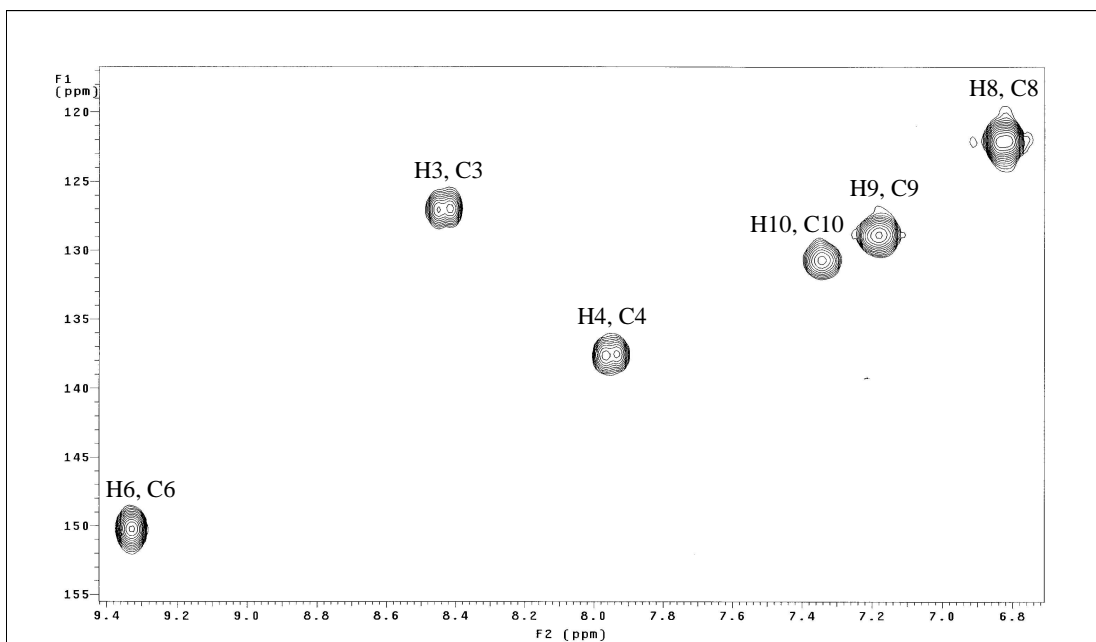
**Figure 3.33** <sup>1</sup>H-<sup>1</sup>H COSY NMR spectrum of *ctc*-[Ru(Clazpy)<sub>2</sub>Cl<sub>2</sub>] in CDCl<sub>3</sub>



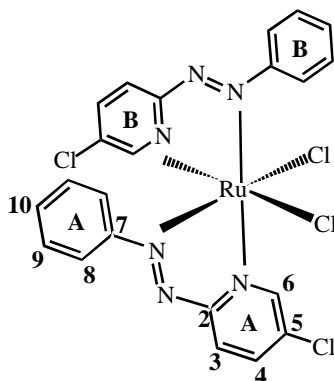
**Figure 3.34** <sup>13</sup>C NMR spectrum of *ctc*-[Ru(Clazpy)<sub>2</sub>Cl<sub>2</sub>] in CDCl<sub>3</sub>



**Figure 3.35** DEPT NMR spectrum of *ctc*-[Ru(Clazpy)<sub>2</sub>Cl<sub>2</sub>] in CDCl<sub>3</sub>



**Figure 3.36** <sup>1</sup>H-<sup>13</sup>C NMR HMQC spectrum of *ctc*-[Ru(Clazpy)<sub>2</sub>Cl<sub>2</sub>] in CDCl<sub>3</sub>

Nuclear magnetic resonance spectroscopy of *ccc*-[Ru(Clazpy)<sub>2</sub>Cl<sub>2</sub>]**Table 3.21** <sup>1</sup>H-<sup>13</sup>C NMR spectroscopic data of *ccc*-[Ru(Clazpy)<sub>2</sub>Cl<sub>2</sub>] in CDCl<sub>3</sub>

H-position	<sup>1</sup> H NMR			<sup>13</sup> C NMR (CH-type)
	δ (ppm)	J (Hz)	Amount of H	
6A	9.72 (dd)	2.5	1	148.62
3A	8.48 (dd)	8.5, 0.5	1	125.22
3B	8.35 (dd)	8.5, 0.5	1	126.57
4A	8.12 (dd)	8.5, 2.5	1	139.10
4B	7.89 (dd)	8.5, 2.0	1	138.55
8B	7.78 (dd)	8.5, 1.0	2	125.70
10B	7.49 (tt)	8.5, 1.0	1	131.54
9B	7.39 (m)		2	127.73
10A			1	130.30
9A	7.22 (t)	8.5	2	128.86
6B	7.20 (dd)	2.0, 0.5	1	147.11
8A	6.72 (dd)	8.5, 1.5	1	121.44
Quaternary carbons (C)				165.24 (C <sub>2A</sub> ), 163.54 (C <sub>2B</sub> ), 157.18 (C <sub>5A</sub> ), 155.53 (C <sub>5B</sub> ), 133.02 (C <sub>7A</sub> ), 132.56 (C <sub>7B</sub> )

dd = doublet of doublet, t = triplet, tt = triplet of triplet, m = multiplet

The  $^1\text{H}$  NMR spectrum (Figure 3.37) of *ccc*-[Ru(Clazpy) $_2$ Cl $_2$ ] showed a doublet set of Clazpy signals due to non-equivalent of ligands on the absence of  $C_2$  axis. From the proposed structure, the pyridine ring of each Clazpy ligand showed distinguish signals due to arrangement of Clazpy molecules around ruthenium center. The pyridine ring A of Clazpy located trans to N=N azo of the other one shows signal at downfield compared with pyridine ring B located trans to chlorine atom. It is to note that the N=N azo unit is  $\pi$ -electron acceptor toward ruthenium center. Consequently, phenyl ring B has more electron density than the ring A. Moreover, all protons were assigned based on  $^1\text{H}$ - $^1\text{H}$  COSY NMR spectrum (Figure 3.38).

The  $^{13}\text{C}$  NMR spectrum (Figure 3.39) showed 12 methine carbons and 6 quaternary carbons. The DEPT spectral data (Figure 3.40) presented only signal of methane carbons. Moreover, the  $^{13}\text{C}$  NMR signals assignments were based on  $^1\text{H}$ - $^{13}\text{C}$  HMQC NMR spectrum (Figure 3.41).

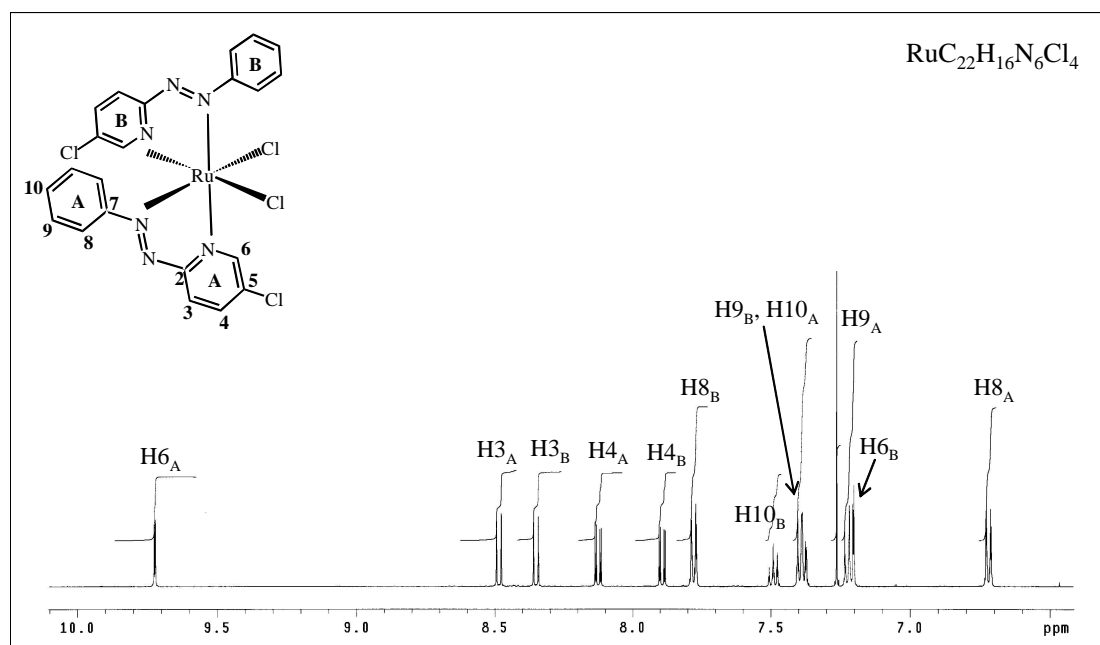


**Figure 3.37**  $^1\text{H}$  NMR spectrum of *ccc*-[Ru(Clazpy) $_2$ Cl $_2$ ] in  $\text{CDCl}_3$

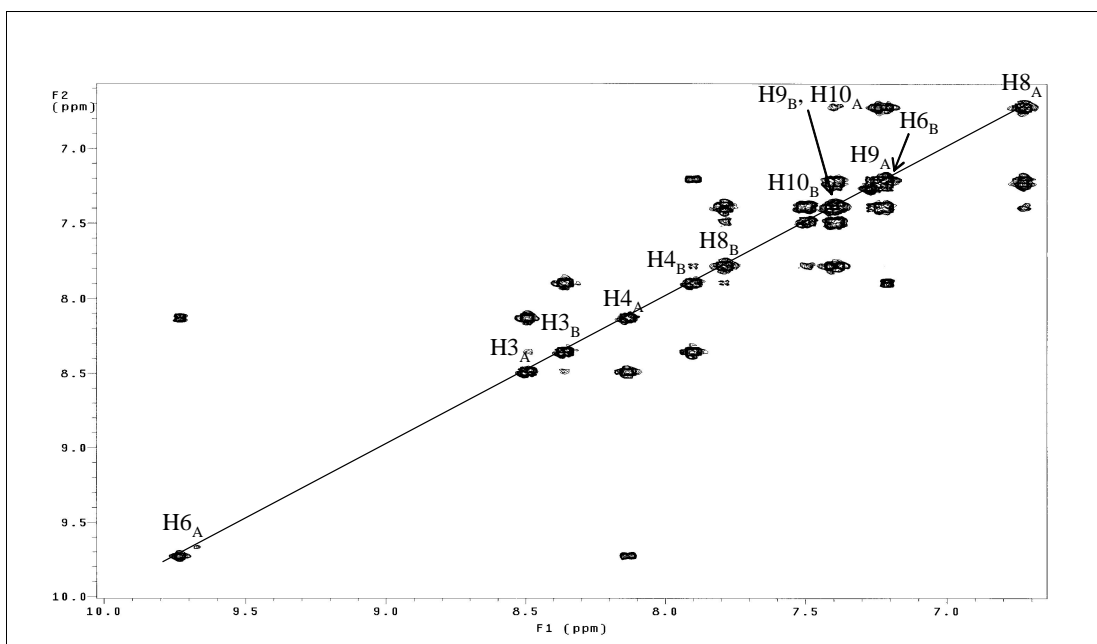


**Figure 3.38**  $^1\text{H}$ - $^1\text{H}$  COSY NMR spectrum of *ccc*-[Ru(Clazpy) $_2$ Cl $_2$ ] in CDCl $_3$

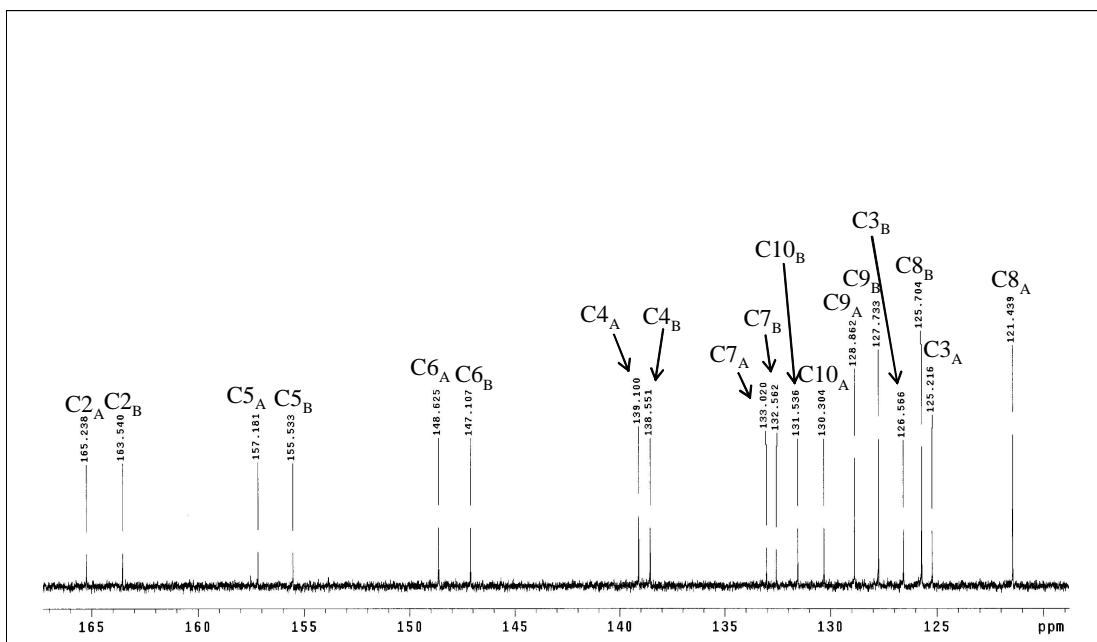


**Figure 3.39**  $^{13}\text{C}$  NMR spectrum of *ccc*-[Ru(Clazpy) $_2$ Cl $_2$ ] in CDCl $_3$

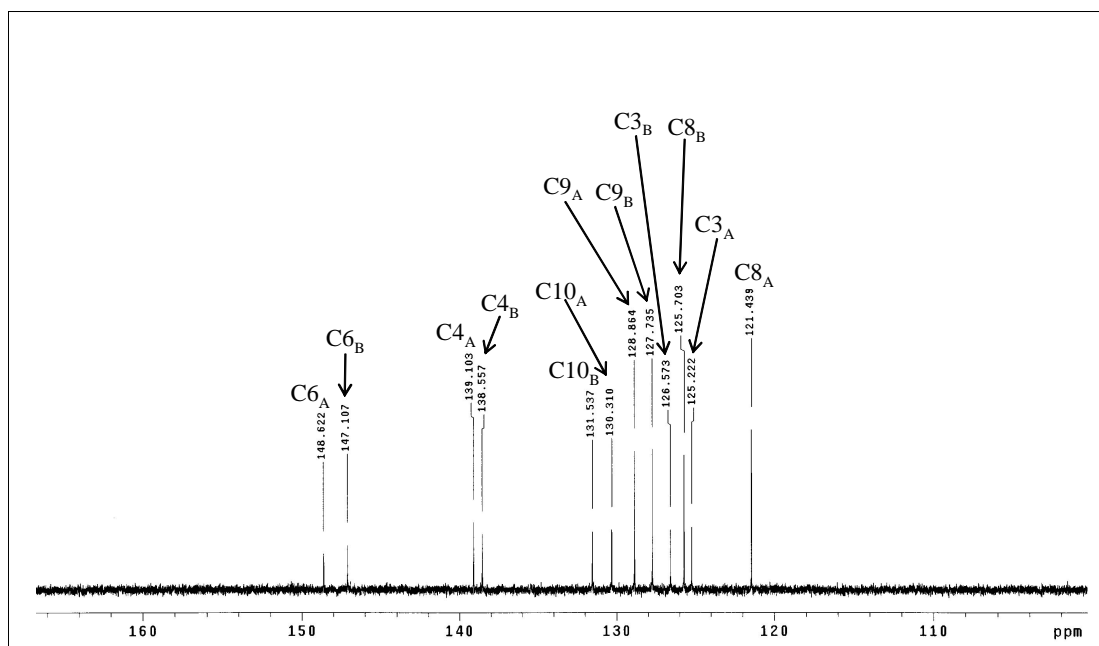


**Figure 3.40** DEPT NMR spectrum of *ccc*-[Ru(Clazpy)<sub>2</sub>Cl<sub>2</sub>] in CDCl<sub>3</sub>

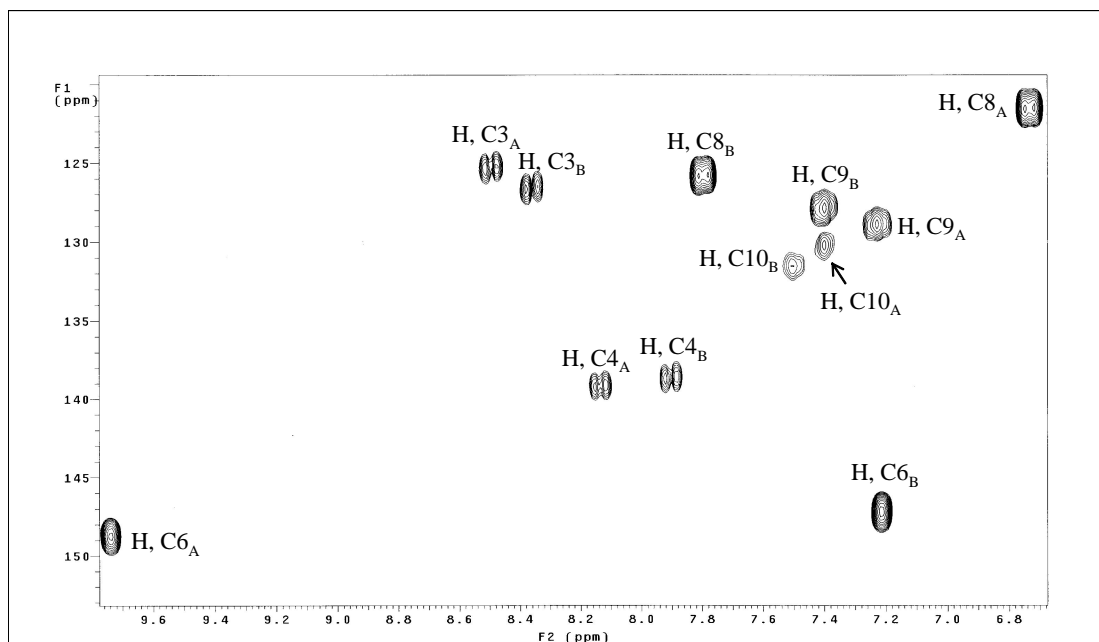


**Figure 3.41** <sup>1</sup>H-<sup>13</sup>C HMQC NMR spectrum of *ccc*-[Ru(Clazpy)<sub>2</sub>Cl<sub>2</sub>] in CDCl<sub>3</sub>

From above results, it is concluded that this method is effective to differentiate between the *cis* and *trans-isomers* of the complex with regard to both symmetrical and unsymmetrical complexes of similar configuration (Farah and Pietro, 2001). In this work, the  $^1\text{H}$  NMR spectra of the ligand compared to complexes displayed the different configuration of the complexes i.e. *tcc* and *ctc* have  $\text{C}_2$  symmetry whereas *ccc* has  $\text{C}_1$  symmetry. This is due to the arrangement of ligand around ruthenium center. For the *tcc* and *ctc*- $[\text{Ru}(\text{clazpy})_2\text{Cl}_2]$ , the Clazpy ligand are equivalents thus they showed 6 signals from sixteen protons whereas in the *ccc*- $[\text{Ru}(\text{clazpy})_2\text{Cl}_2]$ , the pyridine and phenyl rings of each ligand are non-equivalent. Thus NMR spectrum showed all proton as shown in Figure 3.37. Moreover, this technique also illustrates the conformation change of the ligand after metal complexation. In the free ligand, the lowest field resonance is due to H6 (8.69 ppm) of the pyridine whilst in the complex H6 has moved to more downfield (8.80, 9.31, 9.72 ppm in *tcc*-, *ctc*- and *ccc*- respectively). It is due to a change in electron density on the metal center upon chelation of the Clazpy ligand through its nitrogen atoms. In addition, H8 in *tcc*-isomer is shifted to down field whereas shifted to upfield in *ctc*. A change of H6 and H8 shift is caused by metal coordination. On the other hand, *ccc*-isomer is less symmetric than other forms and the signal at higher chemical shift is assigned to the *ccc*-isomer. Again, we can summarize the NMR spectra in Figure 3.42.

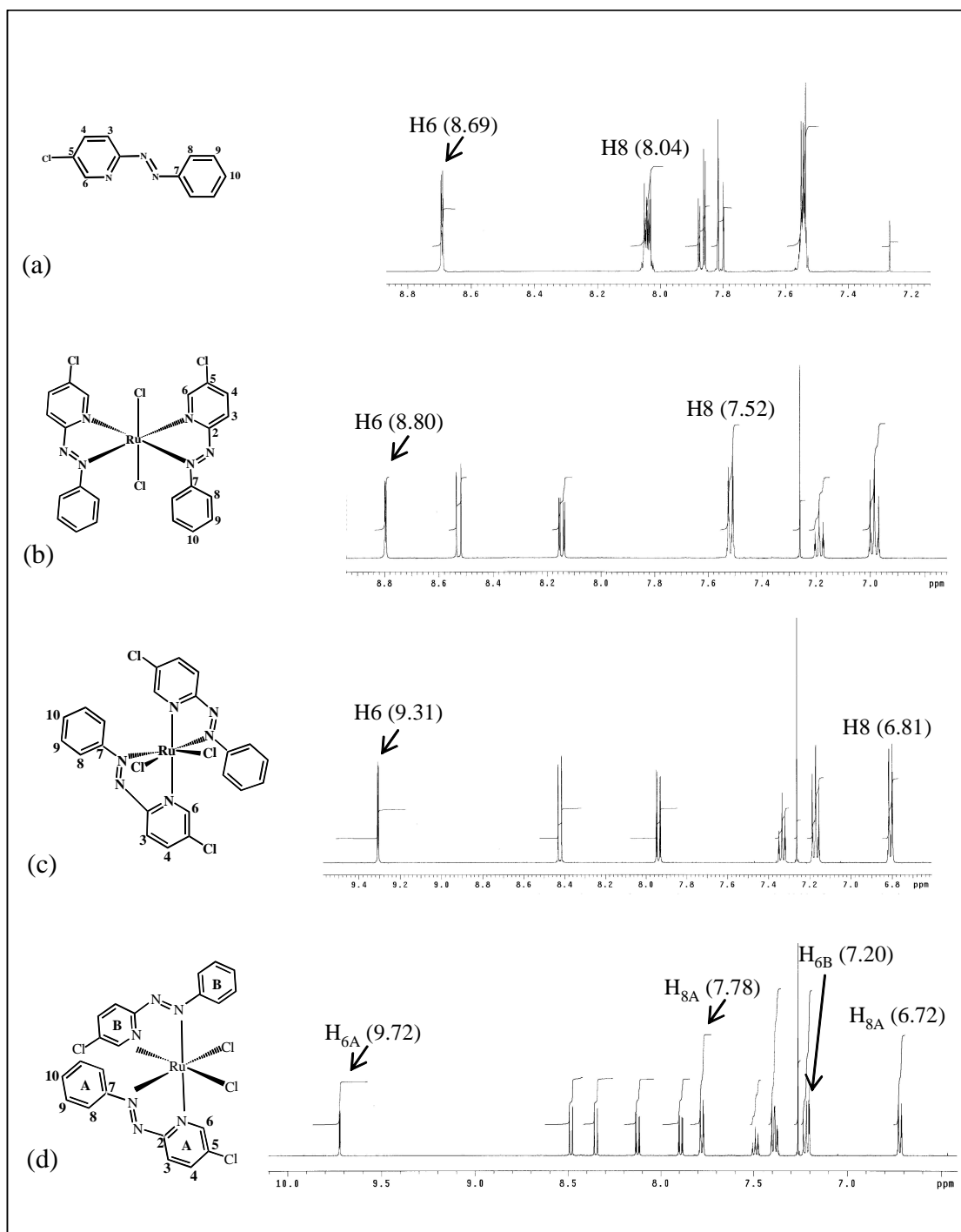


**Figure 3.42**  $^1\text{H}$  NMR spectra of (a) Clazpy; (b) *tcc*; (c) *ctc*; (d) *ccc*-[Ru(Clazpy) $_2$ Cl $_2$ ] in  $\text{CDCl}_3$ .

### 3.2.2.7 Cyclic voltammetry

The electrochemical behavior of the isomeric  $[\text{Ru}(\text{Clazpy})_2\text{Cl}_2]$  complexes has been studied in  $\text{CH}_2\text{Cl}_2$  as a solvent. All complexes exhibited couples corresponding to the metal-based oxidation and successive reduction in the sweep ranging from -2.0 to +2.0 V. The electron transfer properties are shown in Figure 3.43 to 3.45. Furthermore, the measured potentials were compared to the potential of the ferrocene couple. The cyclic voltammetric data of these compounds are listed in Table 3.22.

**Table 3.22** Cyclic voltammetric data of the isomeric  $[\text{Ru}(\text{Clazpy})_2\text{Cl}_2]$  complexes in 0.1 M TBAH  $\text{CH}_2\text{Cl}_2$  at scan rate 50 mV/s.(ferrocene as internal standard)

Compounds	<sup>a</sup> $E_{1/2}$ , V ( $\Delta E_p$ , mV)	
	Oxidation	Reduction
<i>tcc</i> - $[\text{Ru}(\text{Clazpy})_2\text{Cl}_2]$	+0.65 (95)	-0.93 (120), -1.18 <sup>b</sup>
<i>ctc</i> - $[\text{Ru}(\text{Clazpy})_2\text{Cl}_2]$	+0.82 (95)	-0.91 (105), -1.32 <sup>b</sup>
<i>ccc</i> - $[\text{Ru}(\text{Clazpy})_2\text{Cl}_2]$	+0.78 (100)	-0.91 (105), -1.46 <sup>b</sup>

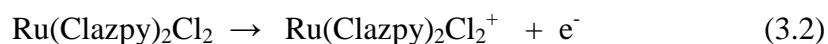
<sup>a</sup> $E_{1/2} = (E_{pa} + E_{pc})/2$ , where  $E_{pa}$  and  $E_{pc}$  are anodic and cathodic peak potentials, respectively;  $\Delta E_p = E_{pa} - E_{pc}$

<sup>b</sup>cathodic peak potential, V

In this work, each complex exhibits one oxidation and two reduction waves in the sweep range from -2.0 to +2.0 V. The pattern is similar to the most  $d^6$  metal bisazoimine complexes,  $[\text{Ru}(\text{L})_2\text{Cl}_2]$  (Misra *et al.*, 1998; Santra *et al.*, 1999). The anodic and cathodic peak separation varies from 95-120 mV.

### Oxidation potential

The potential of the isomeric  $[\text{Ru}(\text{Clazpy})_2\text{Cl}_2]$  complexes were studied in the range 0.00 to +2.00 V and one reversible couple of ruthenium(II)-ruthenium(III) was observed. The potential data of the cis complexes (*ctc*-, *ccc*-  $[\text{Ru}(\text{Clazpy})_2\text{Cl}_2]$ ) exhibited higher redox potentials by 0.1-0.2 V than the trans (*tcc*-  $[\text{Ru}(\text{Clazpy})_2\text{Cl}_2]$ ). An increase in stability of the Ru(II) state in the *ctc* and *ccc*-isomers may be due to a cis-oriented of the azoimine function. In *ctc* and *ccc*-  $[\text{Ru}(\text{Clazpy})_2\text{Cl}_2]$ , the back bonding interactions occur with two different  $d\pi$ -orbitals while in *tcc*-orientation they will compete for the same  $d\pi$ -orbitals. This may be associated with the increase in effective charge on the ruthenium in *ctc* and *ccc*-isomers and may shift the Ru(III)/(II) couple to more positive values than in *tcc* (Byabartta *et al.*, 2001). Moreover, the *ctc*- isomer showed a slightly higher Ru(II)/(III) couple (0.04 V) than that of *ccc*-isomer. The oxidation process is shown in equation 3.2.



As expected, the oxidation potential of each complex is more positive than that of the parent compounds, *ctc*- $[\text{Ru}(\text{azpy})_2\text{Cl}_2]$  (+0.71 V) (Jullapun, 2004) in according with the extension of the corresponding  $\pi$  framework. The present set of Ru(III)/(II) redox potential data of  $[\text{Ru}(\text{Clazpy})_2\text{Cl}_2]$  are higher than  $[\text{Ru}(\text{azpy})_2\text{Cl}_2]$ . This suggests that the  $\pi$ -acidity order of the ligand is arranged as following:



### Reduction potential

In the potential range from 0.00 to - 2.00 V, three isomers showed one reversible couple and one cathodic peak which were referred to the electron acceptance of the azo function in Clazpy ligand follow in equation 3.3.



From Table 3.16, the first reduction potential in *ctc* and *ccc*-[Ru(Calazpy)Cl<sub>2</sub>] (-0.91 V) complexes exhibited slightly higher values than that in *tcc*-[Ru(Clazpy)Cl<sub>2</sub>] (-0.93 V). These results indicate that the *trans*-isomer is easier oxidized than the *cis*-form. Generally, the first reduction potential can be used to determine  $\pi$ -accepting ability of ligand. From previous studies, the first reduction potential occurred at -1.03 V for *ctc*-[Ru(azpy)<sub>2</sub>Cl<sub>2</sub>] (Jullapun, 2004). These results showed that the Clazpy ligand is a better  $\pi$ -acceptor than azpy as listed in Table 3.23.

**Table 3.23** Cyclic voltammetric data of ruthenium(II) complexes in 0.1 M TBAH CH<sub>2</sub>Cl<sub>2</sub> at scan rate 50 mV/s. (ferrocene as internal standard)

Compounds	<sup>a</sup> E <sub>1/2</sub> , V ( $\Delta E_p$ , mV)	
	Oxidation	Reduction
Clazpy	-	-1.57
<i>tcc</i> -[Ru(Clazpy) <sub>2</sub> Cl <sub>2</sub> ]	+0.65 (95)	-0.93 (120), -1.18 <sup>b</sup>
<i>ctc</i> -[Ru(Clazpy) <sub>2</sub> Cl <sub>2</sub> ]	+0.82 (95)	-0.91 (105), -1.32 <sup>b</sup>
<i>ccc</i> -[Ru(Clazpy) <sub>2</sub> Cl <sub>2</sub> ]	+0.78 (100)	-0.91 (105), -1.46 <sup>b</sup>
azpy	-	-1.96 <sup>b</sup>
<i>ctc</i> -[Ru(azpy) <sub>2</sub> Cl <sub>2</sub> ] <sup>c</sup>	+0.71	-1.03, -1.55 <sup>b</sup>

<sup>a</sup>E<sub>1/2</sub> = (E<sub>pa</sub> + E<sub>pc</sub>)/2, where E<sub>pa</sub> and E<sub>pc</sub> are anodic and cathodic peak potentials, respectively;  $\Delta E_p = E_{pa} - E_{pc}$

<sup>b</sup>cathodic peak potential, V

<sup>c</sup>Jullapun, 2004

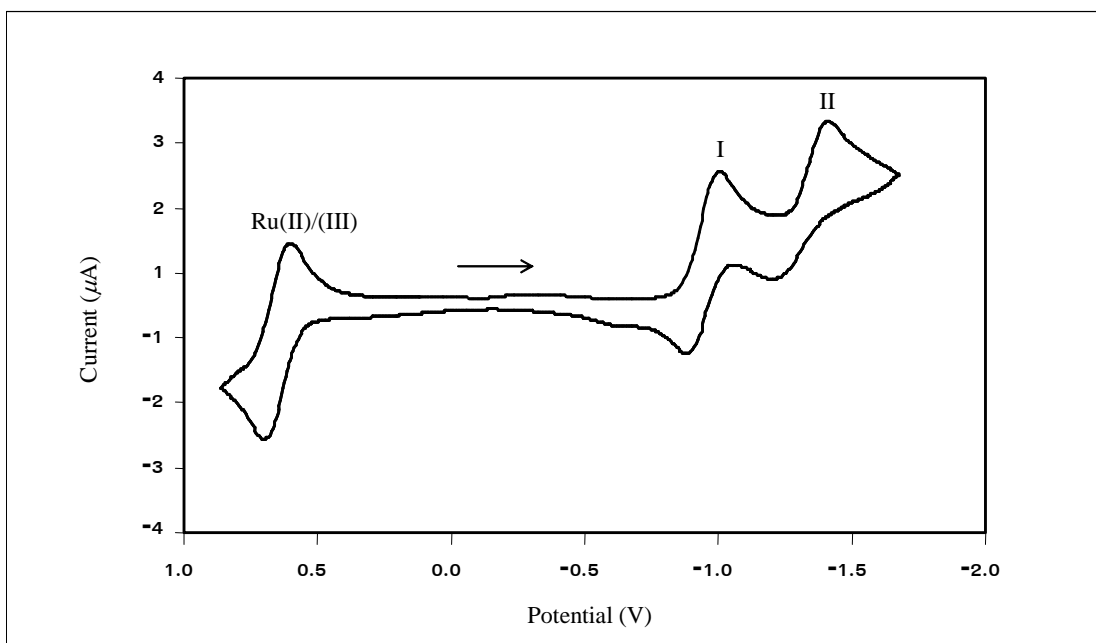


**Figure 3.43** Cyclic voltammogram of *tcc*-[Ru(Clazpy)<sub>2</sub>Cl<sub>2</sub>] in 0.1 M TBAH CH<sub>2</sub>Cl<sub>2</sub> at scan rate 50 mV/s (ferrocene as an internal standard)

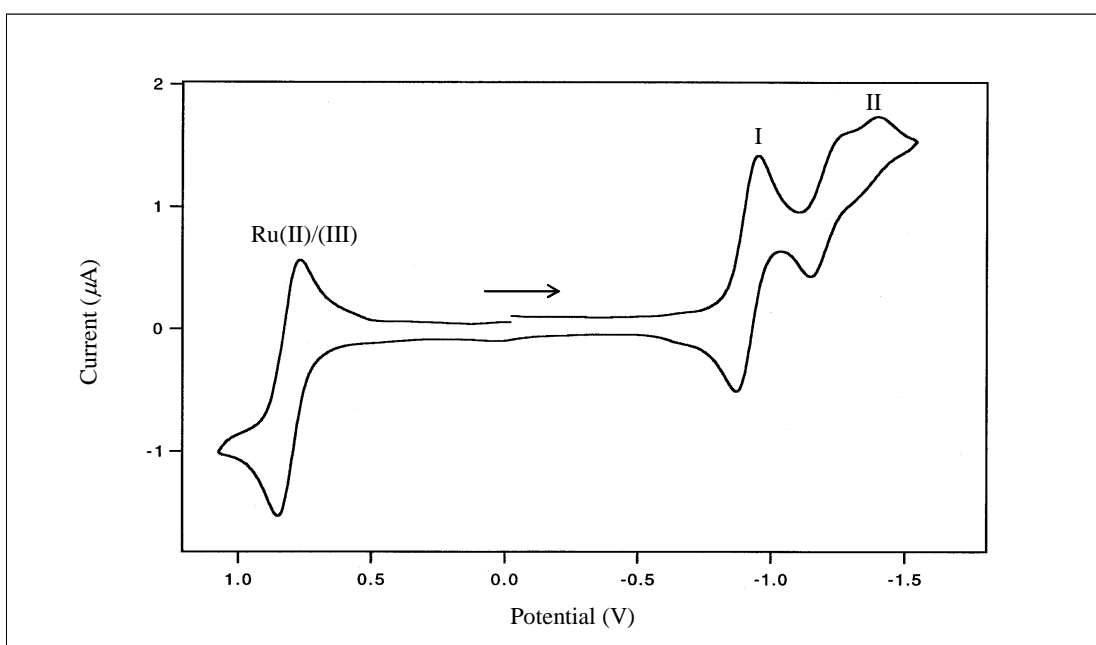


**Figure 3.44** Cyclic voltammogram of *ctcc*-[Ru(Clazpy)<sub>2</sub>Cl<sub>2</sub>] in 0.1 M TBAH CH<sub>2</sub>Cl<sub>2</sub> at scan rate 50 mV/s (ferrocene as an internal standard)

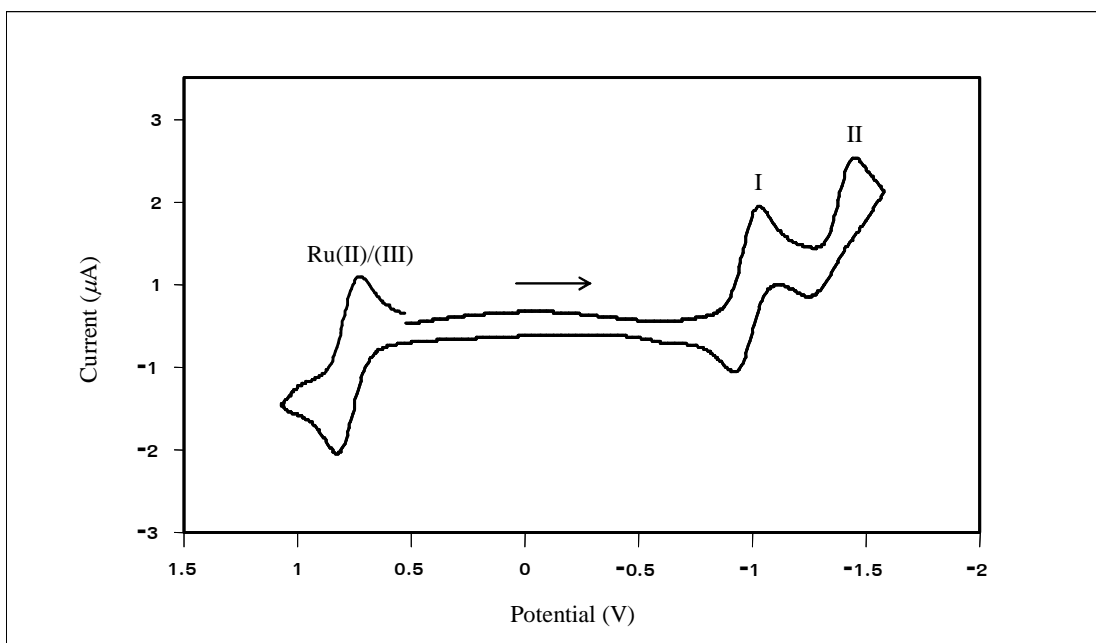


**Figure 3.45** Cyclic voltammogram of *ccc*-[Ru(Clazpy)<sub>2</sub>Cl<sub>2</sub>] in 0.1 M TBAH CH<sub>2</sub>Cl<sub>2</sub> at scan rate 50 mV/s (ferrocene as an internal standard)

### 3.3 Synthesis and characterization of [Ru(Clazpy)(5dmazpy)Cl<sub>2</sub>]

#### 3.3.1 Synthesis of the [Ru(Clazpy)(5dmazpy)Cl<sub>2</sub>] complex

[Ru(Clazpy)(5dmazpy)Cl<sub>2</sub>] was synthesized by the reaction of RuCl<sub>3</sub>·3H<sub>2</sub>O and Clazpy in DMF. First, *ctc*-[Ru(Clazpy)<sub>2</sub>Cl<sub>2</sub>] occurred as a major product like other bisazopyridine ruthenium complexes (Santra *et al.*, 1999). Moreover, if the reaction proceeded for 3 h, the amount of *ctc*-[Ru(Clazpy)<sub>2</sub>Cl<sub>2</sub>] was decreased with increasing the [Ru(Clazpy)(5dmazpy)Cl<sub>2</sub>] as a mixed-azoimine complex. It is interesting to note that the high-boiling point of DMF play a significant role for substitution reaction on a Clazpy ligand by replacing the chloride atom with nucleophile (-N(CH<sub>3</sub>)<sub>2</sub>) dissociated from solvent, followed by the addition-elimination mechanism (Figure 3.46) to give the 5dmazpy ligand within the same molecule.

To prove the occurrence of the [Ru(Clazpy)(5dmazpy)Cl<sub>2</sub>] complex from *ctc*-[Ru(Clazpy)<sub>2</sub>Cl<sub>2</sub>], the monitoring a reaction using TLC of *ctc*-[Ru(Clazpy)<sub>2</sub>Cl<sub>2</sub>] in DMF was studied. The results showed that the solution turned from blue to dark green indicating [Ru(Clazpy)(5dmazpy)Cl<sub>2</sub>], if the reaction proceeded from 5 to 40 min. The desired product was purified by chromatographic process. The neutral-air stable complex is remainly unchanged upon exposure to air even in solution for a month. The physical properties of this complex are summarized in Table 3.24.

**Table 3.24** The physical properties of [Ru(Clazpy)(5dmazpy)Cl<sub>2</sub>]

Complex	Physical properties			
	Appearance	Color	Solution	Melting point (°C)
[Ru(Clazpy)(5dmazpy)Cl <sub>2</sub> ]	solid	dark green	dark green	more than 360

The solubility of 0.0012 g of  $[\text{Ru}(\text{Clazpy})(5\text{dmazpy})\text{Cl}_2]$  was tested in 10 mL of various organic solvents such as hexane, toluene,  $\text{CHCl}_3$ ,  $\text{CH}_2\text{Cl}_2$ , EtOAc,  $\text{CH}_3\text{OCH}_3$ , DMF, DMSO,  $\text{CH}_3\text{CN}$ , EtOH, MeOH and  $\text{H}_2\text{O}$ . The results showed that this complex was slightly soluble in EtOAc, toluene, EtOH and MeOH and it was more soluble in  $\text{CH}_3\text{OCH}_3$ ,  $\text{CHCl}_3$ ,  $\text{CH}_2\text{Cl}_2$ ,  $\text{CH}_3\text{CN}$ , DMF, DMSO but insoluble in hexane and water.

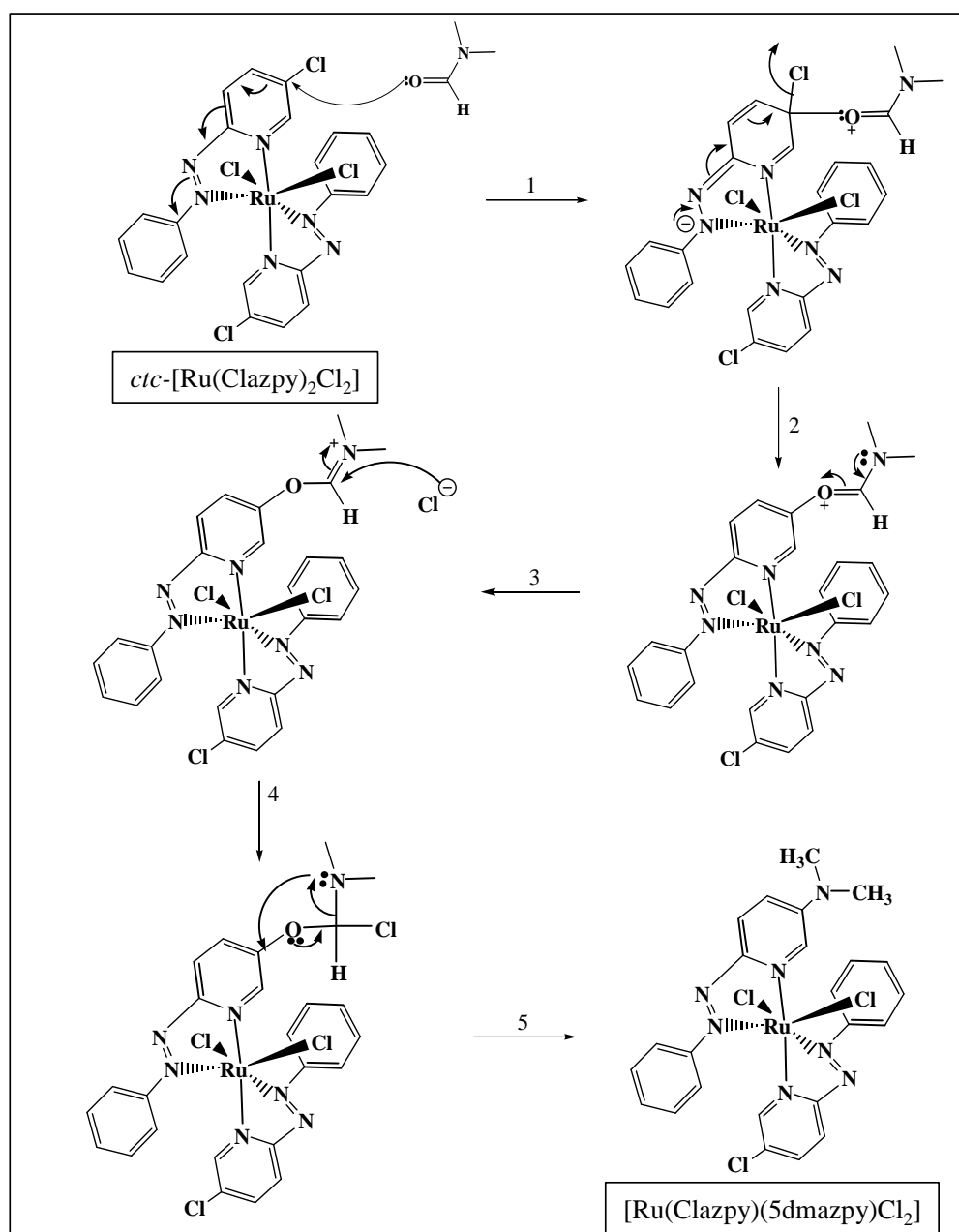


**Figure 3.46** The proposed mechanism of  $[\text{Ru}(\text{Clazpy})(5\text{dmazpy})\text{Cl}_2]$

### 3.3.2 Characterization of [Ru(Clazpy)(5dmazpy)Cl<sub>2</sub>]

The chemistry of [Ru(Clazpy)(5dmazpy)Cl<sub>2</sub>] was characterized by elemental analysis, Mass spectrometry, Infrared spectroscopy, UV-Visible absorption spectroscopy and Nuclear Magnetic Resonance spectroscopy (1D and 2D NMR). The electrochemical property of this complex was studied by using cyclic voltammetric technique.

#### 3.3.2.1 Elemental analysis

The analytical values of [Ru(Clazpy)(5dmazpy)Cl<sub>2</sub>] consistent with the calculated values. The result is given in Table 3.25.

**Table 3.25** Elemental analysis data of the [Ru(Clazpy)(5dmazpy)Cl<sub>2</sub>] complex

Complex	% C		% H		% N	
	Calc.	Found	Calc.	Found	Calc.	Found
[Ru(Clazpy)(5dmazpy)Cl <sub>2</sub> ]	46.80	46.81	3.60	3.59	15.92	15.99

#### 3.3.2.2 X-ray crystallography

The X-ray crystallography is the most important technique to confirm the geometry of compounds. The single crystal of [Ru(Clazpy)(5dmazpy)Cl<sub>2</sub>] showed six coordination around the ruthenium atom.

X-ray structure of [Ru(Clazpy)(5dmazpy)Cl<sub>2</sub>]

Crystals suitable for X-ray analysis were grown by slow diffusion of toluene into a CH<sub>2</sub>Cl<sub>2</sub> solution at room temperature. The crystal structure for [Ru(Clazpy)(5dmazpy)Cl<sub>2</sub>] is shown in Figure 3.47. The crystallographic data are shown in Table 3.26. Selected bond parameters associated with the metal ions are listed in Table 3.27.

**Table 3.26** Crystal data and structure refinement for [Ru(Clazpy)(5dmazpy)Cl<sub>2</sub>]

Empirical formula	C <sub>24</sub> H <sub>22</sub> Cl <sub>3</sub> N <sub>7</sub> Ru
Formula weight	615.95
Temperature	293(2) K
Wavelength	0.71073 Å
Crystal system	Monoclinic
Space group	<i>P</i> 2 <sub>1</sub> / <i>c</i>
Unit cell dimensions	<i>a</i> = 17.4358(13) Å $\alpha$ = 90° <i>b</i> = 10.5913(8) Å $\beta$ = 116.5740(10)° <i>c</i> = 15.7185(12) Å $\gamma$ = 90°
Volume	2596.1(3) Å <sup>3</sup>
<i>Z</i>	4
Density (calculated)	1.576 Mg/m <sup>3</sup>
Absorption coefficient	0.940 mm <sup>-1</sup>
<i>F</i> (000)	1240
Crystal size	0.3 x 0.3 x 0.25 mm <sup>3</sup>
Refinement method	Full-matrix least-squares on <i>F</i> <sup>2</sup>
Goodness-of-fit on <i>F</i> <sup>2</sup>	1.067
Final <i>R</i> indices [ <i>I</i> > 2σ( <i>I</i> )]	<i>R</i> 1 = 0.0322, <i>wR</i> 2 = 0.0765
<i>R</i> indices (all data)	<i>R</i> 1 = 0.0369, <i>wR</i> 2 = 0.0790

**Table 3.27** Selected bond lengths (Å) and angles (°) and estimated standard deviations for [Ru(Clazpy)(5dmazpy)Cl<sub>2</sub>]

Ru(1)-N(1)	2.040(2)	Ru(1)-Cl(1)	2.422(1)
Ru(1)-N(2)	1.943(2)	Ru(1)-Cl(2)	2.401(1)
Ru(1)-N(4)	2.030(2)	N(2)-N(3)	1.293(4)
Ru(1)-N(5)	2.005(2)	N(5)-N(6)	1.288(4)
C(13)-N(7)	1.354(4)	C(2)-Cl(3)	1.725(5)
Angles			
N(1)-Ru(1)-N(4)	172.4(1)	N(1)-Ru(1)-N(5)	101.6(1)
N(2)-Ru(1)-N(4)	96.1(1)	N(2)-Ru(1)-N(5)	100.1(1)
N(4)-Ru(1)-N(5)	76.8(1)	N(1)-Ru(1)-N(2)	76.8(1)
Cl(1)-Ru(1)-Cl(2)	89.86(3)	Cl(1)-Ru(1)-N(1)	96.42(7)
Cl(1)-Ru(1)-N(2)	172.82(9)	Cl(1)-Ru(1)-N(4)	90.77(6)
Cl(1)-Ru(1)-N(5)	83.48(7)	Cl(2)-Ru(1)-N(1)	87.38(9)
Cl(2)-Ru(1)-N(2)	87.50(9)	Cl(2)-Ru(1)-N(4)	95.04(8)
Cl(2)-Ru(1)-N(5)	169.31(6)		

In [Ru(Clazpy)(5dmazpy)Cl<sub>2</sub>], Ru(II) is in octahedral environment bonded to two nitrogen atoms of the Clazpy, two nitrogen atoms of the 5dmazpy and two chloride atoms. The chloro ligands are *cis*, whereas the nitrogen pyridine atoms are *trans*. The pyridine N atom, N(1) of Clazpy is *trans* to that of 5dmazpy, N(4). The Ru(1)-N(4) bond length (2.030(2)Å) of 5dmazpy is shorter than the Ru(1)-N(1) (2.040(2)Å) distance. This shortening may be due to the effect of N(CH<sub>3</sub>)<sub>2</sub> group on the pyridine ring of 5dmazpy. The N(CH<sub>3</sub>)<sub>2</sub> acts as a better electron donating group to the pyridine ring than the chlorine atom and makes the pyridine of 5dmazpy stronger  $\sigma$  donor than that of Clazpy corresponding to the bond length of N(7)-C(13) 1.354(4)Å of 5dmazpy and Cl(3)-C(2) 1.725(5)Å of Clazpy, respectively. In addition, both of the Ru-N(py) from 5dmazpy and Clazpy are shorter than those in

[Ru(azpy)<sub>2</sub>Cl<sub>2</sub>] (2.045(4)Å, 2.051(4)Å) (Seal and Ray, 1984), [Ru(Hsazpy)Cl<sub>2</sub>] (2.032(7)Å) (Hotze *et al.*, 2004) and [Ru(4mazpy)<sub>2</sub>Cl<sub>2</sub>] (2.032(7)Å, 2.057(7)Å) (Hotze *et al.*, 2004) but longer than those in [Ru(azpy)(bpy)Cl<sub>2</sub>] (2.028(2)Å) having an azoimine ligand (Hotze *et al.*, 2004). Moreover, the increasing electron density on ruthenium center gives rise to the shortening Ru-N(2) distance of Clazpy (1.943(2)Å) compared with Ru-N(5) distance of 5dmazpy (2.005(3)Å). The average these bond (1.974(2)Å) in the title compound are comparable to [Ru(4mazpy)<sub>2</sub>Cl<sub>2</sub>] (1.977(6)Å) (Hotze *et al.*, 2004) but shorter than those in [Ru(Hsazpy)<sub>2</sub>Cl<sub>2</sub>] (2.011(7)Å, 1.981(7)Å) (Hotze *et al.*, 2004) and longer than those in [Ru(azpy)(bpy)Cl<sub>2</sub>] (1.937(2)Å) (Hotze *et al.*, 2004). It is noted that the N(2)-N(3) distance (1.293(4)Å) in Clazpy is longer than that of the N(5)-N(6) bond length (1.288(4)Å) in 5dmazpy. This indicates that the Clazpy ligand is a better  $\pi$ -acceptor than the 5dmazpy ligand. Moreover, the Ru-Cl(1) bond (2.422(1)Å) which is trans to N=N(azo) of Clazpy is longer than that in the Ru-Cl(2) bond (2.401(1)Å) which trans to 5dmazpy and comparable to those of [Ru(azpy)<sub>2</sub>Cl<sub>2</sub>] complex (2.401(1), 2.397(1)Å) (Seal and Ray, 1984) and other compounds. The bite angles of Clazpy and 5dmazpy are 76.8(1)<sup>o</sup>. This makes the molecule distorted octahedral.

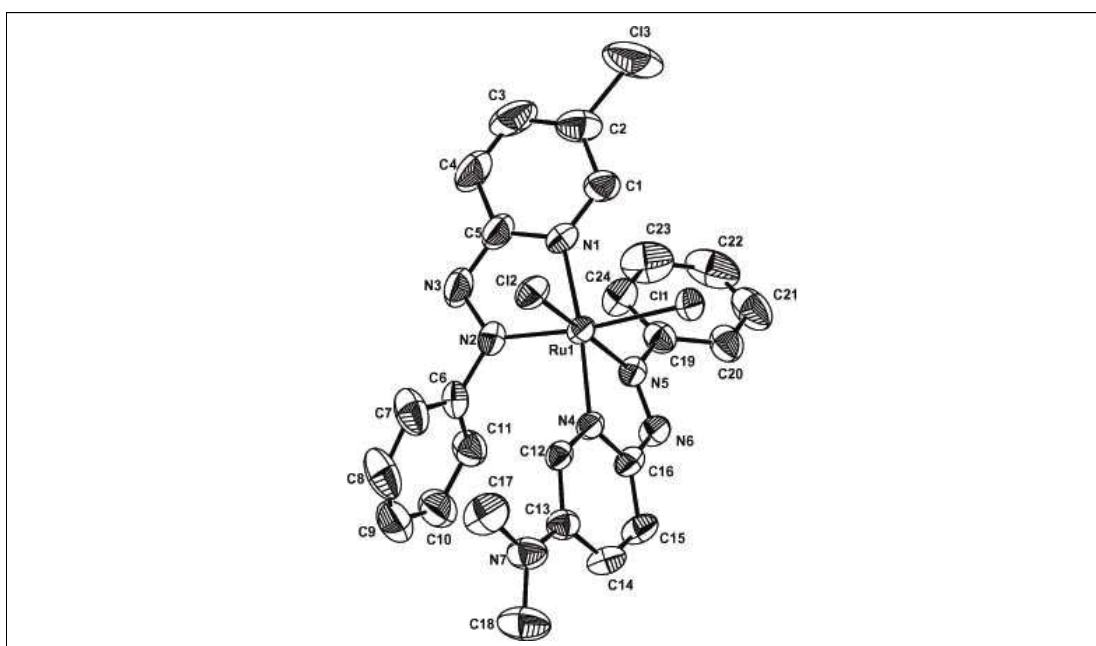


**Figure 3.47** The structure of [Ru(Clazpy)(5dmazpy)Cl<sub>2</sub>] (H-atom omitted)

### 3.3.2.3 Fast- atom bombardment(FAB)

The FAB mass spectrum of  $[\text{Ru}(\text{Clazpy})(5\text{dmazpy})\text{Cl}_2]$  complex is shown in Figure 3.48. The results are given in Table 3.28.

**Table 3.28** FAB mass spectrometric data of  $[\text{Ru}(\text{Clazpy})(5\text{dmazpy})\text{Cl}_2]$

m/z	Stoichiometry	Equivalent species	Rel. Abun. (%)
$[\text{Ru}(\text{Clazpy})(5\text{dmazpy})\text{Cl}_2]$			
617	$[\text{Ru}(\text{Clazpy})(5\text{dmazpy})\text{Cl}_2 + \text{H}]^+$	$[\text{M}+\text{H}]^+$	100
580	$[\text{Ru}(\text{Clazpy})(5\text{dmazpy})\text{Cl}]^+$	$[\text{M}-\text{Cl}]^+$	86

M = molecular weight (MW) of  $[\text{Ru}(\text{Clazpy})(5\text{dmazpy})\text{Cl}_2] = 616.00 \text{ g/mol}$

The FAB mass spectrum of  $[\text{Ru}(\text{Clazpy})(5\text{dmazpy})\text{Cl}_2]$  indicates the presence of two main intense peaks ( $m/z = 617$  and  $580$ ). The first ( $m/z = 617$ ) corresponds to the molecular ion which one protonation. The second ( $m/z = 580$ ) corresponded to the loss of a chloro ligand from  $[\text{Ru}(\text{Clazpy})(5\text{dmazpy})\text{Cl}_2]$  molecule. So, the measured molecular weights were consistent with the expected values. Moreover, a losing chloro ligand from  $[\text{Ru}(\text{Clazpy})(5\text{dmazpy})\text{Cl}_2]$  molecule shown in FAB pattern is similar to be found in *ctc*- $[\text{Ru}(\text{Clazpy})_2\text{Cl}_2]$  patterns that described previously.

Results from X-ray data, the bond distance of Ru-Cl which trans to N=N bond of Clazpy ( $1.293(4)\text{Å}$ ) is longer than that of 5dmazpy ( $1.288(4)\text{Å}$ ). So, it is possible to summarize that the former is more easily to loss from  $[\text{Ru}(\text{Clazpy})(5\text{dmazpy})\text{Cl}_2]$  molecule than the later as shown in Figure 3.49.

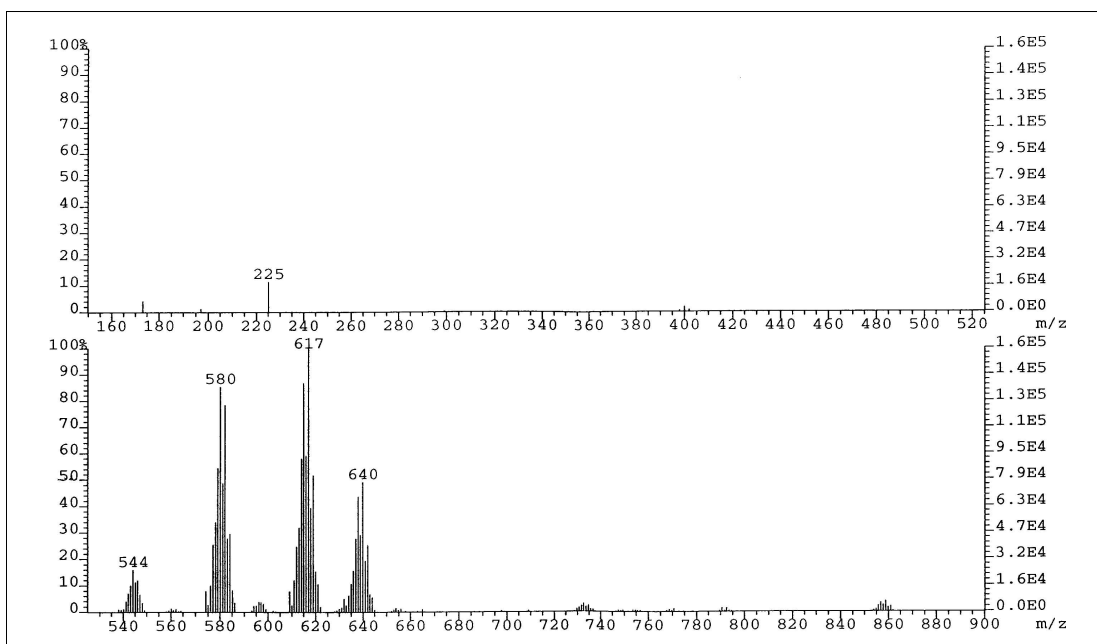


**Figure 3.48** FAB mass spectrum of  $[\text{Ru}(\text{Clazpy})(5\text{dmazpy})\text{Cl}_2]$

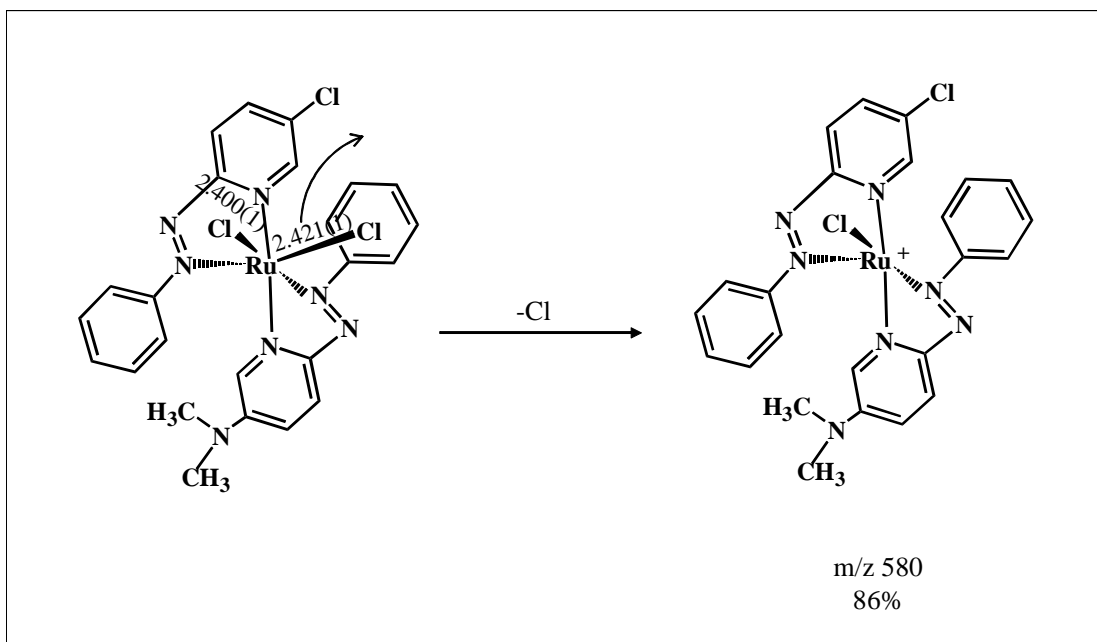


**Figure 3.49** Fragmentation of  $[\text{Ru}(\text{Clazpy})(5\text{dmazpy})\text{Cl}_2]$

### 3.3.2.4 Infrared spectroscopy

The Fourier-transform IR spectrum of  $[\text{Ru}(\text{Clazpy})(5\text{dmazpy})\text{Cl}_2]$  complex was recorded as a KBr disc in 4000-400  $\text{cm}^{-1}$  range. They exhibited many characteristic frequencies such as C=C, C=N, N=N, C-H bending of monosubstituted benzene and C-Cl modes with variable intensities below 1600  $\text{cm}^{-1}$ . The infrared spectroscopic data of  $[\text{Ru}(\text{Clazpy})(5\text{dmazpy})\text{Cl}_2]$  is given in Table 3.29 and this spectrum is shown in Figure 3.50.

**Table 3.29** IR data of the  $[\text{Ru}(\text{Clazpy})(5\text{dmazpy})\text{Cl}_2]$  complexes

Vibration modes	Frequencies ( $\text{cm}^{-1}$ )
C=N stretching and C=C stretching	1589 (s)
	1560 (m)
	1441(m)
$\square_{\text{CH}_3}$ (out of plane bending)	1380 (m)
N=N(azo) stretching	1312 (s)
	1282 (s)
C-N stretching	1130 (m)
C-H out of plane bend in monosubstituted benzene	768 (m)
	693 (m)
C-Cl	596 (s)

s = strong, m = medium

The vibration frequencies below 1600  $\text{cm}^{-1}$  were used to give information about coordinated ligand to the ruthenium center. The N=N stretching is an important peak which used to be considered the  $\pi$ -acid property in azo complexes. This mode exhibited at 1364  $\text{cm}^{-1}$  in the free Clazpy ligand and it was shifted to lower frequencies in the  $[\text{Ru}(\text{Clazpy})(5\text{dmazpy})\text{Cl}_2]$  complexes around 50-80  $\text{cm}^{-1}$  at 1312

and  $1282\text{ cm}^{-1}$  corresponded to the azo moieties in the 5dmazpy and Clazpy, respectively.

In general, the N=N stretching mode in  $[\text{Ru}(\text{L})_2\text{Cl}_2]$  are relative low compared to free ligand values due to  $t_{2g} \rightarrow \pi^*(\text{azo})$  donation ( $\pi$ -backbonding). The extent of this donation would increased with decreasing the N=N frequency. In addition, the trend in N=N frequencies and N=N bond distance are mutually which summarized in Table 3.30.

**Table 3.30** The IR data and X-ray data of N=N in  $[\text{Ru}(\text{Clazpy})(5\text{dmazpy})\text{Cl}_2]$  compared to free Clazpy ligand

Compounds	IR stretching mode ( $\nu_{\text{N=N}}$ , $\text{cm}^{-1}$ )	Bond distances (N=N, Å)
$[\text{Ru}(\text{Clazpy})(5\text{dmazpy})\text{Cl}_2]$	1312 (5dmazpy)	1.288(4)
	1282 (Clazpy)	1.293(4)
Clazpy	1364	-

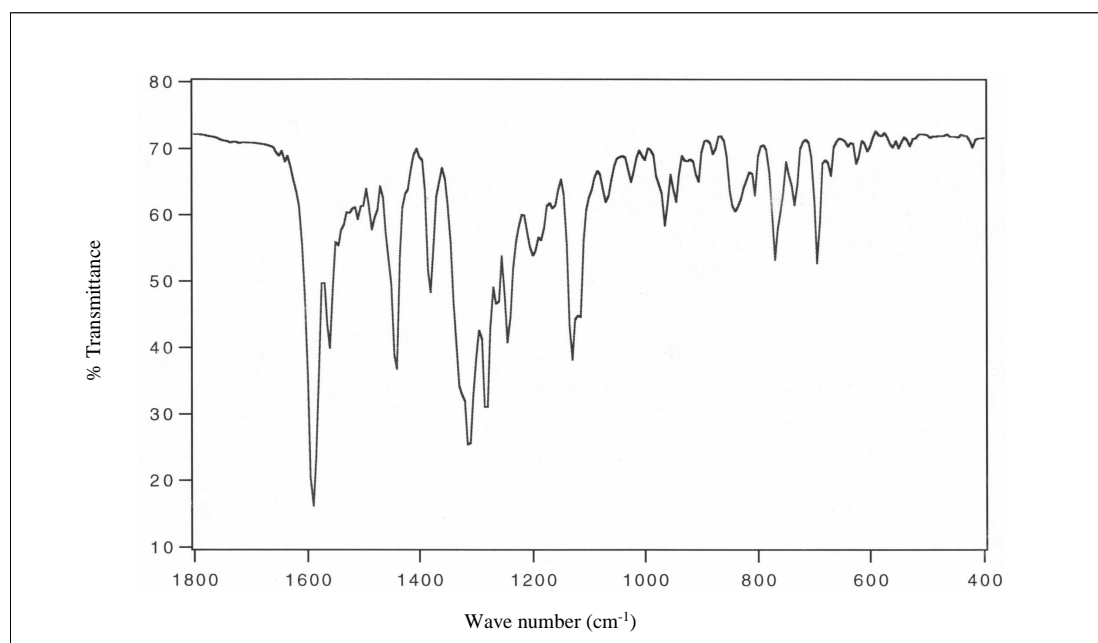


**Figure 3.50** IR spectrum of  $[\text{Ru}(\text{Clazpy})(5\text{dmazpy})\text{Cl}_2]$

### 3.3.2.5 UV-Visible absorption spectroscopy

The UV-Visible absorption spectra of [Ru(Clazpy)(5dmazpy)Cl<sub>2</sub>] complexes were recorded in five solvents; CHCl<sub>3</sub>, CH<sub>2</sub>Cl<sub>2</sub>, DMF, DMSO and CH<sub>3</sub>CN in 200-800 nm range. Electronic spectra of this complex in CH<sub>2</sub>Cl<sub>2</sub> solution are shown in Figure 3.51 and absorption spectroscopic data are listed in Table 3.31.

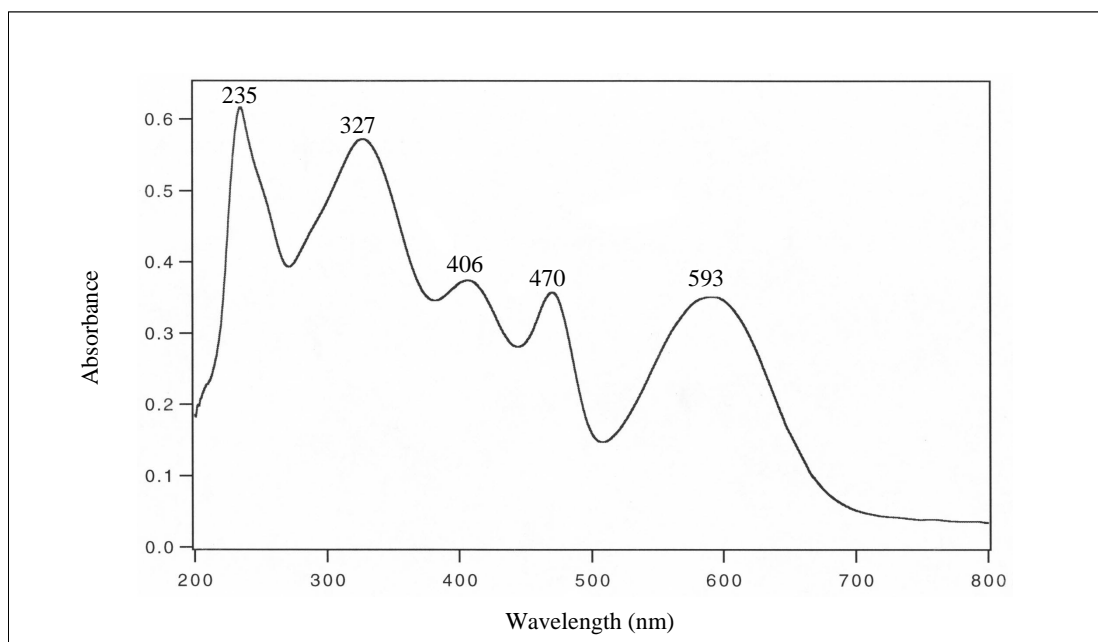
**Table 3.31** UV-Visible absorption spectroscopic data of the [Ru(Clazpy)(5dmazpy)Cl<sub>2</sub>] complex

Solvents	$\lambda_{\max}$ , nm ( $\epsilon^a \times 10^{-4} \text{ M}^{-1}\text{cm}^{-1}$ )
CHCl <sub>3</sub>	246 (1.8), 328 (2.1), 404 (1.4), 469 (1.3), 591 (1.3)
CH <sub>2</sub> Cl <sub>2</sub>	235 (2.6), 327 (2.4), 406 (1.6), 470 (1.5), 593 (1.5)
DMF	323 (2.4), 415 (1.5), 474(1.7), 592 (1.6)
DMSO	265 (1.2), 324 (2.2), 413 (1.4), 475 (1.6), 595 (1.5)
CH <sub>3</sub> CN	207 (2.7), 228 (2.6), 321 (2.4), 410 (1.6), 470 (1.7), 590 (1.6)

<sup>a</sup> Molar extinction coefficient

The absorption spectrum of [Ru(Clazpy)(5dmazpy)Cl<sub>2</sub>] was recorded in UV-Visible region (200-800 nm). From previous studies, the free Clazpy ligand displays two absorption bands at 325 ( $\epsilon \sim 10^4 \text{ M}^{-1}\text{cm}^{-1}$ ) and 450 nm ( $\epsilon \sim 600 \text{ M}^{-1}\text{cm}^{-1}$ ) which have been assigned to  $\pi \rightarrow \pi^*$  transition and  $n \rightarrow \pi^*$  of Clazpy respectively. In [Ru(Clazpy)(5dmazpy)Cl<sub>2</sub>], it displayed five absorption bands in both UV and visible region. These were assigned to intraligand and metal-to-ligand charge transfer (MLCT) transition. The transition energy of these bands varied with the nature of the ligand acting as  $\pi$ -acceptor. Results from X-ray data revealed that Clazpy is a better  $\pi$ -acceptor than 5dmazpy considering the bond distance of N=N 1.293(4)Å and 1.288(4)Å for Clazpy and 5dmazpy, respectively. Therefore, the last MLCT band belong to  $d_{\square}(\text{Ru}) \rightarrow \pi^*(\text{Clazpy})$ . In addition, the lowest energy absorption band of

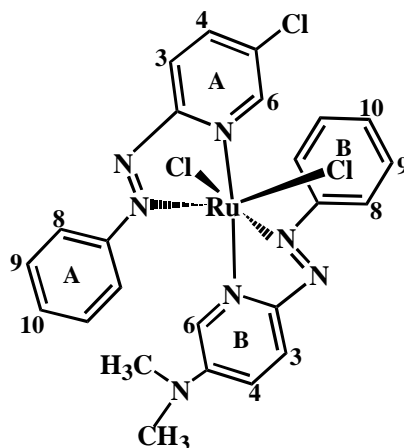
[Ru(Clazpy)(5dmazpy)Cl<sub>2</sub>] were not shifted when the polarity of solvents was increased.



**Figure 3.51** UV-Visible absorption spectrum of [Ru(Clazpy)(5dmazpy)Cl<sub>2</sub>] in CH<sub>2</sub>Cl<sub>2</sub>

### 3.3.2.6 Nuclear magnetic resonance spectroscopy

The stereochemistry of the complex was supported by 1D and 2D NMR (<sup>1</sup>H, <sup>13</sup>C, DEPT, COSY and HMQC NMR) spectral data (Table 3.32) collected in CDCl<sub>3</sub>. Tetramethylsilane (Si(CH<sub>3</sub>)<sub>4</sub>) was used as an internal reference. The signals were assigned on the basis of the spin-spin interaction and on comparing with free ligand values.

**Table 3.32**  $^1\text{H}$ - $^{13}\text{C}$  NMR spectroscopic data of  $[\text{Ru}(\text{Clazpy})(5\text{dmazpy})\text{Cl}_2]$ 

position	$^1\text{H}$ NMR			$^{13}\text{C}$ NMR (CH-type)
	$\delta$ (ppm)	$J$ (Hz)	Amount of H	
6A	9.25 (dd)	2.5, 0.5	1	149.61
6B	8.61 (d)	3.0	1	135.22
3A	8.37 (dd)	8.5, 0.5	1	125.10
3B	8.22 (d)	9.0	1	128.86
4A	7.85 (dd)	8.5, 2.5	1	136.78
10A	7.28 (tt)	8.0, 1.0	1	129.24
10B	7.22 (tt)	8.0, 1.0	1	129.11
9A	7.12 (m)	-	4	128.40
9B				128.25
4B	7.08 (dd)	9.0, 3.0	1	117.35
8A	6.89 (dd)	8.0, 1.0	2	122.06
8B	6.66 (dd)	8.0, 1.0	2	121.93
$\text{CH}_3$	3.09 (s)	-	6	40.26
Quaternary carbons (C)				165.43( $\text{C}_{2\text{A}}$ ), 60.78( $\text{C}_{2\text{B}}$ ), 156.06( $\text{C}_{5\text{A}}$ ), 55.28( $\text{C}_{5\text{B}}$ ), 154.06( $\text{C}_{7\text{A}}$ ), 46.80( $\text{C}_{7\text{B}}$ )

s = singlet, d = doublet, dd = doublet of doublet, tt = triplet of triplet, m = multiplet

From the  $^1\text{H}$  NMR spectrum (Figure 3.52), the H6 signal on pyridine of Clazpy was observed at 9.25 ppm and more downfield than H6 of 5dmazpy due to less electron delocalization in Clazpy compared to 5dmazpy. The methyl proton signals were observed at 3.09 ppm corresponded to the  $\text{N}(\text{CH}_3)_2$  group in 5dmazpy. In addition, the nitrogen pyridine coordinated to ruthenium center caused the protons H3, H4 and H6 occurred at lower downfield than protons H8, H9 and H10 in phenyl ring. Moreover, the peak assignment was supported by results from simple correlation  $^1\text{H}$ - $^1\text{H}$  COSY NMR spectroscopy (Figure 3.53).

The  $^{13}\text{C}$  NMR (Figure 3.54) results correspond to the DEPT NMR (Figure 3.55) showed methine and methyl carbons. The downfield signals below 146 ppm was belong to quaternary carbons (C2, C5 and C7 of Clazpy and 5dmazpy). The high field carbon belonged to methyl carbon at 40.26 ppm. Moreover, the  $^{13}\text{C}$  NMR signals assignments were based on  $^1\text{H}$ - $^{13}\text{C}$  HMQC NMR spectrum (Figure 3.56).

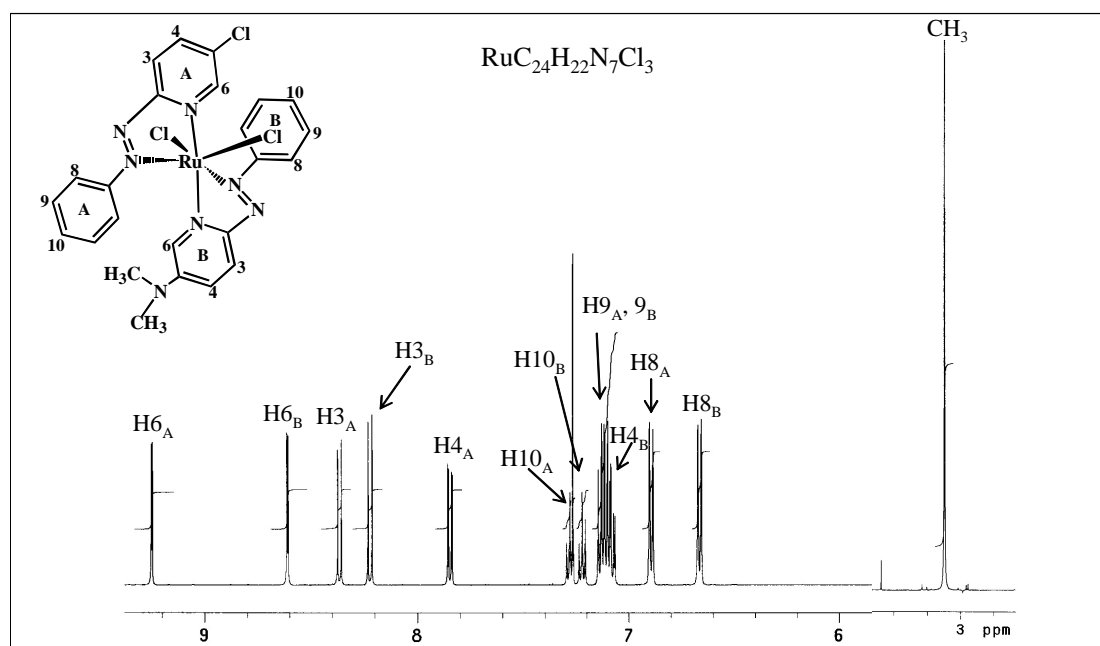


**Figure 3.52**  $^1\text{H}$  NMR spectrum of  $[\text{Ru}(\text{Clazpy})(5\text{dmazpy})\text{Cl}_2]$  in  $\text{CDCl}_3$

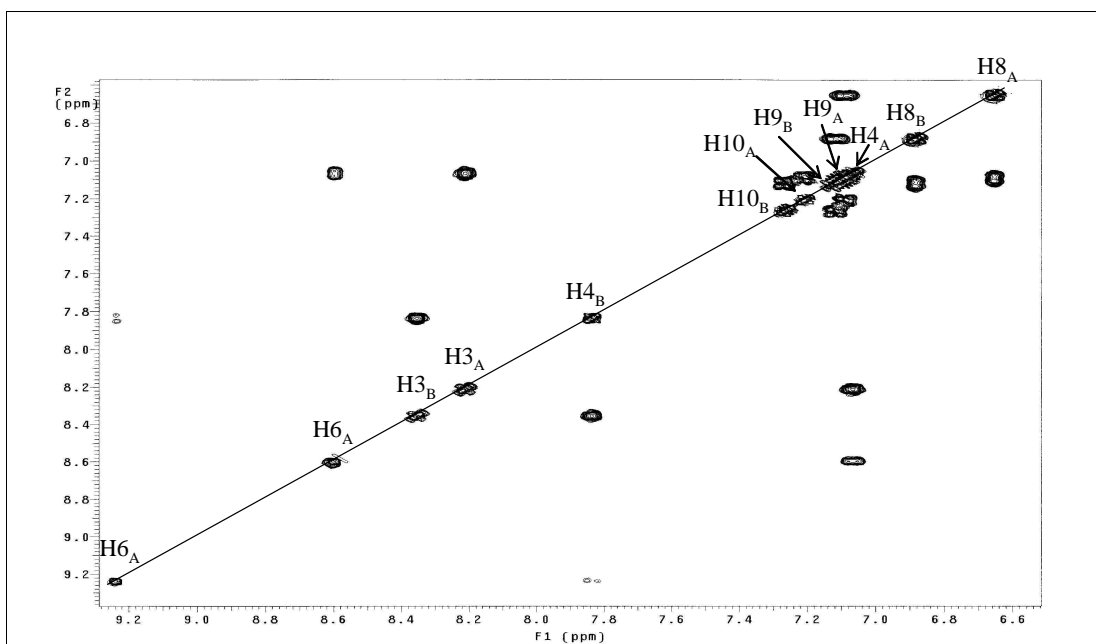


**Figure 3.53**  $^1\text{H}$ - $^1\text{H}$  COSY NMR spectrum of  $[\text{Ru}(\text{Clazpy})(5\text{dmazpy})\text{Cl}_2]$  in  $\text{CDCl}_3$

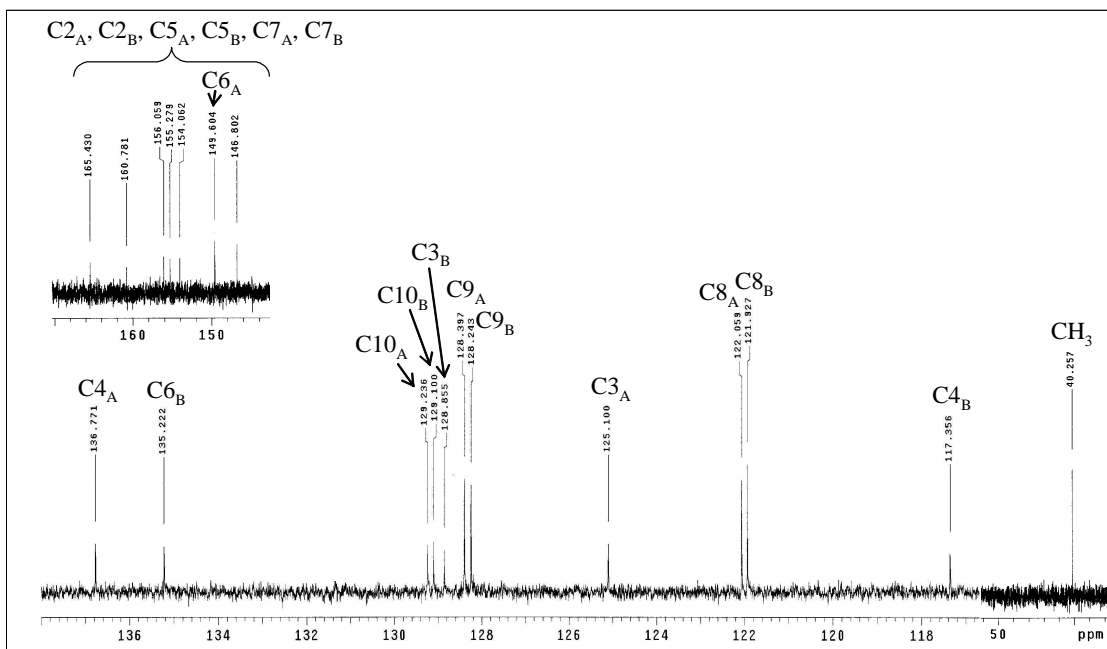


**Figure 3.54**  $^{13}\text{C}$  NMR spectrum of  $[\text{Ru}(\text{Clazpy})(5\text{dmazpy})\text{Cl}_2]$  in  $\text{CDCl}_3$

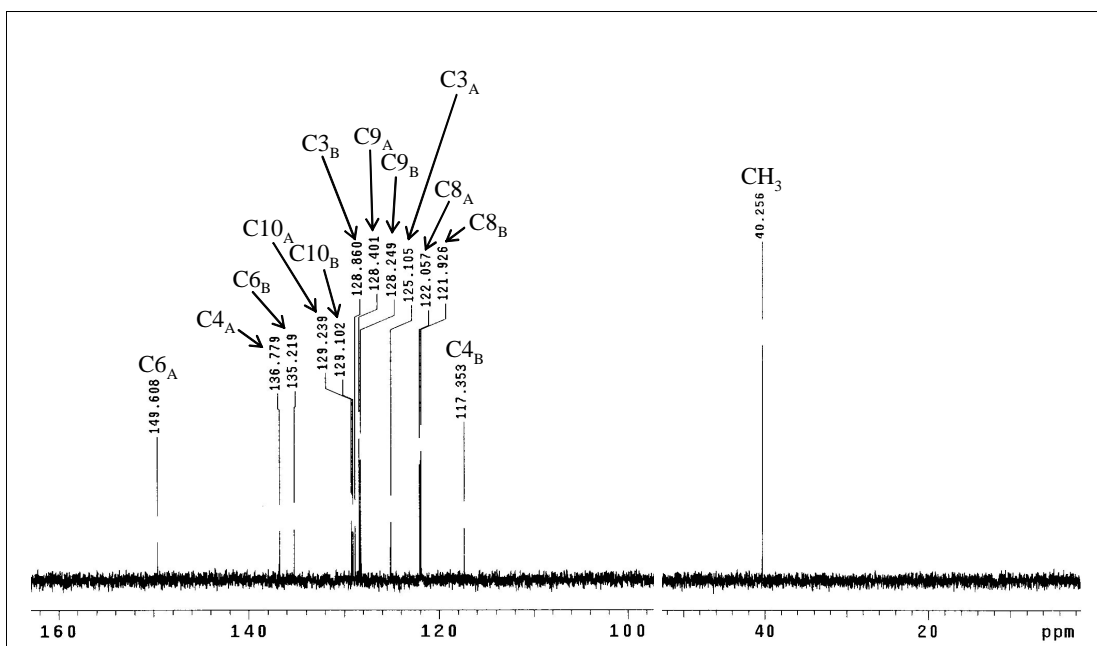


**Figure 3.55** DEPT NMR spectrum of  $[\text{Ru}(\text{Clazpy})(5\text{dmazpy})\text{Cl}_2]$  in  $\text{CDCl}_3$

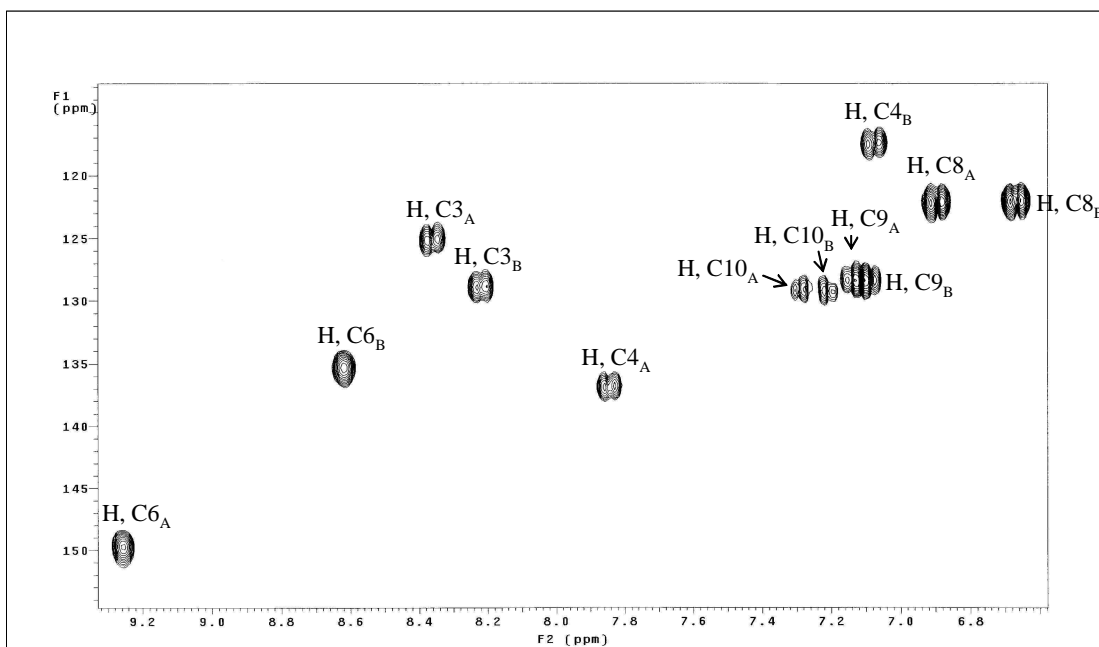


**Figure 3.56**  $^1\text{H}$ - $^{13}\text{C}$  HMQC NMR spectrum of  $[\text{Ru}(\text{Clazpy})(5\text{dmazpy})\text{Cl}_2]$  in  $\text{CDCl}_3$

### 3.3.2.7 Cyclic voltammetry

The electrochemical behavior of the [Ru(Clazpy)(5dmazpy)Cl<sub>2</sub>] complex in CH<sub>2</sub>Cl<sub>2</sub> was examined by cyclic voltammetry (CV). The representative voltammogram (Figure 3.57) displayed metal oxidations on the positive potential and ligand reductions on the negative potential with respect to ferrocene. The result is given in Table 3.33. The measurement was carried out at a scan rate of 50 mV/s in the potential range +2.00 V to -2.00 V.

**Table 3.33** Cyclic voltammetric data of [Ru(Clazpy)(5dmazpy)Cl<sub>2</sub>] in 0.1 M TBAH CH<sub>2</sub>Cl<sub>2</sub> at scan rate 50 mV/s (ferrocene as internal standard)

Compound	<sup>a</sup> E <sub>1/2</sub> , V	
	Oxidation	Reduction
[Ru(Clazpy)(5dmazpy)Cl <sub>2</sub> ]	+0.55 (105), +1.31 <sup>c</sup>	-1.16 (105), -1.58 <sup>b</sup>

<sup>a</sup>E<sub>1/2</sub> = (E<sub>pa</sub> + E<sub>pc</sub>)/2, where E<sub>pa</sub> and E<sub>pc</sub> are anodic and cathodic peak potentials, respectively; ΔE<sub>p</sub> = E<sub>pa</sub> - E<sub>pc</sub>

<sup>b</sup>cathodic peak potential, V

<sup>c</sup>anodic peak potential, V

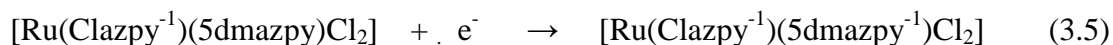
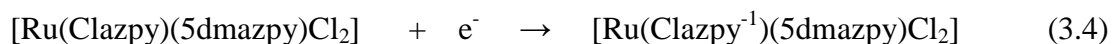
#### Oxidation potential

In this range, the cyclic voltammogram of [Ru(Clazpy)(5dmazpy)Cl<sub>2</sub>] displayed one reversible couple at +0.55 V and anodic peak at +1.31 V. It is believed that the first one belonged to Ru(II)/(III) couples and the later may be due to the substituted (-N(CH<sub>3</sub>)<sub>2</sub>) on pyridine ring compared with the results from *ctc*-[Ru(Clazpy)<sub>2</sub>Cl<sub>2</sub>]. The Ru(II)/(III) couple of [Ru(Clazpy)(5dmazpy)Cl<sub>2</sub>] (+0.55 V) appeared at the most lowest potential compared to *ctc*-[Ru(azpy)<sub>2</sub>Cl<sub>2</sub>] (+0.71 V) and *ctc*-[Ru(Clazpy)<sub>2</sub>Cl<sub>2</sub>] (+0.82 V). These could be explained that 5dmazpy having methyl as electron-donating group increases electron density to the ruthenium center.

Consequently, [Ru(Clazpy)(5dmazpy)Cl<sub>2</sub>] is easier oxidized than *ctc*-[Ru(azpy)<sub>2</sub>Cl<sub>2</sub>] (Jullapan, T., 2004) and *ctc*-[Ru(Clazpy)<sub>2</sub>Cl<sub>2</sub>] which no (-N(CH<sub>3</sub>)<sub>2</sub>) group.

### Reduction potential

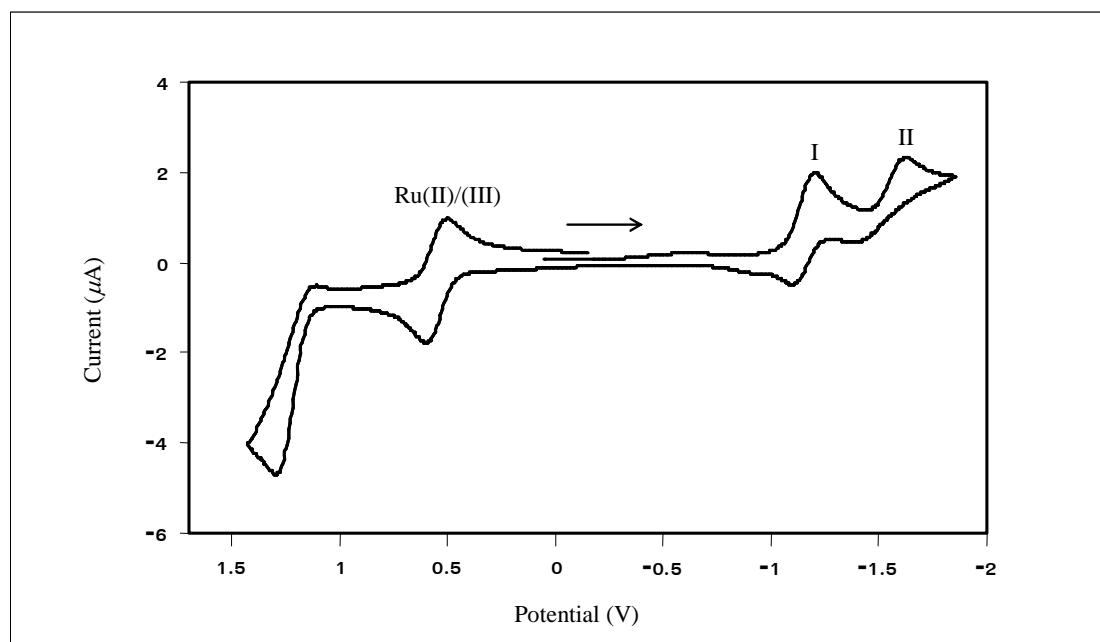
In the negative potential from 0.00 to - 2.00 V, these were assigned to the reduction of coordinated azo (-N=N-) groups. The N=N function in azopyridine ligand was known to be a potential electron transfer center and could accept a maximum of two electrons. Moreover, the first reduction may be expected to involve the ligand having the most stable lowest unoccupied molecular orbital (LUMO), which is dominated by azo function of Clazpy than 5dmazpy (Byabartta *et al.*, 2001). In this work, one reversible couple and one cathodic peak of [Ru(Clazpy)(5dmazpy)Cl<sub>2</sub>] occurred at -1.16 and -1.58 V. The expected reduction processes are displayed in equations 3.4 to 3.5.



These processes revealed that the first reduction potential in [Ru(Calazpy)(5dmazpy)Cl<sub>2</sub>] occurred at -1.16 V referred to more electron accepting ability of Clazpy than 5dmazpy (-1.58 V). This CV result was consistent with the X-ray data which showed longer N=N bond distance of Clazpy than 5dmazpy. The data are summarize in Table 3.34. These results showed that the Clazpy ligand was a better  $\pi$ -acceptor than 5dmazpy within the same molecule.

**Table 3.34** Comparisons of CV and X-ray data in ruthenium azoimine complexes

Complexes	$E_{1/2}$ , V	N=N bond distance, (Å)
[Ru(Clazpy)(5dmazpy)Cl <sub>2</sub> ]	-1.16	1.293(4)
	-1.58	1.288(4)

**Figure 3.57** Cyclic voltammogram of [Ru(Clazpy)(5dmazpy)Cl<sub>2</sub>] in 0.1 M TBAH CH<sub>2</sub>Cl<sub>2</sub> at scan rate 50 mV/s (ferrocene as an internal standard)

### 3.4 Syntheses and characterization of $[\text{Ru}(\text{Clazpy})_2(\text{L})](\text{PF}_6)_2$ (L = bpy, phen, azpy, Clazpy)

#### 3.4.1 Syntheses of $[\text{Ru}(\text{Clazpy})_2(\text{L})](\text{PF}_6)_2$ (L = bpy, phen, azpy, Clazpy)

Dichlorobis(5-chloro-2-(phenylazo)pyridine)ruthenium(II) of *cis-trans-cis* (*ctc*) configuration have been used as the precursor complex for preparation of the ionic compounds,  $[\text{Ru}(\text{Clazpy})_2(\text{L})](\text{PF}_6)_2$  where L is bpy, phen, azpy, Clazpy. The preparation was done by refluxing the precursor, *ctc*- $[\text{Ru}(\text{Clazpy})_2\text{Cl}_2]$ , excess L ligands and  $\text{AgNO}_3$  in methanol. Precipitation of these complexes was carried out by adding  $\text{NH}_4\text{PF}_6$  in the reaction mixture according to procedure shown in Figure 3.58.

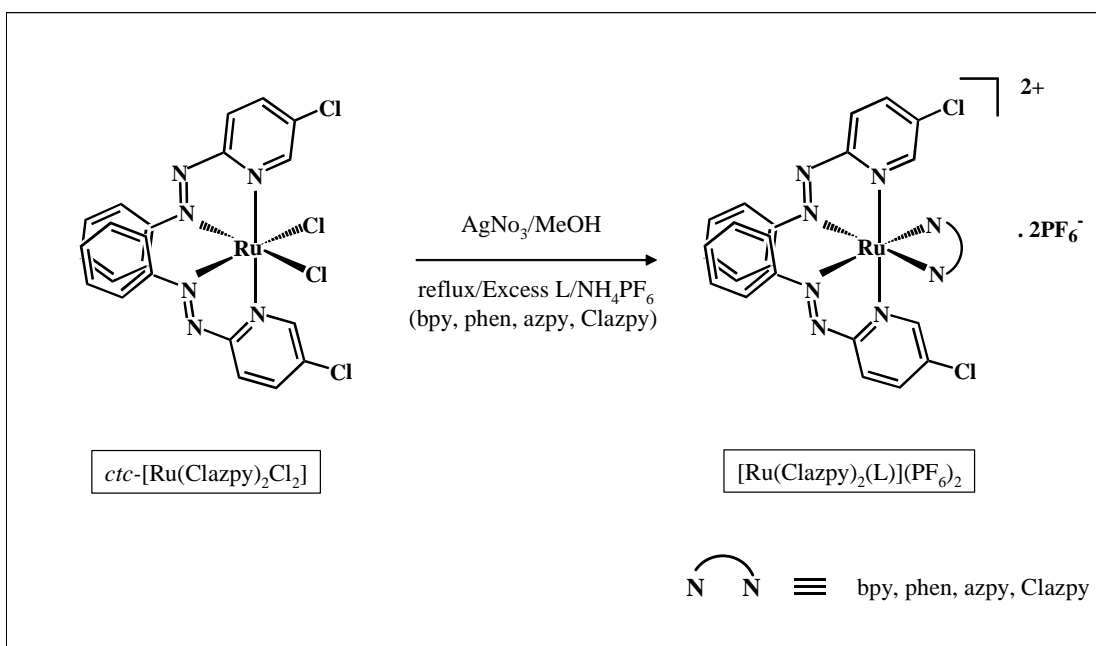


**Figure 3.58** Synthetic routes for the preparation of  $[\text{Ru}(\text{Clazpy})_2(\text{L})](\text{PF}_6)_2$  (L = bpy, phen, azpy, Clazpy)

The physical properties of this complex are summarized in Table 3.35.

**Table 3.35** The physical properties of  $[\text{Ru}(\text{Clazpy})_2(\text{L})](\text{PF}_6)_2$  (L = bpy, phen, azpy, Clazpy)

Complexes	Physical properties			
	Appearance	Color		Melting point (°C)
		solid	solution	
$[\text{Ru}(\text{Clazpy})_2(\text{bpy})](\text{PF}_6)_2$	solid	dark red	red	251-252
$[\text{Ru}(\text{Clazpy})_2(\text{phen})](\text{PF}_6)_2$	solid	dark red	red	209-209
$[\text{Ru}(\text{Clazpy})_2(\text{azpy})](\text{PF}_6)_2$	solid	dark brown	light brown	252-253
$[\text{Ru}(\text{Clazpy})_3](\text{PF}_6)_2$	solid	dark brown	light brown	250-251

The solubility of 0.0012 g of  $[\text{Ru}(\text{Clazpy})_2\text{L}](\text{PF}_6)_2$  (L = bpy, phen, azpy, Clazpy) was tested in 10 mL of various solvents: hexane,  $\text{CHCl}_3$ ,  $\text{CH}_2\text{Cl}_2$ ,  $\text{CH}_3\text{OCH}_3$ , DMF, DMSO,  $\text{CH}_3\text{CN}$ , EtOH, MeOH and  $\text{H}_2\text{O}$ . They are slightly soluble in EtOH and  $\text{H}_2\text{O}$  and they were more soluble in MeOH,  $\text{CHCl}_3$ ,  $\text{CH}_2\text{Cl}_2$ . They were very soluble in  $\text{CH}_3\text{OCH}_3$ , DMF, DMSO,  $\text{CH}_3\text{CN}$  but insoluble in hexane.

### 3.4.2 Characterization of $[\text{Ru}(\text{Clazpy})_2\text{L}](\text{PF}_6)$ (L = bpy, phen, azpy, Clazpy)

The chemistry of  $[\text{Ru}(\text{Clazpy})_2(\text{L})](\text{PF}_6)_2$  complexes were characterized by elemental analysis, Mass spectrometry, Infrared spectroscopy, UV-Visible absorption spectroscopy, Nuclear Magnetic Resonance spectroscopy (1D and 2D NMR). The electrochemical properties of all complexes were studied by using cyclic voltammetric technique.

### 3.4.2.1 Elemental analysis

Elemental analysis was used to confirmed composition of C, H, N in complexes and the results are given in Table 3.36. The analytical values corresponded to the calculated values. Therefore, the composition of  $[\text{Ru}(\text{Clazpy})_2(\text{L})](\text{PF}_6)_2$  was confirmed by this method.

**Table 3.36** Elemental analysis data of  $[\text{Ru}(\text{Clazpy})_2(\text{L})](\text{PF}_6)_2$  (L = bpy, phen, azpy, Clazpy)

Complexes	% C		% H		% N	
	Calc.	Found	Calc.	Found	Calc.	Found
$[\text{Ru}(\text{Clazpy})_2(\text{bpy})](\text{PF}_6)_2$	39.12	38.72	2.46	2.37	11.40	11.58
$[\text{Ru}(\text{Clazpy})_2(\text{phen})](\text{PF}_6)_2$	40.57	40.40	2.40	2.37	11.13	11.53
$[\text{Ru}(\text{Clazpy})_2(\text{azpy})](\text{PF}_6)_2$	39.26	39.07	2.50	2.52	12.49	12.92
$[\text{Ru}(\text{Clazpy})_3](\text{PF}_6)_2$	37.97	37.54	2.32	2.23	12.08	12.54

### 3.4.2.2 X-ray crystallography

In this work, replacing two chlorides by phen and azpy in the parent complex, *ctc*- $[\text{Ru}(\text{Clazpy})_2\text{Cl}_2]$  give a large molecule which difficult to identify the précised structure. Although NMR technique was used to determine the stereochemistry, but overlapping of three pyridines and phenyl rings make it more difficult for interpretation. Fortunately, single-crystal X-ray diffraction studies provide the most convincing evidence for the molecular structures and absolute geometry of  $[\text{Ru}(\text{Clazpy})_2(\text{phen})](\text{PF}_6)_2$  and  $[\text{Ru}(\text{Clazpy})_2(\text{azpy})](\text{PF}_6)_2$ .

X-ray structure of [Ru(Clazpy)<sub>2</sub>(phen)](PF<sub>6</sub>)<sub>2</sub>

Crystals suitable for X-ray analysis were grown by slow diffusion of methanol into an acetone solution at room temperature. The crystal structure of the title compound is shown in Figure 3.59. The crystallographic data are shown in Table 3.37. Selected bond parameters associated with the metal ions are listed in Table 3.38.

**Table 3.37** Crystal data and structure refinement for [Ru(Clazpy)<sub>2</sub>(phen)](PF<sub>6</sub>)<sub>2</sub>

Empirical formula	C <sub>68</sub> H <sub>48</sub> Cl <sub>4</sub> F <sub>24</sub> N <sub>16</sub> P <sub>4</sub> Ru <sub>2</sub>	
Formula weight	2013.04	
Temperature	293(2) K	
Wavelength	0.71073 Å	
Crystal system	Monoclinic	
Space group	P2(1)/n	
Unit cell dimensions	$a = 9.0239(7)$ Å	$\alpha = 90^\circ$
	$b = 18.8634(13)$ Å	$\beta = 98.4710(10)^\circ$
	$c = 22.9819(16)$ Å	$\gamma = 90^\circ$
Volume	3869.3(5) Å <sup>3</sup>	
Z	2	
Density (calculated)	1.728 Mg/m <sup>3</sup>	
Absorption coefficient	0.723 mm <sup>-1</sup>	
$F(0\ 0\ 0)$	2000	
Refinement method	Full-matrix least-squares on F <sup>2</sup>	
Crystal size	0.259 x 0.11 x 0.09 mm <sup>3</sup>	
Goodness-of-fit on F <sup>2</sup>	1.099	
Final R indices [ $I > 2\sigma(I)$ ]	$R1 = 0.0676$ , $wR2 = 0.1261$	
R indices (all data)	$R1 = 0.0986$ , $wR2 = 0.1372$	
Extinction coefficient	0.00000(16)	

**Table 3.38** Selected bond lengths (Å) and angles (°) and estimated standard deviations for [Ru(Clazpy)<sub>2</sub>(phen)](PF<sub>6</sub>)<sub>2</sub>

Ru(1)-N(6)	1.993(4)	Ru(1)-N(3)	2.003(4)
Ru(1)-N(1)	2.051(4)	Ru(1)-N(4)	2.071(4)
Ru(1)-N(8)	2.092(4)	Ru(1)-N(7)	2.100(4)
Cl(1)-C(2)	1.710(6)	Cl(2)-C(13)	1.716(5)
N(2)-N(3)	1.286(5)	N(5)-N(6)	1.287(5)
Angles			
N(1)-Ru(1)-N(3)	76.4(2)	N(1)-Ru(1)-N(4)	101.3(1)
N(1)-Ru(1)-N(6)	96.5(1)	N(1)-Ru(1)-N(7)	92.1(1)
N(1)-Ru(1)-N(8)	169.1(2)	N(3)-Ru(1)-N(4)	176.9(2)
N(3)-Ru(1)-N(6)	101.8(2)	N(3)-Ru(1)-N(7)	86.4(2)
N(3)-Ru(1)-N(8)	97.0(2)	N(4)-Ru(1)-N(6)	76.3(2)
N(4)-Ru(1)-N(7)	95.7(1)	N(4)-Ru(1)-N(8)	85.6(1)
N(6)-Ru(1)-N(7)	169.2(1)	N(6)-Ru(1)-N(8)	93.3(2)
N(7)-Ru(1)-N(8)	78.8(2)		

The ruthenium center is in the distorted octahedral environment with four nitrogens (N1, N3, N4, N6) of two Clazpy ligands and two nitrogens (N7, N8) of one phen ligand. The pyridine ring and azo group of Clazpy are at the cis position and the two pyridine rings of phen are trans to pyridine and the other trans to the azo groups of the Clazpy ligands. Interestingly, the trans-angle around the ruthenium center in the plan range from 169.4(1) to 176.9(2)<sup>o</sup>, indicating enhance distortion from the rectilinear geometry compared to those in [Ru(azpy)<sub>2</sub>(bpy)]<sup>2+</sup> (171.5(16)<sup>o</sup> to 175.6(16)<sup>o</sup> (Hansongnern *et al.*, 2007). Two bite angles extended by two Clazpy and one bpy are 76.4(2)<sup>o</sup>, 76.3(2)<sup>o</sup>, 78.8(2)<sup>o</sup>, respectively. The average bond distance of Ru-N(azo), 1.998(4)Å is shorter than the average Ru-N(pyridine) of 2.061(4)Å. This is due to greater  $\pi$ -backbonding from  $d\pi(\text{Ru}) \rightarrow \pi^*(\text{azo})$ . In addition, it is noted that the Ru-N(phen) distance (average, 2.096(4)Å) is longer than those in [Ru(azpy)<sub>2</sub>(bpy)]<sup>2+</sup> (average, 2.088(4)Å) (Hansongnern *et al.*, 2007). This is probably

due to the competition for the electron density from the metal ion between the Clazpy and phen ligands. Moreover, in the  $[\text{Ru}(\text{Clazpy})_2(\text{phen})](\text{PF}_6)_2$  complex the average N=N distance of Clazpy is 1.286(5) Å which is longer than that of  $[\text{Ru}(\text{azpy})_2(\text{bpy})]^{2+}$  (1.278(4) Å). The coordination of Clazpy lead to a decrease in the N=N bond order due to the  $\sigma$ -donor and  $\pi$ -acceptor character of the ligand. All results from molecular structure of the  $[\text{Ru}(\text{Clazpy})_2(\text{phen})]^{2+}$  complex confirm that Clazpy is a better  $\pi$ -acceptor than azpy and phen.

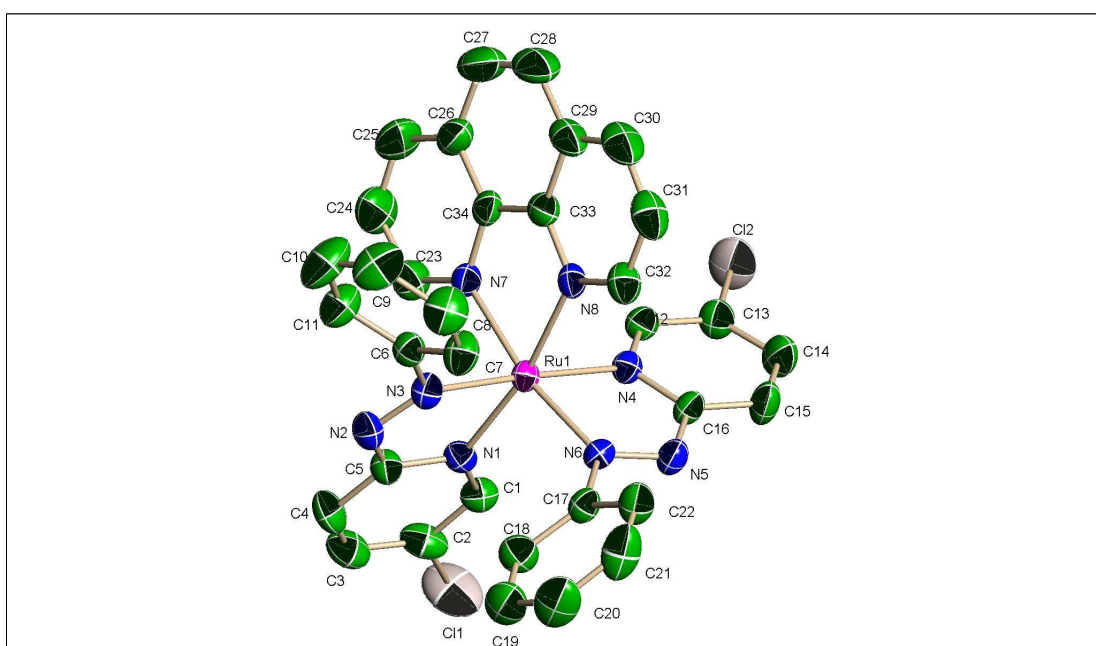


**Figure 3.59** The structure of  $[\text{Ru}(\text{Clazpy})_2(\text{phen})](\text{PF}_6)_2$  (H-atom omitted)

X-ray structure of  $[\text{Ru}(\text{Clazpy})_2(\text{azpy})](\text{PF}_6)_2$

Crystals suitable for X-ray analysis were grown by slow diffusion of methanol into an acetone solution at room temperature. The crystal structure of the title compound is shown in Figure 3.60. The crystallographic data are shown in Table 3.39. Selected bond parameters associated with the metal ions are listed in Table 3.40.

**Table 3.39** Crystal data and structure refinement for [Ru(Clazpy)<sub>2</sub>(azpy)](PF<sub>6</sub>)<sub>2</sub>

Empirical formula	C <sub>33</sub> H <sub>25</sub> Cl <sub>2</sub> F <sub>12</sub> N <sub>9</sub> P <sub>2</sub> Ru	
Formula weight	1009.53	
Temperature	293(2) K	
Wavelength	0.71073 Å	
Crystal system	Orthorhombic	
Space group	<i>Pbca</i>	
Unit cell dimensions	a = 14.8987(13) Å	α = 90°
	b = 14.9395(13) Å	β = 90°
	c = 35.023(3) Å	γ = 90°
Volume	7795.4(12) Å <sup>3</sup>	
Z	8	
Density (calculated)	1.720 Mg/m <sup>3</sup>	
Absorption coefficient	0.719 mm <sup>-1</sup>	
<i>F</i> (0 0 0)	4016	
Goodness-of-fit on <i>F</i> <sup>2</sup>	1.067	
Final R indices [ <i>I</i> > 2σ( <i>I</i> )]	<i>R</i> 1 = 0.0325, <i>wR</i> 2 = 0.0801	
R indices (all data)	<i>R</i> 1 = 0.0373, <i>wR</i> 2 = 0.0830	
Extinction coefficient	0.00000(4)	

**Table 3.40** Selected bond lengths (Å) and angles (°) and estimated standard deviations for [Ru(Clazpy)<sub>2</sub>(azpy)](PF<sub>6</sub>)<sub>2</sub>

Ru(1)-N(3)	2.038(2)	Ru(1)-N(7)	2.054(2)
Ru(1)-N(4)	2.059(2)	Ru(1)-N(1)	2.060(2)
Ru(1)-N(9)	2.070(2)	Ru(1)-N(6)	2.074(2)
N(2)-N(3)	1.274(3)	N(5)-N(6)	1.280(3)
N(8)-N(9)	1.280(3)		
Angles			
N(1)-Ru(1)-N(3)	75.84(8)	N(1)-Ru(1)-N(4)	171.44(8)
N(1)-Ru(1)-N(6)	100.43(7)	N(1)-Ru(1)-N(7)	86.34(7)
N(1)-Ru(1)-N(9)	95.51(7)	N(3)-Ru(1)-N(4)	95.79(8)
N(3)-Ru(1)-N(6)	80.77(8)	N(3)-Ru(1)-N(7)	99.28(8)
N(3)-Ru(1)-N(9)	170.65(8)	N(4)-Ru(1)-N(6)	76.09(7)
N(4)-Ru(1)-N(7)	96.95(7)	N(4)-Ru(1)-N(9)	92.96(7)
N(6)-Ru(1)-N(7)	172.98(7)	N(6)-Ru(1)-N(9)	104.63(7)
N(7)-Ru(1)-N(9)	76.31(8)		

Ru(II) is in a distorted octahedral environment bonded to four nitrogens (N1, N3, N4, N6) of the Clazpy ligand, two nitrogen atoms of the azpy ligand. The pyridine ring of Clazpy is at the trans position and its azo groups are cis. As expected, the Ru-N(pyridine of azpy), 2.054(2)Å gives shortest value of bond length. This phenomenon could be due to the ability of enhance azo group of Clazpy which trans to this bond. The trans-angle around the ruthenium center in the range from 170.6(8) to 173.0(7)°, indicating distortion from the rectilinear geometry. Two bite angles extended by two Clazpy and one azpy are 75.84(8)°, 76.09(7)° and 76.31(8)°, respectively. The average bond distance of Ru-N(azo) of Clazpy, 2.056(2)Å is slightly shorter than the average Ru-N(pyridine of Clazpy) bond length of 2.060(2)Å. This is due to greater  $\pi$ -backbonding from  $d\pi(\text{Ru}) \rightarrow \pi^*(\text{azo})$ .

Moreover, in the  $[\text{Ru}(\text{Clazpy})_2(\text{azpy})](\text{PF}_6)_2$  complex the average N=N distance of Clazpy is 1.277(3)Å which is comparable to those of azpy in the same molecule is 1.280(3)Å and those of azpy in  $[\text{Ru}(\text{azpy})_2(\text{bpy})]^{2+}$  (1.278(4)Å). This is probably due to the competition for the electron density from the metal ion between three azoimine ligands. All results from molecular structure of the  $[\text{Ru}(\text{Clazpy})_2(\text{azpy})]^{2+}$  complex confirm that Clazpy is a  $\pi$ -acceptor ligand like azpy.

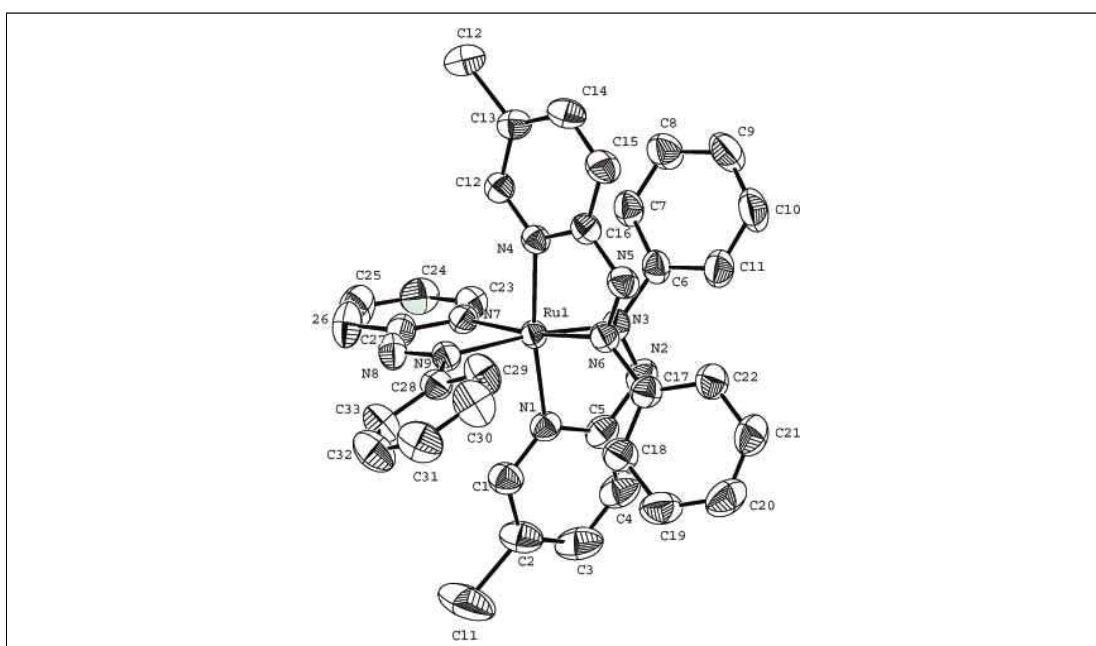


**Figure 3.60** The structure of  $[\text{Ru}(\text{Clazpy})_2(\text{azpy})](\text{PF}_6)_2$  (H-atom omitted)

### 3.4.2.3 Fast-atom bombardment (FAB) and Electrospray (ES) mass spectrometry

The mass spectrum of  $[\text{Ru}(\text{Clazpy})_2(\text{L})](\text{PF}_6)_2$  (L = bpy, phen, azpy, Clazpy) complexes are shown in Figure 3.61 to 3.64. The results are given in Table 3.41.

**Table 3.41** ES mass spectrometric data of  $[\text{Ru}(\text{Clazpy})_2(\text{L})](\text{PF}_6)_2$  (L = bpy, phen, azpy, Clazpy)

m/z	Stoichiometry	Equivalent species	Rel. Abun. (%)
$[\text{Ru}(\text{Clazpy})_2(\text{bpy})](\text{PF}_6)_2$			
345.8	$[\text{Ru}(\text{Clazpy})_2(\text{bpy})]^{2+}$	$[\text{M}-2\text{PF}_6^-]^+$	100
837.2	$[\text{Ru}(\text{Clazpy})_2(\text{bpy})]^+ \text{PF}_6^-$	$[\text{M}-\text{PF}_6^-]^+$	20
$[\text{Ru}(\text{Clazpy})_2(\text{phen})](\text{PF}_6)_2$			
856.3	$[\text{Ru}(\text{Clazpy})_2(\text{phen})]^+ \text{PF}_6^-$	$[\text{M}-\text{PF}_6^-]^+$	100
716.8	$[\text{Ru}(\text{Clazpy})_2(\text{phen})]^{2+}$	$[\text{M}-2\text{PF}_6]^+$	15
$[\text{Ru}(\text{Clazpy})_2(\text{azpy})](\text{PF}_6)_2$			
359.3	$[\text{Ru}(\text{Clazpy})_2(\text{azpy})]^{2+}$	$[\text{M}-2\text{PF}_6^-]^+$	100
719.1	$[\text{Ru}(\text{Clazpy})_2(\text{azpy})]^+ \text{PF}_6^-$	$[\text{M}-\text{PF}_6^-]^+$	30
$[\text{Ru}(\text{Clazpy})_3](\text{PF}_6)_2$			
377.51	$[\text{Ru}(\text{Clazpy})_3]^{2+}$	$[\text{M}-2\text{PF}_6^-]^+$	100
899.99	$[\text{Ru}(\text{Clazpy})_3]^+ \text{PF}_6^-$	$[\text{M}-\text{PF}_6^-]^+$	40

M = molecular weight (MW) of each complexes

MW of  $[\text{Ru}(\text{Clazpy})_2(\text{bpy})](\text{PF}_6)_2 = 982.49$  g/mol

MW of  $[\text{Ru}(\text{Clazpy})_2(\text{phen})](\text{PF}_6)_2 = 1006.52$  g/mol

MW of  $[\text{Ru}(\text{Clazpy})_2(\text{azpy})](\text{PF}_6)_2 = 1009.52$  g/mol

MW of  $[\text{Ru}(\text{Clazpy})_3](\text{PF}_6)_2 = 1043.96$  g/mol

From the data, the parent peak which gave 100% relative abundance of all complexes corresponding to the losing of hexafluorophosphate salts from  $[\text{Ru}(\text{Clazpy})_2(\text{L})](\text{PF}_6)_2$  molecule, except  $[\text{Ru}(\text{Clazpy})_2(\text{phen})](\text{PF}_6)_2$  which showed the ion pair of  $[\text{Ru}(\text{Clazpy})_2(\text{L})]^+(\text{PF}_6)^-$ . So, the proposed formulas of these complexes were confirmed by this technique.

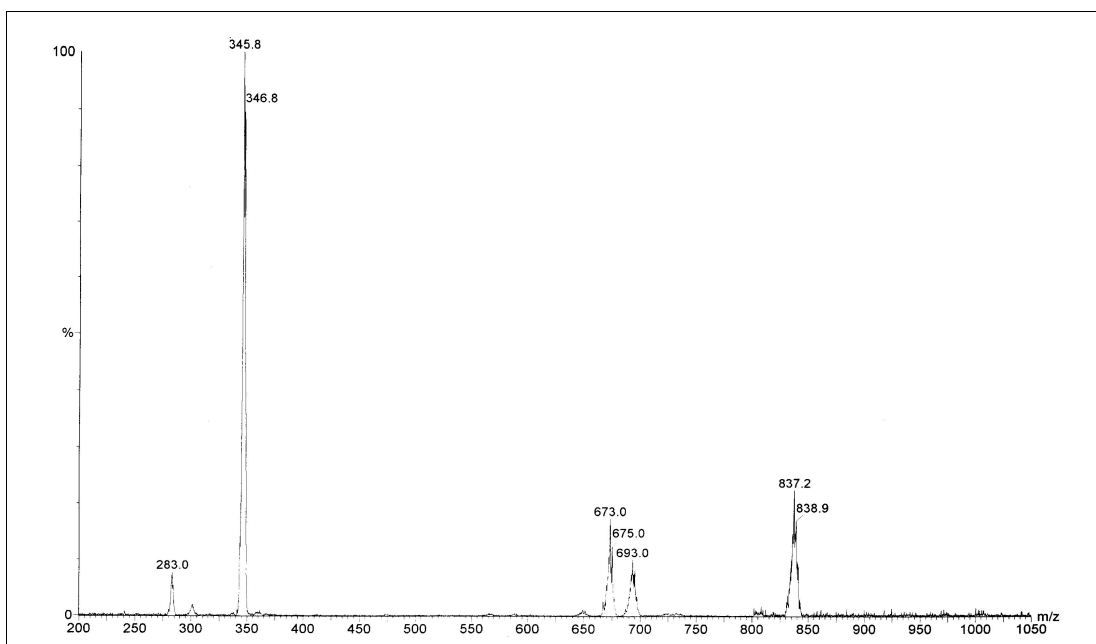


**Figure 3.61** ES mass spectrum of  $[\text{Ru}(\text{Clazpy})_2(\text{bpy})](\text{PF}_6)_2$

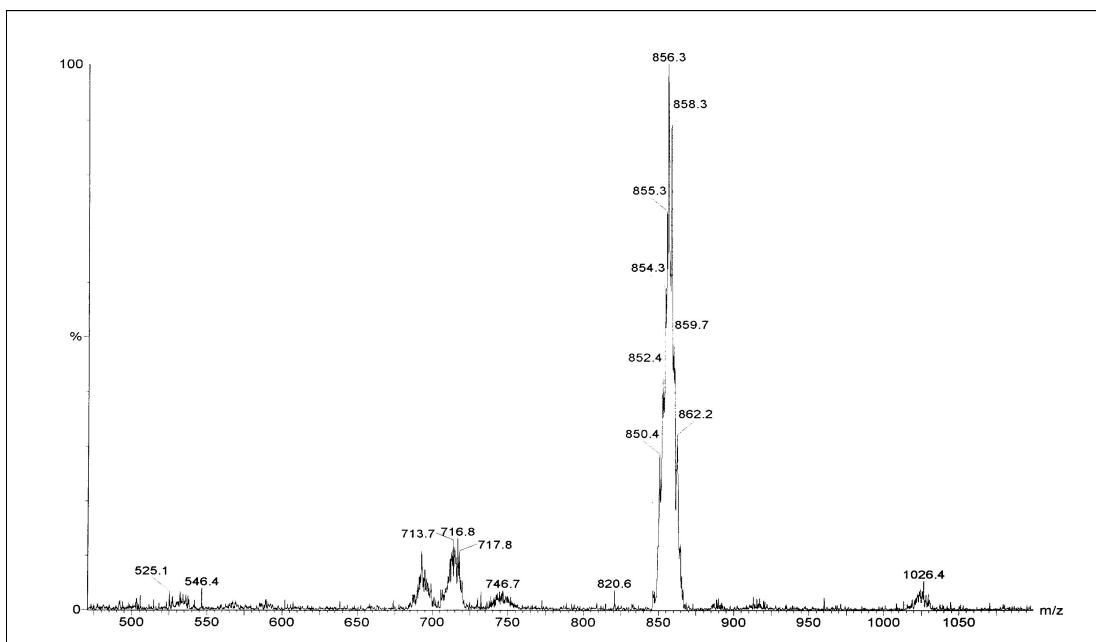


**Figure 3.62** ES mass spectrum of  $[\text{Ru}(\text{Clazpy})_2(\text{phen})](\text{PF}_6)_2$

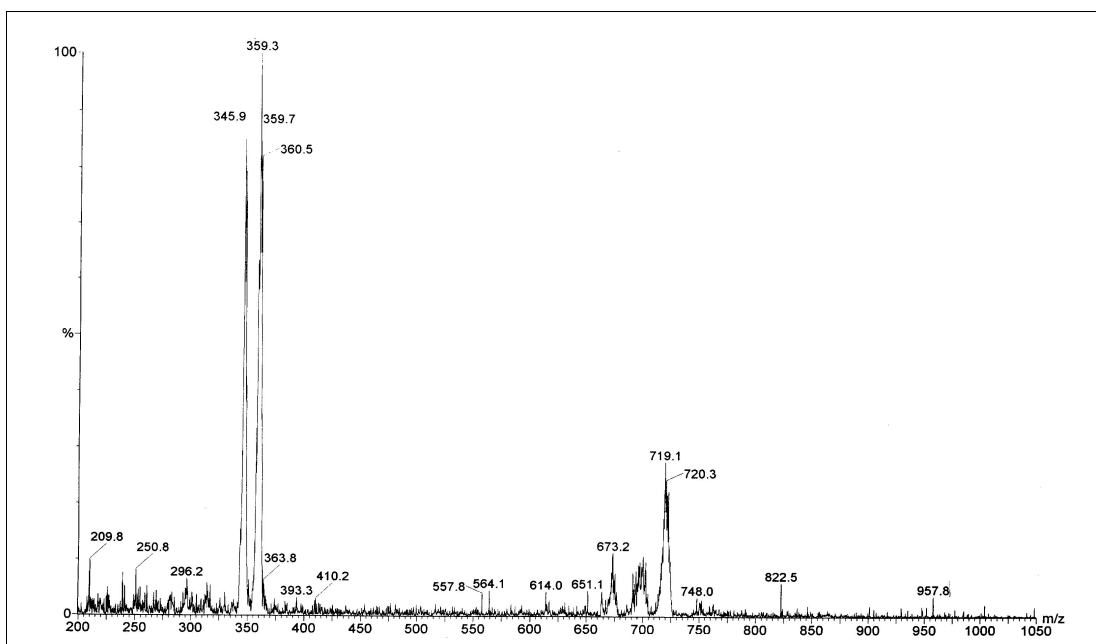


**Figure 3.63** ES mass spectrum of  $[\text{Ru}(\text{Clazpy})_2(\text{azpy})](\text{PF}_6)_2$

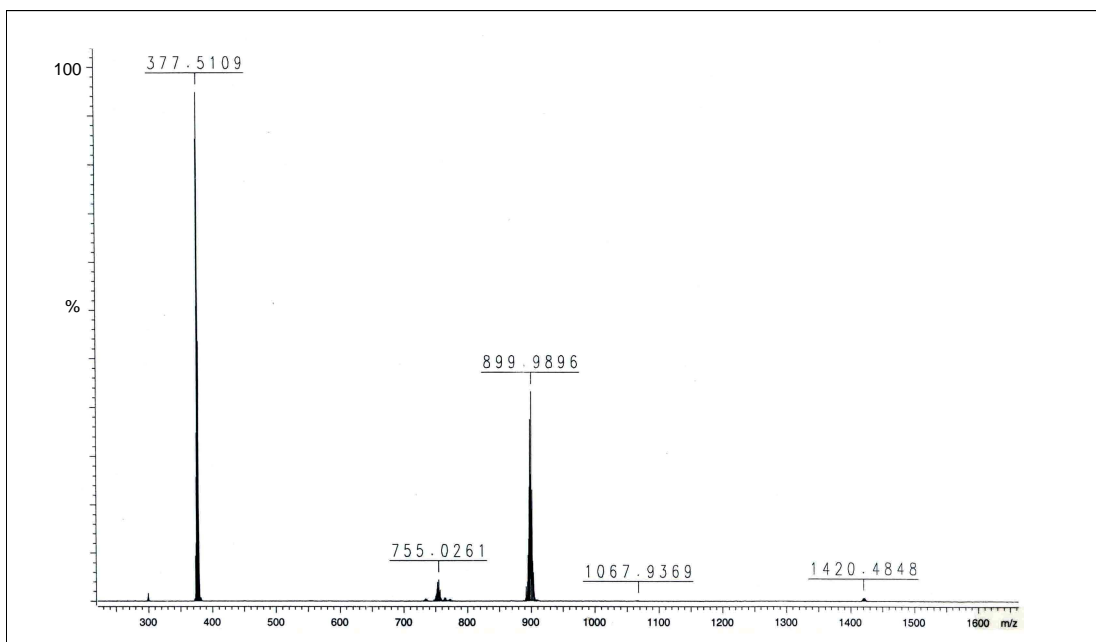


**Figure 3.64** ES mass spectrum of  $[\text{Ru}(\text{Clazpy})_3](\text{PF}_6)_2$

### 3.4.2.4 Infrared spectroscopy

The vibrational spectra of  $[\text{Ru}(\text{Clazpy})_2\text{L}](\text{PF}_6)_2$  (L = bpy, phen, azpy, Clazpy) complex in KBr disc were recorded in  $4000\text{-}400\text{ cm}^{-1}$ . They showed many vibration frequencies such as C=C, C=N, N=N (azo). The IR data of these complexes are given in Table 3.42 and these spectra are shown in Figure 3.65 to 3.68.

**Table 3.42** IR data of  $[\text{Ru}(\text{Clazpy})_2(\text{L})](\text{PF}_6)_2$  (L = bpy, phen, azpy, Clazpy)

Vibrational frequencies	Wave number ( $\text{cm}^{-1}$ ) $[\text{Ru}(\text{Clazpy})_2(\text{L})](\text{PF}_6)_2$ (L = ligands)			
	bpy	phen	azpy	Clazpy
C=N stretching and C=C stretching	1605(m)	1587(m)	1585(m)	1587(m)
	1548(m)	1549(m)	1549(m)	1546(s)
	1450(s)	1455(m)	1454(m)	1452(m)
				1429(m)
N=N(azo) stretching	1350(m)	1350(m)	1383(m) 1358(m)	1368(m)
C-N stretching	1122(s)	1121(s)	1122(s)	1123(s)
C-Cl	558(s)	558(s)	558(s)	578(s)
C-H out of plane bend in monosub.benzene	764 (s)	771(s)	771(m)	772(m)
	740(m)	737(m)	741(m)	739(m)
	691(m)	692(m)	692(m)	691(m)
$\text{PF}_6^-$ stretching	842(s)	838(s)	840(s)	839(s)

s = strong, m = medium

Infrared spectra of all complexes showed many vibrations of different intensities below  $1600\text{ cm}^{-1}$ . The N=N stretching of  $[\text{Ru}(\text{Clazpy})_2(\text{L})](\text{PF}_6)_2$  was shifted to higher frequencies than that of the parent chloro complex,  $[\text{Ru}(\text{Clazpy})_2\text{Cl}_2]$  at  $1336\text{ cm}^{-1}$ . This may be due to the competition between two  $\pi$ -acidic azoimine groups in  $[\text{Ru}(\text{Clazpy})_2(\text{L})]^{2+}$  and one polypyridine or azoimine compared to starting material (Santra, P. K., 2001). Thus, this peak shows a weaker azo coordination to ruthenium(II) in  $[\text{Ru}(\text{Clazpy})_2(\text{L})](\text{PF}_6)_2$  than parent complex. In addition, the most significant feature of these complexes in IR spectrum is the occurrence of a band at  $838\text{-}842\text{ cm}^{-1}$  due to the presence of ionic hexafluorophosphate.

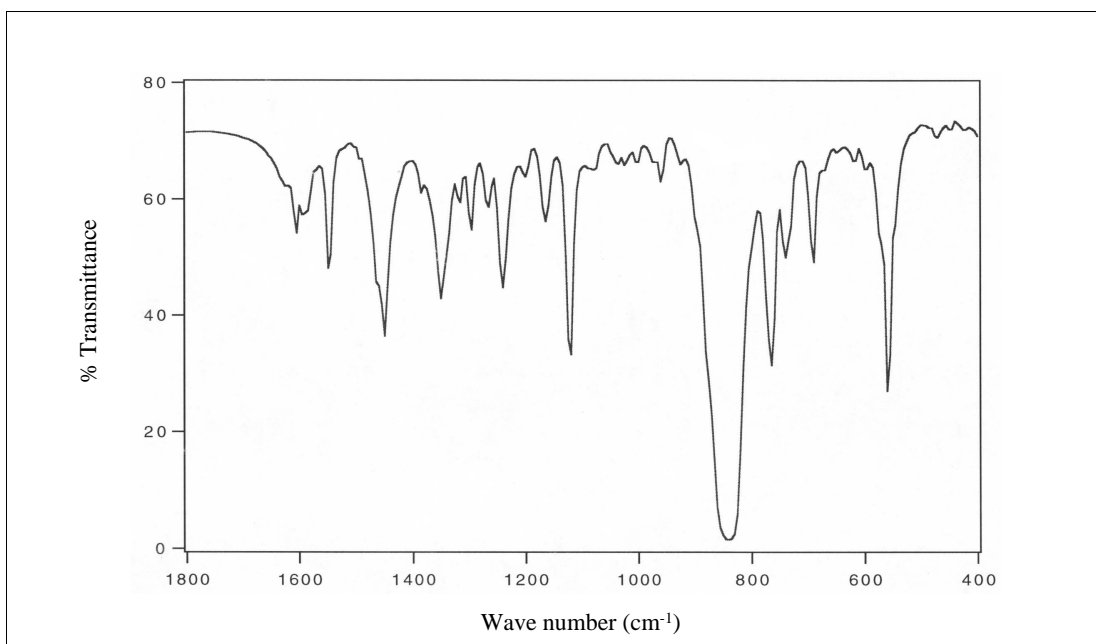


**Figure 3.65** IR spectrum of  $[\text{Ru}(\text{Clazpy})_2(\text{bpy})](\text{PF}_6)_2$

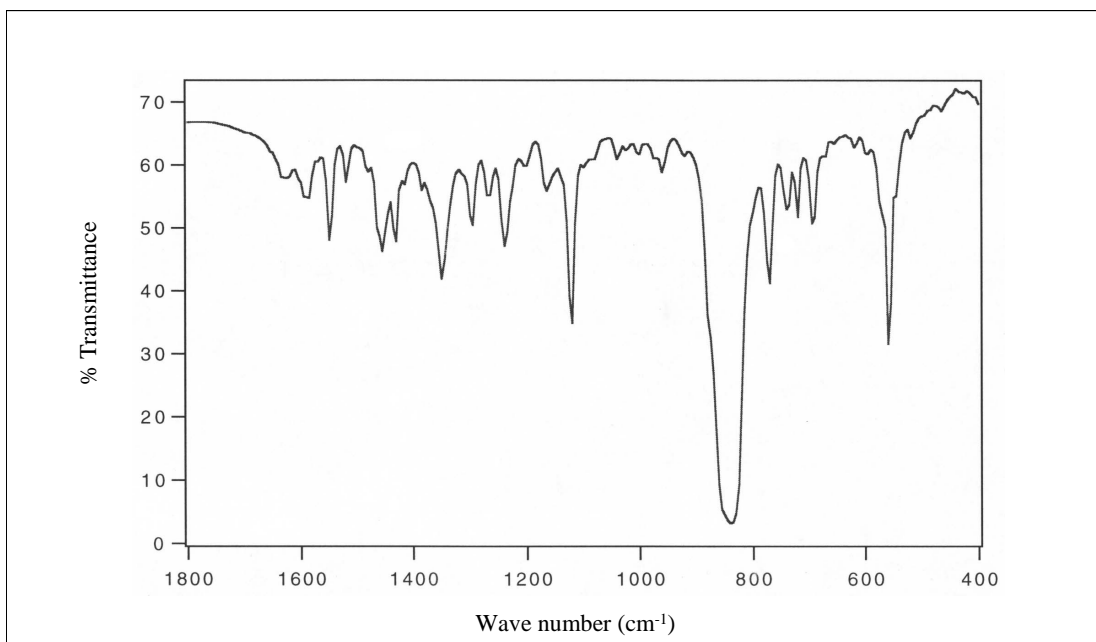


**Figure 3.66** IR spectrum of  $[\text{Ru}(\text{Clazpy})_2(\text{phen})](\text{PF}_6)_2$

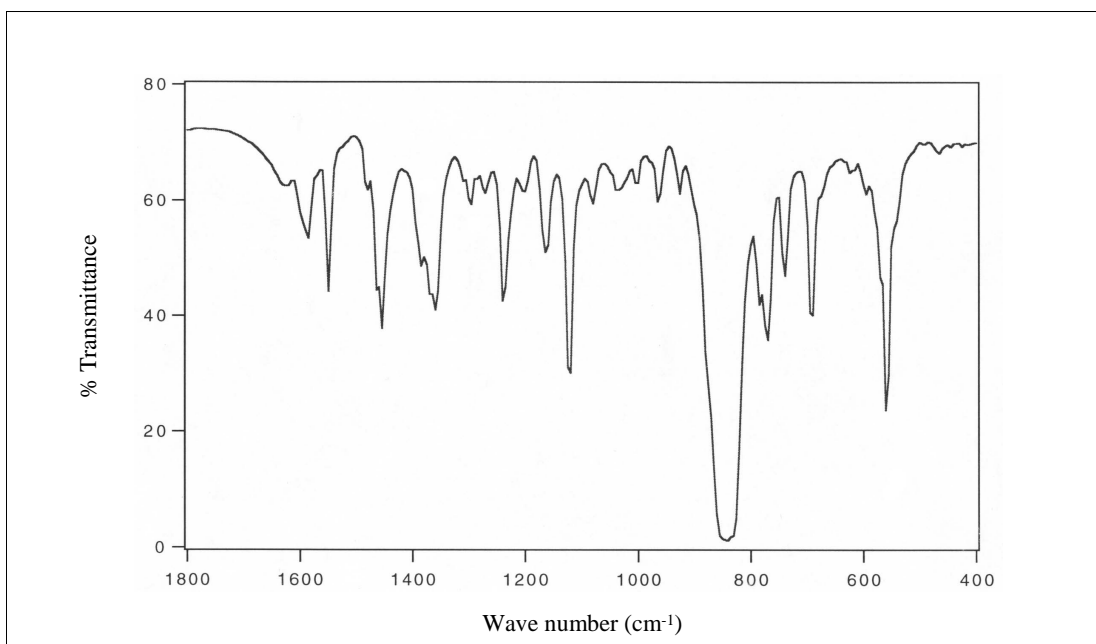


**Figure 3.67** IR spectrum of  $[\text{Ru}(\text{Clazpy})_2(\text{azpy})](\text{PF}_6)_2$

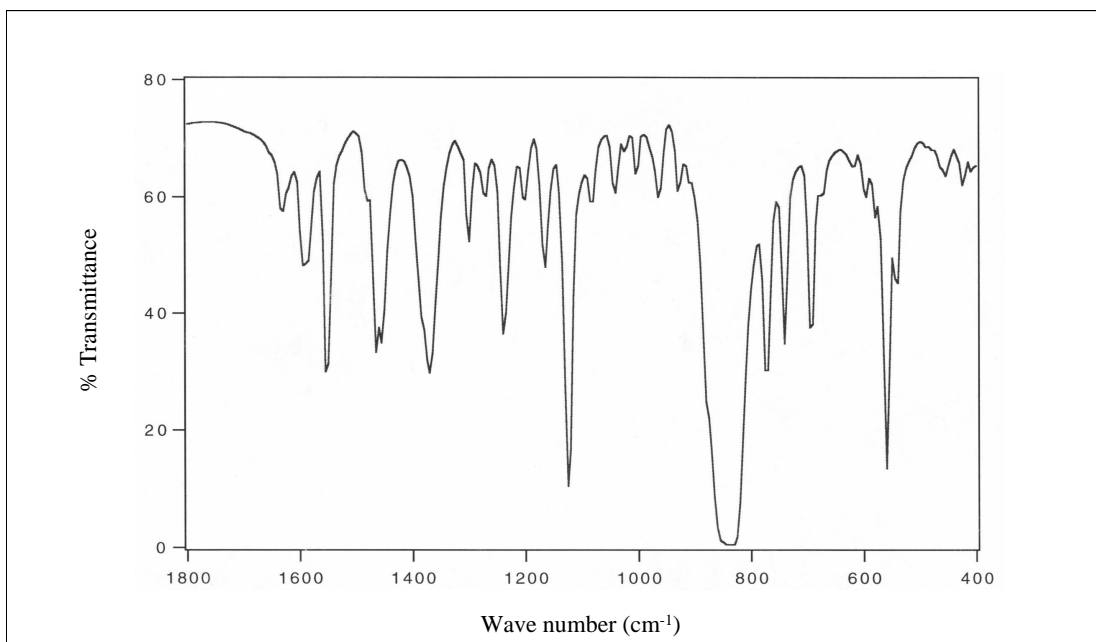


**Figure 3.68** IR spectrum of  $[\text{Ru}(\text{Clazpy})_3](\text{PF}_6)_2$

### 3.4.2.5 UV-Visible absorption spectroscopy

The UV-Visible absorption spectra of  $[\text{Ru}(\text{Clazpy})_2(\text{L})](\text{PF}_6)_2$  are recorded in six solvents;  $\text{CH}_3\text{OCH}_3$ ,  $\text{CH}_2\text{Cl}_2$ , DMF, DMSO,  $\text{CH}_3\text{CN}$  and EtOH in 200-800 nm range. Electronic spectra of these complexes in  $\text{CH}_3\text{CN}$  solution are shown in Figure 3.69 to 3.72 and absorption spectroscopic data are listed in Table 3.43 to 3.44.

**Table 3.43** UV-Visible absorption spectroscopic data of  $[\text{Ru}(\text{Clazpy})_2(\text{L})](\text{PF}_6)_2$   
(L = bpy, phen)

Solvents	$\lambda_{\text{max}}$ , nm ( $\epsilon^{\text{a}} \times 10^{-4} \text{ M}^{-1} \text{ cm}^{-1}$ )			
	$[\text{Ru}(\text{Clazpy})_2(\text{bpy})](\text{PF}_6)_2$			$[\text{Ru}(\text{Clazpy})_2(\text{phen})](\text{PF}_6)_2$
$\text{CH}_2\text{Cl}_2$	234(2.4)	282(2.3)		232(3.7) 277(3.1)
	314(2.2)	388(2.5)	521(1.1)	386(2.7) 516(1.3)
DMF	285(3.1)	382(2.2)		273(3.8) 376(2.4)
	493(1.3)	531(1.2)		525(1.5)
DMSO	319(3.7)	381(3.1)		279(5.4) 377(2.9)
	527(1.5)			524(1.6)
$\text{CH}_3\text{OCH}_3$	338(3.2)	381(3.6)		338(2.5) 378(2.8)
	521(1.6)			520(1.3)
$\text{CH}_3\text{CN}$	204(4.4)	282(2.7)		203(5.5) 223(4.9)
	313(2.8)	380(2.7)	520(1.1)	376(2.7) 516(1.3)
EtOH	207(3.2)	276(2.8)		223(4.2) 276(2.9)
	383(2.0)	520(0.8)		377(2.2) 513(1.0)
MeOH	207(5.1)	314(3.2)		208(3.8) 223(3.6)
	381(3.3)	518(1.3)		378(2.0) 514(0.9)

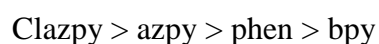
<sup>a</sup> Molar extinction coefficient

**Table 3.44** UV-Visible absorption spectroscopic data of [Ru(Clazpy)<sub>2</sub>(L)](PF<sub>6</sub>)<sub>2</sub>  
(L = azpy, Clazpy)

Solvents	$\lambda_{\max}$ , nm ( $\epsilon^a \times 10^{-4} \text{ M}^{-1} \text{ cm}^{-1}$ )			
	[Ru(Clazpy) <sub>2</sub> (azpy)](PF <sub>6</sub> ) <sub>2</sub>		[Ru(Clazpy) <sub>3</sub> ](PF <sub>6</sub> ) <sub>2</sub>	
CH <sub>2</sub> Cl <sub>2</sub>	233(3.3) 499(1.6)	388(4.9)	233(3.4) 494(1.6)	392(5.0)
DMF	278(3.5) 521(2.3)	365(3.3)	278(4.2) 526(2.4)	371(3.6)
DMSO	280(4.0) 381(4.2)	331(3.3) 504(1.5)	282(4.2) 383(4.8)	326(3.5) 498(1.7)
CH <sub>3</sub> OCH <sub>3</sub>	381(2.9)	499(0.9)	383(3.9)	494(1.3)
CH <sub>3</sub> CN	204(5.3) 495(1.3)	380(4.0)	203(4.9) 493(1.3)	383(4.3)
EtOH	207(2.6) 494(0.7)	382(2.1)	207(2.7) 385(2.3)	276(2.3) 492(0.7)
MeOH	209(5.1) 494(1.3)	382(4.0)	210(4.9) 493(1.3)	383(4.3)

<sup>a</sup> Molar extinction coefficient

The absorption spectra in UV region (200-400 nm) were assigned to  $\pi \rightarrow \pi^*$  transition of ligands ( $\epsilon \sim 22000 - 50000 \text{ M}^{-1} \text{ cm}^{-1}$ ). While, the absorption bands in visible region (400-800 nm) were assigned to metal-to-ligand charge-transfer transition (MLCT) ( $\epsilon \sim 7000 - 50000 \text{ M}^{-1} \text{ cm}^{-1}$ ). The lowest energy absorption bands of MLCT transition of [Ru(Clazpy)<sub>2</sub>(L)](PF<sub>6</sub>)<sub>2</sub> (L = bpy, phen, azpy, Clazpy) increase in order:



In addition, the lowest energy absorption bands of [Ru(Clazpy)<sub>2</sub>(L)](PF<sub>6</sub>)<sub>2</sub> (L = bpy, phen, azpy, Clazpy) were not shifted when the polarity of solvents was increased.

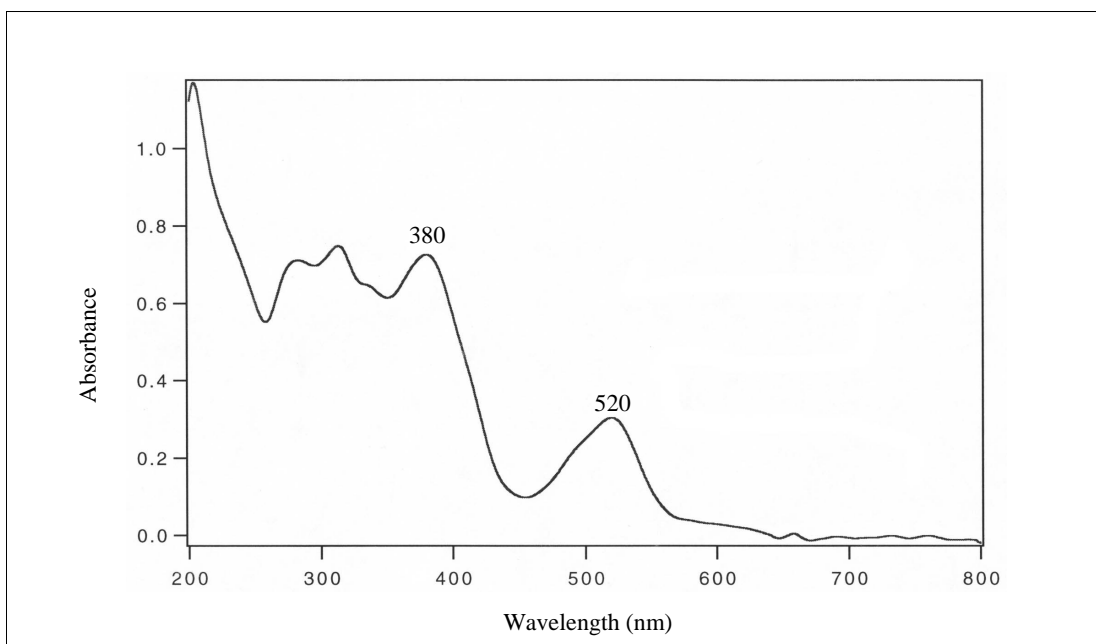


**Figure 3.69** UV-Visible absorption spectrum of  $[\text{Ru}(\text{Clazpy})_2(\text{bpy})](\text{PF}_6)_2$  in  $\text{CH}_3\text{CN}$

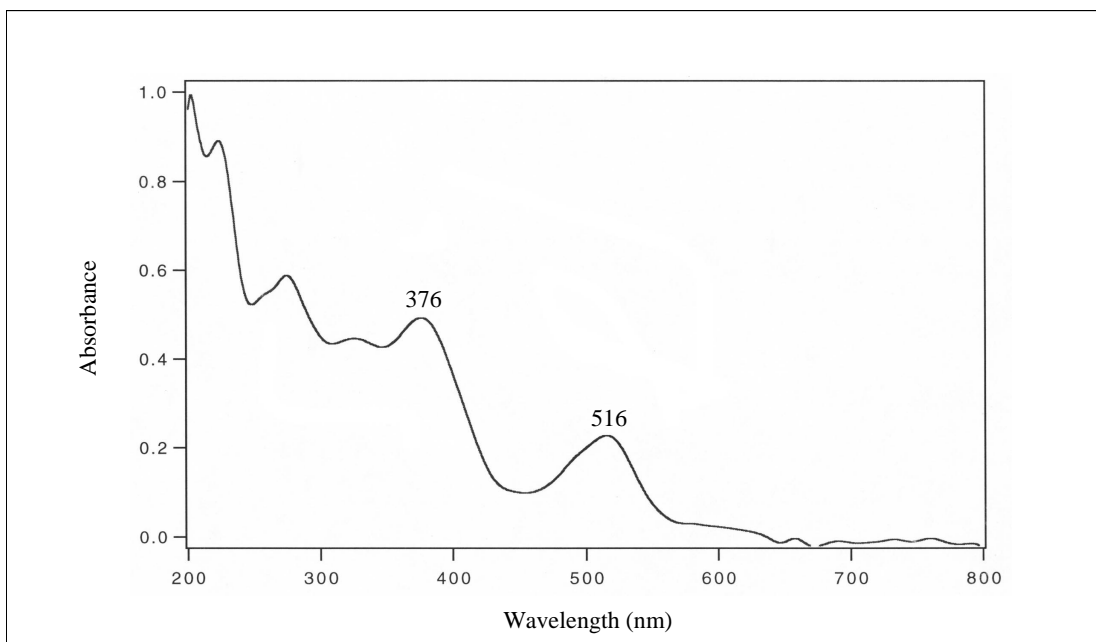


**Figure 3.70** UV-Visible absorption spectrum of  $[\text{Ru}(\text{Clazpy})_2(\text{phen})](\text{PF}_6)_2$  in  $\text{CH}_3\text{CN}$

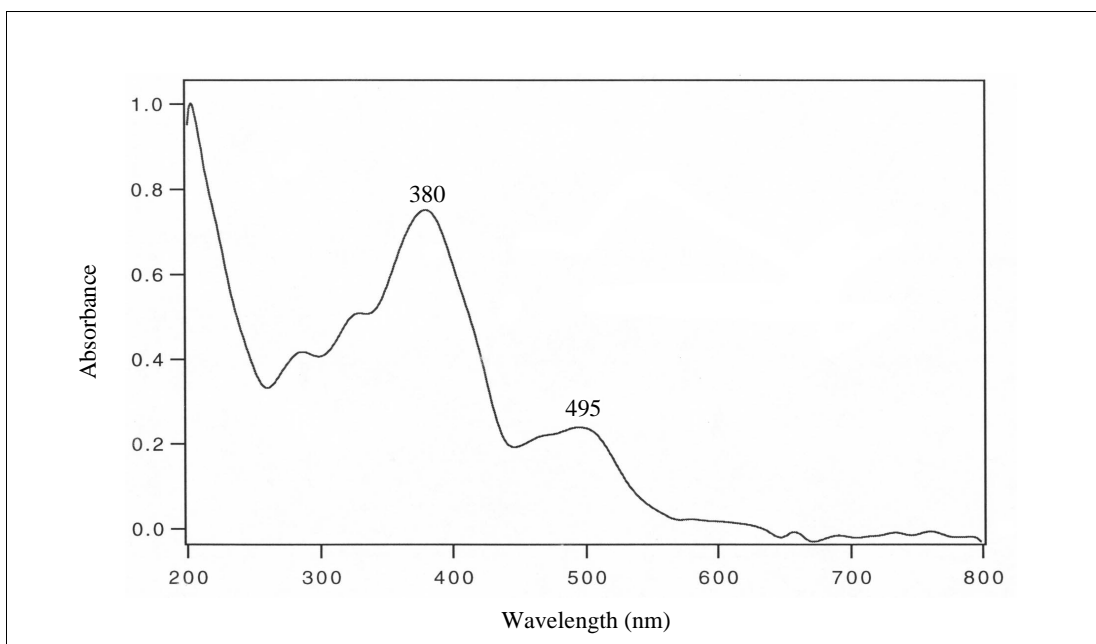


**Figure 3.71** UV-Visible absorption spectrum of  $[\text{Ru}(\text{Clazpy})_2(\text{azpy})](\text{PF}_6)_2$  in  $\text{CH}_3\text{CN}$

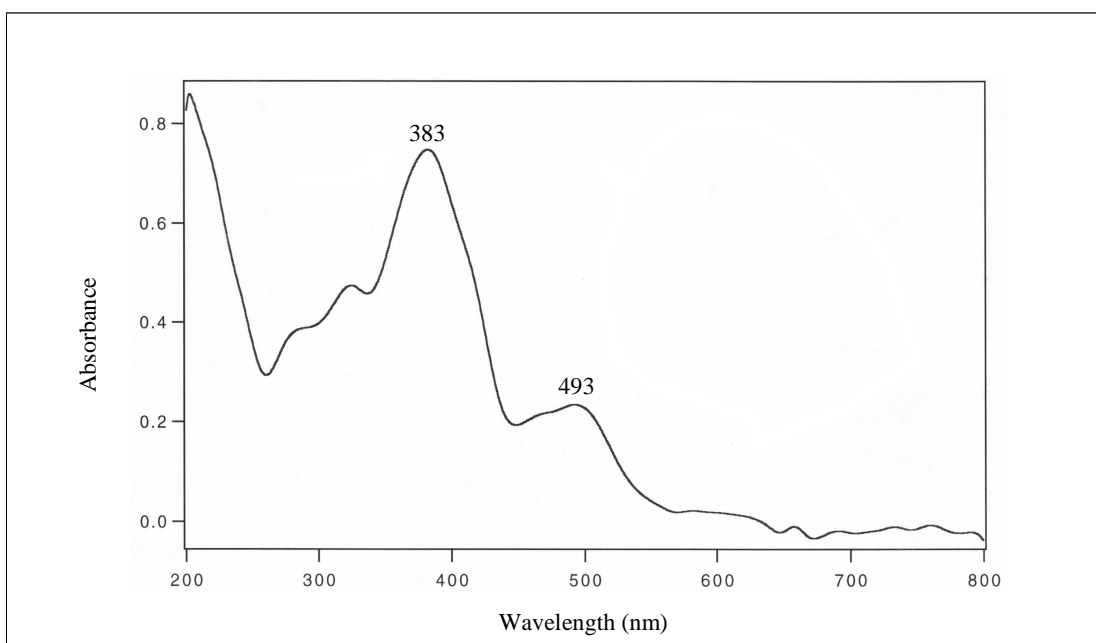


**Figure 3.72** UV-Visible absorption spectrum of  $[\text{Ru}(\text{Clazpy})_3](\text{PF}_6)_2$  in  $\text{CH}_3\text{CN}$

### 3.4.2.6 Nuclear magnetic resonance spectroscopy

The NMR data of  $[\text{Ru}(\text{Clazpy})_2(\text{L})](\text{PF}_6)_2$  ( $\text{L} = \text{bpy}$ , phen, azpy, Clazpy) was explained by using 1D and 2D NMR spectroscopic techniques ( $^1\text{H}$  NMR,  $^1\text{H}$ - $^1\text{H}$  COSY NMR,  $^{13}\text{C}$  NMR, DEPT NMR, and  $^1\text{H}$ - $^{13}\text{C}$  HMQC NMR). The NMR spectra were recorded in acetone- $d_6$  and tetramethylsilane ( $\text{Si}(\text{CH}_3)_4$ ) was used as an internal reference. The NMR spectroscopic data of  $[\text{Ru}(\text{Clazpy})_2(\text{L})](\text{PF}_6)_2$  ( $\text{L} = \text{bpy}$ , phen, azpy, Clazpy) complexes are presented in Table 3.45 to 3.48.

Nuclear magnetic resonance spectroscopy of  $[\text{Ru}(\text{Clazpy})_2(\text{bpy})](\text{PF}_6)_2$

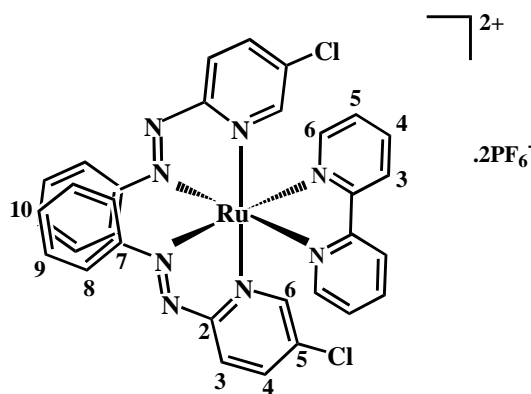


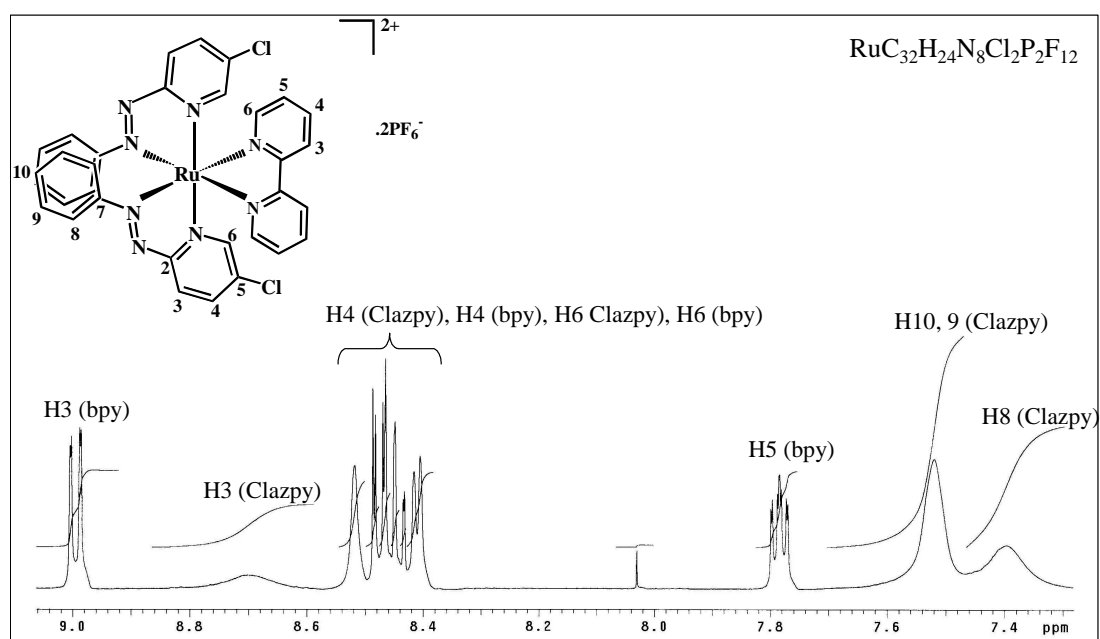
**Table 3.45**  $^1\text{H}$ - $^{13}\text{C}$  NMR spectroscopic data of  $[\text{Ru}(\text{Clazpy})_2(\text{bpy})](\text{PF}_6)_2$ 

H-position	$^1\text{H}$ NMR			$^{13}\text{C}$ NMR (CH-type)
	$\delta$ (ppm)	$J$ (Hz)	Amount of H	
3 (bpy)	8.98 (dd)	8.0, 1.0	1	126.61
3 (Clazpy)	8.76 (b)	-	1	131.50
4 (Clazpy)	8.48 (bs)	8.0, 1.0	1	149.50
4 (bpy)	8.46 (dd)	8.0, 2.5	1	141.68
6 (Clazpy)	8.42 (dd)	7.0, 1.0	1	156.50
6 (bpy)	8.41 (d)	5.5	1	154.35
5 (bpy)	7.78 (ddd)	7.0, 1.0, 5.5	1	129.50
10 (Clazpy)	7.61 (b)	-	3	134.00
9 (Clazpy)				
8 (Clazpy)	7.48 (b)	-	2	130.05
Quaternary carbons (C)				162.77(C2)
				142.27(C5)
				124.71(C7)

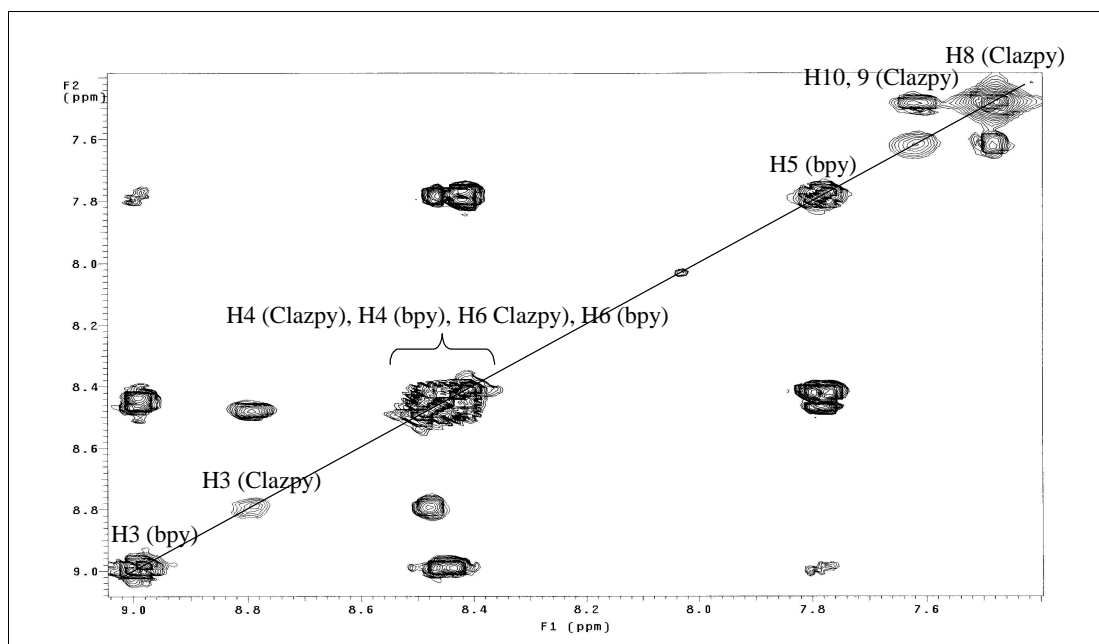
bs = broad of singlet, b = broad, d = doublet, dd = doublet of doublet,  
ddd = doublet of doublet of doublet

The  $^1\text{H}$  NMR spectrum (Figure 3.73) of  $[\text{Ru}(\text{Clazpy})_2(\text{bpy})](\text{PF}_6)_2$  complex showed 10 resonances of 24 protons, six from Clazpy ligand and four from bpy ligand. The spectrum displayed only one set of proton of each ligands (Clazpy and bpy). This result indicated that both Clazpy ligands were equivalent. A chemical shift of proton H3 on the bpy ligand occurred at the lowest field (8.98 ppm) due to trans effect of pyridine of bpy to N=N azo of Clazpy. In addition, others protons in this compound were also studied by using simple correlation  $^1\text{H}$ - $^1\text{H}$  COSY NMR spectroscopy (Figure 3.74).

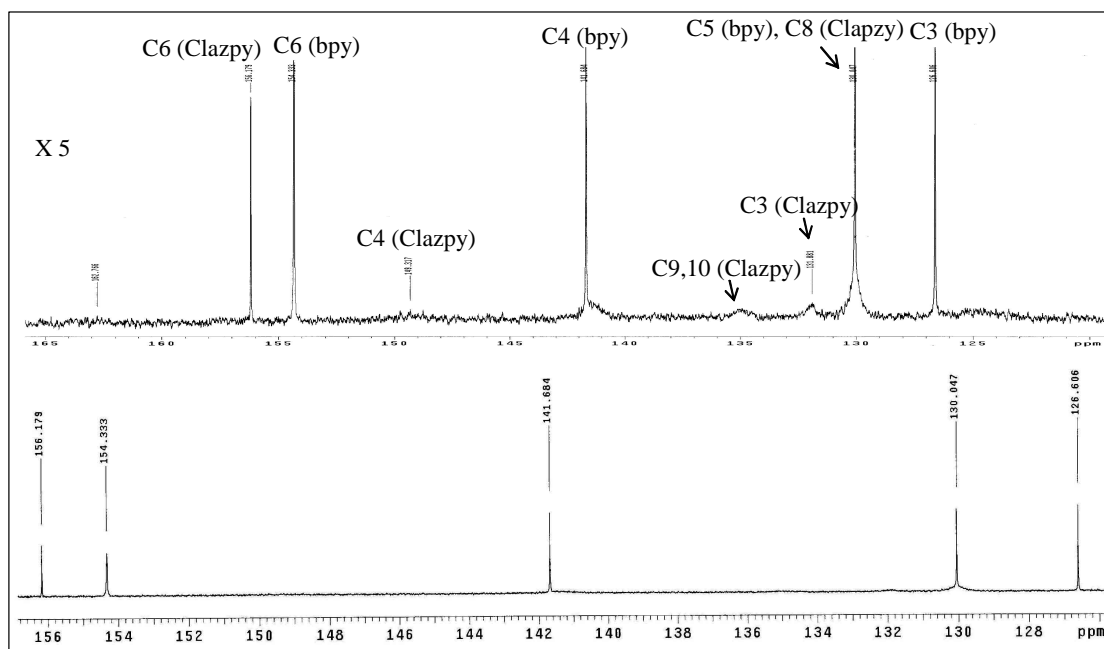
The  $^{13}\text{C}$  NMR (Figure 3.75) results corresponded to the DEPT NMR (Figure 3.76) which showed only one kind of methane carbons. The downfield signals at 156.00 ppm belonged to C2 of bpy. The signals at 162.77, 142.27 and 124.71 ppm were assigned to two quaternary carbons C2, C5 and C7 of Clazpy ligand. Moreover, the other  $^{13}\text{C}$  NMR signal assignments were based on  $^1\text{H}$ - $^{13}\text{C}$  HMQC NMR spectrum (Figure 3.77).



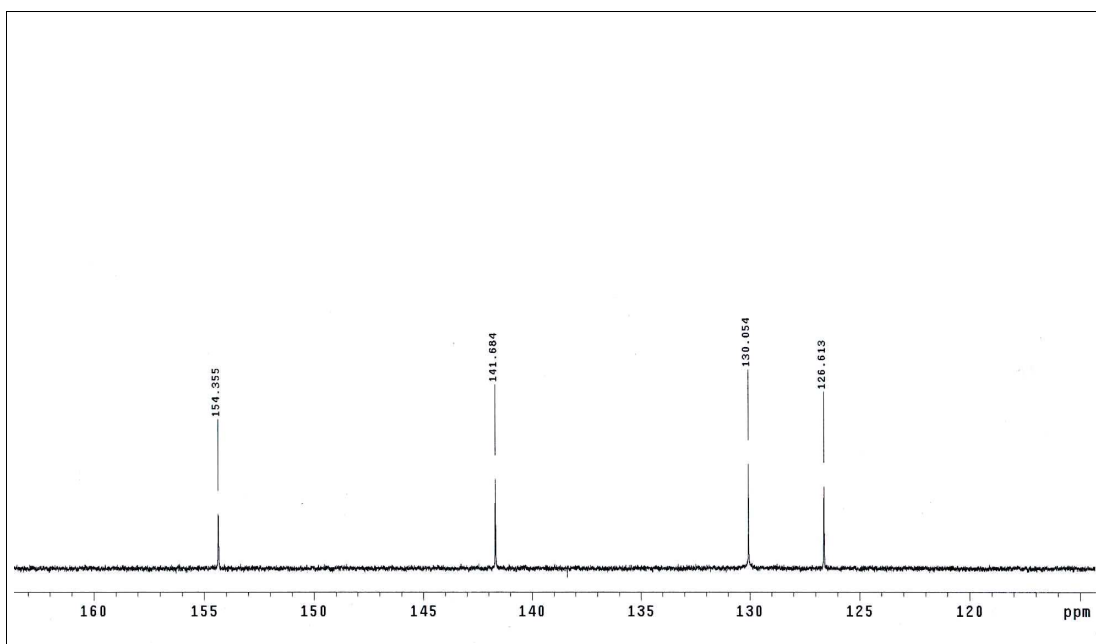
**Figure 3.73**  $^1\text{H}$  NMR spectrum of  $[\text{Ru}(\text{Clazpy})_2(\text{bpy})](\text{PF}_6)_2$  in acetone- $d_6$



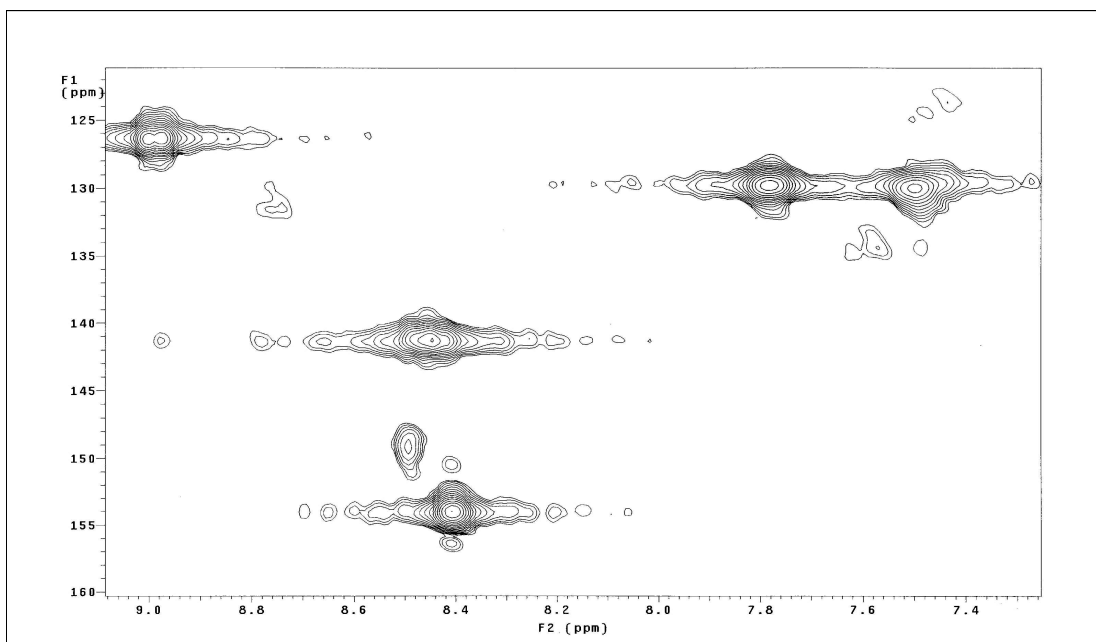
**Figure 3.74**  $^1\text{H}$ - $^1\text{H}$  COSY NMR spectrum of  $[\text{Ru}(\text{Clazpy})_2(\text{bpy})](\text{PF}_6)_2$  in acetone- $d_6$



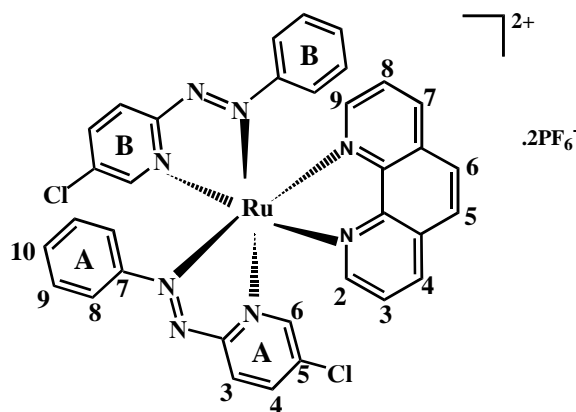
**Figure 3.75**  $^{13}\text{C}$  NMR spectrum of  $[\text{Ru}(\text{Clazpy})_2(\text{bpy})](\text{PF}_6)_2$  in acetone- $d_6$



**Figure 3.76** DEPT NMR spectrum of  $[\text{Ru}(\text{Clazpy})_2(\text{bpy})](\text{PF}_6)_2$  in acetone- $d_6$



**Figure 3.77**  $^1\text{H}$ - $^{13}\text{C}$  HMQC NMR spectrum of  $[\text{Ru}(\text{Clazpy})_2(\text{bpy})](\text{PF}_6)_2$  in acetone- $d_6$

Nuclear magnetic resonance spectroscopy of  $[\text{Ru}(\text{Clazpy})_2(\text{phen})](\text{PF}_6)_2$ 

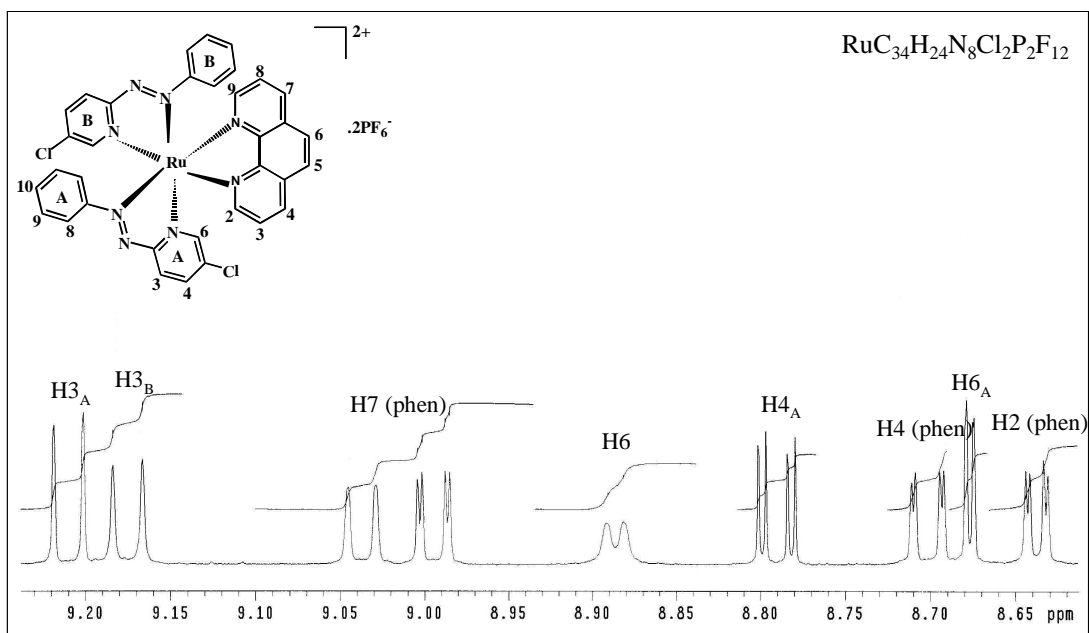
The  $^1\text{H}$  NMR spectrum (Figure 3.78 -3.79) of  $[\text{Ru}(\text{Clazpy})_2(\text{phen})](\text{PF}_6)_2$  showed 20 resonances of 24 protons (twelve signals from Clazpy ligand and eight signals from phen ligand). This result indicated that the Clazpy ligands were not equivalent. Besides, the  $^1\text{H}$  NMR signals of phen showed no equivalent. In addition, the first signal exhibited at the lowest field was proton 3A (9.21 ppm) on pyridine ring of Clazpy which trans to N=N azo function of Clazpy. In addition, others protons in this compound were also studied by using simple correlation  $^1\text{H}$ - $^1\text{H}$  COSY NMR spectroscopy (Figure 3.80).

The  $^{13}\text{C}$  NMR (Figure 3.81) results corresponded to the DEPT NMR (Figure 3.82) which showed only one kind of methane carbons. All quaternary carbons at 164.75, 163.22, 158.32, 154.06, 146.75, 146.54, 146.45, 138.35, 132.67 belonged to C2, C5, C7 of Clazpy and C10, C11, C12, C13 of phen. Moreover, the others  $^{13}\text{C}$  NMR signals assignments were based on  $^1\text{H}$ - $^{13}\text{C}$  HMQC NMR spectrum (Figure 3.83).

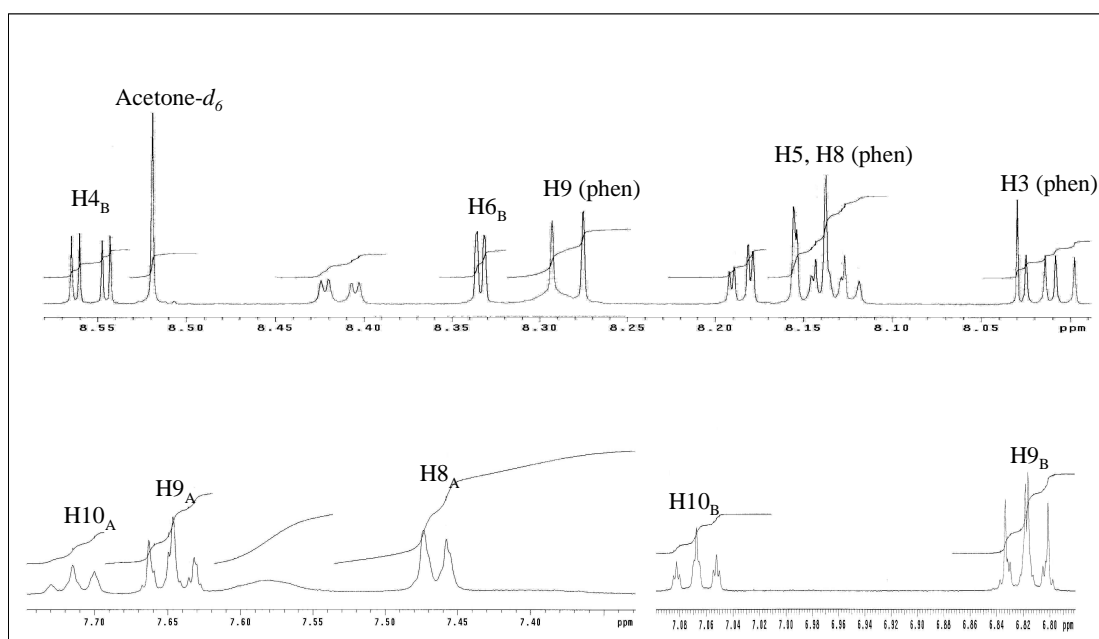
**Table 3.46**  $^1\text{H}$ - $^{13}\text{C}$  NMR spectroscopic data of  $[\text{Ru}(\text{Clazpy})_2(\text{phen})](\text{PF}_6)_2$ 

H-position	$^1\text{H}$ NMR			$^{13}\text{C}$ NMR (CH-type)
	$\delta$ (ppm)	$J$ (Hz)	Amount of H	
3A	9.21 (d)	9.0	1	131.96
3B	9.18 (d)	9.0	1	131.81
7	9.04 (d)	8.0	1	141.12
6	8.88 (d)	4.5	1	155.23
4A	8.79 (dd)	2.0, 9.0	1	143.14
4	8.70 (dd)	8.5, 1.0	1	139.93
2	8.64 (dd)	5.0, 1.0	1	153.38
6A	8.68 (dd)	2.0	1	140.62
4B	8.56 (dd)	9.0, 2.5	1	142.18
6B	8.33 (d)	1.5	1	150.56
9	8.19 (d)	9.0	1	128.93
5	8.16 (d)	1.0	1	153.39
8	8.14 (dd)	8.5, 5.0	1	128.36
3	8.01 (dd)	8.5, 5.0	1	128.16
10A	7.72 (t)	7.5	1	134.27
9A	7.65 (tt)	7.5, 1.5	2	131.10
8A	7.47 (d)	7.5	2	124.19
10B	7.07 (tt)	7.5, 1.5	1	132.57
9B	6.82 (tt)	7.5, 1.5	2	129.50
8B	6.38 (dd)	7.5, 1.5	2	121.99
Quaternary carbons (C)				164.78, 163.22, 158.32, 154.02, 146.82, 146.58, 146.52, 138.48, 132.77

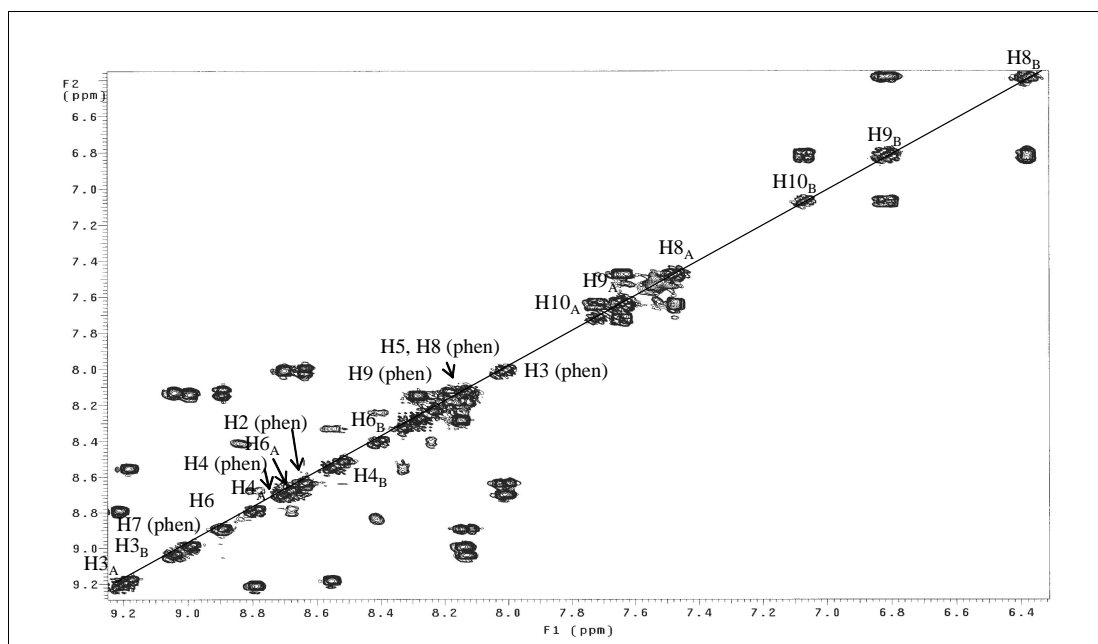
d = doublet, dd = doublet of doublet, t = triplet, tt = triplet of triplet



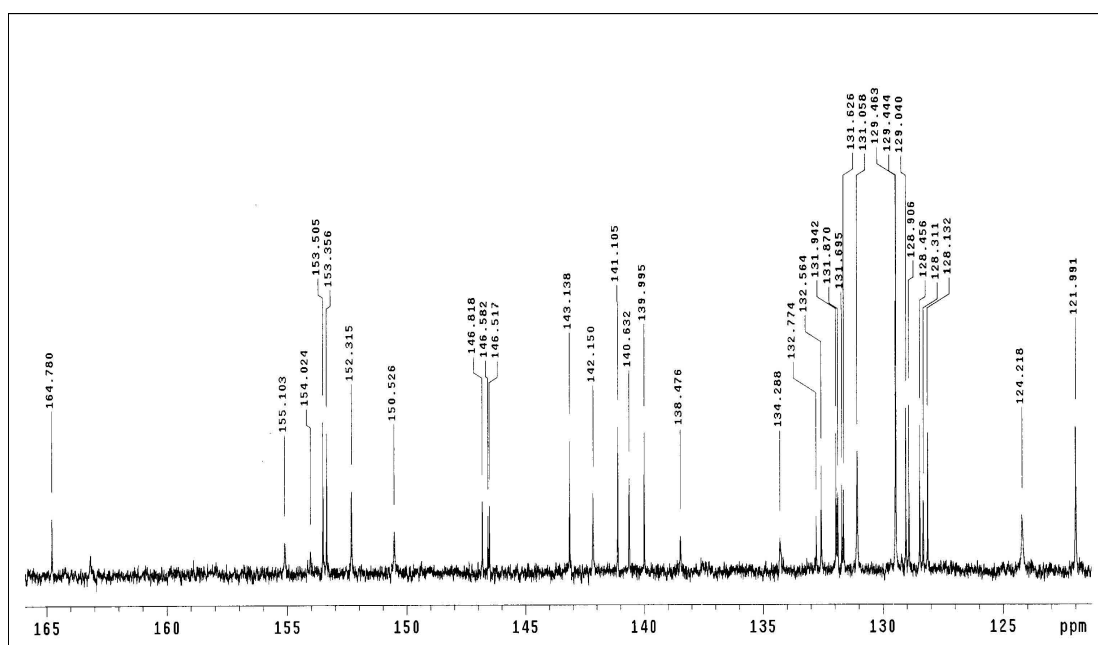
**Figure 3.78**  $^1\text{H}$  NMR spectrum of  $[\text{Ru}(\text{Clazpy})_2(\text{phen})](\text{PF}_6)_2$  in  $\text{acetone-}d_6$



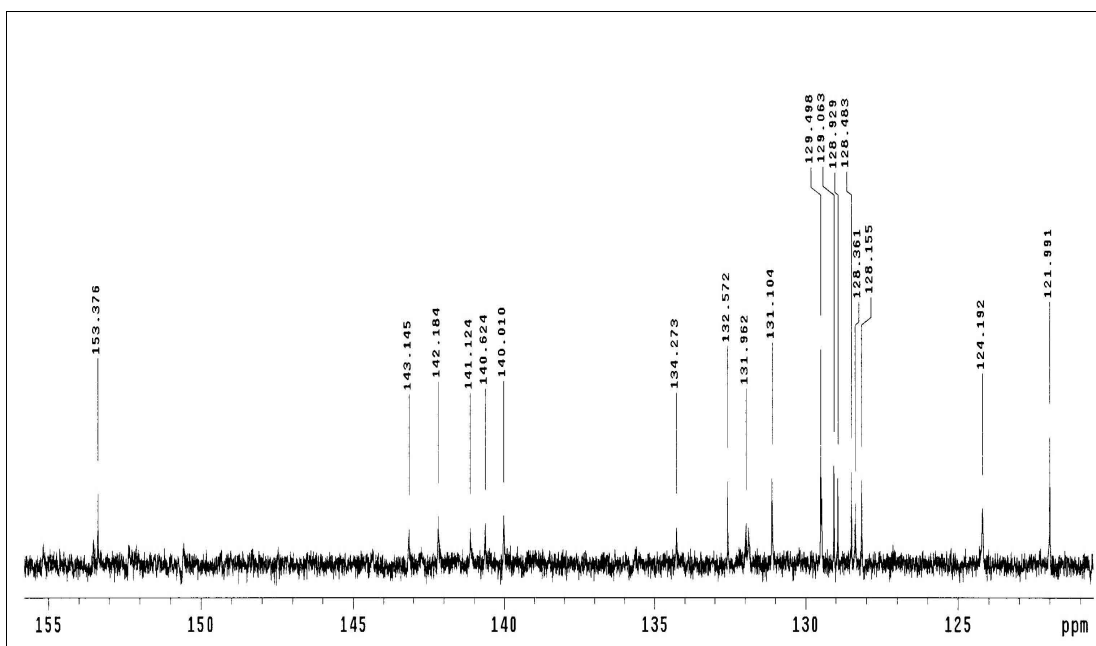
**Figure 3.79**  $^1\text{H}$  NMR spectrum of  $[\text{Ru}(\text{Clazpy})_2(\text{phen})](\text{PF}_6)_2$  in  $\text{acetone-}d_6$



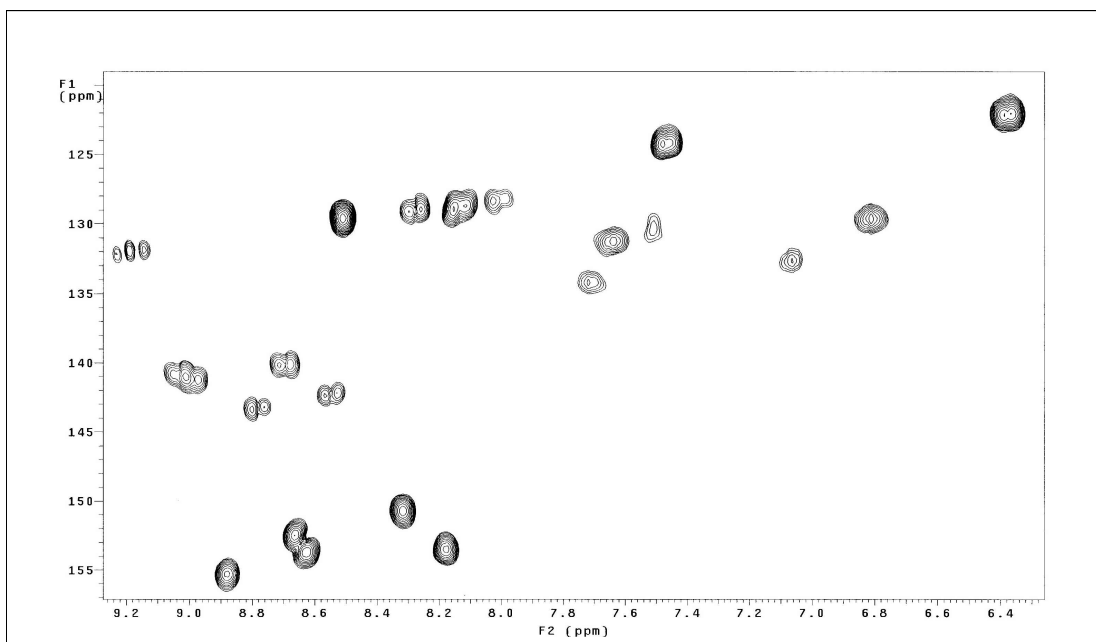
**Figure 3.80**  $^1\text{H}$ - $^1\text{H}$  COSY NMR spectrum of  $[\text{Ru}(\text{Clazpy})_2(\text{phen})](\text{PF}_6)_2$  in acetone- $d_6$



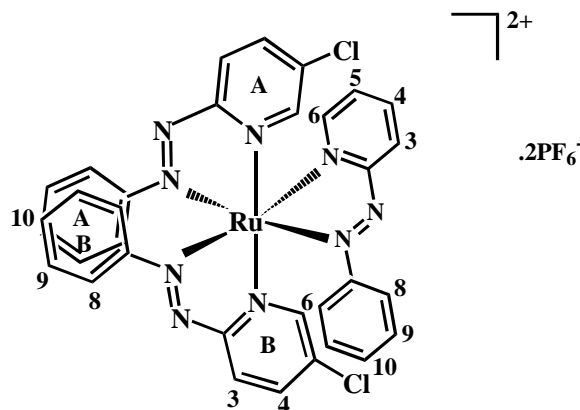
**Figure 3.81**  $^{13}\text{C}$  NMR spectrum of  $[\text{Ru}(\text{Clazpy})_2(\text{phen})](\text{PF}_6)_2$  in acetone- $d_6$



**Figure 3.82** DEPT NMR spectrum of  $[\text{Ru}(\text{Clazpy})_2(\text{phen})](\text{PF}_6)_2$  in acetone- $d_6$



**Figure 3.83**  $^1\text{H}$ - $^{13}\text{C}$  NMR spectrum of  $[\text{Ru}(\text{Clazpy})_2(\text{phen})](\text{PF}_6)_2$  in acetone- $d_6$

Nuclear magnetic resonance spectroscopy of  $[\text{Ru}(\text{Clazpy})_2(\text{azpy})](\text{PF}_6)_2$ 

The  $^1\text{H}$  NMR spectrum (Figure 3.84) of  $[\text{Ru}(\text{Clazpy})_2(\text{azpy})](\text{PF}_6)_2$  complex showed 14 resonances of 25 protons because some resonances were overlapped. This result indicated that three of ligands are unsymmetrical molecules. In addition, the first signal exhibited at the lowest field was proton H3 (azpy) (9.27 ppm) on pyridine ring of azpy ligand which trans to N=N azo function of Clazpy. In addition, others protons in this compound were also studied by using simple correlation  $^1\text{H}$ - $^1\text{H}$  COSY NMR spectroscopy (Figure 3.85).

The  $^{13}\text{C}$  NMR (Figure 3.86) results corresponded to the DEPT NMR (Figure 3.87) which showed only one kind of methane carbons. All quaternary carbons at 163.93, 155.98, 133.91, 123.5, 135.5 belonged to C2, C7 of azpy ligand and C2, C5, C7 of Clazpy ligand. Moreover, the others  $^{13}\text{C}$  NMR signals assignments were based on  $^1\text{H}$ - $^{13}\text{C}$  HMQC NMR spectrum (Figure 3.88).

**Table 3.47**  $^1\text{H}$ - $^{13}\text{C}$  NMR spectroscopic data of  $[\text{Ru}(\text{Clazpy})_2(\text{azpy})](\text{PF}_6)_2$ 

H-position	$^1\text{H}$ NMR			$^{13}\text{C}$ NMR (CH-type)
	$\delta$ (ppm)	$J$ (Hz)	Amount of H	
3 (azpy)	9.27 (d)	8.0	1	133.48
6 (azpy)	8.80 (d)	5.0	1	154.13
4 (azpy)	8.72 (t)	8.0	4	143.45
3B	8.70 (m)	-		143.45
6A				143.45
3A				143.45
4B	8.60 (dd)		8.5, 2.0	1
4A	8.51 (dd)	8.5, 2.0	1	142.91
6B	8.44 (dd)	2.0	1	151.09
5 (azpy)	7.98 (t)	-	1	132.31
10 (azpy)	7.69 (t)	8.0	1	135.02
9A	7.58 (t)	8.0	5	124.36
9 (azpy)				131.05
10A				124.36
8A	7.49 (d)	8.5	3	130.47
10B				124.36
9B	7.43 (t)	8.0	4	130.70
8 (azpy)				130.70
8B	7.08 (b)	-	2	124.40
Quaternary carbons (C)				163.93, 155.98, 133.91, 123.5, 135.5

S = singlet, d = doublet, dd = doublet of doublet, t = triplet, m = multiplet

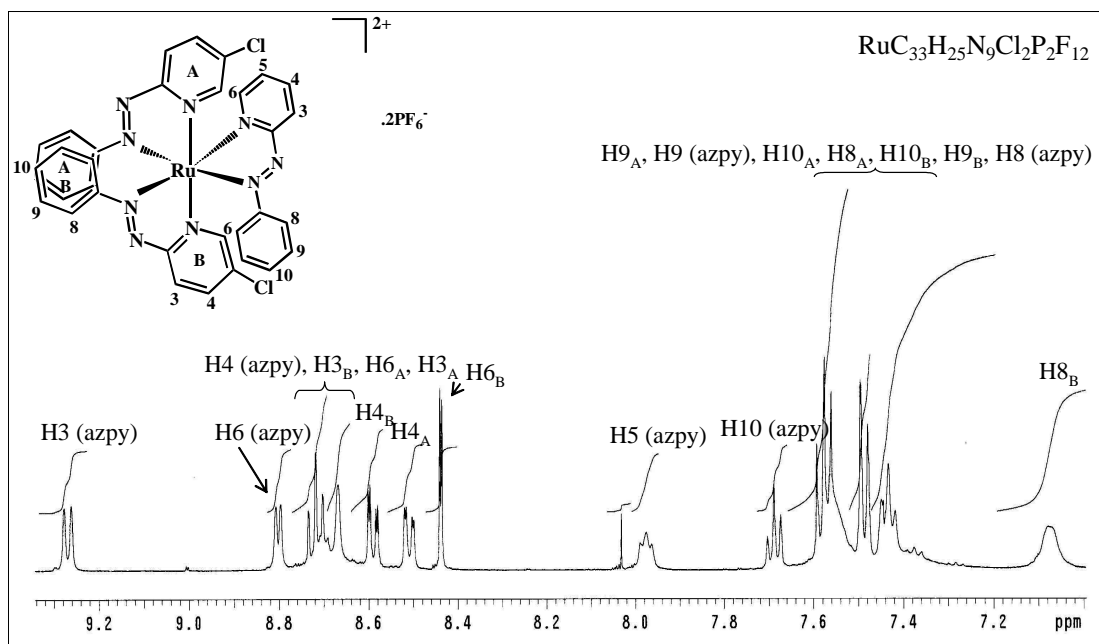


**Figure 3.84**  $^1\text{H}$  NMR spectrum of  $[\text{Ru}(\text{Clazpy})_2(\text{azpy})](\text{PF}_6)_2$  in acetone- $d_6$

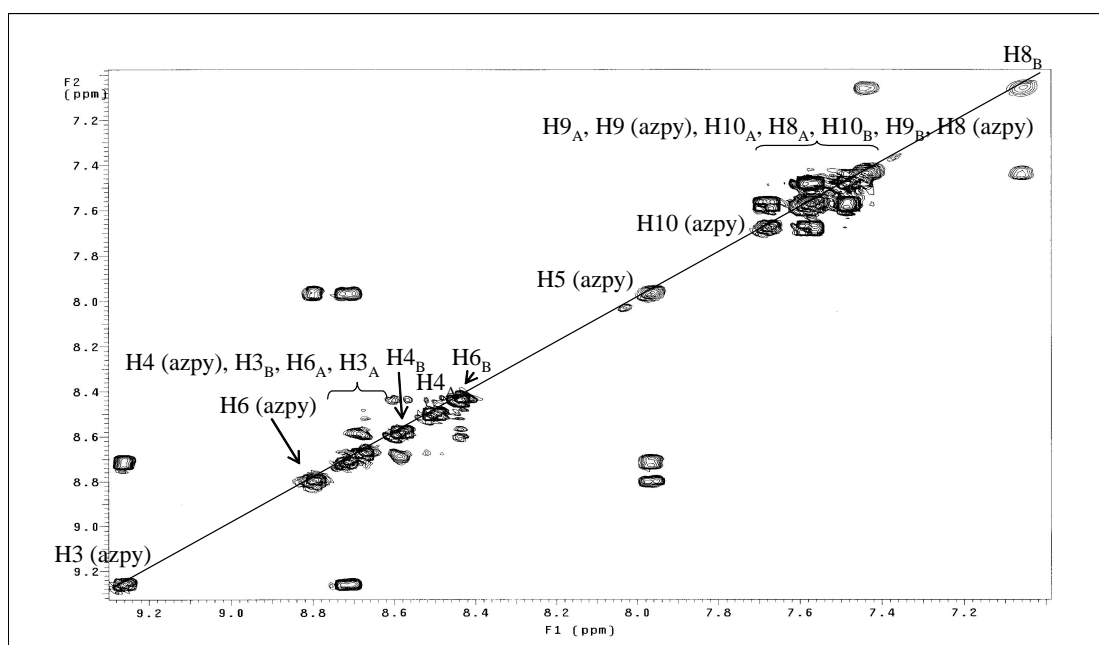


**Figure 3.85**  $^1\text{H}$ - $^1\text{H}$  COSY NMR spectrum of  $[\text{Ru}(\text{Clazpy})_2(\text{azpy})](\text{PF}_6)_2$  in acetone- $d_6$

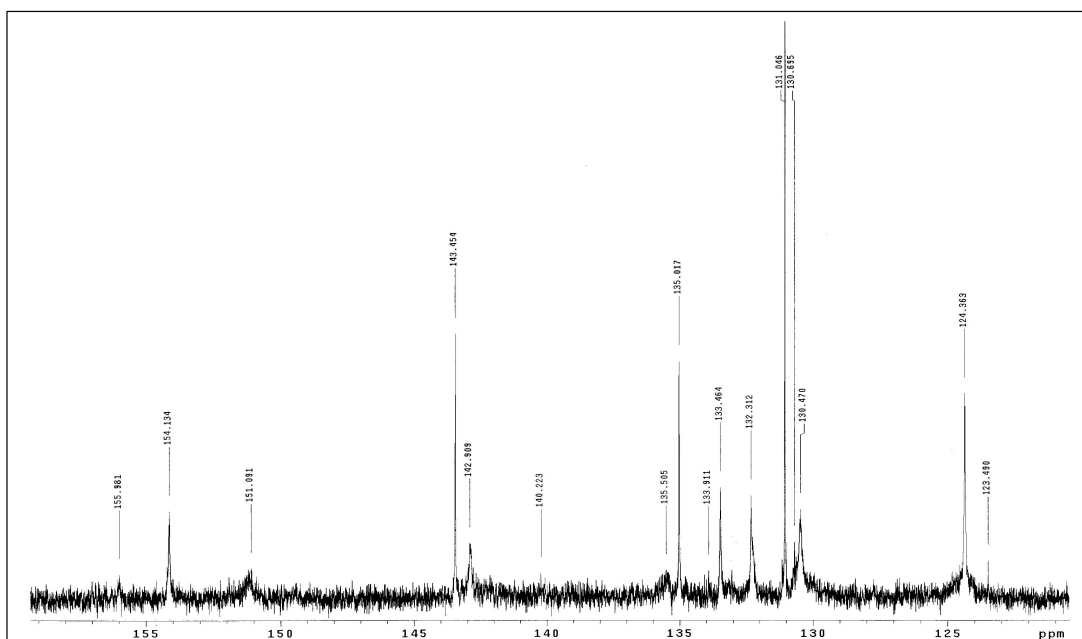


**Figure 3.86**  $^{13}\text{C}$  NMR spectrum of  $[\text{Ru}(\text{Clazpy})_2(\text{azpy})](\text{PF}_6)_2$  in acetone- $d_6$

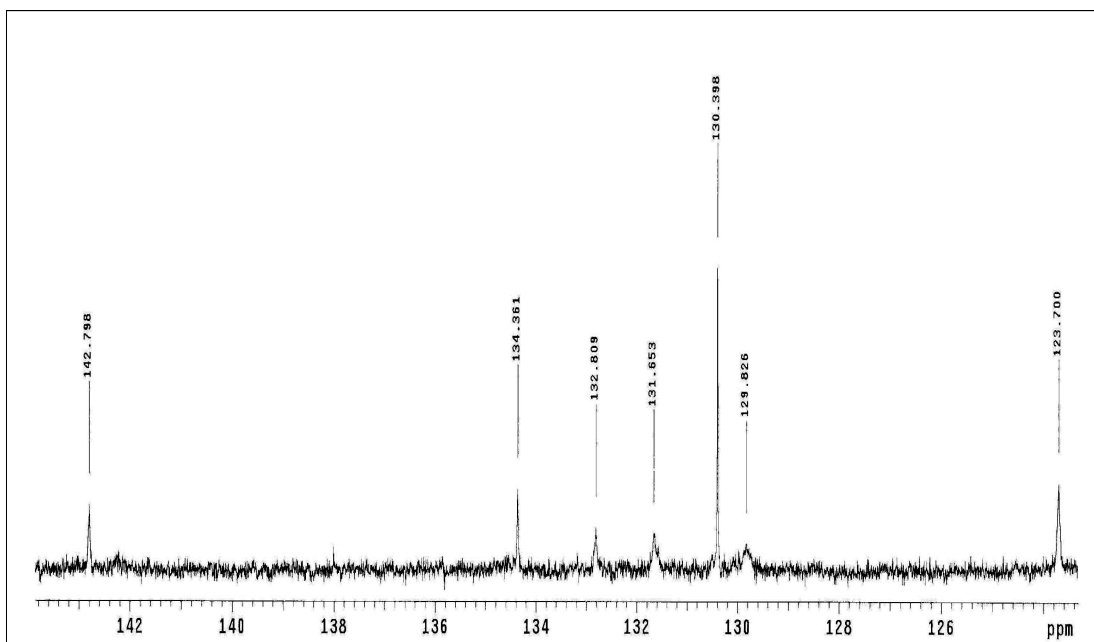


**Figure 3.87** DEPT NMR spectrum of  $[\text{Ru}(\text{Clazpy})_2(\text{azpy})](\text{PF}_6)_2$  in acetone- $d_6$

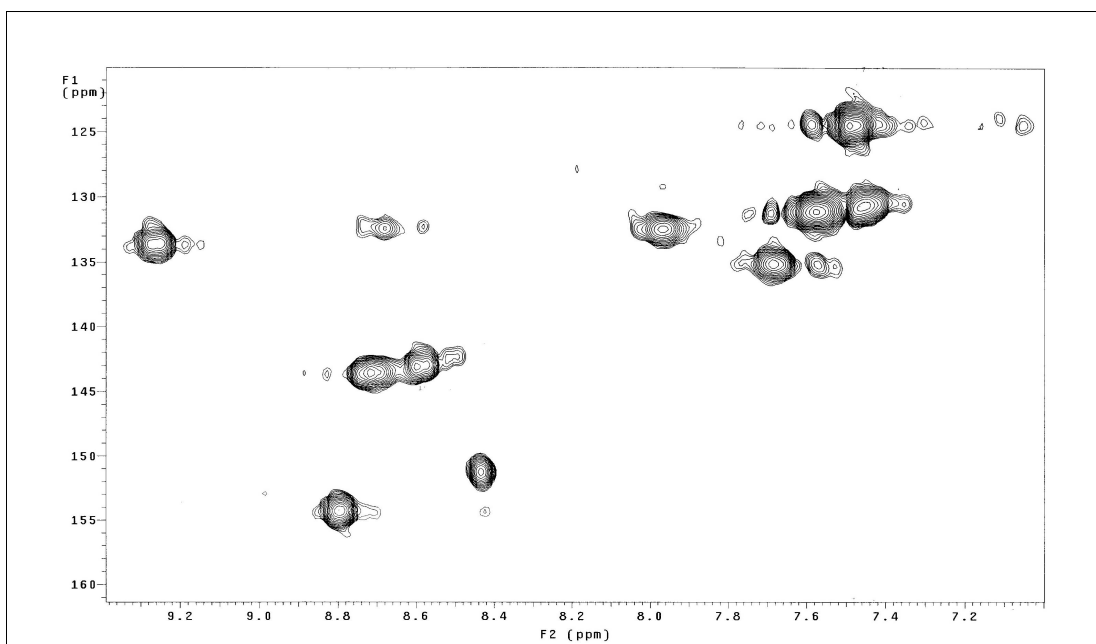


**Figure 3.88**  $^1\text{H}$ - $^{13}\text{C}$  HMQC NMR spectrum of  $[\text{Ru}(\text{Clazpy})_2(\text{azpy})](\text{PF}_6)_2$  in acetone- $d_6$

Nuclear magnetic resonance spectroscopy of  $[\text{Ru}(\text{Clazpy})_3](\text{PF}_6)_2$

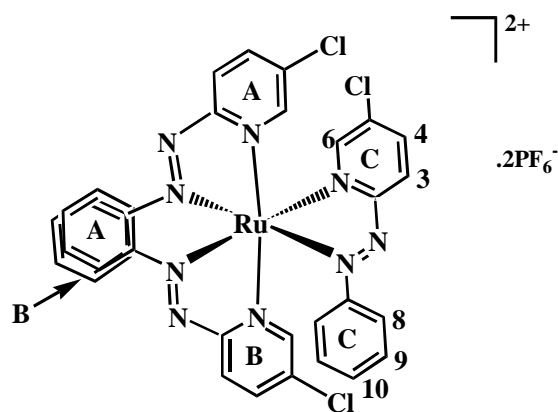


**Table 3.48**  $^1\text{H}$ - $^{13}\text{C}$  NMR spectroscopic data of  $[\text{Ru}(\text{Clazpy})_3](\text{PF}_6)_2$ 

H-position	$^1\text{H}$ NMR			$^{13}\text{C}$ NMR (CH-type)
	$\delta$ (ppm)	$J$ (Hz)	Amount of H	
3C	9.29 (d)	9.0	1	133.57
6C	8.96 (d)	2.0	1	153.16
4C	8.76 (dd)	9.0, 2.0	1	143.16
3A, 3B	8.74 (d)	8.5	2	131.04
6A	8.62 (dd)	2.0	1	143.16
4A	8.60 (dd)	9.0, 2.0	1	151.84
6B	8.58 (dd)	2.0	1	142.88
4B	8.51 (dd)	9.0, 2.0	1	141.50
10A, 10C	7.68 (t)	7.5	2	135.20
9A, 9C	7.57 (t)	7.5	4	130.63
8A, 10B	7.53 (m)	-	3	135.20
8C	7.48 (d)	8.0	2	124.50
9B	7.40 (t)	8.0	2	130.00
8B	7.10 (d)	8.0	2	124.00
Quaternary carbons (C)				162.59, 139.51, 135.34

d = doublet, dd = doublet of doublet, t = triplet, m = multiplet

The  $^1\text{H}$  NMR spectrum (Figure 3.89) of  $[\text{Ru}(\text{Clazpy})_3](\text{PF}_6)_2$  complex showed 12 resonances of 24 protons. Some appeared to be multiple signals due to overlap of resonances. In addition, the protons H3, H4 and H6 on pyridine ring appear at lower downfield than protons H8, H9 and H10 on phenyl ring. This may be due to the pyridine protons having less electron density than the phenyl protons.

From the correlation  $^1\text{H}$ - $^1\text{H}$  COSY NMR spectroscopy (Figure 3.90), the three set of Clazpy pyridine signals have been distinguished. Since two of the three Clazpy pyridine rings (A and B) are trans to each other, the protons are slightly

different and this result similar to the situation of the  $[\text{Ru}(\text{azpy})_3](\text{PF}_6)_2$  complex. In contrast to the protons in the Clazpy pyridine ring (C), the chemical shift appeared at the lowest field due to trans to N=N azo function. These data confirmed the configuration of N(py) and N(azo) orientation from the starting material, *ctc*- $[\text{Ru}(\text{Clazpy})_2\text{Cl}_2]$ .

The  $^{13}\text{C}$  NMR (Figure 3.91) and DEPT (Figure 3.92) signals assignments were based on the  $^1\text{H}$ - $^{13}\text{C}$  HMQC spectrum (Figure 3.93) which was generally used for studying large and complicated molecule. The  $^{13}\text{C}$  NMR spectrum showed 14 signals from 24 methine carbons and three signals of six quaternary carbons. The signals at 162.59, 139.54 and 135.34 ppm was assigned to the quaternary carbons C2, C5 and C7, respectively. Since C2 was located between nitrogen atoms, the chemical shift occurred at the lowest field.

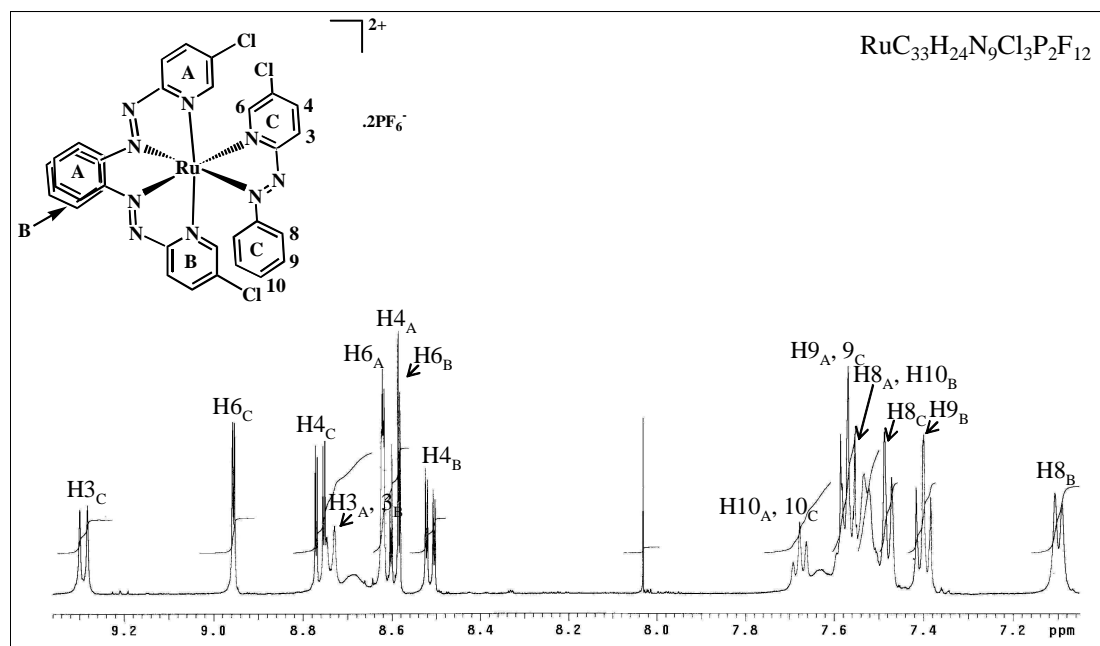


**Figure 3.89**  $^1\text{H}$  NMR spectrum of  $[\text{Ru}(\text{Clazpy})_3](\text{PF}_6)_2$  in acetone- $d_6$

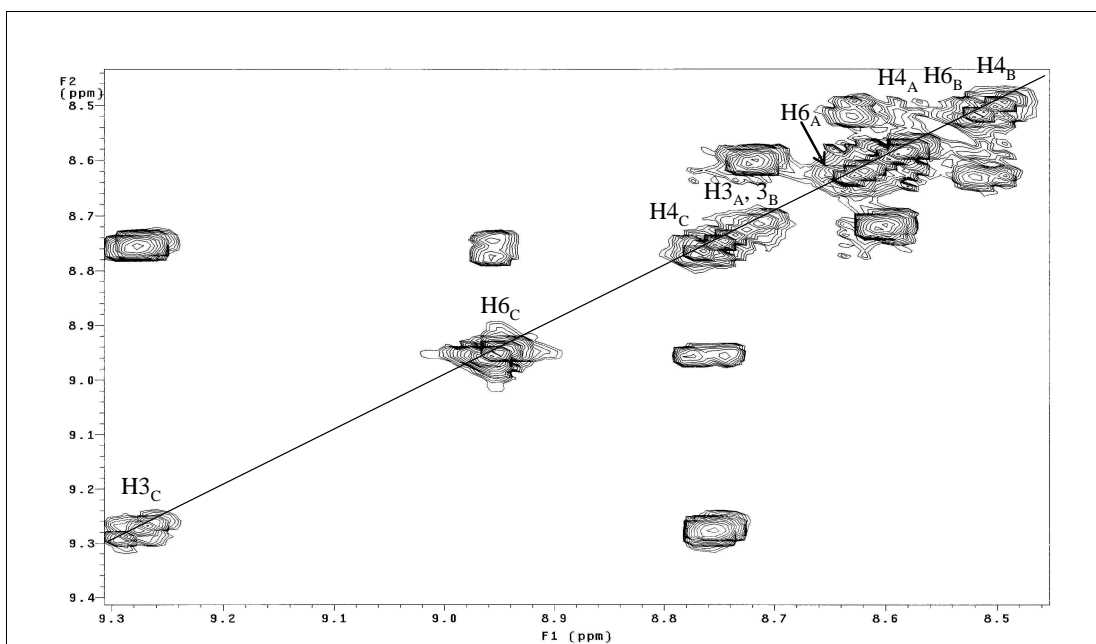


**Figure 3.90**  $^1\text{H}$ - $^1\text{H}$  COSY NMR spectrum of  $[\text{Ru}(\text{Clazpy})_3](\text{PF}_6)_2$  in acetone- $d_6$

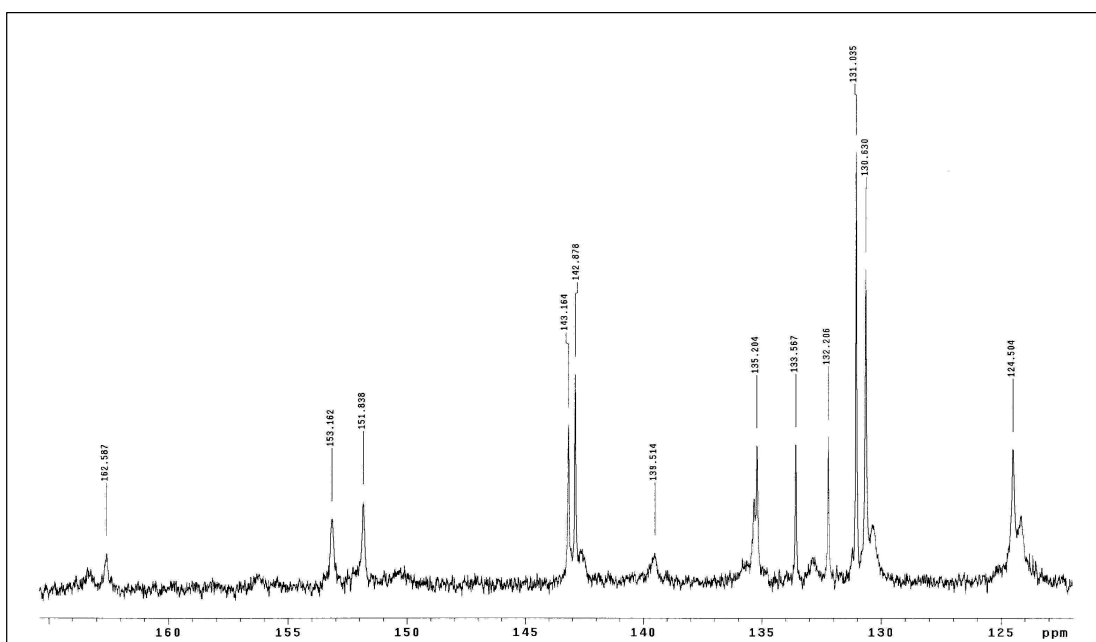


**Figure 3.91**  $^{13}\text{C}$  NMR spectrum of  $[\text{Ru}(\text{Clazpy})_3](\text{PF}_6)_2$  in acetone- $d_6$

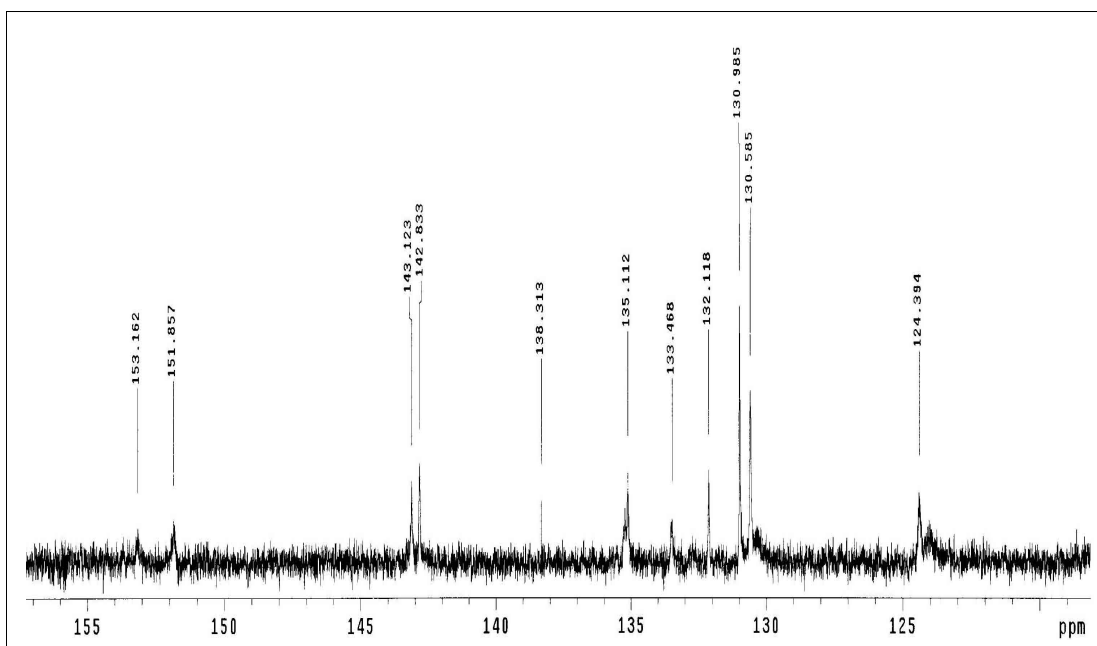


**Figure 3.92** DEPT NMR spectrum of  $[\text{Ru}(\text{Clazpy})_3](\text{PF}_6)_2$  in acetone- $d_6$

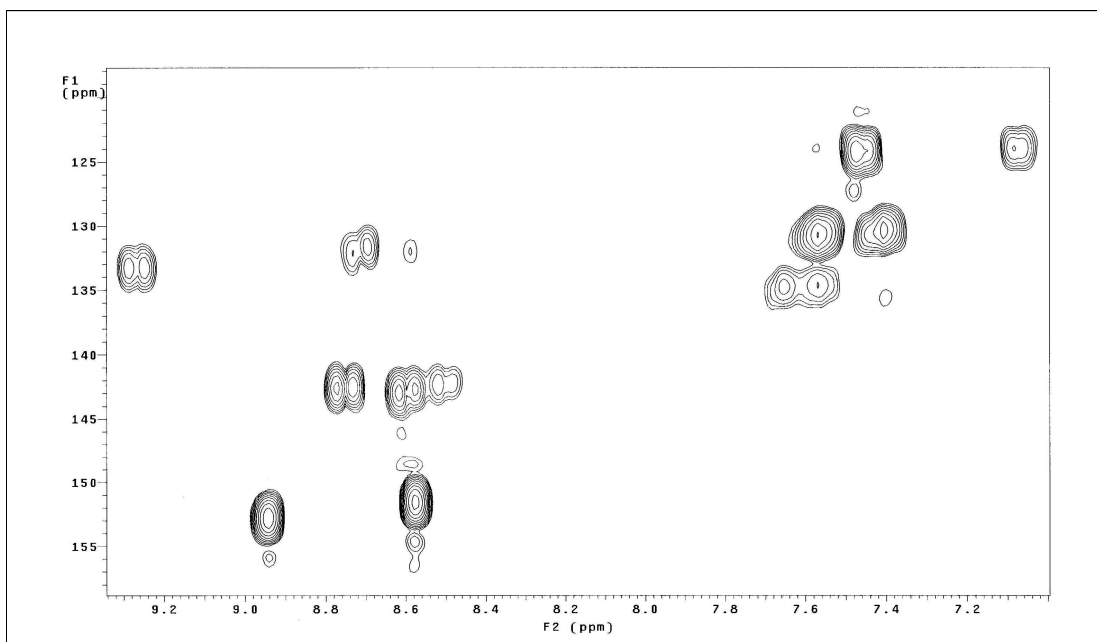


**Figure 3.93**  $^1\text{H}$ - $^{13}\text{C}$  HMQC NMR spectrum of  $[\text{Ru}(\text{Clazpy})_3](\text{PF}_6)_2$  in acetone- $d_6$

### 3.4.2.7 Cyclic voltammetry

Cyclic voltammetry is a convenient method to study the electrochemical properties of  $[\text{Ru}(\text{Clazpy})_2(\text{L})](\text{PF}_6)_2$  ( $\text{L} = \text{bpy}, \text{phen}, \text{azpy}, \text{Clazpy}$ ) The electron transfer properties are shown in Figure 3.94 to 3.97 and the cyclic voltammetric data of these compounds are summarized in Table 3.49.

**Table 3.49** Cyclic voltammetric data of  $[\text{Ru}(\text{Clazpy})_2(\text{L})](\text{PF}_6)_2$  ( $\text{L} = \text{bpy}, \text{phen}, \text{azpy}, \text{Clazpy}$ ) in 0.1 M TBAH  $\text{CH}_3\text{CN}$  at scan rate 50 mV/s (ferrocene as used an internal standard)

Compounds	<sup>a</sup> $E_{1/2}$ , V						
	Oxidation	Reduction					
	Ru(II)/(III)	I	II	III	IV	V	VI
$[\text{Ru}(\text{Clazpy})_2(\text{bpy})](\text{PF}_6)_2$	+1.58 (175)	-0.46 (95)	-0.94 (95)	-1.72 (90)	-2.02 (110)	-2.45 (250)	-
$[\text{Ru}(\text{Clazpy})_2(\text{phen})](\text{PF}_6)_2$	+1.62 (145)	-0.49 (120)	-0.93 (90)	-1.70 (100)	-2.01 (75)	-2.46 (285)	-
$[\text{Ru}(\text{Clazpy})_2(\text{azpy})](\text{PF}_6)_2$	n	-0.33 (95)	-0.66 (85)	-1.10 (100)	-1.78 (100)	-2.19 (125)	- 2.56 <sup>b</sup>
$[\text{Ru}(\text{Clazpy})_3](\text{PF}_6)_2$	n	-0.32 (95)	-0.60 (95)	-1.05 (100)	-1.70 (85)	-2.03 <sup>c</sup>	- 2.52 <sup>b</sup>

<sup>a</sup> $E_{1/2} = (E_{\text{pa}} + E_{\text{pc}})/2$ , where  $E_{\text{pa}}$  and  $E_{\text{pc}}$  are anodic and cathodic peak potentials, respectively;  $\Delta E_{\text{p}} = E_{\text{pa}} - E_{\text{pc}}$

<sup>b</sup>cathodic peak potential, V

<sup>c</sup>anodic peak potential, V

The electrochemical behavior of the  $[\text{Ru}(\text{Clazpy})_2(\text{L})](\text{PF}_6)_2$  ( $\text{L} = \text{bpy}, \text{phen}, \text{azpy}, \text{Clazpy}$ ) complexes in  $\text{CH}_3\text{CN}$  have been rationalized in terms of a metal-based oxidation and a series of reductions which are ligand-based occurring in a stepwise manner for each  $\pi^*$  system.

### Oxidation potential

The cyclic voltammogram of  $[\text{Ru}(\text{Clazpy})_2(\text{L})](\text{PF}_6)_2$  ( $\text{L} = \text{bpy}, \text{phen}, \text{azpy}, \text{Clazpy}$ ) complexes displayed metal oxidation range. The oxidation process of these complexes was studied in the range 0.00 to +2.00 V. In  $[\text{Ru}(\text{Clazpy})_2(\text{bpy})](\text{PF}_6)_2$  and  $[\text{Ru}(\text{Clazpy})_2(\text{phen})](\text{PF}_6)_2$  complexes, the couple of Ru(II)/(III) occurred at +1.58 and +1.68 V, which more positive potential than the parent compound, *ctc*- $[\text{Ru}(\text{Clazpy})_2\text{Cl}_2]$ . This phenomenon may be described in term of chelating effect which can stabilize the  $d\pi$  orbital of metal center and make azoimine moiety to accept electron. In the other hand, the Ru(II)/(III) couple of  $[\text{Ru}(\text{Clazpy})_2(\text{azpy})](\text{PF}_6)_2$  and  $[\text{Ru}(\text{Clazpy})_3](\text{PF}_6)_2$  were not observed because the redox of Ru(II)/(III) was too positive to be observed within solvent window. The cyclic voltammetric data results were corresponded to the electronic absorption spectral data shown in Table 3.50.

From data, it was noting that replacing two chloride atoms in the parent compound, *ctc*- $[\text{Ru}(\text{Clazpy})_2\text{Cl}_2]$  by other bidentate ligand resulted in the increasing redox potential of Ru(II)/(III) in  $[\text{Ru}(\text{Clazpy})_2(\text{L})](\text{PF}_6)_2$  especially, where the third ligand as azpy and Clazpy exhibited higher potential than those ligand as bpy and phen.

**Table 3.50** Comparison of electronic and redox properties of the  $[\text{Ru}(\text{Clazpy})_2(\text{L})](\text{PF}_6)_2$  and *ctc*- $[\text{Ru}(\text{Clazpy})_2\text{Cl}_2]$

Complexes	Ru(II)/(III), $E_{1/2}$ (V)	<sup>a</sup> MLCT bands, $\lambda_{\text{max}}$ , (nm)
<i>ctc</i> - $[\text{Ru}(\text{Clazpy})_2\text{Cl}_2]$	+0.82	584
$[\text{Ru}(\text{Clazpy})_2(\text{bpy})](\text{PF}_6)_2$	+1.58	520
$[\text{Ru}(\text{Clazpy})_2(\text{phen})](\text{PF}_6)_2$	+1.68	520
$[\text{Ru}(\text{Clazpy})_2(\text{azpy})](\text{PF}_6)_2$	n	495
$[\text{Ru}(\text{Clazpy})_3](\text{PF}_6)_2$	n	493

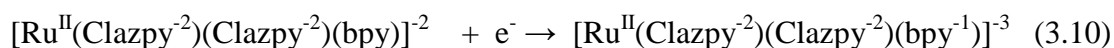
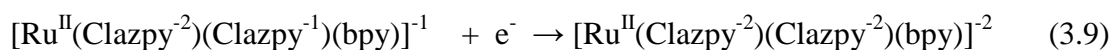
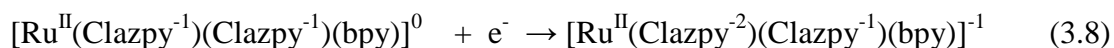
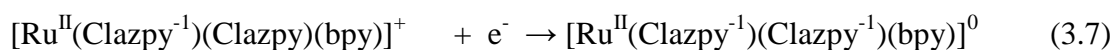
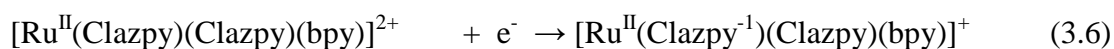
<sup>a</sup>in acetonitrile, n = not observed

From data revealed that the more positive potential of Ru(II)/(III) couple showed the greater blue shift of MLCT bands in comparison.

### Reduction potential

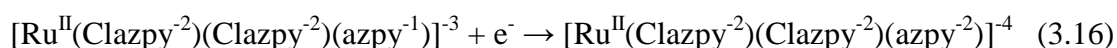
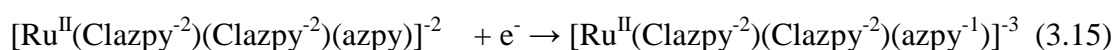
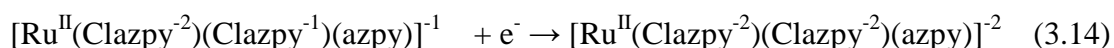
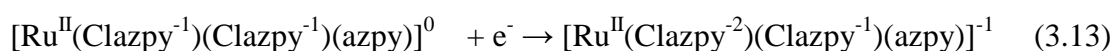
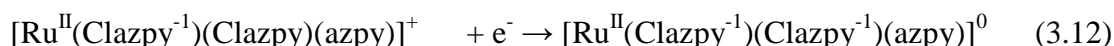
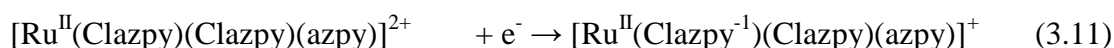
The electron accepting capability of  $[\text{Ru}(\text{Clazpy})_2(\text{L})](\text{PF}_6)_2$  (L = bpy, phen, azpy, Clazpy) were considered in the range 0.00 to - 2.60 V. The more positive potential was the greater electron accepting ability. The negative value of  $[\text{Ru}(\text{Clazpy})_2(\text{L})](\text{PF}_6)_2$  are listed in Table 3.49. In this experiment, five couples have been detected in  $[\text{Ru}(\text{Clazpy})_2(\text{bpy})](\text{PF}_6)_2$  and  $[\text{Ru}(\text{Clazpy})_2(\text{phen})](\text{PF}_6)_2$  whereas, six couples have been observed in  $[\text{Ru}(\text{Clazpy})_2(\text{azpy})](\text{PF}_6)_2$  and  $[\text{Ru}(\text{Clazpy})_3](\text{PF}_6)_2$  within the specified potential range.

From the previous work, Krause and Krause (1980) reported that polypyridyl ligands such as bpy and phen were capable of accepting electron, but azopyridine ligands were better  $\pi$ -acceptors and underwent easier reduction than those of the pyridine ligands. In addition, azopyridine ligand is known to accept successively two electron in its lowest unoccupied molecular orbital (Goswami *et al.*, 1983). Therefore, six successive one electron azo reductions were expected in the  $[\text{Ru}(\text{Clazpy})_2(\text{L})]^{2+}$  (L = bpy, phen, azpy, Clazpy) complexes. However, in this work five couple has been detected in bpy and phen complexes and the expected reduction processes of  $[\text{Ru}(\text{Clazpy})_2(\text{bpy})](\text{PF}_6)_2$  are displayed in equation 3.6 to 3.10.



The  $[\text{Ru}(\text{Clazpy})_2(\text{phen})](\text{PF}_6)_2$  complex also had similar reduction behavior and reduction potential values to the  $[\text{Ru}(\text{Clazpy})_2(\text{bpy})](\text{PF}_6)_2$  complex (Table 3.49). Moreover, the expected five reductions were similar to those of the  $[\text{Ru}(\text{Clazpy})_2(\text{bpy})](\text{PF}_6)_2$  complex.

In the case of the  $[\text{Ru}(\text{Clazpy})_2(\text{azpy})](\text{PF}_6)_2$  and  $[\text{Ru}(\text{Clazpy})_3](\text{PF}_6)_2$  complexes, five reversible couple and one cathodic peak (at scan rate 50 mV/s) was observed. Since the Clazpy ligand could accept electron better than azpy in the parent complex,  $[\text{Ru}(\text{L})_2\text{Cl}_2]$  (L = azpy, Clazpy; Table 3.23). The reduction processes of  $[\text{Ru}(\text{Clazpy})_2(\text{azpy})](\text{PF}_6)_2$  displayed as in followed equations 3.11 to 3.16.



The  $[\text{Ru}(\text{Clazpy})_3](\text{PF}_6)_2$  complex also had similar reduction behavior and reduction potential values to the  $[\text{Ru}(\text{Clazpy})_2(\text{bpy})](\text{PF}_6)_2$  complex (Table 3.49). Moreover, the expected six reductions were similar to those of the  $[\text{Ru}(\text{Clazpy})_2(\text{azpy})](\text{PF}_6)_2$  complex.

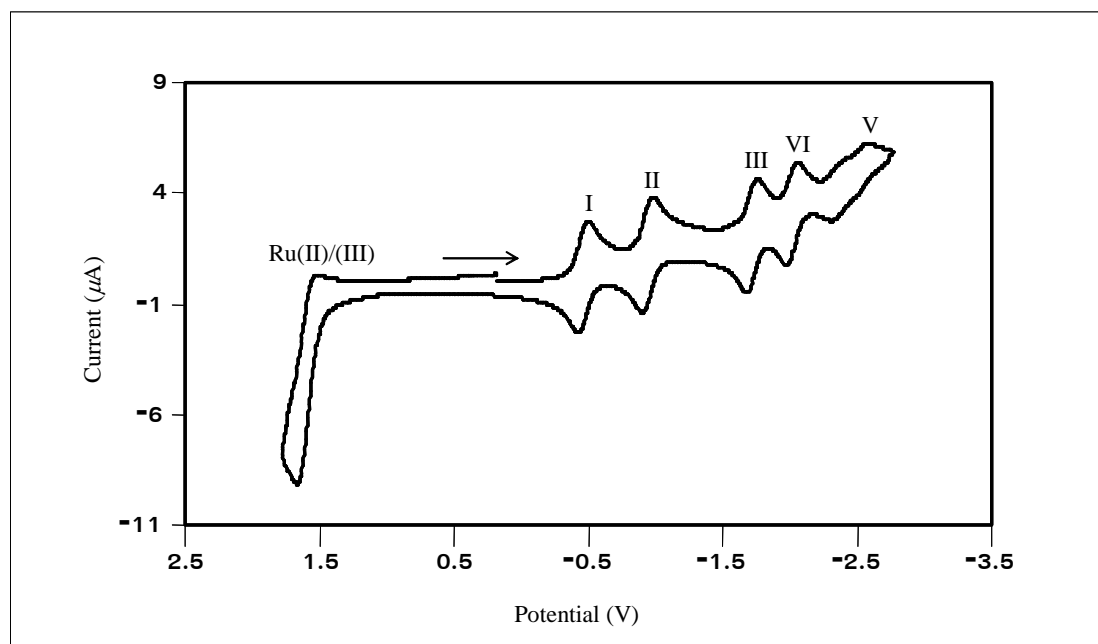


**Figure 3.94** Cyclic voltammogram of  $[\text{Ru}(\text{Clazpy})_2(\text{bpy})](\text{PF}_6)_2$  in 0.1 M TBAH  $\text{CH}_3\text{CN}$  at scan rate 50 mV (ferrocene as an internal standard)

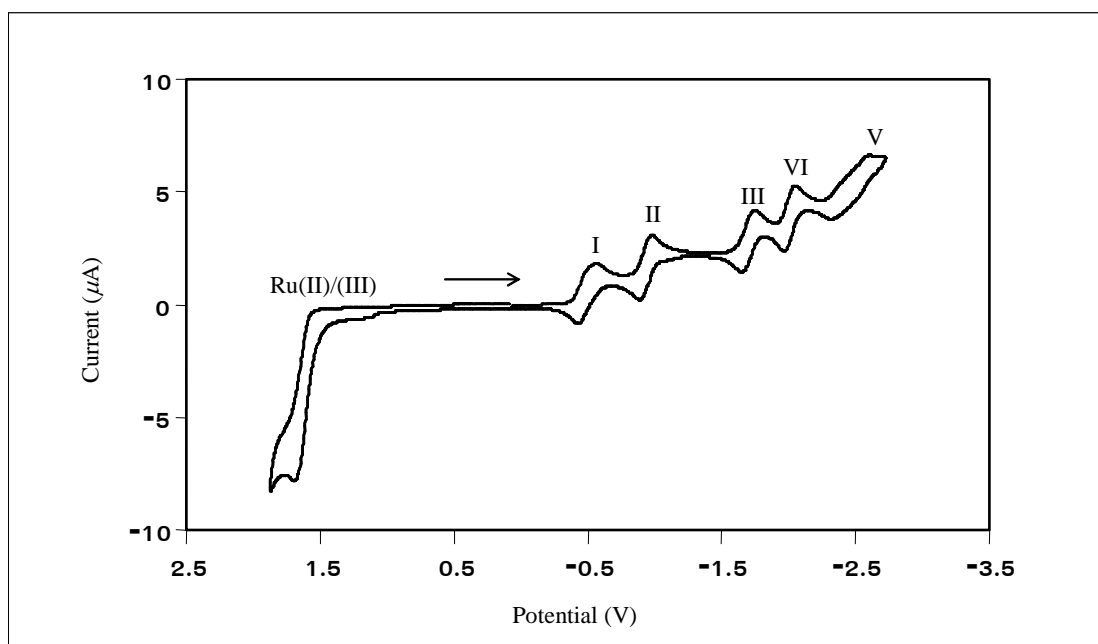


**Figure 3.95** Cyclic voltammogram of  $[\text{Ru}(\text{Clazpy})_2(\text{phen})](\text{PF}_6)_2$  in 0.1 M TBAH  $\text{CH}_3\text{CN}$  at scan rate 50 mV/s (ferrocene as an internal standard)

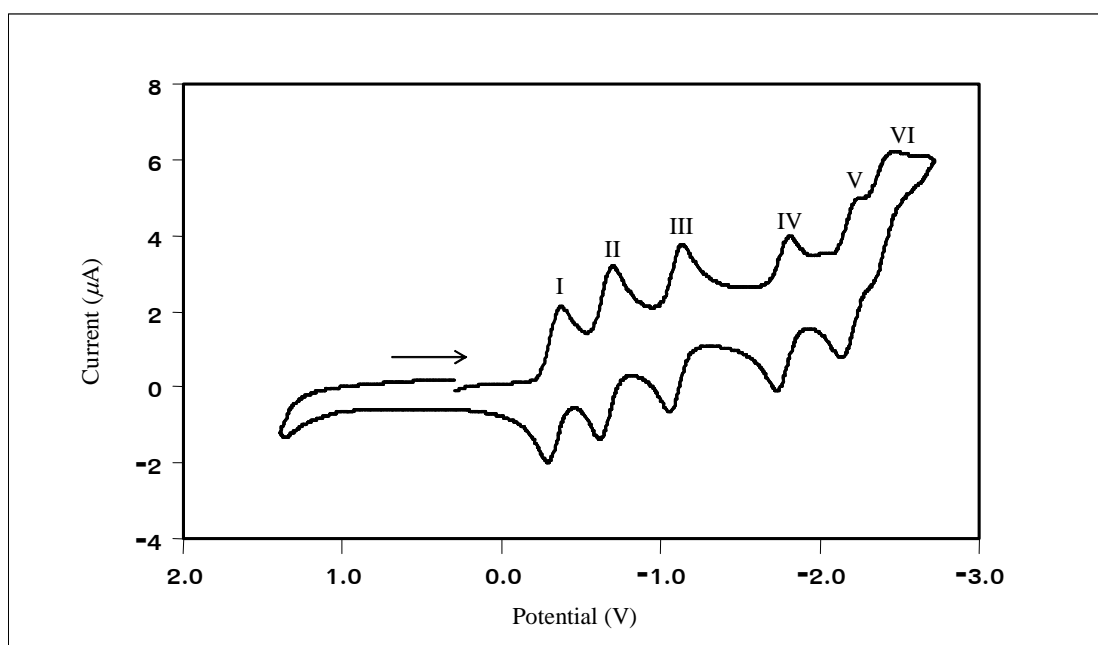


**Figure 3.96** Cyclic voltammogram of  $[\text{Ru}(\text{Clazpy})_2(\text{azpy})](\text{PF}_6)_2$  in 0.1 M TBAH  $\text{CH}_3\text{CN}$  at scan rate 50 mV/s (ferrocene as an internal standard)

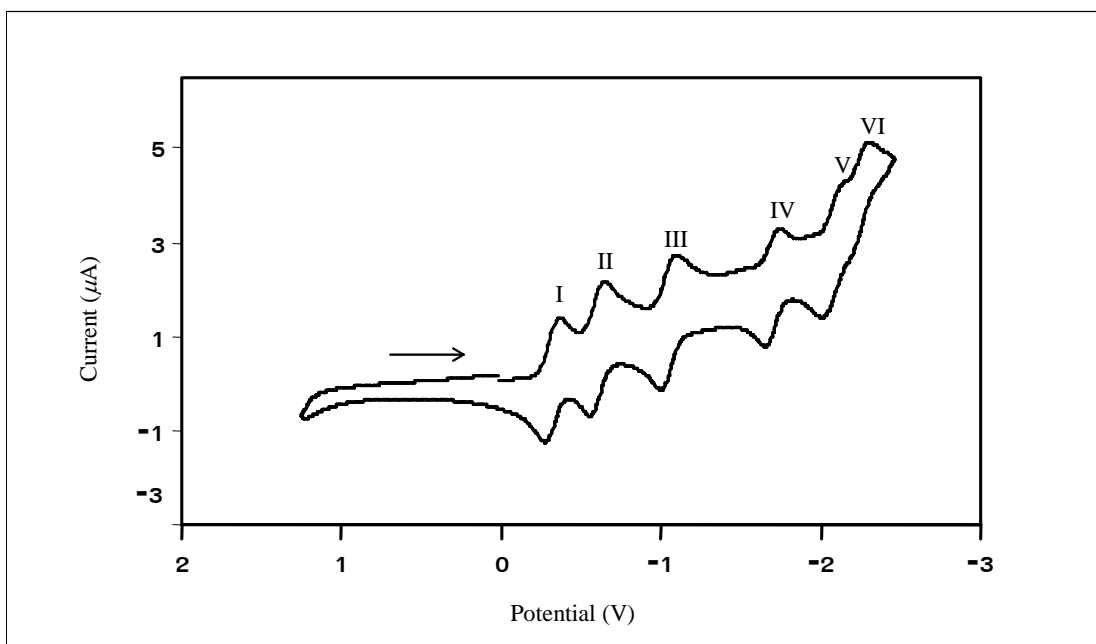


**Figure 3.97** Cyclic voltammogram of [Ru(Clazpy)<sub>3</sub>](PF<sub>6</sub>)<sub>2</sub> in 0.1 M TBAH CH<sub>3</sub>CN at scan rate 50 mV/s (ferrocene as an internal standard)

### 3.5 Syntheses and characterization of $[\text{Ru}(\text{Clazpy})_2(\text{L})](\text{NO}_3)_2 \cdot x\text{H}_2\text{O}$ (L = bpy, phen, azpy, Clazpy)

#### 3.5.1 Syntheses of $[\text{Ru}(\text{Clazpy})_2(\text{L})](\text{NO}_3)_2 \cdot x\text{H}_2\text{O}$ (L = bpy, phen, azpy, Clazpy)

The synthesis of  $[\text{Ru}(\text{Clazpy})_2(\text{L})](\text{NO}_3)_2 \cdot x\text{H}_2\text{O}$  complexes (where L = bpy, phen, azpy, Clazpy) was achieved by the stepwise addition of equimolar amounts of excess L and  $\text{AgNO}_3$  in refluxing methanol which have the solution of precursor complex, *ctc*- $[\text{Ru}(\text{Clazpy})_2\text{Cl}_2]$  as outline in Figure 3.98. The expected of these complexes were recrystallized by the mixing of ethanol and ether where L are azpy and Clazpy whereas using the mixture of ethanol and hexane where L are bpy and phen.

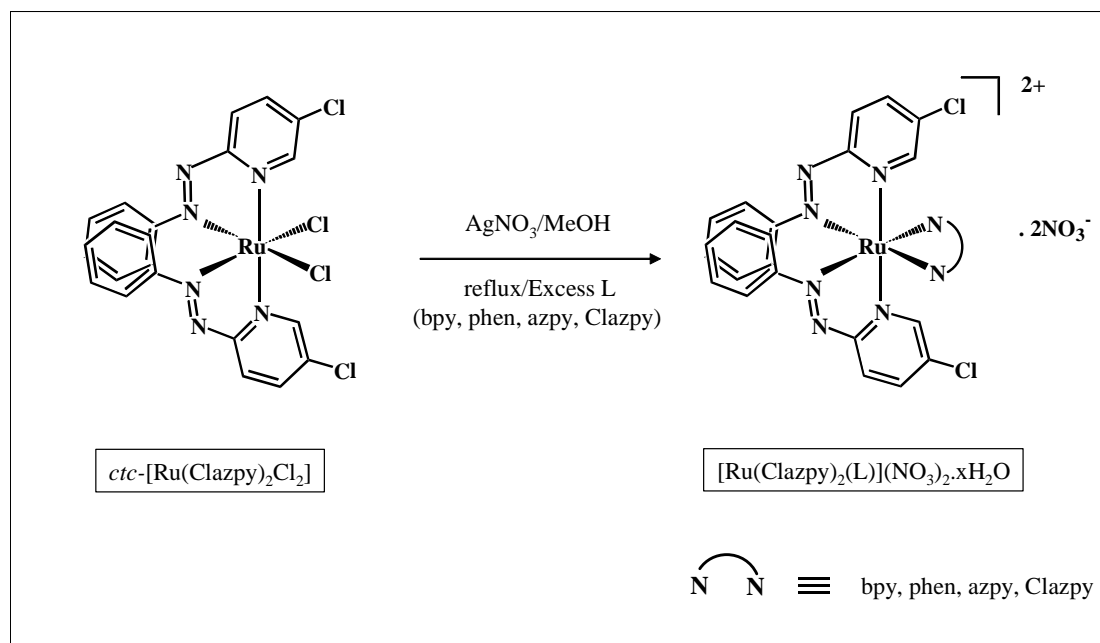


**Figure 3.98** Synthetic route of the preparation of  $[\text{Ru}(\text{Clazpy})_2(\text{L})](\text{NO}_3)_2 \cdot x\text{H}_2\text{O}$  (L = bpy, phen, azpy, Clazpy)

The physical properties of this complex are summarized in Table 3.51.

**Table 3.51** The physical properties of  $[\text{Ru}(\text{Clazpy})_2(\text{L})](\text{NO}_3)_2$  complexes  
(where L = bpy, phen, azpy, Clazpy)

Complexes	Physical properties			
	Appearance	Color		Melting point (°C)
		solid	solution	
$[\text{Ru}(\text{Clazpy})_2(\text{bpy})](\text{NO}_3)_2 \cdot 5\text{H}_2\text{O}$	solid	dark brown	red brown	more than 360
$[\text{Ru}(\text{Clazpy})_2(\text{phen})](\text{NO}_3)_2 \cdot 3\text{H}_2\text{O}$	solid	dark brown	red brown	more than 360
$[\text{Ru}(\text{Clazpy})_2(\text{azpy})](\text{NO}_3)_2 \cdot \text{H}_2\text{O}$	solid	dark brown	light brown	186-187
$[\text{Ru}(\text{Clazpy})_3](\text{NO}_3)_2 \cdot 5\text{H}_2\text{O}$	solid	dark brown	light brown	185-186

The solubility of 0.0012 g of  $[\text{Ru}(\text{Clazpy})_2(\text{L})](\text{NO}_3)_2$  (L = bpy, phen, azpy, Clazpy) was tested in 10 mL of various solvents *e.g.* hexane,  $\text{CH}_2\text{Cl}_2$ ,  $\text{CH}_3\text{OCH}_3$ , DMF,  $\text{CH}_3\text{CN}$ , MeOH and water. The results showed that four complexes were slightly soluble in  $\text{CH}_3\text{OCH}_3$ ,  $\text{CH}_2\text{Cl}_2$ . They were very soluble in DMF, DMSO,  $\text{CH}_3\text{CN}$ , MeOH and  $\text{H}_2\text{O}$  but insoluble in hexane.

### 3.5.2 Characterization of $[\text{Ru}(\text{Clazpy})_2(\text{L})](\text{NO}_3)_2 \cdot x\text{H}_2\text{O}$ (L = bpy, phen, azpy, Clazpy)

The chemistry of  $[\text{Ru}(\text{Clazpy})_2(\text{L})](\text{NO}_3)_2 \cdot x\text{H}_2\text{O}$  (L = bpy, phen, azpy, Clazpy) complexes have been fully characterized by elemental analysis, Mass spectrometry, Infrared spectroscopy, UV-Visible absorption spectroscopy, Nuclear Magnetic Resonance spectroscopy (1D and 2D NMR) and electrochemical method.

### 3.5.2.1 Elemental analysis

Elemental analysis was used to confirmed composition of C, H, N in complexes. From data, the analytical values corresponded to the calculated values. Therefore, the composition of  $[\text{Ru}(\text{Clazpy})_2(\text{L})](\text{NO}_3)_2 \cdot x\text{H}_2\text{O}$  was confirmed by this method. The results are given in Table 3.52.

**Table 3.52** Elemental analysis data of the  $[\text{Ru}(\text{Clazpy})_2(\text{L})](\text{NO}_3)_2 \cdot x\text{H}_2\text{O}$  complexes (L = bpy, phen, azpy, Clazpy)

Complexes	% C		% H		% N	
	Calc.	Found	Calc.	Found	Calc.	Found
$[\text{Ru}(\text{Clazpy})_2(\text{bpy})](\text{NO}_3)_2 \cdot 5\text{H}_2\text{O}$	42.39	42.69	3.78	3.81	15.45	15.20
$[\text{Ru}(\text{Clazpy})_2(\text{phen})](\text{NO}_3)_2 \cdot 3\text{H}_2\text{O}$	45.65	45.42	3.38	3.83	15.66	15.36
$[\text{Ru}(\text{Clazpy})_2(\text{azpy})](\text{NO}_3)_2 \cdot \text{H}_2\text{O}$	46.00	45.87	3.16	3.01	17.88	17.64
$[\text{Ru}(\text{Clazpy})_3](\text{NO}_3)_2 \cdot 5\text{H}_2\text{O}$	40.94	40.99	3.54	3.46	15.91	15.57

### 3.5.2.2 X-ray Crystallography

The X-ray crystallography is the most important technique to confirm the geometry of compounds. The single crystal of  $[\text{Ru}(\text{Clazpy})_2(\text{phen})](\text{NO}_3)_2 \cdot 3.5\text{H}_2\text{O}$  was determined and it showed six coordination around the ruthenium atom.

X-ray structure of  $[\text{Ru}(\text{Clazpy})_2(\text{phen})](\text{NO}_3)_2 \cdot 3.5\text{H}_2\text{O}$

Crystals suitable for X-ray analysis were grown by slow diffusion of ether into a mixture of methanol and acetone solution at room temperature. The crystal structure of the title compound is shown in Figure 3.99. The crystallographic data are shown in Table 3.53. Selected bond parameters associated with the metal ions are listed in Table 3.54.

**Table 3.53** Crystal data and structure refinement for


---

Empirical formula	$\text{C}_{34}\text{H}_{31}\text{Cl}_2\text{N}_{10}\text{O}_{9.50}\text{Ru}$
Chemical formula	$\text{C}_{34}\text{H}_{24}\text{Cl}_2\text{N}_8\text{Ru}, 2(\text{NO}_3), 3.5(\text{H}_2\text{O})$
Formula weight	903.66
Temperature	100(2)
Wavelength	0.71073 Å
Crystal system	monoclinic
Space group	P 1 21/n 1
Unit cell dimensions	$a = 13.6561(8) \quad \alpha = 90^\circ$ $b = 16.8955(4) \quad \beta = 91.691(4)^\circ$ $c = 16.3230(7) \quad \gamma = 90^\circ$
Volume	$3764.5(3) \text{ \AA}^3$
Z	4
Density	$1.594 \text{ Mg/m}^3$
Absorption coefficient	$0.628 \text{ mm}^{-1}$
F(000)	1836
Goodness-of-fit on $F^2$	0.961
Final R indices [ $I > 2\sigma(I)$ ]	$R1 = 0.0670, wR2 = 0.1277$
R indices (all data)	$R1 = 0.2079, wR2 = 0.1858$

---

**Table 3.54** Selected bond lengths (Å) and angles (°) and estimated standard deviations for [Ru(Clazpy)<sub>2</sub>(phen)](NO<sub>3</sub>)<sub>2</sub>·3.5H<sub>2</sub>O

Ru1-N22	2.004(4)	Ru1-N12	2.020(4)
Ru1-N211	2.043(4)	Ru1-N111	2.052(4)
Ru1-N311	2.065(4)	Ru1-N321	2.074(4)
N11-N12	1.279(6)	N21-N22	1.284(5)
Angles			
N22-Ru1-N12	84.20(16)	N22-Ru1-N211	76.30(16)
N12-Ru1-N211	100.36(16)	N22-Ru1-N111	97.84(16)
N12-Ru1-N111	75.92(17)	N211-Ru1-N111	173.47(16)
N22-Ru1-N311	99.09(16)	N12-Ru1-N311	173.54(15)
N211-Ru1-N311	85.86(15)	N111-Ru1-N311	98.05(16)
N22-Ru1-N321	174.36(15)	N12-Ru1-N321	98.05(17)
N211-Ru1-N321	98.17(15)	N111-Ru1-N321	87.73(15)
N311-Ru1-N321	79.20(16)		

The ruthenium center is in the distorted octahedral environment with four nitrogens (N111, N211, N12, N22) of two Clazpy ligands and two nitrogens (N311, 321) of one phen ligand. The pyridine ring of Clazpy are at the trans position and the two pyridine rings of phen are trans to the azo groups of the Clazpy ligands. The trans-angle around the ruthenium center in the range from 173.4(16) to 174.4(15)°, indicating distortion from the rectilinear geometry. Two bite angles extended by two Clazpy and one bpy are 75.92(17)°, 76.30(16)°, 79.20(16)°, respectively. The average bond distance of Ru-N(azo), 2.012(14)Å is shorter than the average Ru-N(pyridine of Clazpy) bond length of 2.048(4)Å. This is due to greater  $\pi$ -backbonding from  $d\pi(\text{Ru}) \rightarrow \pi^*(\text{azo})$ . In addition, it is noted that the Ru-N(bpy) distance (average, 2.069(4)Å) is shorter than those in [Ru(azpy)<sub>2</sub>(bpy)]<sup>2+</sup> (average, 2.088(4)Å) (Hansongnern *et al.*, 2007). This was probably due to the effect of chloride atom at the fifth position increasing electron density on pyridine ring and this enhanced  $\sigma$ -donor property of the N(pyridine of Clazpy). Moreover, in this complex the average

N=N distance of Clazpy is 1.281(6)Å which is slightly longer than that of [Ru(azpy)<sub>2</sub>(bpy)]<sup>2+</sup> (1.278(4)Å). The coordination of Clazpy led to a decrease in the N=N bond order due to the σ-donor and π-acceptor character of the ligand. All results from molecular structure of the [Ru(Clazpy)<sub>2</sub>(phen)]<sup>2+</sup> complex confirm that Clazpy is a better π-acceptor than azpy and phen.

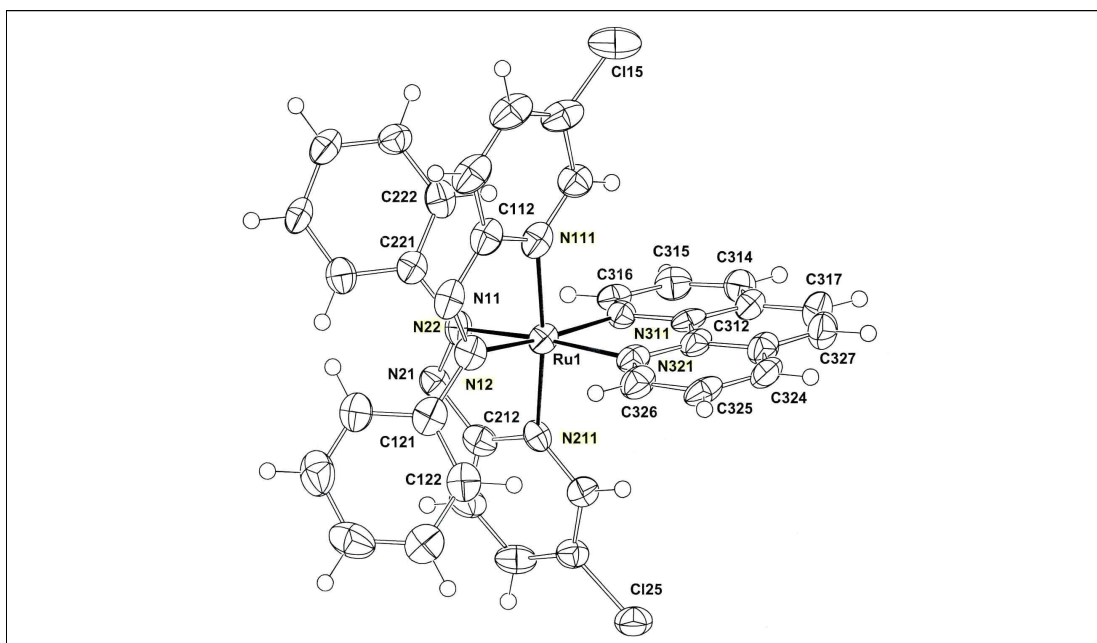


**Figure 3.99** Crystal structure of [Ru(Clazpy)<sub>2</sub>(phen)](NO<sub>3</sub>)<sub>2</sub>·3.5H<sub>2</sub>O

### 3.5.2.3 Electrospray mass (ES) spectrometry

The ES-MS spectrometric data of [Ru(Clazpy)<sub>2</sub>(L)](NO<sub>3</sub>)<sub>2</sub>·xH<sub>2</sub>O (L = bpy, phen, azpy, Clazpy) are shown in Figure 3.100 to 3.103. The results are given in Table 3.55.

**Table 3.55** ES mass spectrometric data of  $[\text{Ru}(\text{Clazpy})_2(\text{L})](\text{NO}_3)_2 \cdot x\text{H}_2\text{O}$  (L = bpy, phen, azpy, Clazpy)

m/z	Stoichiometry	Rel. Abun. (%)
$[\text{Ru}(\text{Clazpy})_2(\text{bpy})](\text{NO}_3)_2 \cdot 5\text{H}_2\text{O}$		
692.0530	$[\text{M}-2\text{NO}_3-5\text{H}_2\text{O}-\text{H}^+]^+$	25
346.02	$[\text{M}-2\text{NO}_3-5\text{H}_2\text{O}]^{2+}$	100
$[\text{Ru}(\text{Clazpy})_2(\text{phen})](\text{NO}_3)_2 \cdot 3\text{H}_2\text{O}$		
716.05	$[\text{M}-2\text{NO}_3-3\text{H}_2\text{O}+\text{H}^+]^+$	35
358.02	$[\text{M}-2\text{NO}_3-3\text{H}_2\text{O}]^{2+}$	100
$[\text{Ru}(\text{Clazpy})_2(\text{azpy})](\text{NO}_3)_2 \cdot \text{H}_2\text{O}$		
719.0651	$[\text{M}-2\text{NO}_3-\text{H}_2\text{O}+\text{H}^+]^+$	70
359.53	$[\text{M}-2\text{NO}_3-\text{H}_2\text{O}]^{2+}$	100
$[\text{Ru}(\text{Clazpy})_3](\text{NO}_3)_2 \cdot 5\text{H}_2\text{O}$		
753.0275	$[\text{M}-2\text{NO}_3-5\text{H}_2\text{O}+\text{H}^+]^+$	100
377.51	$[\text{M}-2\text{NO}_3-5\text{H}_2\text{O}]^{2+}$	80

M = molecular weight (MW) of each complexes

MW of  $[\text{Ru}(\text{Clazpy})_2(\text{bpy})](\text{NO}_3)_2 \cdot 5\text{H}_2\text{O} = 906.66 \text{ g/mol}$

MW of  $[\text{Ru}(\text{Clazpy})_2(\text{phen})](\text{NO}_3)_2 \cdot 3\text{H}_2\text{O} = 894.65 \text{ g/mol}$

MW of  $[\text{Ru}(\text{Clazpy})_2(\text{azpy})](\text{NO}_3)_2 \cdot \text{H}_2\text{O} = 879.64 \text{ g/mol}$

MW of  $[\text{Ru}(\text{Clazpy})_3](\text{NO}_3)_2 \cdot 5\text{H}_2\text{O} = 968.12 \text{ g/mol}$

From the data, the parent peak which gave 100% relative abundance of all complexes corresponded to the loss of nitrate and aqua molecules from each of  $[\text{Ru}(\text{Clazpy})_2(\text{L})](\text{NO}_3)_2 \cdot x\text{H}_2\text{O}$ . The measured molecular weights were consistent with expected values.

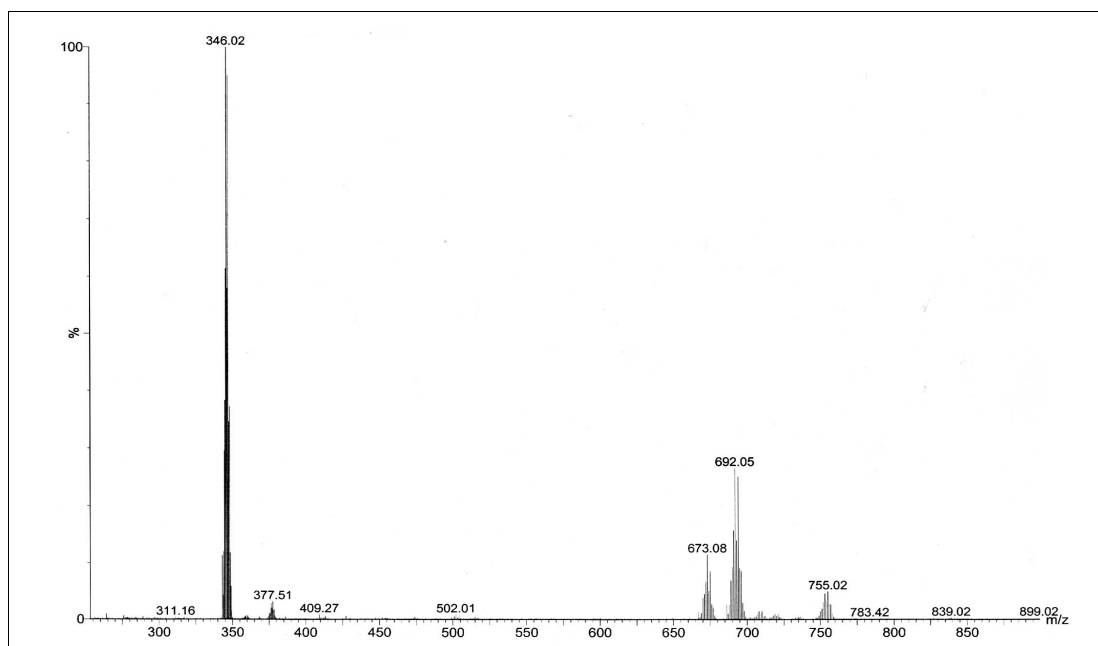


**Figure 3.100** ES mass spectrum of [Ru(Clazpy)<sub>2</sub>(bpy)](NO<sub>3</sub>)<sub>2</sub>.5H<sub>2</sub>O

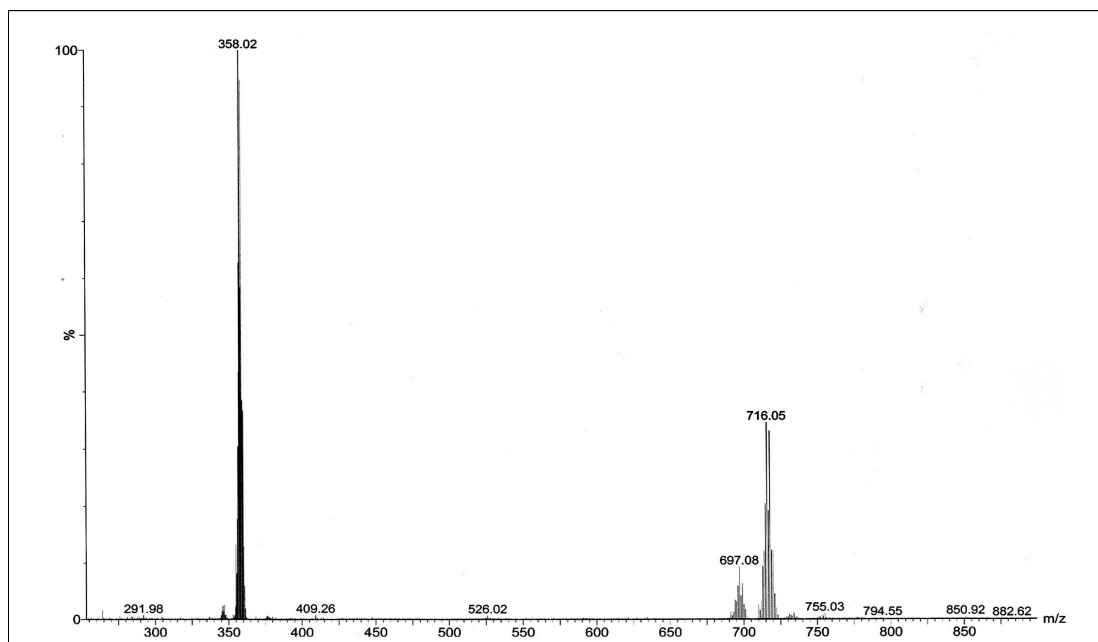


**Figure 3.101** ES mass spectrum of [Ru(Clazpy)<sub>2</sub>(phen)](NO<sub>3</sub>)<sub>2</sub>.3H<sub>2</sub>O

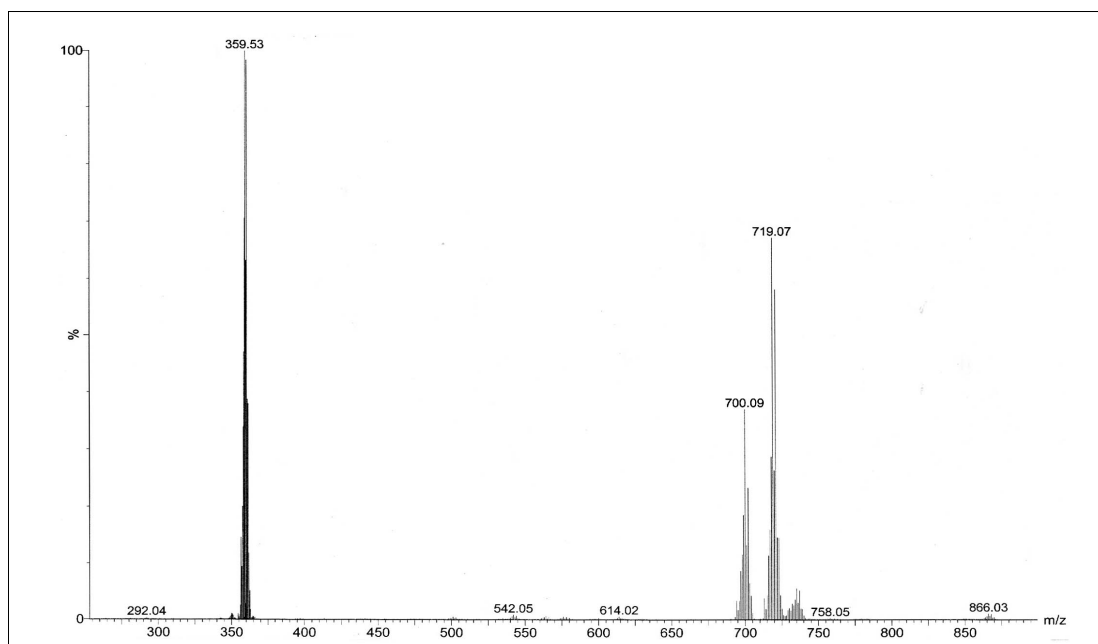


**Figure 3.102** ES mass spectrum of  $[\text{Ru}(\text{Clazpy})_2(\text{azpy})](\text{NO}_3)_2 \cdot \text{H}_2\text{O}$

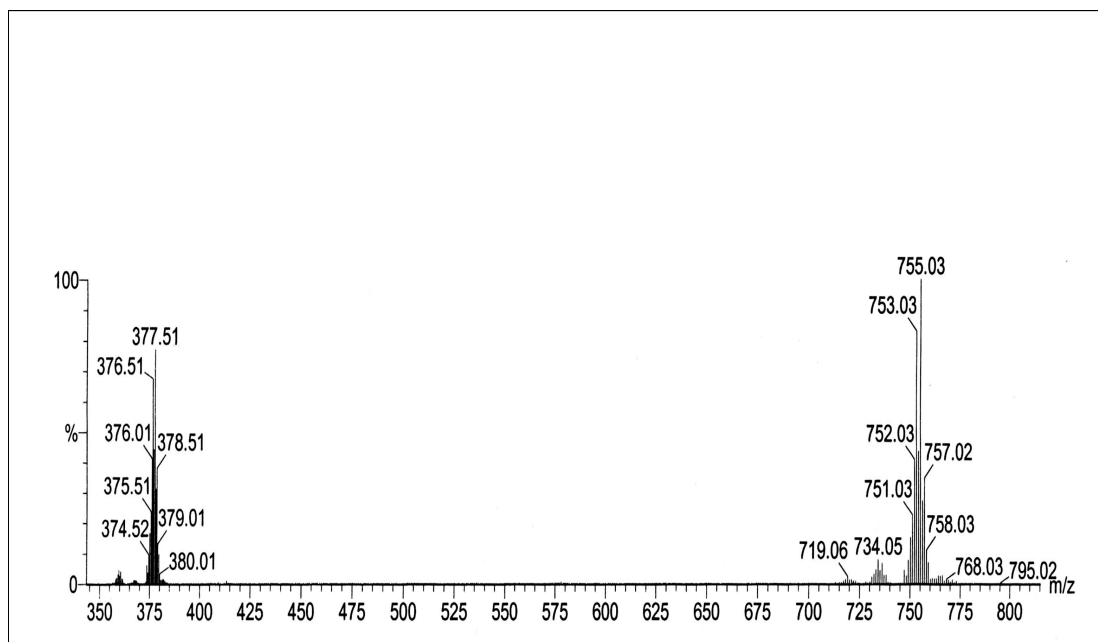


**Figure 3.103** ES mass spectrum of  $[\text{Ru}(\text{Clazpy})_3](\text{NO}_3)_2 \cdot 5\text{H}_2\text{O}$

### 3.5.2.4 Infrared spectroscopy

Vibrational spectra in the region 4000-400  $\text{cm}^{-1}$  could be used to give information about ligands coordination to the ruthenium center. Infrared spectroscopic spectra of  $[\text{Ru}(\text{Clazpy})_2(\text{L})](\text{NO}_3)_2 \cdot x\text{H}_2\text{O}$  (L = bpy, phen, azpy, Clazpy) displayed important peaks in 1600-400  $\text{cm}^{-1}$  range with KBr disc. The infrared spectroscopic data are given in Table 3.56 and their spectra are shown in Figure 3.104 to 3.107.

**Table 3.56** IR data of  $[\text{Ru}(\text{Clazpy})_2(\text{L})](\text{NO}_3)_2 \cdot x\text{H}_2\text{O}$  (L = bpy, phen, azpy, Clazpy)

Vibrational frequencies	Wave number ( $\text{cm}^{-1}$ ) $[\text{Ru}(\text{Clazpy})_2(\text{L})](\text{NO}_3)_2 \cdot x\text{H}_2\text{O}$ (L = ligands)			
	bpy	phen	azpy	Clazpy
C=N stretching and C=C stretching	1605(m)	1632(m)	1574(m)	1583(m)
	1548(m)	1594(m)	1454(m)	1549(m)
	1448(m)	1566(m) 1548(m)		1454(m)
N=N(azo) stretching	1351(m)	1350(m)	1353(s)	1361(s)
C-N stretching	1119(m)	1119(m)	1120(m)	1346(s)
C-Cl	575(s)	573(m)	550(m)	559(s)
C-H out of plane bend in monosub. benzene	765 (s)	771(m)	770(m)	771(m)
	736(m)	735(m)	740(m)	738(m)
	696(m)	696(m)	692(m)	692(m)
$\text{NO}_3^-$ stretching	1384(s)	1385(s)	1384(s)	1384(s)

s = strong, m = medium

Infrared spectra of all complexes showed many vibrations of different intensities below 1600  $\text{cm}^{-1}$ . The N=N stretching of complexes where L are bpy, phen and azpy exhibited around 1350-1353  $\text{cm}^{-1}$  which shifted to lower wave numbers than that of the free Clazpy ligand (1364  $\text{cm}^{-1}$ ). This is a criterion of the coordination of both azoimine nitrogen atoms of the Clazpy ligand to the metal ion. In  $[\text{Ru}(\text{Clazpy})_3]^{2+}$ , the vibrational frequency appeared at the same position of the free Clazpy ligand. This result may be due to the competition of three azoimine Clazpy ligand in molecule. In addition, a strong vibration around 1384  $\text{cm}^{-1}$  is observed due to the presence of ionic nitrate salts (ตั้งคนานุรักษ์, 2547).

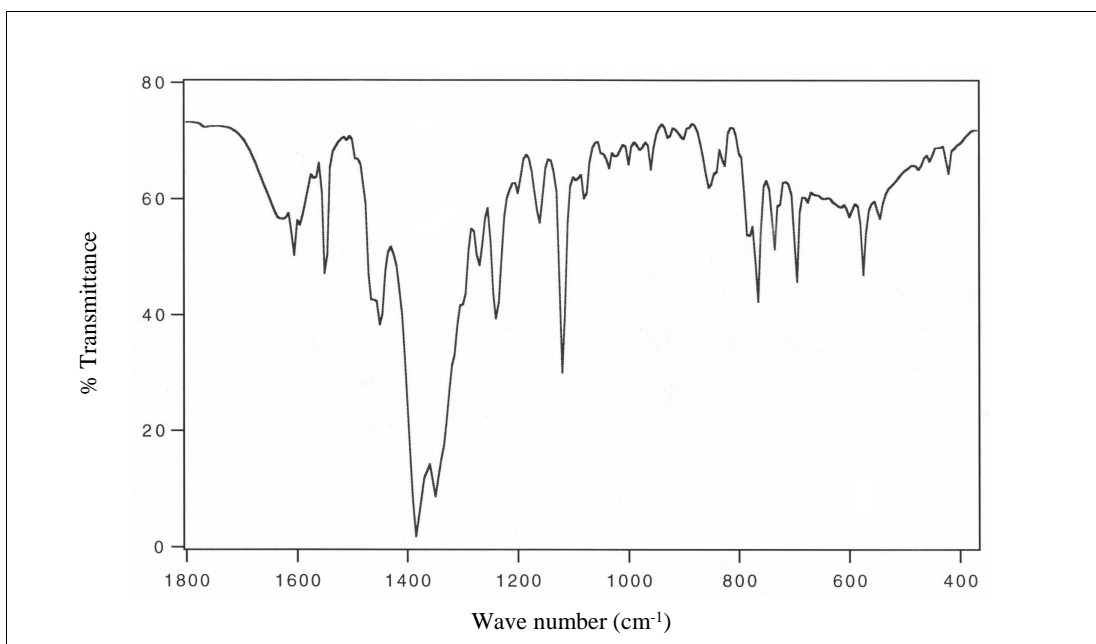


**Figure 3.104** IR spectrum of  $[\text{Ru}(\text{Clazpy})_2(\text{bpy})](\text{NO}_3)_2 \cdot 5\text{H}_2\text{O}$

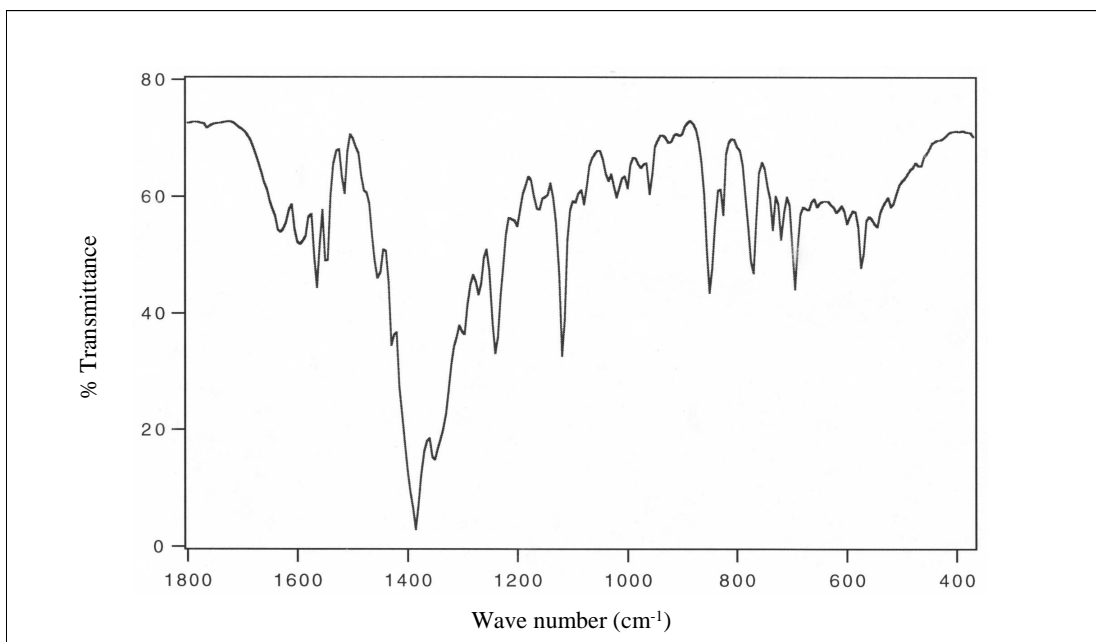


**Figure 3.105** IR spectrum of  $[\text{Ru}(\text{Clazpy})_2(\text{phen})](\text{NO}_3)_2 \cdot 3\text{H}_2\text{O}$

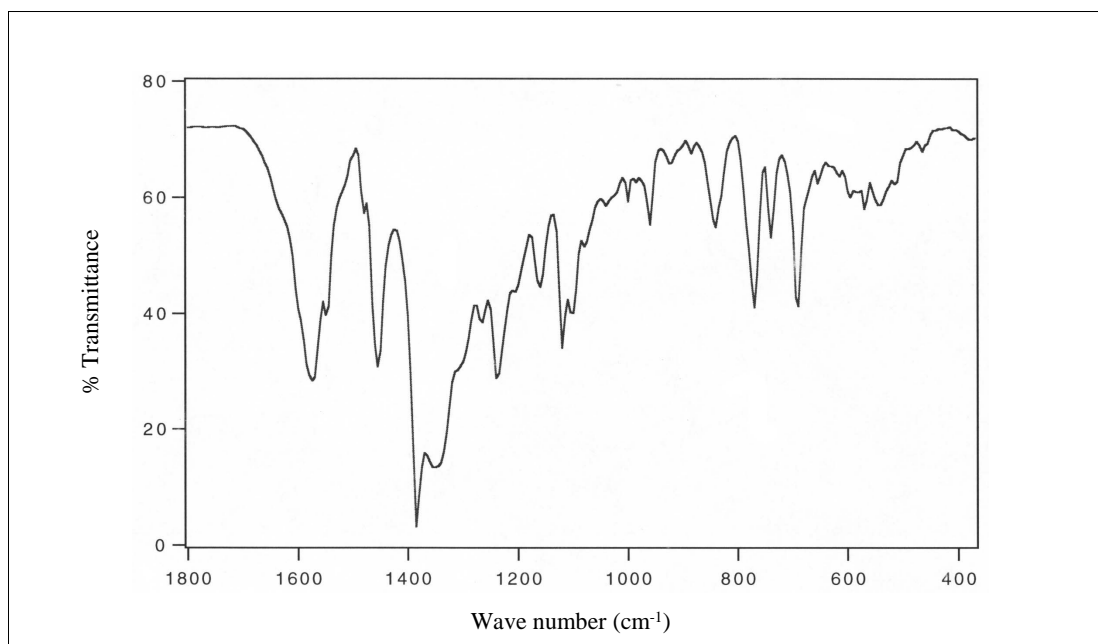


**Figure 3.106** IR spectrum of  $[\text{Ru}(\text{Clazpy})_2(\text{azpy})](\text{NO}_3)_2 \cdot \text{H}_2\text{O}$

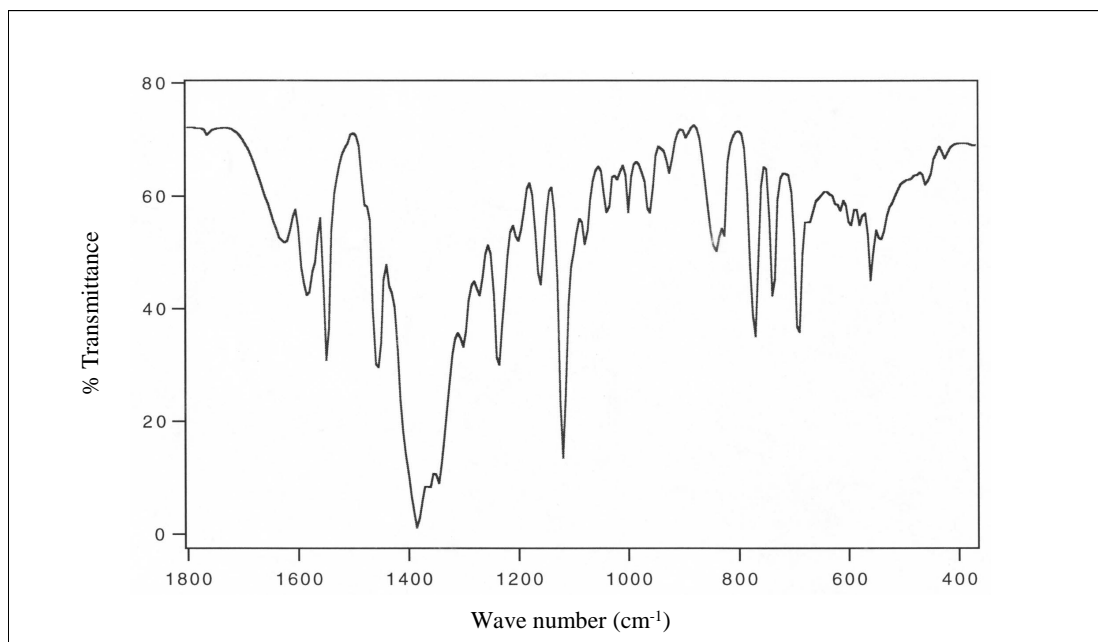


**Figure 3.107** IR spectrum of  $[\text{Ru}(\text{Clazpy})_3](\text{NO}_3)_2 \cdot 5\text{H}_2\text{O}$

### 3.5.2.5 UV-Visible absorption spectroscopy

The solution electronic spectra of  $[\text{Ru}(\text{Clazpy})_2(\text{L})](\text{NO}_3)_2 \cdot x\text{H}_2\text{O}$  ( $\text{L} = \text{bpy}, \text{phen}, \text{azpy}, \text{Clazpy}$ ) were measured using a variety of solvents;  $\text{CH}_2\text{Cl}_2$ , DMF, DMSO,  $\text{CH}_3\text{OCH}_3$ ,  $\text{CH}_3\text{CN}$ , EtOH, MeOH, and  $\text{H}_2\text{O}$  in 200-800 nm range. The band positions of these complexes are shown in Figure 3.108 to 3.111 and absorption spectroscopic data are listed in Table 3.57 and 3.58.

**Table 3.57** UV-Visible absorption spectroscopic data of  $[\text{Ru}(\text{Clazpy})_2(\text{L})](\text{NO}_3)_2 \cdot x\text{H}_2\text{O}$  ( $\text{L} = \text{bpy}, \text{phen}$ )

Solvents	$\lambda_{\text{max}}, \text{nm} (\epsilon^{\text{a}} \times 10^{-4} \text{M}^{-1} \text{cm}^{-1})$					
	$[\text{Ru}(\text{Clazpy})_2(\text{bpy})](\text{NO}_3)_2 \cdot 5\text{H}_2\text{O}$			$[\text{Ru}(\text{Clazpy})_2(\text{phen})](\text{NO}_3)_2 \cdot 3\text{H}_2\text{O}$		
$\text{CH}_2\text{Cl}_2$	232(2.5)	283(2.4)		232(5.1)	278(3.6)	
	318(2.3)	388(2.4)	523(1.0)	383(3.4)	520(1.4)	
DMF	284(2.2)	315(2.2)		276(5.0)	376(2.7)	
	382(1.9)	525(0.9)		520(1.4)		
DMSO	279(3.6)	316(3.0)		278(6.0)	377(2.8)	
	381(2.5)	527(1.2)		523(1.5)		
$\text{CH}_3\text{OCH}_3$	336(1.9)	381(2.1)		337(1.9)	378(2.1)	
	521(0.9)			519(1.0)		
$\text{CH}_3\text{CN}$	279(3.4)	380(2.6)	520(1.1)	274(4.5)	376(2.8)	517(1.3)
EtOH	208(5.4)	277(3.6)		207(7.9)	274(6.8)	
	383(2.4)	520(1.1)		380(3.1)	517(1.5)	
MeOH	208(6.0)	285(2.9)		208(6.7)	258(3.6)	
	315(2.7)	382(3.1)	518(1.3)	275(3.4)	378(3.0)	516(1.2)
Water	284(2.5)	313(2.5)	383(2.6)	258(3.3)	275(3.6)	
	518(1.1)			378(2.9)	514(1.4)	

<sup>a</sup> Molar extinction coefficient

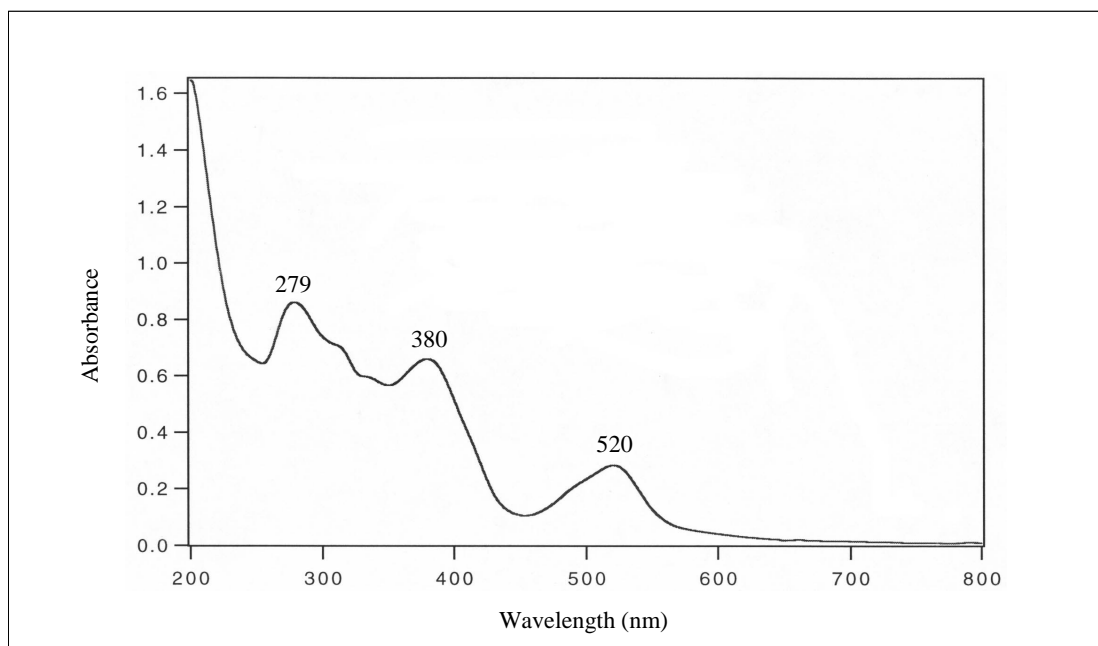
**Table 3.58** UV-Visible absorption spectroscopic data of  
 $[\text{Ru}(\text{Clazpy})_2(\text{L})](\text{NO}_3)_2 \cdot x\text{H}_2\text{O}$  (L = azpy, Clazpy)

Solvents	$\lambda_{\text{max}}$ , nm ( $\epsilon^a \times 10^4 \text{ M}^{-1}\text{cm}^{-1}$ )			
	$[\text{Ru}(\text{Clazpy})_2(\text{azpy})](\text{NO}_3)_2 \cdot \text{H}_2\text{O}$		$[\text{Ru}(\text{Clazpy})_3](\text{NO}_3)_2 \cdot 5\text{H}_2\text{O}$	
CH <sub>2</sub> Cl <sub>2</sub>	232(4.4) 387(5.6)	287(3.2) 491(1.7)	232(4.4) 502(1.7)	390(5.6)
DMF	280(3.7)	378(4.0) 506(1.8)	279(3.7) 506(1.7)	381(3.8)
DMSO	282(2.8)	381(3.4) 502(1.3)	280(3.9) 498(1.5)	383(4.3)
CH <sub>3</sub> OCH <sub>3</sub>	380(3.1)	501(1.1)	382(2.9)	499(1.0)
CH <sub>3</sub> CN	279(3.8) 499(1.5)	379(4.3)	381(3.4)	495(1.2)
EtOH	208(8.4) 383(4.9)	275(5.5) 497(1.7)	207(6.5) 385(3.9)	275(4.3) 494(1.4)
MeOH	208(8.3) 381(5.2)	279(3.8) 492(1.7)	208(7.5) 327(3.3)	280(3.3) 383(5.1) 492(1.6)
Water	275(3.0) 383(4.5)	328(2.9) 496(1.5)	325(3.3)	385(5.7) 493(1.9)

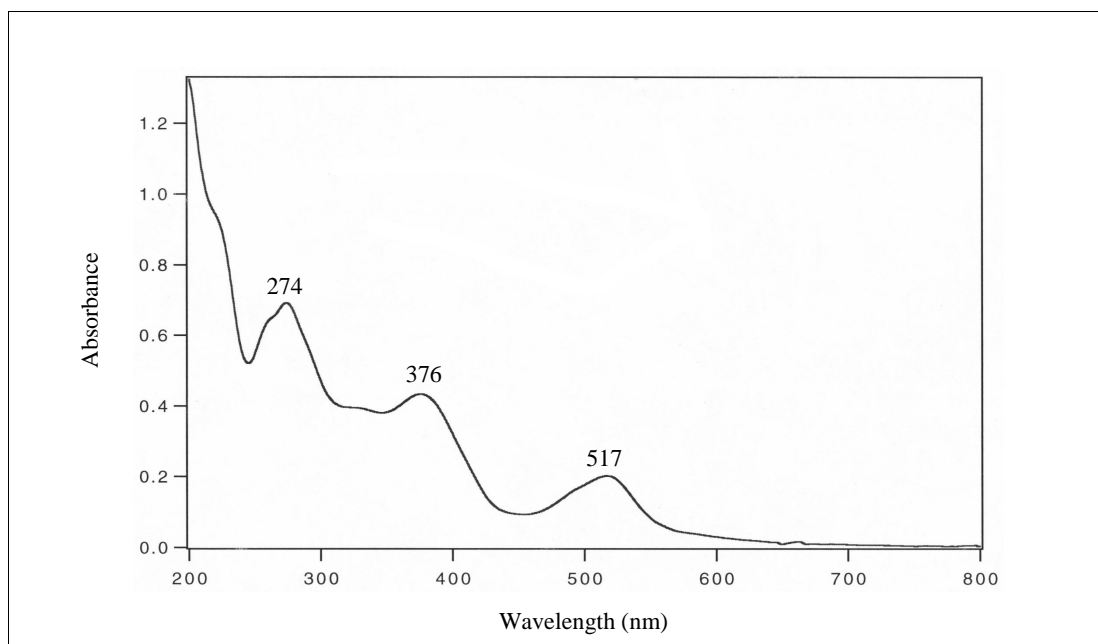
<sup>a</sup> Molar extinction coefficient

The absorption spectra in UV region (200-400 nm) were assigned to  $\pi \rightarrow \pi^*$  transition of ligands ( $\epsilon \sim 22000 - 84000 \text{ M}^{-1}\text{cm}^{-1}$ ). While, the absorption bands in visible region (400-800 nm) were assigned to metal-to-ligand charge transfer transition (MLCT) ( $\epsilon \sim 9000 - 19000 \text{ M}^{-1}\text{cm}^{-1}$ ). From previous discuss of the parent complex, *ctc*- $[\text{Ru}(\text{Clazpy})_2\text{Cl}_2]$ , transition band in the visible region at 584 nm in CH<sub>3</sub>CN was shifted to shorter wavelength in  $[\text{Ru}(\text{Clazpy})_2(\text{L})]^{2+}$  (L = bpy, phen, azpy, Clazpy) because each L ligand increased stability of d-orbital of Ru(II). However, the

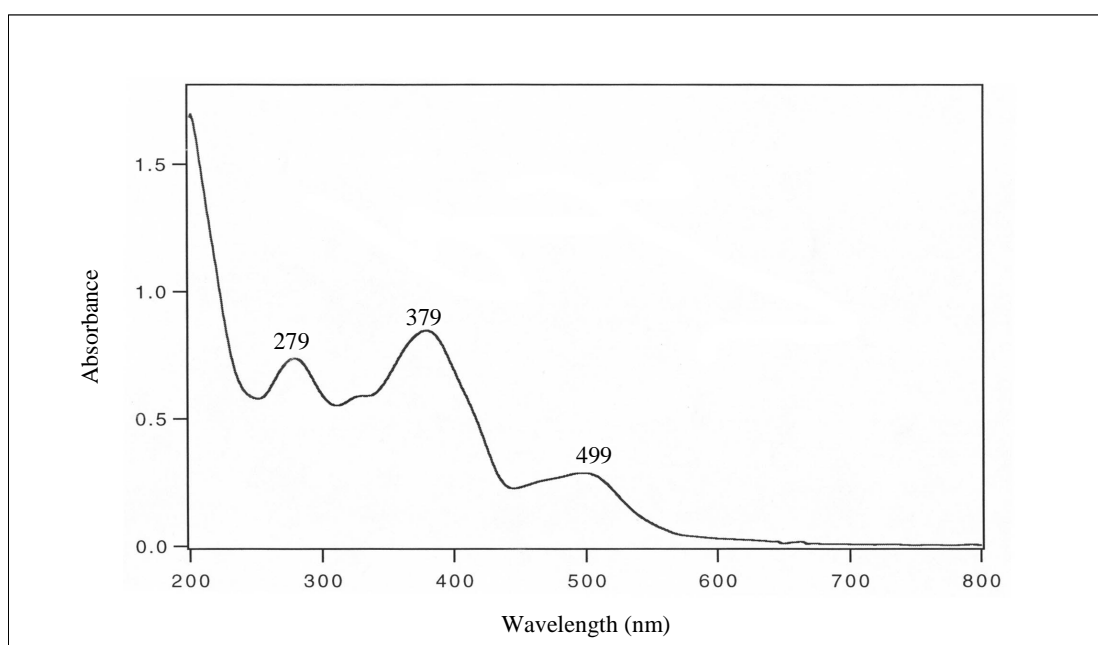
lowest energy absorption band of  $[\text{Ru}(\text{Clazpy})_2(\text{L})](\text{NO}_3)_2 \cdot x\text{H}_2\text{O}$  ( $\text{L} = \text{bpy}$ , phen, azpy, Clazpy) were not shifted when the polarity of solvents was increased.



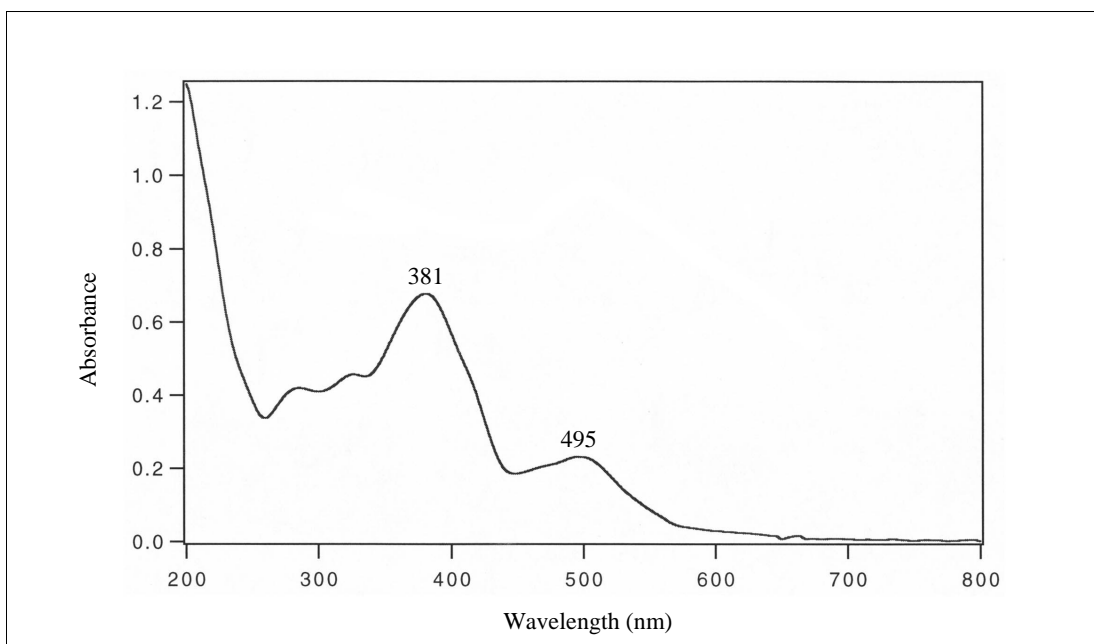
**Figure 3.108** UV-Visible absorption spectrum of  $[\text{Ru}(\text{Clazpy})_2(\text{bpy})](\text{NO}_3)_2 \cdot 5\text{H}_2\text{O}$  in  $\text{CH}_3\text{CN}$



**Figure 3.109** UV-Visible absorption spectrum of  $[\text{Ru}(\text{Clazpy})_2(\text{phen})](\text{NO}_3)_2 \cdot 3\text{H}_2\text{O}$  in  $\text{CH}_3\text{CN}$



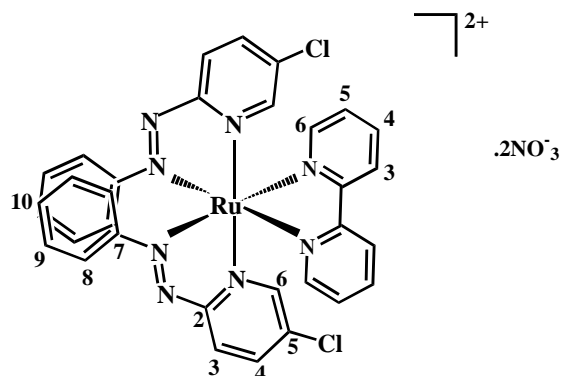
**Figure 3.110** UV-Visible absorption spectrum of  $[\text{Ru}(\text{Clazpy})_2(\text{azpy})](\text{NO}_3)_2 \cdot \text{H}_2\text{O}$  in  $\text{CH}_3\text{CN}$



**Figure 3.111** UV-Visible absorption spectrum of  $[\text{Ru}(\text{Clazpy})_3](\text{NO}_3)_2 \cdot 5\text{H}_2\text{O}$  in  $\text{CH}_3\text{CN}$

### 3.5.2.6 Nuclear magnetic resonance spectroscopy

Nuclear Magnetic Resonance (NMR) spectroscopy is a technique to determine the stereochemistry of compound. The structures of complexes were studied by using 1D and 2D NMR spectroscopic techniques i.e.  $^1\text{H}$  NMR,  $^1\text{H}$ - $^1\text{H}$  COSY NMR,  $^{13}\text{C}$  NMR, DEPT NMR and  $^1\text{H}$ - $^{13}\text{C}$  HMQC NMR. Their NMR spectra were recorded in methanol- $d_4$  and tetramethylsilane ( $\text{Si}(\text{CH}_3)_4$ ) was used as an internal reference. The NMR spectroscopic data of  $[\text{Ru}(\text{Clazpy})_2(\text{L})](\text{NO}_3)_2 \cdot x\text{H}_2\text{O}$  (L = bpy, phen, azpy, Clazpy) complexes are presented in Table 3.59 to 3.62.

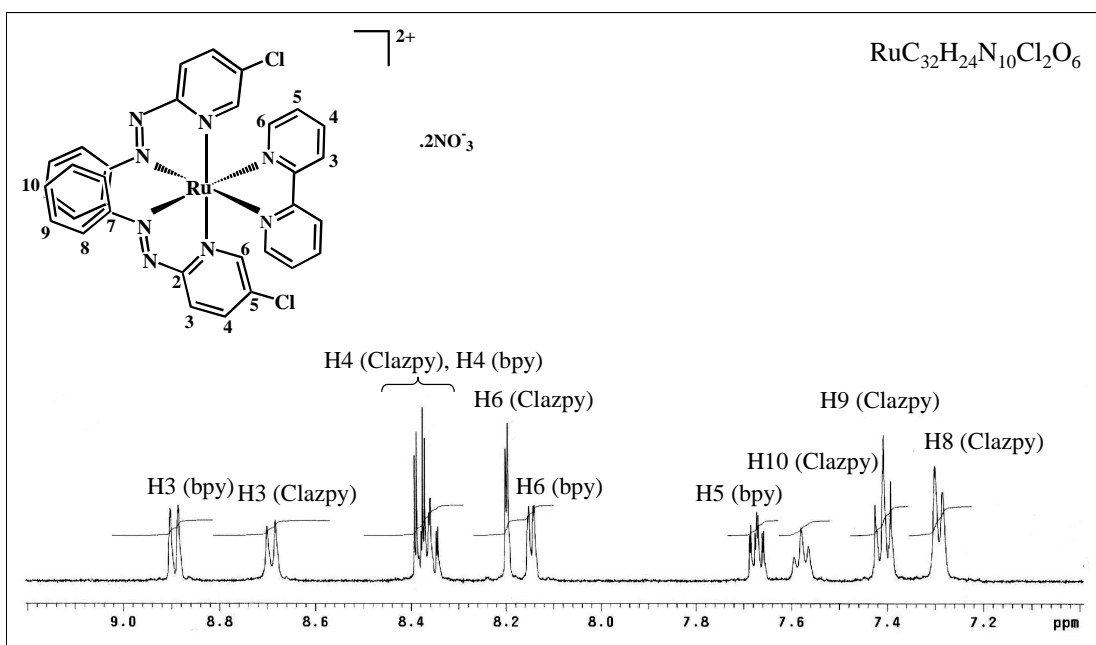
Nuclear magnetic resonance spectroscopy of  $[\text{Ru}(\text{Clazpy})_2(\text{bpy})](\text{NO}_3)_2 \cdot 5\text{H}_2\text{O}$ **Table 3.59**  $^1\text{H}$ - $^{13}\text{C}$  NMR spectroscopic data of  $[\text{Ru}(\text{Clazpy})_2(\text{bpy})](\text{NO}_3)_2 \cdot 5\text{H}_2\text{O}$ 

H-position	$^1\text{H}$ NMR			$^{13}\text{C}$ NMR (CH-type)
	$\delta$ (ppm)	$J$ (Hz)	Amount of H	
3 (bpy)	8.89 (dd)	8.0, 1.0	1	126.89
3 (Clazpy)	8.69 (d)	9.0	1	131.62
4 (Clazpy)	8.39 (dd)	9.0, 2.0	1	142.32
4 (bpy)	8.36 (dt)	8.0, 1.0	1	142.03
6 (Clazpy)	8.20 (d)	2.0	1	150.01
6 (bpy)	8.15 (dt)	8.0, 1.0	1	154.12
5 (bpy)	7.67 (ddd)	5.5, 1.0	1	130.22
10 (Clazpy)	7.58 (t)	8.0	1	134.72
9 (Clazpy)	7.41 (t)	8.0	2	130.85
8 (Clazpy)	7.30 (d)	8.0	2	123.89
Quaternary carbons (C)				164.80, 156.54, 154.51

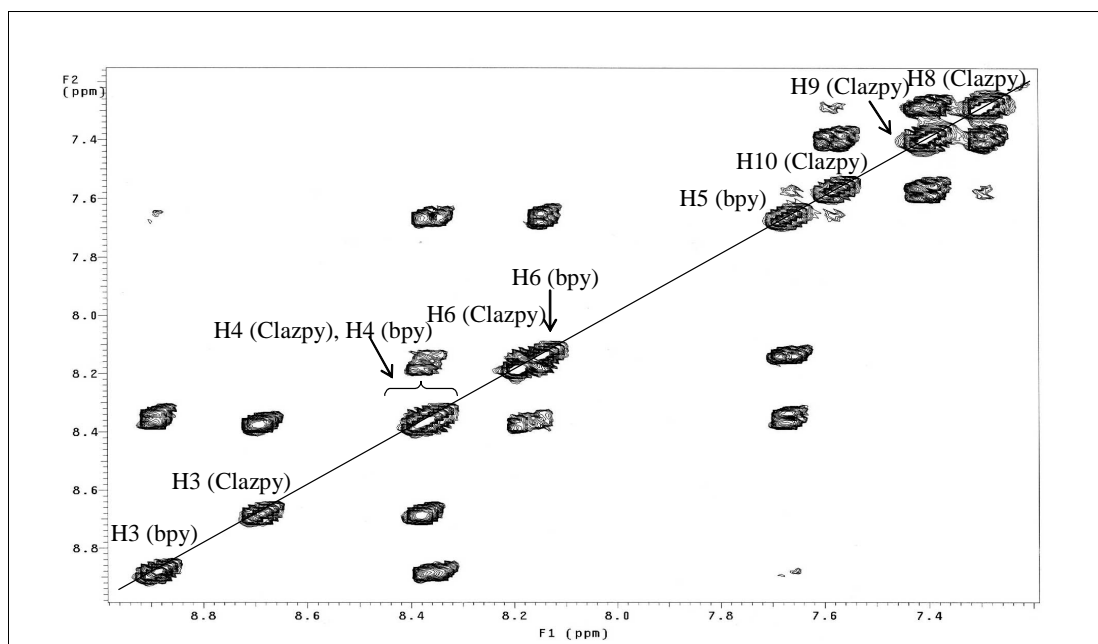
d = doublet, dd = doublet of doublet, ddd = doublet of doublet of doublet, dt = doublet of triplet, t = triplet

The  $^1\text{H}$  NMR spectrum (Figure 3.112) of  $[\text{Ru}(\text{Clazpy})_2(\text{bpy})](\text{NO}_3)_2 \cdot 5\text{H}_2\text{O}$  complex showed 10 resonances of 24 protons, six from Clazpy ligand and four from bpy ligand. The spectrum displayed only one set of proton of each ligands (Clazpy and bpy). This result indicated that both Clazpy are equivalent. A chemical shift of proton H3 on bpy ligand occurred at the lowest field (8.89 ppm) due to trans effect of pyridine of coordinated bpy to N=N azo of Clazpy. In addition, others protons in this compound were also studied by using simple correlation  $^1\text{H}$ - $^1\text{H}$  COSY NMR spectroscopy (Figure 3.113).

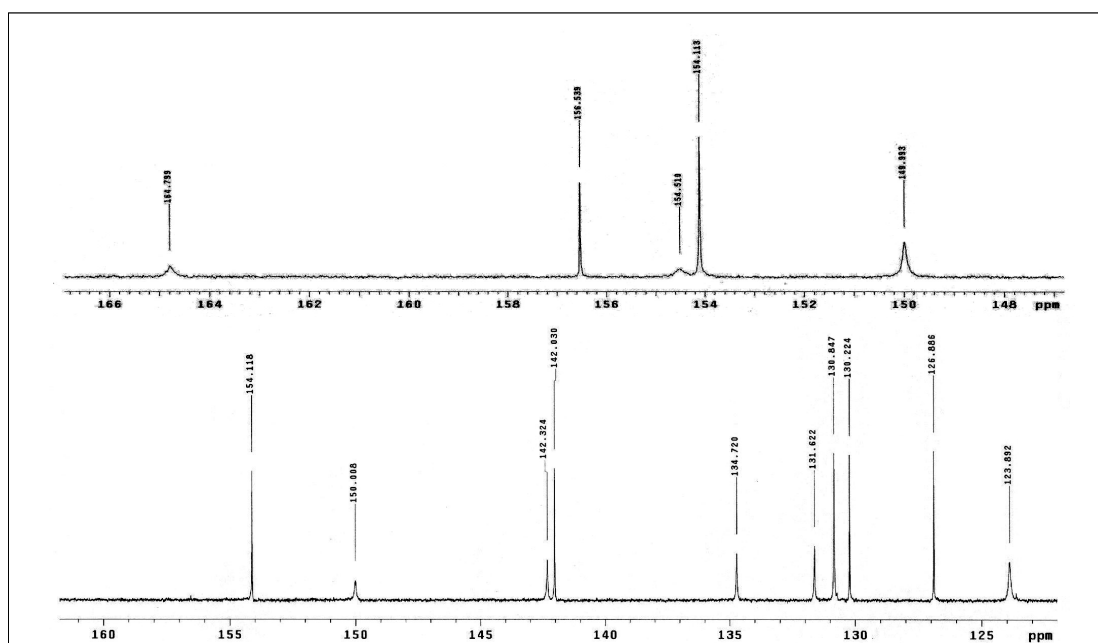
The  $^{13}\text{C}$  NMR (Figure 3.114) results corresponded to the DEPT NMR (Figure 3.115) which showed only one kind of methane carbons. The signals at 164.80, 156.54 and 154.51 ppm were assigned to two quaternary carbons C2, C5 and C7 of Clazpy ligand. Moreover, the others  $^{13}\text{C}$  NMR signals assignments were based on  $^1\text{H}$ - $^{13}\text{C}$  HMQC NMR spectrum (Figure 3.116).



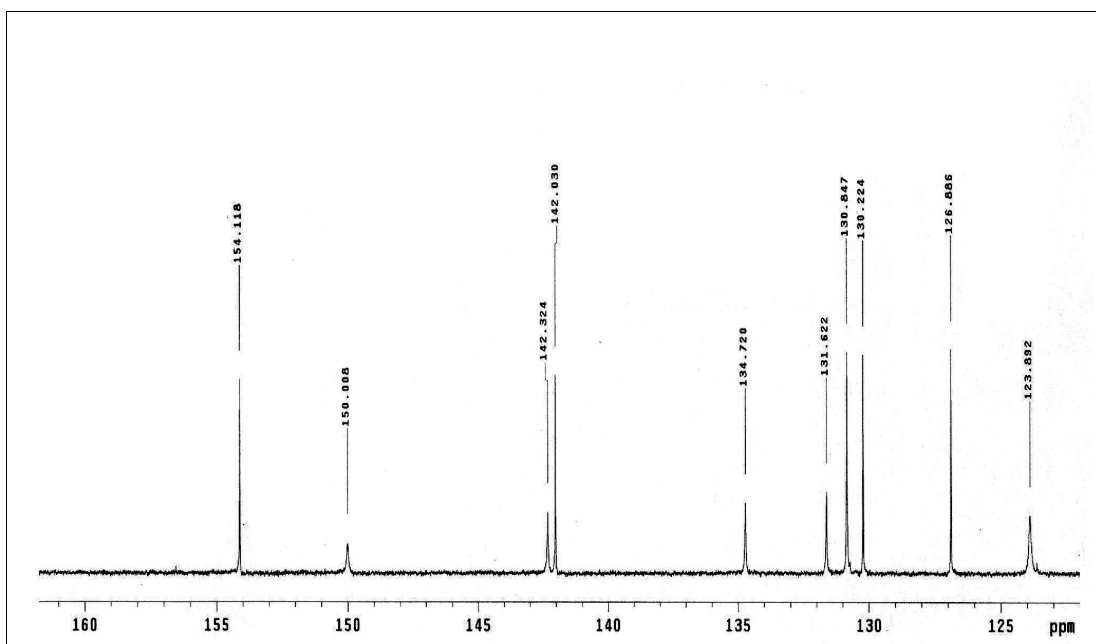
**Figure 3.112**  $^1\text{H}$  NMR spectrum of  $[\text{Ru}(\text{Clazpy})_2(\text{bpy})](\text{NO}_3)_2 \cdot 5\text{H}_2\text{O}$  in methanol- $d_4$



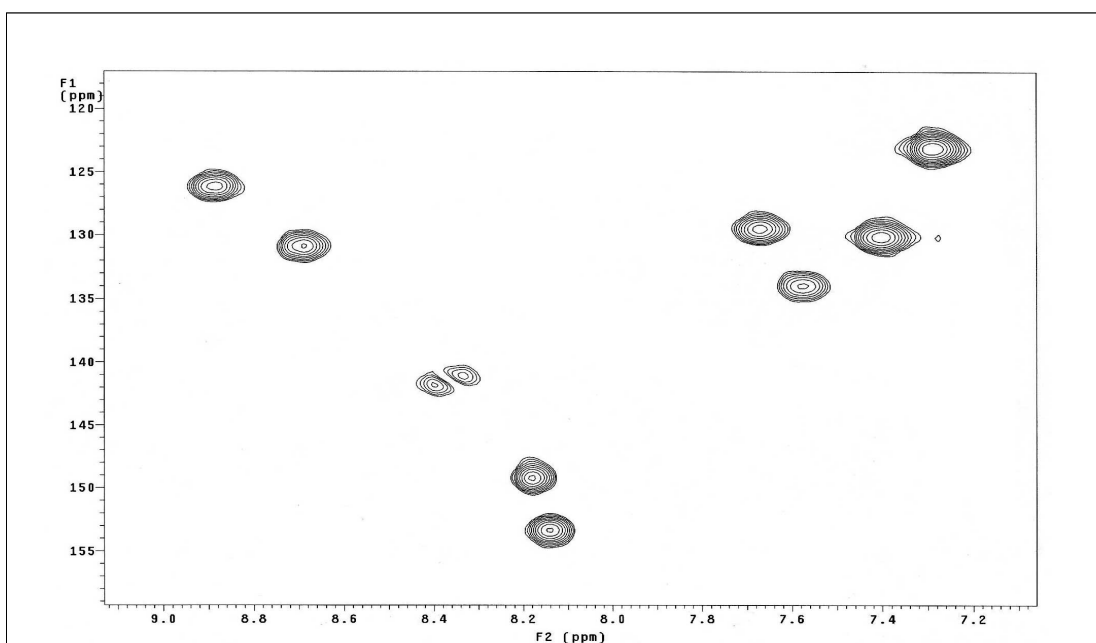
**Figure 3.113**  $^1\text{H}$ - $^1\text{H}$  COSY NMR spectrum of  $[\text{Ru}(\text{Clazpy})_2(\text{bpy})](\text{NO}_3)_2 \cdot 5\text{H}_2\text{O}$  in methanol- $d_4$



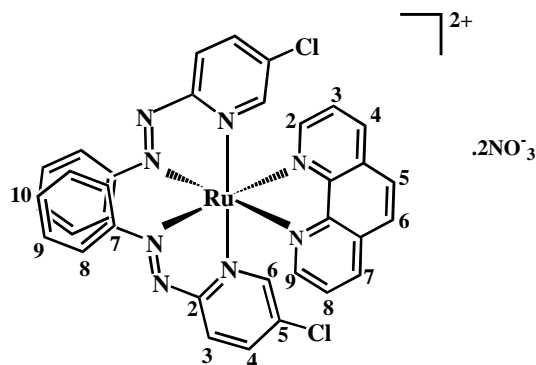
**Figure 3.114**  $^{13}\text{C}$  NMR spectrum of  $[\text{Ru}(\text{Clazpy})_2(\text{bpy})](\text{NO}_3)_2 \cdot 5\text{H}_2\text{O}$  in methanol- $d_4$



**Figure 3.115** DEPT NMR spectrum of [Ru(Clazpy)<sub>2</sub>(bpy)](NO<sub>3</sub>)<sub>2</sub>·5H<sub>2</sub>O in methanol-*d*<sub>4</sub>



**Figure 3.116** <sup>1</sup>H-<sup>13</sup>C HMQC NMR spectrum of [Ru(Clazpy)<sub>2</sub>(bpy)](NO<sub>3</sub>)<sub>2</sub>·5H<sub>2</sub>O in methanol-*d*<sub>4</sub>

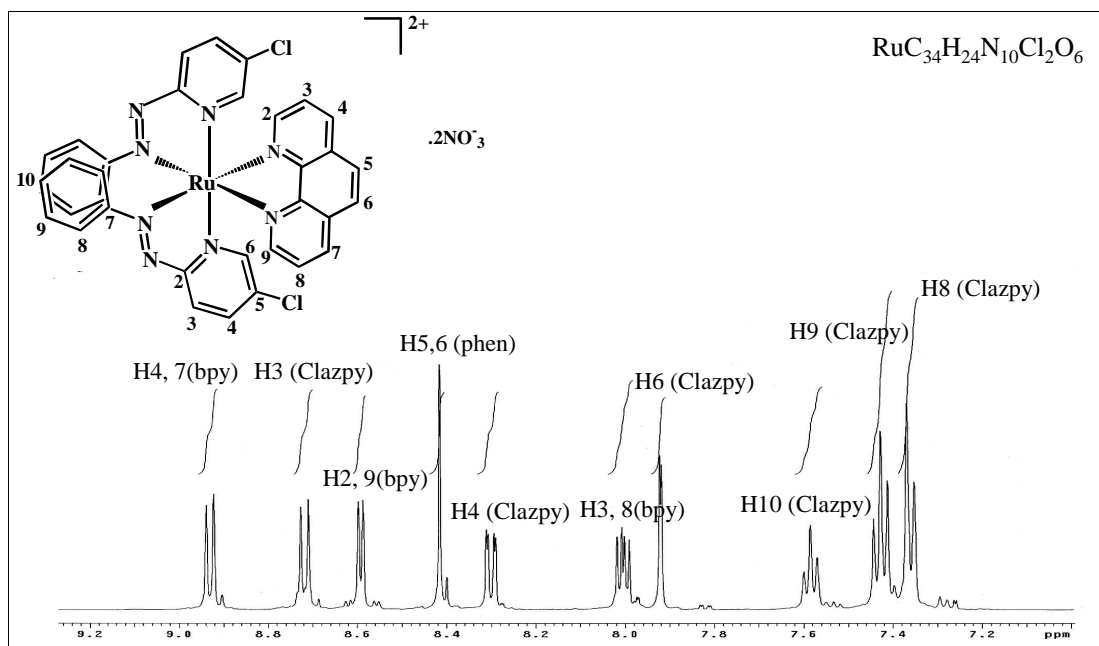
Nuclear magnetic resonance spectroscopy of  $[\text{Ru}(\text{Clazpy})_2(\text{phen})](\text{NO}_3)_2 \cdot 3\text{H}_2\text{O}$ **Table 3.60**  $^1\text{H}$ - $^{13}\text{C}$  NMR spectroscopic data of  $[\text{Ru}(\text{Clazpy})_2(\text{phen})](\text{NO}_3)_2 \cdot 3\text{H}_2\text{O}$ 

H-position	$^1\text{H}$ NMR			$^{13}\text{C}$ NMR (CH-type)
	$\delta$ (ppm)	$J$ (Hz)	Amount of H	
4,7 (phen)	8.93 (d)	8.5	1	141.09
3 (Clazpy)	8.72 (d)	9.0	1	131.65
2,9 (phen)	8.59 (d)	5.0	1	154.98
5,6 (phen)	8.42	-	1	129.73
4 (Clazpy)	8.30 (dd)	9.0, 2.0	1	142.18
3,8 (phen)	8.00 (dd)	8.5, 5.0	1	128.42
6 (Clazpy)	7.92 (d)	2.0	1	150.18
10 (Clazpy)	7.58 (t)	8.0	1	134.52
9 (Clazpy)	7.43 (t)	8.0	2	130.87
8 (Clazpy)	7.36 (d)	8.0	2	123.85
Quaternary carbons (C)				164.80, 146.75, 138.80, 133.22, 154.98

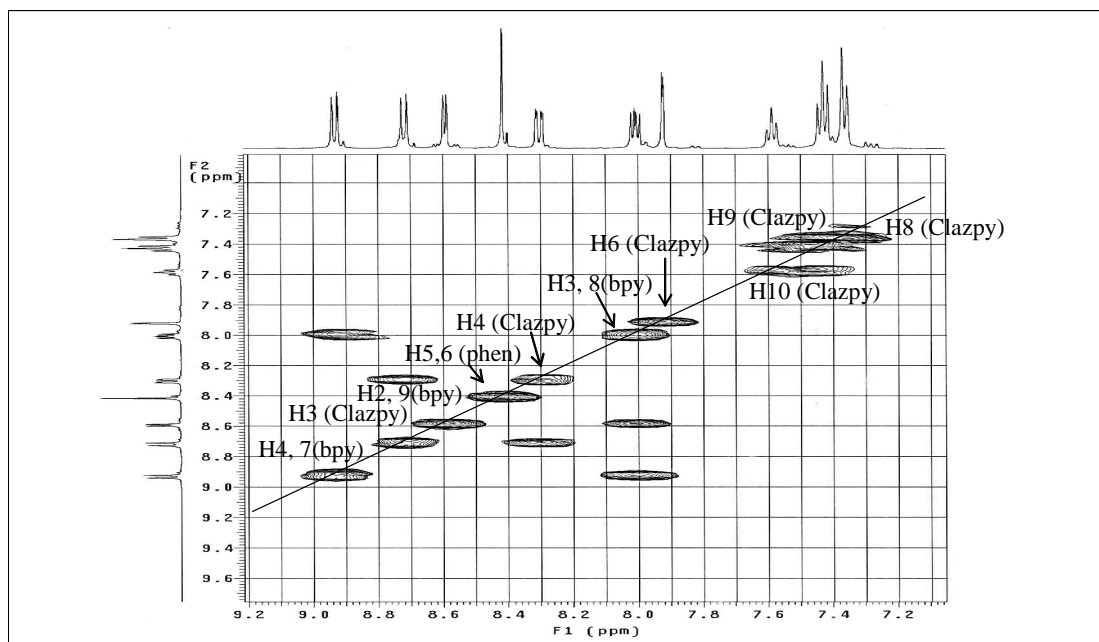
d = doublet, dd = doublet of doublet, t = triplet

The  $^1\text{H}$  NMR spectrum (Figure 3.117) of  $[\text{Ru}(\text{Clazpy})_2(\text{phen})](\text{NO}_3)_2 \cdot 3\text{H}_2\text{O}$  complex showed two sets of ligands (Clazpy and phen). They displayed 12 resonances of 24 protons, eight from Clazpy ligand and four from phen ligand. This indicated the molecule has  $\text{C}_2$  symmetry. The proton 4, 7 occurred at the lowest field due to its position trans to the  $\text{N}=\text{N}$  azo function. In addition, others protons in this compound were also studied by using simple correlation  $^1\text{H}$ - $^1\text{H}$  COSY NMR spectroscopy (Figure 3.118) and  $^1\text{H}$ - $^1\text{H}$  TOCSY NMR (Figure 3.119). The later techniques give detail about the correlation between proton-proton which none directly bonded such as H3, H4 and H6. Moreover,  $^1\text{H}$ - $^1\text{H}$  ROESY NMR (Figure 3.120) supported the interaction between proton-proton in space such as H3, H8 of phen correlated with H8 of Clazpy ligand.

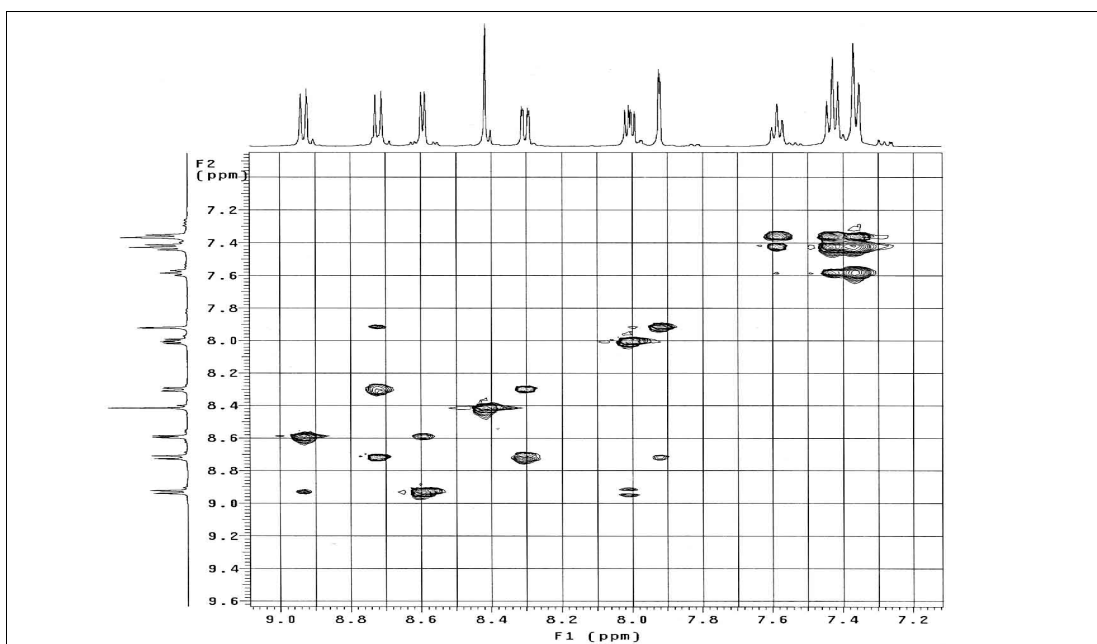
The  $^{13}\text{C}$  NMR (Figure 3.121) results corresponded to the DEPT NMR (Figure 3.122) which showed only one kind of methane carbons. All quaternary carbons at 164.80, 146.75, 138.80, 133.22, 154.98 belonged to C2, C5, C7 of Clazpy and C10, C11, C12, C13 of phen. Moreover, the othres  $^{13}\text{C}$  NMR signals assignments were based on  $^1\text{H}$ - $^{13}\text{C}$  HSQC NMR spectrum (Figure 3.123). In addition, to monitoring the correlation between carbon and proton as long range coupling  $^1\text{H}$ - $^{13}\text{C}$  HMBC NMR (Figure 3.124) techniques was used.



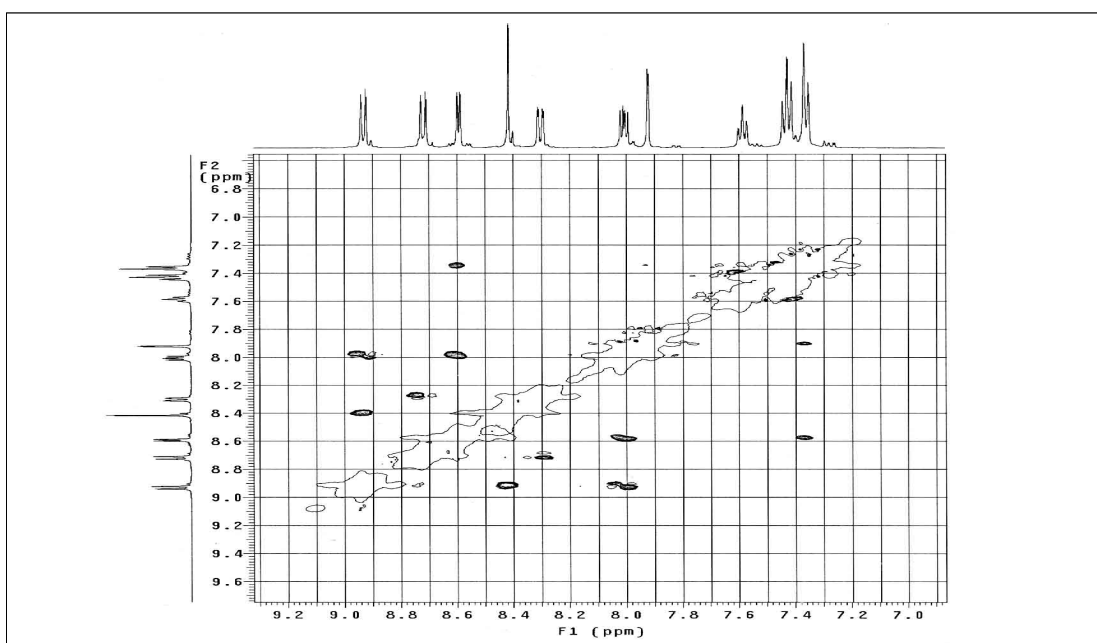
**Figure 3.117**  $^1\text{H}$  NMR spectrum of  $[\text{Ru}(\text{Clazpy})_2\text{phen}](\text{NO}_3)_2 \cdot 3\text{H}_2\text{O}$  in methanol- $d_4$



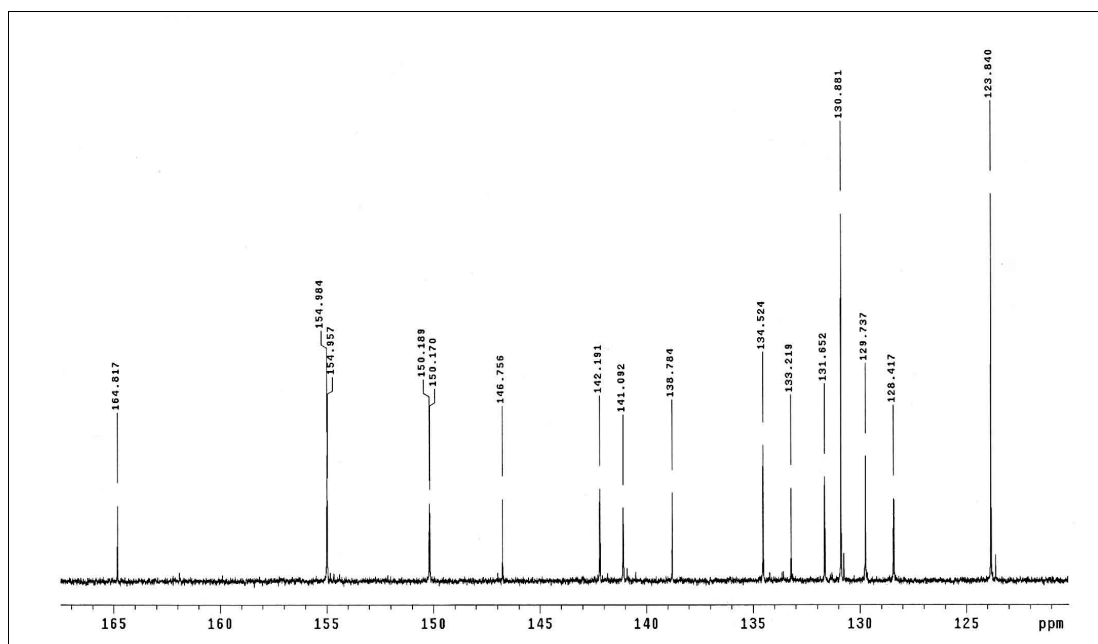
**Figure 3.118**  $^1\text{H}$ - $^1\text{H}$  COSY NMR spectrum of  $[\text{Ru}(\text{Clazpy})_2(\text{phen})](\text{NO}_3)_2 \cdot 3\text{H}_2\text{O}$  in methanol- $d_4$



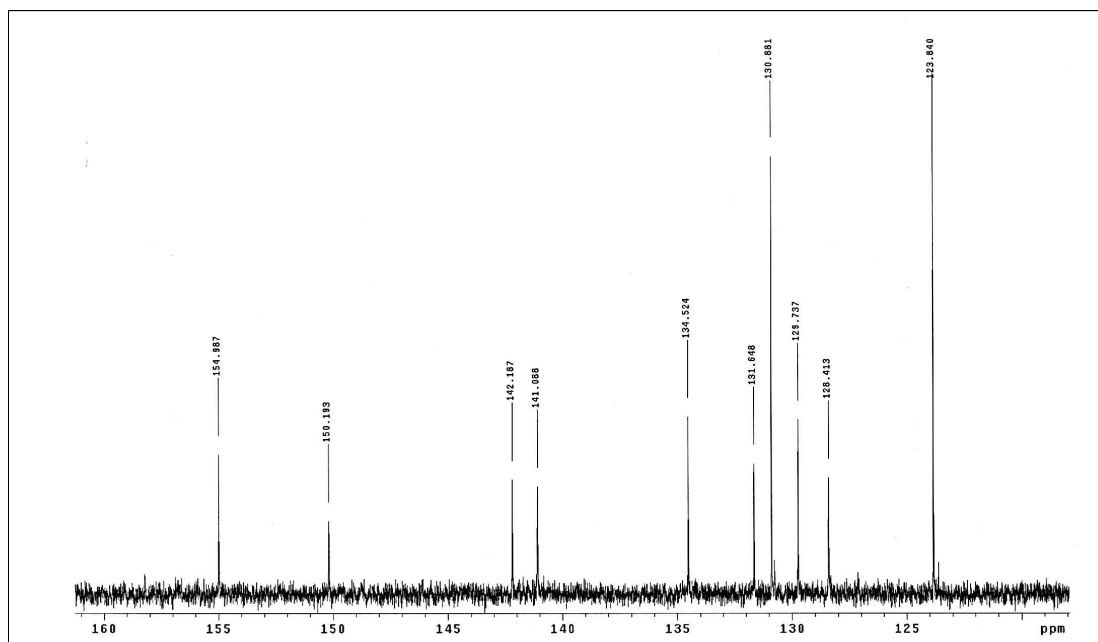
**Figure 3.119**  $^1\text{H}$ - $^1\text{H}$  TOCSY NMR spectrum of  $[\text{Ru}(\text{Clazpy})_2(\text{phen})](\text{NO}_3)_2 \cdot 3\text{H}_2\text{O}$  in methanol- $d_4$



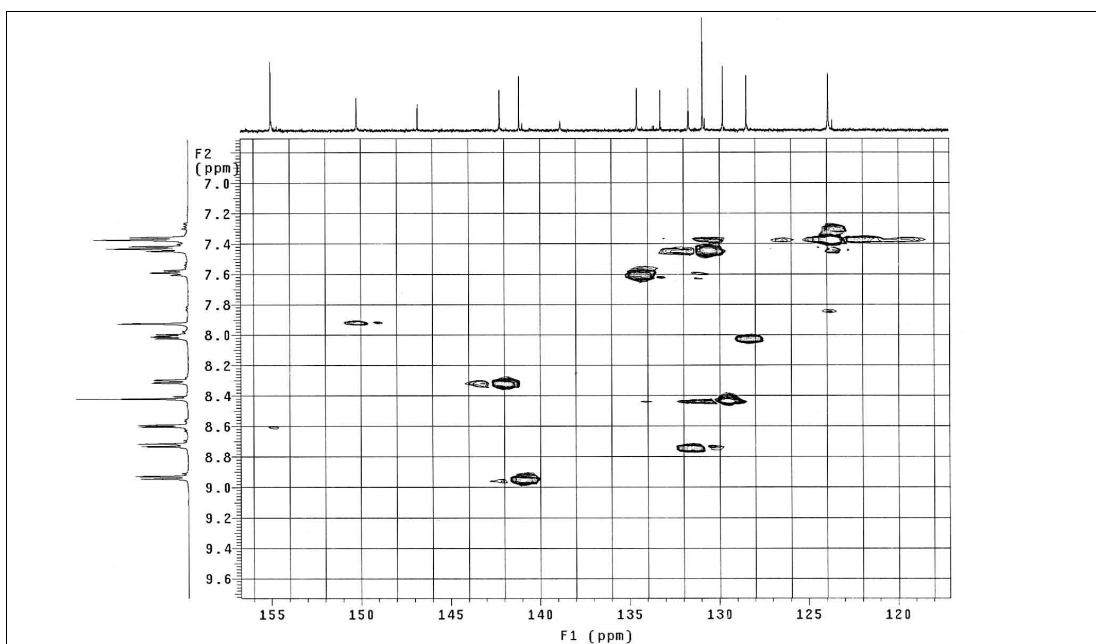
**Figure 3.120**  $^1\text{H}$ - $^1\text{H}$  ROESY NMR spectrum of  $[\text{Ru}(\text{Clazpy})_2(\text{phen})](\text{NO}_3)_2 \cdot 3\text{H}_2\text{O}$  in methanol- $d_4$



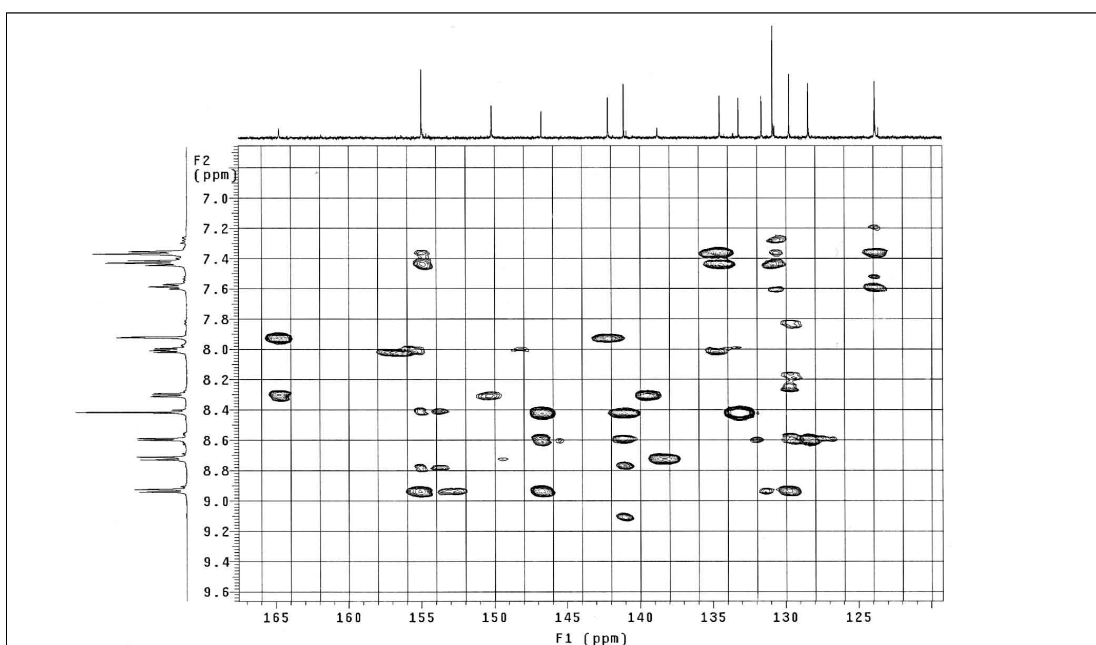
**Figure 3.121**  $^{13}\text{C}$  NMR spectrum of  $[\text{Ru}(\text{Clazpy})_2(\text{phen})](\text{NO}_3)_2 \cdot 3\text{H}_2\text{O}$  in methanol- $d_4$



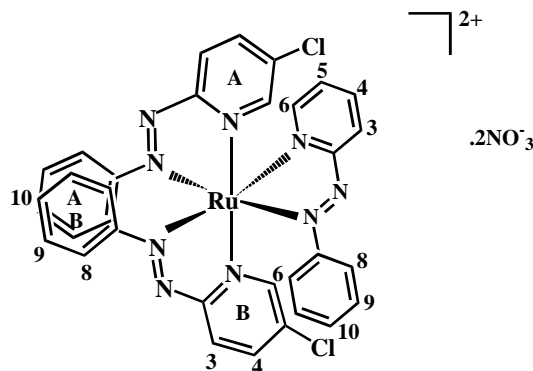
**Figure 3.122** DEPT NMR spectrum of  $[\text{Ru}(\text{Clazpy})_2(\text{phen})](\text{NO}_3)_2 \cdot 3\text{H}_2\text{O}$  in methanol- $d_4$



**Figure 3.123**  $^1\text{H}$ - $^{13}\text{C}$  HSQC NMR spectrum of  $[\text{Ru}(\text{Clazpy})_2(\text{phen})](\text{NO}_3)_2 \cdot 3\text{H}_2\text{O}$  in methanol- $d_4$



**Figure 3.124**  $^1\text{H}$ - $^{13}\text{C}$  HMBC NMR spectrum of  $[\text{Ru}(\text{Clazpy})_2(\text{phen})](\text{NO}_3)_2 \cdot 3\text{H}_2\text{O}$  in methanol- $d_4$

Nuclear magnetic resonance spectroscopy of  $[\text{Ru}(\text{Clazpy})_2(\text{azpy})](\text{NO}_3)_2 \cdot \text{H}_2\text{O}$ 

The  $^1\text{H}$  NMR spectrum (Figure 3.125) of  $[\text{Ru}(\text{Clazpy})_2(\text{azpy})](\text{NO}_3)_2 \cdot \text{H}_2\text{O}$  complex showed 13 resonances of 25 protons because some resonances were overlapped. This result indicated that three ligands are unsymmetrical molecules. In addition, the first signal exhibited at the lowest field was proton H6 (azpy) (9.25 ppm) on the pyridine ring of azpy ligand which located near coordinated nitrogen on pyridine ring. In addition, others protons in this compound were also studied by using simple correlation  $^1\text{H}$ - $^1\text{H}$  COSY NMR spectroscopy (Figure 3.126).

The  $^{13}\text{C}$  NMR (Figure 3.127) results corresponded to the DEPT NMR (Figure 3.128) which showed only one kind of methane carbons. All quaternary carbons at 164.82, 164.21, 164.00, 156.91, 153.56, 152.93, 140.09, 139.95 belonged to C2, C7 of azpy ligand and C2, C5, C7 of Clazpy ligand. Moreover, the others  $^{13}\text{C}$  NMR signals assignments were based on  $^1\text{H}$ - $^{13}\text{C}$  HMQC NMR spectrum (Figure 3.129).

**Table 3.61**  $^1\text{H}$ - $^{13}\text{C}$  NMR spectroscopic data of  $[\text{Ru}(\text{Clazpy})_2(\text{azpy})](\text{NO}_3)_2 \cdot \text{H}_2\text{O}$ 

H-position	$^1\text{H}$ NMR			$^{13}\text{C}$ NMR (CH-type)
	$\delta$ (ppm)	$J$ (Hz)	Amount of H	
6 (azpy)	9.25 (d)	6.5, 1.0	1	132.62
5 (azpy)	8.63 (m)	-	3	132.13
3A				143.78
3B				
4 (azpy)	8.55 (d)	6.0, 1.5	1	154.06
4B	8.50 (dd)	9.0, 2.5	1	143.20
4A	8.42 (dd)	8.5, 2.0	1	143.49
6A	8.37 (d)	2.0	1	150.80
6B	8.25 (d)	2.0	1	151.70
3 (azpy)	7.90 (dt)	7.5, 1.5	1	132.05
8, 10	7.63 (m)	-	13	131.09, 135.07
9, 9, 8 (azpy)	7.52 (m)	-		131.36, 135.24, 124.07
10B	7.43 (t)	8.5		123.87
9B, 10	7.08 (m)	-		130.91, 133.50
8B	6.90 (d)	7.5		123.74
Quaternary carbons (C)				164.82, 164.21, 164.00, 156.91, 153.56, 152.93, 140.09, 139.95

d = doublet, dd = doublet of doublet, t = triplet, tt = triplet of triplet, m = multiplet

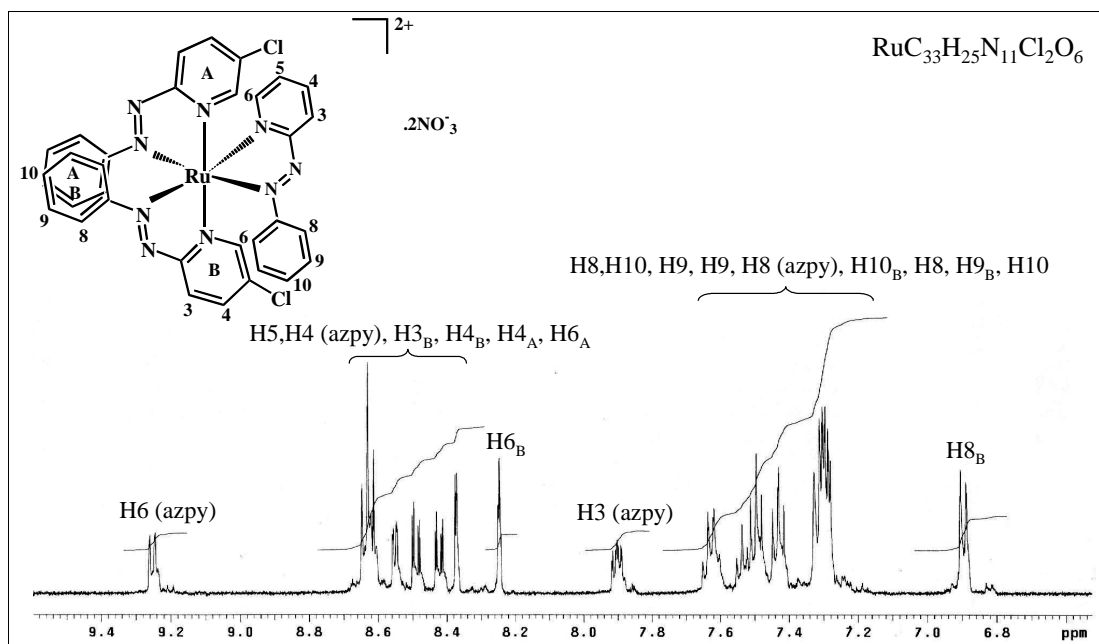


**Figure 3.125**  $^1\text{H}$  NMR spectrum of  $[\text{Ru}(\text{Clazpy})_2(\text{azpy})](\text{NO}_3)_2 \cdot \text{H}_2\text{O}$  in  $\text{methanol-}d_4$

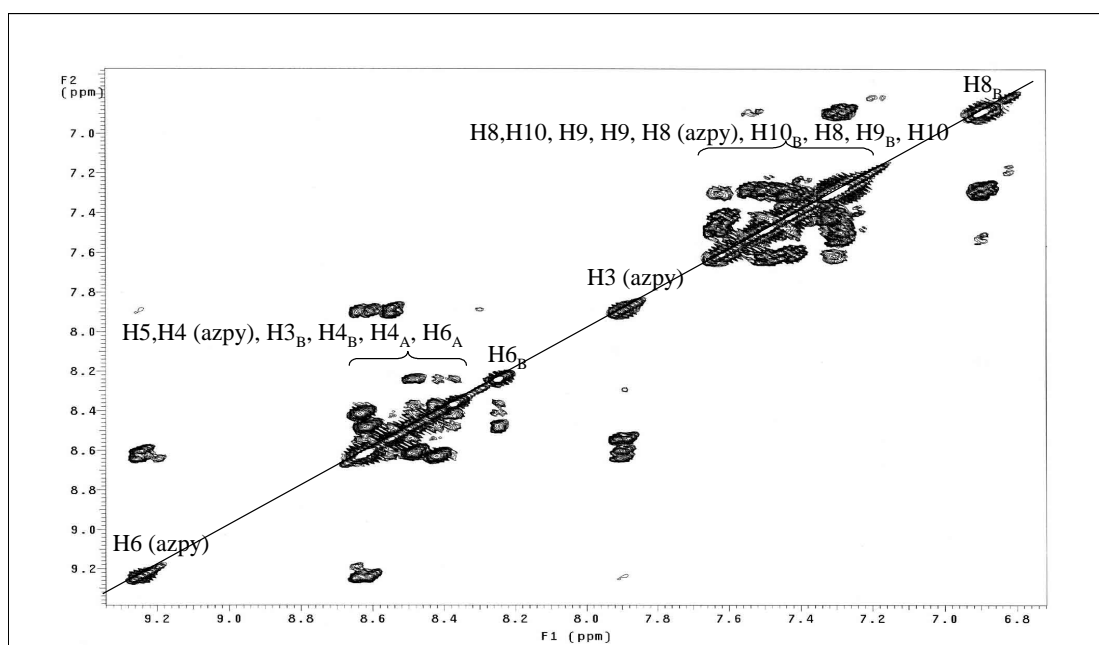


**Figure 3.126**  $^1\text{H}$ - $^1\text{H}$  COSY NMR spectrum of  $[\text{Ru}(\text{Clazpy})_2(\text{azpy})](\text{NO}_3)_2 \cdot \text{H}_2\text{O}$  in  $\text{methanol-}d_4$

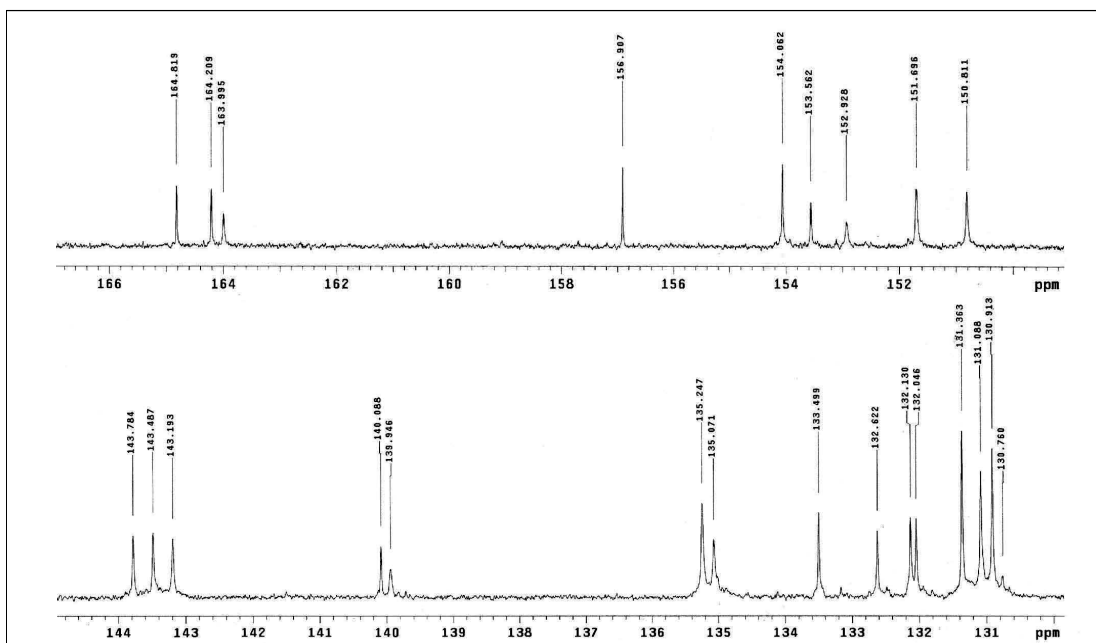


**Figure 3.127**  $^{13}\text{C}$  NMR spectrum of  $[\text{Ru}(\text{Clazpy})_2(\text{azpy})](\text{NO}_3)_2 \cdot \text{H}_2\text{O}$  in methanol- $d_4$

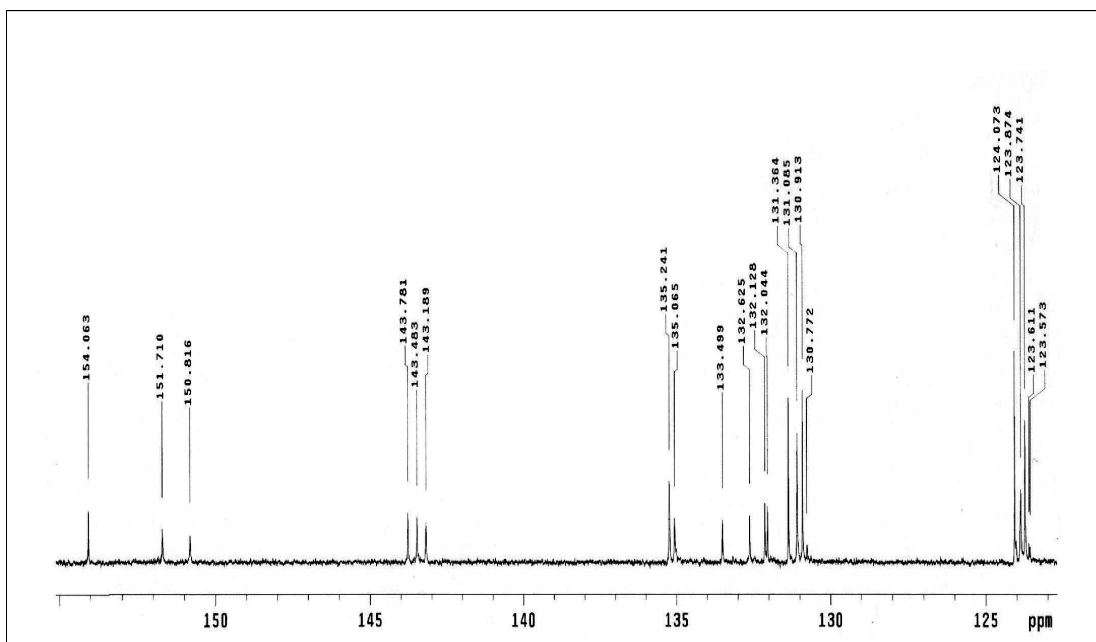


**Figure 3.128** DEPT NMR spectrum of  $[\text{Ru}(\text{Clazpy})_2(\text{azpy})](\text{NO}_3)_2 \cdot \text{H}_2\text{O}$  in methanol- $d_4$



**Table 3.62**  $^1\text{H}$ - $^{13}\text{C}$  NMR spectroscopic data of  $[\text{Ru}(\text{Clazpy})_3](\text{NO}_3)_2 \cdot 5\text{H}_2\text{O}$ 

H-position	$^1\text{H}$ NMR			$^{13}\text{C}$ NMR (CH-type)
	$\delta$ (ppm)	J (Hz)	Amount of H	
3C	9.21 (d)	8.5	1	133.44
4C	8.68 (dd)	8.5, 2.0	1	143.56
6C	8.63 (d)	2.0	1	153.29
3A	8.61 (d)	8.5	1	132.59
3B	8.58 (d)	8.5	1	132.07
4A	8.50 (dd)	8.5, 2.0	1	143.43
6A	8.44 (d)	2.0	1	152.28
4B	8.41 (dd)	8.5, 2.0	1	143.17
6B	8.32 (d)	2.0	1	150.83
10C, 10A	7.63 (t)	7.5	2	135.32, 135.21
10B, 9C	7.51 (m)	-	3	135.08, 131.42
9A	7.44 (t)	8.5, 1.0	1	131.08
8C	7.36 (dd)	7.5	2	124.07
8A	7.27 (m)	-	4	124.00
9B				130.88
8B	6.85 (dd)		2	123.63
Quaternary carbons (C)				164.11, 164.06, 163.21, 157.24, 152.73, 140.26, 140.03, 139.91

d = doublet, dd = doublet of doublet, t = triplet, m = multiplet

The  $^1\text{H}$  NMR spectrum (Figure 3.130) of  $[\text{Ru}(\text{Clazpy})_3](\text{NO}_3)_2 \cdot 5\text{H}_2\text{O}$  complex showed 15 resonances of 24 protons. Some appeared to be multiple signals due to overlap of resonances. In addition, the protons H3, H4 and H6 on pyridine ring appeared at lower downfield than protons H8, H9 and H10 on phenyl ring. This may be due to the pyridine protons having less electron density than the phenyl protons. From the correlation  $^1\text{H}$ - $^1\text{H}$  COSY NMR spectroscopy (Figure 3.131), the three sets of Clazpy pyridine signals have been distinguished. Since two of the three Clazpy pyridine rings (A and B) are trans to each other, the protons are slightly different similar to the situation of the  $[\text{Ru}(\text{Clazpy})_3](\text{PF}_6)_2$  complex. In contrast to the protons in the Clazpy pyridine ring (C), the chemical shift appeared at the lowest field due to trans to N=N azo function. These data confirmed the retained configuration of N(py) and N(azo) orientation from the starting material, *ctc*- $[\text{Ru}(\text{Clazpy})_2\text{Cl}_2]$ .

The  $^{13}\text{C}$  NMR signals assignments (Figure 3.132) correlated with DEPTNMR(spectrum (Figure 3.133) were based on the  $^1\text{H}$ - $^{13}\text{C}$  HMQC spectrum (Figure 3.134) which is generally used for studying large and complicated molecules. The  $^{13}\text{C}$  NMR spectrum showed 18 signals from 24 methine carbons and six signals of six quaternary carbons. The signals at 162.59, 139.54 and 135.34 ppm were assigned to the quaternary carbons C2, C5 and C7, respectively. Since C2 was located between nitrogen atoms, the chemical shift occurred at the lowest field.

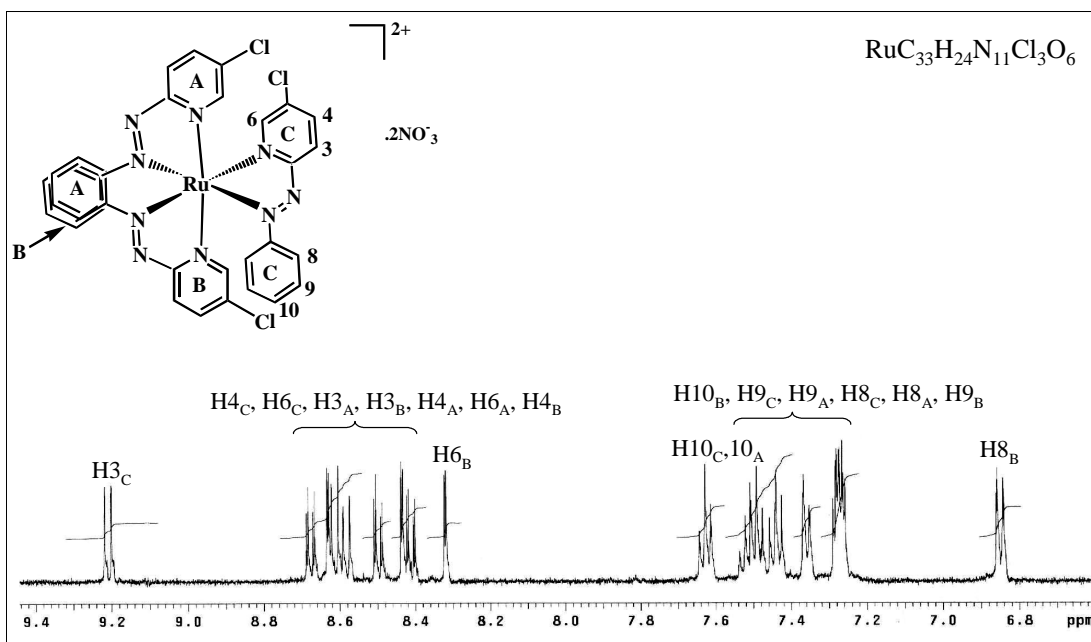


**Figure 3.130**  $^1\text{H}$  NMR spectrum of  $[\text{Ru}(\text{Clazpy})_3](\text{NO}_3)_2 \cdot 5\text{H}_2\text{O}$  in methanol- $d_4$

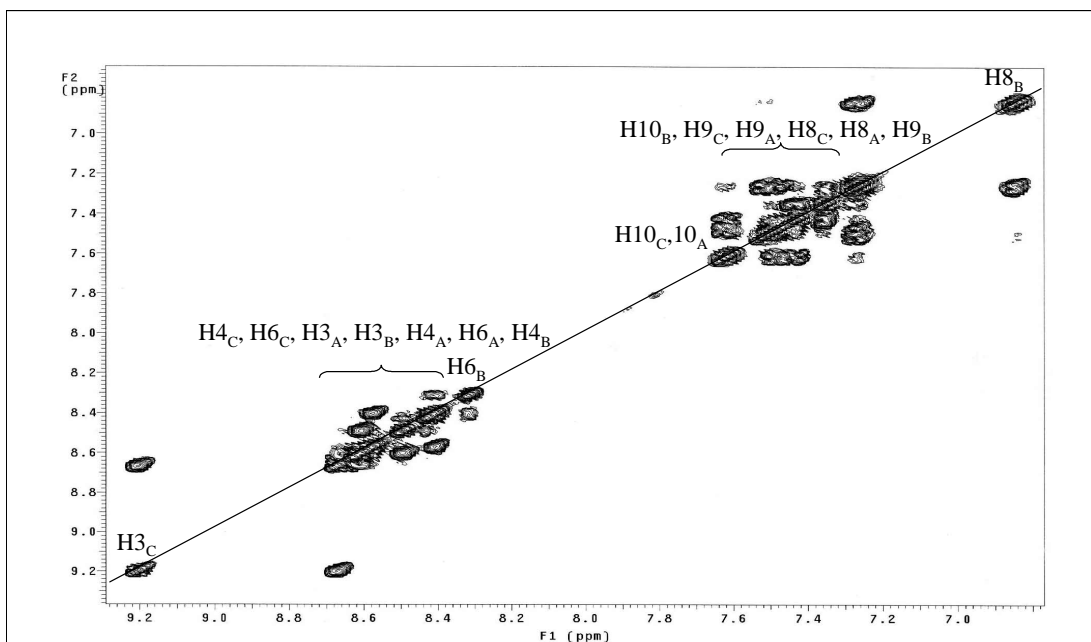


**Figure 3.131**  $^1\text{H}$ - $^1\text{H}$  COSY NMR spectrum of  $[\text{Ru}(\text{Clazpy})_3](\text{NO}_3)_2 \cdot 5\text{H}_2\text{O}$  in methanol- $d_4$

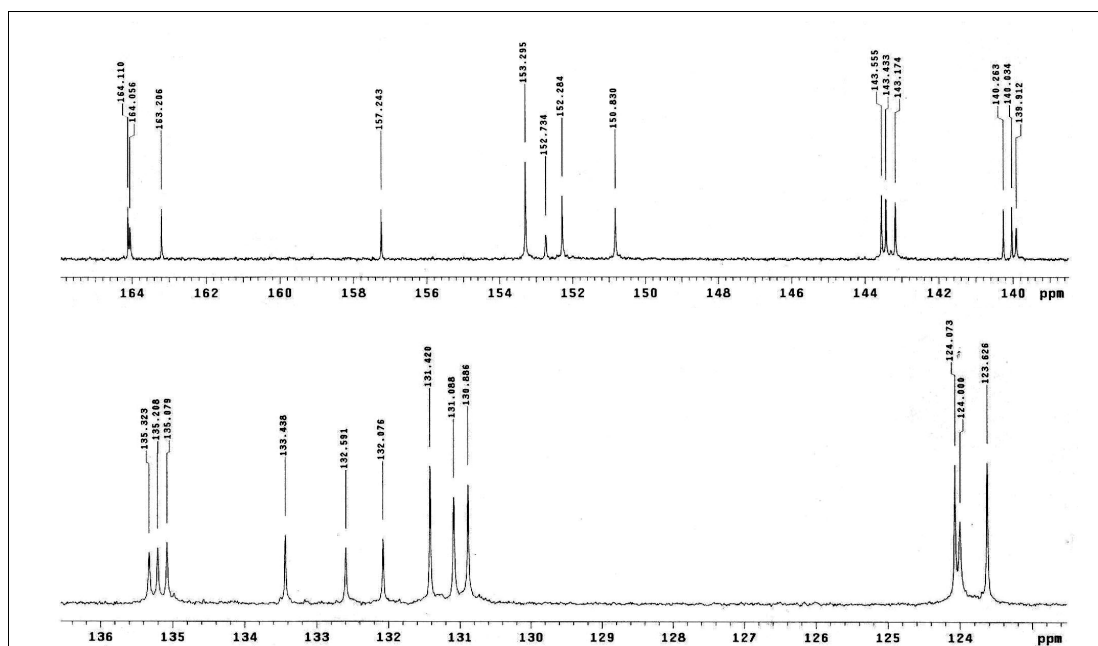


**Figure 3.132**  $^{13}\text{C}$  NMR spectrum of  $[\text{Ru}(\text{Clazpy})_3](\text{NO}_3)_2 \cdot 5\text{H}_2\text{O}$  in  $\text{methanol-}d_4$

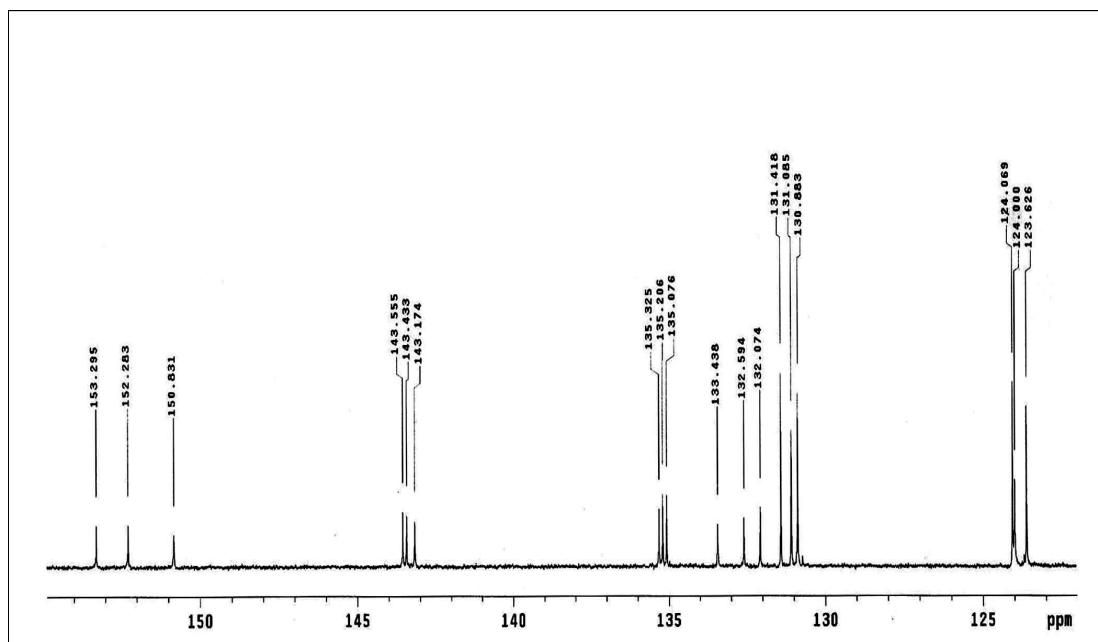


**Figure 3.133** DEPT NMR spectrum of  $[\text{Ru}(\text{Clazpy})_3](\text{NO}_3)_2 \cdot 5\text{H}_2\text{O}$  in  $\text{methanol-}d_4$

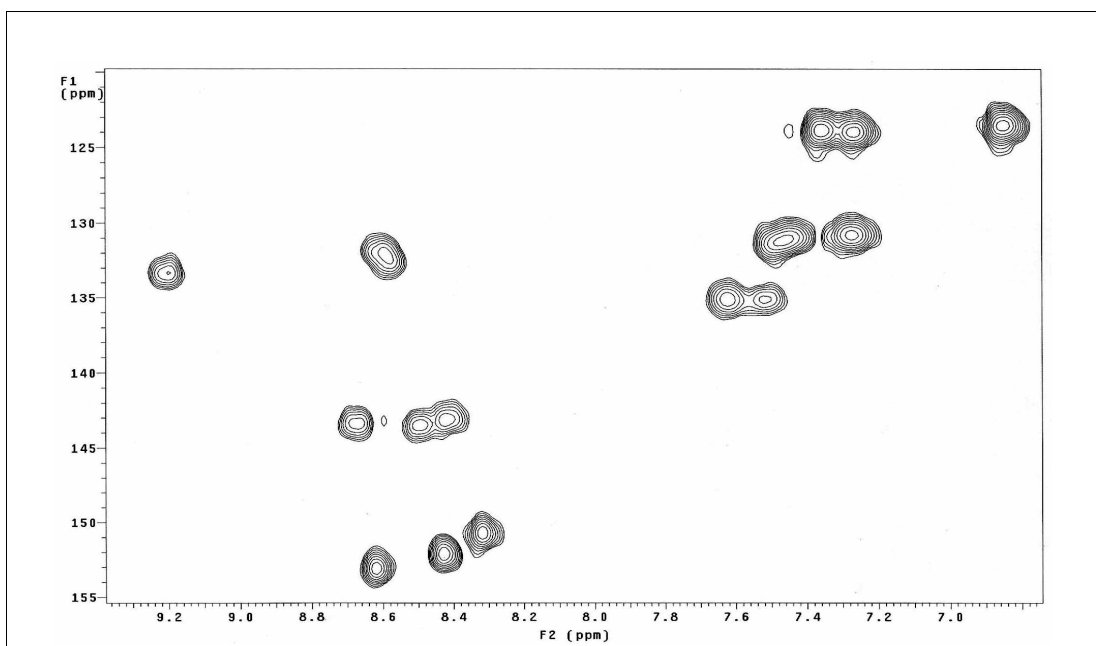


**Figure 3.134**  $^1\text{H}$ - $^{13}\text{C}$  HMQC NMR spectrum of  $[\text{Ru}(\text{Clazpy})_3](\text{NO}_3)_2 \cdot 5\text{H}_2\text{O}$  in methanol- $d_4$

### 3.5.2.7 Cyclic voltammetry

Cyclic voltammetry is the most widely used technique providing information about electrochemical reactions. The electrochemical behavior of the  $[\text{Ru}(\text{Clazpy})_2(\text{L})](\text{NO}_3)_2 \cdot x\text{H}_2\text{O}$  ( $\text{L} = \text{bpy}$ ,  $\text{phen}$ ,  $\text{azpy}$ ,  $\text{Clazpy}$ ) complexes were carried out in 0.1 M TBAH using  $\text{CH}_3\text{CN}$  as solvent. The electron transfer properties are shown in Figure 3.135 to 3.138 with corresponding half-wave potentials. The cyclic voltammetric data of these compounds are listed in Table 3.63.

**Table 3.63** Cyclic voltammetric data of  $[\text{Ru}(\text{Clazpy})_2(\text{L})](\text{NO}_3)_2 \cdot x\text{H}_2\text{O}$  (L = bpy, phen, azpy, Clazpy) in 0.1 M TBAH  $\text{CH}_3\text{CN}$  at scan rate 50 mV/s (ferrocene as used an internal standard)

Compounds	<sup>a</sup> $E_{1/2}$ , V						
	Oxidation	Reduction					
	Ru(II)/(III)	I	II	III	IV	V	VI
$[\text{Ru}(\text{Clazpy})_2(\text{bpy})](\text{NO}_3)_2 \cdot 5\text{H}_2\text{O}$	n	-0.44 (95)	-0.93 (85)	-1.70 (90)	-1.98 (80)	-2.28 (95)	-
$[\text{Ru}(\text{Clazpy})_2(\text{phen})](\text{NO}_3)_2 \cdot 3\text{H}_2\text{O}$	n	-0.49 (140)	-0.93 (95)	-1.71 (87)	-1.99 (85)	-2.38 (235)	-
$[\text{Ru}(\text{Clazpy})_2(\text{azpy})](\text{NO}_3)_2 \cdot \text{H}_2\text{O}$	n	-0.34 (85)	-0.67 (80)	-1.10 (95)	-1.78 (95)	- 2.11 <sup>b</sup>	-2.48 <sup>a</sup>
$[\text{Ru}(\text{Clazpy})_3](\text{NO}_3)_2 \cdot 5\text{H}_2\text{O}$	n	-0.33 (85)	-0.61 (80)	-1.06 (80)	-1.72 (75)	- 2.10 <sup>b</sup>	-2.44 <sup>a</sup>

<sup>a</sup> $E_{1/2} = (E_{\text{pa}} + E_{\text{pc}})/2$ , where  $E_{\text{pa}}$  and  $E_{\text{pc}}$  are anodic and cathodic peak potentials, respectively;  $\Delta E_{\text{p}} = E_{\text{pa}} - E_{\text{pc}}$

<sup>b</sup>cathodic peak potential, V

<sup>c</sup>anodic peak potential, V

### Oxidation potential

The cyclic voltammogram of  $[\text{Ru}(\text{Clazpy})_2(\text{L})](\text{NO}_3)_2 \cdot x\text{H}_2\text{O}$  complexes where L = bpy, phen, azpy, Clazpy were studied in the range 0.00 to +2.00 V. This couple cannot be observed in all complexes because the redox of Ru(II)/(III) could occur at positive potential greater than +2.00 V which is out of the solvent window.

### Reduction potential

The reduction potential of  $[\text{Ru}(\text{Clazpy})_2(\text{L})](\text{NO}_3)_2 \cdot x\text{H}_2\text{O}$  complexes where  $\text{L} = \text{bpy}$ ,  $\text{phen}$ ,  $\text{azpy}$ ,  $\text{Clazpy}$  were studied in the range 0.00 to -2.60 V. The cyclic voltammogram of these complexes where  $\text{L} = \text{bpy}$  and  $\text{phen}$  displayed five couples, whereas where  $\text{L} = \text{azpy}$  and  $\text{Clazpy}$  appeared six couples. The first reduction which was usually controlled by the ligand which have the most stable lower unoccupied molecular orbital (LUMO), was assigned to a reduction centered on  $\text{Clazpy}$ . It is well known that azoimine moiety could accept maximum two electron so that the last reduction peak may be the reduction of  $\text{bpy}$  or  $\text{phen}$  in  $[\text{Ru}(\text{Clazpy})_2(\text{L})](\text{NO}_3)_2 \cdot x\text{H}_2\text{O}$ . Meanwhile, two last reduction potential of  $[\text{Ru}(\text{Clazpy})_2(\text{azpy})](\text{NO}_3)_2 \cdot x\text{H}_2\text{O}$  belonged to two couple of  $\text{azpy}$ . The results were similar to the cyclic voltammogram of  $[\text{Ru}(\text{Clazpy})_2(\text{L})](\text{PF}_6)_2$  ( $\text{L} = \text{bpy}$ ,  $\text{phen}$ ,  $\text{azpy}$ ,  $\text{Clazpy}$ ).

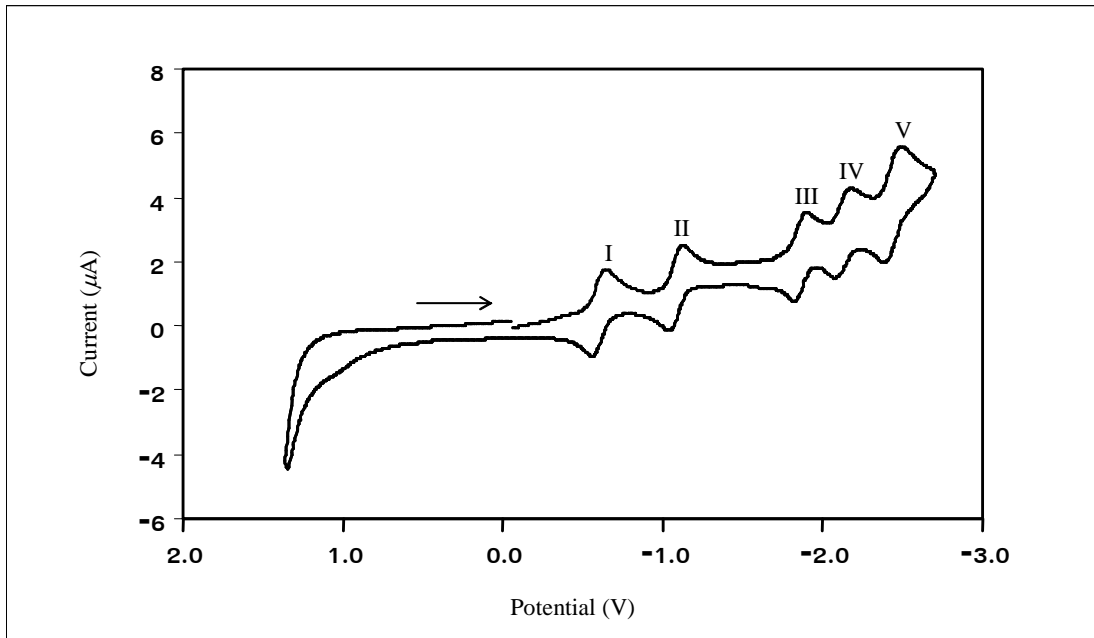


**Figure 3.135** Cyclic voltammogram of  $[\text{Ru}(\text{Clazpy})_2(\text{bpy})](\text{NO}_3)_2 \cdot 5\text{H}_2\text{O}$  in 0.1 M TBAH  $\text{CH}_3\text{CN}$  at scan rate 50 mV/s (ferrocene as an internal standard)

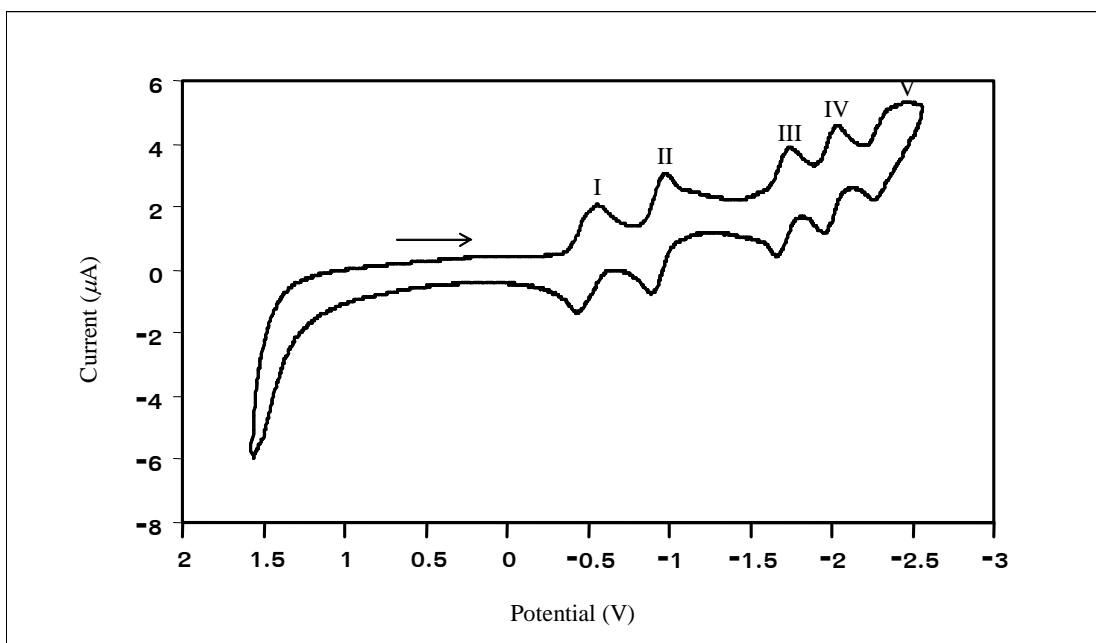


**Figure 3.136** Cyclic voltammogram of  $[\text{Ru}(\text{Clazpy})_2(\text{phen})](\text{NO}_3)_2 \cdot 3\text{H}_2\text{O}$  in 0.1 M TBAH  $\text{CH}_3\text{CN}$  at scan rate 50 mV/s (ferrocene as an internal standard)

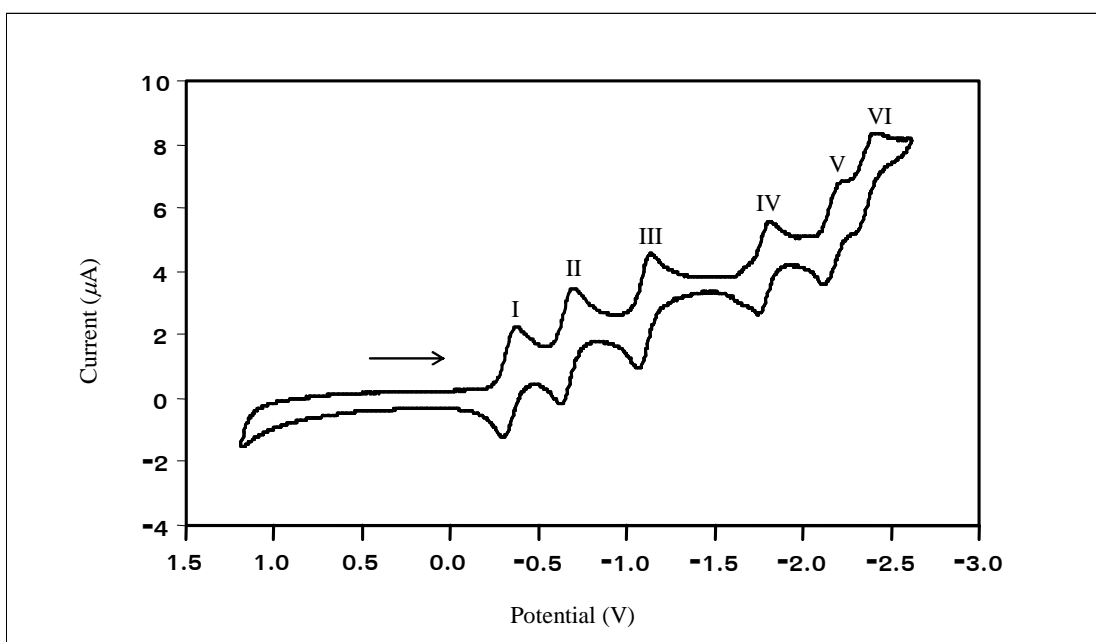


**Figure 3.137** Cyclic voltammogram of  $[\text{Ru}(\text{Clazpy})_2(\text{azpy})](\text{NO}_3)_2 \cdot \text{H}_2\text{O}$  in 0.1 M TBAH  $\text{CH}_3\text{CN}$  at scan rate 50 mV/s (ferrocene as an internal standard)

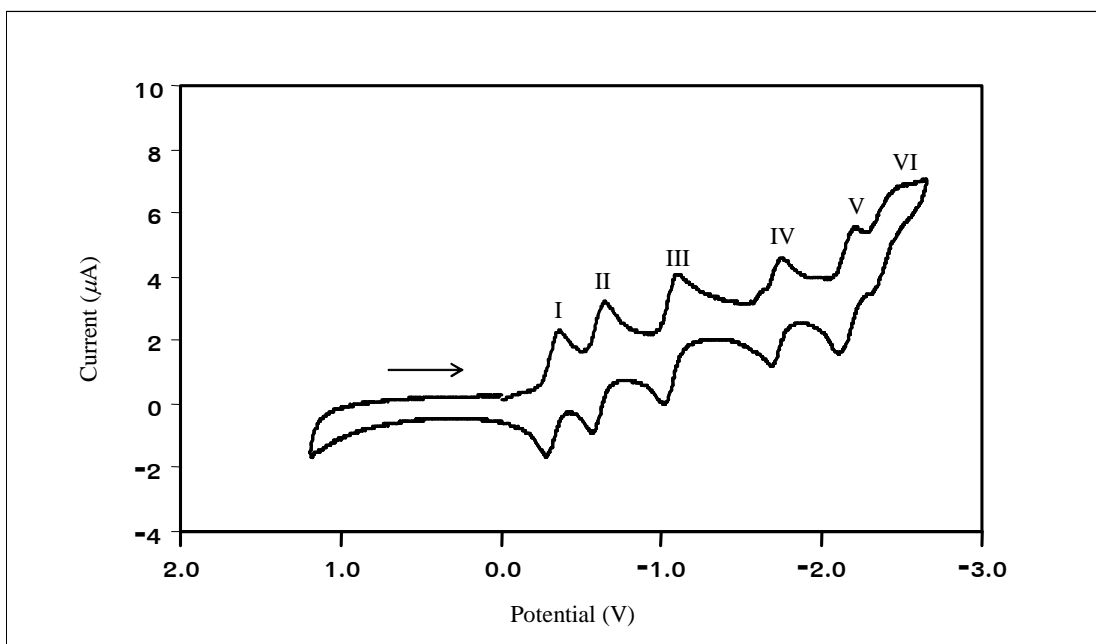


**Figure 3.138** Cyclic voltammogram of  $[\text{Ru}(\text{Clazpy})_3](\text{NO}_3)_2 \cdot 3\text{H}_2\text{O}$  in 0.1 M TBAH  $\text{CH}_3\text{CN}$  at scan rate 50 mV/s (ferrocene as an internal standard)

### 3.6 Syntheses and characterization of $[\text{Ru}(\text{Clazpy})_2(\text{L})]\text{Cl}_2 \cdot x\text{H}_2\text{O}$ (L = bpy, phen, azpy, Clazpy)

#### 3.6.1 Syntheses of $[\text{Ru}(\text{Clazpy})_2(\text{L})]\text{Cl}_2 \cdot x\text{H}_2\text{O}$ (L = bpy, phen, azpy, Clazpy)

The  $[\text{Ru}(\text{Clazpy})_2(\text{L})]\text{Cl}_2 \cdot x\text{H}_2\text{O}$  (L = bpy, phen, azpy, Clazpy) complexes was prepared by converted  $[\text{Ru}(\text{Clazpy})_2(\text{L})](\text{PF}_6)_2$  into chloride salts by treating hexafluorophosphate salts in acetone with tetra-*n*-butylammonium chloride (TBACl) also dissolved in acetone. The obtained complexes were recrystallized by the mixing of ethanol and ether. The synthesis route is presented in Figure 3.139.

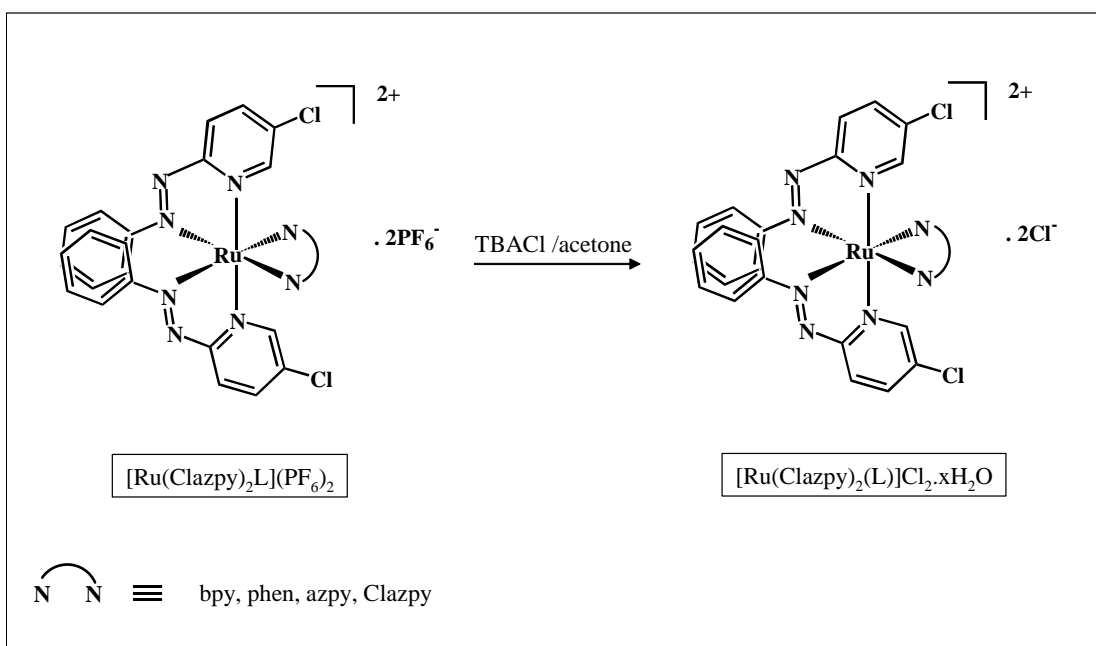


**Figure 3.139** Synthetic route for the preparation of  $[\text{Ru}(\text{Clazpy})_2(\text{L})]\text{Cl}_2 \cdot x\text{H}_2\text{O}$

The physical properties of these complexes are summarized in Table 3.64.

**Table 3.64** The physical properties of  $[\text{Ru}(\text{Clazpy})_2(\text{L})]\text{Cl}_2 \cdot x\text{H}_2\text{O}$  complexes

(L = bpy, phen, azpy, Clazpy)

Complexes	Physical properties			
	Appearance	Color		Melting point (°C)
		solid	solution	
$[\text{Ru}(\text{Clazpy})_2(\text{bpy})]\text{Cl}_2 \cdot 7\text{H}_2\text{O}$	solid	dark red	dark red	186-187
$[\text{Ru}(\text{Clazpy})_2(\text{phen})]\text{Cl}_2 \cdot 8\text{H}_2\text{O}$	solid	dark red	dark red	188-189
$[\text{Ru}(\text{Clazpy})_2(\text{azpy})]\text{Cl}_2 \cdot 3\text{H}_2\text{O}$	solid	dark brown	light brown	185-186
$[\text{Ru}(\text{Clazpy})_3]\text{Cl}_2 \cdot 4\text{H}_2\text{O}$	solid	dark brown	light brown	186-187

The ruthenium(II) complexes are thermally stable and show no reactivity towards air or moisture, except for L are azpy and Clazpy, which are stable in the solid state but decompose slowly in solution after several days. The color of the complexes varied from dark-red to light-brown depending on L ligand.

The  $[\text{Ru}(\text{Clazpy})_2(\text{L})]\text{Cl}_2 \cdot x\text{H}_2\text{O}$  (L = bpy, phen, azpy, Clazpy) are soluble in polar organic solvents such as MeOH, EtOH,  $\text{CH}_3\text{CN}$ ,  $\text{H}_2\text{O}$  and are less soluble in  $\text{CH}_2\text{Cl}_2$  and acetone.

### 3.6.2 Characterization of $[\text{Ru}(\text{Clazpy})_2(\text{L})]\text{Cl}_2 \cdot x\text{H}_2\text{O}$ (L = bpy, phen, azpy, Clazpy)

The chemistry of  $[\text{Ru}(\text{Clazpy})_2(\text{L})]\text{Cl}_2 \cdot x\text{H}_2\text{O}$  (L = bpy, phen, azpy, Clazpy) complexes was characterized by elemental analysis, Mass spectrometry, Infrared spectroscopy, UV-Visible absorption spectroscopy, Nuclear Magnetic Resonance spectroscopy (1D and 2D NMR). The electrochemical properties of all complexes were studied by using cyclic voltammetric technique.

### 3.6.2.1 Elemental analysis

Elemental analysis was used to confirm composition of C, H, N in complexes. The results are given in Table 3.65.

**Table 3.65** Elemental analysis data of  $[\text{Ru}(\text{Clazpy})_2(\text{L})]\text{Cl}_2 \cdot x\text{H}_2\text{O}$  (L = bpy, phen, azpy, Clazpy)

Complexes	% C		% H		% N	
	Calc.	Found	Calc.	Found	Calc.	Found
$[\text{Ru}(\text{Clazpy})_2(\text{bpy})]\text{Cl}_2 \cdot 7\text{H}_2\text{O}$	43.21	43.54	4.31	4.03	12.60	12.43
$[\text{Ru}(\text{Clazpy})_2(\text{phen})]\text{Cl}_2 \cdot 8\text{H}_2\text{O}$	43.84	43.74	4.33	4.40	12.03	11.68
$[\text{Ru}(\text{Clazpy})_2(\text{azpy})]\text{Cl}_2 \cdot 4\text{H}_2\text{O}$	45.95	46.04	3.86	3.64	14.61	14.37
$[\text{Ru}(\text{Clazpy})_3]\text{Cl}_2 \cdot 3\text{H}_2\text{O}$	45.09	45.11	3.44	3.46	14.34	13.64

### 3.6.2.2 Electrospray (ES) mass spectrometry

The ES mass spectra of  $[\text{Ru}(\text{Clazpy})_2(\text{L})]\text{Cl}_2 \cdot x\text{H}_2\text{O}$  (L = bpy, phen, azpy, Clazpy) complexes are displayed in Figure 3.140 to 3.143. The important ES mass data of complexes with the corresponding relative abundance are listed in Table 3.66.

**Table 3.66** ES mass spectrometric data of  $[\text{Ru}(\text{Clazpy})_2(\text{L})]\text{Cl}_2 \cdot x\text{H}_2\text{O}$  (L = bpy, phen, azpy, Clazpy)

m/z	Stoichiometry	Rel. Abun. (%)
$[\text{Ru}(\text{Clazpy})_2(\text{bpy})]\text{Cl}_2 \cdot 7\text{H}_2\text{O}$		
692.05	$[\text{M}-2\text{Cl}-7\text{H}_2\text{O}-\text{H}^+]^+$	85
346.02	$[\text{M}-2\text{Cl}-7\text{H}_2\text{O}]^{2+}$	100
$[\text{Ru}(\text{Clazpy})_2(\text{phen})]\text{Cl}_2 \cdot 8\text{H}_2\text{O}$		
716.0542	$[\text{M}-2\text{Cl}-8\text{H}_2\text{O}-\text{H}^+]^+$	25
358.02	$[\text{M}-2\text{Cl}-8\text{H}_2\text{O}]^{2+}$	100
$[\text{Ru}(\text{Clazpy})_2(\text{azpy})]\text{Cl}_2 \cdot 4\text{H}_2\text{O}$		
719.06	$[\text{M}-2\text{Cl}-4\text{H}_2\text{O}-\text{H}^+]^+$	60
359.53	$[\text{M}-2\text{Cl}-4\text{H}_2\text{O}]^{2+}$	100
$[\text{Ru}(\text{Clazpy})_3]\text{Cl}_2 \cdot 3\text{H}_2\text{O}$		
755.02	$[\text{M}-2\text{Cl}-3\text{H}_2\text{O}-\text{H}^+]^+$	30
377.51	$[\text{M}-2\text{Cl}-3\text{H}_2\text{O}]^{2+}$	100

M = molecular weight (MW) of each complexes

MW of  $[\text{Ru}(\text{Clazpy})_2(\text{bpy})]\text{Cl}_2 \cdot 5\text{H}_2\text{O} = 889.58$  g/mol

MW of  $[\text{Ru}(\text{Clazpy})_2(\text{phen})]\text{Cl}_2 \cdot 3\text{H}_2\text{O} = 931.62$  g/mol

MW of  $[\text{Ru}(\text{Clazpy})_2(\text{azpy})]\text{Cl}_2 \cdot \text{H}_2\text{O} = 862.56$  g/mol

MW of  $[\text{Ru}(\text{Clazpy})_3]\text{Cl}_2 \cdot 5\text{H}_2\text{O} = 878.99$  g/mol

In all the cases, the loss of chlorine ions was detected with 100% relative abundance of the parent peak. So, expected structures were confirmed by this technique.

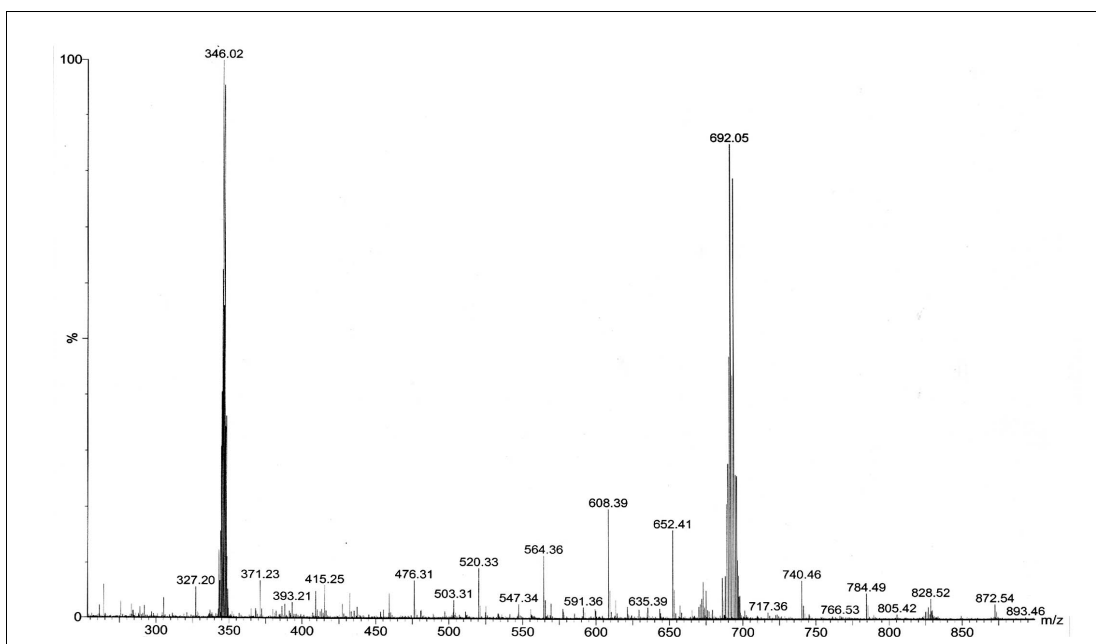


**Figure 3.140** ES mass spectrum of  $[\text{Ru}(\text{Clazpy})_2(\text{bpy})]\text{Cl}_2 \cdot 7\text{H}_2\text{O}$

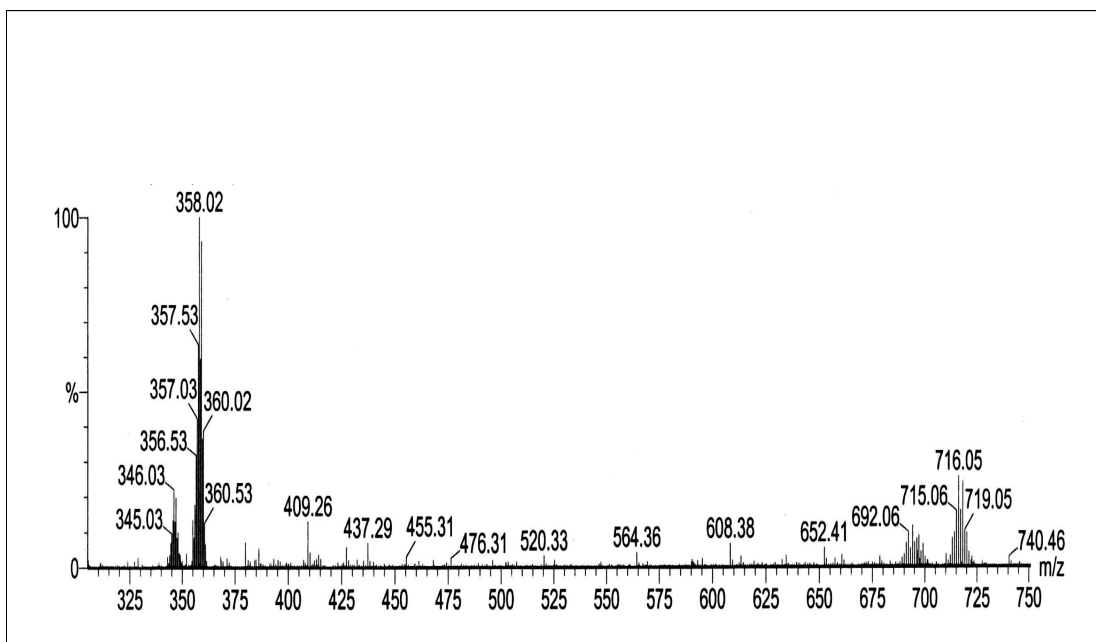


**Figure 3.141** ES mass spectrum of  $[\text{Ru}(\text{Clazpy})_2(\text{phen})]\text{Cl}_2 \cdot 8\text{H}_2\text{O}$

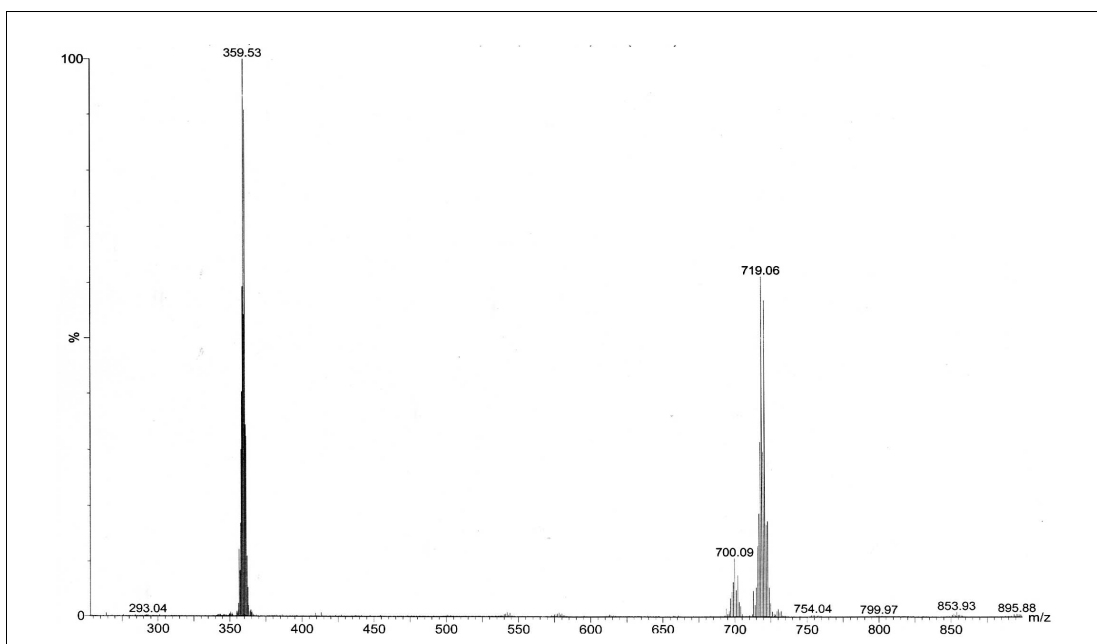


**Figure 3.142** ES mass spectrum of  $[\text{Ru}(\text{Clazpy})_2(\text{azpy})]\text{Cl}_2 \cdot 4\text{H}_2\text{O}$

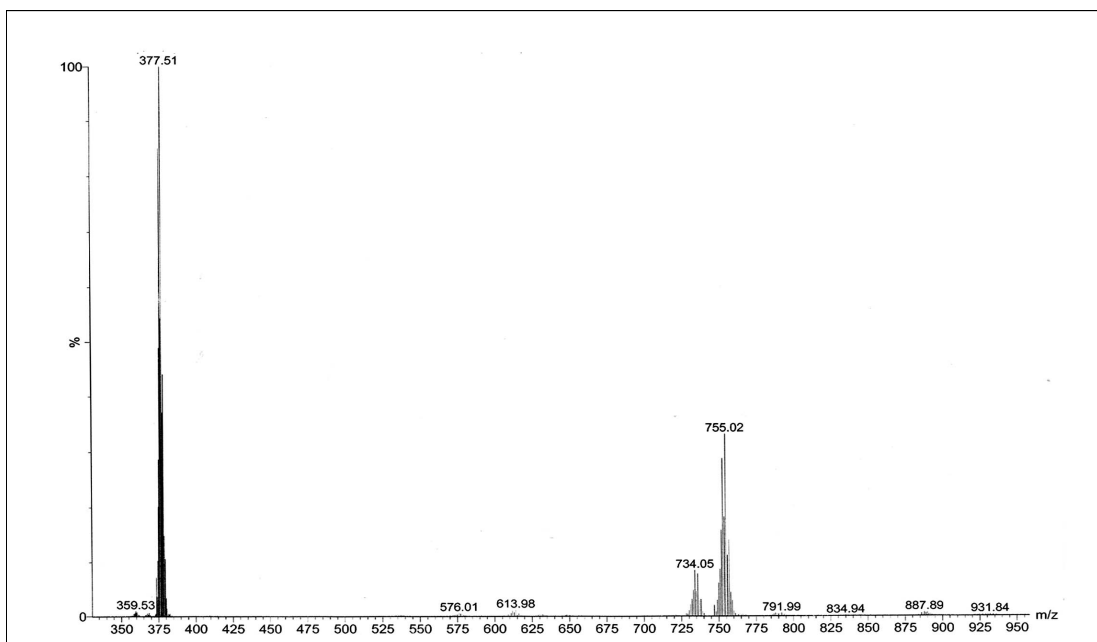


**Figure 3.143** ES mass spectrum of  $[\text{Ru}(\text{Clazpy})_3]\text{Cl}_2 \cdot 3\text{H}_2\text{O}$

### 3.6.2.3 Infrared spectroscopy

The vibrational spectra of  $[\text{Ru}(\text{Clazpy})_2(\text{L})]\text{Cl}_2 \cdot x\text{H}_2\text{O}$  (L = bpy, phen, azpy, Clazpy) complexes were recorded in 4000-400  $\text{cm}^{-1}$ . They showed many vibration frequencies such as C=C, C=N, N=N (azo), C-H bending of monosubstituted benzene and C-Cl in this range. The infrared spectroscopic data of these complexes are given in Table 3.67 and these spectra are shown in Figure 3.144 to 3.147.

**Table 3.67** IR data of  $[\text{Ru}(\text{Clazpy})_2(\text{L})]\text{Cl}_2 \cdot x\text{H}_2\text{O}$  (L = bpy, phen, azpy, Clazpy)

Vibrational frequencies	Wave number ( $\text{cm}^{-1}$ ) [ $\text{Ru}(\text{Clazpy})_2(\text{L})]\text{Cl}_2 \cdot x\text{H}_2\text{O}$ (L = ligands)			
	bpy	phen	azpy	Clazpy
C=N stretching and C=C stretching	1615(m)	1587(m)	1587(m)	1584(m)
	1548(m)	1546(m)	1548(s)	1548(s)
	1450(s)	1452(m)	1451(s)	1457(s)
		1429(m)		
N=N(azo) stretching	1339(s)	1336(s)	1364(s)	1368(s) 1351(s)
C-N stretching	1120(s)	1120(s)	1120(s)	1120(s)
C-H out of plane bend in monosub. benzene	772(s)	773(m)	768(s)	774(s)
	736(m)	723(m)	737(s)	738(s)
	694(m)	694(m)	691(s)	693(s)
C-Cl	576(s)	578(s)	570(s)	560(s)

s = strong, m = medium

Infrared spectra of the complexes exhibited sharp intense bands at 3400-3420  $\text{cm}^{-1}$  and supported the presence of water in the molecule (Nakamoto, 1986). Moreover, IR spectra showed many vibrations of different intensities below 1600  $\text{cm}^{-1}$ . The N=N bands of these complexes where L were bpy and phen exhibited around 1336-1339  $\text{cm}^{-1}$  which was shifted to lower frequencies than that of the free ligand (1360  $\text{cm}^{-1}$ ). The red shift may result from better  $\pi$ -backbonding,  $t_{2g} \rightarrow \pi^*(\text{azo})$  in these complexes. Meanwhile, where L were azpy and Clazpy, this vibrational frequency appeared around the same position of the free ligand. This result

may be due to the competition of three azoimine ligand in molecule. In addition, a strong vibration around  $840\pm 2\text{ cm}^{-1}$  ( $\square_{\text{P-F}}$ ) observing in  $[\text{Ru}(\text{Clazpy})_2(\text{L})](\text{PF}_2)_6$  were not observed in  $[\text{Ru}(\text{Clazpy})_2(\text{L})]\text{Cl}_2 \cdot x\text{H}_2\text{O}$ .

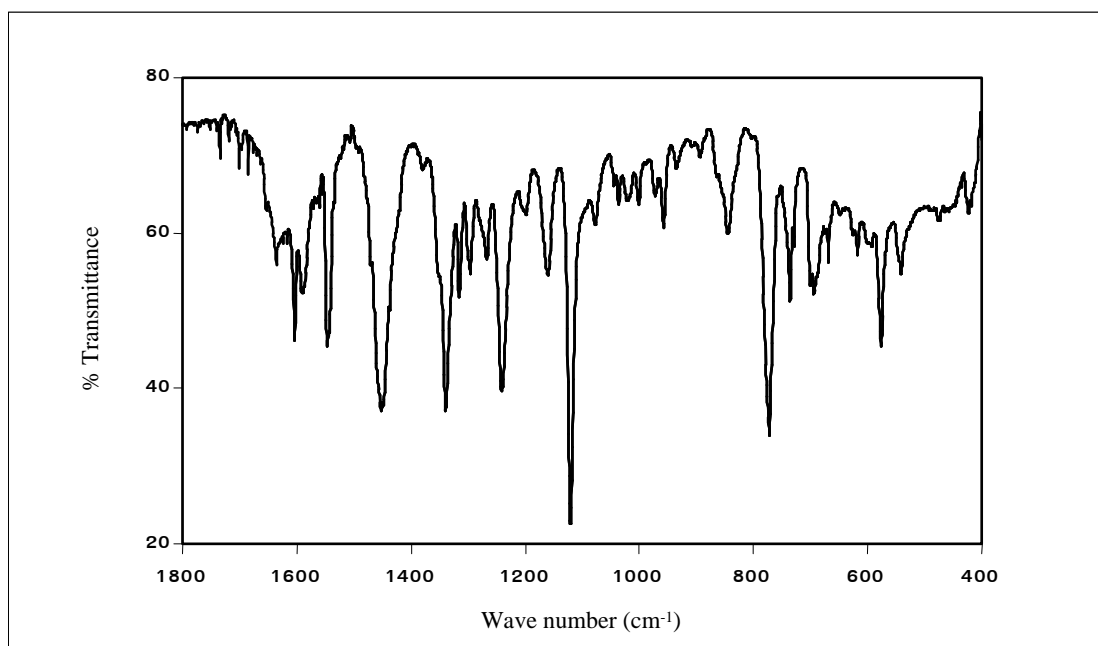


**Figure 3.144** IR spectrum of  $[\text{Ru}(\text{Clazpy})_2(\text{bpy})]\text{Cl}_2 \cdot 7\text{H}_2\text{O}$

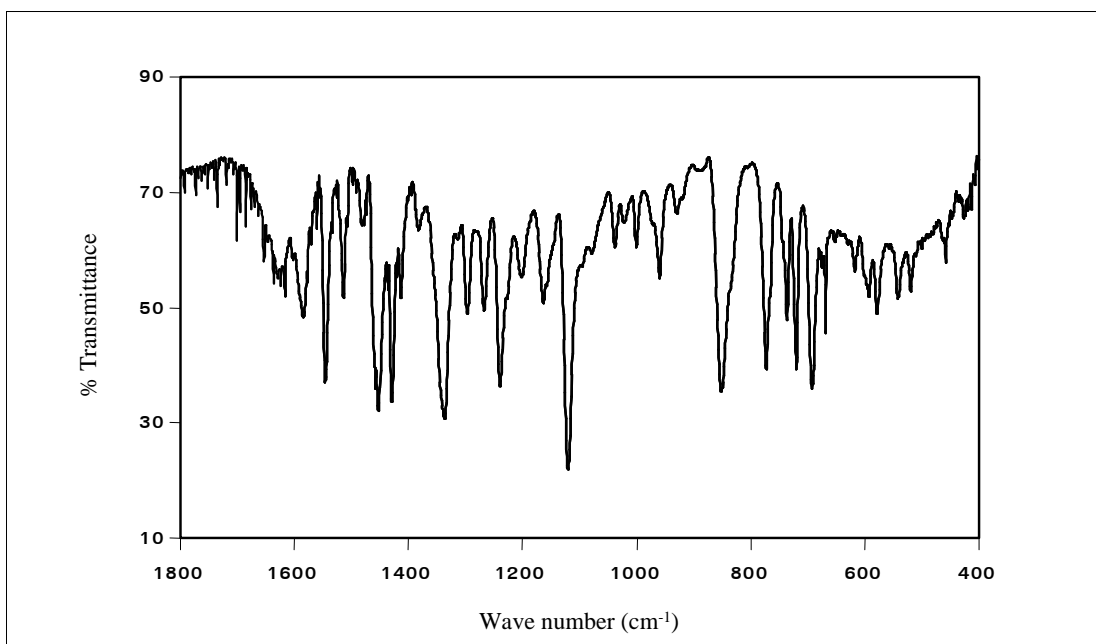


**Figure 3.145** IR spectrum of  $[\text{Ru}(\text{Clazpy})_2(\text{phen})]\text{Cl}_2 \cdot 8\text{H}_2\text{O}$

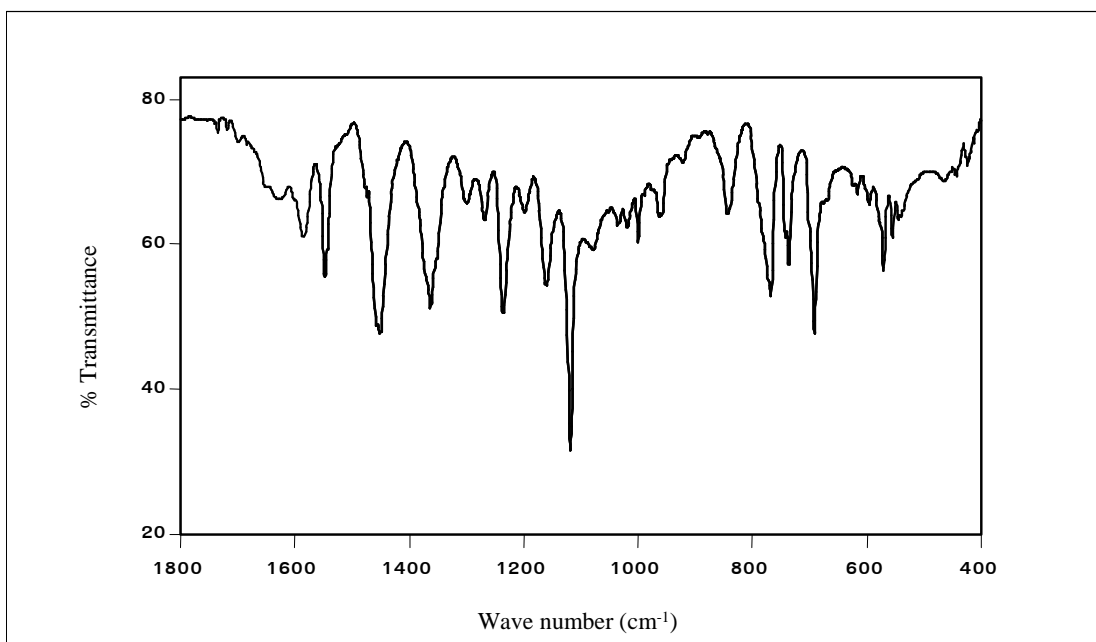


**Figure 3.146** IR spectrum of  $[\text{Ru}(\text{Clazpy})_2(\text{azpy})]\text{Cl}_2 \cdot 4\text{H}_2\text{O}$

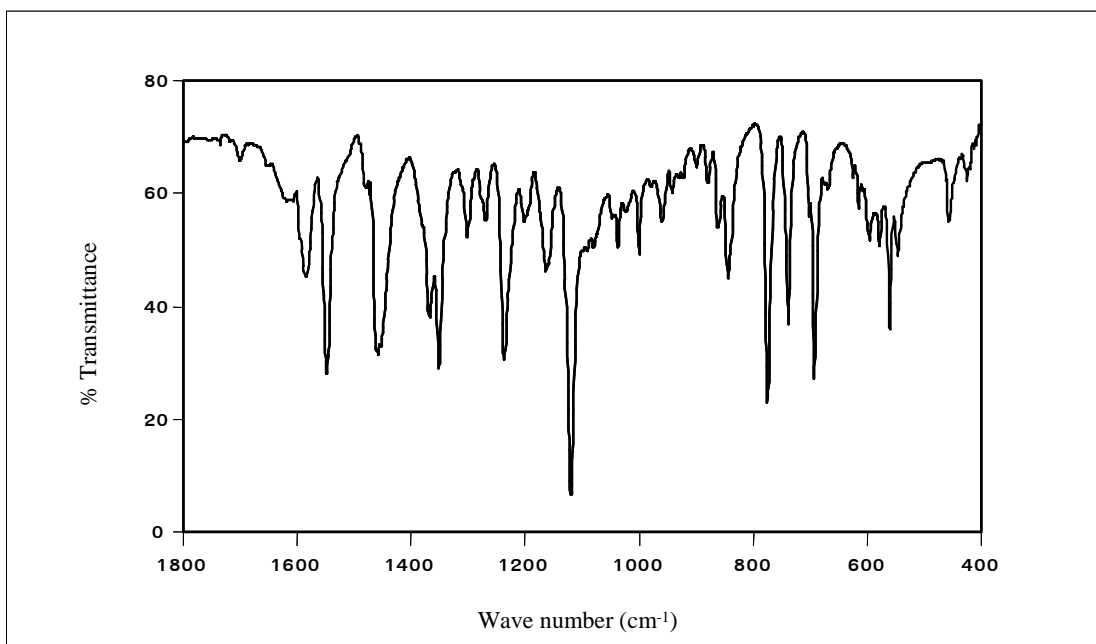


**Figure 3.147** IR spectrum of  $[\text{Ru}(\text{Clazpy})_3]\text{Cl}_2 \cdot 3\text{H}_2\text{O}$

#### 3.6.2.4 UV-Visible absorption spectroscopy

The optical absorption spectra of  $[\text{Ru}(\text{Clazpy})_2(\text{L})]\text{Cl}_2 \cdot x\text{H}_2\text{O}$  complexes were recorded in eight solvents;  $\text{CH}_2\text{Cl}_2$ , DMF, DMSO,  $\text{CH}_3\text{OCH}_3$ ,  $\text{CH}_3\text{CN}$ , EtOH, MeOH, and  $\text{H}_2\text{O}$  in 200-800 nm range. Electronic spectra of this complex in  $\text{CH}_3\text{CN}$  solution are shown in Figure 3.148 to 3.151 and absorption spectroscopic data are listed in Table 3.68-3.69.

**Table 3.68** UV-Visible absorption spectroscopic data of  $[\text{Ru}(\text{Clazpy})_2(\text{L})]\text{Cl}_2 \cdot x\text{H}_2\text{O}$   
(L = bpy, phen)

Solvents	$\lambda_{\text{max}}$ , nm ( $\epsilon^{\text{a}}$ x $10^{-4}$ M $^{-1}$ cm $^{-1}$ )	
	$[\text{Ru}(\text{Clazpy})_2(\text{bpy})]\text{Cl}_2 \cdot 7\text{H}_2\text{O}$	$[\text{Ru}(\text{Clazpy})_2(\text{phen})]\text{Cl}_2 \cdot 8\text{H}_2\text{O}$
CH <sub>2</sub> Cl <sub>2</sub>	232(2.5) 275(2.1)	232(4.4) 256(3.8)
	320(2.3) 388(2.3) 525(1.0)	385(2.9) 522(1.4)
DMF	286(2.2) 382(1.8)	272(3.1) 381(2.2)
	528(0.9)	528(1.1)
DMSO	321(2.4) 381(2.0)	263(2.5) 283(2.6)
	526(0.9)	380(2.1) 526(0.9)
CH <sub>3</sub> OCH <sub>3</sub>	338(1.7) 521(0.8)	337(2.2) 521(1.1)
CH <sub>3</sub> CN	285(2.3) 316(2.4)	225(4.9) 258(3.7)
	380(2.3) 520(0.9)	274(3.7) 378(2.8) 520(1.2)
EtOH	207(4.3) 285(2.6)	206(5.5) 225(5.2)
	317(2.6) 383(2.6) 520(1.1)	259(3.6) 275(3.4) 381(3.0)
MeOH	207(4.2) 286(2.4)	204(5.5) 223(4.9) 259(3.3)
	316(2.5) 382(2.6) 520(1.0)	275(3.1) 380(2.8) 520(1.2)
Water	285(2.2) 382(2.3)	225(4.4) 257(3.0)
	314(2.2) 520(0.9)	274(2.8) 381(2.6) 520(1.1)

<sup>a</sup> Molar extinction coefficient

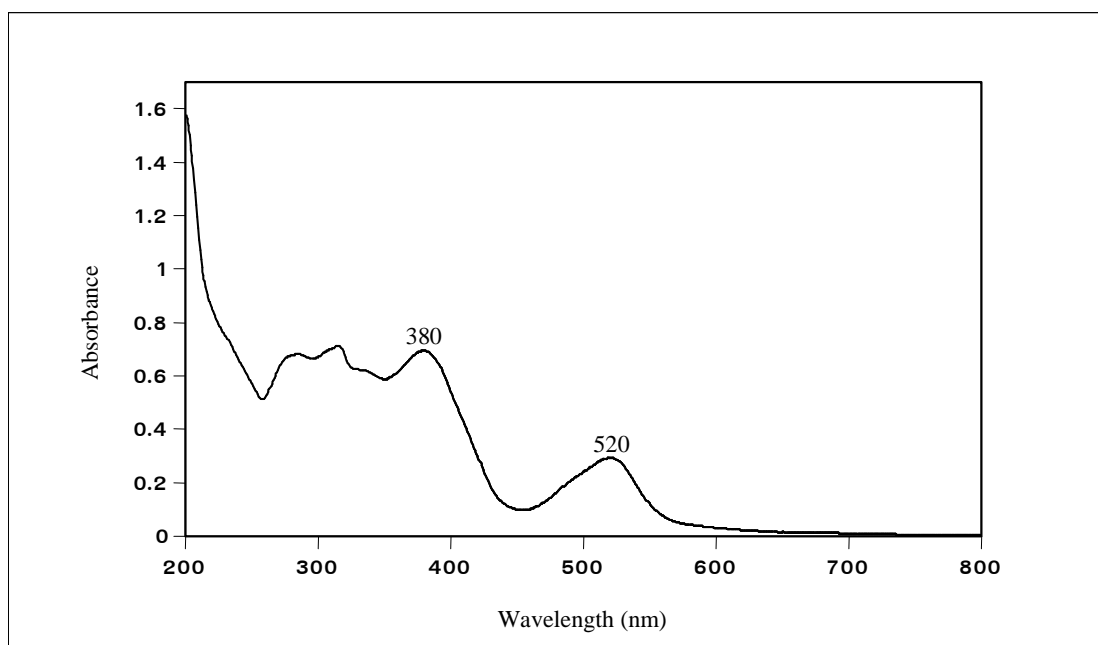
**Table 3.69** UV-Visible absorption spectroscopic data of  $[\text{Ru}(\text{Clazpy})_2(\text{L})]\text{Cl}_2 \cdot x\text{H}_2\text{O}$   
(L = azpy, Clazpy)

Solvents	$\lambda_{\text{max}}$ , nm ( $\epsilon^{\text{a}}$ x $10^{-4}$ M <sup>-1</sup> cm <sup>-1</sup> )	
	$[\text{Ru}(\text{Clazpy})_2(\text{azpy})]\text{Cl}_2 \cdot 4\text{H}_2\text{O}$	$[\text{Ru}(\text{Clazpy})_3]\text{Cl}_2 \cdot 3\text{H}_2\text{O}$
CH <sub>2</sub> Cl <sub>2</sub>	232(3.1) 386(3.6) 504(1.2)	232(3.6) 386(4.0) 502(1.2)
DMF	281(2.2) 371(2.7) 514(1.5)	282(3.6) 378(4.1) 514(2.1)
DMSO	285(2.5) 332(2.6) 382(3.3) 503(1.4)	288(3.1) 327(3.4) 383(4.6) 501(1.6)
acetone	378(4.0) 5.2(1.3)	379(4.0) 498(1.3)
CH <sub>3</sub> CN	287(2.4) 330(2.9) 380(4.2) 498(1.4)	294(2.5) 326(3.0) 382(4.7) 494(1.5)
EtOH	206(4.2) 287(2.2) 329(2.7) 380(3.9) 498(1.3)	205(5.5) 327(2.9) 382(4.5) 494(1.4)
MeOH	206(5.1) 286(2.1) 330(2.6) 381(3.8) 496(1.2)	206(7.9) 327(4.2) 383(6.5) 492(2.0)
Water	285(2.3) 328(2.7) 383(4.0) 492(1.3)	287(2.1) 325(2.5) 385(3.9) 491(1.3)

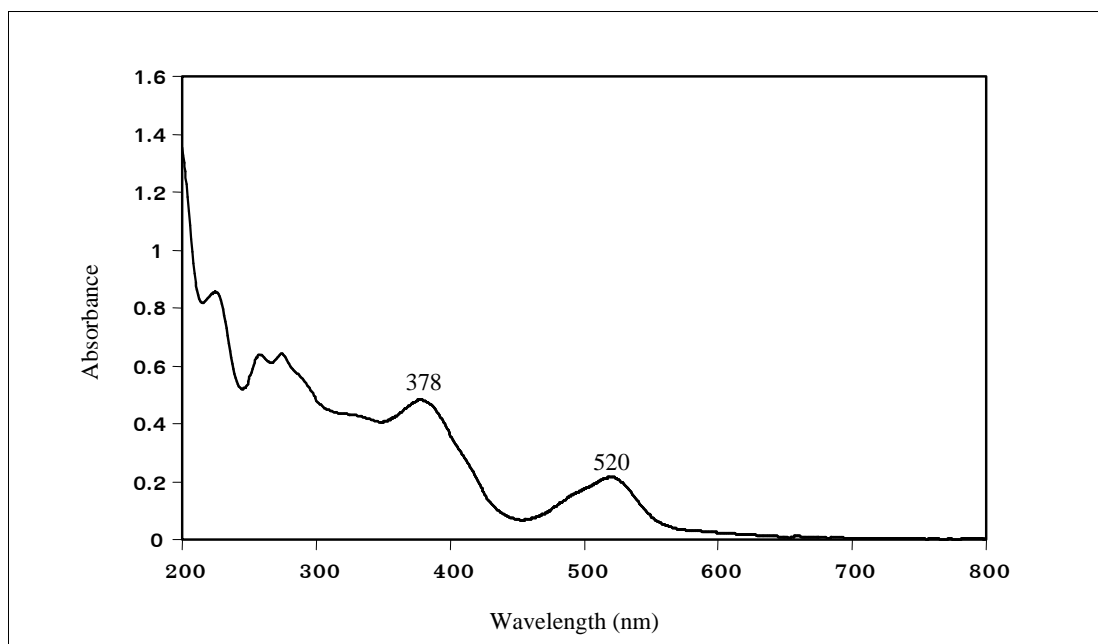
<sup>a</sup> Molar extinction coefficient

In generally, the electronic transitions in ruthenium(II) tris-chelate complexes can be classified as metal centered (d-d), ligand centered ( $\pi \rightarrow \pi^*$ ) and metal-to-ligand charge transfer (Yang *et al.*, 2001). In this work, the complexes exhibited multiple transitions in this region. Multiple transitions in mixed-ligand complexes may result from the lower symmetry splitting of the metal dominated molecular orbitals. The weak band at longer wavelength,  $497 \pm 7$  nm, may be associated with a spin forbidden transition in spin-orbit coupled states of ruthenium 4d orbitals (Byabartta *et al.*, 2003). All complexes displayed absorption spectra in

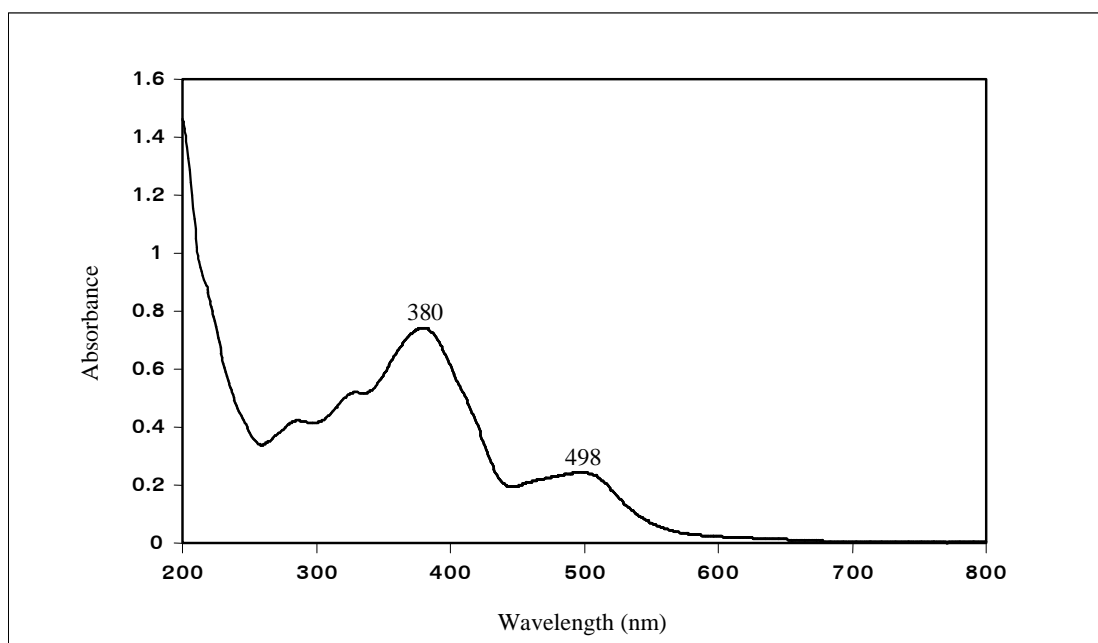
UV-Visible region (200-800 nm) which were assigned to  $\pi \rightarrow \pi^*$  transitions of ligands ( $\epsilon \sim 22000 - 45000 \text{ M}^{-1}\text{cm}^{-1}$ ) and metal-to-ligand charge transfer (MLCT) transitions ( $\epsilon \sim 12000 - 20000 \text{ M}^{-1}\text{cm}^{-1}$ ). In addition, the lowest energy absorption band of  $[\text{Ru}(\text{Clazpy})_2(\text{L})]\text{Cl}_2 \cdot x\text{H}_2\text{O}$  ( $\text{L} = \text{bpy}, \text{phen}, \text{azpy}, \text{Clazpy}$ ) were not shifted when the polarity of solvents was increased.



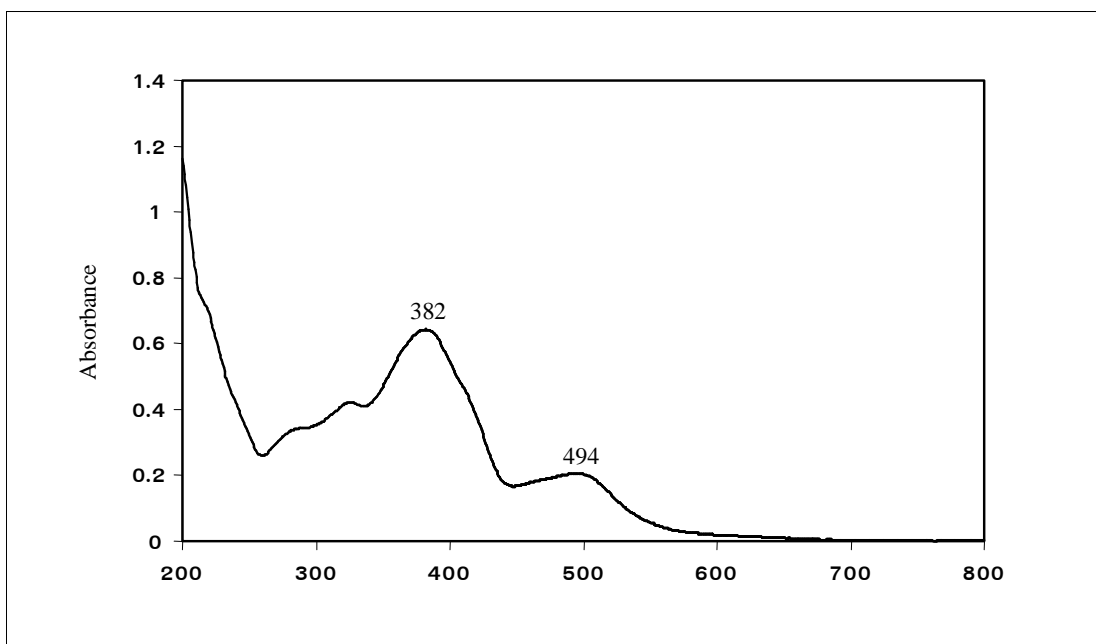
**Figure 3.148** UV-Visible absorption spectrum of  $[\text{Ru}(\text{Clazpy})_2(\text{bpy})]\text{Cl}_2 \cdot 7\text{H}_2\text{O}$  in  $\text{CH}_3\text{CN}$



**Figure 3.149** UV-Visible absorption spectrum of [Ru(Clazpy)<sub>2</sub>(phen)]Cl<sub>2</sub>·8H<sub>2</sub>O in CH<sub>3</sub>CN



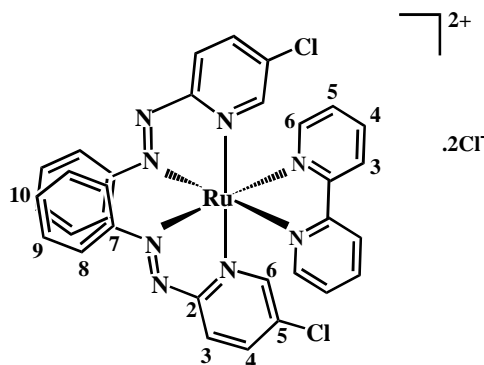
**Figure 3.150** UV-Visible absorption spectrum of [Ru(Clazpy)<sub>2</sub>(azpy)]Cl<sub>2</sub>·4H<sub>2</sub>O in CH<sub>3</sub>CN



**Figure 3.151** UV-Visible absorption spectrum of  $[\text{Ru}(\text{Clazpy})_3]\text{Cl}_2 \cdot 3\text{H}_2\text{O}$  in  $\text{CH}_3\text{CN}$

### 3.6.2.5 Nuclear magnetic resonance spectroscopy

The NMR spectra of  $[\text{Ru}(\text{Clazpy})_2(\text{L})]\text{Cl}_2 \cdot x\text{H}_2\text{O}$  ( $\text{L} = \text{bpy}, \text{phen}, \text{azpy}, \text{Clazpy}$ ) was prepared in methanol- $d_4$  and tetramethylsilane ( $\text{Si}(\text{CH}_3)_4$ ) was used as an internal reference. Their structures were confirmed by using 1D and 2D NMR spectroscopic techniques ( $^1\text{H}$  NMR,  $^1\text{H}$ - $^1\text{H}$  COSY NMR,  $^{13}\text{C}$  NMR, DEPT NMR and  $^1\text{H}$ - $^{13}\text{C}$  HMQC NMR). The signals were assigned on the basis of spin-spin interaction, and comparative integration between aliphatic and aromatic regions. The structure and stereochemistry of these complexes were established by  $^1\text{H}$  NMR spectral data on comparison with the spectra of parent complex, *ctc*- $[\text{Ru}(\text{Clazpy})_2\text{Cl}_2]$ . The NMR spectroscopic data of complexes are presented in Table 3.70 to 3.73.

Nuclear magnetic resonance spectroscopy of  $[\text{Ru}(\text{Clazpy})_2(\text{bpy})]\text{Cl}_2 \cdot 7\text{H}_2\text{O}$ **Table 3.70**  $^1\text{H}$ - $^{13}\text{C}$  NMR spectroscopic data of  $[\text{Ru}(\text{Clazpy})_2(\text{bpy})]\text{Cl}_2 \cdot 7\text{H}_2\text{O}$ 

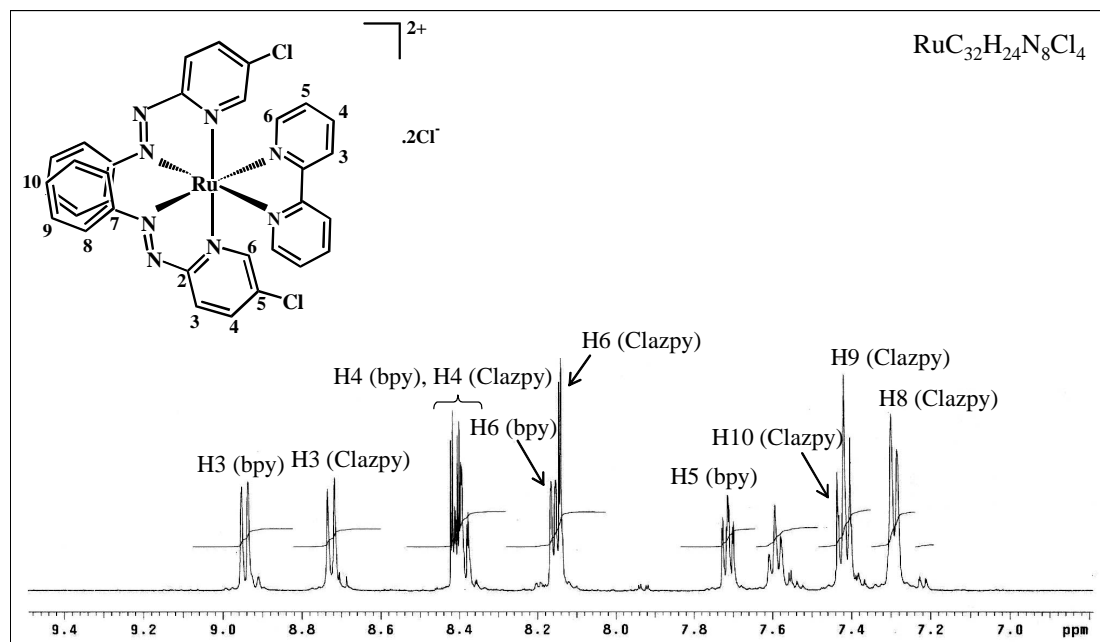
H-position	$^1\text{H}$ NMR			$^{13}\text{C}$ NMR (CH-type)
	$\delta$ (ppm)	$J$ (Hz)	Amount of H	
3 (bpy)	8.84 (d)	8.5, 1.0	1	126.96
3 (Clazpy)	8.73 (d)	8.0	1	131.69
4 (bpy)	8.41 (ddd)	5.5, 1.5	1	142.39
4 (Clazpy)	8.39 (dd)	8.0, 2.0	1	142.10
6 (bpy)	8.16 (dd)	5.5, 1.0	1	150.10
6 (Clazpy)	8.14 (d)	2.0	1	154.80
5 (bpy)	7.71 (dt)	5.5, 1.0	1	130.34
10 (Clazpy)	7.60 (t)	8.0	1	134.73
9 (Clazpy)	7.42 (dt)	8.0, 1.5	2	130.85
8 (Clazpy)	7.29 (d)	8.0	2	123.85
Quaternary carbons (C)				164.78, 156.46, 154.52, 138.94

d = doublet, dd = doublet of doublet, ddd = doublet of doublet of doublet,

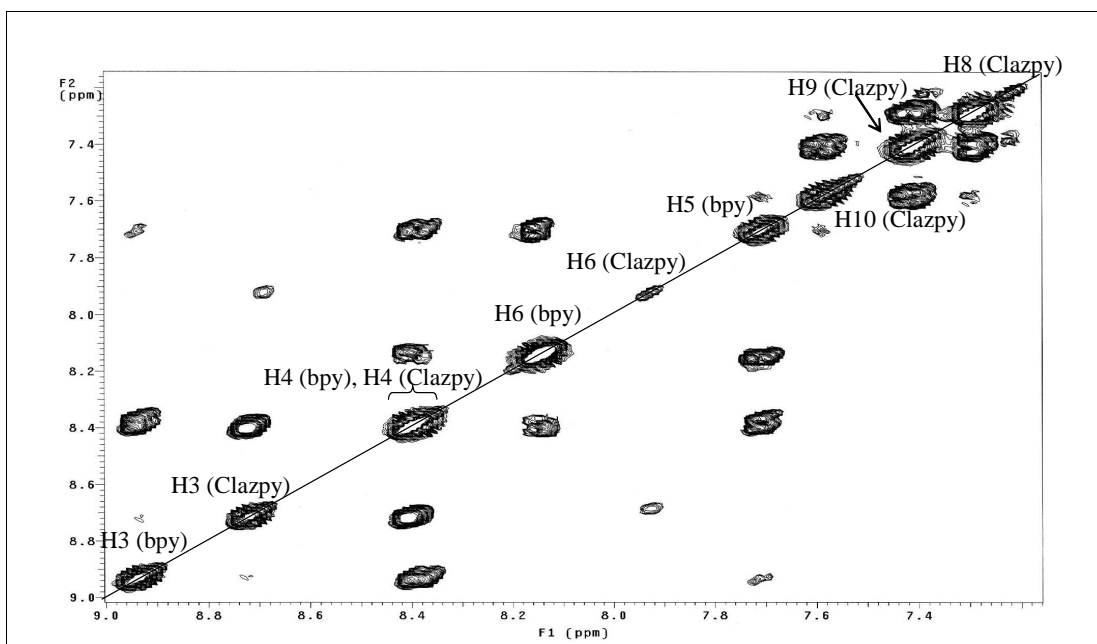
dt = doublet of triplet, t = triplet

The  $^1\text{H}$  NMR spectrum (Figure 3.152) of  $[\text{Ru}(\text{Clazpy})_2(\text{bpy})]\text{Cl}_2 \cdot 7\text{H}_2\text{O}$  complex displayed only one set of proton of each ligands (Clazpy and bpy) with 10 resonances of 24 protons, six signals from Clazpy ligand and four signals from bpy ligand. This result indicated that both Clazpy ligands were equivalent. A chemical shift of proton H3 on bpy ligand occurred at the lowest field (8.94 ppm) due to trans effect of pyridine of bpy to N=N azo of Clazpy. In addition, other protons in this compound were also studied by using simple correlation  $^1\text{H}$ - $^1\text{H}$  COSY NMR spectroscopy (Figure 3.153).

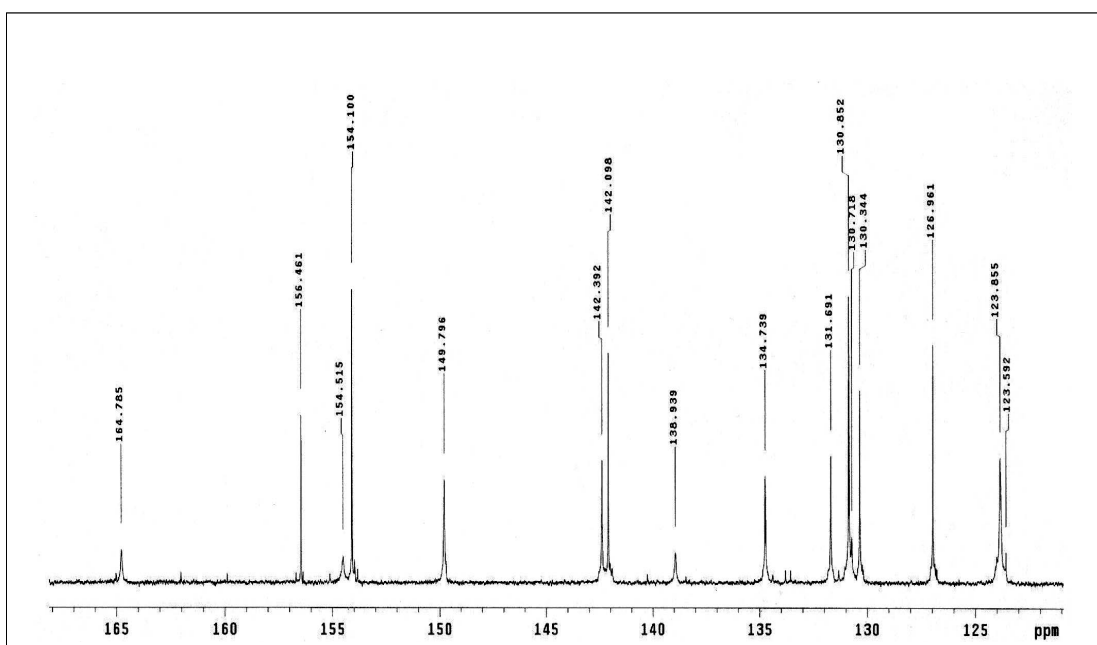
The  $^{13}\text{C}$  NMR (Figure 3.154) results corresponded to the DEPT NMR (Figure 3.155) which showed only one kind of methane carbons. The downfield signals at 156.00 ppm belonged to C2 of bpy. The signals at 164.78, 156.46, 154.52 and 138.94 ppm were assigned to two quaternary carbons C2, C5 and C7 of Clazpy ligand and bpy, respectively. Moreover, the others  $^{13}\text{C}$  NMR signal assignments were based on  $^1\text{H}$ - $^{13}\text{C}$  HMQC NMR spectrum (Figure 3.156).



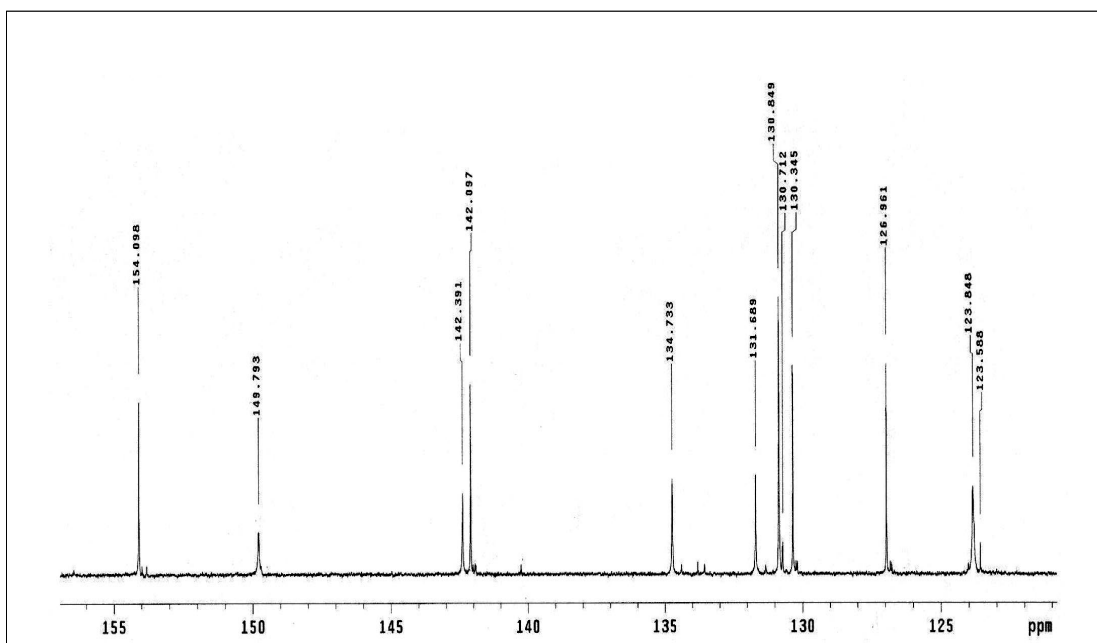
**Figure 3.152**  $^1\text{H}$  NMR spectrum of  $[\text{Ru}(\text{Clazpy})_2(\text{bpy})]\text{Cl}_2 \cdot 7\text{H}_2\text{O}$  in methanol- $d_4$



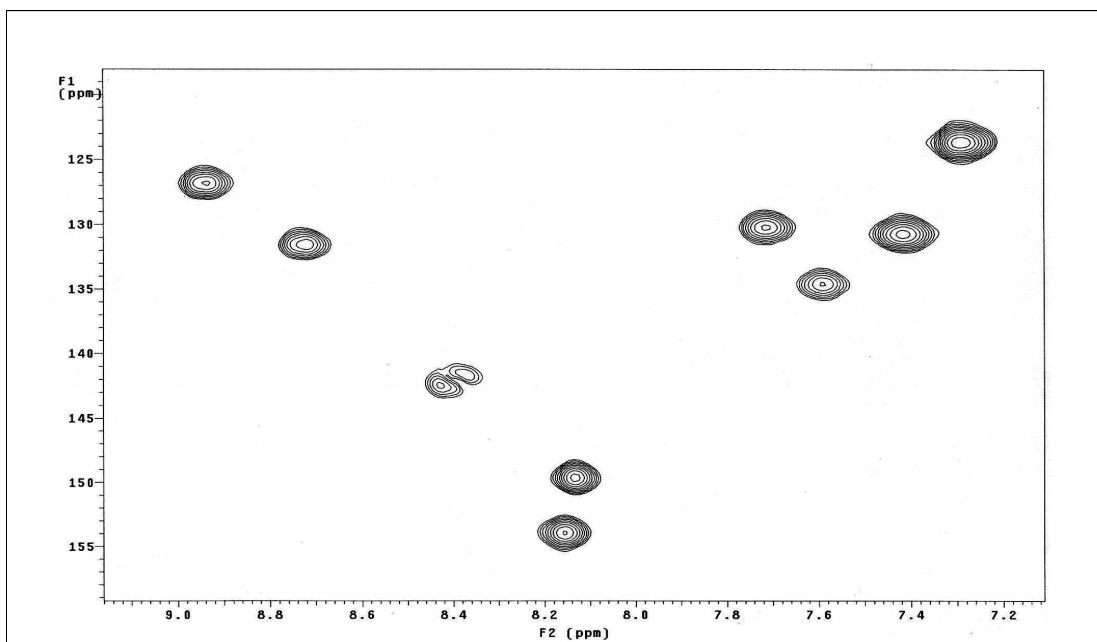
**Figure 3.153**  $^1\text{H}$ - $^1\text{H}$  COSY NMR spectrum of  $[\text{Ru}(\text{Clazpy})_2(\text{bpy})]\text{Cl}_2 \cdot 7\text{H}_2\text{O}$  methanol- $d_4$



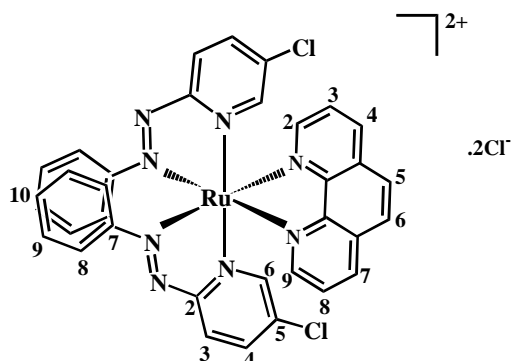
**Figure 3.154**  $^{13}\text{C}$  NMR spectrum of  $[\text{Ru}(\text{Clazpy})_2(\text{bpy})]\text{Cl}_2 \cdot 7\text{H}_2\text{O}$  in methanol- $d_4$



**Figure 3.155** DEPT NMR spectrum of  $[\text{Ru}(\text{Clazpy})_2(\text{bpy})]\text{Cl}_2 \cdot 7\text{H}_2\text{O}$  in methanol- $d_4$



**Figure 3.156**  $^1\text{H}$ - $^{13}\text{C}$  HMQC NMR spectrum of  $[\text{Ru}(\text{Clazpy})_2(\text{bpy})]\text{Cl}_2 \cdot 7\text{H}_2\text{O}$  in methano- $d_4$

Nuclear magnetic resonance spectroscopy of  $[\text{Ru}(\text{Clazpy})_2(\text{phen})]\text{Cl}_2 \cdot 8\text{H}_2\text{O}$ **Table 3.71**  $^1\text{H}$  and  $^{13}\text{C}$  NMR spectroscopic data of  $[\text{Ru}(\text{Clazpy})_2(\text{phen})]\text{Cl}_2 \cdot 8\text{H}_2\text{O}$ 

H-position	$^1\text{H}$ NMR			$^{13}\text{C}$ NMR (CH-type)
	$\delta$ (ppm)	$J$ (Hz)	Amount of H	
4,7 (phen)	8.93 (d)	8.5	1	141.09
3 (Clazpy)	8.72 (d)	9.0	1	131.65
2,9 (phen)	8.59 (d)	5.0	1	154.98
5,6 (phen)	8.42	-	1	129.73
4 (Clazpy)	8.30 (dd)	9.0, 2.0	1	142.18
3,8 (phen)	8.00 (dd)	8.5, 5.5	1	128.42
6 (Clazpy)	7.92 (d)	2.0	1	150.18
10 (Clazpy)	7.58 (t)	8.0	1	134.52
9 (Clazpy)	7.43 (t)	8.0	2	130.87
8 (Clazpy)	7.36 (d)	8.0	2	123.85
Quaternary carbons (C)				164.80, 146.75, 138.80, 133.22, 154.98

S = singlet, d = doublet, dd = doublet of doublet, t = triplet

The  $^1\text{H}$  NMR spectrum (Figure 3.157) of  $[\text{Ru}(\text{Clazpy})_2(\text{phen})]\text{Cl}_2 \cdot 8\text{H}_2\text{O}$  complex showed one set of each ligands (Clazpy and phen). They displayed 10 resonances of 24 protons, eight from Clazpy ligand and four from phen ligand. This make molecule has  $\text{C}_2$  symmetry. The proton H4, H7 of bpy occurred at the lowest field due to its position are trans to  $\text{N}=\text{N}$  azo function. The 2D COSY NMR (Figure 3.158) connectivities result in the assignment of other protons. Results from  $^1\text{H}$ - $^1\text{H}$  ROESY NMR (Figure 3.160) showed interaction through space between some proton on the bipyridine rings of phen and the groups of Clazpy especially H3, H8 of phen and H8 of Clazpy. Moreover, the long-range coupling of proton by  $^1\text{H}$ - $^1\text{H}$  TOCSY NMR (Figure 3.159) supported that result as well.

The  $^{13}\text{C}$  NMR (Figure 3.161) results corresponded to the DEPT NMR (Figure 3.162) which showed only one kind of methane carbons. All quaternary carbons at 164.80, 146.75, 138.80, 133.22, 154.98 belonged to C2, C5, C7 of Clazpy and C10, C11, C12, C13 of phen. Moreover, the othres  $^{13}\text{C}$  NMR signals assignments were based on  $^1\text{H}$ - $^{13}\text{C}$  HSQC NMR spectrum (Figure 3.163) and the long-range coupling of carbon-proton was determined by  $^1\text{H}$ - $^{13}\text{C}$  HMBC NMR spectrum (Figure 3.164).

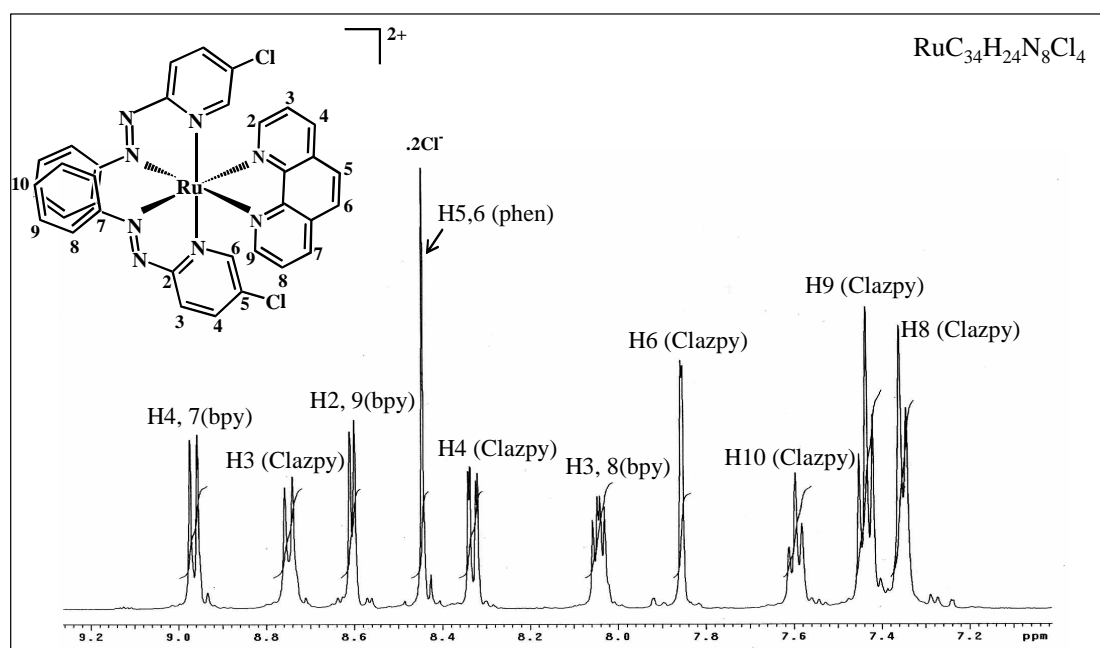


**Figure 3.157**  $^1\text{H}$  NMR spectrum of  $[\text{Ru}(\text{Clazpy})_2(\text{phen})]\text{Cl}_2 \cdot 8\text{H}_2\text{O}$  in methanol- $d_4$

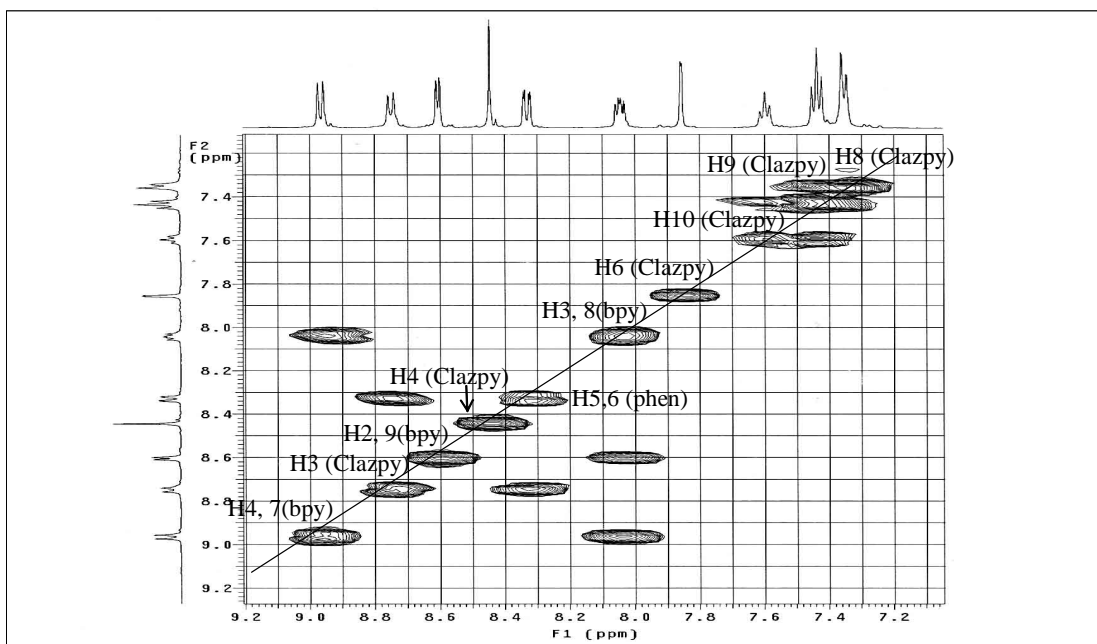


**Figure 3.158** <sup>1</sup>H-<sup>1</sup>H COSY NMR spectrum of [Ru(Clazpy)<sub>2</sub>(phen)]Cl<sub>2</sub>·8H<sub>2</sub>O in methanol-*d*<sub>4</sub>

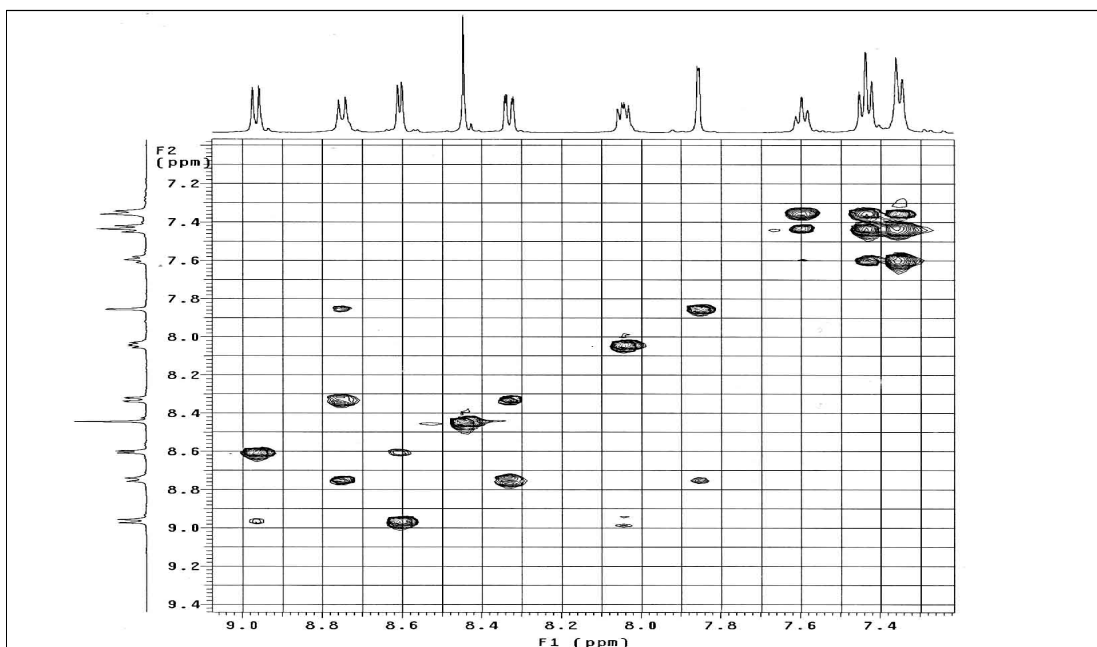


**Figure 3.159** <sup>1</sup>H-<sup>1</sup>H TOCSY NMR spectrum of [Ru(Clazpy)<sub>2</sub>(phen)]Cl<sub>2</sub>·8H<sub>2</sub>O in methanol-*d*<sub>4</sub>

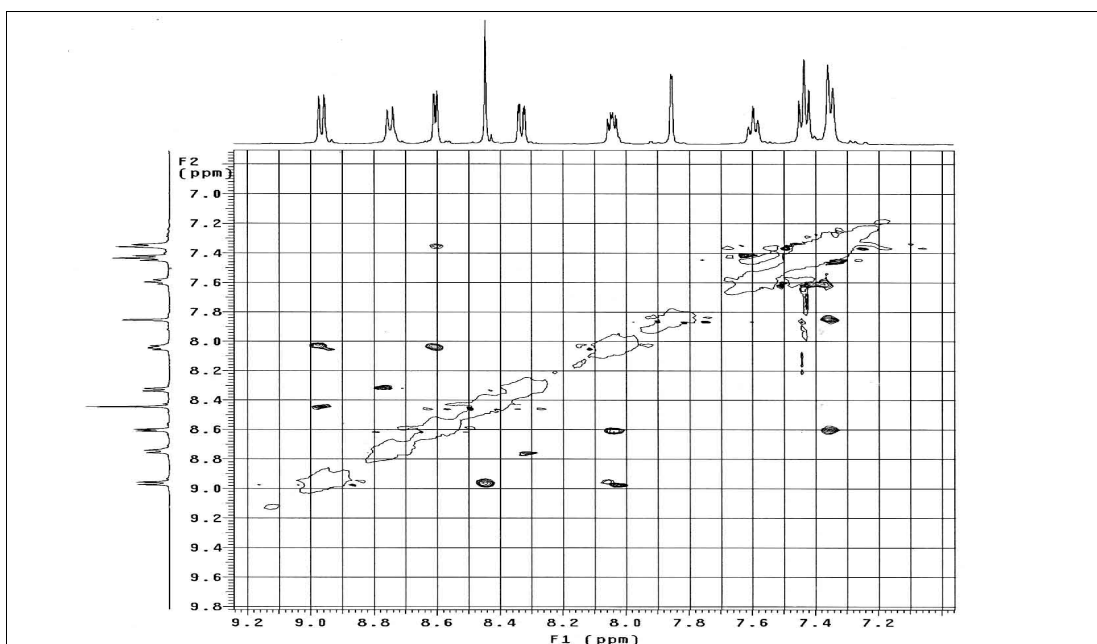


**Figure 3.160**  $^1\text{H}$ - $^1\text{H}$  ROESY NMR spectrum of  $[\text{Ru}(\text{Clazpy})_2(\text{phen})]\text{Cl}_2 \cdot 8\text{H}_2\text{O}$  in methanol- $d_4$

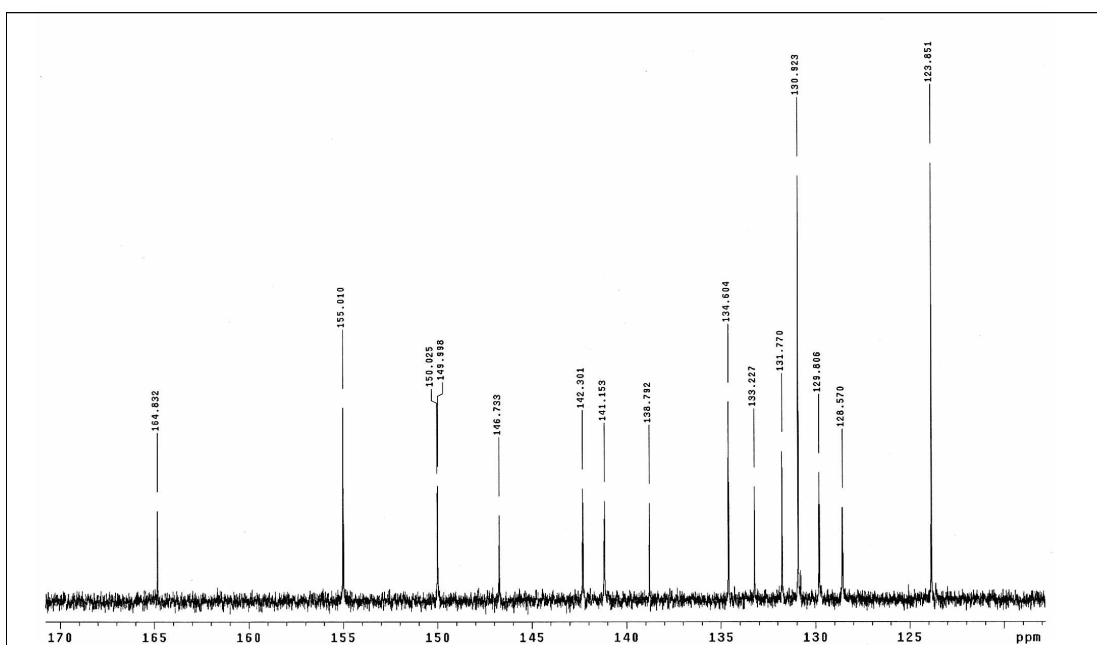


**Figure 3.161**  $^{13}\text{C}$  NMR spectrum of  $[\text{Ru}(\text{Clazpy})_2(\text{phen})]\text{Cl}_2 \cdot 8\text{H}_2\text{O}$  in methanol- $d_4$

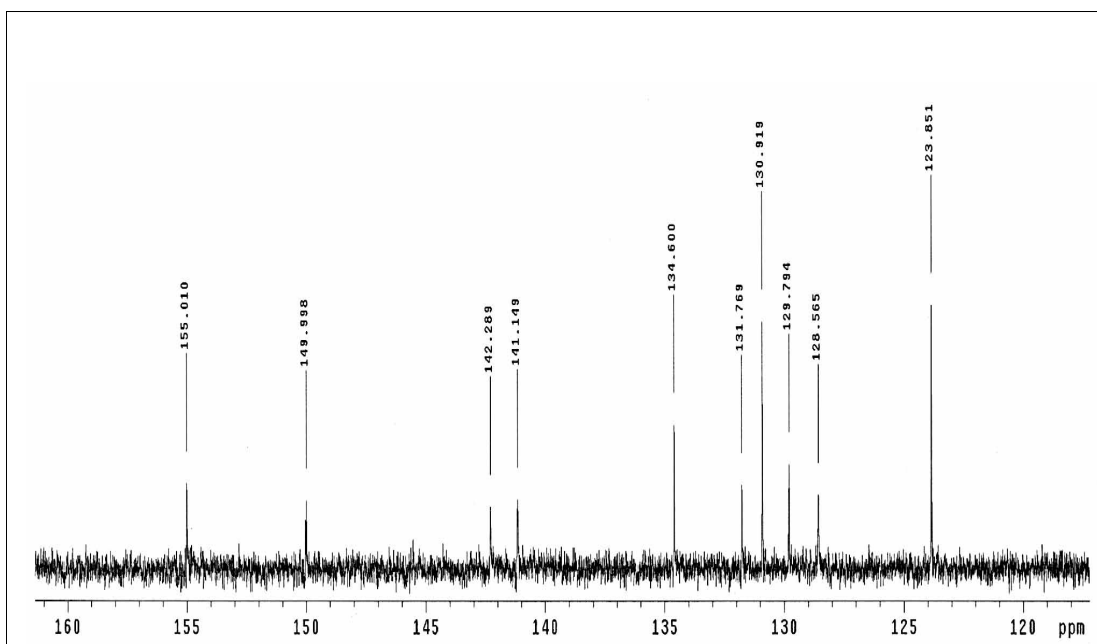


**Figure 3.162** DEPT NMR spectrum of  $[\text{Ru}(\text{Clazpy})_2(\text{phen})]\text{Cl}_2 \cdot 8\text{H}_2\text{O}$  in methanol- $d_4$

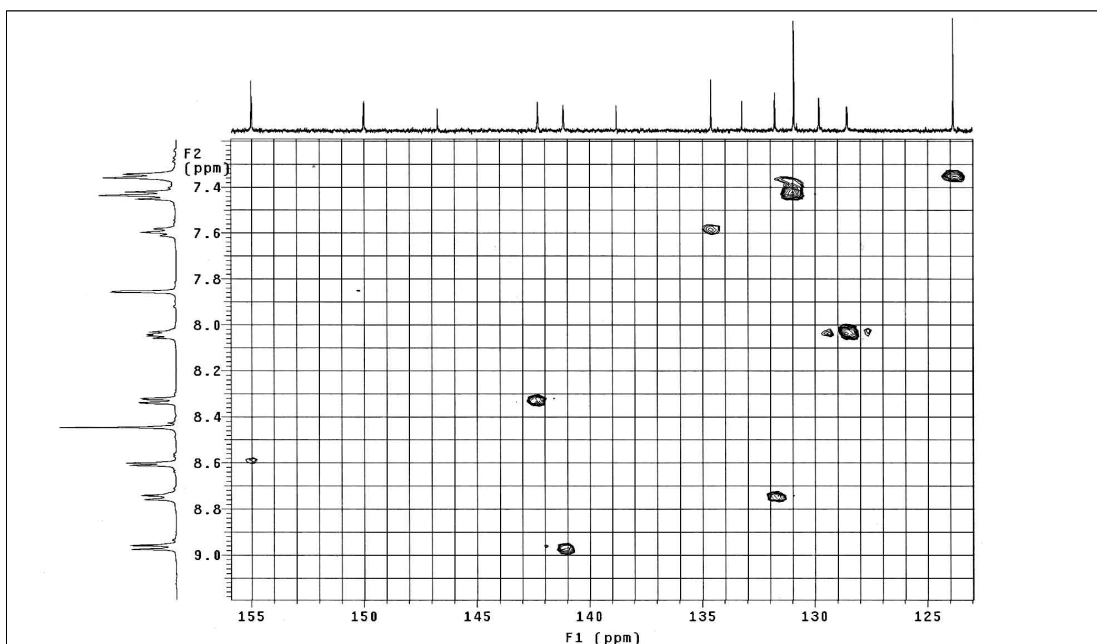


**Figure 3.163**  $^1\text{H}$ - $^{13}\text{C}$  HSQC NMR spectrum of  $[\text{Ru}(\text{Clazpy})_2(\text{phen})]\text{Cl}_2 \cdot 8\text{H}_2\text{O}$  in methanol- $d_4$

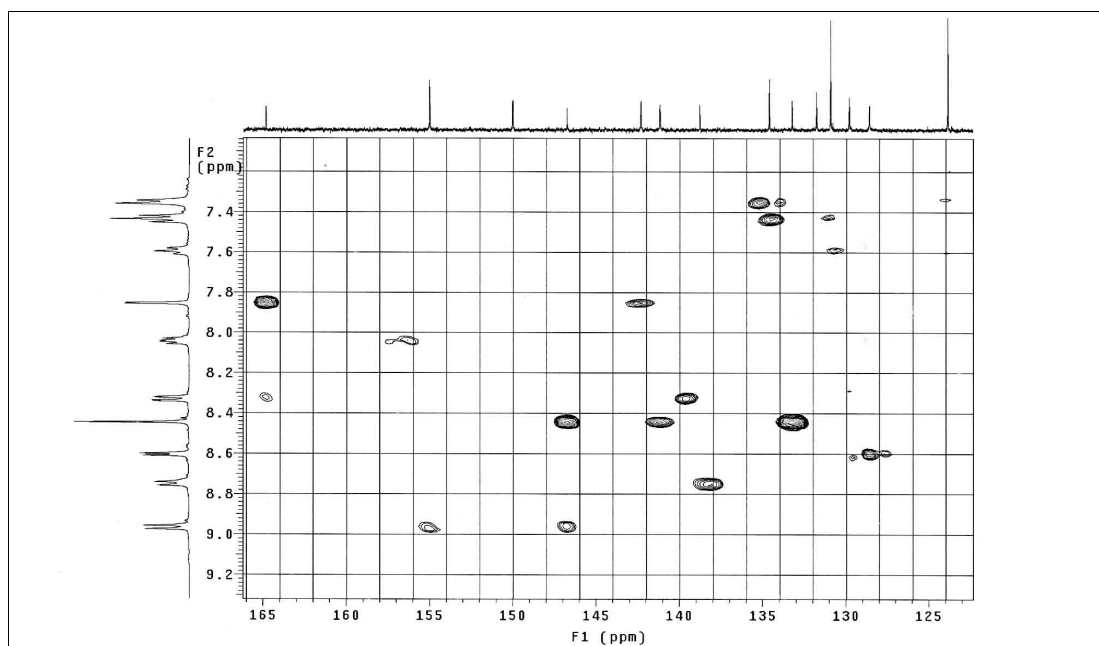


**Figure 3.164**  $^1\text{H}$ - $^{13}\text{C}$  HMBC NMR spectrum of  $[\text{Ru}(\text{Clazpy})_2(\text{phen})]\text{Cl}_2 \cdot 8\text{H}_2\text{O}$  in methanol- $d_4$

Nuclear magnetic resonance spectroscopy of  $[\text{Ru}(\text{Clazpy})_2(\text{azpy})]\text{Cl}_2 \cdot 4\text{H}_2\text{O}$

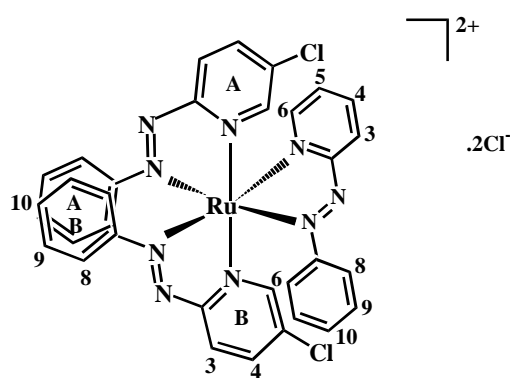


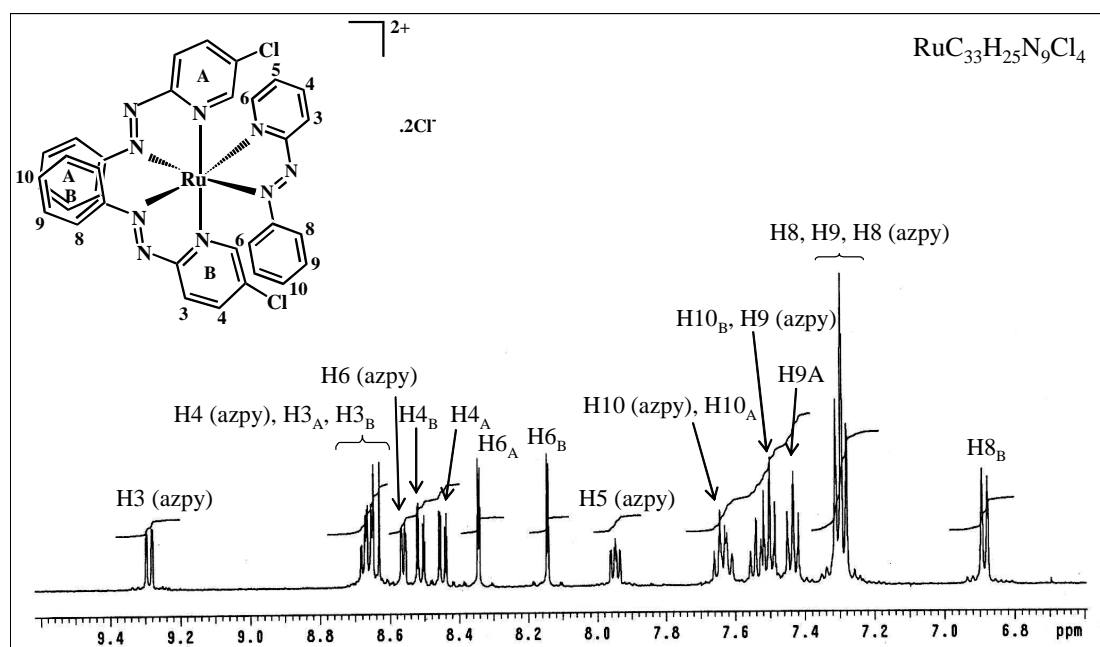
**Table 3.72**  $^1\text{H}$ - $^{13}\text{C}$  NMR spectroscopic data of  $[\text{Ru}(\text{Clazpy})_2(\text{azpy})]\text{Cl}_2 \cdot 4\text{H}_2\text{O}$ 

H-position	$^1\text{H}$ NMR			$^{13}\text{C}$ NMR (CH-type)
	$\delta$ (ppm)	$J$ (Hz)	Amount of H	
3 (azpy)	9.29 (dd)	8.0, 1.0	1	132.75
4 (azpy)	8.68 (dd)	6.0, 2.0	1	143.87
3A	8.68 (d)	6.5	1	143.87
3B	8.64 (d)	8.5	1	132.17
6 (azpy)	8.56 (dd)	5.5, 1.0	1	154.10
4B	8.51 (dd)	8.0, 2.0	1	143.32
4A	8.45 (dd)	8.5, 2.0	1	143.62
6A	8.37(d)	2.0	1	150.66
6B	8.14 (d)	2.0	1	151.43
5 (azpy)	7.95 (ddd)	5.5, 1.0	1	132.33
10 (azpy)	7.64 (t)	8.0	1	135.33
10A	7.62 (t)	7.5	1	135.18
10B	7.54 (t)	7.5	1	133.59
9 (azpy)	7.50 (t)	8.5	2	131.42
9A	7.43 (t)	8.5	2	130.95
8A	7.305 (d)	8.0	2	123.88
9B	7.30 (t)	8.0	2	124.07
8 (azpy)	7.29 (d)	7.5	2	131.12
8B	6.89 (dd)	7.5, 1.0	2	123.75
Quaternary carbons (C)				164.80, 164.22, 164.00, 156.88, 153.56, 152.93, 140.08, 139.99

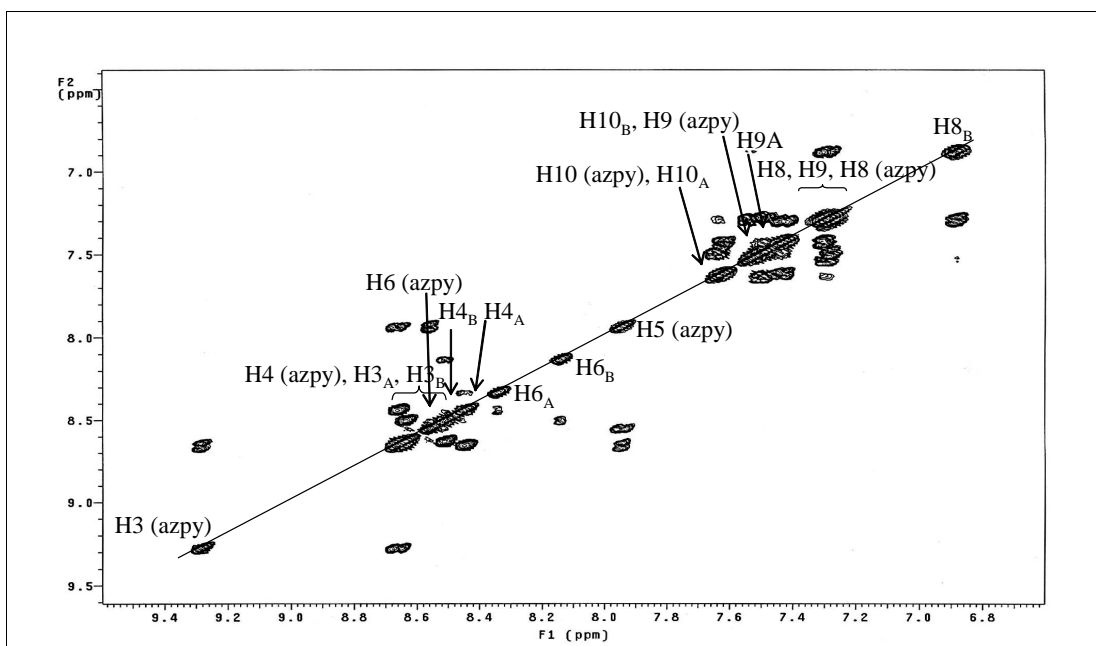
d = doublet, dd = doublet of doublet, ddd = doublet of doublet of doublet, t = triplet

The  $^1\text{H}$  NMR spectrum (Figure 3.165) of  $[\text{Ru}(\text{Clazpy})_2(\text{azpy})]\text{Cl}_2 \cdot 4\text{H}_2\text{O}$  complex showed 13 resonances of 25 protons because some resonances are overlapping. This result indicated that three of ligands are unsymmetrical molecules. The first signal appeared at the lowest field was proton H6 (9.25 ppm) which located near coordinated nitrogen on pyridine ring of azpy. Since aromatic regions of the spectra are very complex owing to the large number of protons from Clazpy and azpy rings, others protons in this complex were also studied by using simple correlation  $^1\text{H}$ - $^1\text{H}$  COSY NMR spectroscopy (Figure 3.166).

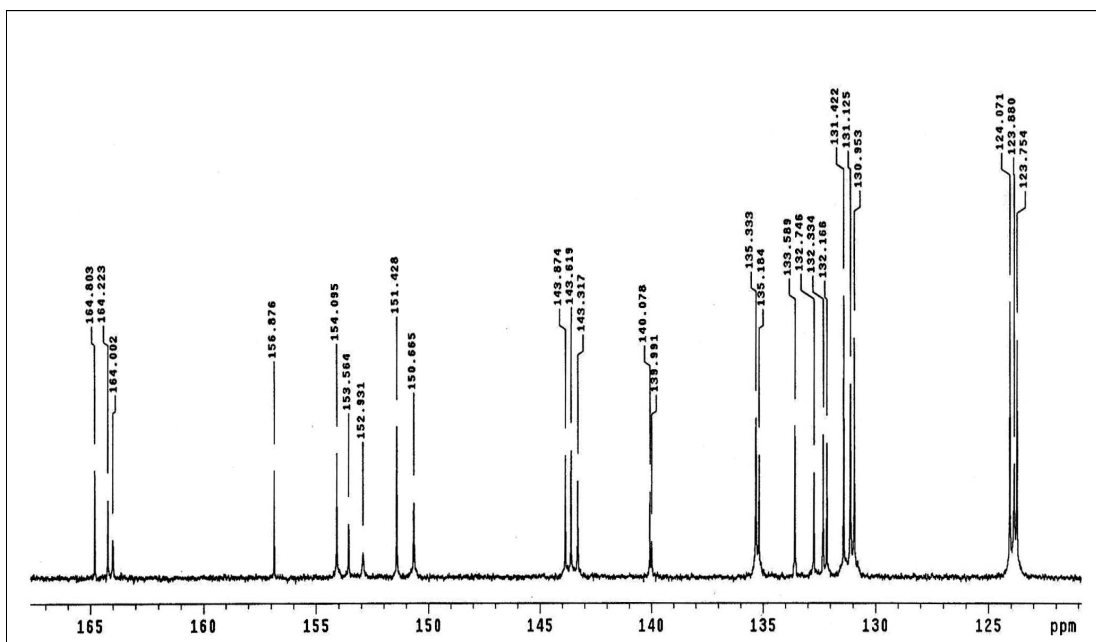
The  $^{13}\text{C}$  NMR (Figure 3.167) results corresponded to the DEPT NMR (Figure 3.168) which showed only one kind of methane carbons. All quaternary carbons at 164.80, 164.22, 164.00, 156.88, 153.56, 152.93, 140.08, 139.99 belonged to C2, C7 of azpy ligand and C2, C5, C7 of two Clazpy ligands. Moreover, the others  $^{13}\text{C}$  NMR signals assignments were based on  $^1\text{H}$ - $^{13}\text{C}$  HMQC NMR spectrum (Figure 3.169).



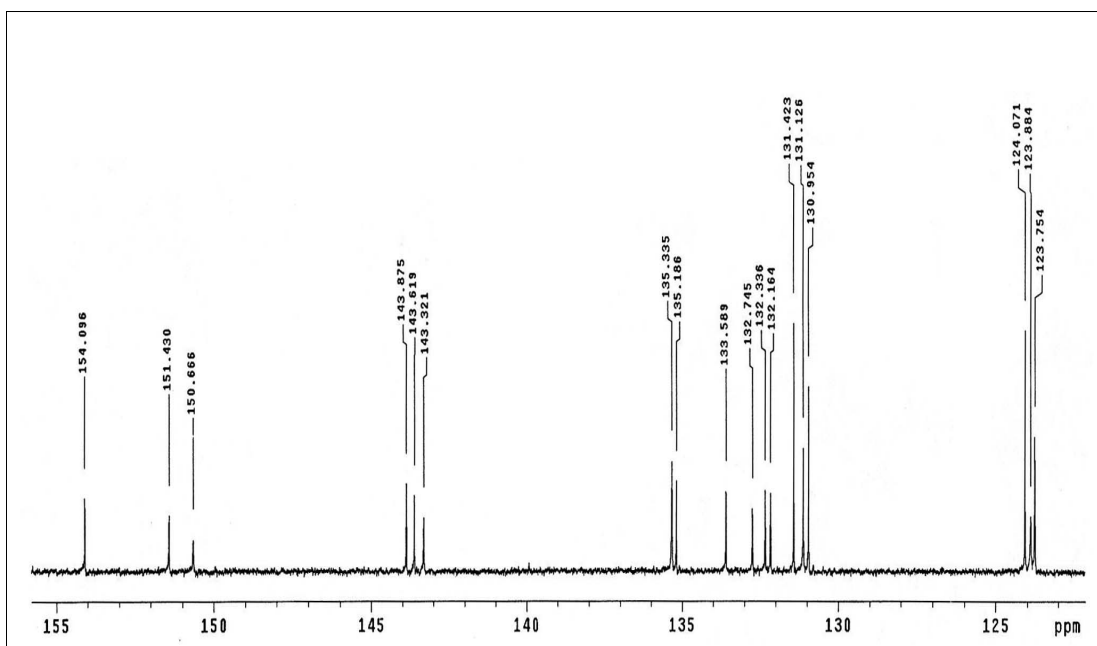
**Figure 3.165**  $^1\text{H}$  NMR spectrum of  $[\text{Ru}(\text{Clazpy})_2(\text{azpy})]\text{Cl}_2 \cdot 4\text{H}_2\text{O}$  in methanol- $d_4$



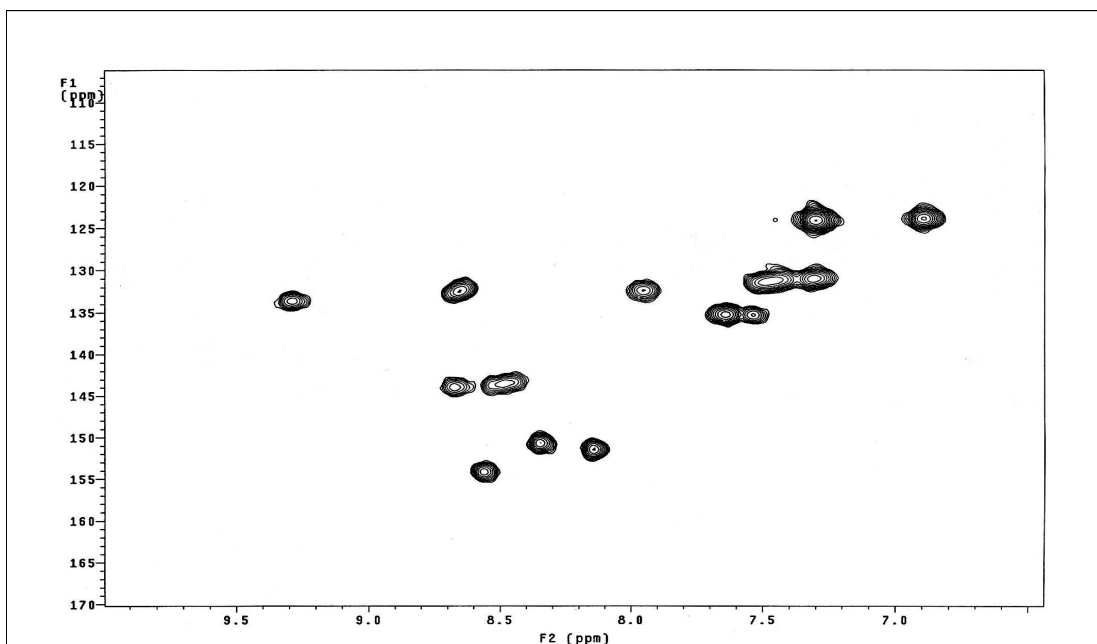
**Figure 3.166**  $^1\text{H}$ - $^1\text{H}$  COSY NMR spectrum of  $[\text{Ru}(\text{Clazpy})_2(\text{azpy})]\text{Cl}_2 \cdot 4\text{H}_2\text{O}$  in methanol- $d_4$



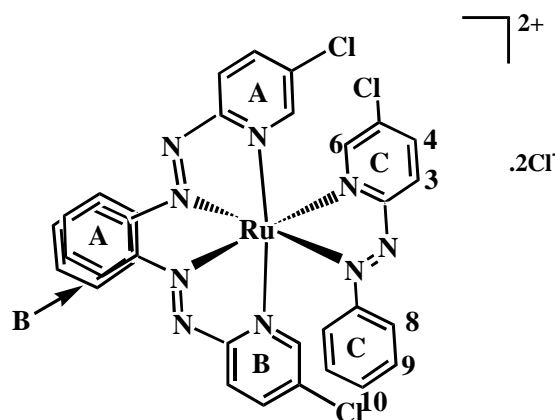
**Figure 3.167**  $^{13}\text{C}$  NMR spectrum of  $[\text{Ru}(\text{Clazpy})_2(\text{azpy})]\text{Cl}_2 \cdot 4\text{H}_2\text{O}$  in methanol- $d_4$



**Figure 3.168** DEPT NMR spectrum of  $[\text{Ru}(\text{Clazpy})_2(\text{azpy})]\text{Cl}_2 \cdot 4\text{H}_2\text{O}$  in methanol- $d_4$



**Figure 3.169**  $^1\text{H}$ - $^{13}\text{C}$  HMQC NMR spectrum of  $[\text{Ru}(\text{Clazpy})_2(\text{azpy})]\text{Cl}_2 \cdot 4\text{H}_2\text{O}$  in methanol- $d_4$

Nuclear magnetic resonance spectroscopy of  $[\text{Ru}(\text{Clazpy})_3]\text{Cl}_2 \cdot 3\text{H}_2\text{O}$ 

As  $[\text{Ru}(\text{Clazpy})_3]\text{Cl}_2 \cdot 3\text{H}_2\text{O}$  has  $C_1$  symmetry, all three Clazpy ligands are not equivalent, resulting in 15 resonances, which have fully been assigned by using 2D COSY NMR spectroscopy. First 2D COSY NMR, the three sets of Clazpy pyridine signals and three sets of azpy phenyl signals have been distinguished.

The  $^1\text{H}$  NMR spectrum (Figure 3.170) of  $[\text{Ru}(\text{Clazpy})_3]\text{Cl}_2 \cdot 3\text{H}_2\text{O}$  complex showed 15 resonances of 24 protons. Some appeared to be multiple signals due to overlap of resonances. In addition, the protons H3, H4 and H6 on pyridine ring appear at lower downfield than protons H8, H9 and H10 on phenyl ring. This may be due to the pyridine protons having less electron density than the phenyl protons. From the correlation  $^1\text{H}$ - $^1\text{H}$  COSY NMR spectroscopy (Figure 3.171), the three set of Clazpy pyridine signals have been distinguished. Since two of the three Clazpy pyridine rings (A and B) are trans to each other, the protons are slightly different similar to the situation of the  $[\text{Ru}(\text{Clazpy})_3](\text{PF}_6)_2$  complex. In contrast to the protons in the Clazpy pyridine ring (C), the chemical shift appeared at the lowest field due to trans to N=N azo function. These data confirm the configuration of N(py) and N(azo) orientation from the starting material, *cis*- $[\text{Ru}(\text{Clazpy})_2\text{Cl}_2]$ .

The  $^{13}\text{C}$  NMR signals assignments (Figure 3.172) and DEPT (Figure 3.373) were based on the  $^1\text{H}$ - $^{13}\text{C}$  HMQC spectrum (Figure 3.174) which was generally used for studying large and complicated molecules. The  $^{13}\text{C}$  NMR spectrum showed 14 signals from 24 methine carbons and three signals of six quaternary carbons. The signals at 164.09, 163.07, 157.17, 140.29 and 140.13 ppm was assigned

to the quaternary carbons C2, C5 and C7, respectively. Since C2 was located between nitrogen atoms, the chemical shift occurred at the lowest field.

**Table 3.73**  $^1\text{H}$ - $^{13}\text{C}$  NMR spectroscopic data of  $[\text{Ru}(\text{Clazpy})_3]\text{Cl}_2 \cdot 3\text{H}_2\text{O}$

H-position	$^1\text{H}$ NMR			$^{13}\text{C}$ NMR (CH-type)
	$\delta$ (ppm)	$J$ (Hz)	Amount of H	
3C	9.26 (d)	8.5	1	133.58
4C	8.72 (dd)	8.5, 2.0	1	143.29
6C	8.63 (d)	7.5	3	132.75
3A	8.62 (d)	1.0		153.19
3B	8.60 (d)	9.0		153.19
4A	8.52 (dd)	8.5, 2.0	1	143.55
4B	8.44 (d)	8.5, 2.0	1	143.71
6A	8.32 (d)	2.0	1	151.95
6B	8.30 (d)	2.0	1	150.66
10C	7.63 (tt)	7.5	2	135.46
10A				135.31
10B	7.53 (t)	7.5	5	135.22
9C	7.50 (t)	7.5, 2.0		132.22
9A	7.45 (t)	8.0		131.10
8A	7.33 (d)	7.5	6	124.09
9B	7.28 (-)	7.5		131.47
8C	7.27 (dd)	7.5, 1.0		130.92
8B	6.84 (d)	8.0	2	123.66
Quaternary carbons (C)				164.09, 163.07, 157.17, 140.29, 140.13

d = doublet, dd = doublet of doublet, t = triplet, tt = triplet

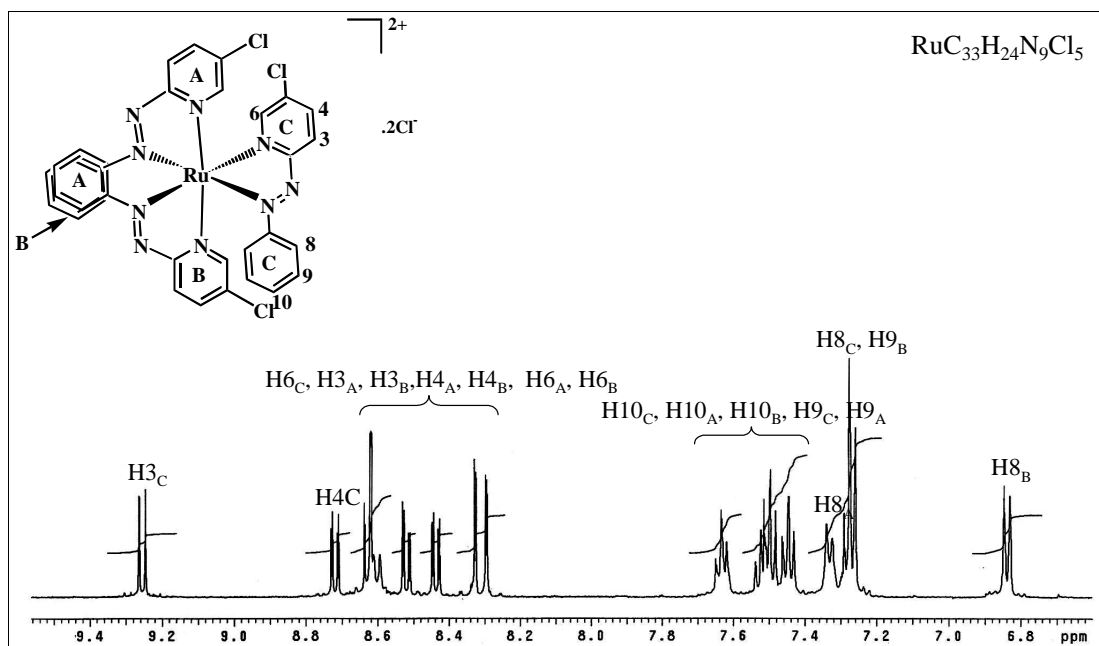


**Figure 3.170**  $^1\text{H}$  NMR spectrum of  $[\text{Ru}(\text{Clazpy})_3]\text{Cl}_2 \cdot 4\text{H}_2\text{O}$  in methanol- $d_4$

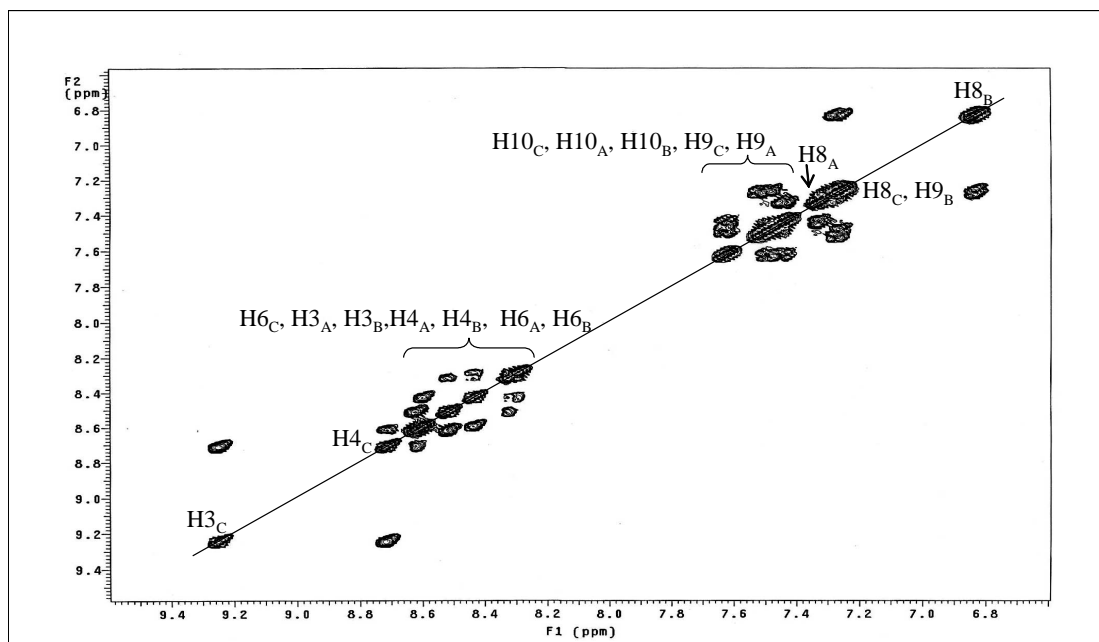


**Figure 3.171**  $^1\text{H}$ - $^1\text{H}$  COSY NMR spectrum of  $[\text{Ru}(\text{Clazpy})_3]\text{Cl}_2 \cdot 4\text{H}_2\text{O}$  in methanol- $d_4$

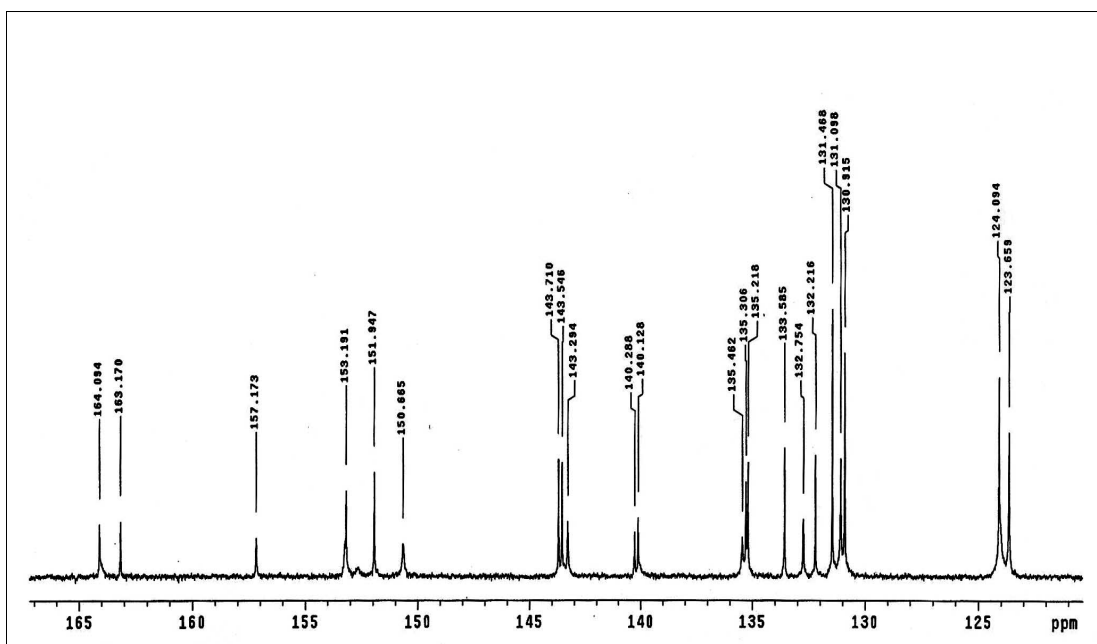


**Figure 3.172**  $^{13}\text{C}$  NMR spectrum of  $[\text{Ru}(\text{Clazpy})_3]\text{Cl}_2 \cdot 4\text{H}_2\text{O}$  in methanol- $d_4$

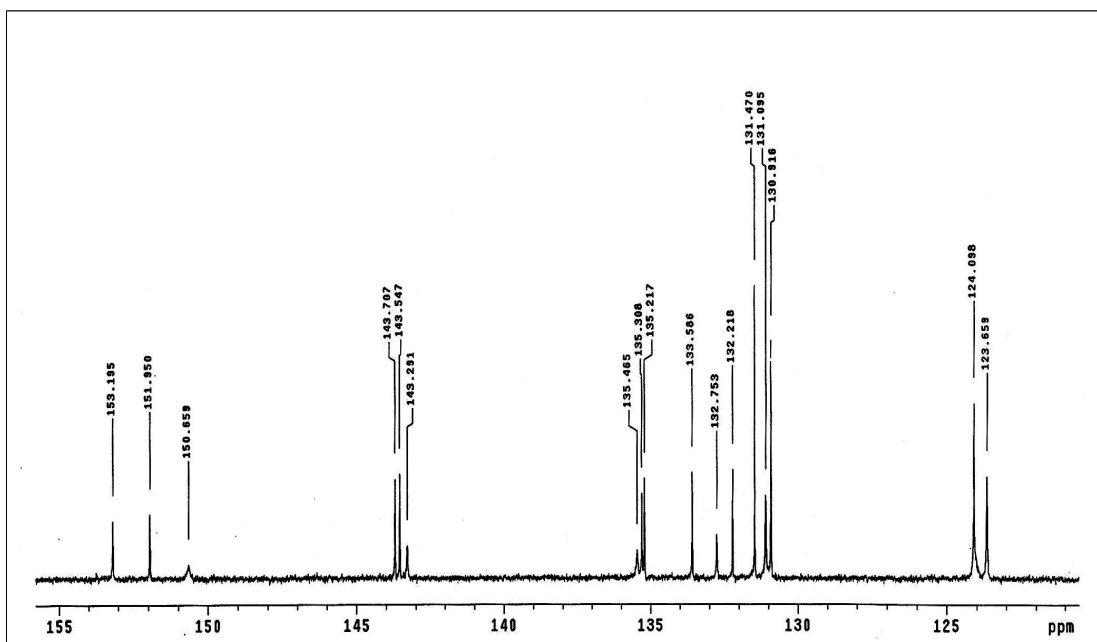


**Figure 3.173** DEPT NMR spectrum of  $[\text{Ru}(\text{Clazpy})_3]\text{Cl}_2 \cdot 4\text{H}_2\text{O}$  in methanol- $d_4$

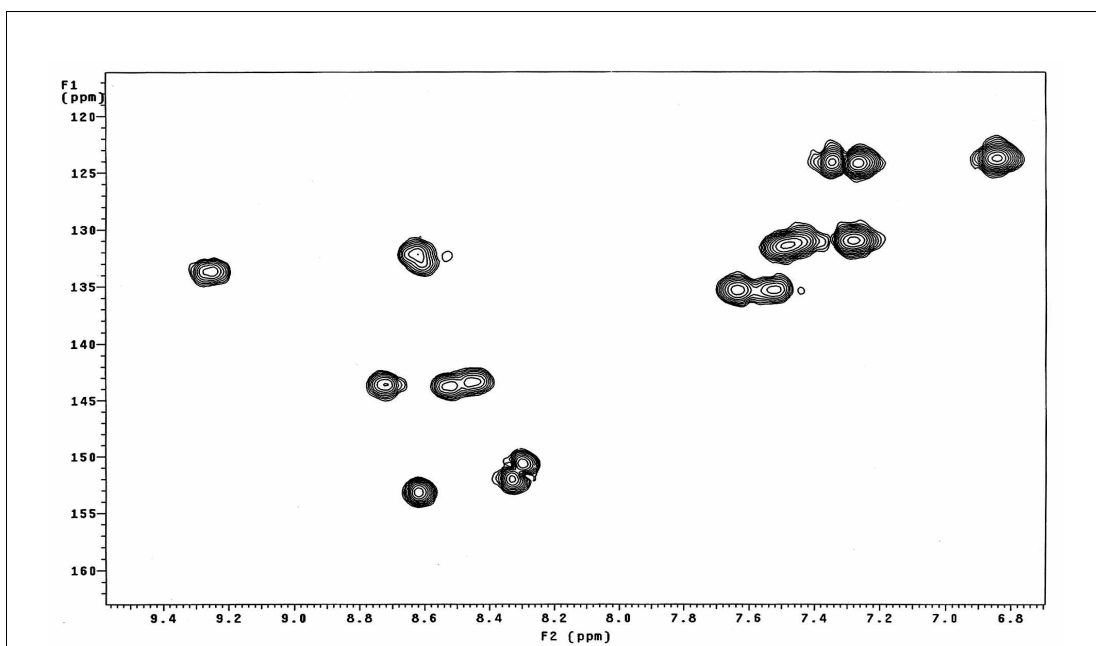


**Figure 3.174**  $^1\text{H}$ - $^{13}\text{C}$  HMQC NMR spectrum of  $[\text{Ru}(\text{Clazpy})_3]\text{Cl}_2 \cdot 4\text{H}_2\text{O}$  in methanol- $d_4$

### 3.4.2.6 Cyclic voltammetry

Redox properties of the  $[\text{Ru}(\text{Clazpy})_2(\text{L})]\text{Cl}_2 \cdot x\text{H}_2\text{O}$  ( $\text{L} = \text{bpy}$ ,  $\text{phen}$ ,  $\text{azpy}$ ,  $\text{Clazpy}$ ) were examined by cyclic voltammetry using glassy carbon electrode in  $\text{CH}_3\text{CN}$  in the presence of tetra-*n*-butylammonium hexafluorophosphate (TBAH) as supporting electrolyte. The potentials were compared to the potential of the ferrocene couple as used an internal standard. Cyclic voltammograms of  $\text{CH}_3\text{CN}$  solution of the complexes are shown in Figure 3.175 to 3.178. The cyclic voltammetric data are summarized in Table 3.74.

**Table 3.74** Cyclic voltammetric data of  $[\text{Ru}(\text{Clazpy})_2(\text{L})]\text{Cl}_2 \cdot x\text{H}_2\text{O}$  (L = bpy, phen, azpy, Clazpy) in 0.1 M TBAH  $\text{CH}_3\text{CN}$  at scan rate 50 mV/s (ferrocene as used an internal standard)

Compounds	<sup>a</sup> $E_{1/2}$ , V					
	Oxidation Ru(II)/(III)	Reduction				
		I	II	III	IV	V
$[\text{Ru}(\text{Clazpy})_2(\text{bpy})]\text{Cl}_2 \cdot 7\text{H}_2\text{O}$	+0.68 <sup>c</sup>	-0.45 (75)	-0.93 (70)	-1.71 (75)	-2.02 (80)	-2.37 (135)
$[\text{Ru}(\text{Clazpy})_2(\text{phen})]\text{Cl}_2 \cdot 8\text{HO}$	+0.71 <sup>c</sup>	-0.46 (75)	-0.95 (85)	-1.71 (85)	-2.01 (85)	-2.42 (225)
$[\text{Ru}(\text{Clazpy})_2(\text{azpy})]\text{Cl}_2 \cdot 4\text{H}_2\text{O}$	+0.55 <sup>c</sup>	-0.34 (75)	-0.66 (80)	-1.10 (75)	-1.78 (75)	-2.23 (135)
$[\text{Ru}(\text{Clazpy})_3]\text{Cl}_2 \cdot 3\text{HO}$	+0.67 <sup>c</sup>	-0.33 (80)	-0.61 (85)	-1.06 (75)	-1.72 (75)	-2.18 (110)

<sup>a</sup> $E_{1/2} = (E_{\text{pa}} + E_{\text{pc}})/2$ , where  $E_{\text{pa}}$  and  $E_{\text{pc}}$  are anodic and cathodic peak potentials, respectively;  $\Delta E_{\text{p}} = E_{\text{pa}} - E_{\text{pc}}$

<sup>b</sup>cathodic peak potential, V

<sup>c</sup>anodic peak potential, V

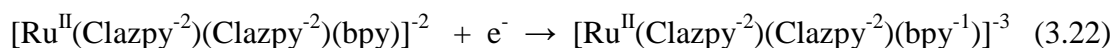
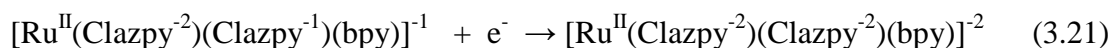
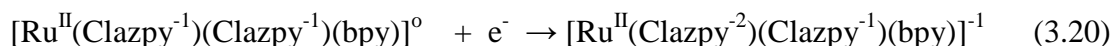
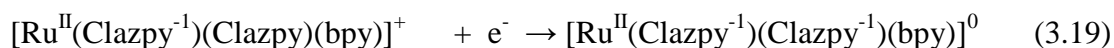
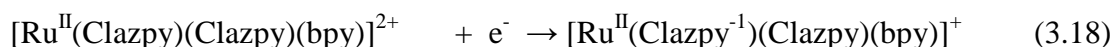
### Oxidation potential

The cyclic voltammogram of  $[\text{Ru}(\text{Clazpy})_2(\text{L})]\text{Cl}_2 \cdot x\text{H}_2\text{O}$  complexes where L = bpy, phen, azpy, Clazpy were studied in the range 0.00 to +1.50 V. These complexes exhibited only anodic peak at +0.55 to +0.71 which less value than the parent complex, *ctc*- $[\text{Ru}(\text{Clazpy})_2\text{Cl}_2]$  (+0.82 V). It was observed that chloride salt complexes are easily to be oxidized from Ru(II) to Ru(III) as shown in equation 3.17.

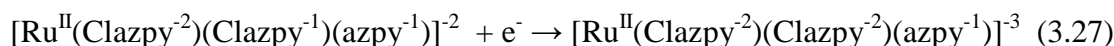
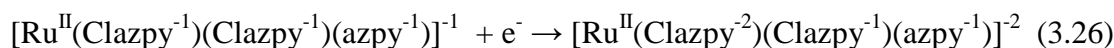
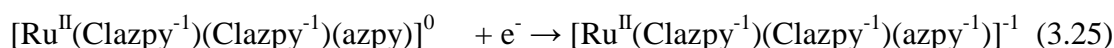
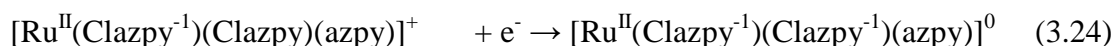
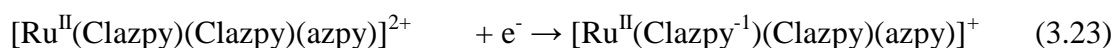


### Reduction potential

The reduction potential of  $[\text{Ru}(\text{Clazpy})_2(\text{L})]\text{Cl}_2 \cdot x\text{H}_2\text{O}$  complexes where L are bpy, phen, azpy, Clazpy were studied in the range 0.00 to -2.60 V. All complexes exhibit five reductive response negative values at the scan rate 50 mV/s, four redox couple were observed; one of them was quasireversible as evident from peak-to-peak separation value,  $\Delta E_p > 110$  mV. The first reductive reversible couple showed at less negative potential than that of the parent complexes, *ctc*- $[\text{Ru}(\text{Clazpy})_2\text{Cl}_2]$ . Since both polypyridyl and azoimine compounds are  $\pi$ -acidic ligands, azoimine unit can accommodate two electrons at LUMO mostly characterized by azo groups (Goswami *et al.*, 1982). First four couples occurred due to  $\text{azo}^-/\text{azo}$  reduction of two coordinated Clazpy and the fifth response was referred to bpy or phen in  $[\text{Ru}(\text{Clazpy})_2(\text{L})]\text{Cl}_2 \cdot x\text{H}_2\text{O}$  and to azpy or Clazpy in  $[\text{Ru}(\text{Clazpy})_2(\text{L})]\text{Cl}_2 \cdot x\text{H}_2\text{O}$  such equation 3.18 to 3.27.



and



*etc.*

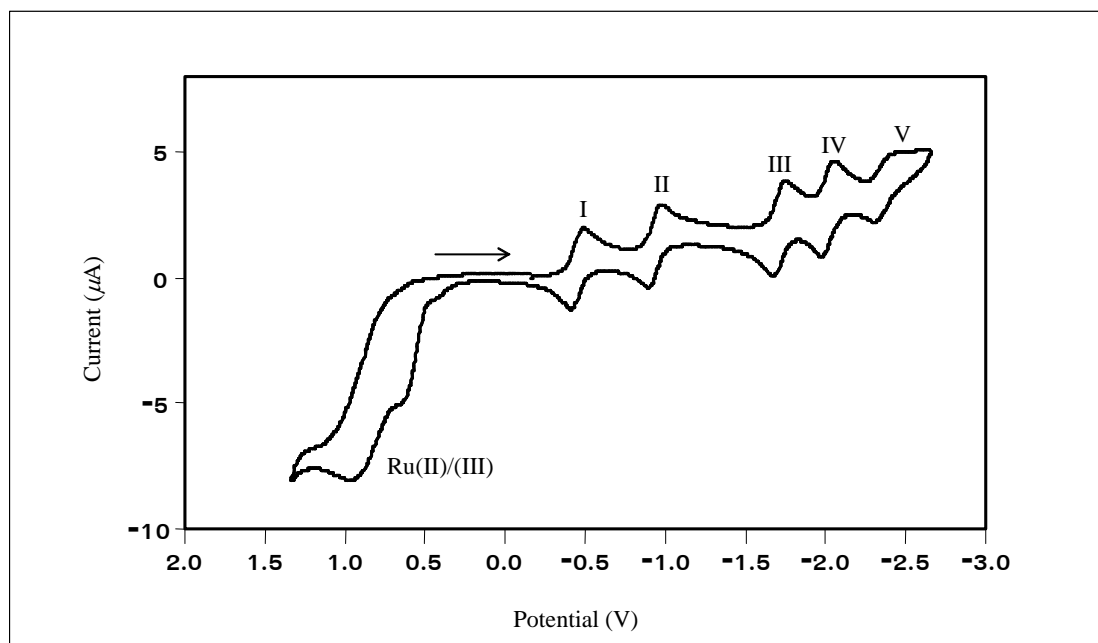


**Figure 3.175** Cyclic voltammogram of  $[\text{Ru}(\text{Clazpy})_2(\text{bpy})]\text{Cl}_2 \cdot 7\text{H}_2\text{O}$  in 0.1 M TBAH  $\text{CH}_3\text{CN}$  at scan rate 50 mV/s (ferrocene as an internal standard)

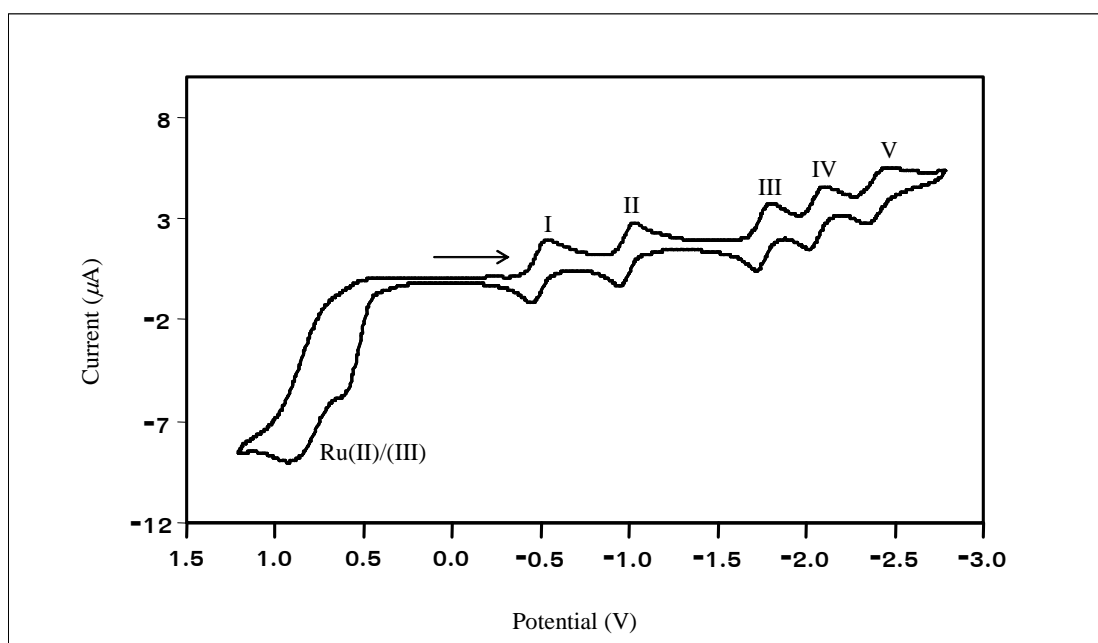


**Figure 3.176** Cyclic voltammogram of  $[\text{Ru}(\text{Clazpy})_2(\text{phen})]\text{Cl}_2 \cdot 8\text{H}_2\text{O}$  in 0.1 M TBAH  $\text{CH}_3\text{CN}$  at scan rate 50 mV/s (ferrocene as an internal standard)

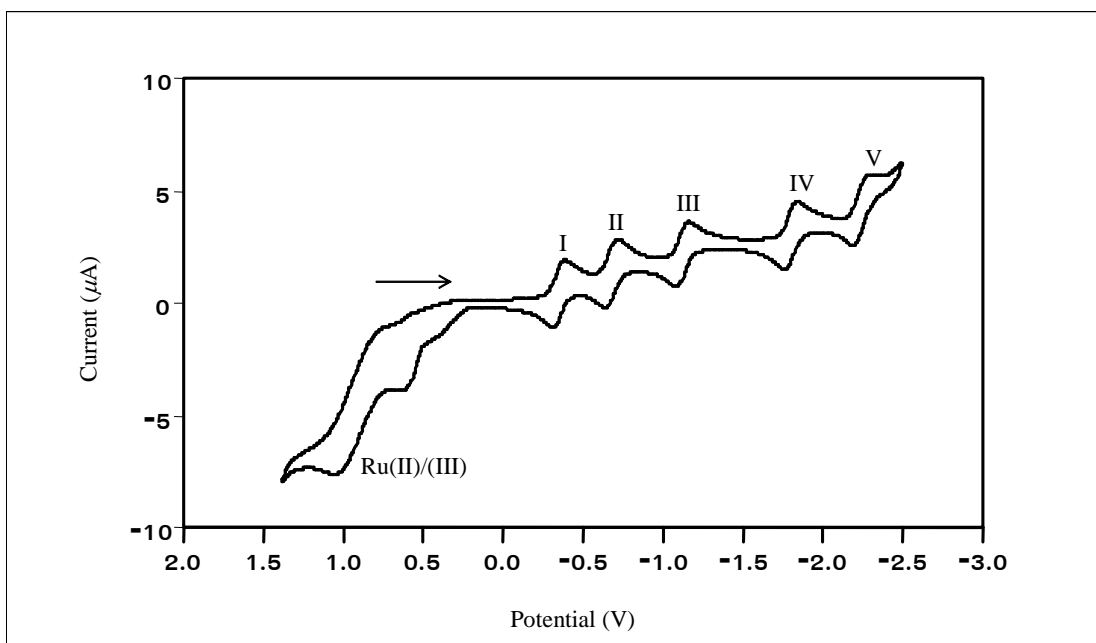


**Figure 3.177** Cyclic voltammogram of  $[\text{Ru}(\text{Clazpy})_2(\text{azpy})]\text{Cl}_2 \cdot 4\text{H}_2\text{O}$  in 0.1 M TBAH  $\text{CH}_3\text{CN}$  at scan rate 50 mV/s (ferrocene as an internal standard)

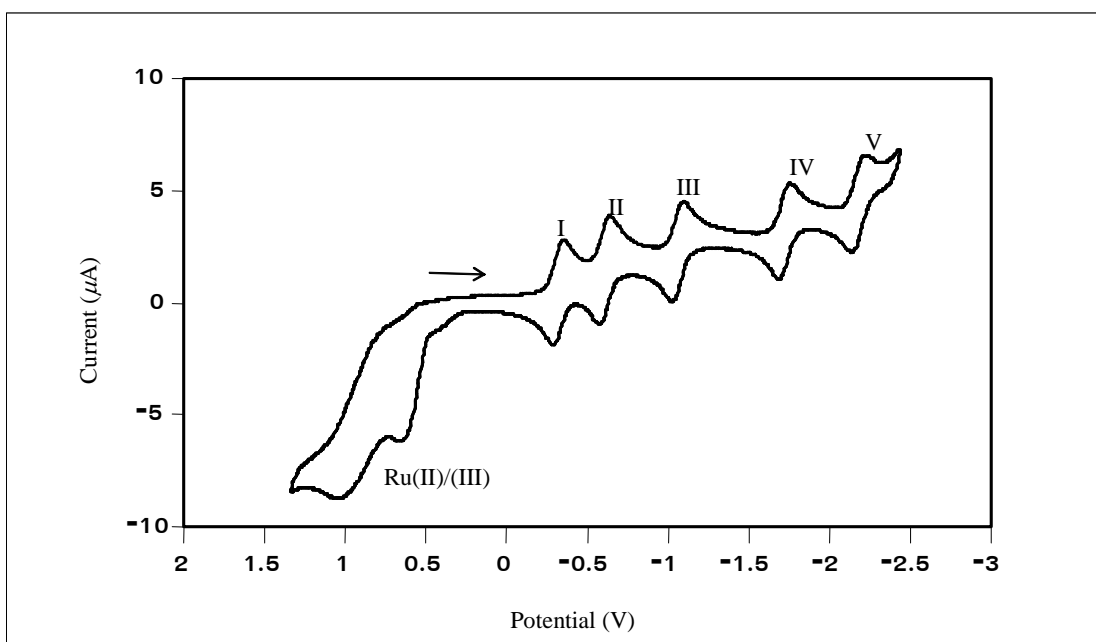


**Figure 3.178** Cyclic voltammogram of  $[\text{Ru}(\text{Clazpy})_3]\text{Cl}_2 \cdot 3\text{H}_2\text{O}$  in 0.1 M TBAH  $\text{CH}_3\text{CN}$  at scan rate 50 mV/s (ferrocene as an internal standard)

### 3.7 Syntheses and characterization of $[\text{Ru}(\text{bpy})_2(\text{Clazpy})]\text{X}_2$ and $[\text{Ru}(\text{phen})_2(\text{Clazpy})]\text{X}_2$ ( $\text{X} = \text{PF}_6^-, \text{Cl}^-$ )

#### 3.7.1 Syntheses of $[\text{Ru}(\text{bpy})_2(\text{Clazpy})]\text{X}_2$ and $[\text{Ru}(\text{phen})_2(\text{Clazpy})]\text{X}_2$ ( $\text{X} = \text{PF}_6^-, \text{Cl}^-$ )

Ruthenium trichloride hydrate was refluxed in DMF in the presence of excess stoichiometric amount of 1,10-phenanthroline/ 2,2'-bipyridine. This afforded the final product *cis*-bis(1,10-phenanthroline)ruthenium/ *cis*-bis(2,2'-bipyridine)ruthenium (Figure 3.179).

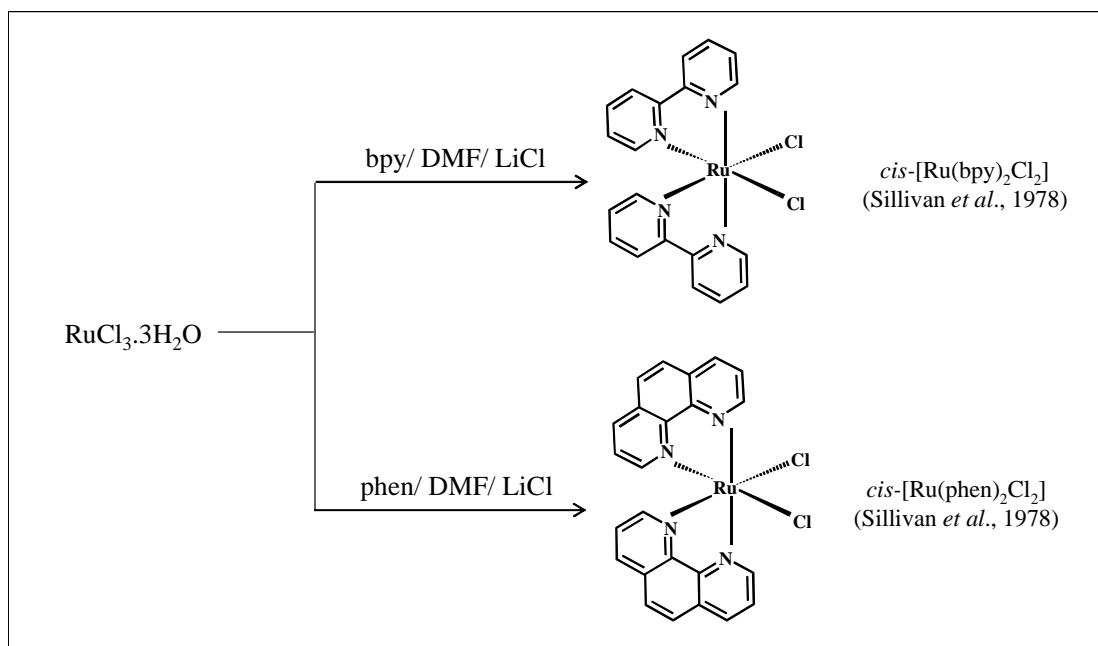


**Figure 3.179** Synthetic routes for the preparation of *cis*-[Ru(bpy)<sub>2</sub>Cl<sub>2</sub>] and *cis*-[Ru(phen)<sub>2</sub>Cl<sub>2</sub>]

The synthesized *cis*-[Ru(bpy)<sub>2</sub>Cl<sub>2</sub>] or *cis*-[Ru(phen)<sub>2</sub>Cl<sub>2</sub>] complexes were used as precursors to prepare the mixed-ligand complexes. The third chelate ligand used was Clazpy and was introduced in the presence of alcohol and AgNO<sub>3</sub> (Figure 3.180). The expected compounds precipitated as [Ru(bpy)<sub>2</sub>(Clazpy)](PF<sub>6</sub>)<sub>2</sub>

and  $[\text{Ru}(\text{phen})_2(\text{Clazpy})](\text{PF}_6)_2$ . Finally, the  $\text{PF}_6^-$  complexes were converted to the water-soluble chloride salts by the standard procedure using TBACl.

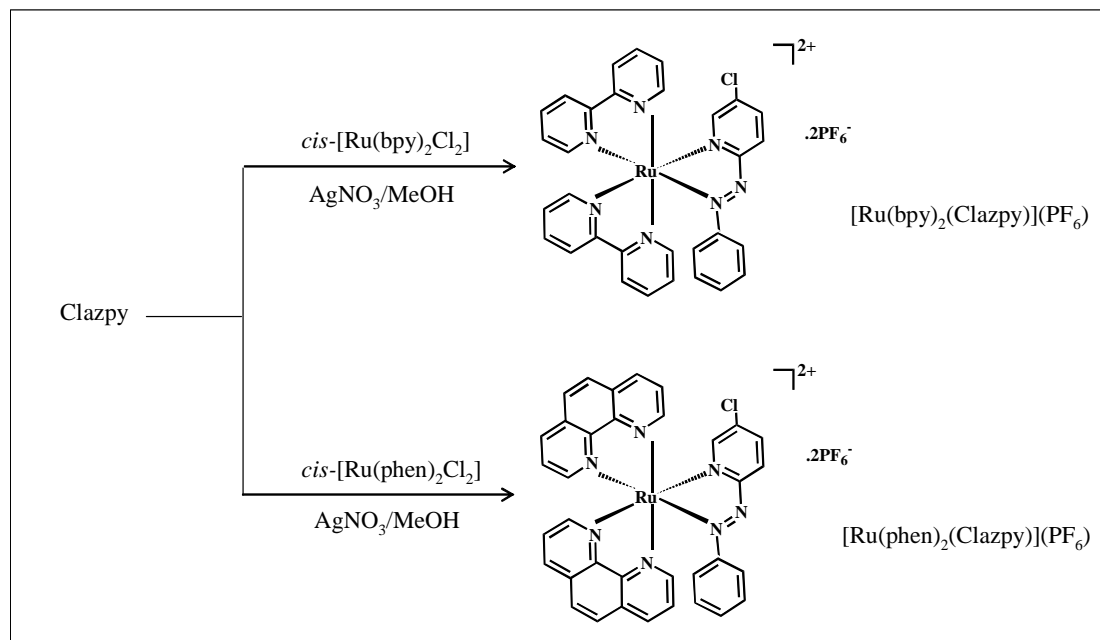


**Figure 3.180** Synthetic routes for the preparation of  $[\text{Ru}(\text{bpy})_2(\text{Clazpy})](\text{PF}_6)_2$  and  $[\text{Ru}(\text{phen})_2(\text{Clazpy})](\text{PF}_6)_2$

The physical properties of these complexes are summarized in Table 3.75.

**Table 3.75** The physical properties of  $[\text{Ru}(\text{bpy})_2(\text{Clazpy})]\text{X}_2$  and  $[\text{Ru}(\text{phen})_2(\text{Clazpy})]\text{X}_2$  ( $\text{X} = \text{PF}_6^-, \text{Cl}^-$ )

Complexes	Physical properties			
	Appearance	Color		Melting point ( $^\circ\text{C}$ )
		solid	solution	
$[\text{Ru}(\text{bpy})_2(\text{Clazpy})](\text{PF}_6)_2$	solid	dark red	dark red	248-249
$[\text{Ru}(\text{phen})_2(\text{Clazpy})](\text{PF}_6)_2$	solid	dark red	dark red	246-247
$[\text{Ru}(\text{bpy})_2(\text{Clazpy})]\text{Cl}_2 \cdot 7\text{H}_2\text{O}$	solid	dark red	dark red	235-236
$[\text{Ru}(\text{phen})_2(\text{Clazpy})]\text{Cl}_2 \cdot 8\text{H}_2\text{O}$	solid	dark red	dark red	252-253

The  $[\text{Ru}(\text{bpy})_2(\text{Clazpy})]\text{X}_2$  and  $[\text{Ru}(\text{phen})_2(\text{Clazpy})]\text{X}_2$  ( $\text{X} = \text{PF}_6^-$ ) were very soluble in acetone, DMF, DMSO; less soluble in  $\text{CH}_2\text{Cl}_2$ , EtOH and MeOH. In contrast to these complexes where X is  $\text{Cl}^-$ , they were very soluble in alcohol but less soluble in acetone.

### 3.7.2 Characterization of $[\text{Ru}(\text{bpy})_2(\text{Clazpy})]\text{X}_2$ and $[\text{Ru}(\text{phen})_2(\text{Clazpy})]\text{X}_2$ ( $\text{X} = \text{PF}_6^-, \text{Cl}^-$ )

The chemistry of  $[\text{Ru}(\text{bpy})_2(\text{Clazpy})]\text{X}_2$  and  $[\text{Ru}(\text{phen})_2(\text{Clazpy})]\text{X}_2$  ( $\text{X} = \text{PF}_6^-, \text{Cl}^-$ ) complexes were characterized by elemental analysis, Mass spectrometry, Infrared spectroscopy, UV-Visible absorption spectroscopy, Nuclear Magnetic Resonance spectroscopy (1D and 2D NMR). The electrochemical properties of all complexes were studied by using cyclic voltammetric technique.

#### 3.7.2.1 Elemental analysis

The composition of  $[\text{Ru}(\text{L})_2(\text{Clazpy})]\text{X}_2$  ( $\text{X} = \text{PF}_6^-, \text{Cl}^-$ ) was formulated by microanalytical data. The result showed the analytical values consistent with the proposed formulas. The results are given in Table 3.76.

**Table 3.76** Elemental analysis data of the  $[\text{Ru}(\text{bpy})_2(\text{Clazpy})]\text{X}_2$  and  $[\text{Ru}(\text{phen})_2(\text{Clazpy})]\text{X}_2$  ( $\text{L} = \text{PF}_6^-, \text{Cl}^-$ )

Complexes	% C		% H		% N	
	Calc.	Found	Calc.	Found	Calc.	Found
$[\text{Ru}(\text{bpy})_2(\text{Clazpy})](\text{PF}_6)_6$	40.43	40.82	2.63	2.56	10.64	9.55
$[\text{Ru}(\text{phen})_2(\text{Clazpy})](\text{PF}_6)_6$	43.38	42.50	2.50	2.30	10.12	8.90
$[\text{Ru}(\text{bpy})_2(\text{Clazpy})]\text{Cl}_2 \cdot 7\text{H}_2\text{O}$	44.96	45.80	4.62	4.30	11.84	11.71
$[\text{Ru}(\text{phen})_2(\text{Clazpy})]\text{Cl}_2 \cdot 8\text{H}_2\text{O}$	47.01	47.11	4.51	4.99	10.96	10.61

### 3.7.2.2 Electrospray (ES) mass spectrometry

The electrospray mass spectrum of  $[\text{Ru}(\text{bpy})_2(\text{Clazpy})]\text{X}_2$  and  $[\text{Ru}(\text{phen})_2(\text{Clazpy})]\text{X}_2$  ( $\text{X} = \text{PF}_6^-, \text{Cl}^-$ ) complexes are shown in Figure 3.181 to 3.184. The results are given in Table 3.77.

**Table 3.77** ES mass spectrometric data of the  $[\text{Ru}(\text{bpy})_2(\text{Clazpy})]\text{X}_2$  and  $[\text{Ru}(\text{phen})_2(\text{Clazpy})]\text{X}_2$  ( $\text{X} = \text{PF}_6^-, \text{Cl}^-$ )

m/z	Stoichiometry	Rel. Abun. (%)
$[\text{Ru}(\text{bpy})_2(\text{Clazpy})](\text{PF}_6)_2$		
776.05	$[\text{M}-\text{PF}_6]^+$	35
315.54	$[\text{M}-2\text{PF}_6]^{2+}$	100
$[\text{Ru}(\text{phen})_2(\text{Clazpy})](\text{PF}_6)_2$		
824.05	$[\text{M}-\text{PF}_6]^+$	50
339.54	$[\text{M}-2\text{PF}_6]^{2+}$	100
$[\text{Ru}(\text{bpy})_2(\text{Clazpy})]\text{Cl}_2 \cdot 7\text{H}_2\text{O}$		
315.53	$[\text{M}-2\text{Cl}-7\text{H}_2\text{O}]^{2+}$	100
$[\text{Ru}(\text{phen})_2(\text{Clazpy})]\text{Cl}_2 \cdot 8\text{H}_2\text{O}$		
339.54	$[\text{M}-2\text{Cl}-8\text{H}_2\text{O}]^{2+}$	100

M = molecular weight (MW) of each complexes

MW of  $[\text{Ru}(\text{bpy})_2(\text{Clazpy})](\text{PF}_6)_2 = 921.03 \text{ g/mol}$

MW of  $[\text{Ru}(\text{phen})_2(\text{Clazpy})](\text{PF}_6)_2 = 969.07 \text{ g/mol}$

MW of  $[\text{Ru}(\text{bpy})_2(\text{Clazpy})]\text{Cl}_2 \cdot 7\text{H}_2\text{O} = 828.11 \text{ g/mol}$

MW of  $[\text{Ru}(\text{phen})_2(\text{Clazpy})]\text{Cl}_2 \cdot 8\text{H}_2\text{O} = 894.17 \text{ g/mol}$

In  $[\text{Ru}(\text{bpy})_2(\text{Clazpy})](\text{PF}_6)_2$  and  $[\text{Ru}(\text{phen})_2(\text{Clazpy})](\text{PF}_6)_2$ , the first fragment was due to ion pair of  $[\text{Ru}(\text{L})_2(\text{Clazpy})]^{2+}(\text{PF}_6)^-$ . The second one showed of the complex cation  $[\text{Ru}(\text{L})_2(\text{Clazpy})]^{2+}$  which gave 100% relative abundance. This

pattern of fragmentation was similarly to for  $[\text{Ru}(\text{L})_2(\text{azpy})]^{2+}$  (Tempiam, S., 2002; Rattanawit, N., 2002). In contrast to the  $[\text{Ru}(\text{bpy})_2(\text{Clazpy})]\text{Cl}_2 \cdot x\text{H}_2\text{O}$  and  $[\text{Ru}(\text{phen})_2(\text{Clazpy})]\text{Cl}_2 \cdot x\text{H}_2\text{O}$  complexes, only one fragment was observed which lossing of water molecule in each complexes. The ES-MS thus confirms the authenticity of the complex.

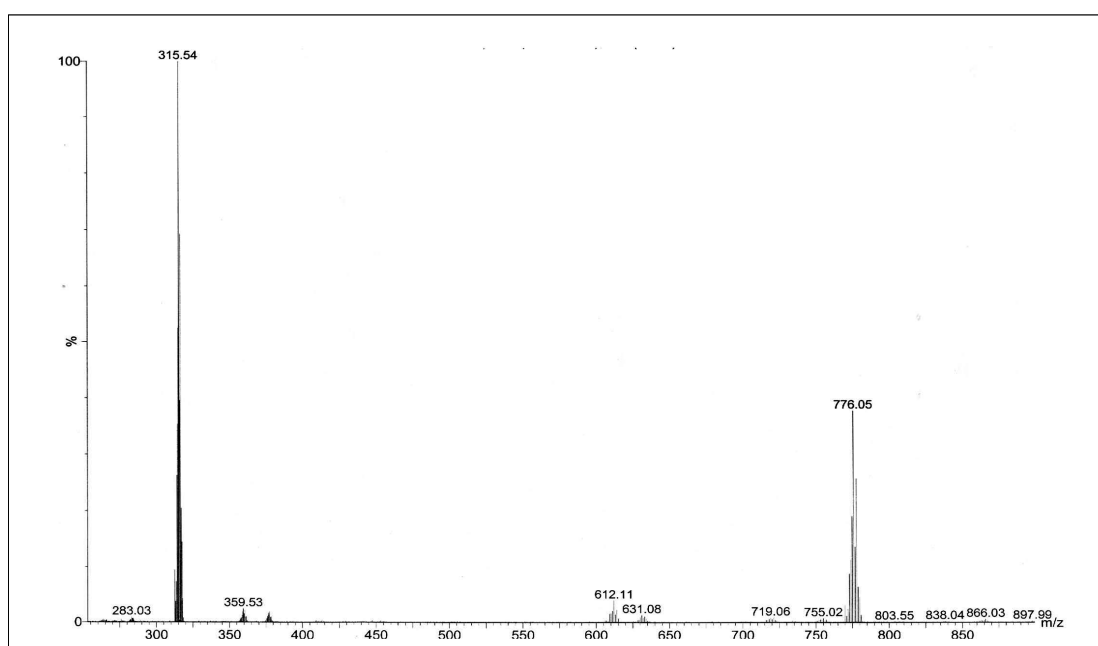


**Figure 3.181** ES mass spectrum of  $[\text{Ru}(\text{bpy})_2(\text{Clazpy})](\text{PF}_6)_2$

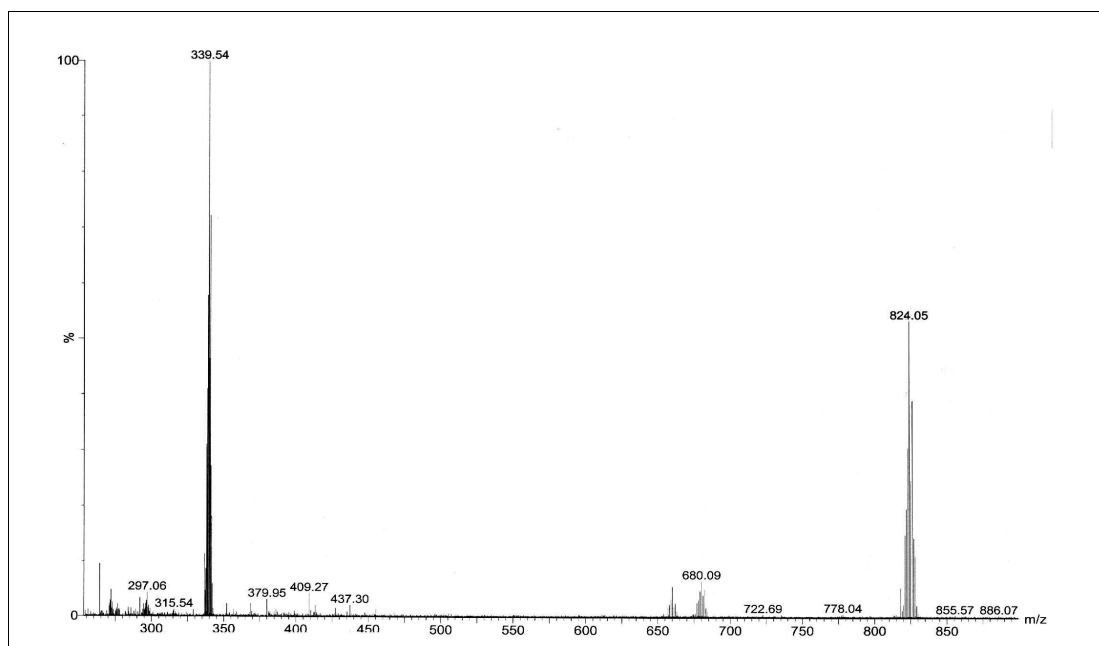


**Figure 3.182** ES mass spectrum of  $[\text{Ru}(\text{phen})_2(\text{Clazpy})](\text{PF}_6)_2$

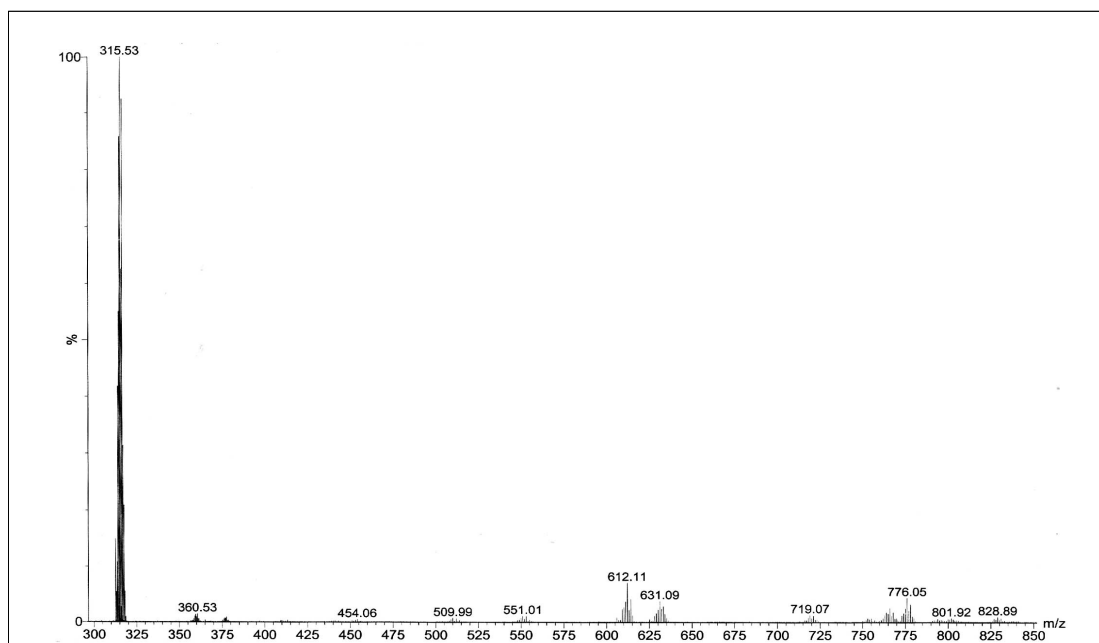


**Figure 3.183** ES mass spectrum of  $[\text{Ru}(\text{bpy})_2(\text{Clazpy})]\text{Cl}_2 \cdot 7\text{H}_2\text{O}$

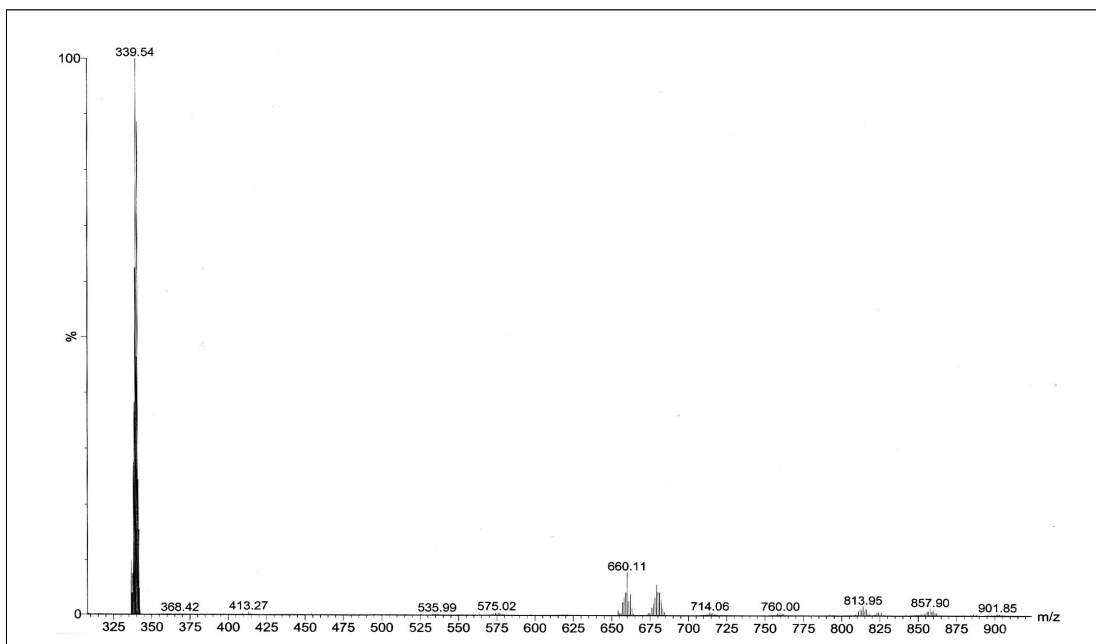


**Figure 3.184** ES mass spectrum of  $[\text{Ru}(\text{phen})_2(\text{Clazpy})]\text{Cl}_2 \cdot 8\text{H}_2\text{O}$

### 3.7.2.3 Infrared spectroscopy

The infrared spectroscopic data in the region  $4000\text{--}400\text{ cm}^{-1}$  could be used to give information about coordinated ligand to metal center. The important vibrational frequencies below  $1800\text{ cm}^{-1}$  was used to assigned significant peak such as C=C, C=N especially N=N stretching of  $[\text{Ru}(\text{bpy})_2(\text{Clazpy})]\text{X}_2$  and  $[\text{Ru}(\text{phen})_2(\text{Clazpy})]\text{X}_2$  ( $\text{X} = \text{PF}_6^-, \text{Cl}^-$ ) complexes in KBr. The infrared spectra of complexes are shown in Figure 3.185 to 3.188. The summaries of the infrared spectroscopic data are listed in Table 3.78.

**Table 3.78** IR data of  $[\text{Ru}(\text{bpy})_2(\text{Clazpy})]\text{X}_2$  and  $[\text{Ru}(\text{phen})_2(\text{Clazpy})]\text{X}_2$  ( $\text{X} = \text{PF}_6^-$ ,  $\text{Cl}^-$ )

Vibrational frequencies	Wave number ( $\text{cm}^{-1}$ )			
	$[\text{Ru}(\text{bpy})_2(\text{Clazpy})]\text{X}_2$		$[\text{Ru}(\text{phen})_2(\text{Clazpy})]\text{X}_2$	
	$\text{PF}_6^-$	$\text{Cl}^-$	$\text{PF}_6^-$	$\text{Cl}^-$
C=N stretching and C=C stretching	1542 (m)	1603 (m)	1541 (m)	1542 (m)
	1517 (m)	1543 (m)	1452 (m)	1513 (m)
	1457 (s)	1467 (m)	1432 (s)	1450 (m)
	1432 (m)	1448 (m)		1428 (m)
N=N(azo) stretching	1329 (s)	1307 (s)	1328 (s)	1304 (s)
C-N stretching	1121 (s)	1121 (s)	1121 (s)	1120 (s)
C-H out of plane bend in monosub. benzene	769 (s)	771 (m)	770 (s)	774 (m)
	723 (m)	729 (m)	723 (m)	721 (m)
	698 (m)	701 (m)	668 (m)	699 (m)
$\text{PF}_6^-$ strextching	842 (s)	-	841 (s)	-
C-Cl	558 (s)	545 (s)	558 (s)	523 (s)

s = strong, m = medium

Infrared spectra of all complexes showed many vibrations of different intensities below  $1600 \text{ cm}^{-1}$ . The N=N stretching of  $[\text{Ru}(\text{bpy})_2(\text{Clazpy})](\text{PF}_6)_2$  and  $[\text{Ru}(\text{phen})_2(\text{Clazpy})](\text{PF}_6)_2$  complexes appeared at  $1329$  and  $1328 \text{ cm}^{-1}$ , respectively. Whereas, this peak was shifted to lower energy in  $[\text{Ru}(\text{bpy})_2(\text{Clazpy})]\text{Cl}_2 \cdot 7\text{H}_2\text{O}$  and  $[\text{Ru}(\text{phen})_2(\text{Clazpy})]\text{Cl}_2 \cdot 8\text{H}_2\text{O}$  at  $1307$  and  $1304 \text{ cm}^{-1}$ , respectively. In addition, the  $\nu_{\text{P-F}}$  in  $[\text{Ru}(\text{L})_2(\text{Clazpy})](\text{PF}_6)_2$  showed band in the  $841\text{-}842 \text{ cm}^{-1}$  was absent for the corresponding chloride salts,  $[\text{Ru}(\text{L})_2(\text{Clazpy})]\text{Cl}_2 \cdot x\text{H}_2\text{O}$ .

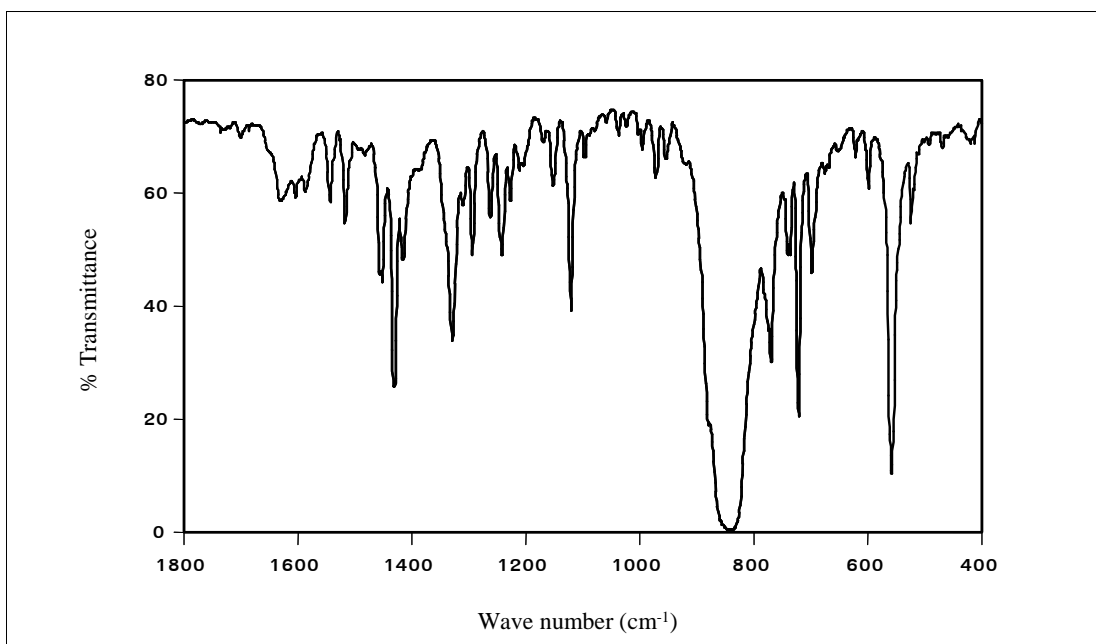


**Figure 3.185** IR spectrum of  $[\text{Ru}(\text{bpy})_2(\text{Clazpy})](\text{PF}_6)_2$

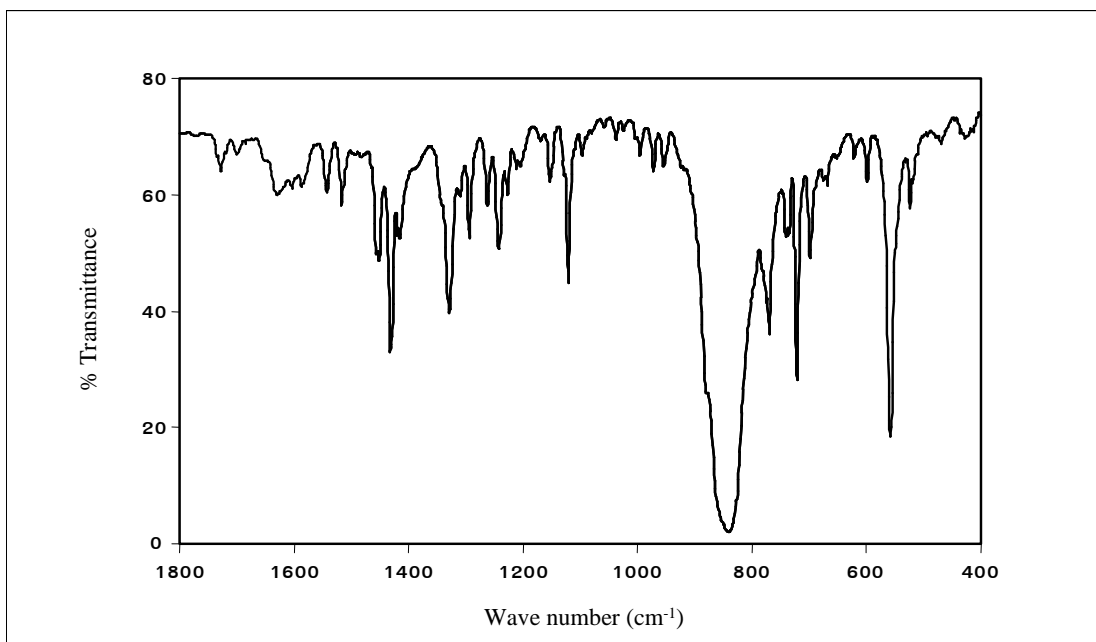


**Figure 3.186** IR spectrum of  $[\text{Ru}(\text{phen})_2(\text{Clazpy})](\text{PF}_6)_2$

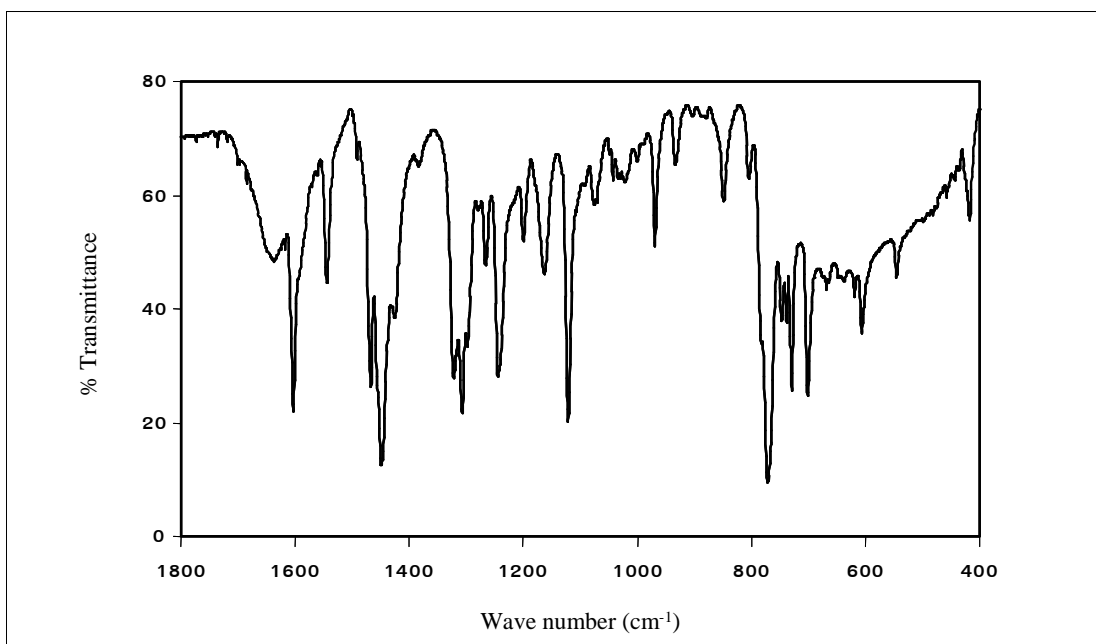


**Figure 3.187** IR spectrum of  $[\text{Ru}(\text{bpy})_2(\text{Clazpy})]\text{Cl}_2 \cdot 8\text{H}_2\text{O}$

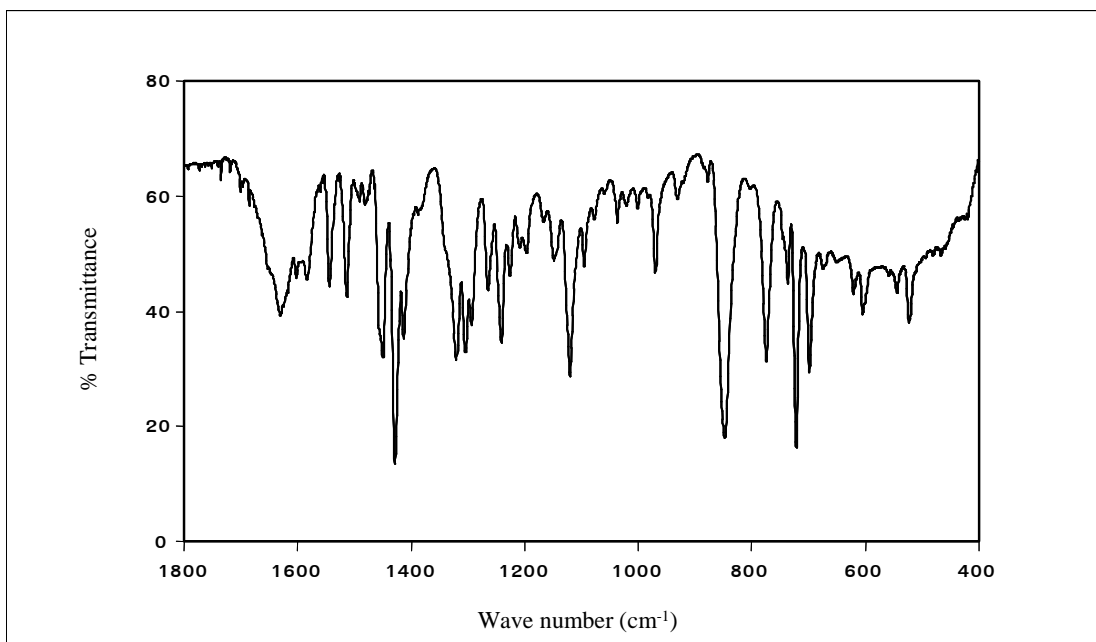


**Figure 3.188** IR spectrum of  $[\text{Ru}(\text{phen})_2(\text{Clazpy})]\text{Cl}_2 \cdot 8\text{H}_2\text{O}$

### 3.7.2.4 UV-Visible absorption spectroscopy

The UV-Visible absorption spectra of  $[\text{Ru}(\text{bpy})_2(\text{Clazpy})]\text{X}_2$  and  $[\text{Ru}(\text{phen})_2(\text{Clazpy})]\text{X}_2$  ( $\text{X} = \text{PF}_6^-, \text{Cl}^-$ ) complexes are recorded in various solvents in 200-800 nm range. Electronic spectra of these compounds in  $\text{CH}_3\text{CN}$  solution are shown in Figure 3.189 to 3.193 and the positions of the electronic absorption maxima and the extinction coefficients are listed in Table 3.79 - 3.80.

**Table 3.79** UV-Visible absorption spectroscopic data of  $[\text{Ru}(\text{bpy})_2(\text{Clazpy})](\text{PF}_6)_2$  and  $[\text{Ru}(\text{phen})_2(\text{Clazpy})](\text{PF}_6)_2$

Solvents	$\lambda_{\text{max}}$ , nm ( $\epsilon^{\text{a}}$ x $10^{-4}$ $\text{M}^{-1}\text{cm}^{-1}$ )	
	$[\text{Ru}(\text{bpy})_2(\text{Clazpy})](\text{PF}_6)_2$	$[\text{Ru}(\text{phen})_2(\text{Clazpy})](\text{PF}_6)_2$
$\text{CH}_2\text{Cl}_2$	232(6.4) 264(8.7)	232(5.5) 264(8.0)
	352(2.8) 502(1.4)	352(2.3) 502(1.1)
DMF	270(5.4) 351(1.7)	270(6.8) 351(2.2)
	502(1.0)	502(1.3)
DMSO	265(6.8) 351(2.4)	265(7.0) 351(2.4)
	502(1.1)	502(1.1)
$\text{CH}_3\text{OCH}_3$	348(2.6) 502(1.3)	348(2.2) 502(1.1)
$\text{CH}_3\text{CN}$	224(6.3) 261(6.2)	224(6.5) 262(7.5)
	347(2.0) 500(1.0)	345(2.1) 500(1.0)
EtOH	224(6.1) 263(6.3)	207(1.2) 263(1.3)
	350(2.0) 500(0.9)	349(4.2) 495(2.0)
MeOH	207(6.3) 223(6.4)	207(7.9) 223(8.1)
	262(6.1) 351(1.9) 500(1.0)	262(7.6) 350(2.5) 495(1.9)

<sup>a</sup> Molar extinction coefficient

**Table 3.80** UV-Visible absorption spectroscopic data of  $\text{Ru}(\text{bpy})_2(\text{Clazpy})\text{Cl}_2 \cdot 7\text{H}_2\text{O}$  and  $[\text{Ru}(\text{phen})_2(\text{Clazpy})]\text{Cl}_2 \cdot 8\text{H}_2\text{O}$

Solvents	$\lambda_{\text{max}}$ , nm ( $\epsilon^{\text{a}}$ x $10^{-4}$ M $^{-1}$ cm $^{-1}$ )	
	$[\text{Ru}(\text{bpy})_2(\text{Clazpy})]\text{Cl}_2 \cdot 7\text{H}_2\text{O}$	$[\text{Ru}(\text{phen})_2(\text{Clazpy})]\text{Cl}_2 \cdot 8\text{H}_2\text{O}$
$\text{CH}_2\text{Cl}_2$	278(4.5) 369(1.7)	232(4.8) 264(5.5)
	506(0.9)	352(1.9) 504(0.9)
DMF	283(4.1) 363(1.4)	269(5.4) 352(1.7)
	503(0.9)	500(1.0)
DMSO	281(4.0) 362(1.5)	266(5.3) 351(1.8)
	507(0.9)	507(0.8)
$\text{CH}_3\text{OCH}_3$	363(1.9) 502(1.1)	347(1.9) 502(0.9)
$\text{CH}_3\text{CN}$	244(2.7) 277(4.2)	222(6.1) 262(6.2)
	363(1.5) 502(0.9)	347(1.9) 502(0.9)
EtOH	206(4.9) 245(3.1)	224(6.5) 263(6.5)
	279(4.8) 368(1.8) 501(1.0)	349(2.1) 500(1.0)
MeOH	206(3.9) 243(2.4)	206(6.3) 223(6.4)
	278(3.7) 368(1.4) 502(0.9)	262(6.2) 349(2.0) 500(1.4)
$\text{H}_2\text{O}$	244(2.7) 276(4.0)	224(5.8) 261(5.5)
	363(1.5) 502(0.9)	345(1.8) 502(0.9)

<sup>a</sup> Molar extinction coefficient

The absorption spectra of  $\text{Ru}(\text{bpy})_2(\text{Clazpy})\text{X}_2$  and  $[\text{Ru}(\text{phen})_2(\text{Clazpy})]\text{X}_2$  ( $\text{X} = \text{PF}_6^-, \text{Cl}^-$ ) exhibited several bands in UV-Visible region (200-800 nm). In the  $[\text{Ru}(\text{bpy})_2(\text{Clazpy})]^{2+}$  complexes the UV region showed the bands around  $219 \pm 12$  and  $265 \pm 4$  nm were assigned to  $\pi \rightarrow \pi^*$  charge transfer transition. The same transition was found in free bipyridine at 236 and 280 nm (Changsaluk, 2002). There are also two bands at around  $358 \pm 3$  and  $503 \pm 3$  nm, which were attributed to metal-to-ligand charge transfer transitions (MLCT) involving 2,2'-bipyridine (bpy) and Clazpy ligands.

Similar to  $[\text{Ru}(\text{phen})_2(\text{Clazpy})]^{2+}$ , the UV region showed the bands around  $215\pm 8$  and  $265\pm 5$  nm were assigned to the phenanthroline ligand. The same transition was found in free phenanthroline at 232 and 264 nm (Rattanawit, 2002), so that coordination of the ligands result in a slightly red shift in the transition energy. There are also two bands at around  $351\pm 2$  and  $498\pm 3$  nm, which were attributed to metal-to-ligand charge transfer transitions (MLCT) involving Clazpy ligands. In addition, the lowest energy absorption band was not shifted when the polarity of solvents was increased.

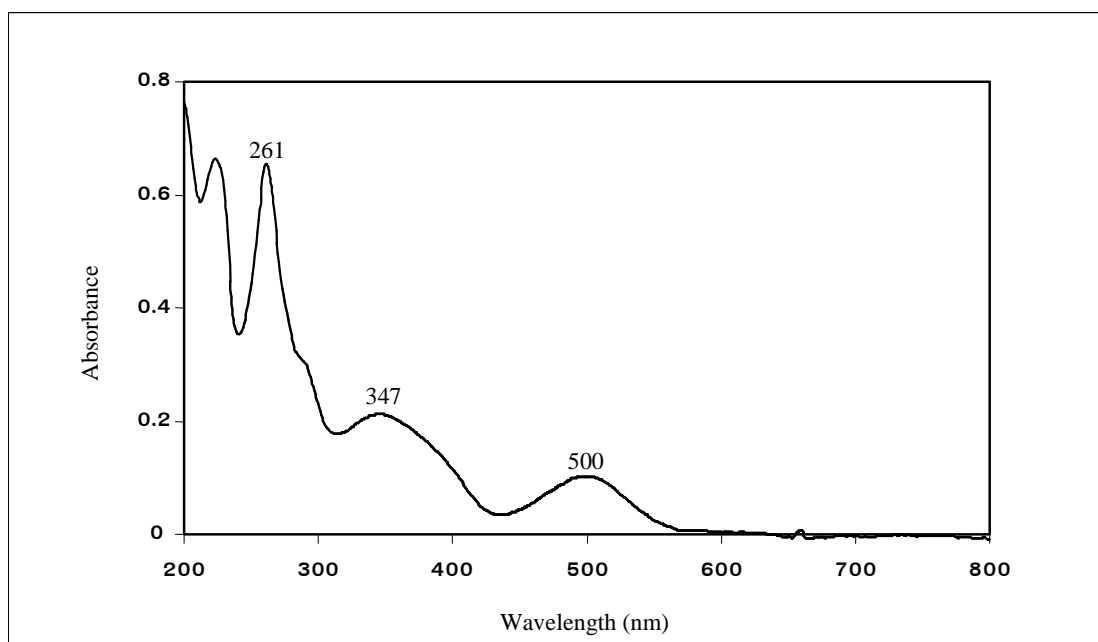


**Figure 3.189** UV-Visible absorption spectrum of  $[\text{Ru}(\text{bpy})_2(\text{Clazpy})](\text{PF}_6)_2$  in  $\text{CH}_3\text{CN}$

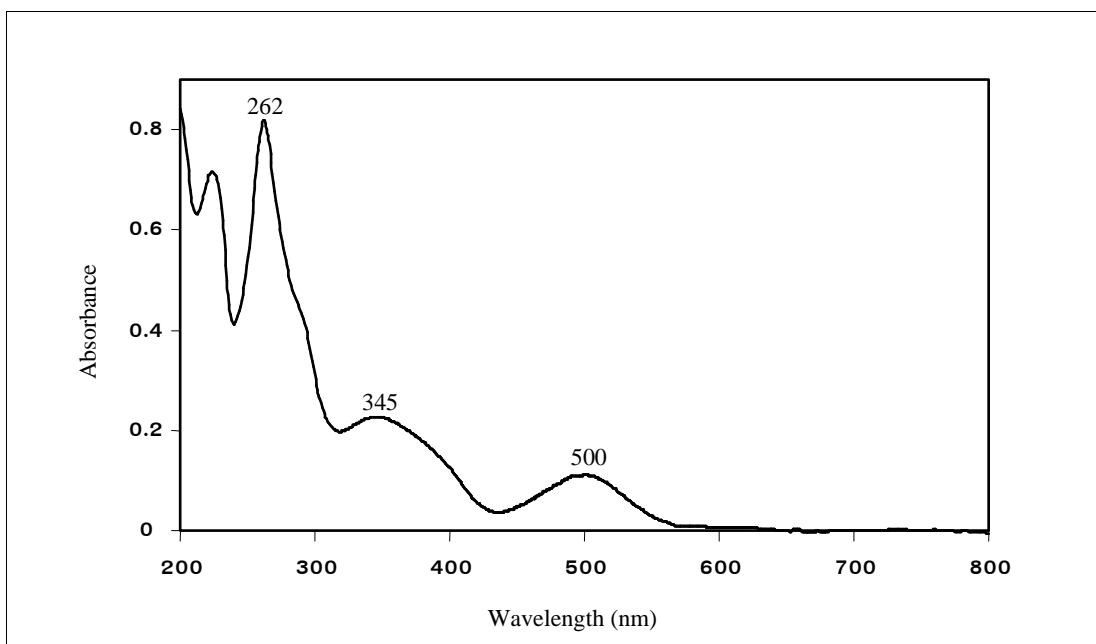


**Figure 3.190** UV-Visible absorption spectrum of [Ru(phen)<sub>2</sub>(Clazpy)](PF<sub>6</sub>)<sub>2</sub> in CH<sub>3</sub>CN

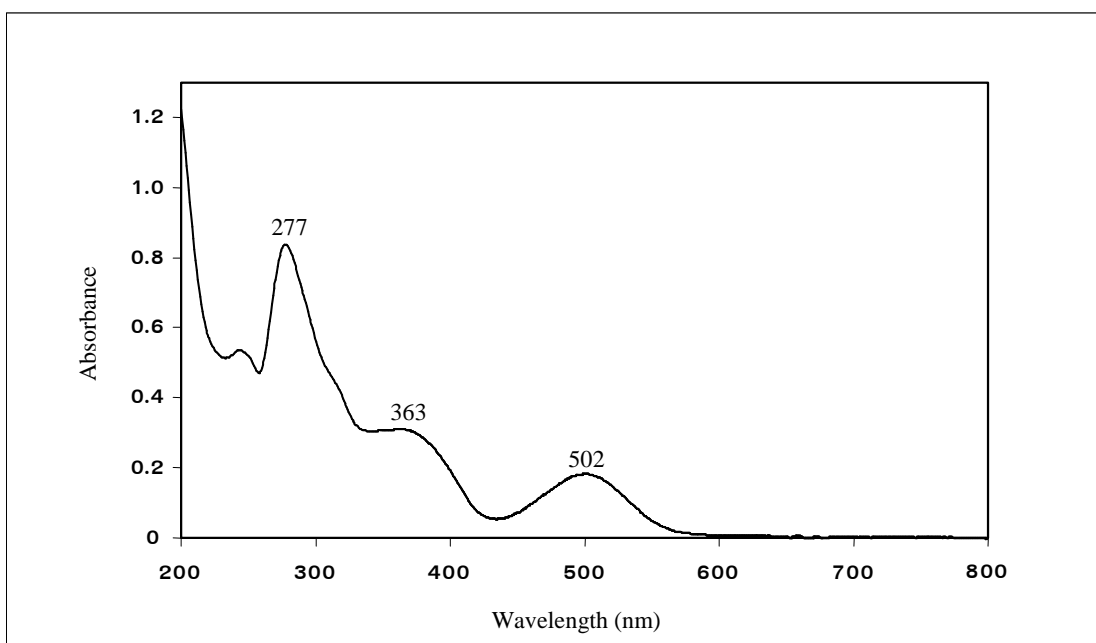


**Figure 3.191** UV-Visible absorption spectrum of [Ru(bpy)<sub>2</sub>(Clazpy)]Cl<sub>2</sub>·7H<sub>2</sub>O in CH<sub>3</sub>CN

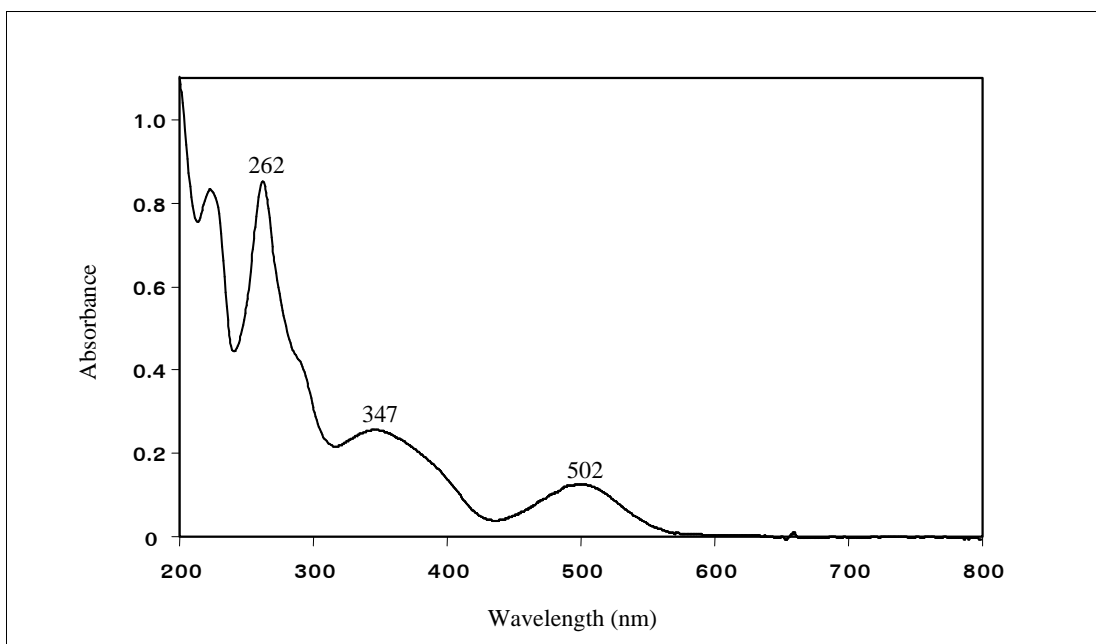


**Figure 3.192** UV-Visible absorption spectrum of  $[\text{Ru}(\text{phen})_2(\text{Clazpy})]\text{Cl}_2 \cdot 8\text{H}_2\text{O}$  in  $\text{CH}_3\text{CN}$

### 3.7.2.5 Nuclear magnetic resonance spectroscopy

The structure of  $[\text{Ru}(\text{bpy})_2(\text{Clazpy})]\text{X}_2$  and  $[\text{Ru}(\text{phen})_2(\text{Clazpy})]\text{X}_2$  ( $\text{X} = \text{PF}_6^-, \text{Cl}^-$ ) complexes was explained by using 1D and 2D NMR spectroscopic techniques. Its NMR spectra was recorded in methanol- $d_4$  and tetramethylsilane ( $\text{Si}(\text{CH}_3)_4$ ) was used as an internal reference. The NMR spectroscopic data of are presented in Table 3.81-3.84.

Nuclear magnetic resonance spectroscopy of  $[\text{Ru}(\text{bpy})_2(\text{Clazpy})](\text{PF}_6)_2$

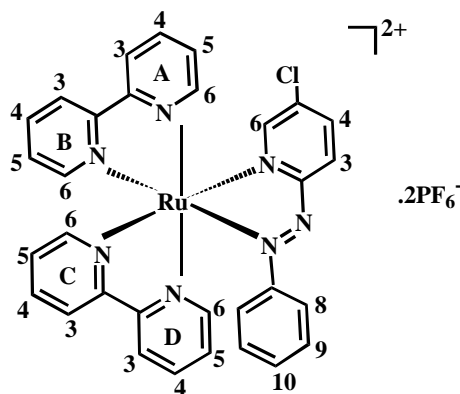


**Table 3.81**  $^1\text{H}$ - $^{13}\text{C}$  NMR spectroscopic data of  $[\text{Ru}(\text{bpy})_2(\text{Clazpy})](\text{PF}_6)_2$ 

position	$^1\text{H}$ NMR			$^{13}\text{C}$ NMR (CH-type)
	$\delta$ (ppm)	$J$ (Hz)	Amount of H	
3(Clazpy)	9.01(d)	8.5	1	129.41
3B, 3C	8.94 (td)	8.0, 1.0	2	126.35 125.98
3A	8.63 (d)	8.0	1	125.41
3D	8.49 (d)	8.0	1	125.17
4(Clazpy)	8.46 (dd)	8.5, 2.0	1	140.87
4B	8.39 (dd)	8.0, 1.0	1	141.06
4C	8.36 (dd)	8.0, 1.0	2	141.40
6(Clazpy)	8.37 (d)	2.0	1	141.11
6B	8.32 (m)	-	1	154.25
4A	8.34 (m)	-	1	149.76
4D	8.11 (td)	8.0	1	140.29
6C	8.01 (dt)	5.0, 1.0	1	152.00
6D	7.94 (dt)	5.0, 1.0	1	152.55
6A	7.84 (dt)	5.0, 1.0	1	153.76
5C	7.68 (m)	-	3	129.74
5B	7.76 (m)	-		129.84
5A	7.74 (dd)	5.5, 1.0		129.77
5D	7.54 (td)	8.0, 1.0	1	129.23
10(Clazpy)	7.42 (tt)	7.5, 1.5	1	132.07
9(Clazpy)	7.24 (tt)	7.5, 1.5	2	130.89
8(Clazpy)	7.17 (dd)	7.5, 1.5	2	123.05
Quaternary carbons (C)				165.95, 157.58, 157.22, 156.93, 155.99, 155.76, 136.25

d = doublet, dd = doublet of doublet, td = triplet of doublet, dt = doublet of triplet ,  
tt = triplet of triplet, m = multiplet

The  $^1\text{H}$  NMR spectrum (Figure 3.193) of  $[\text{Ru}(\text{bpy})_2(\text{Clazpy})](\text{PF}_6)_2$  were based on 14 resonances of 24 protons and some of these proton appeared at the same position due to overlapping. For the expected complexes, the pyridine ring C is trans to the pyridine ring of Clazpy ligand, while pyridine ring B is trans to the N=N group. Thus the protons on the pyridine ring C and B may be shifted to lower field than those of other ring. The chemical shift of proton H3 on pyridine ring of Clazpy ligand having strong  $\pi$ -donor to ruthenium center occurs at the lowest field (9.01 ppm) following the H3 in ring B and ring C. In addition, three resonances occurring at 7.42 (tt), 7.24 (tt), 7.11 (dd) ppm can be assigned to the protons H10, H9, H8 of Clazpy ligand, respectively which due to electron rich in ring. Other protons were also studied by using simple correlation  $^1\text{H}$ - $^1\text{H}$  COSY NMR spectroscopy (Figure 3.194).

The  $^{13}\text{C}$  NMR (Figure 3.195) results corresponded to the DEPT NMR (Figure 3.196) showed only one kind of methane carbons. The signals at 165.95, 157.58, 157.22, 156.93, 155.99, 155.76 and 136.25 ppm were assigned to two quaternary carbons C2, C5, C7 of Clazpy ligand and C2 of bpy, respectively. Moreover, the other  $^{13}\text{C}$  NMR signals assignments were based on  $^1\text{H}$ - $^{13}\text{C}$  HMQC NMR spectrum (Figure 3.197).

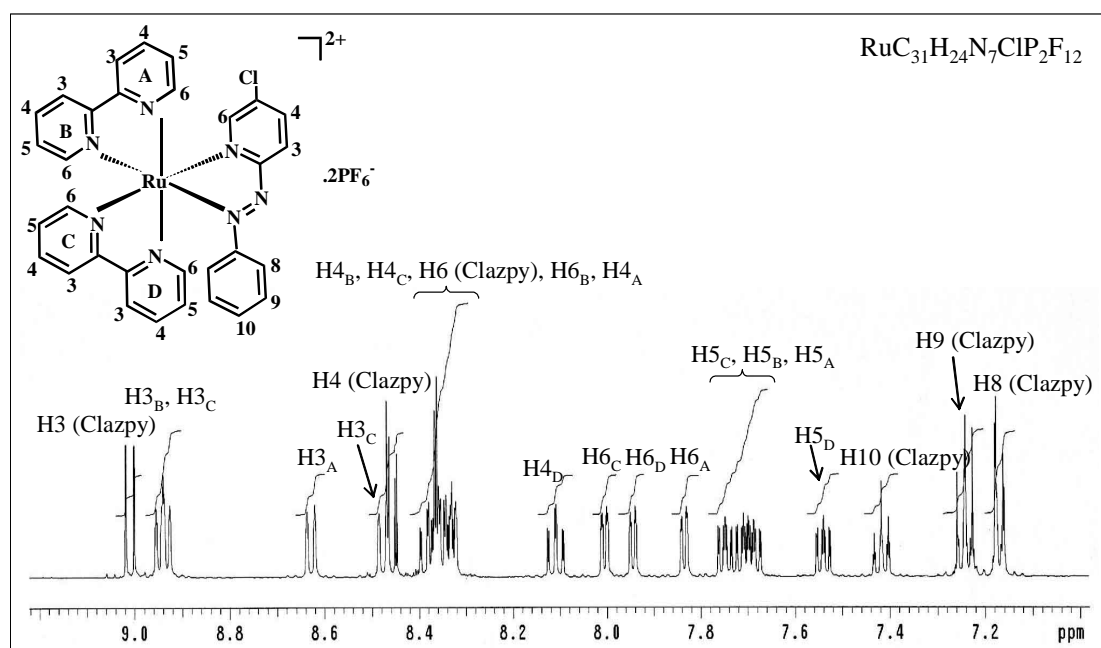


**Figure 3.193**  $^1\text{H}$  NMR spectrum of  $[\text{Ru}(\text{bpy})_2(\text{Clazpy})](\text{PF}_6)_2$  in acetone- $d_6$

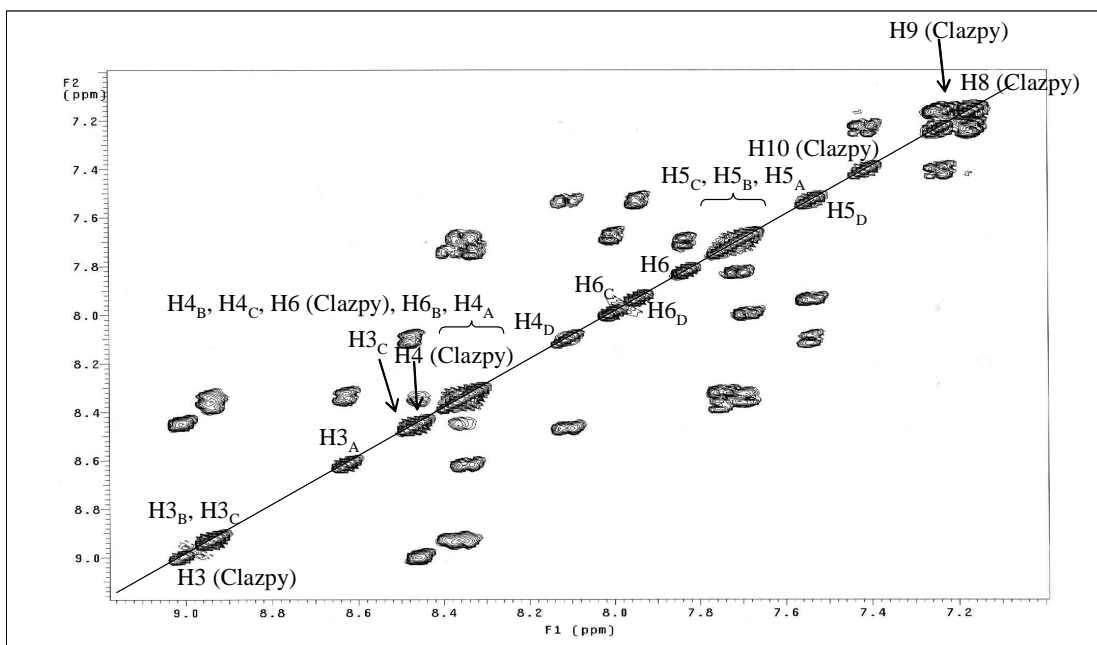


**Figure 3.194**  $^1\text{H}$ - $^1\text{H}$  NMR spectrum of  $[\text{Ru}(\text{bpy})_2(\text{Clazpy})](\text{PF}_6)_2$  in acetone- $d_6$

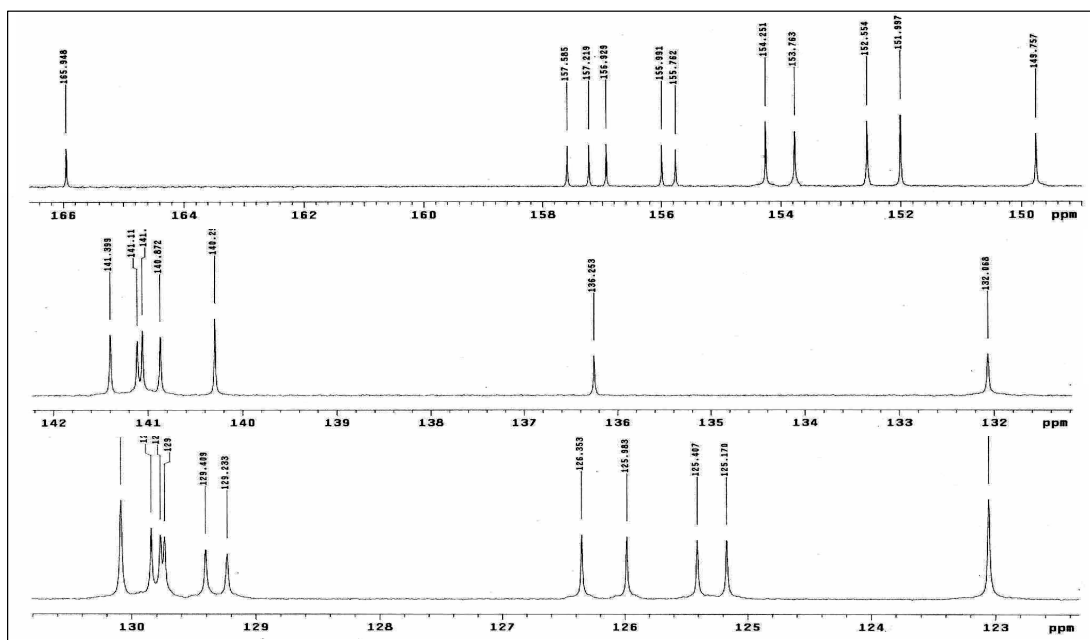


**Figure 3.195**  $^{13}\text{C}$  NMR spectrum of  $[\text{Ru}(\text{bpy})_2(\text{Clazpy})](\text{PF}_6)_2$  in acetone- $d_6$

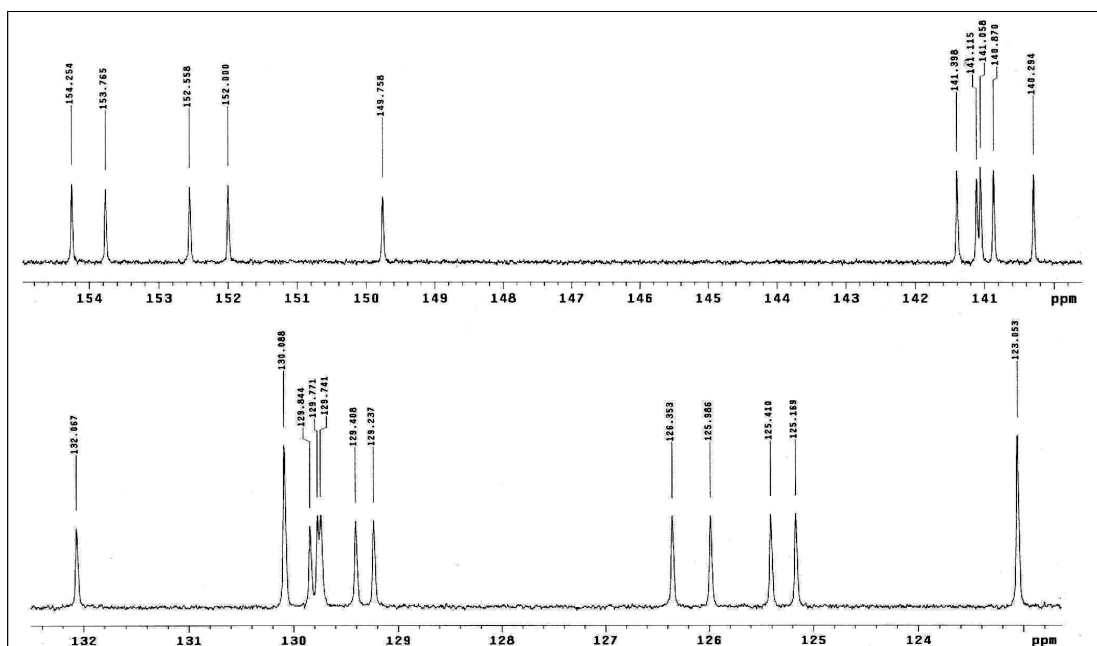


**Figure 3.196** DEPT NMR spectrum of  $[\text{Ru}(\text{bpy})_2(\text{Clazpy})](\text{PF}_6)_2$  in acetone- $d_6$

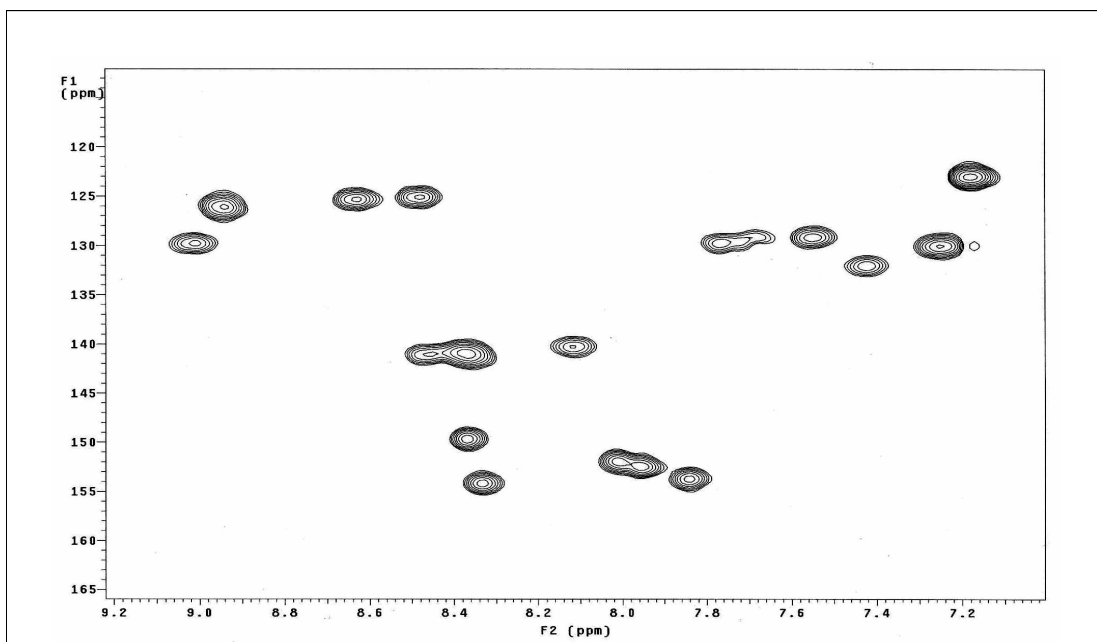


**Figure 3.197**  $^1\text{H}$ - $^{13}\text{C}$  HMQC NMR spectrum of  $[\text{Ru}(\text{bpy})_2(\text{Clazpy})](\text{PF}_6)_2$  in acetone- $d_6$



**Table 3.82**  $^1\text{H}$  and  $^{13}\text{C}$  NMR spectroscopic data of  $[\text{Ru}(\text{phen})_2(\text{Clazpy})](\text{PF}_6)_2$ 

position	$^1\text{H}$ NMR			$^{13}\text{C}$ NMR (CH-type)
	$\delta$ (ppm)	$J$ (Hz)	Amount of H	
3(Clazpy)	9.04 (d)	8.5	1	129.74
4A	9.03 (dd)	8.5, 1.0	1	139.86
7A	9.00 (dd)	8.5, 1.0	1	139.84
2A	8.96 (dd)	5.5, 1.0	1	155.68
4B	8.90 (dd)	8.5, 1.0	1	140.34
7B	8.64 (dd)	8.0, 1.0	1	138.96
5A	8.51 (d)	8.5	1	129.47
6A	8.48 (d)	8.5	1	129.33
4(Clazpy)	8.44 (dd)	8.5, 2.0	1	141.04
9A	8.42 (dd)	5.5, 1.0	1	155.07
5B	8.34 (d)	9.0	1	128.91
6(Clazpy)	8.33 (d)	2.0	1	150.32
2B	8.30 (dd)	5.5, 1.0	1	153.23
6B	8.22 (d)	9.0	1	129.18
3A	8.14 (dd)	8.5, 5.5	1	128.13
9B	8.12 (dd)	8.0, 1.0	1	153.67
8A	8.10 (dd)	8.5, 5.5	1	127.94
3B	7.85 (dd)	8.5, 5.5	1	127.57
8B	7.66 (dd)	8.0	1	127.39
10 (Clazpy)	7.19 (tt)	7.0, 1.5	1	131.93
8 (Clazpy)	7.08 (dd)	7.0, 1.5	2	122.58
9 (Clazpy)	7.01 (tt)	7.0, 1.5	2	129.63
Quaternary carbons (C)				166.28, 155.71, 148.03, 147.77, 147.46, 146.73, 136.08, 132.59, 132.44, 131.72, 131.69

d = doublet, dd = doublet of doublet, tt = triplet of triplet

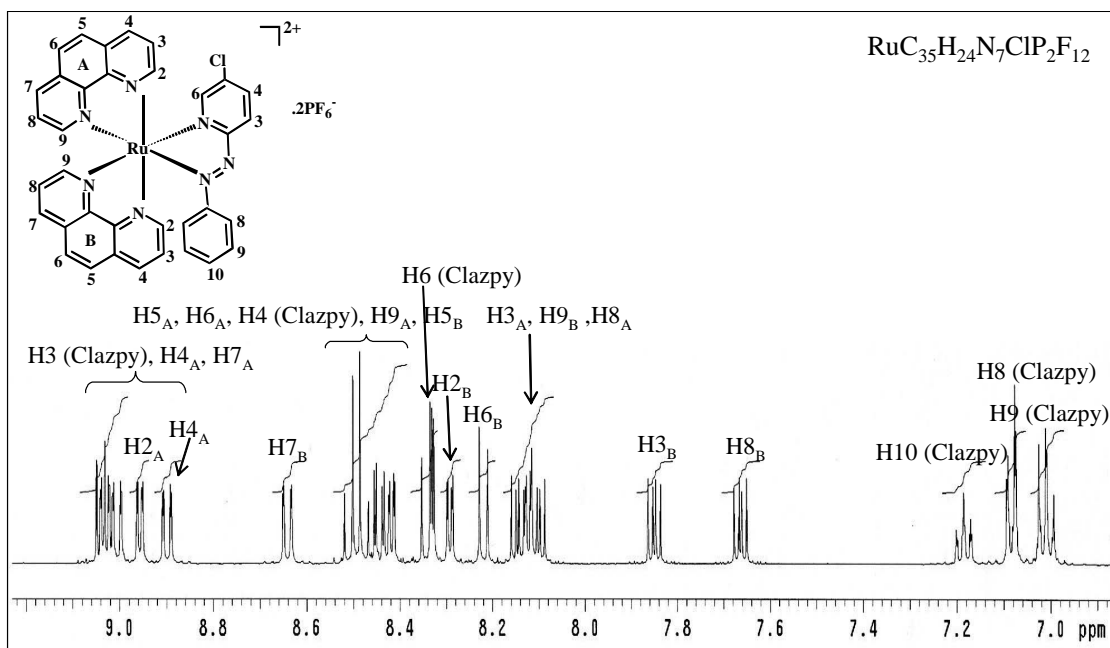


**Figure 3.198**  $^1\text{H}$  NMR spectrum of  $[\text{Ru}(\text{phen})_2(\text{Clazpy})](\text{PF}_6)_2$  in  $\text{acetone-}d_6$

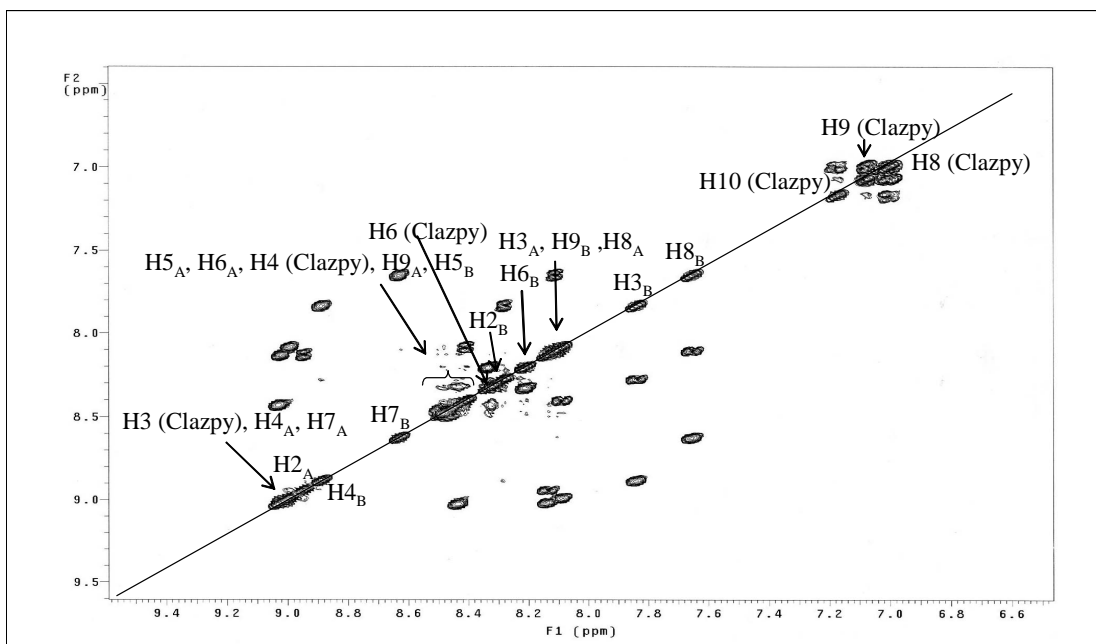


**Figure 3.199**  $^1\text{H}$ - $^1\text{H}$  COSY NMR spectrum of  $[\text{Ru}(\text{phen})_2(\text{Clazpy})](\text{PF}_6)_2$  in  $\text{acetone-}d_6$

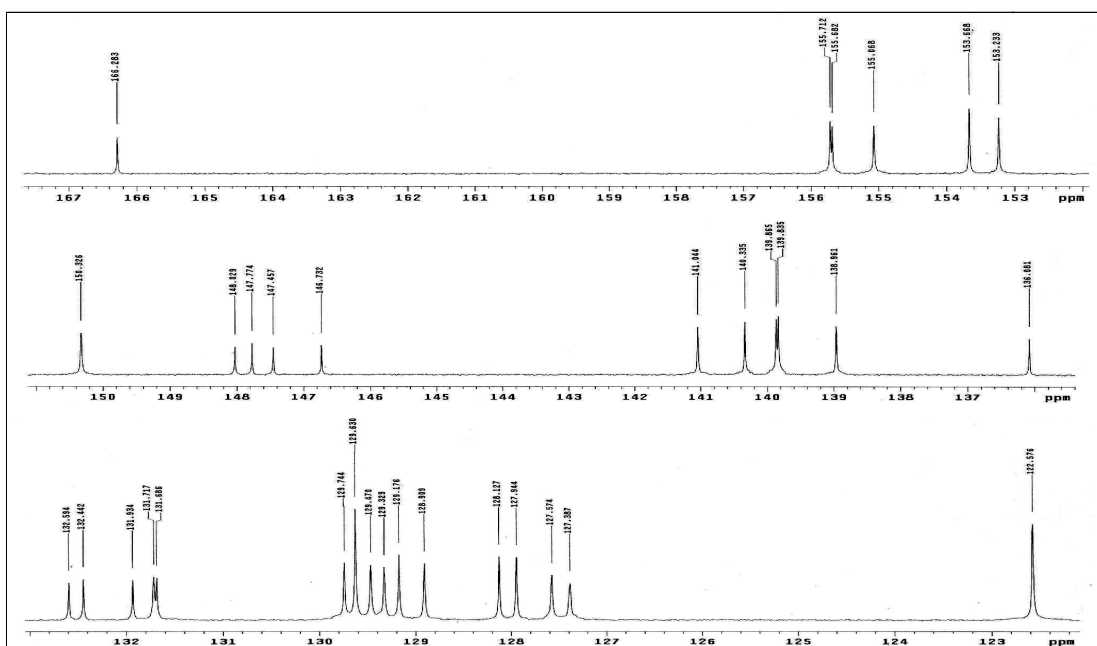


Figure 3.200  $^{13}\text{C}$  NMR spectrum of  $[\text{Ru}(\text{phen})_2(\text{Clazpy})](\text{PF}_6)_2$  in acetone- $d_6$

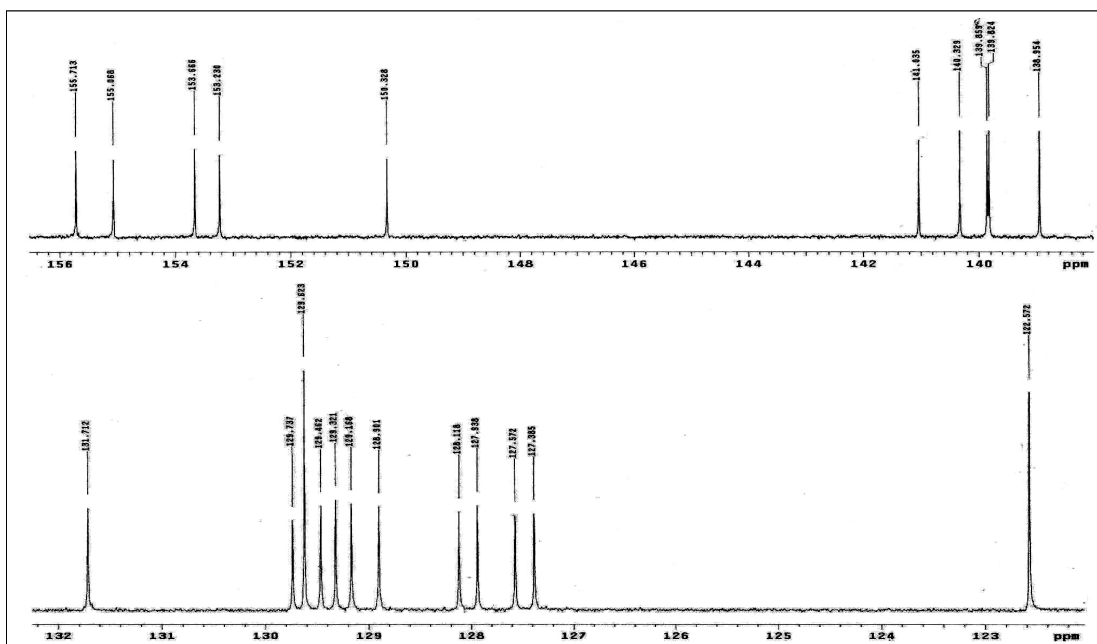
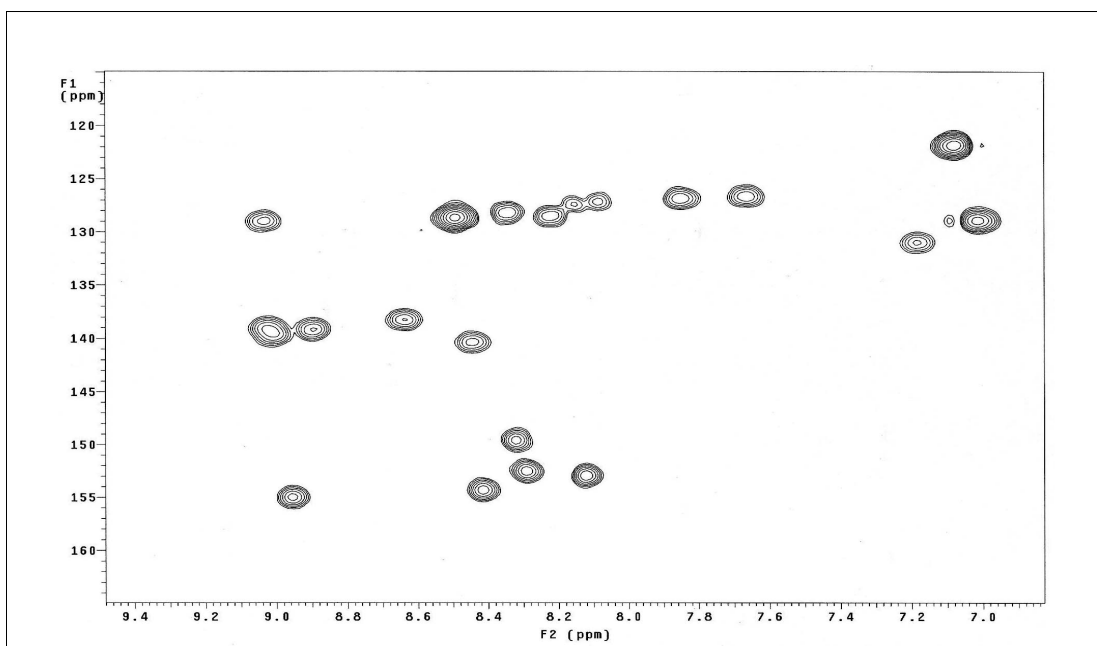
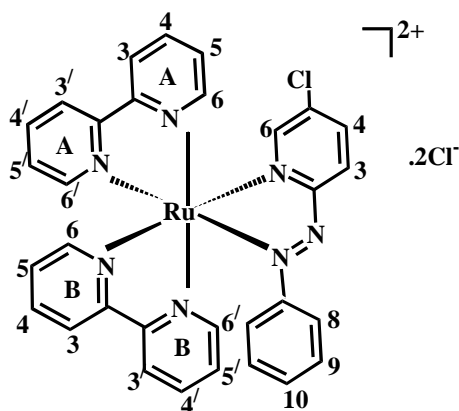


Figure 3.201 DEPT NMR spectrum of  $[\text{Ru}(\text{phen})_2(\text{Clazpy})](\text{PF}_6)_2$  in acetone- $d_6$



**Figure 3.202**  $^1\text{H}$ - $^{13}\text{C}$  HMQC NMR spectrum of  $[\text{Ru}(\text{phen})_2(\text{Clazpy})](\text{PF}_6)_2$  in acetone- $d_6$

Nuclear magnetic resonance spectroscopy of  $[\text{Ru}(\text{bpy})_2(\text{Clazpy})]\text{Cl}_2 \cdot 7\text{H}_2\text{O}$



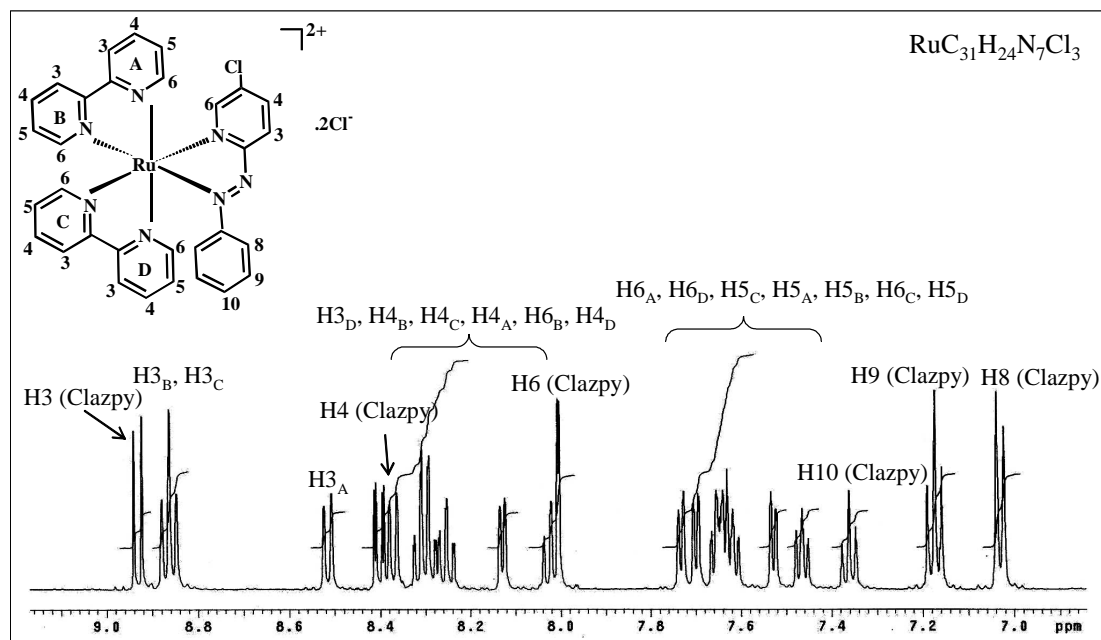
**Table 3.83**  $^1\text{H}$ - $^{13}\text{C}$  NMR spectroscopic data of  $[\text{Ru}(\text{bpy})_2(\text{Clazpy})]\text{Cl}_2 \cdot 7\text{H}_2\text{O}$ 

position	$^1\text{H}$ NMR			$^{13}\text{C}$ NMR (CH-type)
	$\delta$ (ppm)	$J$ (Hz)	Amount of H	
3(Clazpy)	8.93 (d)	8.5	1	129.54
3A', 3B	8.86 (t)	8.0	2	126.60 125.24
3A	8.52 (d)	8.0	1	125.62
4(Clazpy)	8.40 (dd)	9.0, 2.0	1	141.50
3B'	8.37 (d)	8.0	1	125.45
4A'	8.30 (d)	8.0	1	141.44
4B	8.26 (m)	-	2	141.30
4A	8.24 (m)	-		141.14
6A'	8.13 (d)	5.5	1	154.14
4B'	8.03 (dd)	8.0, 1.0	1	140.47
6(Clazpy)	8.00 (d)	2.0	1	149.18
6A	7.73 (d)	5.5	1	151.76
6B'	7.70 (d)	6.0, 1.0	1	152.38
5B	7.62 (m)	-	3	130.03
5A	7.64 (m)	-		129.86
5A'	7.65 (m)	-		129.86
6B	7.53 (d)	5.5	1	153.53
5B'	7.46 (tt)	5.5, 1.0	1	129.28
10(Clazpy)	7.36 (t)	8.0	1	132.34
9(Clazpy)	7.17 (t)	8.0	2	130.23
8(Clazpy)	7.03 (d)	8.0	2	123.12
Quaternary carbons (C)			166.22, 157.95, 157.42, 157.90, 156.23, 156.03, 137.04	

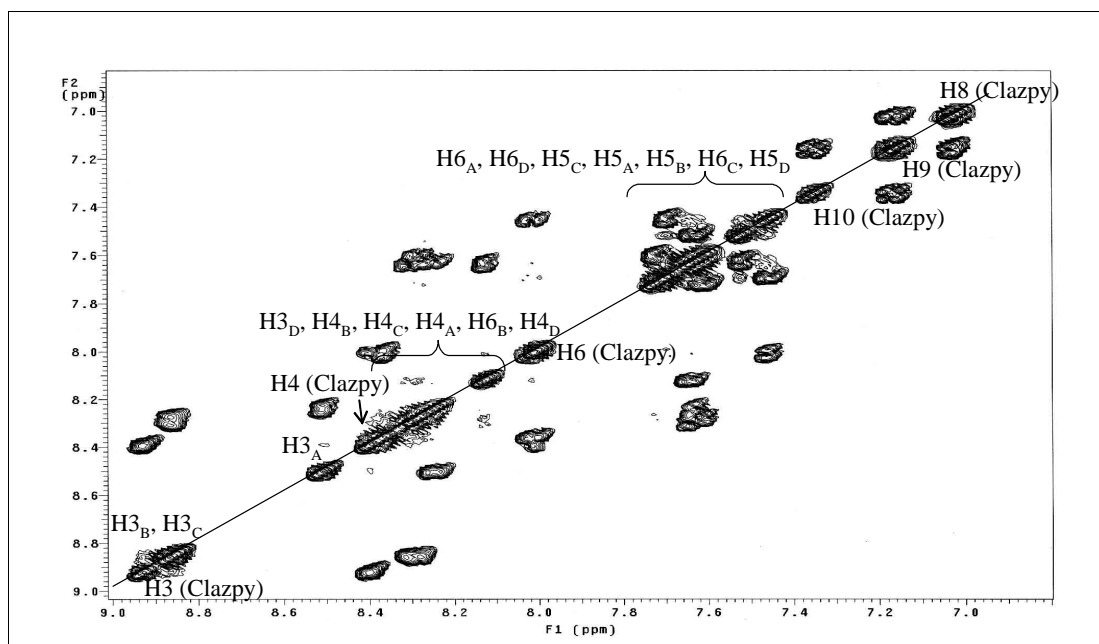
d = doublet, dd = doublet of doublet, t = triplet, tt = triplet of triplet, m = multiplet

The  $^1\text{H}$  NMR spectrum (Figure 3.203) of  $[\text{Ru}(\text{bpy})_2(\text{Clazpy})]\text{Cl}_2 \cdot 7\text{H}_2\text{O}$  complex showed 14 resonances of 24 protons because some resonances are overlapping. This result indicated that three of ligands are unsymmetrical molecules supported  $\text{C}_1$  symmetry. It is interesting to note that, due to the asymmetry of the complex, the protons in different positions (H3, H4, H5, H6) on different pyridine ring (A, B, C, D) are distinguished as defined in the structure. The coordination of nitrogen on pyridine ring of Clazpy to ruthenium(II) may lead to downfield shifting of H3 signal (8.93 ppm) as well. Others protons in this compound were also studied by using simple correlation  $^1\text{H}$ - $^1\text{H}$  COSY NMR spectroscopy (Figure 3.204).

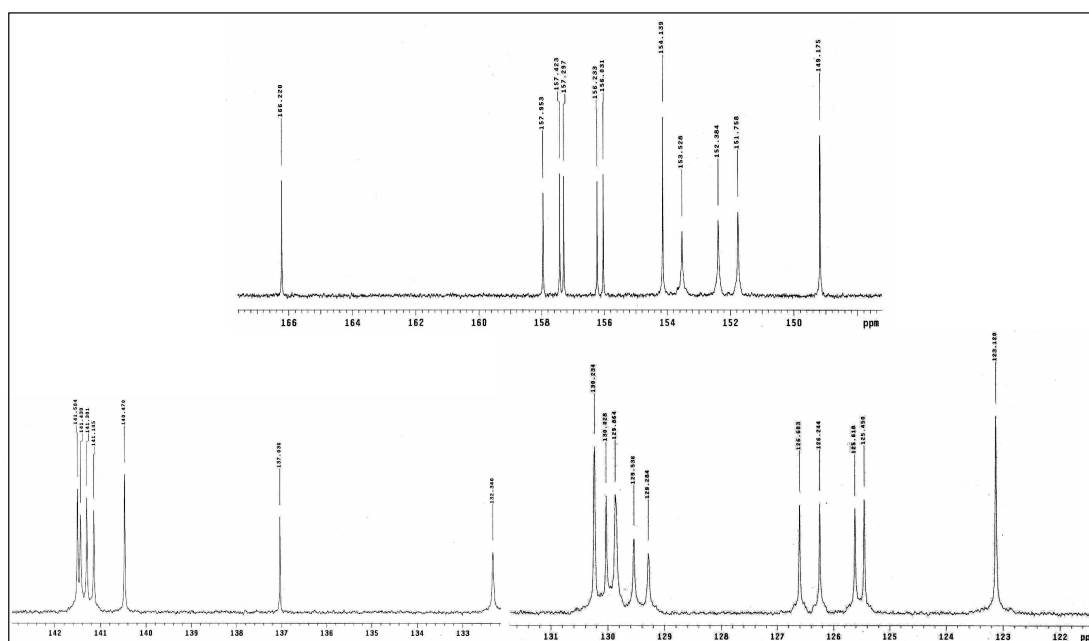
The  $^{13}\text{C}$  NMR (Figure 3.205) results corresponded to the DEPT NMR (Figure 3.206) which showed only one kind of methane carbons. All quaternary carbons at 166.22, 157.95, 157.42, 157.90, 156.23, 156.03 and 137.04 belonged to C2, C5, C7 of Clazpy ligand and C2 of two bpy ligands. Moreover, the others  $^{13}\text{C}$  NMR signals assignments were based on  $^1\text{H}$ - $^{13}\text{C}$  HMQC NMR spectrum (Figure 3.207).



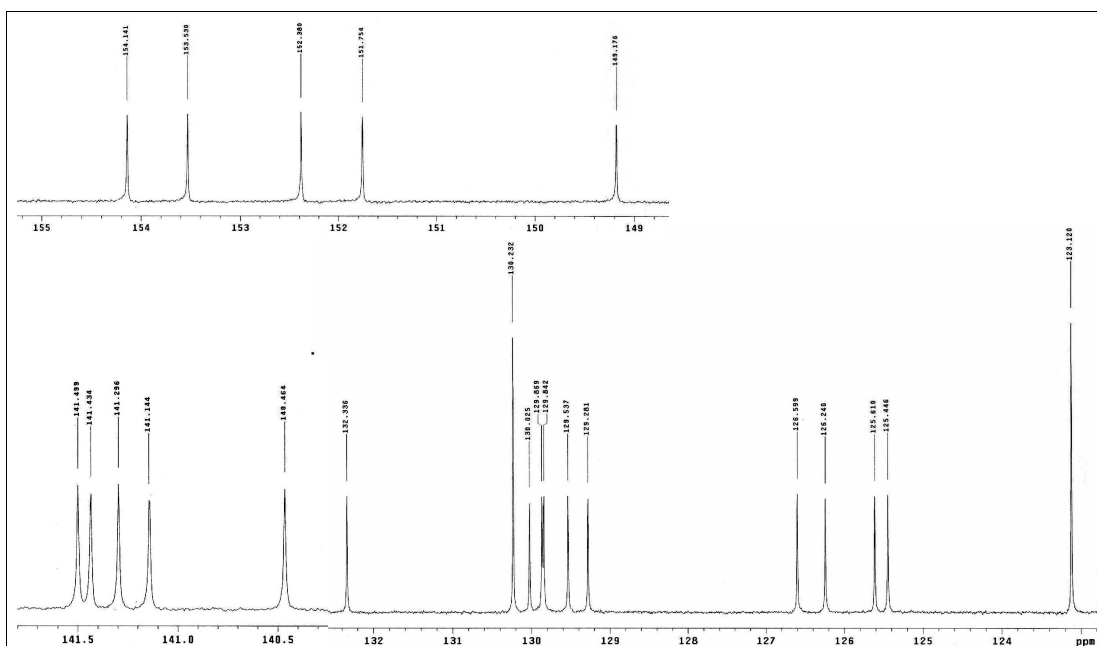
**Figure 3.203**  $^1\text{H}$  NMR spectrum of  $[\text{Ru}(\text{bpy})_2(\text{Clazpy})]\text{Cl}_2 \cdot 7\text{H}_2\text{O}$  in methanol- $d_4$



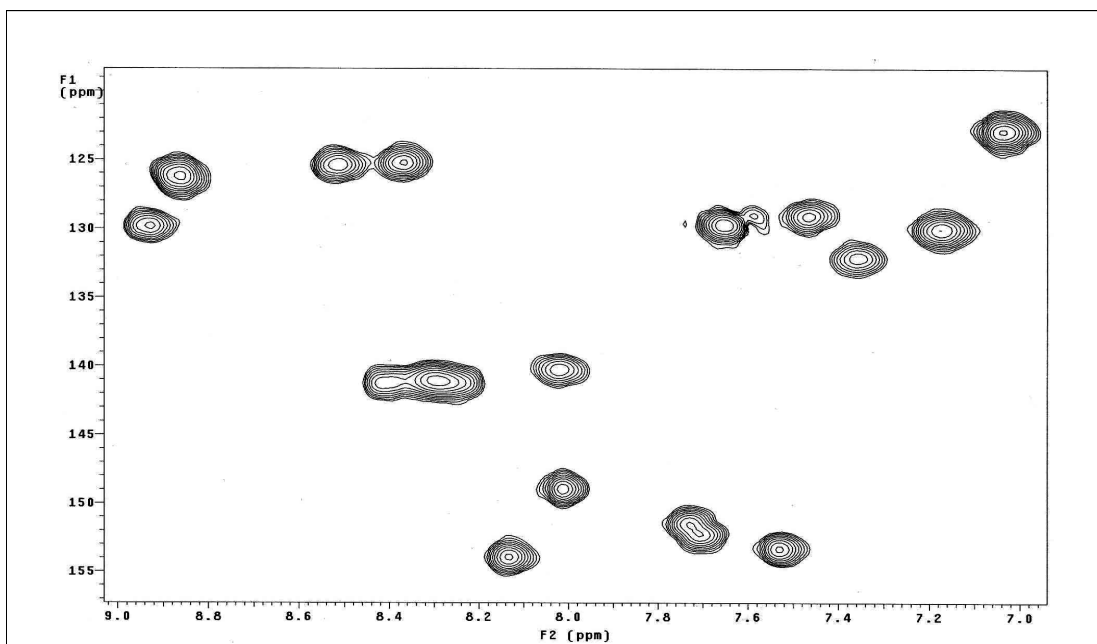
**Figure 3.204**  $^1\text{H}$ - $^1\text{H}$  COSY NMR spectrum of  $[\text{Ru}(\text{bpy})_2(\text{Clazpy})]\text{Cl}_2 \cdot 7\text{H}_2\text{O}$  in methanol- $d_4$



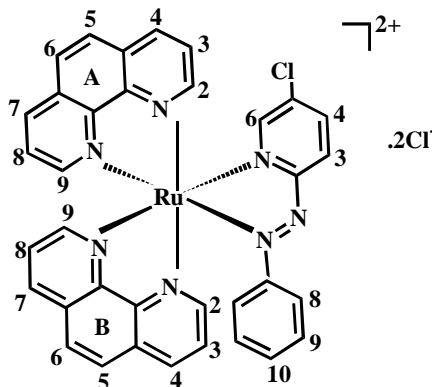
**Figure 3.205**  $^{13}\text{C}$  NMR spectrum of  $[\text{Ru}(\text{bpy})_2(\text{Clazpy})]\text{Cl}_2 \cdot 7\text{H}_2\text{O}$  in methanol- $d_4$



**Figure 3.206** DEPT NMR spectrum of  $[\text{Ru}(\text{bpy})_2(\text{Clazpy})]\text{Cl}_2 \cdot 7\text{H}_2\text{O}$  in methanol- $d_4$



**Figure 3.207**  $^1\text{H}$ - $^{13}\text{C}$  HMQC NMR spectrum of  $[\text{Ru}(\text{bpy})_2(\text{Clazpy})]\text{Cl}_2 \cdot 7\text{H}_2\text{O}$  in methanol- $d_4$

Nuclear magnetic resonance spectroscopy of  $[\text{Ru}(\text{phen})_2(\text{Clazpy})]\text{Cl}_2 \cdot 8\text{H}_2\text{O}$ 

The  $^1\text{H}$  NMR spectrum (Figure 3.208) of  $[\text{Ru}(\text{phen})_2(\text{Clazpy})]\text{Cl}_2 \cdot 8\text{H}_2\text{O}$  complex showed 14 resonances of 24 protons. Some appeared to be multiple signals due to overlap of resonances. This result indicated that three of ligands are unsymmetrical molecules. In addition, the first signal exhibited at the lowest field was proton H3 (Clazpy) (8.97 ppm) on pyridine ring of Clazpy ligand which located near coordinated nitrogen on pyridine ring. In addition,  $^1\text{H}$ - $^1\text{H}$  COSY NMR spectrum (Figure 3.209) also turn out very helpful in the accurate assignment of proton resonance in the aromatic region. Other protons in this compound were also studied by using this simple correlation spectroscopy.

The  $^{13}\text{C}$  NMR (Figure 3.210) results corresponded to the DEPT NMR (Figure 3.211) which showed only one kind of methane carbons. All quaternary carbons at 166.55, 155.94, 148.27, 147.85, 147.70, 146.84, 136.98, 133.00, 132.84, 132.28 and 132.12 belonged to C2, C5, C7 of Clazpy ligand and C2 of two phen ligands. Moreover, the others  $^{13}\text{C}$  NMR signals assignments were based on  $^1\text{H}$ - $^{13}\text{C}$  HMQC NMR spectrum (Figure 3.212) which provided information regarding the interaction between the protons and the carbon atoms to which they are directly attached.

**Table 3.84**  $^1\text{H}$ - $^{13}\text{C}$  NMR spectroscopic data of  $[\text{Ru}(\text{phen})_2(\text{Clazpy})]\text{Cl}_2 \cdot 8\text{H}_2\text{O}$ 

position	$^1\text{H}$ NMR			$^{13}\text{C}$ NMR (CH-type)
	$\delta$ (ppm)	$J$ (Hz)	Amount of H	
3(Clazpy)	8.97 (d)	9.0	1	126.78
7A	8.95 (dd)	9.0, 1.0	1	140.52
4A	8.90 (dd)	9.0, 1.0	1	140.24
4B	8.83 (dd)	9.0, 1.0	1	140.22
9A	8.74 (dd)	5.0, 1.0	1	155.80
7B	8.54 (dd)	9.0, 1.5	1	139.23
5B	8.44(d)	9.0	1	129.72
6B	8.41(d)	9.0	1	129.61
4(Clazpy)	8.40 (dd)	9.0, 2.0	1	141.44
6A	8.23 (d)	9.0	1	129.09
5A	8.11 (d)	9.0	1	129.37
2A	8.09 (t)	1.0	1	154.79
8A	8.05 (-)	5.0	1	128.16
3A	8.02 (-)	3.0	1	128.08
2B	8.00 (m)	-	1	152.90
6(Clazpy)	7.97 (d)	2.0	1	149.70
9B	7.84 (d)	5.0	1	153.40
3B	7.79 (dd)	8.0, 5.0	1	127.73
8B	7.60 (dd)	8.0, 5.0	1	127.50
10	7.19 (m)	-	1	130.85
9, 8	6.94 (d)	8.0	4	129.98 122.58
Quaternary carbons (C)				166.55, 155.94, 148.27, 147.85, 147.70, 146.84, 136.98, 133.00, 132.84, 132.28, 132.12

d = doublet, dd = doublet of doublet, t = triplet, tt = triplet

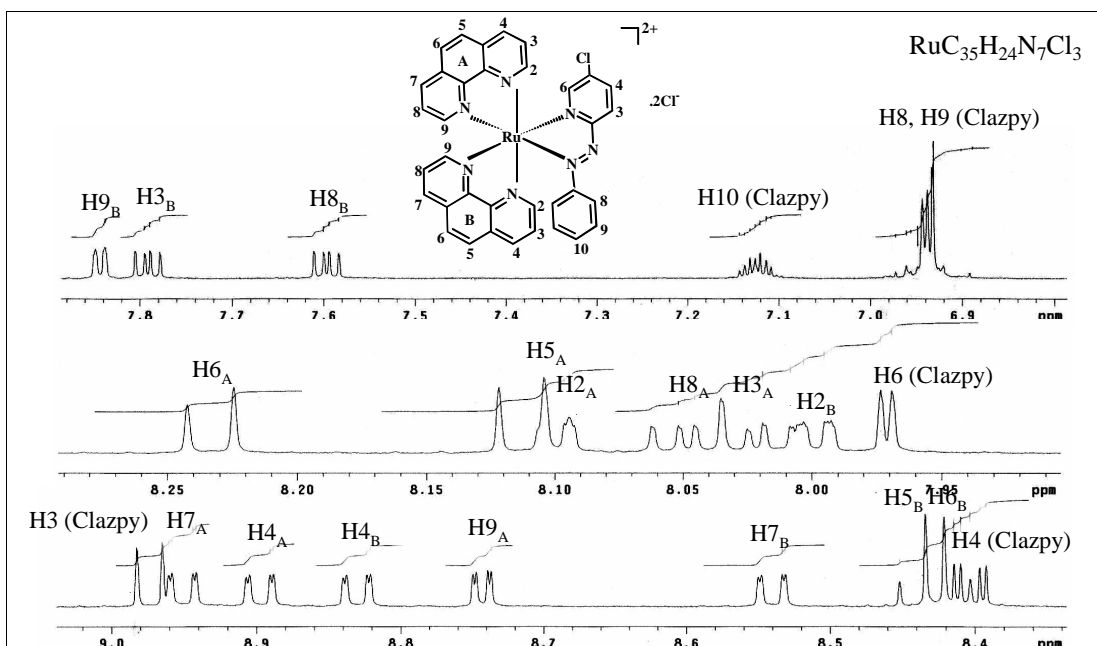


**Figure 3.208**  $^1\text{H}$  NMR spectrum of  $[\text{Ru}(\text{phen})_2(\text{Clazpy})]\text{Cl}_2 \cdot 8\text{H}_2\text{O}$  in methanol- $d_4$

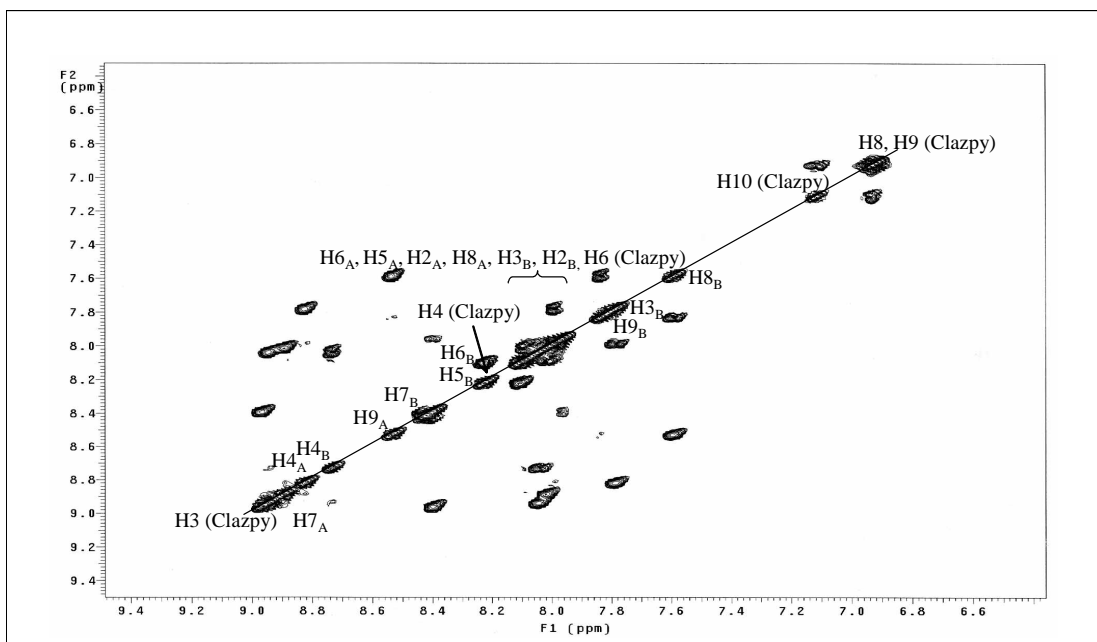


**Figure 3.209**  $^1\text{H}$ - $^1\text{H}$  COSY NMR spectrum of  $[\text{Ru}(\text{phen})_2(\text{Clazpy})]\text{Cl}_2 \cdot 8\text{H}_2\text{O}$  in methanol- $d_4$



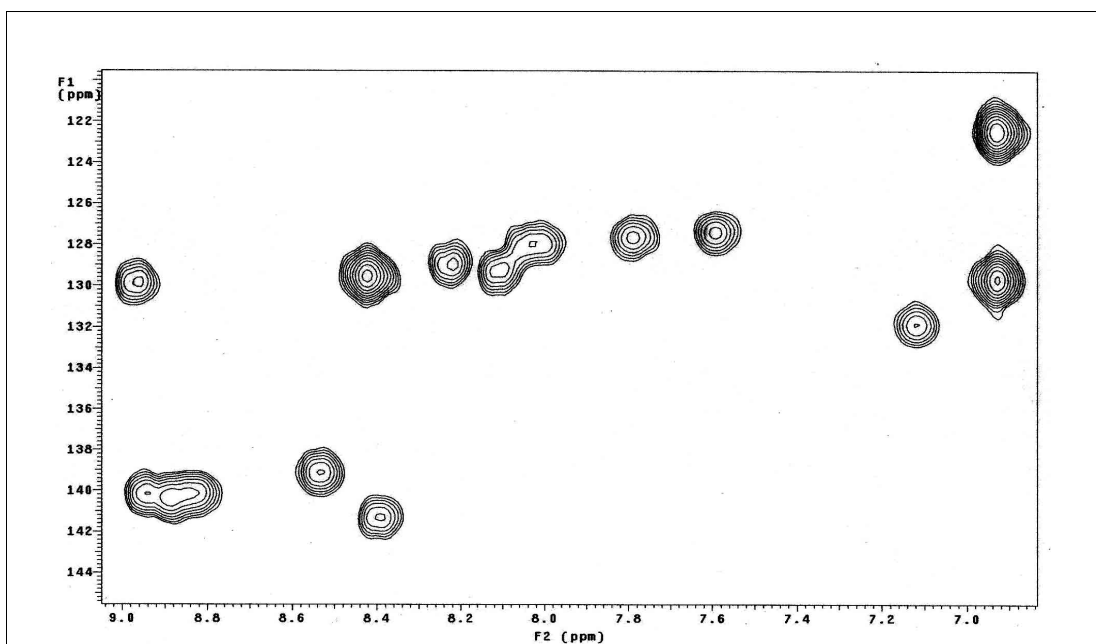


**Figure 3.212**  $^1\text{H}$ - $^{13}\text{C}$  HMQC NMR spectrum of  $[\text{Ru}(\text{phen})_2(\text{Clazpy})]\text{Cl}_2 \cdot 8\text{H}_2\text{O}$  in methanol- $d_4$

### 3.7.2.6 Cyclic voltammetry

The electrochemical activity of  $[\text{Ru}(\text{bpy})_2(\text{Clazpy})]\text{X}_2$  and  $[\text{Ru}(\text{phen})_2(\text{Clazpy})]\text{X}_2$  ( $\text{X} = \text{PF}_6^-, \text{Cl}^-$ ) was studied in  $\text{CH}_3\text{CN}$  solution by cyclic voltammetry. The results are summarized in Table 3.85 and representative voltammograms are shown in Figure 3.213 to 3.216.

**Table 3.85** Cyclic voltammetric data of [Ru(bpy)<sub>2</sub>(Clazpy)]X<sub>2</sub> and [Ru(phen)<sub>2</sub>Clazpy]X<sub>2</sub> (X = PF<sub>6</sub><sup>-</sup>, Cl<sup>-</sup>) in 0.1 M TBAH CH<sub>3</sub>CN at scan rate 50 mV/s (ferrocene as used an internal standard)

Compounds	<sup>a</sup> E <sub>1/2</sub> , V				
	Oxidation Ru(II)/(III)	Reduction			
		I	II	III	IV
[Ru(bpy) <sub>2</sub> (Clazpy)](PF <sub>6</sub> ) <sub>2</sub>	-	-0.80 (90)	-1.5 (70)	-2.01 (70)	-2.34 (110)
[Ru(phen) <sub>2</sub> (Clazpy)](PF <sub>6</sub> ) <sub>2</sub>	-	-0.81 (75)	-1.52 (75)	-2.0 (70)	-2.35 (125)
[Ru(bpy) <sub>2</sub> (Clazpy)]Cl <sub>2</sub> .7H <sub>2</sub> O	+0.86 <sup>c</sup>	-0.79 (65)	-1.52 (70)	-2.02 (80)	-2.37 (105)
[Ru(phen) <sub>2</sub> (Clazpy)]Cl <sub>2</sub> .8HO	+0.98 <sup>c</sup>	-0.80 (85)	-1.53 (75)	-2.02 (65)	-2.38 (105)

<sup>a</sup>E<sub>1/2</sub> = (E<sub>pa</sub> + E<sub>pc</sub>)/2, where E<sub>pa</sub> and E<sub>pc</sub> are anodic and cathodic peak potentials, respectively; ΔE<sub>p</sub> = E<sub>pa</sub> - E<sub>pc</sub>

<sup>b</sup>cathodic peak potential, V

<sup>c</sup>anodic peak potential, V

It is well-known that the electrochemical behavior of ruthenium(II) polypyridyl observed as a metal centered oxidation and a series of ligand-centered reduction.

### Oxidation potential

The cyclic voltammogram of [Ru(bpy)<sub>2</sub>(Clazpy)]X<sub>2</sub> and [Ru(phen)<sub>2</sub>(Clazpy)]X<sub>2</sub> (X = PF<sub>6</sub><sup>-</sup>, Cl<sup>-</sup>) complexes were studied in the range 0.00 to +1.50 V. This couple cannot be observed in PF<sub>6</sub><sup>-</sup> complexes because the redox of Ru(II)/(III) could occurred at positive potential greater than +1.50 V which is out of

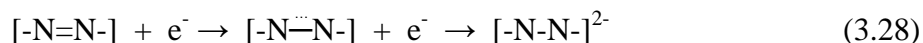
the solvent window. Whereas, the Cl<sup>-</sup> complexes show the anodic peak in this range at +0.86, +0.98 V for [Ru(bpy)<sub>2</sub>(Clazpy)]<sup>2+</sup> and [Ru(phen)<sub>2</sub>(Clazpy)]<sup>2+</sup>, respectively. Thus the chloride complexes could be easily to oxidize.

In chloride salts complexes, [Ru(bpy)<sub>2</sub>(Clazpy)]<sup>2+</sup> and [Ru(phen)<sub>2</sub>(Clazpy)]<sup>2+</sup>, the ancillary ligand phen of the later expands the  $\pi$ -delocalization and thus decreases the  $\pi$ -donor capacity coordination to central Ru ion, leading greater  $\pi$ -accepting ability stabilize to Ru(II) center. As a result, the oxidation potential of complex [Ru(phen)<sub>2</sub>(Clazpy)]<sup>2+</sup> is more positively.

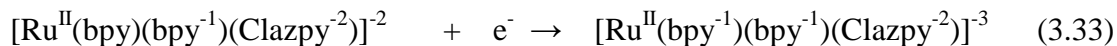
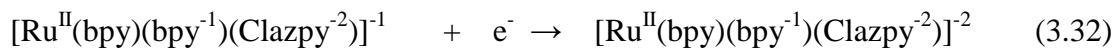
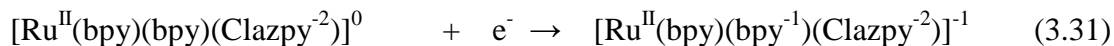
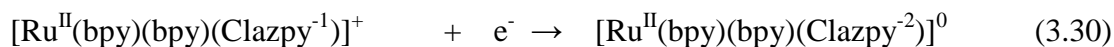
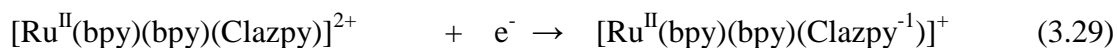
As expected, the combination of two L ligands and one Clazpy around the Ru(II) center, the oxidation potential of [Ru(L)<sub>2</sub>(Clazpy)](PF<sub>6</sub>)<sub>2</sub> (L = bpy and phen) was more positive than that of [Ru(bpy)<sub>3</sub>]<sup>2+</sup> (+1.09 V) and [Ru(phen)<sub>3</sub>]<sup>2+</sup> (+1.08 V). Consequently, the oxidative Ru(III)/(II) couple of [Ru(L)<sub>2</sub>(Clazpy)](PF<sub>6</sub>)<sub>2</sub> (L = bpy and phen) occurred out of solvent window in the same condition.

### Reduction potential

In the range 0.00 to -2.60 V, four successive reduction responses of [Ru(bpy)<sub>2</sub>(Clazpy)]X<sub>2</sub> and [Ru(phen)<sub>2</sub>(Clazpy)]X<sub>2</sub> (X = PF<sub>6</sub><sup>-</sup>, Cl<sup>-</sup>) were observed under similar condition. Moreover, the first reduction potential of all compounds appeared in the same range 0.79-0.81 V with separation peak by 65-110 mV. The first reduction is controlled by the ligand having the most lowest unoccupied molecular orbital (LUMO) which possible characterized by the azoimine function (Pal *et al.*, 2000). It was assigned to a reduction centered on Clazpy, and the last reduction is characterized of the co-ligand (bpy or phen). The azo group can accommodate up to two electrons stepwise at the LUMO as in following equation:



The expected reduction processes of [Ru(bpy)<sub>2</sub>(Clazpy)]<sup>2+</sup> are displayed in equation 3.29 to 3.33.



In the case of  $[\text{Ru}(\text{phen})_2(\text{Clazpy})]^{2+}$ , the process also had similar reduction behavior and reduction potential values to the  $[\text{Ru}(\text{bpy})_2(\text{Clazpy})]^{2+}$ . Moreover, the expected four reductions was also similar to those of the above complex.

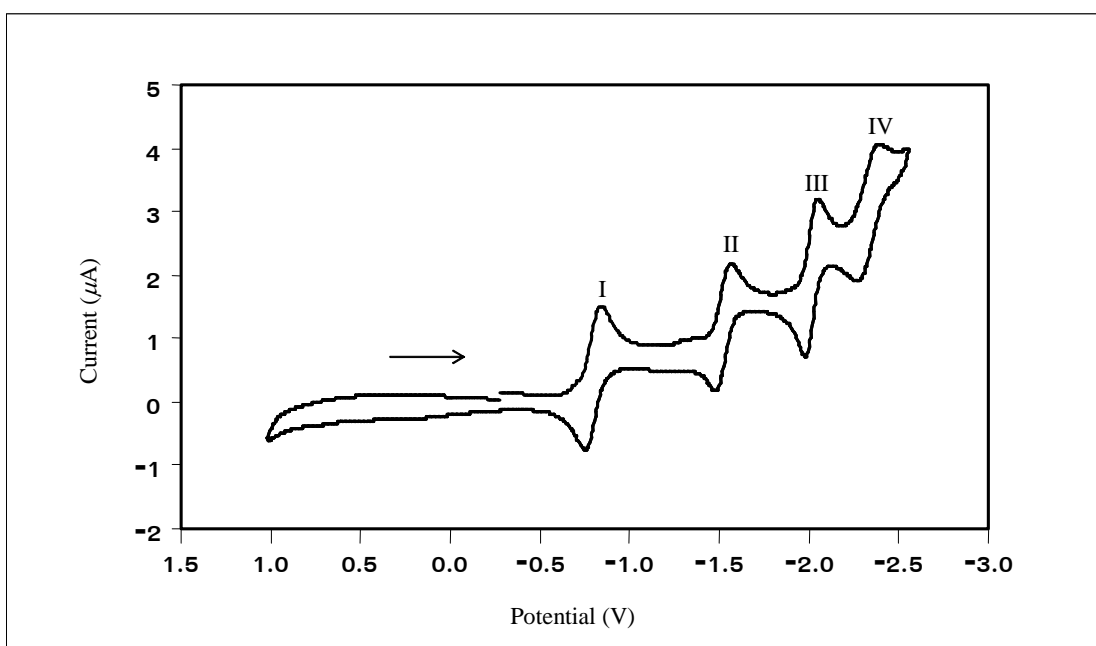


**Figure 3.213** Cyclic voltammogram of  $[\text{Ru}(\text{bpy})_2(\text{Clazpy})](\text{PF}_6)_2$  in 0.1 M TBAH  $\text{CH}_3\text{CN}$  at scan rate 50 mV/s (ferrocene as an internal standard)

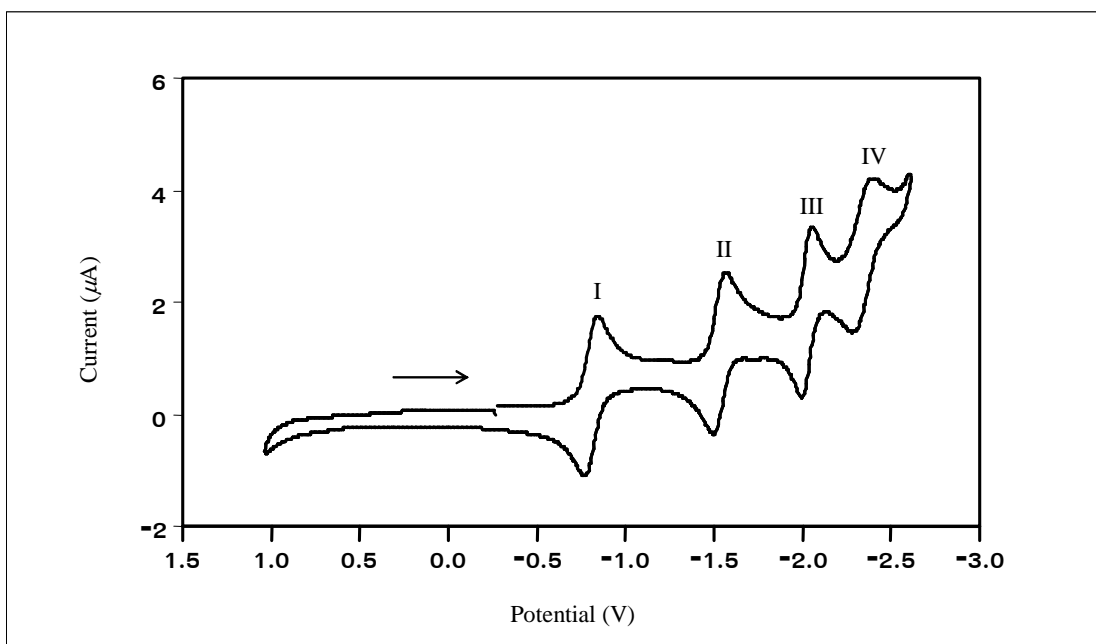


**Figure 3.214** Cyclic voltammogram of  $[\text{Ru}(\text{phen})_2(\text{Clazpy})](\text{PF}_6)_2$  in 0.1 M TBAH  $\text{CH}_3\text{CN}$  at scan rate 50 mV/s (ferrocene as an internal standard)

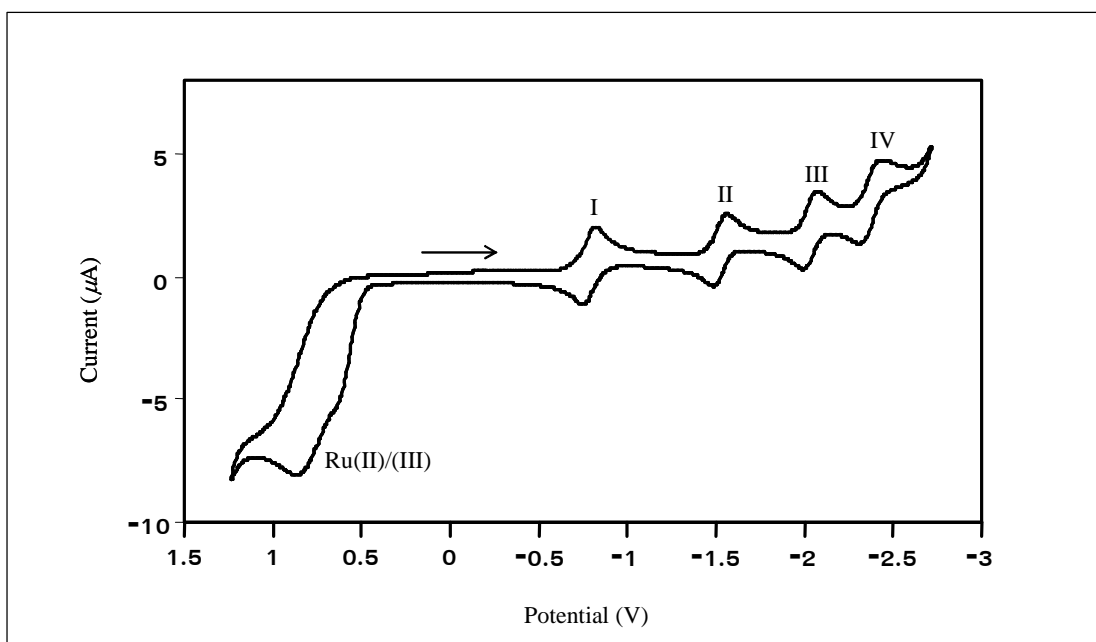


**Figure 3.215** Cyclic voltammogram of  $[\text{Ru}(\text{bpy})_2(\text{Clazpy})]\text{Cl}_2 \cdot 7\text{H}_2\text{O}$  in 0.1 M TBAH  $\text{CH}_3\text{CN}$  at scan rate 50 mV/s (ferrocene as an internal standard)

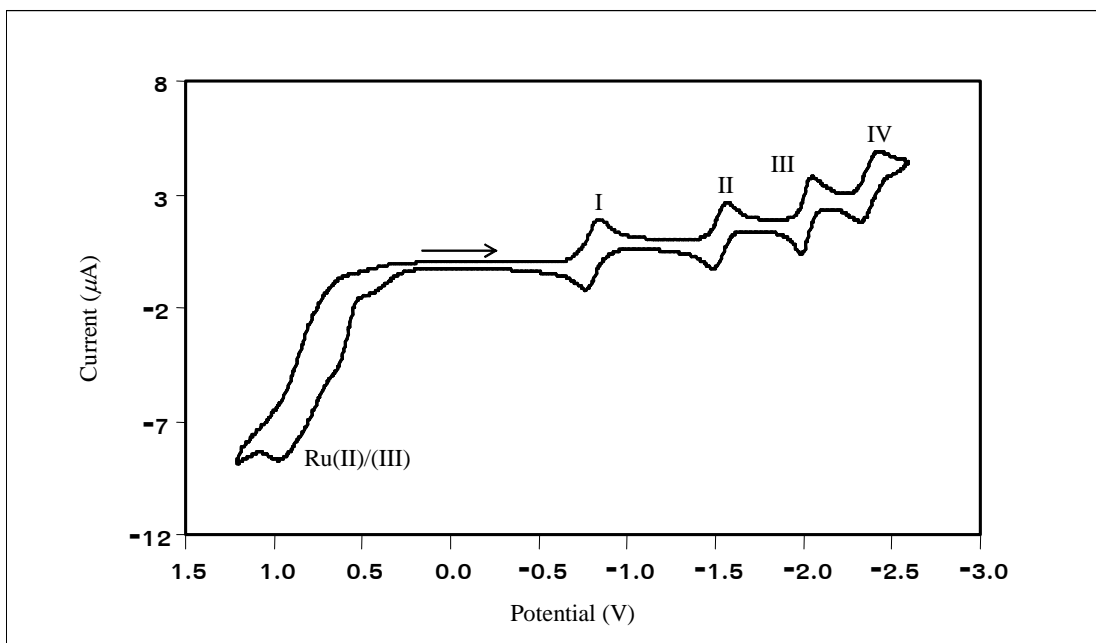


**Figure 3.216** Cyclic voltammogram of  $[\text{Ru}(\text{phen})_2(\text{Clazpy})]\text{Cl}_2 \cdot 8\text{H}_2\text{O}$  in 0.1 M TBAH  $\text{CH}_3\text{CN}$  at scan rate 50 mV/s (ferrocene as an internal standard)

### 3.8 DNA-binding experiment

In present work, new water-soluble complexes of Ru(II) were prepared and successfully characterized. Their interaction with CT-DNA was carried out.

- 1  $[\text{Ru}(\text{Clazpy})_2(\text{bpy})]\text{Cl}_2 \cdot 7\text{H}_2\text{O}$
- 2  $[\text{Ru}(\text{Clazpy})_2(\text{phen})]\text{Cl}_2 \cdot 8\text{H}_2\text{O}$
- 3  $[\text{Ru}(\text{Clazpy})_2(\text{azpy})]\text{Cl}_2 \cdot 4\text{H}_2\text{O}$
- 4  $[\text{Ru}(\text{Clazpy})_3]\text{Cl}_2 \cdot 3\text{H}_2\text{O}$
- 5  $[\text{Ru}(\text{Clazpy})_2(\text{bpy})](\text{NO}_3)_2 \cdot 5\text{H}_2\text{O}$
- 6  $[\text{Ru}(\text{Clazpy})_2(\text{phen})](\text{NO}_3)_2 \cdot 3\text{H}_2\text{O}$
- 7  $[\text{Ru}(\text{Clazpy})_2(\text{azpy})](\text{NO}_3)_2 \cdot \text{H}_2\text{O}$
- 8  $[\text{Ru}(\text{Clazpy})_3](\text{NO}_3)_2 \cdot 5\text{H}_2\text{O}$
- 9  $[\text{Ru}(\text{bpy})_2(\text{Clazpy})]\text{Cl}_2 \cdot 7\text{H}_2\text{O}$
- 10  $[\text{Ru}(\text{phen})_2(\text{Clazpy})]\text{Cl}_2 \cdot 8\text{H}_2\text{O}$

It should be noted that all ten new complexes were isolated in their racemic forms and that the DNA-binding behaviors described below are a composite of those of two enantiomer. The interaction of these new complexes with DNA was monitored by the absorption titration method, viscosity measurement, emission study and electrochemical behaviors using chloride and nitrate salts complexes as described previously. The absorption spectra of which in aqueous buffered solutions were found to be nearly identical to the corresponding spectra of the  $\text{PF}_6^-$  salts in  $\text{CH}_3\text{CN}$ .

#### 3.8.1 Absorption spectroscopic studies

The application of electronic absorption spectroscopy in DNA-binding studies is one of the most useful techniques (Barton *et al.*, 1984) which can monitor the interaction of a metal complexes and DNA. In general, complex bound to DNA through intercalation resulting in hypochromism and red shift (bathochromism), due

to the strong stacking interaction between aromatic chromophore of the complex and the base pair of DNA (Wang *et al.*, 2004).

The absorption spectra of all complexes with increasing concentration of calf thymus DNA were shown in 3.217 to 3.226. In all cases, although no obvious red shift was found, hypochromicities were observed. For example, when the amount of DNA was increased, a decrease of 6.42% and 6.88% in the  $\pi \rightarrow \pi^*$  and MLCT transition are found for complex  $[\text{Ru}(\text{Clazpy})_2(\text{bpy})]\text{Cl}_2 \cdot 7\text{H}_2\text{O}$ . These spectroscopic changes suggest that there are some interactions between the Ru(II) complex and DNA. This result could explain that since DNA is a polyanion composed of two complementary, polymeric subunit hydrogen bonded together in the form of right-handed double helix, cationic binding agent of  $[\text{Ru}(\text{Clazpy})_2(\text{L})]^{2+}$  or  $[\text{Ru}(\text{L}')_2(\text{Clazpy})]^{2+}$  ( $\text{L}' = \text{bpy}, \text{phen}$ ) bind to DNA via replace its from the compact inner (stern) layer or the diffuse outer layer surrounding DNA and interact with the anionic phosphate residues of DNA (Mahadevan and Palaniandavar, 1998).

To compare quantitatively the affinity of the complexes bound to CT-DNA, the intrinsic binding constant  $K_b$  of all complexes with DNA were obtained by monitoring the changes of absorbance with increasing concentration of DNA using the following equation (3.34) and are listed in Table 3.86.

$$[\text{DNA}]/(\varepsilon_a - \varepsilon_f) = [\text{DNA}]/(\varepsilon_b - \varepsilon_f) + 1/[K_b(\varepsilon_b - \varepsilon_f)] \quad (3.34)$$

where  $[\text{DNA}]$  is the concentration of DNA in base pair, the apparent absorption coefficients  $\varepsilon_a$ ,  $\varepsilon_f$  and  $\varepsilon_b$  correspond to  $A_{\text{obsd}}/[\text{Ru}]$ , the extinction coefficient for the free ruthenium complex and in the fully bound form, respectively. In plot  $[\text{DNA}]/(\varepsilon_a - \varepsilon_f)$  vs  $[\text{DNA}]$ ,  $K_b$  is given by the ratio of slope to the y intercept (Nair *et al.*, 1998).

**Table 3.86** UV-Visible absorption spectroscopic data of Ru(II) complexes upon addition of CT-DNA in 5 mM Tris/ 50 mM NaCl pH 7.1

Complexes	$\lambda_{\max}$		Binding constant, $K_b$ ( $M^{-1}$ )
	nm	Hypochromism <sup>a</sup> (%)	
[Ru(Clazpy) <sub>2</sub> (bpy)]Cl <sub>2</sub> .7H <sub>2</sub> O	382	6.42	(6.2±0.1) x 10 <sup>4</sup>
	518	6.88	(1.2±0.1) x 10 <sup>5</sup>
[Ru(Clazpy) <sub>2</sub> (phen)]Cl <sub>2</sub> .8H <sub>2</sub> O	380	6.36	(6.4±0.5) x 10 <sup>4</sup>
	518	6.56	(1.4±0.2) x 10 <sup>5</sup>
[Ru(Clazpy) <sub>2</sub> (azpy)]Cl <sub>2</sub> .4H <sub>2</sub> O	382	7.66	(4.6±0.5) x 10 <sup>4</sup>
	494	5.74	(1.1±0.1) x 10 <sup>5</sup>
[Ru(Clazpy) <sub>3</sub> ]Cl <sub>2</sub> .3H <sub>2</sub> O	384	8.96	(7.1±0.6) x 10 <sup>4</sup>
	491	6.17	(1.2 ±0.1)x 10 <sup>5</sup>
[Ru(Clazpy) <sub>2</sub> (bpy)](NO <sub>3</sub> ) <sub>2</sub> .5H <sub>2</sub> O	381	7.38	(8.2±0.2) x 10 <sup>4</sup>
	518	7.56	(1.0±0.1) x 10 <sup>5</sup>
[Ru(Clazpy) <sub>2</sub> (phen)](NO <sub>3</sub> ) <sub>2</sub> .3H <sub>2</sub> O	380	8.43	(5.5±0.7) x 10 <sup>4</sup>
	518	8.58	(7.4±0.6) x 10 <sup>4</sup>
[Ru(Clazpy) <sub>2</sub> (azpy)](NO <sub>3</sub> ) <sub>2</sub> .H <sub>2</sub> O	381	7.56	(4.5±0.7) x 10 <sup>4</sup>
	494	6.74	(1.2±0.1) x 10 <sup>5</sup>
[Ru(Clazpy) <sub>3</sub> ](NO <sub>3</sub> ) <sub>2</sub> .5H <sub>2</sub> O	384	9.21	(4.5±0.7) x 10 <sup>4</sup>
	490	7.42	(1.3±0.2) x 10 <sup>5</sup>
[Ru(bpy) <sub>2</sub> (Clazpy)]Cl <sub>2</sub> .7H <sub>2</sub> O	361	4.17	(6.5±0.1) x 10 <sup>4</sup>
	449	5.52	(8.8±0.4) x 10 <sup>4</sup>
[Ru(phen) <sub>2</sub> (Clazpy)]Cl <sub>2</sub> .8H <sub>2</sub> O	344	5.73	(1.8±0.6) x 10 <sup>5</sup>
	498	5.27	(1.8±0.2) x 10 <sup>5</sup>

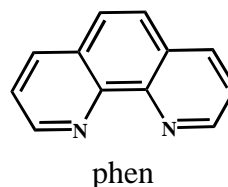
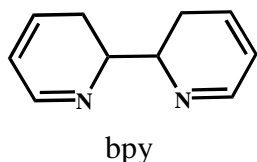
<sup>a</sup> Hypochromism =  $[(A_{\text{free}} - A_{\text{bound}})/A_{\text{free}}] \times 100 \%$

The typical plot of [DNA] versus [DNA]/( $\epsilon_a - \epsilon_f$ ) are shown for the titration of CT-DNA in Figure 3.217-3.226. The plots were constructed according to eq. (3.34), affording the ratio of the slope to the intercept *i.e.* binding constant ( $K_b$ ).

### 3.8.1.1 Complexes containing the [Ru<sup>II</sup>(Clazpy)<sub>2</sub>] center

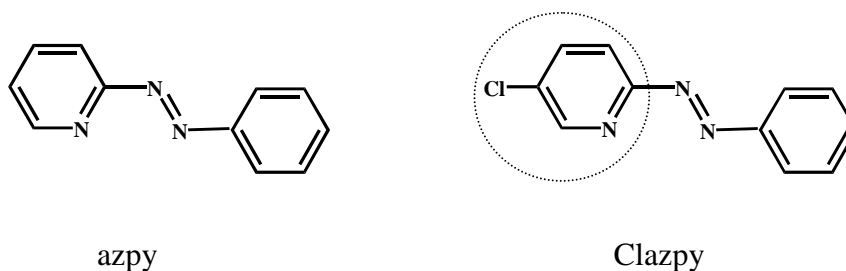
For the [Ru(Clazpy)<sub>2</sub>(L)]<sup>2+</sup> (L = bpy, phen, azpy, Clazpy) complexes, the extent of this effect greatly depended on the nature of the ligand attached to the [Ru<sup>II</sup>(Clazpy)<sub>2</sub>] center. This group can be divided into two parts according to the third ligand (polypyridyl and azoimine) for discussion and comparison.

The first part contains polypyridyl ligand as the third ligand, [Ru(Clazpy)<sub>2</sub>(bpy)]<sup>2+</sup> and [Ru(Clazpy)<sub>2</sub>(phen)]<sup>2+</sup>. The interaction of the later complex with CT-DNA is slightly greater than that of the former. This may be due to the different shape and planarity of the main ligand. From structure, the phen ligand has more fit planarity than bpy to stack or overlap with the base pair of DNA resulting in more  $K_b$  values of [Ru(Clazpy)<sub>2</sub>(phen)]<sup>2+</sup> than that of [Ru(Clazpy)<sub>2</sub>(bpy)]<sup>2+</sup>. It is concluded that the DNA-binding mode involving the complete insertion of the planar molecule between the base pairs.



However, the complexes with NO<sub>3</sub><sup>-</sup> salt give conversely result. It is to assume that the NO<sub>3</sub><sup>-</sup> group employs in ionic interaction with Na<sup>+</sup> on the surface of DNA may obstruct the interaction of complexes having more hydrophobicity with CT-DNA.

In the case of [Ru(Clazpy)<sub>2</sub>(azpy)]<sup>2+</sup> and [Ru(Clazpy)<sub>3</sub>]<sup>2+</sup>, containing only azoimine ligands, the binding of [Ru(Clazpy)<sub>3</sub>]<sup>2+</sup> with DNA is grater than that of [Ru(Clazpy)<sub>2</sub>(azpy)]<sup>2+</sup>. It is interesting that the Clazpy having chloride atom on pyridine ring may be more assist them into base pair of DNA than azpy resulting in increasing of binding affinity.



From absorption spectroscopic data, we summarized the interaction of  $[\text{Ru}(\text{Clazpy})_2]^{2+}$  core center where L are azpy and Clazpy with DNA is stronger than that of those complexes where L are bpy and phen.

### 3.8.1.2 Complexes containing the $[\text{Ru}^{\text{II}}(\text{bpy})_2]$ and $[\text{Ru}^{\text{II}}(\text{phen})_2]$

In the case of  $[\text{Ru}(\text{L})_2(\text{Clazpy})]^{2+}$  (L = bpy, phen), addition of CT-DNA to  $[\text{Ru}(\text{phen})_2(\text{Clazpy})]^{2+}$  resulted in different absorption changes than  $[\text{Ru}(\text{bpy})_2(\text{Clazpy})]^{2+}$  in UV-Visible region. The results from Table 3.86 showed that the interaction of  $[\text{Ru}(\text{phen})_2(\text{Clazpy})]^{2+}$  with DNA was greater than that of  $[\text{Ru}(\text{bpy})_2(\text{Clazpy})]^{2+}$ . In addition, the  $K_b$  values for  $[\text{Ru}(\text{L})_2(\text{Clazpy})]^{2+}$  (L = bpy, phen) were more than 10 times larger than those obtained for  $[\text{Ru}(\text{bpy})_3]^{2+}$  and  $[\text{Ru}(\text{phen})_3]^{2+}$ . Thus the presence of the Clazpy ligand had an effect to increase affinity toward the CT-DNA. Moreover, the steric interaction between nonintercalated (ancillary ligand) two ligands and the outer region of DNA is expected to have a prominent effect (Naing *et al.*, 1995). We summarized related structures of ancillary ligand bpy and phen in Table 3.87.

**Table 3.87** Electronic absorption spectral data upon addition of CT-DNA

Complexes	$K_b$	Kind of interaction
$[\text{Ru}(\text{bpy})_3]^{2+}$	-	electrostatic interaction (Yang <i>et al.</i> , 1997)
$[\text{Ru}(\text{bpy})_2(\text{NMIP})]^{2+}$ (NMIP = 2'-(2''-nitro-3'',4''-methylenedioxy phenyl)imidazo-[4',5'-f][1,10]-phenanthroline)	$1.15 \pm 0.5 \times 10^4$	Partial intercalation (Tan and Chao, 2007)
$[\text{Ru}(\text{bpy})_2(\text{dpq})]^{2+}$ (dpq = dipyrido[3,2-d:2',3'-f]quinoxaline)	$5.9 \times 10^4$	Intercalation (Han <i>et al.</i> , 2004)
$[\text{Ru}(\text{bpy})_2(\text{dppz})]^{2+}$ (dppz = dipyridophenazine)	$4.9 \times 10^6$	Intercalation (Liu <i>et al.</i> , 1999)
$[\text{Ru}(\text{bpy})_2(\text{MPPIP})]^{2+}$ MPPIP = 2-(3'-phenoxyphenyl)imidazo[4,5-f]-[1,10]phenanthroline)	$4.11 \times 10^4$	Intercalation (Tan <i>et al.</i> , 2007)
$[\text{Ru}(\text{bpy})_2(\text{BPIP})]^{2+}$ BPIP = 2-(4'-benzyloxyphenyl)imidazo[4,5-f]-[1,10]phenanthroline)	$2.97 \times 10^4$	Intercalation (Tan <i>et al.</i> , 2007)
$[\text{Ru}(\text{bpy})_2(\text{BPIP})]^{2+}$ BPIP = 2-(4'-biphenyl)imidazo[4,5-f][1,10]phenanthroline)	$7.1 \times 10^4$	Intercalation (Tan <i>et al.</i> , 2007)
$[\text{Ru}(\text{phen})_3]^{2+}$	$5.5 \times 10^3$	Intercalation (Pyle <i>et al.</i> , 1989)
$[\text{Ru}(\text{phen})_2(\text{NMIP})]^{2+}$ (NMIP = 2'-(2''-nitro-3'',4''-methylenedioxy phenyl)imidazo-[4',5'-f][1,10]-phenanthroline)	$2.1 \pm 0.3 \times 10^4$	Partial intercalation (Tan <i>et al.</i> , 2005)
$[\text{Ru}(\text{phen})_2(\text{dppz})]^{2+}$	$> 10^6$	Intercalation (Friedman <i>et al.</i> , 1990)

**Table 3.87** (continued)

Complexes	$K_b$	Kind of interaction
[Ru(phen) <sub>2</sub> (MPPIP)] <sup>2+</sup> MPPIP = 2-(3'-phenoxyphenyl)imidazo[4,5-f]- [1,10]phenanthroline)	6.08 x 10 <sup>4</sup>	Intercalation (Tan <i>et al.</i> , 2007)
[Ru(phen) <sub>2</sub> (BPIP)] <sup>2+</sup> BPIP = 2-(4'-benzyloxyphenyl)imidazo[4,5-f]- [1,10]phenanthroline)	3.96 x 10 <sup>4</sup>	Intercalation (Tan <i>et al.</i> , 2007)
[Ru(phen) <sub>2</sub> (BPIP)] <sup>2+</sup> BPIP = 2-(4'-biphenyl)imidazo[4,5-f][1,10] phenanthroline)	1.7 x 10 <sup>5</sup>	Intercalation (Tan <i>et al.</i> , 2007)
EB	1.4 x 10 <sup>6</sup>	Intercalation (Gao <i>et al.</i> , 2006)

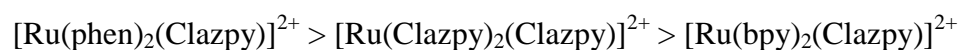
Interestingly, some complexes (Table 3.87) containing three or four fused rings have no such interaction and they behave as good intercalator. Additionally, when one of the bpy and phen in [RuL<sub>3</sub>]<sup>2+</sup> (L = bpy, phen) was replaced with a ligand with more extended fused rings such as dppz or phi, the steric interaction can be reduced by this substitution. Similarly, the planar of azopyridine ring of the Clazpy ligand in complexes may also have an effect to the DNA-binding affinity.

In addition, to further exploring the ancillary ligand effect to the DNA-binding affinity, the bpy and phen ligands are chosen to describe in distinguishing the small differences of interaction of the complexes. The spectrophotometric data of three complexes was listed in Table 3.88.

**Table 3.88** Different ancillary ligand effect to interaction with CT-DNA

Complexes	$\lambda_{\max}$		Binding constant, $K_b$ ( $M^{-1}$ )
	nm	Hypochromism <sup>a</sup> (%)	
[Ru( <b>bpy</b> ) <sub>2</sub> (Clazpy)]Cl <sub>2</sub> .7H <sub>2</sub> O	361	4.17	(6.5±0.1) x 10 <sup>4</sup>
	449	5.52	(8.8±0.4) x 10 <sup>4</sup>
[Ru( <b>phen</b> ) <sub>2</sub> (Clazpy)]Cl <sub>2</sub> .8H <sub>2</sub> O	344	5.73	(1.8±0.6) x 10 <sup>5</sup>
	498	5.27	(1.8±0.2) x 10 <sup>5</sup>
[Ru( <b>Clazpy</b> ) <sub>2</sub> (Clazpy)]Cl <sub>2</sub> .3H <sub>2</sub> O	384	8.96	(7.1±0.6) x 10 <sup>4</sup>
	491	6.17	(1.2 ±0.1)x 10 <sup>5</sup>

This trend may be explained that the plane area and hydrophobicity increase leading to greater binding affinity to DNA. Comparison further of that ancillary ligand with Clazpy, its result shows that the DNA-binding affinity of ancillary Clazpy ligand is greater than that of bpy but less than phen in order to:



These results supported that the size and shape of the ancillary ligand had a significant effect on the strength on DNA binding, and the most suitable intercalating ligand led to the highest affinity of complexes with DNA (Gao *et al.*, 2006).

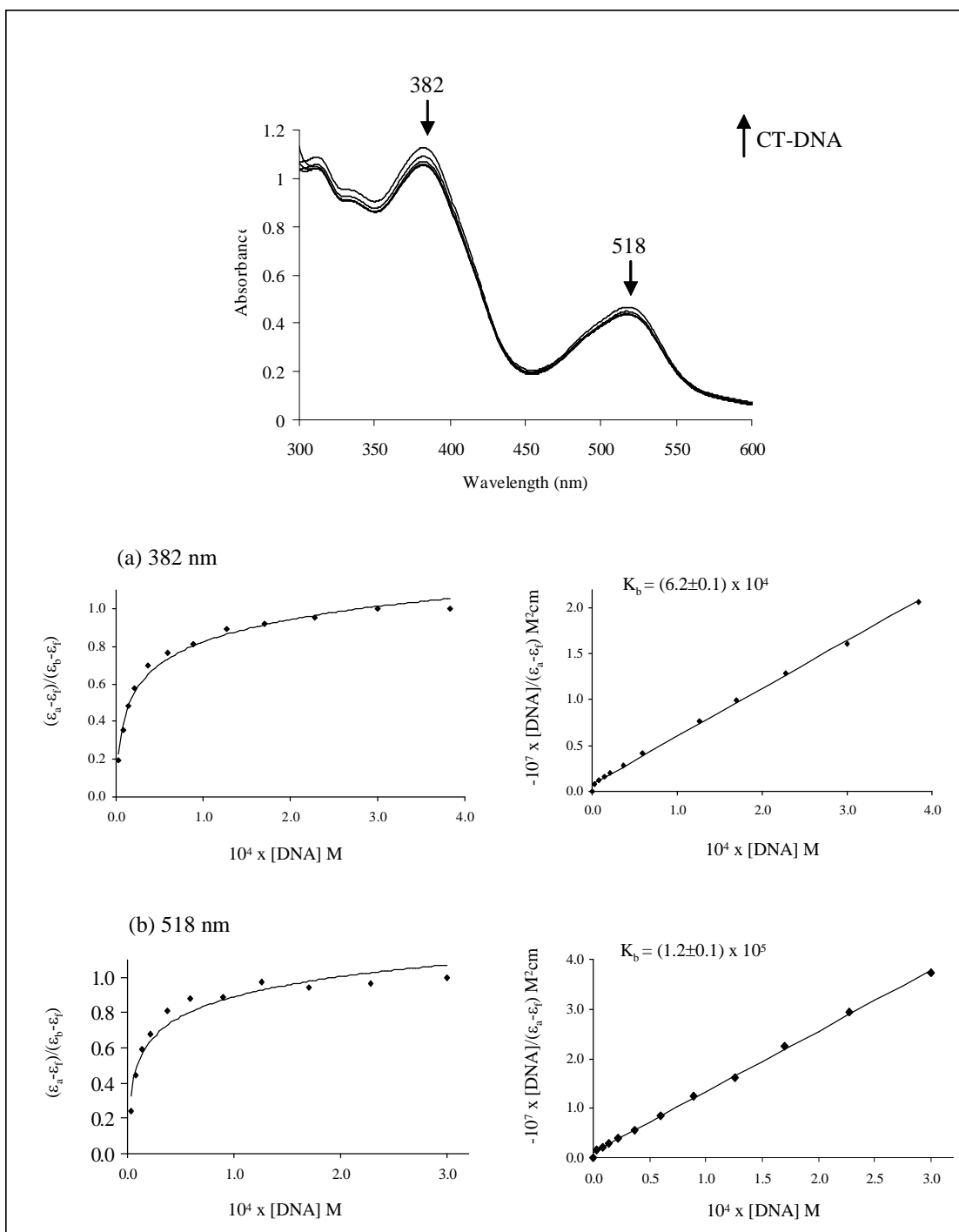


**Figure 3.217** Absorption spectra of  $[\text{Ru}(\text{Clazpy})_2(\text{bpy})]\text{Cl}_2 \cdot 7\text{H}_2\text{O}$  in 5 mM Tris/ 50 mM NaCl buffer pH 7.1 upon addition of calf thymus DNA.  $[\text{Ru}] = 4 \times 10^{-4} \text{ M}$ ,  $[\text{DNA}] = (0-30) \times 10^{-5} \text{ M}$ . Arrows show the absorbance changing upon increasing DNA concentrations. Inset plots of  $[\text{DNA}]/(\epsilon_a - \epsilon_f)$  versus  $[\text{DNA}]$  for the titration of DNA with the complex.

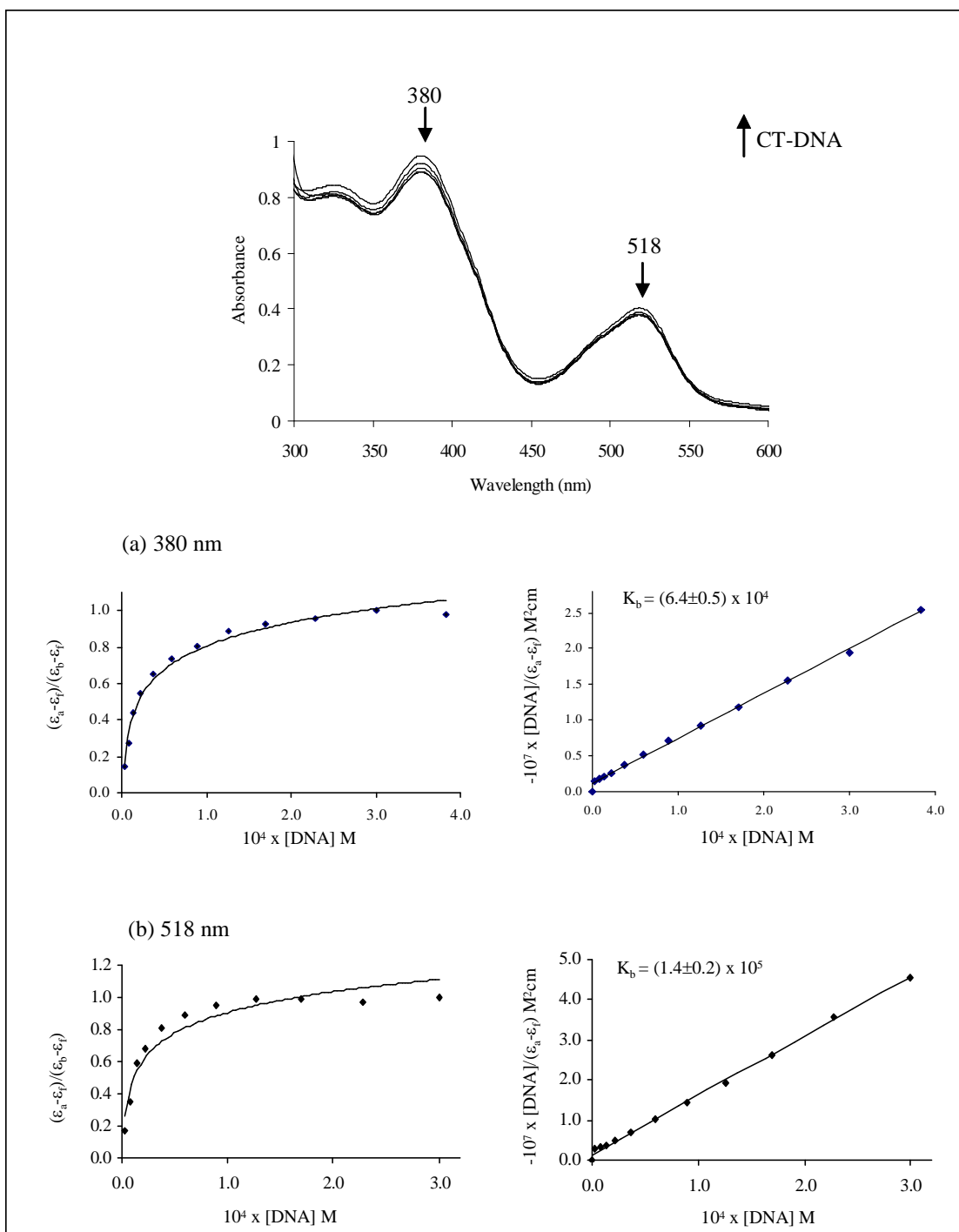


**Figure 3.218** Absorption spectra of  $[\text{Ru}(\text{Clazpy})_2(\text{phen})]\text{Cl}_2 \cdot 8\text{H}_2\text{O}$  in 5 mM Tris/ 50 mM NaCl buffer pH 7.1 upon addition of calf thymus DNA.  $[\text{Ru}] = 4 \times 10^{-4}$  M,  $[\text{DNA}] = (0-30) \times 10^{-5}$  M. Arrows show the absorbance changing upon increasing DNA concentrations. Inset plots of  $[\text{DNA}]/(\epsilon_a - \epsilon_f)$  versus  $[\text{DNA}]$  for the titration of DNA with the complex.

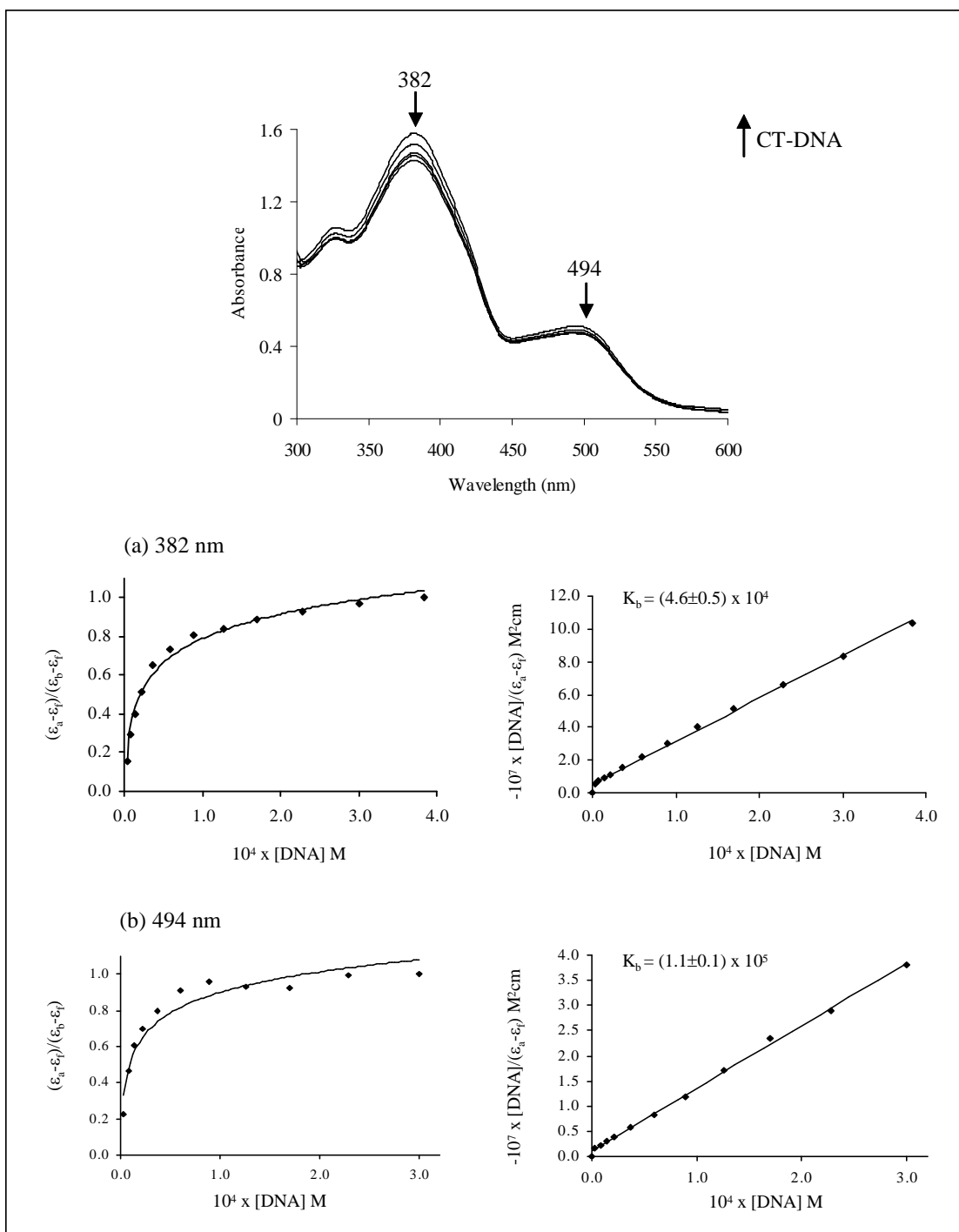


**Figure 3.219** Absorption spectra of  $[\text{Ru}(\text{Clazpy})_2(\text{azpy})]\text{Cl}_2 \cdot 4\text{H}_2\text{O}$  in 5 mM Tris/ 50 mM NaCl buffer pH 7.1 upon addition of calf thymus DNA.  $[\text{Ru}] = 4 \times 10^{-4} \text{ M}$ ,  $[\text{DNA}] = (0-30) \times 10^{-5} \text{ M}$ . Arrows show the absorbance changing upon increasing DNA concentrations. Inset plots of  $[\text{DNA}] / (\epsilon_a - \epsilon_f)$  versus  $[\text{DNA}]$  for the titration of DNA with the complex.

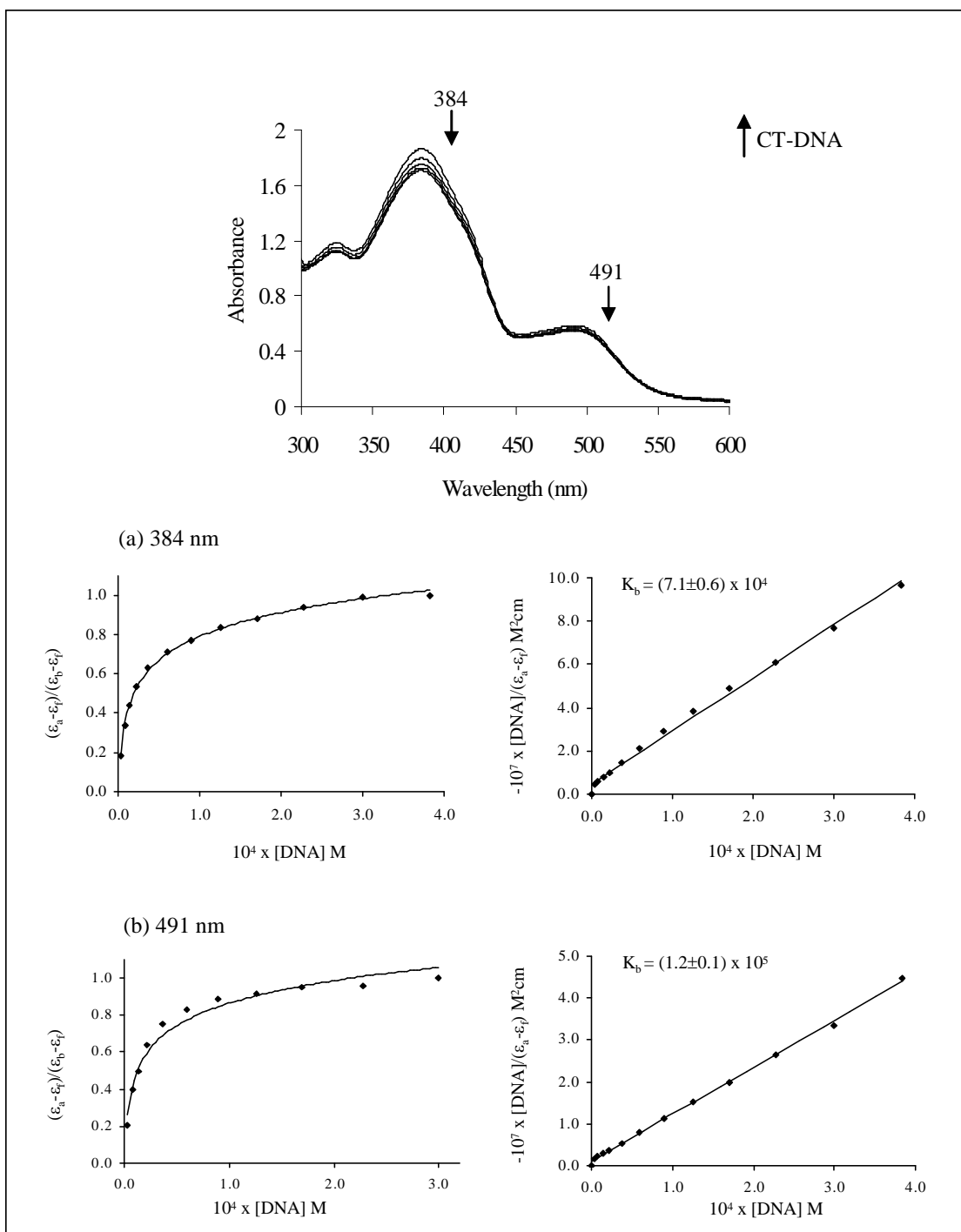


**Figure 3.220** Absorption spectra of  $[\text{Ru}(\text{Clazpy})_3]\text{Cl}_2 \cdot 3\text{H}_2\text{O}$  in 5 mM Tris/ 50 mM NaCl buffer pH 7.1 upon addition of calf thymus DNA.  $[\text{Ru}] = 4 \times 10^{-4} \text{ M}$ ,  $[\text{DNA}] = (0-30) \times 10^{-5} \text{ M}$ . Arrows show the absorbance changing upon increasing DNA concentrations. Inset plots of  $[\text{DNA}] / (\epsilon_a - \epsilon_f)$  versus  $[\text{DNA}]$  for the titration of DNA with the complex.

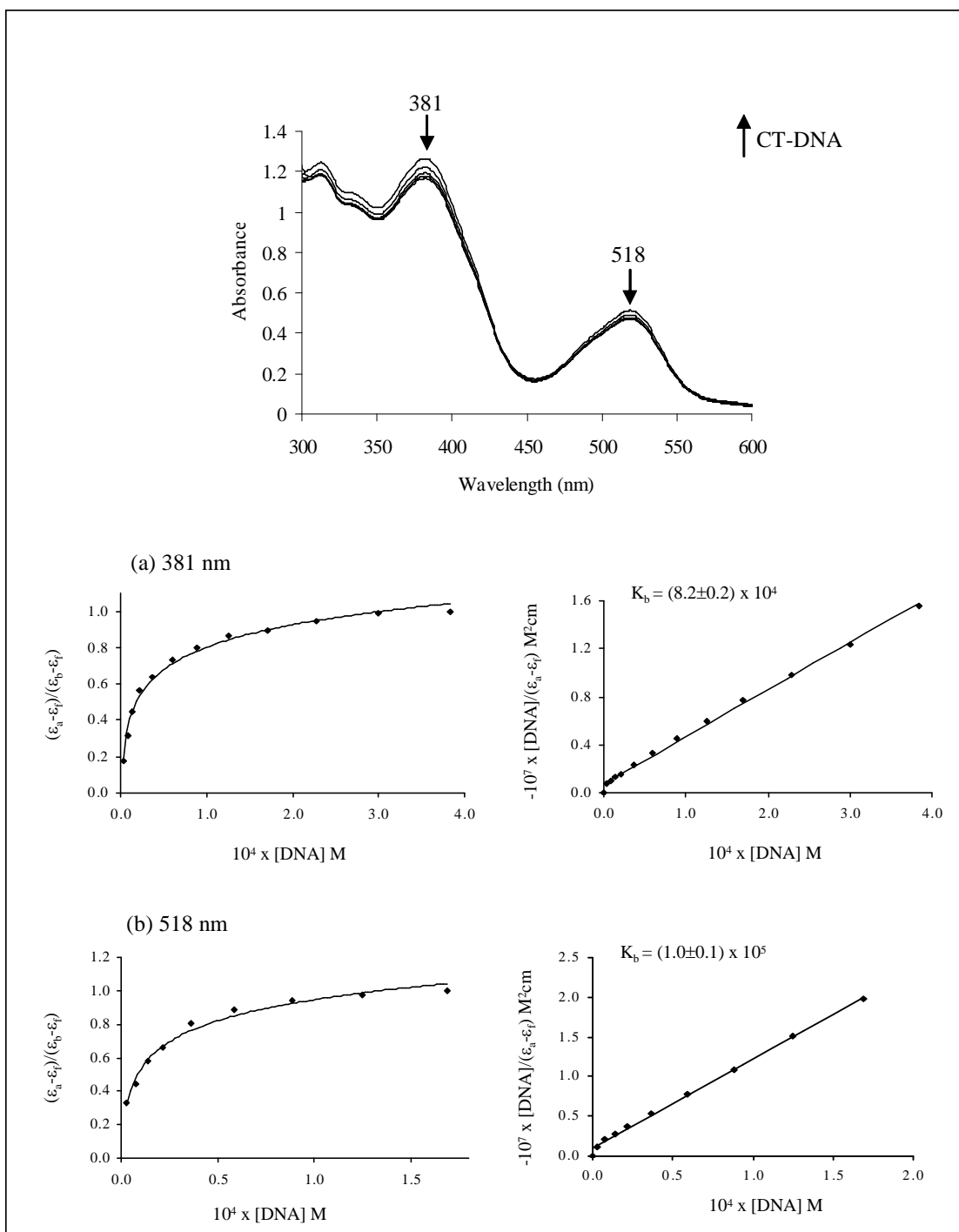


**Figure 3.221** Absorption spectra of  $[\text{Ru}(\text{Clazpy})_2(\text{bpy})](\text{NO}_3)_2 \cdot 5\text{H}_2\text{O}$  in 5 mM Tris/50 mM NaCl buffer pH 7.1 upon addition of calf thymus DNA.  $[\text{Ru}] = 4 \times 10^{-4} \text{ M}$ ,  $[\text{DNA}] = (0-30) \times 10^{-5} \text{ M}$ . Arrows show the absorbance changing upon increasing DNA concentrations. Inset plots of  $[\text{DNA}] / (\epsilon_a - \epsilon_f)$  versus  $[\text{DNA}]$  for the titration of DNA with the complex.

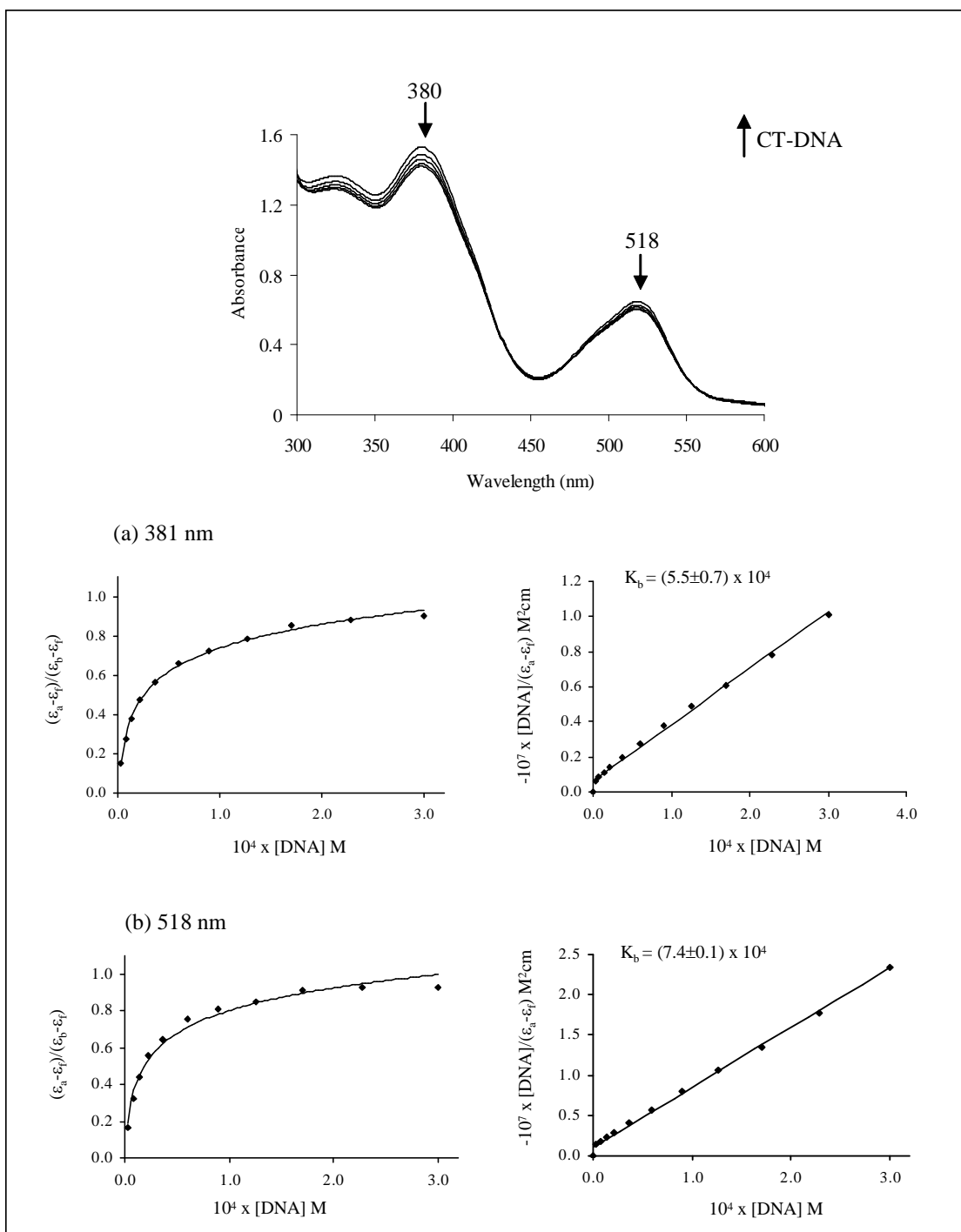


**Figure 3.222** Absorption spectra of  $[\text{Ru}(\text{Clazpy})_2(\text{phen})](\text{NO}_3)_2 \cdot 3\text{H}_2\text{O}$  in 5 mM Tris/50 mM NaCl buffer pH 7.1 upon addition of calf thymus DNA.  $[\text{Ru}] = 4 \times 10^{-4}$  M,  $[\text{DNA}] = (0-30) \times 10^{-5}$  M. Arrows show the absorbance changing upon increasing DNA concentrations. Inset plots of  $[\text{DNA}]/(\epsilon_a - \epsilon_f)$  versus  $[\text{DNA}]$  for the titration of DNA with the complex.

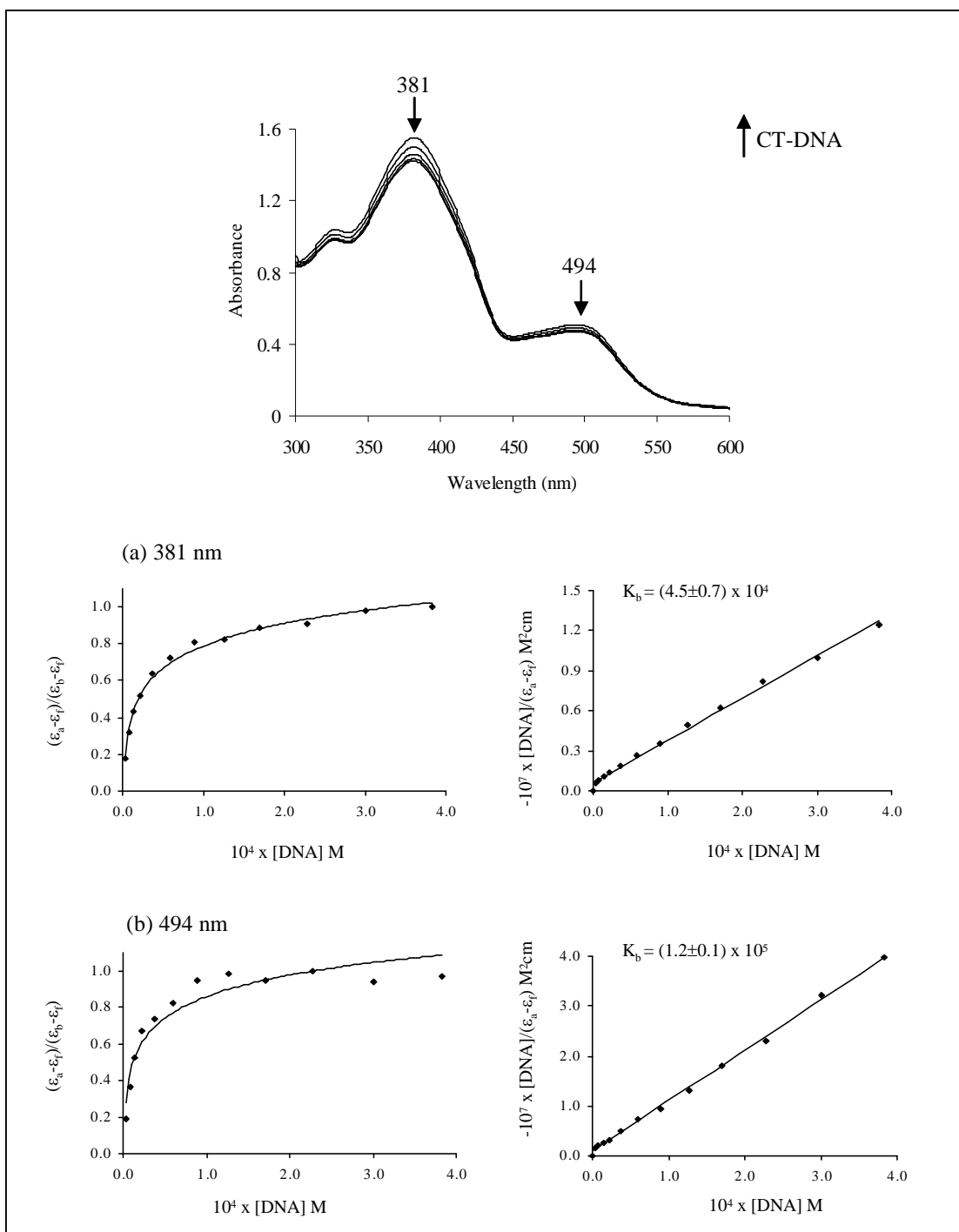


**Figure 3.223** Absorption spectra of  $[\text{Ru}(\text{Clazpy})_2(\text{azpy})](\text{NO}_3)_2 \cdot \text{H}_2\text{O}$  in 5 mM Tris/50 mM NaCl buffer pH 7.1 upon addition of calf thymus DNA.  $[\text{Ru}] = 4 \times 10^{-4} \text{ M}$ ,  $[\text{DNA}] = (0-30) \times 10^{-5} \text{ M}$ . Arrows show the absorbance changing upon increasing DNA concentrations. Inset plots of  $[\text{DNA}] / (\epsilon_a - \epsilon_f)$  versus  $[\text{DNA}]$  for the titration of DNA with the complex.

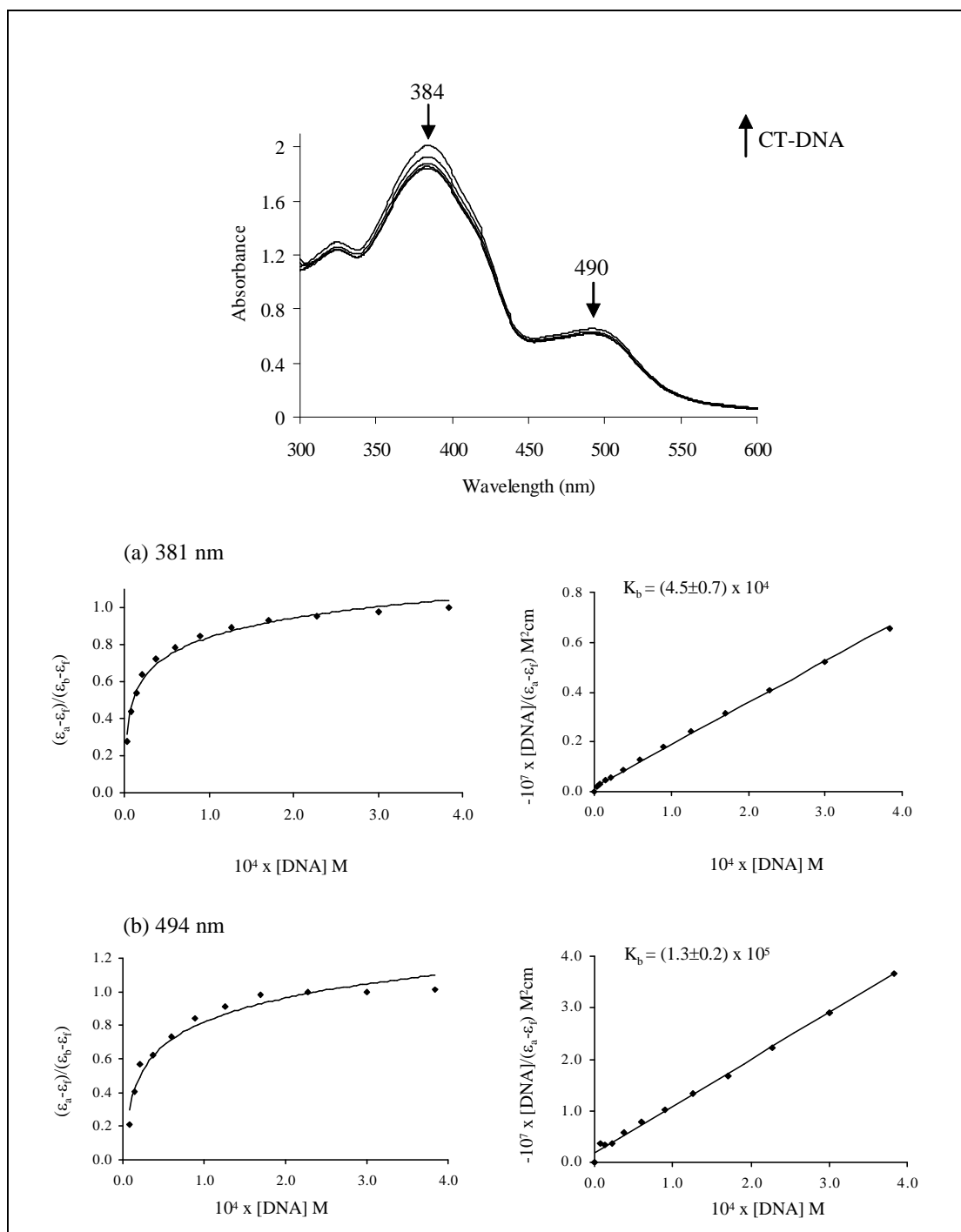


**Figure 3.224** Absorption spectra of [Ru(Clazpy)<sub>3</sub>](NO<sub>3</sub>)<sub>2</sub>·3H<sub>2</sub>O in 5 mM Tris/ 50 mM NaCl buffer pH 7.1 upon addition of calf thymus DNA. [Ru] =  $4 \times 10^{-4}$  M, [DNA] = (0-30)  $\times 10^{-5}$  M. Arrows show the absorbance changing upon increasing DNA concentrations. Inset plots of [DNA]/( $\epsilon_a - \epsilon_f$ ) versus [DNA] for the titration of DNA with the complex.

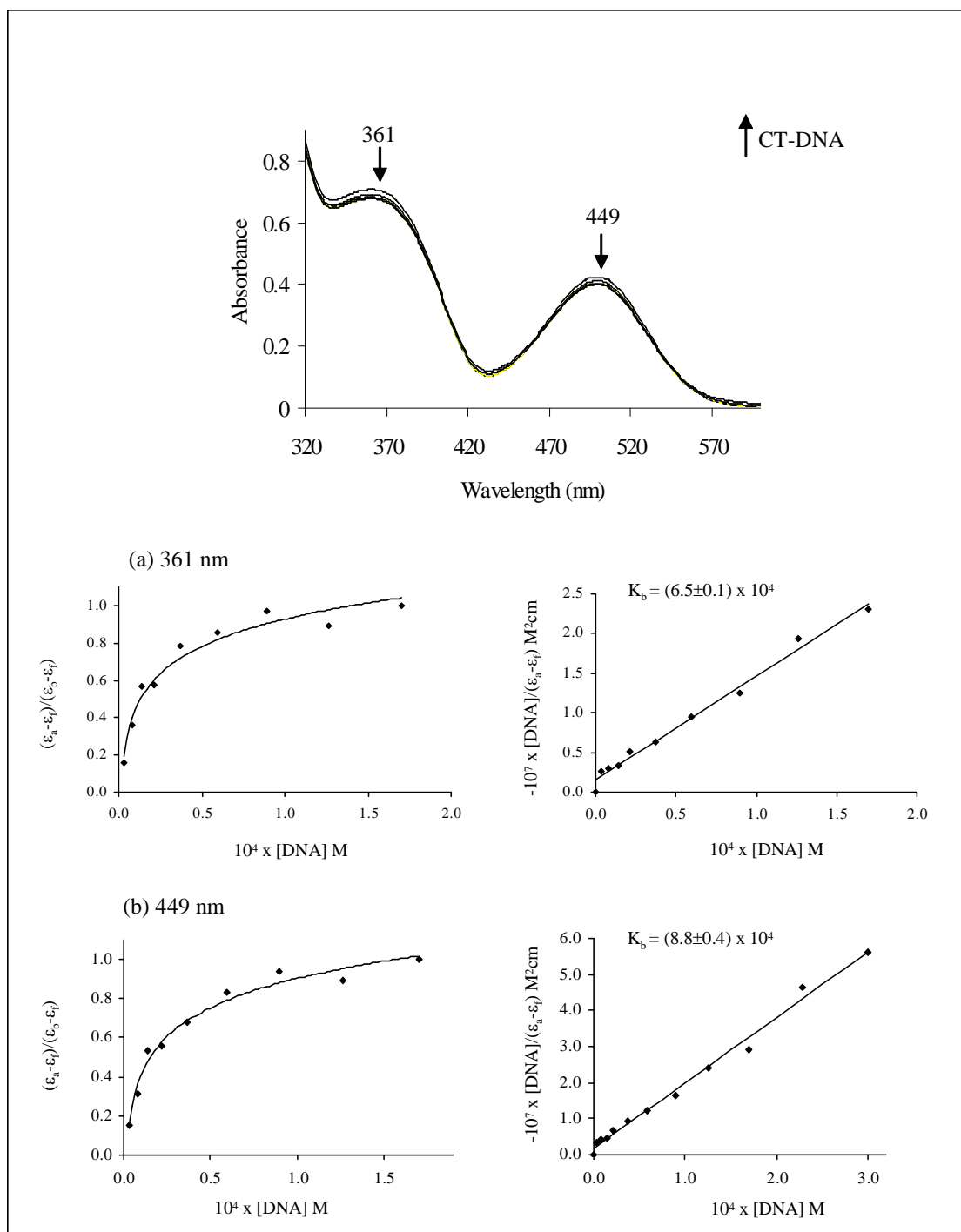


**Figure 3.225** Absorption spectra of  $[\text{Ru}(\text{bpy})_2(\text{Clazpy})]\text{Cl}_2 \cdot 7\text{H}_2\text{O}$  in 5 mM Tris/ 50 mM NaCl buffer pH 7.1 upon addition of calf thymus DNA.  $[\text{Ru}] = 4 \times 10^{-4} \text{ M}$ ,  $[\text{DNA}] = (0-30) \times 10^{-5} \text{ M}$ . Arrows show the absorbance changing upon increasing DNA concentrations. Inset plots of  $[\text{DNA}] / (\epsilon_a - \epsilon_f)$  versus  $[\text{DNA}]$  for the titration of DNA with the complex.

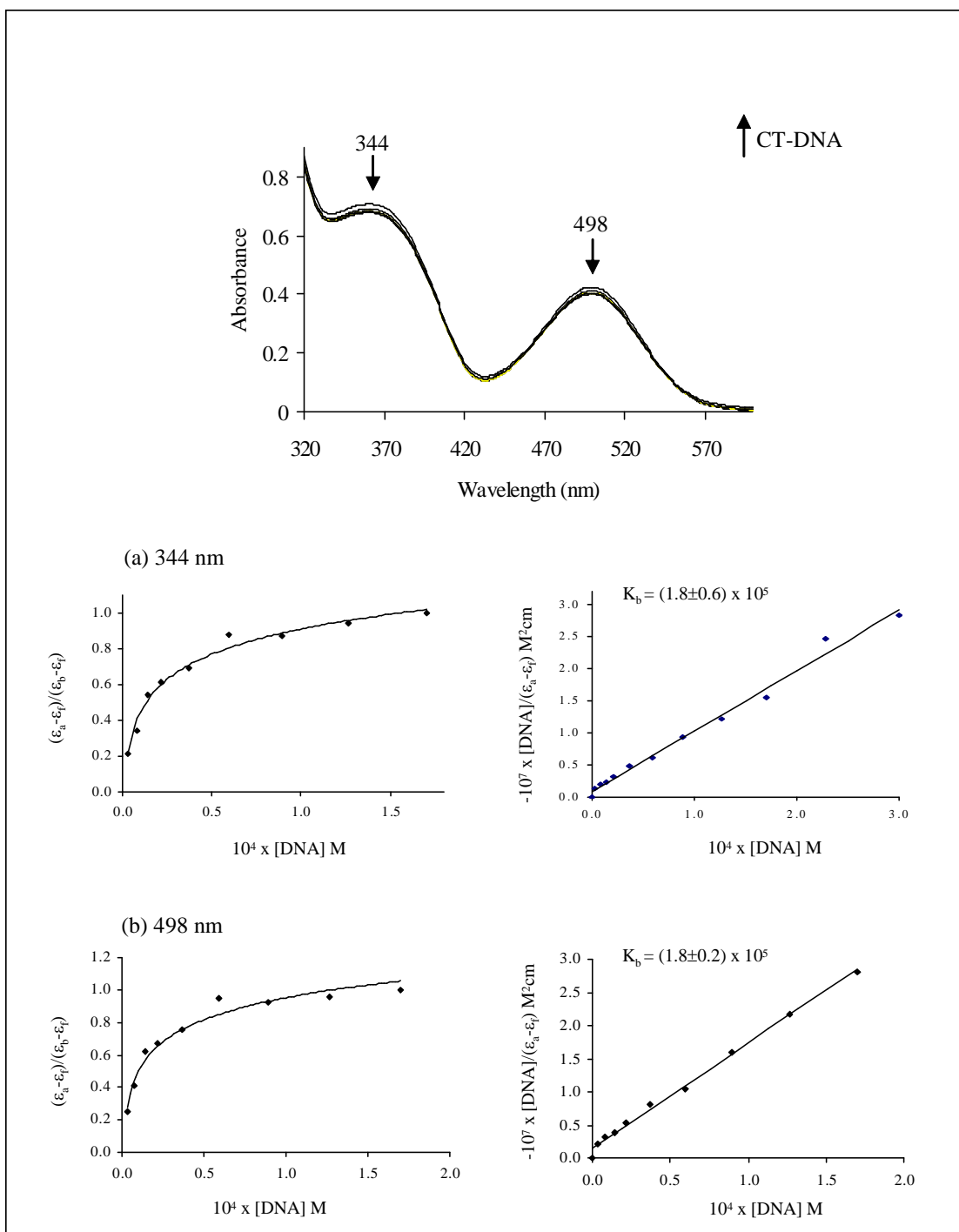


**Figure 3.226** Absorption spectra of  $[\text{Ru}(\text{phen})_2(\text{Clazpy})]\text{Cl}_2 \cdot 8\text{H}_2\text{O}$  in 5 mM Tris/ 50 mM NaCl buffer pH 7.1 upon addition of calf thymus DNA.  $[\text{Ru}] = 4 \times 10^{-4} \text{ M}$ ,  $[\text{DNA}] = (0-30) \times 10^{-5} \text{ M}$ . Arrows show the absorbance changing upon increasing DNA concentrations. Inset plots of  $[\text{DNA}]/(\epsilon_a - \epsilon_f)$  versus  $[\text{DNA}]$  for the titration of DNA with the complex.

### 3.8.2 Viscosity measurement

To further explore the binding modes of the complexes, viscosity measurements were carried out on CT-DNA bound to varying concentration of the added complexes. The lengthening of DNA occurred when DNA base pairs separate to accommodate the aromatic chromophore of the bound ligands. Intercalation is expected to lengthen the DNA helix leading to an increase in the DNA viscosity. In contrast, a partial or non-classical intercalation of ligand, it could bend (or kink) the DNA helix which was reduced its effective length and its viscosity. In present work, we examined the effect on the specific relative viscosity of DNA upon addition of the complexes by measuring of the flow rate of DNA solution through a viscometer.

In this work, the effect of  $[\text{Ru}(\text{Clazpy})_2(\text{L})](\text{X}_2)$  ( $\text{L} = \text{bpy}, \text{phen}, \text{azpy}, \text{Clazpy}$ ;  $\text{X} = \text{Cl}^-, \text{NO}_3^-$ ) complexes together with  $[\text{Ru}(\text{phen})_3]^{2+}$  and EB on viscosity of CT-DNA are shown in Figure 3.227-3.231. As expected, EB increases the relative specific viscosity for the lengthening of the DNA double helix resulting from intercalation. On increasing the amount of  $[\text{Ru}(\text{Clazpy})_2(\text{bpy})]^{2+}$ , the relative viscosity of DNA initially increased and decreased later. Similar behavior has been observed on the addition of  $[\text{Ru}(\text{Clazpy})_2(\text{phen})]^{2+}$ ,  $[\text{Ru}(\text{Clazpy})_2(\text{azpy})]^{2+}$  and  $[\text{Ru}(\text{Clazpy})_3]^{2+}$  to CT-DNA. Since the DNA-binding affinity of the present complexes is less than observed in an intercalator like EB, the mode of binding is partial intercalation.

In the previous work, there are reported that at least two hypothesized about phases of binding for complexes was occurred. The hydrophobic interaction of  $[\text{Ru}(\text{Clazpy})_2(\text{L})]^{2+}$  ( $\text{L} = \text{bpy}, \text{phen}, \text{azpy}, \text{Clazpy}$ ) with DNA occurred first, which is followed by the bridging of duplexes involving all the ligand. In fact, at higher concentrations of the complex, DNA gets precipitated. Similar lowering of viscosity and precipitation at higher concentrations has been reported previously (Selvi *et al.*, 2005).

In the case of  $[\text{Ru}(\text{bpy})_2(\text{Clazpy})]^{2+}$  and  $[\text{Ru}(\text{phen})_2(\text{Clazpy})]^{2+}$ , similarly trend that observed in  $[\text{Ru}(\text{Clazpy})_2(\text{L})]^{2+}$  by readily first increasing but then decreasing later. They could bind to DNA by the partial intercalation via the flexible Clazpy ligand into the base pairs of DNA supporting by the ancillary ligand bpy and phen. This may be related to the molecular structure of the complex.

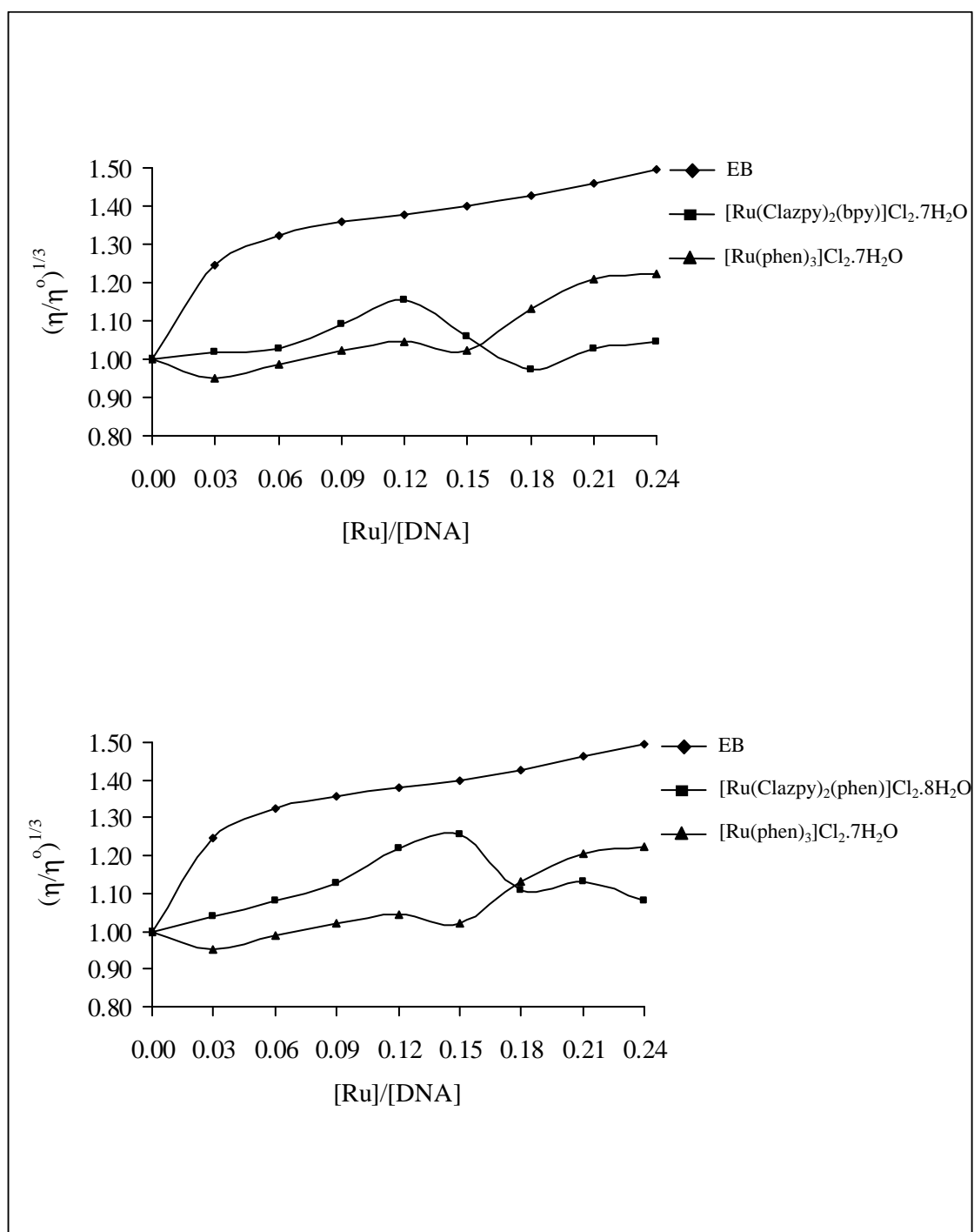


**Figure 3.227** Effect of increasing amount of  $[\text{Ru}(\text{Clazpy})_2(\text{bpy})]\text{Cl}_2 \cdot 7\text{H}_2\text{O}$  and  $[\text{Ru}(\text{Clazpy})_2(\text{phen})]\text{Cl}_2 \cdot 8\text{H}_2\text{O}$  compared with EB and  $[\text{Ru}(\text{phen})_3]\text{Cl}_2 \cdot 7\text{H}_2\text{O}$  on the relative viscosity of calf thymus DNA at  $29 (\pm 0.5) ^\circ\text{C}$ . The total concentration of DNA is 0.3 mM

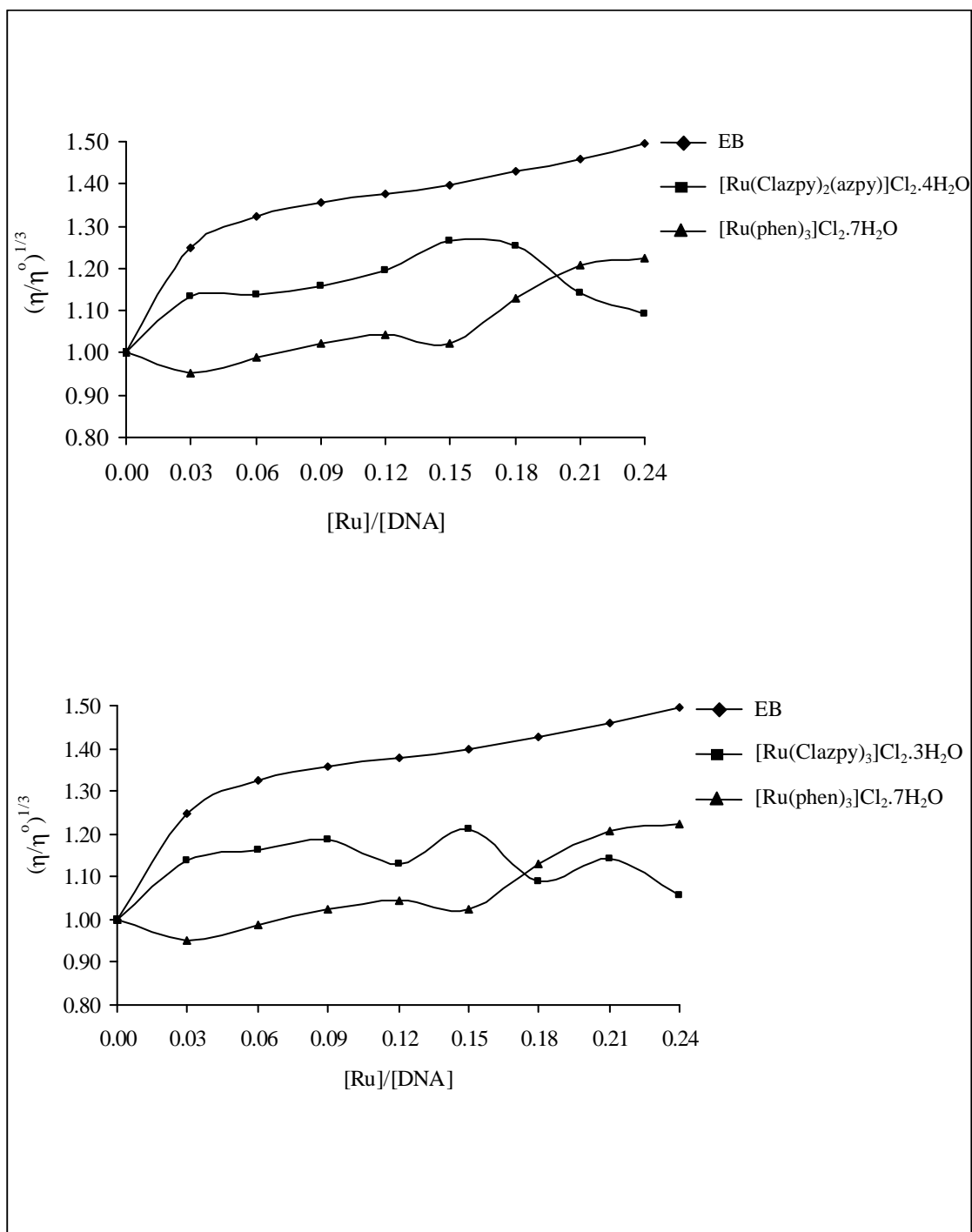


**Figure 3.228** Effect of increasing amount of  $[Ru(Clazpy)_2(azpy)]Cl_2 \cdot 4H_2O$  and  $[Ru(Clazpy)_3]Cl_2 \cdot 3H_2O$  compared with EB and  $[Ru(phen)_3]Cl_2 \cdot 7H_2O$  on the relative viscosity of calf thymus DNA at  $29(\pm 0.5)^\circ C$ . The total concentration of DNA is 0.3 mM

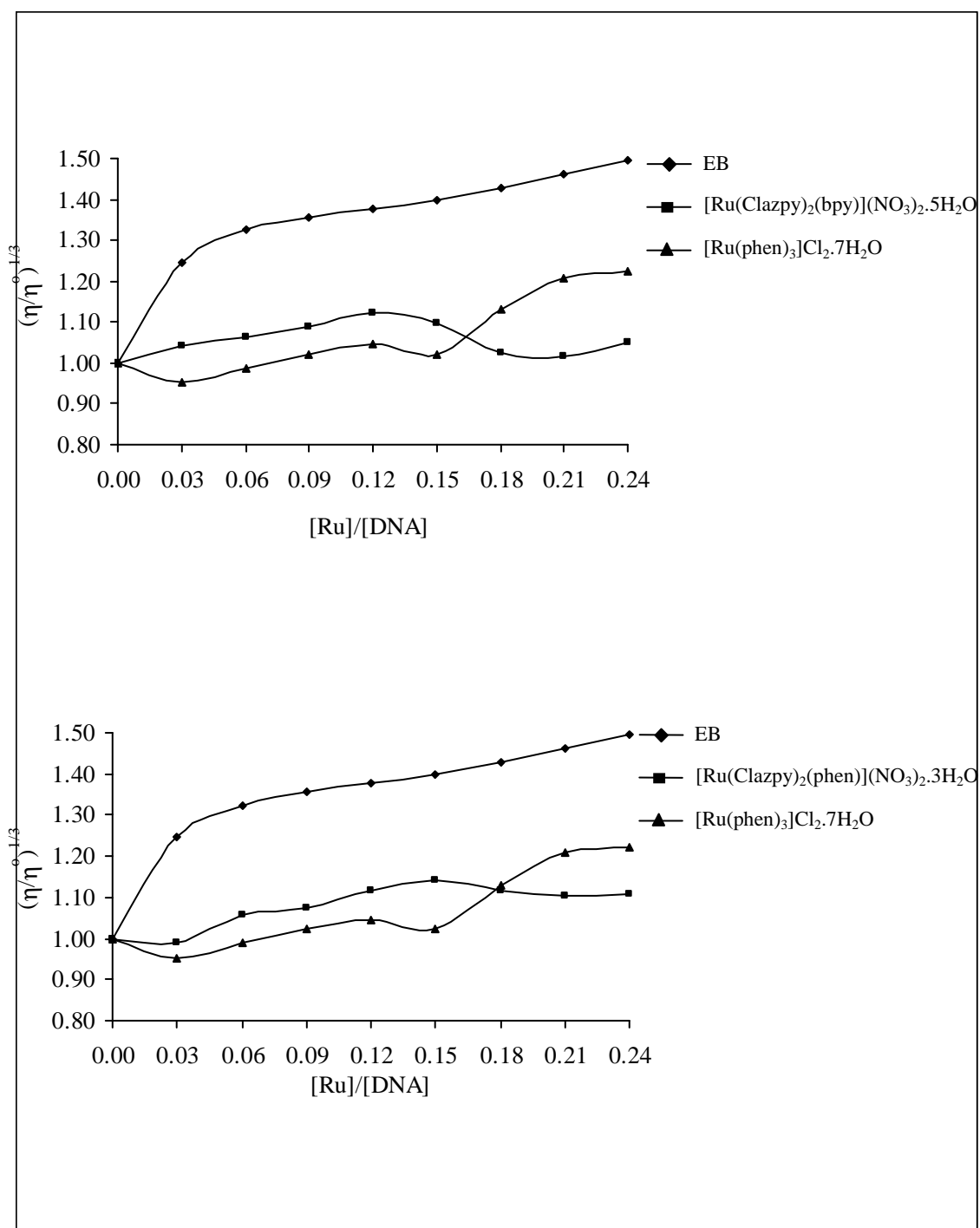


**Figure 3.229** Effect of increasing amount of  $[Ru(Clazpy)_2(bpy)](NO_3)_2 \cdot 5H_2O$  and  $[Ru(Clazpy)_2(phen)](NO_3)_2 \cdot 3H_2O$  compared with EB and  $[Ru(phen)_3]Cl_2 \cdot 7H_2O$  on the relative viscosity of calf thymus DNA at  $29(\pm 0.5)^\circ C$ . The total concentration of DNA is 0.3 mM

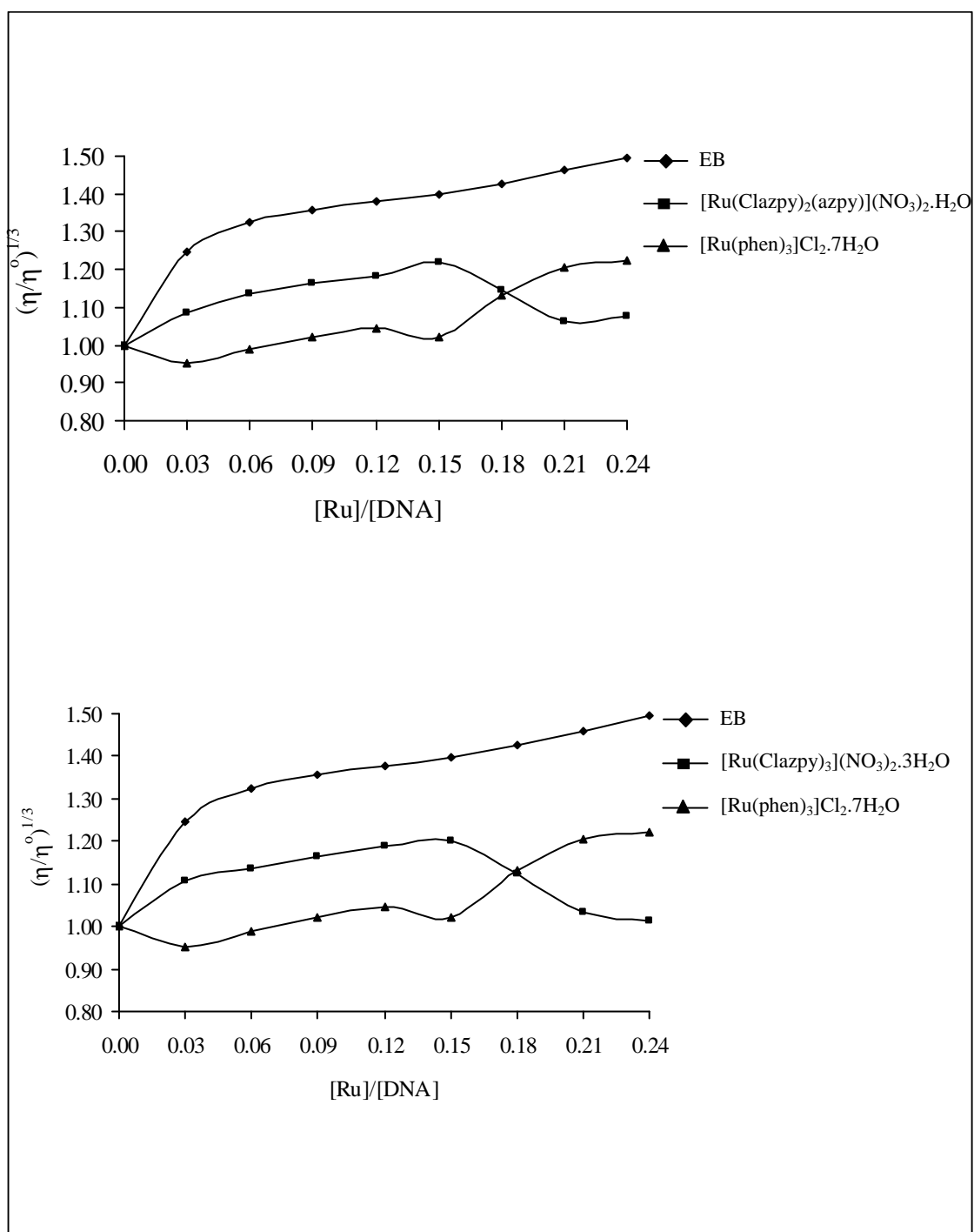


**Figure 3.230** Effect of increasing amount of  $[Ru(Clazpy)_2(azpy)](NO_3)_2 \cdot H_2O$  and  $[Ru(Clazpy)_3](NO_3)_2 \cdot 3H_2O$  compared with EB and  $[Ru(phen)_3]Cl_2 \cdot 7H_2O$  on the relative viscosity of calf thymus DNA at  $29(\pm 0.5)^\circ C$ . The total concentration of DNA is 0.3 mM

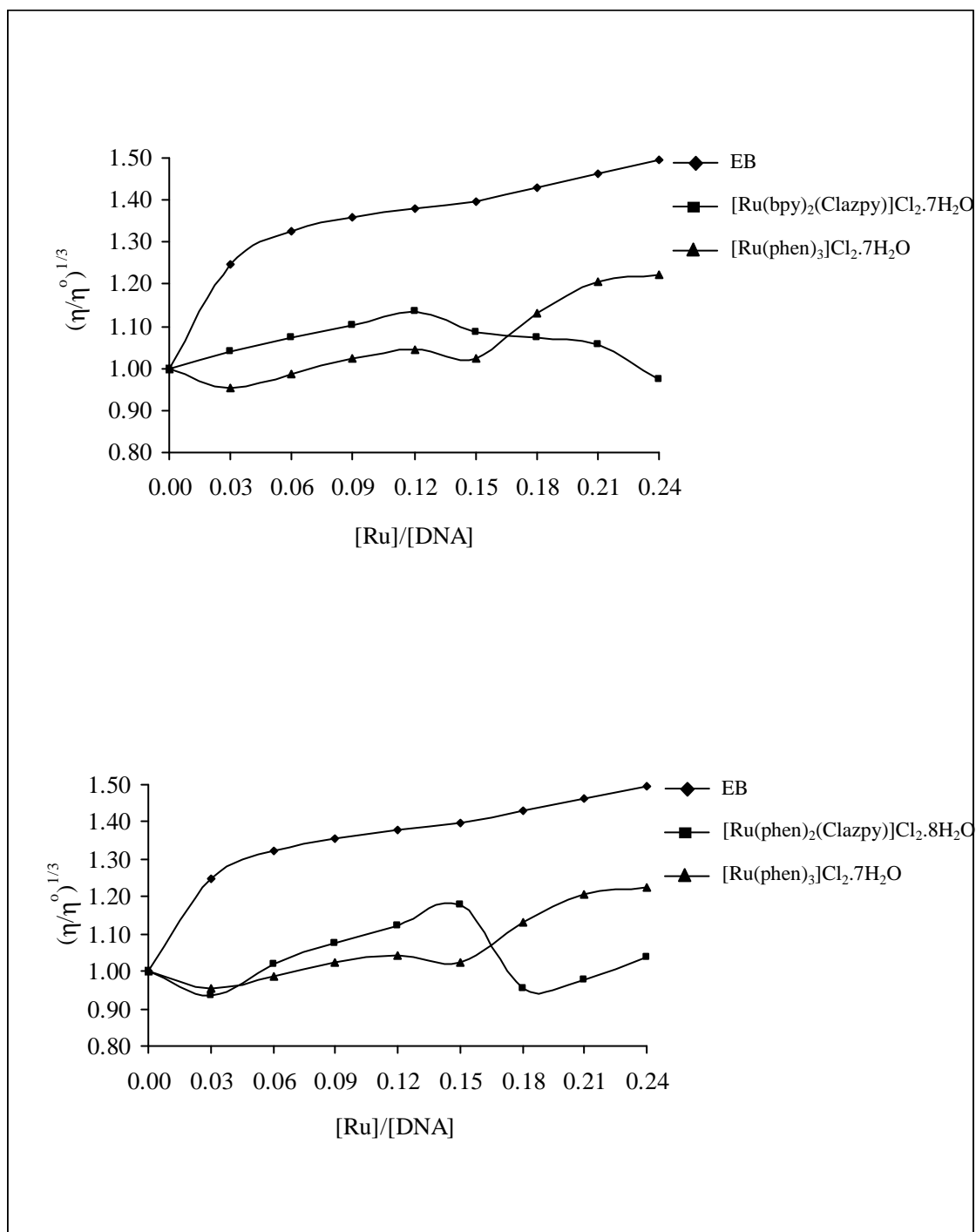


**Figure 3.231** Effect of increasing amount of  $[\text{Ru}(\text{bpy})_2(\text{Clazpy})]\text{Cl}_2 \cdot 7\text{H}_2\text{O}$  and  $[\text{Ru}(\text{phen})_2(\text{Clazpy})]\text{Cl}_2 \cdot 8\text{H}_2\text{O}$  compared with EB and  $[\text{Ru}(\text{phen})_3]\text{Cl}_2 \cdot 7\text{H}_2\text{O}$  on the relative viscosity of calf thymus DNA at  $29(\pm 0.5)^\circ\text{C}$ . The total concentration of DNA is 0.3 mM

### 3.8.3 Fluorescence quenching studies

Since water-soluble Ru(II) complexes are non-emissive both in the presence and absence of CT-DNA at room temperature, the binding of Ru(II) complexes and DNA cannot be directly presented in the emission spectra. As we known, ethidium bromide (EB) emit intense fluorescence light in the presence of DNA, due to its strong intercalation between the adjacent DNA base pair (Tan *et al.*, 2007). Thus, competitive binding studies using an EB bound to DNA was carried out for these complexes. The quenching extent of fluorescence of EB binding to DNA is used to determine the extent the binding of the second molecule to DNA. Binding of the complex resulted in the displacement of DNA bound EB molecule with a reduction of emission intensity due to fluorescence quenching of free EB by water (Ghosh *et al.*, 2006). According to the classical Stern-Volmer equation (Wang *et al.*, 2004) :

$$I_0/I = 1 + Kr \quad (3.35)$$

Where  $I_0$  and  $I$  are the fluorescence intensities in the absence and the presence of complex, respectively.  $K$  is the Stern-Volmer constant of quenching on the ratio of  $r_{be}$  (the ratio of the bound concentration of EB to the concentration DNA).  $r$  is the ratio of the total concentration of complex to that of DNA.

In this work, the fluorescence quenching curves of EB bound to DNA by the Ru(II) complexes and a plot of ruthenium(II) complexes caused fluorescence quenching of EB-DNA complex are shown in Figure 3.232-3.236. From data, we can see that the addition of these complexes to DNA pretreated EB caused appreciable reduction in the emission intensity.

The quenching plot illustrate that the quenching of EB bound to DNA by all complexes are in good agreement with the linear Stern-Volmer equation (eq 3.35) which also indicates that all of complexes bind to DNA. In the plot of  $I_0/I$  versus  $[\text{complex}]/[\text{DNA}]$ ,  $K$  is given by the ratio of the slope to intercept. The  $K$  values for  $[\text{Ru}(\text{Clazpy})_2(\text{L})]^{2+}$  ( $\text{L} = \text{bpy}, \text{phen}, \text{azpy}, \text{Clazpy}$ ),  $[\text{Ru}(\text{bpy})_2(\text{Clazpy})]^{2+}$  and  $[\text{Ru}(\text{phen})_2(\text{Clazpy})]^{2+}$  are listed in Table 3.89. The  $R$  values of their linear fit plot of  $I_0/I$  versus  $[\text{complex}]/[\text{DNA}]$  are also listed. When the present complexes were added

to CT-DNA incubated with EB, the emission of EB is quenched by all complexes. These data is consistent with the above absorption spectral results.

**Table 3.89** Fluorescence quenching values of complexes

Complexes	$K_q$ values (% <sup>a</sup> )	$R^2$
[Ru(Clazpy) <sub>2</sub> (bpy)]Cl <sub>2</sub> .7H <sub>2</sub> O	8.47 (13.55)	0.9988
[Ru(Clazpy) <sub>2</sub> (phen)]Cl <sub>2</sub> .8H <sub>2</sub> O	8.14 (13.65)	0.9900
[Ru(Clazpy) <sub>2</sub> (azpy)]Cl <sub>2</sub> .4H <sub>2</sub> O	8.12 (13.26)	0.9930
[Ru(Clazpy) <sub>3</sub> ]Cl <sub>2</sub> .3H <sub>2</sub> O	9.66 (15.49)	0.9983
[Ru(bpy) <sub>2</sub> (Clazpy)]Cl <sub>2</sub> .7H <sub>2</sub> O	7.28 (10.19)	0.9910
[Ru(phen) <sub>2</sub> (Clazpy)]Cl <sub>2</sub> .8H <sub>2</sub> O	8.16 (11.98)	0.9905
[Ru(Clazpy) <sub>2</sub> (bpy)](NO <sub>3</sub> ) <sub>2</sub> .5H <sub>2</sub> O	10.33 (13.37)	0.9985
[Ru(Clazpy) <sub>2</sub> (phen)](NO <sub>3</sub> ) <sub>2</sub> .3H <sub>2</sub> O	8.00 (13.94)	0.9920
[Ru(Clazpy) <sub>2</sub> (azpy)](NO <sub>3</sub> ) <sub>2</sub> .H <sub>2</sub> O	8.77 (13.80)	0.9956
[Ru(Clazpy) <sub>3</sub> ](NO <sub>3</sub> ) <sub>2</sub> .5H <sub>2</sub> O	9.09 (14.76)	0.9966

<sup>a</sup> the amount of decreasing in emission intensity

In the case of [Ru(bpy)<sub>2</sub>(Clazpy)]Cl<sub>2</sub>.7H<sub>2</sub>O and [Ru(phen)<sub>2</sub>(Clazpy)]Cl<sub>2</sub>.8H<sub>2</sub>O, the  $K$  value were 7.28 and 8.16 corresponding to the  $R$  values as 0.9910 and 0.9905, respectively. The data suggested that the interaction of [Ru(phen)<sub>2</sub>(Clazpy)]<sup>2+</sup> with DNA was stronger than that [Ru(bpy)<sub>2</sub>(Clazpy)]<sup>2+</sup>, which was consistent with the above absorption spectral results.

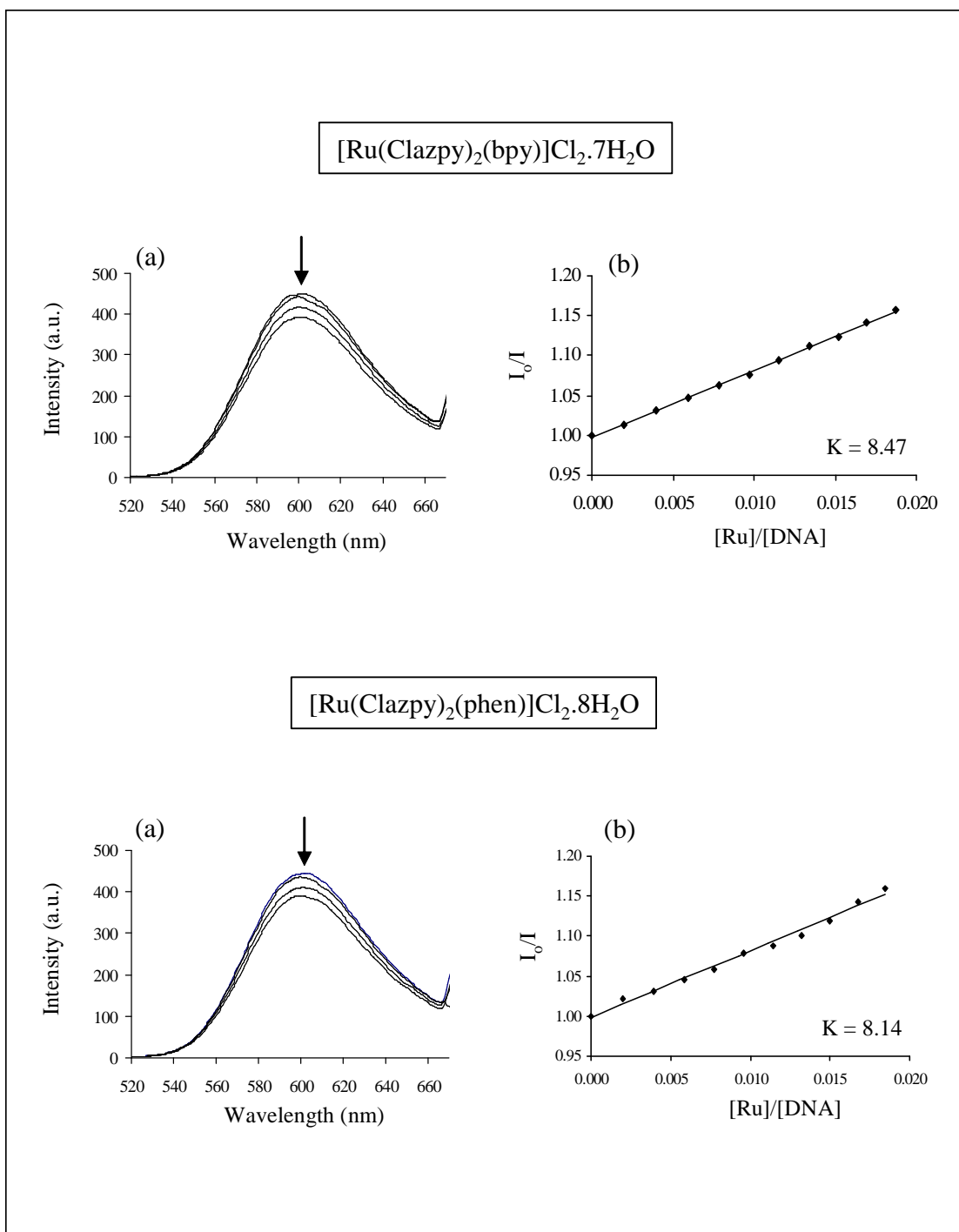


**Figure 3.232** (a) Fluorescence quenching curve of EB bound to DNA in the absence and presence of  $[\text{Ru}(\text{Clazpy})_2(\text{bpy})]\text{Cl}_2 \cdot 7\text{H}_2\text{O}$  and  $[\text{Ru}(\text{Clazpy})_2(\text{phen})]\text{Cl}_2 \cdot 8\text{H}_2\text{O}$ ,  $[\text{EB}] = 2.0 \mu\text{M}$ ,  $[\text{DNA}] = 40 \mu\text{M}$ ,  $[\text{Ru}] = 0, 0.1, 0.3, 0.6 \mu\text{M}$ ; (b) in the plot of  $[\text{Ru}(\text{Clazpy})_2(\text{bpy})]\text{Cl}_2 \cdot 7\text{H}_2\text{O}$  and  $[\text{Ru}(\text{Clazpy})_2(\text{phen})]\text{Cl}_2 \cdot 8\text{H}_2\text{O}$  of  $I_0/I$  versus  $[\text{Ru}]/[\text{DNA}] = 0 - 0.02$ .

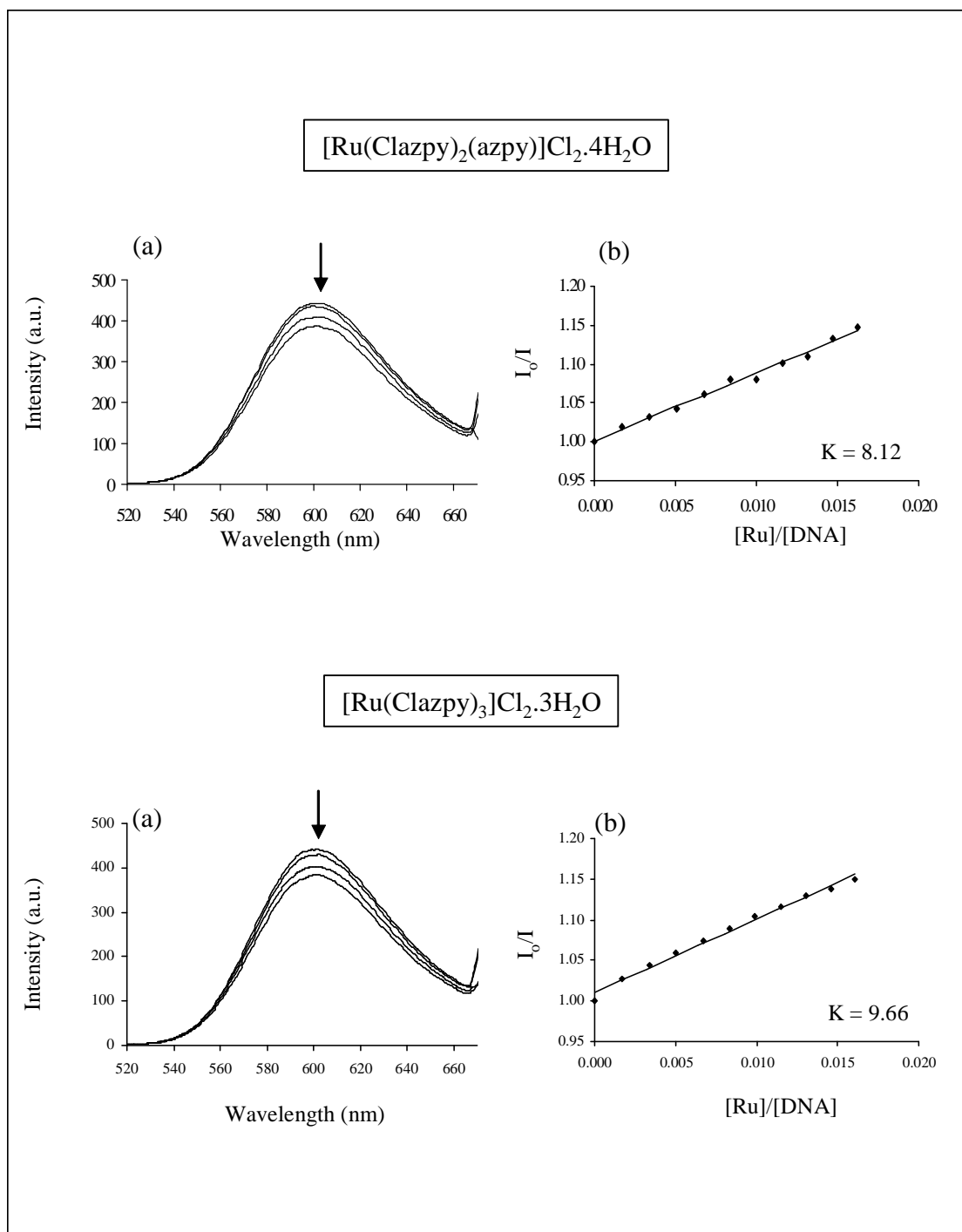


**Figure 3.233** (a) Fluorescence quenching curve of EB bound to DNA in the absence and presence of  $[\text{Ru}(\text{Clazpy})_2(\text{azpy})]\text{Cl}_2 \cdot 4\text{H}_2\text{O}$  and  $[\text{Ru}(\text{Clazpy})_3]\text{Cl}_2 \cdot 3\text{H}_2\text{O}$ ,  $[\text{EB}] = 2.0 \mu\text{M}$ ,  $[\text{DNA}] = 40 \mu\text{M}$ ,  $[\text{Ru}] = 0, 0.1, 0.3, 0.6 \mu\text{M}$ ; (b) in the plot of  $[\text{Ru}(\text{Clazpy})_2(\text{azpy})]\text{Cl}_2 \cdot 4\text{H}_2\text{O}$  and  $[\text{Ru}(\text{Clazpy})_3]\text{Cl}_2 \cdot 3\text{H}_2\text{O}$  of  $I_0/I$  versus  $[\text{Ru}]/[\text{DNA}] = 0 - 0.02$ .

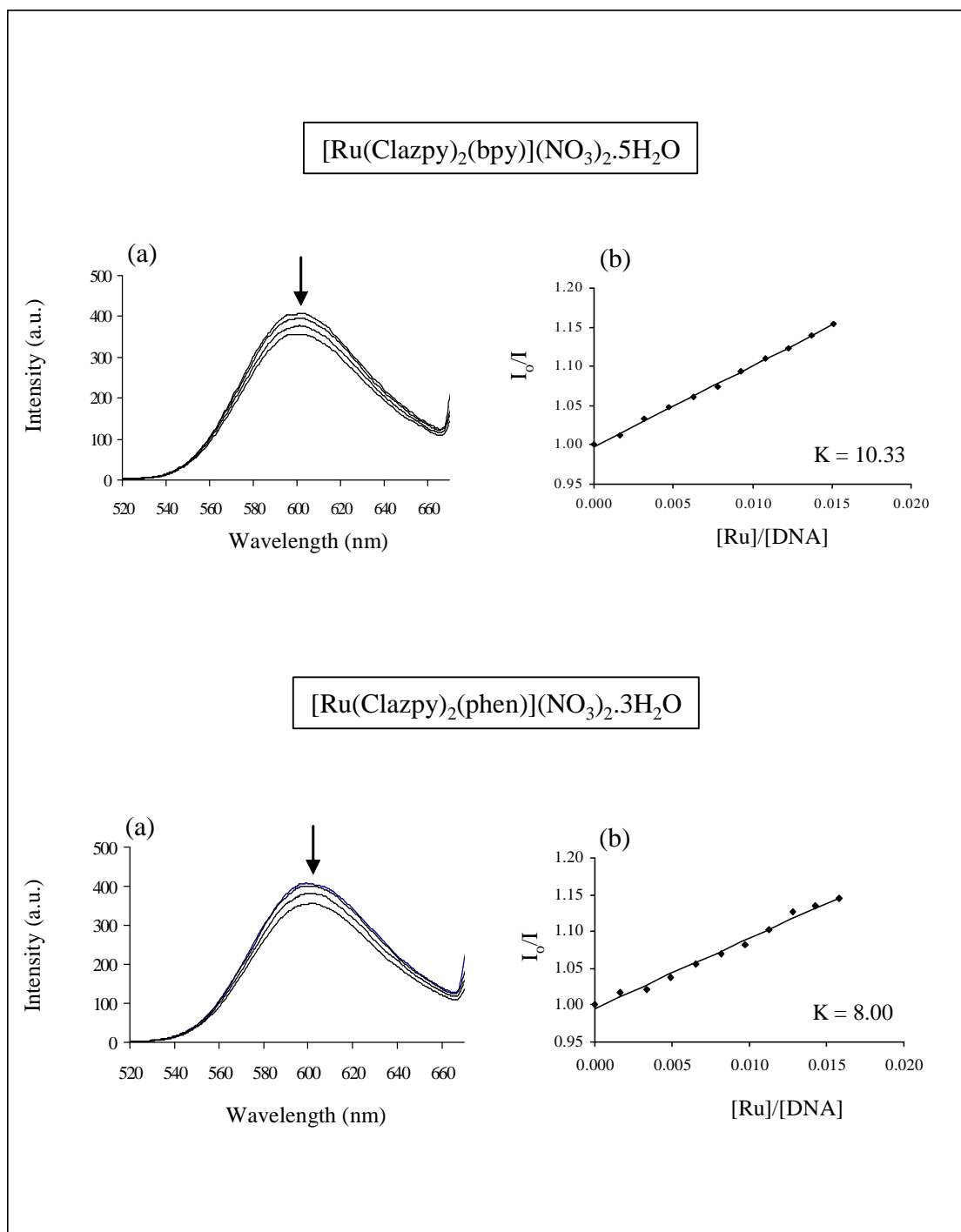


**Figure 3.234** (a) Fluorescence quenching curve of EB bound to DNA in the absence and presence of [Ru(Clazpy)<sub>2</sub>(bpy)](NO<sub>3</sub>)<sub>2</sub>·5H<sub>2</sub>O and [Ru(Clazpy)<sub>2</sub>(phen)](NO<sub>3</sub>)<sub>2</sub>·3H<sub>2</sub>O, [EB] = 2.0 μM, [DNA] = 40 μM, [Ru] = 0, 0.1, 0.3, 0.6 μM; (b) in the plot of [Ru(Clazpy)<sub>2</sub>(bpy)](NO<sub>3</sub>)<sub>2</sub>·5H<sub>2</sub>O and [Ru(Clazpy)<sub>2</sub>(phen)](NO<sub>3</sub>)<sub>2</sub>·3H<sub>2</sub>O of I<sub>0</sub>/I versus [Ru]/[DNA] = 0 - 0.02.

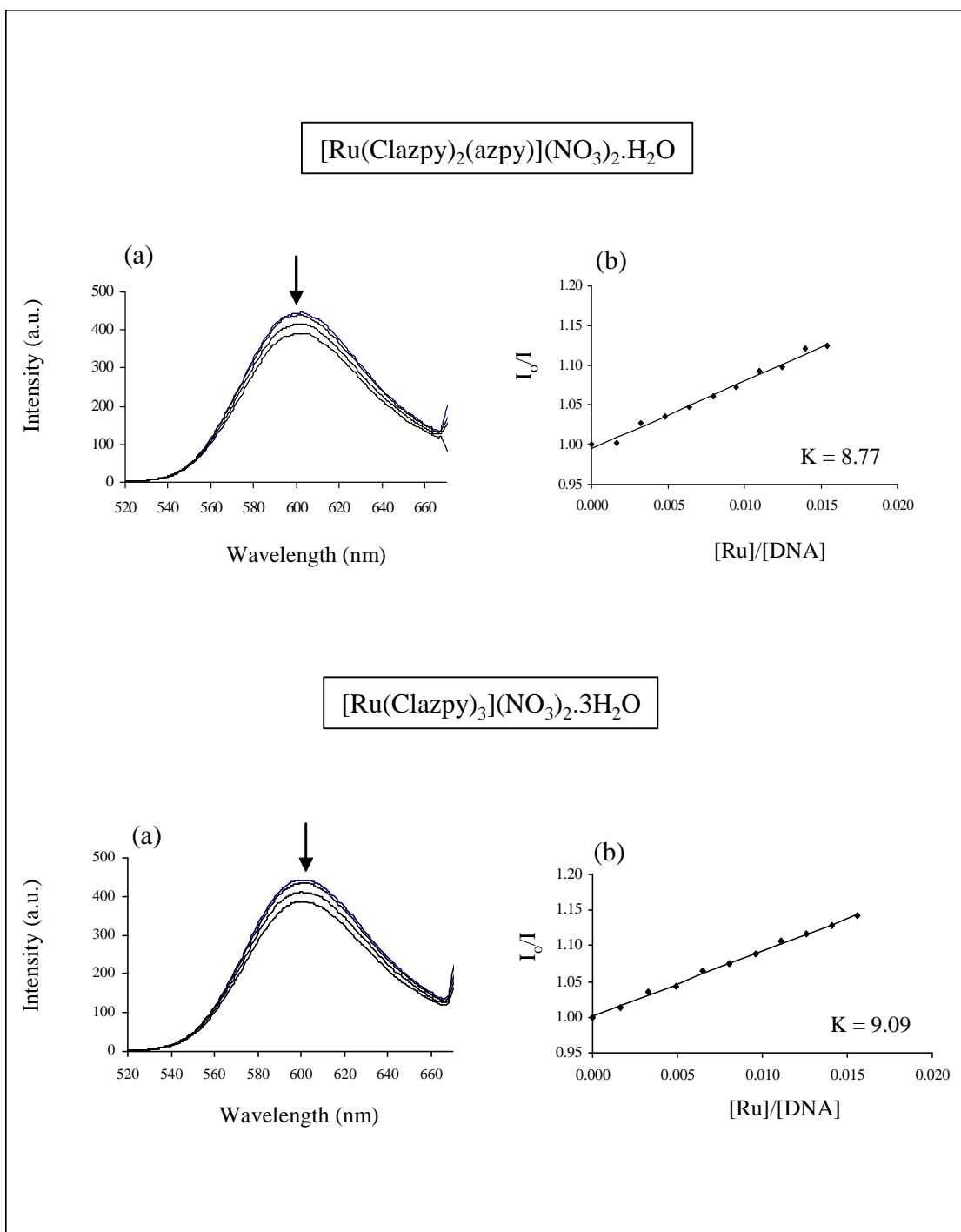


**Figure 3.235** (a) Fluorescence quenching curve of EB bound to DNA in the absence and presence of  $[Ru(Clazpy)_2(azpy)](NO_3)_2 \cdot H_2O$  and  $[Ru(Clazpy)_3](NO_3)_2 \cdot 3H_2O$ ,  $[EB] = 2.0 \mu M$ ,  $[DNA] = 40 \mu M$ ,  $[Ru] = 0, 0.1, 0.3, 0.6 \mu M$ ; (b) in the plot of  $[Ru(Clazpy)_2(azpy)](NO_3)_2 \cdot H_2O$  and  $[Ru(Clazpy)_3](NO_3)_2 \cdot 3H_2O$  of  $I_0/I$  versus  $[Ru]/[DNA] = 0 - 0.02$ .

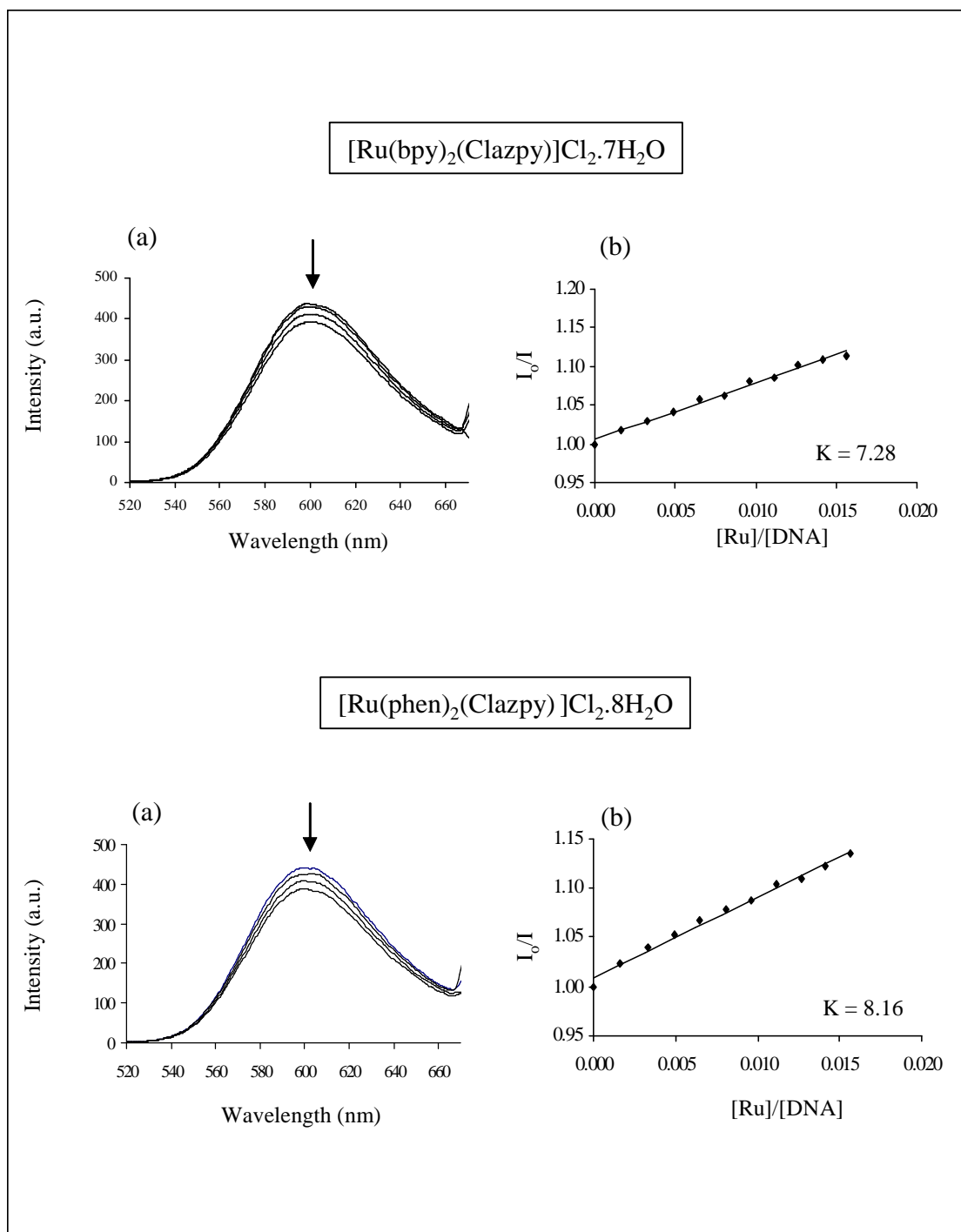


**Figure 3.236** (a) Fluorescence quenching curve of EB bound to DNA in the absence and presence of  $[\text{Ru}(\text{bpy})_2(\text{Clazpy})]\text{Cl}_2 \cdot 7\text{H}_2\text{O}$  and  $[\text{Ru}(\text{phen})_2(\text{Clazpy})]\text{Cl}_2 \cdot 8\text{H}_2\text{O}$ ,  $[\text{EB}] = 2.0 \mu\text{M}$ ,  $[\text{DNA}] = 40 \mu\text{M}$ ,  $[\text{Ru}] = 0, 0.1, 0.3, 0.6 \mu\text{M}$ ; (b) in the plot of  $[\text{Ru}(\text{bpy})_2(\text{Clazpy})]\text{Cl}_2 \cdot 7\text{H}_2\text{O}$  and  $[\text{Ru}(\text{phen})_2(\text{Clazpy})]\text{Cl}_2 \cdot 8\text{H}_2\text{O}$  of  $I_0/I$  versus  $[\text{Ru}]/[\text{DNA}] = 0 - 0.02$ .

### 3.8.4 Electrochemical studies

Cyclic voltammetric (CV) technique has been employed to study the interaction of the redox active Ru(II) complexes with DNA in order to further verify the DNA-binding modes assessed from the above spectral and viscosimeter studies. The cyclic voltammetric results of these complexes in the absence and presence of DNA in a mixture of DMSO and 5 mM Tris/50 mM NaCl buffer (pH 7.2) are given in Table 3.90. These data in the absence of DNA featured the reduction of +3 to +2 form at a cathodic peak potential (Wang *et al.*, 2004).

In this work, the presence of CT-DNA in the solution ( $R = 5$ ) at the same concentration of these complexes caused a considerable decrease in the voltammetric current. In addition, the peak potential,  $E_{p_c}$  and  $E_{p_a}$ , as well as  $E_{1/2}$  were shifted to more positive value. The drop of voltammetric currents in the presence of CT-DNA can be attributed to the diffusion of the metal complex bound to the large, slowly diffusing DNA molecule (Wang *et al.*, 2004) or due to diffusion of an equilibrium mixture of free and DNA-bound metal complex to the electrode surface (Arjmand *et al.*, 2005). The results parallel to the above spectroscopic and viscosity data of these complexes in the presence of DNA.

**Table 3.90** Cyclic voltammetric behavior for the Ru(II) complexes on interaction with CT-DNA

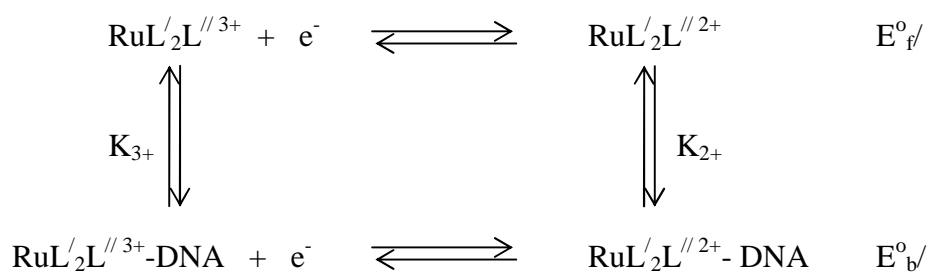
Complexes	R	E <sub>pa</sub> (V)	E <sub>pc</sub> (V)	<sup>a</sup> E <sub>1/2</sub> (V)	ΔE <sub>p</sub> (mV)	K <sub>2+</sub> /K <sub>3+</sub> (R = 0)
[Ru(Clazpy) <sub>2</sub> (bpy)]Cl <sub>2</sub> .7H <sub>2</sub> O	0	-0.397	-0.465	-0.431	68	1.66
	5	-0.378	-0.458	-0.418	80	
[Ru(Clazpy) <sub>2</sub> (phen)]Cl <sub>2</sub> .8H <sub>2</sub> O	0	-0.426	-0.496	-0.461	70	6.16
	5	-0.381	-0.447	-0.414	66	
[Ru(Clazpy) <sub>2</sub> (azpy)]Cl <sub>2</sub> .4H <sub>2</sub> O	0	-0.351	-0.409	-	-	-
	5	-0.308	-0.356	-	-	
[Ru(Clazpy) <sub>3</sub> ]Cl <sub>2</sub> .3H <sub>2</sub> O	0	-0.237	-0.293	-	-	-
	5	-0.232	-0.288	-	-	
[Ru(Clazpy) <sub>2</sub> (bpy)](NO <sub>3</sub> ) <sub>2</sub> .5H <sub>2</sub> O	0	-0.555	-0.605	-0.579	48	64.64
	5	-0.443	-0.501	-0.472	58	
[Ru(Clazpy) <sub>2</sub> (phen)](NO <sub>3</sub> ) <sub>2</sub> .3H <sub>2</sub> O	0	-0.398	-0.468	-0.433	70	1.36
	5	-0.380	-0.470	-0.425	110	
[Ru(Clazpy) <sub>2</sub> (azpy)](NO <sub>3</sub> ) <sub>2</sub> .H <sub>2</sub> O	0	-0.329	-0.455	-	-	-
	5	-0.287	-0.425	-	-	
[Ru(bpy) <sub>2</sub> (Clazpy)]Cl <sub>2</sub> .7H <sub>2</sub> O	0	-0.633	-0.821	-0.727	188	1.08
	5	-0.659	-0.791	-0.725	132	
[Ru(phen) <sub>2</sub> (Clazpy)]Cl <sub>2</sub> .8H <sub>2</sub> O	0	-0.664	-0.800	-0.732	136	3.48
	5	-0.618	-0.782	-0.700	164	

<sup>a</sup> measured versus ferrocene, using glassy carbon electrode, scan rate 50 mV s<sup>-1</sup>;  
 supporting electrolyte 5 mM Tris base/ 50 mM NaCl; complex concentration = 5 x  
 10<sup>-4</sup> M; R = [DNA]/[Ru]

To elucidate the binding mechanism involving the Ru(III) or Ru(II) forms of complex to CT-DNA (Scheme 1), the net shift in  $E_{1/2}$  can be used to estimate the ratio of equilibrium constants,  $K_{2+}/K_{3+}$  by the following equation.

$$E_b^{\circ'} - E_f^{\circ'} = 0.0591 \log (K_{2+}/K_{3+}) \quad (3.36)$$

where  $E_b^{\circ'}$  and  $E_f^{\circ'}$  are the formal potentials of the redox couple in the DNA bound and free form, respectively. It has been used to estimate the ratio of binding constant of the Ru(II) form and Ru(III) form to DNA (Vaidyanathan and Nair, 2003). The ratio of binding constants of +2 and +3 species was more than 1, suggesting that Ru(II) form interact with DNA is greater than Ru(III) (scheme I). For example, -13 mV shift in the Ru(III)/Ru(II) potential on binding of the  $[\text{Ru}(\text{Clazpy})_2(\text{bpy})]\text{Cl}_2 \cdot 7\text{H}_2\text{O}$  complex to DNA is indicative of the fact that the Ru(II) state of the complex is more easily reducible upon binding to DNA compared to the free complex. Treatment of the electrochemical data gave a value of 1.66 for  $K_{2+}/K_{3+}$  suggesting that this complex is binding to DNA in the ruthenium(II) state.



**Scheme 1**

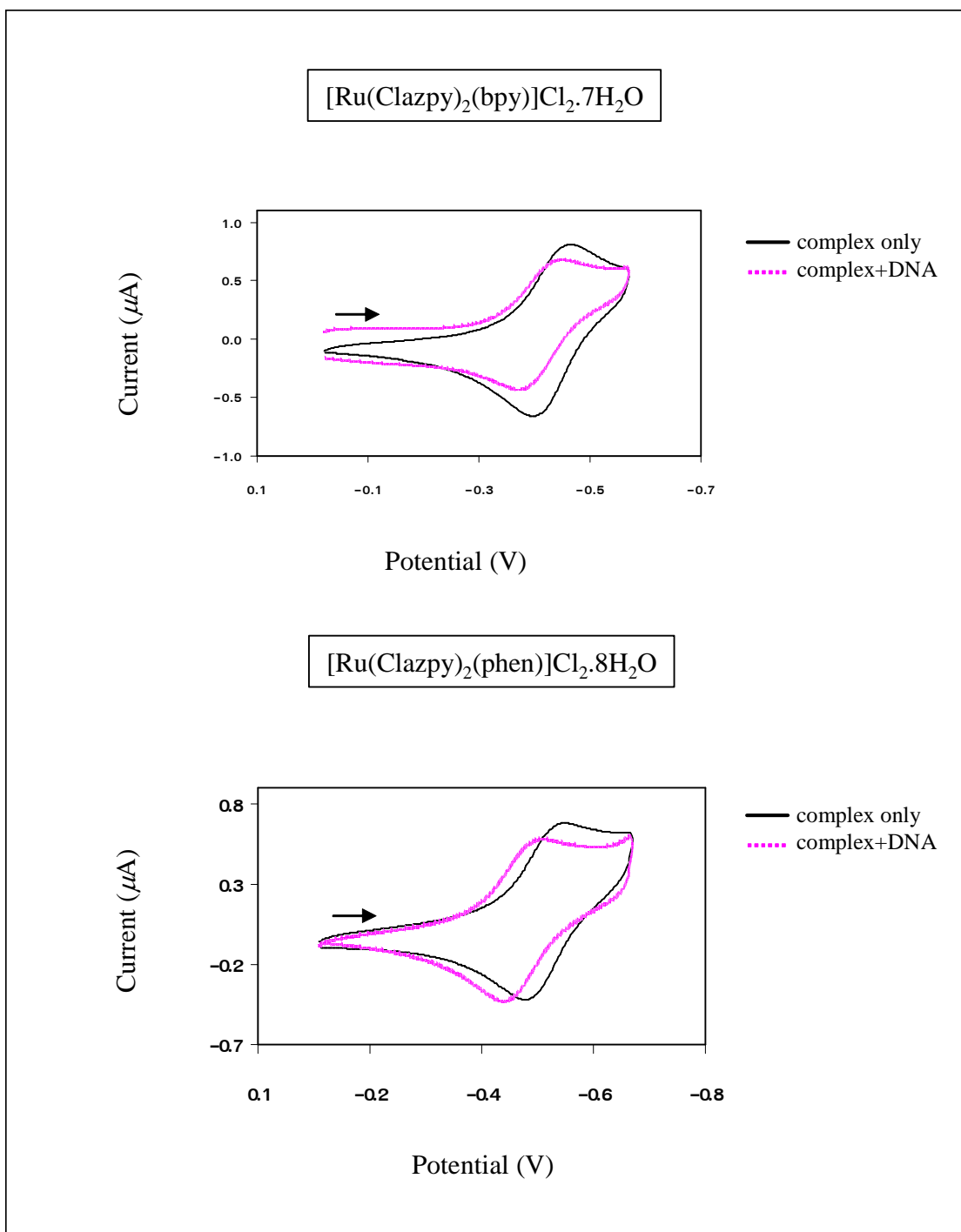


**Figure 3.237** Cyclic voltammogram of 0.5 mM  $[\text{Ru}(\text{Clazpy})_2(\text{bpy})]\text{Cl}_2 \cdot 7\text{H}_2\text{O}$  and  $[\text{Ru}(\text{Clazpy})_2(\text{phen})]\text{Cl}_2 \cdot 8\text{H}_2\text{O}$  in the absence and presence of 2.5 mM DNA. Supporting electrolyte, 5 mM Tris base/50 mM NaCl, pH 7.2 ( $\text{H}_2\text{O}:\text{DMSO}$  100:5),  $[\text{DNA}]/[\text{Ru}] = 5$ , scan rate 50 mV/s

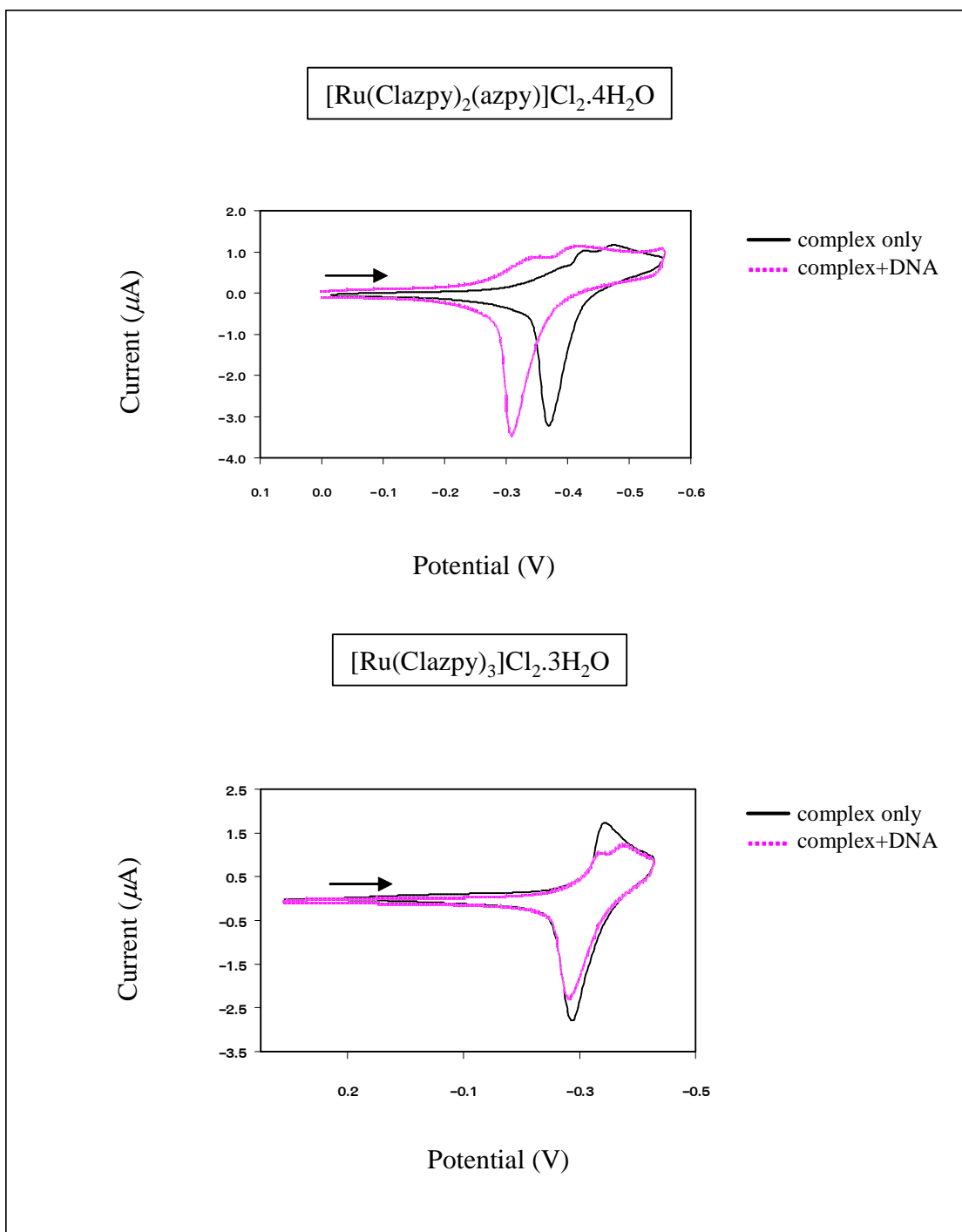


**Figure 3.238** Cyclic voltammogram of 0.5 mM  $[\text{Ru}(\text{Clazpy})_2(\text{azpy})]\text{Cl}_2 \cdot 4\text{H}_2\text{O}$  and  $[\text{Ru}(\text{Clazpy})_3]\text{Cl}_2 \cdot 3\text{H}_2\text{O}$  in the absence and presence of 2.5 mM DNA. Supporting electrolyte, 5 mM Tris base/50 mM NaCl, pH 7.2 ( $\text{H}_2\text{O}$ :DMSO 100:5),  $[\text{DNA}]/[\text{Ru}] = 5$ , scan rate 50 mV/s

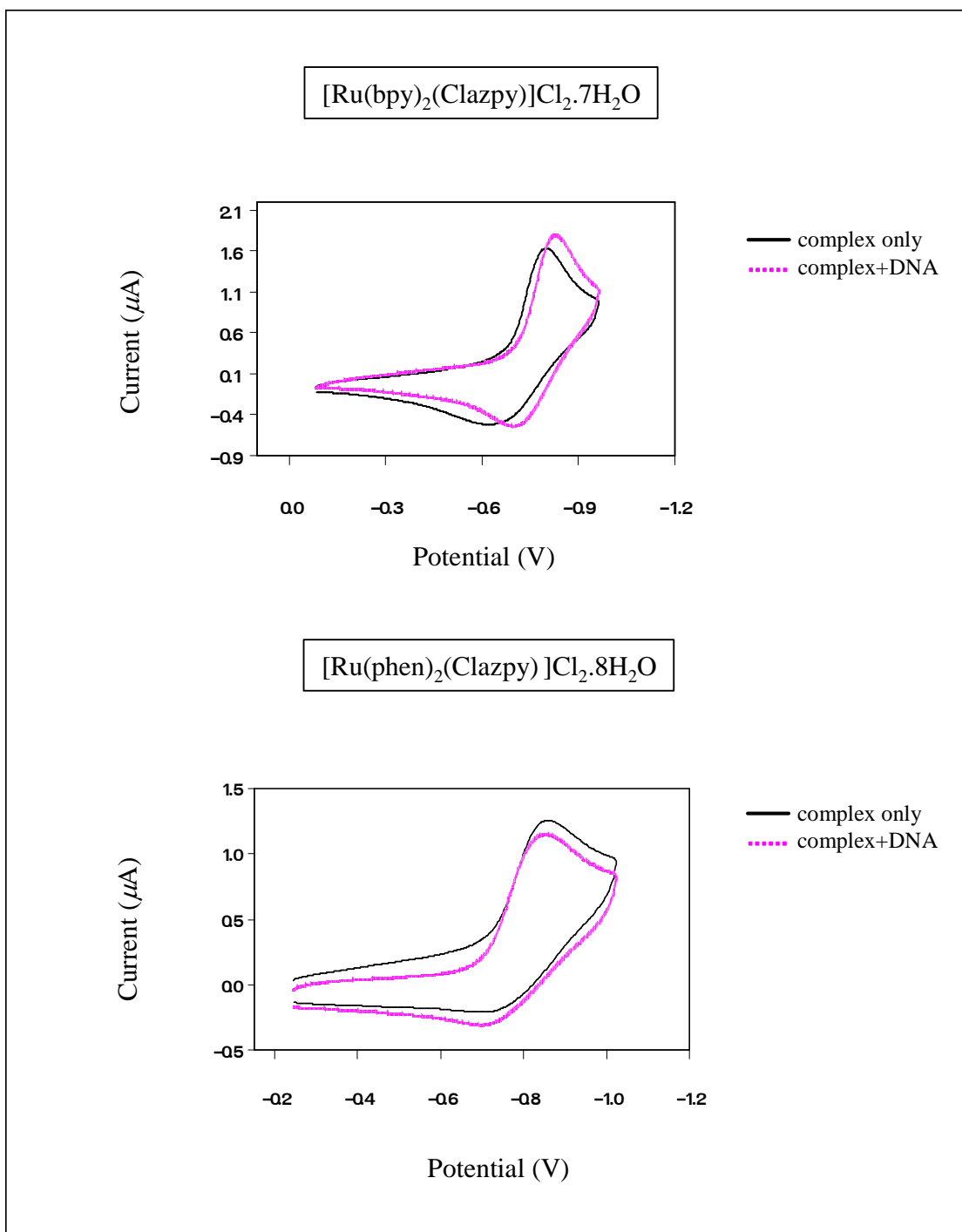


**Figure 3.239** Cyclic voltammogram of 0.5 mM  $[\text{Ru}(\text{bpy})_2(\text{Clazpy})]\text{Cl}_2 \cdot 7\text{H}_2\text{O}$  and  $[\text{Ru}(\text{phen})_2(\text{Clazpy})]\text{Cl}_2 \cdot 8\text{H}_2\text{O}$  in the absence and presence of 2.5 mM DNA. Supporting electrolyte, 5 mM Tris base/50 mM NaCl, pH 7.2 ( $\text{H}_2\text{O}:\text{DMSO}$  100:5),  $[\text{DNA}]/[\text{Ru}] = 5$ , scan rate 50 mV/s

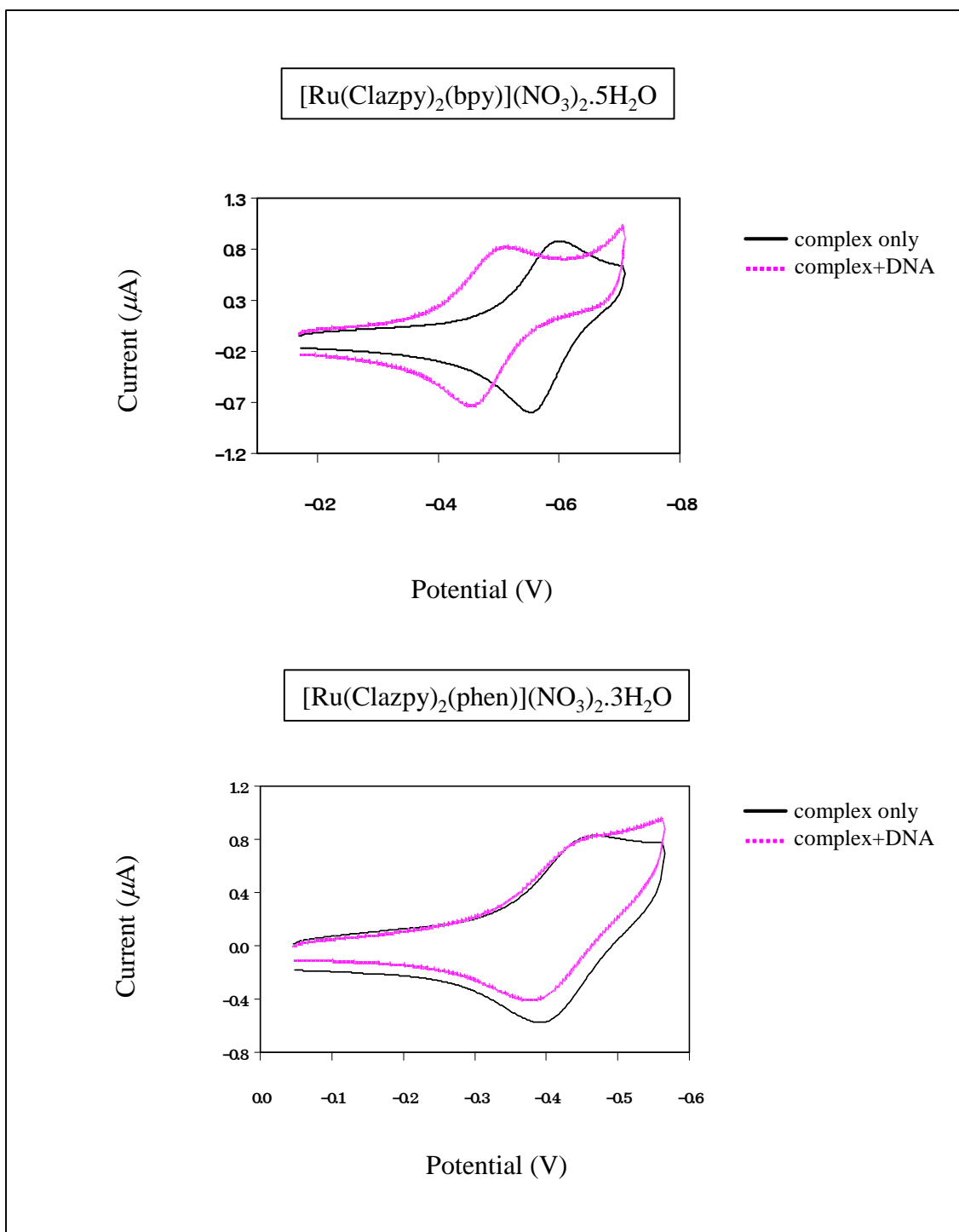


**Figure 3.240** Cyclic voltammogram of 0.5 mM  $[\text{Ru}(\text{Clazpy})_2(\text{bpy})](\text{NO}_3)_2 \cdot 5\text{H}_2\text{O}$  and  $[\text{Ru}(\text{Clazpy})_2(\text{phen})](\text{NO}_3)_2 \cdot 3\text{H}_2\text{O}$  in the absence and presence of 2.5 mM DNA. Supporting electrolyte, 5 mM Tris base/50 mM NaCl, pH 7.2 ( $\text{H}_2\text{O}:\text{DMSO}$  100:5),  $[\text{DNA}]/[\text{Ru}] = 5$ , scan rate 50 mV/s

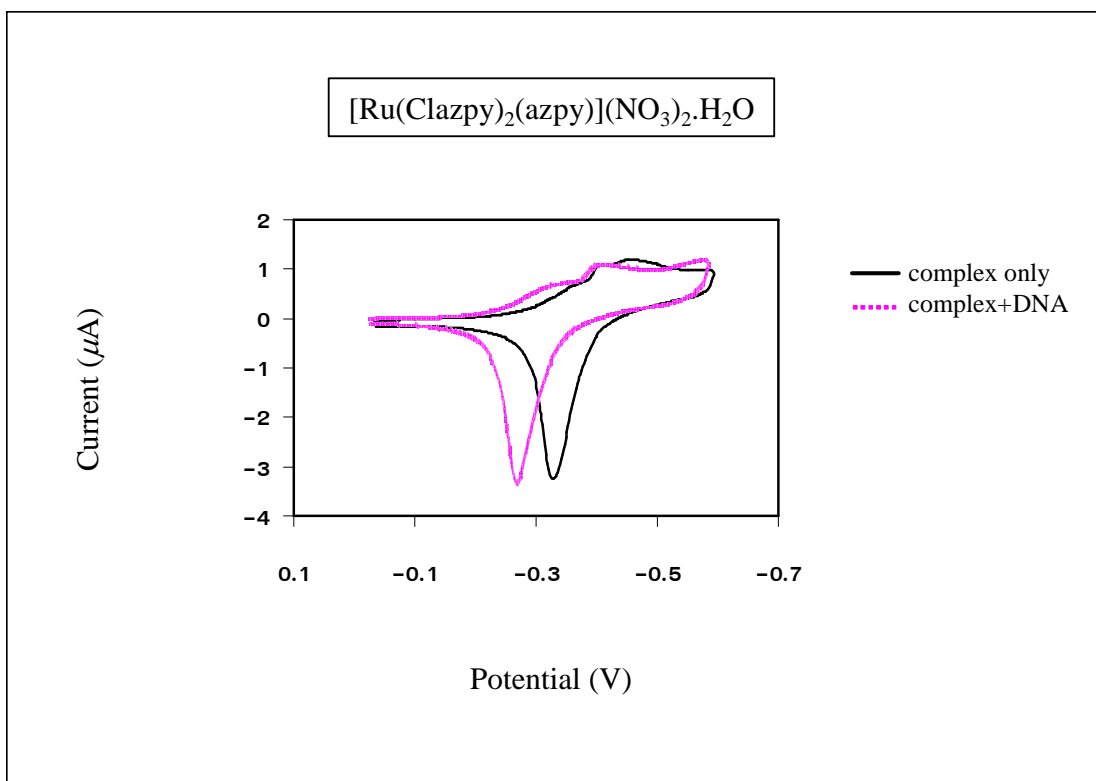


**Figure 3.241** Cyclic voltammogram of 0.5 mM  $[\text{Ru}(\text{Clazpy})_2(\text{azpy})](\text{NO}_3)_2 \cdot \text{H}_2\text{O}$  in the absence and presence of 2.5 mM DNA. Supporting electrolyte, 5 mM Tris base/50 mM NaCl, pH 7.2 ( $\text{H}_2\text{O}:\text{DMSO}$  100:5),  $[\text{DNA}]/[\text{Ru}] = 5$ , scan rate 50 mV/s

### 3.9 Cytotoxicity test

The cytotoxicity of the ruthenium complexes tested in this work can be compared with the known compound, cisplatin. The cytotoxicity has been evaluated by means of IC<sub>50</sub> values (the concentration of the drug required to inhibit cell growth by 50%) in the human three cancer cell lines i.e. Oral human epidermal carcinoma (Anti-NCI-H187), breast cancer (BC), small cell lung cancer (KB). The IC<sub>50</sub> values corresponding to cisplatin are summarized in Table 3.91.

**Table 3.91** IC<sub>50</sub> values in  $\mu\text{g/mL}$  ( $\mu\text{M}$ ) of Clazpy and its complexes against a series of tumor cell lines

Compounds	Anti-NCI-H187		BC		KB	
	IC <sub>50</sub> ( $\mu\text{g/ml}$ )	IC <sub>50</sub> ( $\mu\text{M}$ )	IC <sub>50</sub> ( $\mu\text{g/ml}$ )	IC <sub>50</sub> ( $\mu\text{M}$ )	IC <sub>50</sub> ( $\mu\text{g/ml}$ )	IC <sub>50</sub> ( $\mu\text{M}$ )
cisplatin	inactive	inactive	inactive	inactive	inactive	inactive
Clazpy	7.51	34.53	inactive	inactive	inactive	inactive
$\gamma$ -[Ru(Clazpy) <sub>2</sub> Cl <sub>2</sub> ]	7.65	12.59	18.4	30.29	inactive	inactive
$\alpha$ -[Ru(Clazpy) <sub>2</sub> Cl <sub>2</sub> ]	5.7	9.38	12.67	20.86	inactive	inactive
$\beta$ -[Ru(Clazpy) <sub>2</sub> Cl <sub>2</sub> ]	0.671	1.10	1.2	1.98	1.46	2.40
[Ru(Clazpy)(dmazpy)Cl <sub>2</sub> ]	inactive	inactive	inactive	inactive	inactive	inactive
[Ru(Clazpy) <sub>2</sub> bpy](PF <sub>6</sub> ) <sub>2</sub>	5.466	5.56	8.95	9.11	3.52	3.58
[Ru(Clazpy) <sub>2</sub> phen](PF <sub>6</sub> ) <sub>2</sub>	3.542	3.52	7.37	7.32	1.82	1.81
[Ru(Clazpy) <sub>2</sub> azpy](PF <sub>6</sub> ) <sub>2</sub>	0.694	0.69	1.84	1.82	1.68	1.66
[Ru(Clazpy) <sub>3</sub> ](PF <sub>6</sub> ) <sub>2</sub>	0.286	0.27	0.73	0.70	0.886	0.85
[Ru(Clazpy) <sub>2</sub> bpy](NO <sub>3</sub> ) <sub>2</sub> ·5H <sub>2</sub> O	5.847	6.45	7.13	7.86	3.29	3.63
[Ru(Clazpy) <sub>2</sub> phen](NO <sub>3</sub> ) <sub>2</sub> ·3H <sub>2</sub> O	2.799	3.13	3.86	4.31	2.18	2.44
[Ru(Clazpy) <sub>2</sub> azpy](NO <sub>3</sub> ) <sub>2</sub> ·H <sub>2</sub> O	0.669	0.76	1.93	2.19	1.52	1.73
[Ru(Clazpy) <sub>3</sub> ](NO <sub>3</sub> ) <sub>2</sub> ·5H <sub>2</sub> O	0.449	0.46	0.695	0.72	0.693	0.72
[Ru(Clazpy) <sub>2</sub> bpy]Cl <sub>2</sub> ·7H <sub>2</sub> O	5.477	6.16	7.85	8.82	3.09	3.47
[Ru(Clazpy) <sub>2</sub> phen]Cl <sub>2</sub> ·8H <sub>2</sub> O	2.5	2.68	4.88	5.24	2.23	2.39
[Ru(Clazpy) <sub>2</sub> azpy]Cl <sub>2</sub> ·4H <sub>2</sub> O	0.614	0.71	1.66	1.92	1.76	2.04
[Ru(Clazpy) <sub>3</sub> ]Cl <sub>2</sub> ·3H <sub>2</sub> O	0.195	0.22	0.685	0.78	0.753	0.86
[Ru(bpy) <sub>2</sub> Clazpy](PF <sub>6</sub> ) <sub>2</sub>	inactive	inactive	inactive	inactive	inactive	inactive
[Ru(phen) <sub>2</sub> Clazpy](PF <sub>6</sub> ) <sub>2</sub>	inactive	inactive	inactive	inactive	inactive	inactive
[Ru(bpy) <sub>2</sub> Clazpy]Cl <sub>2</sub> ·7H <sub>2</sub> O	inactive	inactive	inactive	inactive	inactive	inactive
[Ru(phen) <sub>2</sub> Clazpy]Cl <sub>2</sub> ·8H <sub>2</sub> O	inactive	inactive	inactive	inactive	inactive	inactive

\* IC<sub>50</sub> ( $\mu\text{g/mL}$ ) interpretation

> 20 Inactive; 10-20 Weakly active; 5-10 Moderately active; < 5 Strongly active

The cytotoxicity data of all complexes compared with well-known compound cisplatin, in a series of human tumor cell lines, are listed in Table 3.91. As reported earlier (Velder *et al.*, 2000), the *ctc*- or  $\alpha$ -[Ru(azpy)<sub>2</sub>Cl<sub>2</sub>] shows a very pronounced cytotoxicity, higher than that of cisplatin and others isomers in all cell line.

From Table 3.91, it is indicated that although the Clazpy ligand showed only active in Anti-NCI-H187 cell line, but its complexes, [Ru(Clazpy)<sub>2</sub>Cl<sub>2</sub>] showed a moderate to strongly active for all cell lines. On the other hand, the [Ru(Clazpy)(5dmazpy)Cl<sub>2</sub>] complex showed no effect to cancer cell lines. This result is similar to the data of [Ru(azpy)(bpy)Cl<sub>2</sub>] which displayed less cytotoxic activity than the parent compound, *ctc*-[Ru(azpy)<sub>2</sub>Cl<sub>2</sub>] (Hotze *et al.*, 2004). It can be summarized that the two ancillary ligands (Clazpy or azpy) in the complexes has an effect to cytotoxic activity in cancer cell lines. Moreover, replacing two chloro ligands in the precursor complex, *ctc*-[Ru(Clazpy)<sub>2</sub>Cl<sub>2</sub>] give rise the ionic compounds of [Ru(Clazpy)<sub>2</sub>(L)]X<sub>2</sub> (L = bpy, phen, azpy, Clazpy; X = PF<sub>6</sub><sup>-</sup>, NO<sub>3</sub><sup>-</sup>, Cl<sup>-</sup>) which showed higher cytotoxic activity than *ctc*-[Ru(Clazpy)<sub>2</sub>Cl<sub>2</sub>], especially tris-chelate complexes [Ru(Clazpy)<sub>3</sub>]X<sub>2</sub> (X = PF<sub>6</sub><sup>-</sup>, NO<sub>3</sub><sup>-</sup>, Cl<sup>-</sup>). Therefore, it is concluded that

- (1) only a Clazpy ligand has slightly effect to human tumor cell lines
- (2) in three dimensional structure of ruthenium(II) complex with Clazpy, [Ru(Clazpy)<sub>2</sub>Cl<sub>2</sub>] play an interesting role to different kind of cell lines with different activity like the previous reported (Velder *et al.*, 2000; Hotze *et al.*, 2004; Haatnoot *et al.*, 2004)
- (3) replacing a Clazpy ligand with 5dmazpy in *ctc*-[Ru(Clazpy)<sub>2</sub>Cl<sub>2</sub>] having no effect to cancer cell lines
- (4) the [Ru(Clazpy)<sub>2</sub>(L)]<sup>2+</sup> (L = bpy, phen, azpy, Clazpy) complexes showed higher cytotoxic activity for cancer cell lines than the parent compounds, *ctc*-[Ru(Clazpy)<sub>2</sub>Cl<sub>2</sub>] in absence of chloro ligands
- (5) the different salts of PF<sub>6</sub><sup>-</sup>, NO<sub>3</sub><sup>-</sup>, Cl<sup>-</sup>, [Ru(Clazpy)<sub>2</sub>(L)]<sup>2+</sup> complexes have no effect for the cytotoxic activity with similarity of IC<sub>50</sub> values. However, PF<sub>6</sub><sup>-</sup> complexes are water- insoluble and NO<sub>3</sub><sup>-</sup> complexes is highly toxic in cell (Wong and Giandomenico, 1999). Thus, Cl<sup>-</sup>

complexes are suitable for further studying in physiological condition in the future

- (6) on the other hand, if bpy and phen as an ancillary ligand in  $[\text{Ru}(\text{L})_2(\text{Clazpy})]^{2+}$  (L = bpy and phen), they showed no effect to cancer cell lines although having a Clazpy ligand

In addition, the cytotoxic ruthenium(II) complexes were tested further with Vero cells and the results are listed Table 3.92.

**Table 3.92** IC<sub>50</sub> values in  $\mu\text{g/mL}$  ( $\mu\text{M}$ ) of some ruthenium(II) complexes against a vero cell

Compounds	Cytotoxicity	
	IC <sub>50</sub> mg/mL	IC <sub>50</sub> mM
$[\text{Ru}(\text{Clazpy})_2(\text{bpy})](\text{PF}_6)_2$	> 50	> 50.89
$[\text{Ru}(\text{Clazpy})_2(\text{phen})](\text{PF}_6)_2$	> 50	> 49.68
$[\text{Ru}(\text{Clazpy})_2(\text{azpy})](\text{PF}_6)_2$	19.39	19.21
$[\text{Ru}(\text{Clazpy})_3](\text{PF}_6)_2$	1.38	1.32
$[\text{Ru}(\text{Clazpy})_2(\text{bpy})](\text{NO}_3)_2 \cdot 5\text{H}_2\text{O}$	> 50	> 55.15
$[\text{Ru}(\text{Clazpy})_2(\text{phen})](\text{NO}_3)_2 \cdot 3\text{H}_2\text{O}$	> 50	> 55.89
$[\text{Ru}(\text{Clazpy})_2(\text{azpy})](\text{NO}_3)_2 \cdot 2\text{H}_2\text{O}$	15.84	18.01
$[\text{Ru}(\text{Clazpy})_3](\text{NO}_3)_2 \cdot 5\text{H}_2\text{O}$	2.95	3.05
$[\text{Ru}(\text{Clazpy})_2(\text{bpy})]\text{Cl}_2 \cdot 7\text{H}_2\text{O}$	> 50	> 56.21
$[\text{Ru}(\text{Clazpy})_2(\text{phen})]\text{Cl}_2 \cdot 8\text{H}_2\text{O}$	> 50	> 53.67
$[\text{Ru}(\text{Clazpy})_2(\text{azpy})]\text{Cl}_2 \cdot 4\text{H}_2\text{O}$	22.13	25.66
$[\text{Ru}(\text{Clazpy})_3]\text{Cl}_2 \cdot 3\text{H}_2\text{O}$	2.44	2.78

From data, the complexes of  $[\text{Ru}(\text{Clazpy})_2]^{2+}$  (L = bpy and phen) has no side effect to normal cell in contrast to the complexes as L are azpy and Clazpy which show a very toxic in normal cell.

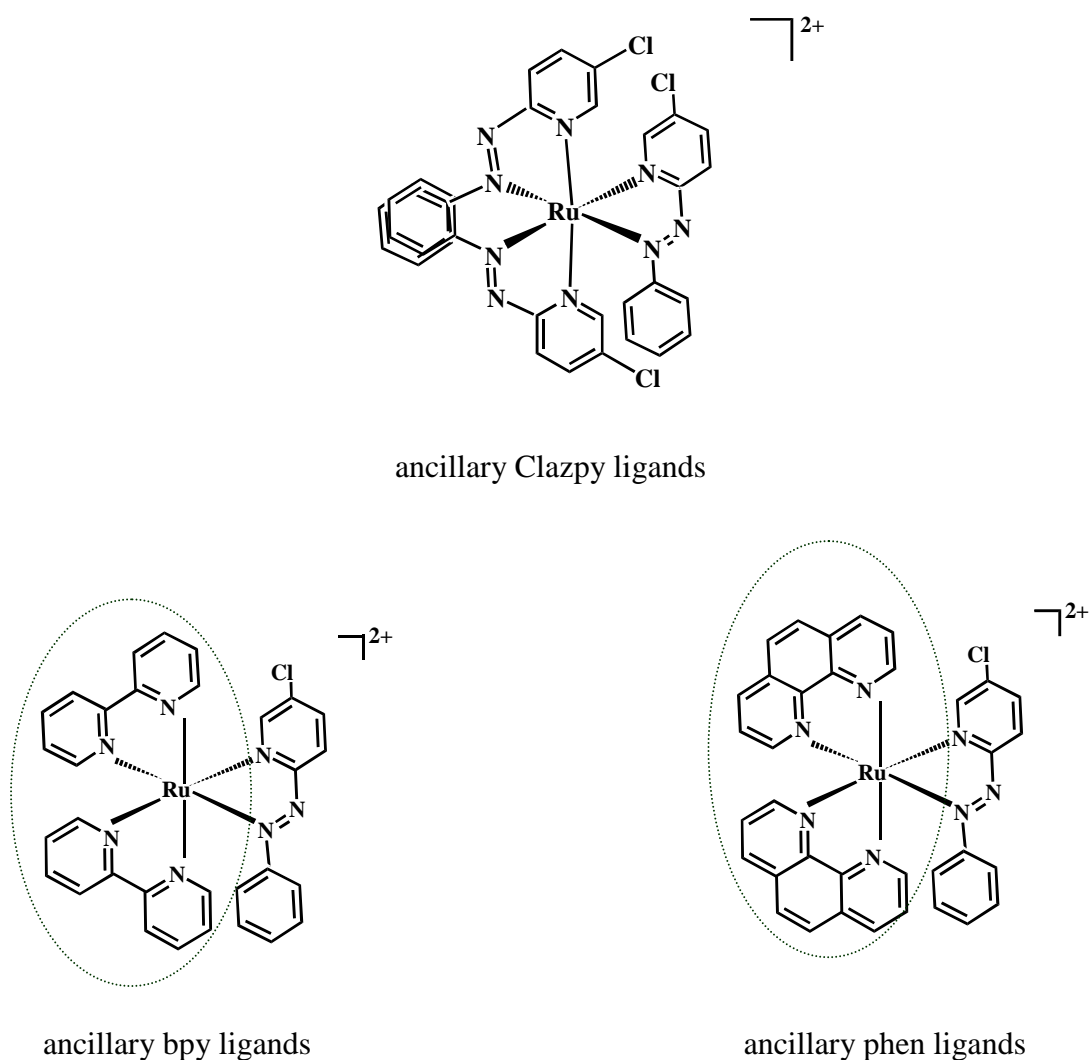
It is summarized that the influence of cytotoxic activity of these series of compounds depend on structural differences such as isomeric structures ( $\alpha$  and  $\beta$  backbones) and variation of ligands around metal center. However, the reason of all factors having influence of the activity of these compounds is not yet far from understood, and more in vitro and in vivo studies are needed in the search for structure-activity relationships for these kind of the isomeric  $[\text{Ru}(\text{L})_2\text{Cl}_2]$  complexes and ionic  $[\text{Ru}(\text{L})_2\text{L}']^{2+}$  in the future further.

## CHAPTER 4 CONCLUSION

In this work the syntheses and characterization of the new bidentate azoimine ligand 5-Chloro-2-(phenylazo)pyridine or Clazpy and the corresponding three isomeric ruthenium(II) compounds,  $[\text{Ru}(\text{Clazpy})_2\text{Cl}_2]$  have been described. The structure of such ligand is similar to, a good  $\pi$ -acceptor, 2-(phenylazo)pyridine or azpy but the hydrogen atom at the fifth position on pyridine ring is replaced by electronegativity chlorine atom. All isomers have been obtained pure and have been confirmed structure by X-ray Crystallography. The result from IR and X-ray data supported that the Clazpy ligand is stronger  $\sigma$ -donor properties than azpy and comparable a  $\pi$ -acceptor properties to azpy. In addition, the mixed-azoimine ligand,  $[\text{Ru}(\text{Clazpy})(5\text{dmazpy})\text{Cl}_2]$  (5dmazpy = 5-*N,N*-dimethyl-2-(phenylazo)pyridine) was observed in during isomerization process by addition-elimination mechanism on a pyridine ring and its structure can be also supposed by X-ray diffraction analysis. It is noting that results from X-ray data of the Clazpy ligand have also a better  $\pi$ -acceptor properties than the 5dmazpy ligand within the same molecule corresponding to IR data that described previously. The electrochemical behavior showed the most stable compound is *cis*-form of *ctc*- $[\text{Ru}(\text{Clazpy})_2\text{Cl}_2]$ .

Variation of bidentate ligands in  $[\text{Ru}(\text{Clazpy})_2(\text{L})](\text{X})_2$  (L = bpy, phen, azpy, Clazpy; X =  $\text{PF}_6^-$ ,  $\text{NO}_3^-$ , Cl) afforded from the reaction between *ctc*- $[\text{Ru}(\text{Clazpy})_2\text{Cl}_2]$  and L in ethanol give interesting chemical properties differed from the parent complex. Results from spectroscopic data and electrochemical studies showed that the increasing chelate ligand in molecule of tris and mixed-ligand complexes the compounds more stable are. It was found that although the different salts have no effected to the  $\pi$ -accepting ability of ligands, the stability depends on the potential value of Ru(II)/(III) couple. The chloride complexes were sensitively or easily oxidized compared to nitrate and hexafluorophosphate complexes. A changing pure form with impurity in a few weeks of chloride salts complexes supported their CV data.

The interaction between water-soluble compounds,  $[\text{Ru}(\text{Clazpy})_2(\text{L})](\text{X})_2$  ( $\text{L} = \text{bpy}, \text{phen}, \text{azpy}, \text{Clazpy}; \text{X} = \text{NO}_3^-, \text{Cl}^-$ ) and  $[\text{Ru}(\text{L})_2(\text{Clazpy})]\text{Cl}_2 \cdot x\text{H}_2\text{O}$  ( $\text{L} = \text{bpy}, \text{phen}$ ) with CT-DNA were investigated. Spectroscopic studies, viscosity measurements together with fluorescence quenching and electrochemical behavior indicate that the  $[\text{Ru}(\text{Clazpy})_2(\text{L})]^{2+}$  complexes can bind to CT-DNA better than that of  $[\text{Ru}(\text{L})_2\text{Clazpy}]^{2+}$ . Additionally, as the ancillary ligand varies from phen, Clazpy to bpy, the DNA binding affinity of their ruthenium(II) complexes declines.



**Scheme 2** The structure of  $[\text{Ru}(\text{L})_2(\text{Clazpy})]^{2+}$  ( $\text{L} = \text{bpy}, \text{phen}, \text{Clazpy}$ )

Moreover, the DNA binding affinity of  $[\text{Ru}(\text{Clazpy})_2(\text{azpy})]^{2+}$  and  $[\text{Ru}(\text{Clazpy})_3]^{2+}$  is slightly better than that of  $[\text{Ru}(\text{Clazpy})_2(\text{bpy})]^{2+}$  and  $[\text{Ru}(\text{Clazpy})_2(\text{phen})]^{2+}$ . Thus, it is summarized that the effect of azoimine ligand has an influence to binding properties with CT-DNA. The results from viscosity showed that  $[\text{Ru}(\text{Clazpy})_2(\text{L})](\text{X})_2$  could be intercalate to DNA as partial intercalation mode by  $\pi$ - $\pi$  stacking interaction binding base pair and also including generally electrostatic of cationic ruthenium(II) complexes with anionic DNA and groove binding modes by the large of molecules.

Preliminary evaluation of the cytotoxicity by means of the  $\text{IC}_{50}$  value with Anti-NCI-H187, KB and BC cell lines classified almost compounds as being cytotoxic excepting  $[\text{Ru}(\text{Clazpy})(5\text{dmazpy})\text{Cl}_2]$  and  $[\text{Ru}(\text{L})_2(\text{Clazpy})](\text{X})_2$  ( $\text{L} = \text{bpy}$ ,  $\text{phen}$ ;  $\text{PF}_6^-$ ,  $\text{Cl}^-$ ). From data, it is concluded that the complexes contained two Clazpy ligands play a significant role to cytotoxic activity in cancer cell lines. These data agree well with the above biological experiments.

## BIBLIOGRAPHY

- คณาจารย์ภาควิชาชีวเคมี คณะวิทยาศาสตร์ จุฬาลงกรณ์มหาวิทยาลัย. 2541. ตำราปฏิบัติการชีวเคมีเบื้องต้น. พิมพ์ครั้งที่ 3. ศูนย์หนังสือจุฬาลงกรณ์มหาวิทยาลัย.: กรุงเทพฯ.
- นิพนธ์ ตั้งคณานุรักษ์ และคณิตา ตั้งคณานุรักษ์. 2547. สเปกโทรสโกปีด้านการวิเคราะห์ (Analytical Spectroscopy). ศูนย์หนังสือมหาวิทยาลัยเกษตรศาสตร์.: กรุงเทพฯ.
- Al-Noaimi, M.Z., Abdel-Jalil, R.J., Haddad, S.F., Al-Far, R.H. and Crutchley, R.J. 2006. Ruthenium(II) Complex of the Novel Azoimine Ligand,  $\alpha$ -Acetyl- $\alpha$ -phenylazo-4-chlorophenylazomethine. Inorg. Chim. Acta. 359, 2395-2399.
- Arjmand, F., Mohani, B. and Ahmad, S. 2005. Synthesis, Antibacterial, Antifungal Activity and Interaction of CT-DNA with a New Benzimidazole Derived Cu(II) Complex. Eur. J. Med. Chem. 40, 1103-1110.
- Aslanoglu, M. 2006. Electrochemical and Spectroscopic Studies of the Interaction of Proflavine with DNA. Anal. Sci. 22, 439-443.
- Barton, J.K., Danishefsky, A.T. and Goldberg, J.M. 1984. Tris(phenanthroline) Ruthenium(II): Stereoselectivity in Binding to DNA. J. Am. Chem. Soc. 106, 2172-2176.
- Barf, G.A. and Sheldon, R.A. 1995. Ruthenium(II) 2-(Phenylazo)pyridine Complexes as Epoxidation Catalysts. J. Mol. Catal. 98, 143-146.
- Brabec, V. and Nováková, O. 2006. DNA Binding Mode of Ruthenium Complexes and Relationship to Tumor Cell Toxicity. Drug Resist. Updates. 9, 111-122.
- Butler, J.N., and Cogley, D.R. 1998. Ionic Equilibrium Solubility and pH Calculations. John Wiley & Sons.: New York.

- Byabartta, P., Santra, P.K., Misra, T.K., Sinha, C. and Kennard, C.H.L. 2001. Synthesis, Spectral Characterization, Redox Studies of Isomeric Dichloro-bis-[1-alkyl-2-(naphthyl-( $\alpha/\beta$ )-azo)imidazole]ruthenium(II). Single Crystal X-ray Structure of Blue-green Dichloro-bis-[1-ethyl-2-(naphthyl- $\alpha$ -azo)imidazole] Ruthenium(II). *Polyhedron*. 20, 905-913.
- Byabartta, P., Jasimuddin, S.K., Mostafa, G., Lu, T.-H. and Sinha, C. 2003. The Synthesis, Spectral Studies and Electrochemistry of 1,10-(Phenanthroline)-bis-{1-alkyl-2-(arylo)imidazole}ruthenium(II) Perchlorate. Single Crystal X-ray Structure of  $[\text{Ru}(\text{phen})(\text{HaaiMe})_2](\text{ClO}_4)_2$  [Phen = 1,10-Phenanthroline, HaaiMe = 1-Methyl-2-(phenylazo)imidazole]. *Polyhedron*. 22, 849-859.
- Byabartta, P. 2007. Heteroleptic Tris-chelates of Ruthenium(II): Synthesis, Spectral Characterization and Electrochemical Properties. *Spectrochim. Acta Part A*. 66, 521-533.
- Changsaluk, U. 2003. Chemistry of Bis[2-(phenylazo)pyridine]ruthenium(II) Complexes with 1,10-Phenanthroline and Other Ligands. Master of Science Thesis, Prince of Songkla University, Songkhla, Thailand.
- Chao, H., Mei, W.-J., Huang, Q.-W. and Ji, L.-N. 2002. DNA Binding Studies of Ruthenium(II) Complexes Containing Asymmetric Tridentate Ligands. *J. Inorg. Biochem.* 92, 165-170.
- Chen, J., Li, J., Wu, W. and Zheng, K. 2006. Structures and Anticancer Activities of a Series of Isomeric Complexes  $\text{Ru}(\text{azpy})_2\text{Cl}_2$ . *Acta Phys.-Chim. Sin.* 22(4), 391-396.
- Clarke, M.J. 2002. Ruthenium Metallopharmaceuticals. *Coord. Chem. Rev.* 232, 69-93.

- Clarke, M.J. 2003. Ruthenium Metallopharmaceuticals. *Coord. Chem. Rev.* 236, 209-233.
- Dougan, S.J., Melchart, M., Habtemariam, A., Parsons, S. and Sadler, P.J. 2006. Phenylazo-pyridine and Phenylazo-pyrazole Chlorido Ruthenium(II) Arene Complexes: Arene Loss, Aquation, and Cancer Cell Cytotoxicity. *Inorg. Chem.* 45, 10882-10894.
- Erkkila, K.E., Odam, D.T. and Barton, J.K. 1999. Recognition and Reaction of Metallointercalators with DNA. *Chem. Rev.* 99, 2777-2795.
- Farah, A.A. and Pietro, W. 2001. *Cis*-dichloro-bis-2-(2-pyridyl)-4-(methylcarboxy) quinoline Ruthenium (II): a Novel Ruthenium (II) Tris-chelated Building Precursor. *Inorg. Chem. Commun.* 4, 237-240.
- Friedman, A.E., Turro, N.J. and Barton, J.K. 1991. The Recognition of DNA Structure by a "Molecular Light Switch"  $[\text{Ru}(\text{N-N})_2(\text{DPPZ})]^{2+}$ . *J. Inorg. Biochem.* 43(2-3), 442.
- Gao, F., Chao, H., Zhou, F., Yuan, Y.-X., Peng, B. and Ji, L.-N. 2006. DNA Interactions of a Functionalized Ruthenium(II) Mixed-polypyridyl Complex  $[\text{Ru}(\text{bpy})_2\text{ppd}]^{2+}$ . *J. Inorg. Biochem.* 100, 1487-1494.
- Ghosh, S., Barve, A.C., Kumbhar, A.A., Kumbhar, A.S., Puranik, V.G., Datar, P.A., Sonawane, U.B., and Joshi, R.R. 2006. Synthesis, Characterization, X-ray Structure and DNA Photocleavage by *cis*-Dichloro Bis(diimine) Co(III) Complexes. *Biochemistry.* 100, 331-343.
- Gordon, A.J., and Richard, A.F. 1972. *The Chemist's Companion a Hand Book of Practical Data, Techniques and Reference.* John Wiley & Sons.: New York.

- Goswami, S., Chakravarty, A.R. and Chakravorty, A. 1981. Chemistry of Ruthenium. 2.<sup>1</sup> Synthesis, Structure, and Redox Properties of 2-(Arylazo)pyridine Complexes. *Inorg. Chem.* 20, 2246-2250.
- Goswami, S., Chakravarty, A.R. and Chakravorty, A. 1982. Chemistry of Ruthenium. 5.<sup>1</sup> Reaction of trans-Dichlorobis[2-(arylazo)pyridine]ruthenium(II) with Tertiary Phosphines: Chemical, Spectroelectrochemical, and Mechanistic Characterization of Geometrically Isomerized Substitution Products. *Inorg. Chem.* 21, 2737-2742.
- Goswami, S., Mukherjee, R. and Chakravorty, A. 1983. Chemistry of ruthenium. 12.<sup>1</sup> Reactions of Bidentate Ligands with Diaquobis[2-(arylazo)pyridine] Ruthenium(II) Cation. Stereoretentive Synthesis of Tris Chelates and Their Characterization: Metal Oxidation, Ligand Reduction, and Spectroelectrochemical Correlation. *Inorg. Chem.* 22, 2825-2832.
- Han, D., Wang, H. and Ren, N. 2004. Molecular Modeling Study on the Binding Mode of Polypyridyl Transition Ru Metal Complexes with B-DNA. *J. Molecular Struct: THEOCHEM.* 711, 185-192.
- Hansongnern, K., Changsaluk, U., Wu, J.-S. and Lu, T.-H. 2007. Crystal Structure of the [Ru(azpy)<sub>2</sub>bpy](PF<sub>6</sub>)<sub>2</sub> Complex (azpy = 2-(Phenylazo)pyridine, bpy = 2,2'-Bipyridine). *Anal. Sci.* 23, x131-1132.
- Hoffmann, E.D., Charette, J., and Stroobant, V. 1996. Mass spectrometry: Principles and Applications. John Wiley & Sons.: Chichester.
- Hong, J., Yang, G.-S., Duan, C.-Y., Guo, Z.-J. and Zhu, L.-G. 2005. Fluorescence Quenching of EB-DNA Complex by a Novel di-Bipyridyl Ruthenium(II) Complex of *p*-tert-Butyltetrathiacalix[4]arene. *Inorg. Chem. Commun.* 8, 988-991.

- Horton, H.R., Moran, L.A., Ochs, R.S., Rawn, J.D. and Scrimgeour, K.G. 1996. Principles of Biochemistry. 2<sup>nd</sup> ed. Upper Saddle River, N.J.: Prentice Hall.
- Hotze, A.C.G., Velders, A.H., Ugozzoli, F., Biagini-Cingi, M., Manotti-Lanfredi, A.M., Haasnoot, J.G. and Reedijk, J. 2000. Synthesis, Characterization, and Crystal Structure of  $\square$ -[Ru(azpy)<sub>2</sub>(NO<sub>3</sub>)<sub>2</sub>] (azpy = 2-(Phenylazo)pyridine) and the Products of Its Reactions with Guanine Derivatives. *Inorg. Chem.* 39, 3838-3844.
- Hotze, A.C.G., Broekhuisen, M.E.T., Velder, A.H., Schilden, K.V.D., Haasnoot, J.G. and Reedijk, J. 2002. Unusual Coordination of the Rare Neutral Imine Tautomer of 9-Methyladenine Chelating in the *N*6,*N*7-Mode to Ruthenium(II) Complexes. *Eur. J. Inorg. Chem.* 369-376.
- Hotze, A.C.G., Bacac, M., Velders, A.H., Jansen, B.A.J., Kooijman, H., Spek, A.L., Haasnoot, J.G. and Reedijk, J. 2003. New Cytotoxic and Water-soluble Bis(2-phenylazopyridine)ruthenium(II) Complexes. *J. Med. Chem.* 46, 1743-1750.
- Hotze, A.C.G., Caspers, S.E., De Vos, D., Kooijman, H., Spek, A.L., Flamigni, A., Bacao, M., Sava, G., Haasnoot, J.G. and Reedijk, J. 2004. Structure-dependent in Vitro Cytotoxicity of the Isomeric Complexes [Ru(L)<sub>2</sub>Cl<sub>2</sub>] (L = *o*-Tolylazopyridine and 4-Methy-2-phenylazopyridine) in Comparison to [Ru(azpy)<sub>2</sub>Cl<sub>2</sub>]. *J. Biol. Inorg. Chem.* 9, 354-364.
- Hotze, A.C.G., Kooijman, H., Spek, A.L., Haasnoot, J.G., Reedijk, J. 2004. Synthesis and Characterization of Ruthenium(II) Complexes with the New Ligand 2-Phenylazopyridine-5-sulfonic acid (Hsazpy): in Search for New Anticancer Agents. *New. J. Chem.* 28, 565-569.

- Hotze, A.C.G., Ven Der Geer, E.P.L., Caspers, S.E., Kooijman, H., Spek, A.L., Haasnoot, J.G. and Reedijk, J. 2004. Coordination of 9-Ethylguanine to the Mixed-Ligand Compound  $\alpha$ -[Ru(azpy)(bpy)Cl<sub>2</sub>] (azpy = 2-Phenylazopyridine and bpy = 2,2'-Bipyridine). An Unprecedented Ligand Positional Shift, Correlated to the Cytotoxicity of This Type of [RuL<sub>2</sub>Cl<sub>2</sub>] (with L = azpy or bpy) Complex. *Inorg. Chem.* 43, 4935-4943.
- Hotze, A.C.G., Van der Geer, E.P.L., Kooijman, H., Spek, A.L., Haasnoot, J.G. and Reedijk, J. 2005. Characterization by NMR Spectroscopy, X-ray Analysis and Cytotoxic Activity of the Ruthenium(II) Compounds [RuL<sub>3</sub>](PF<sub>6</sub>)<sub>2</sub> (L = 2-Phenylazopyridine or o-Tolylazopyridine) and [RuL'<sub>2</sub>L'']<sub>2</sub>(PF<sub>6</sub>)<sub>2</sub> (L', L'' = 2-Phenylazopyridine, 2,2-Bibyrindine. *Eur. J. Inorg. Chem.* 2648-2657.
- Jamieson, E.R., Lippard, S.J. 1999. Structure, Recognition, and Processing of Cisplatin DNA Adducts. *Chem. Rev.* 99, 2467-2498.
- Ji, L.-N., Liu, J.-G. and Ye, B.-H. 1999. Studies of Molecular Recognition Mechanism in Supramolecular System of Ruthenium(II) Polypyridyl Complexes and DNA. *Materials Science and Engineering.* C10, 51-57.
- Ji, Z., Huang, S.D. and Guadalupe, A.R. 2000. Synthesis, X-ray Structure, Spectroscopic and Electrochemical Properties of Ruthenium(II) Complexes Containing 2,2'-Bipyrimidine. *Inorg. Chim. Acta.* 305, 127-134.
- Jiang, C.-W., Chao, H., Li, H. and Ji, L.-N. 2003. Syntheses, Characterization and DNA-binding Studies of Ruthenium(II) Terpyridine Complexes: [Ru(tpy)(PHBI)]<sup>2+</sup> and [Ru(tpy)(PHNI)]<sup>2+</sup>. *J. Inorg. Biochem.* 93, 247-255.
- Jiang, C.-W. 2004. Homoleptic Ruthenium (II) Complexes Containing Asymmetric Tridentate 2-(Benzimidazole-2-yl)-1,10-phenanthroline Likes Ligands: Syntheses, Characterization and DNA Binding. *J. Inorg. Biochem.* 98, 1399-1404.

- Jing, B., Zhang, M. and Shen, T. 2004. [Ruthenium(II)(bpy)<sub>2</sub>L]<sup>2+</sup>, Where L are Imidazo[f]-1,10-phenanthrolines: Synthesis, Photophysics and Binding with DNA. *Spectrochim. Acta Part A.* 60, 2635-2641.
- Jullapan, T. 2004. Synthesis and Characterization of Ruthenium with 2-(Phenylazo) Benzothiazole Ligands. Master of Science Thesis, Prince of Songkla University, Songkhla, Thailand.
- Krause, R.A. and Krause, K. 1980. Chemistry of Bipyridyl-like Ligands. Isomeric Complexes of Ruthenium(II) with 2-(Phenylazo)pyridine<sup>1</sup>. *Inorg. Chem.* 19, 2600-2603.
- Krause, R.A. and Krause, K. 1984. Chemistry of Bipyridyl-like Ligands. 3. Complexes of Ruthenium(II) with 2-((4-Nitrophenyl)azo)pyridine<sup>1</sup>. *Inorg. Chem.* 23, 2195-2198.
- Kooijman, H., Hotze, A.C.G., Caspers, S.E., Haasnoot, J.G., Reedijk, J. and Spek, A.L. 2004.  $\alpha$ -Dichlorobis(2-phenylazo-4,6-dimethylpyridine)ruthenium(II) Chloroform Solvate. *Acta Cryst. Sect E.* E60, m247-m249).
- Liu, J.-G., Zhang, Q.-L., Shi, X.-F. and Ji, L.-N. 2001. Interaction of [Ru(dmp)<sub>2</sub>(dppz)]<sup>2+</sup> and [Ru(dmb)<sub>2</sub>(dppz)]<sup>2+</sup> with DNA: Effects of the Ancillary Ligands on the DNA-binding Behaviors. *Inorg. Chem.* 40, 5045-5050.
- Liu, Y.-J., Chao, H., Yuan, Y.-X., Yu, H.-J. and Ji, L.-N. 2006. Ruthenium(II) Mixed-ligand Complexes Containing 2-(6-Methyl-3-chromonyl)imidazo[4,5-f][1,10]-phenanthroline: Synthesis, DNA-binding and Photocleavage Studies. *Inorg. Chim. Acta.* 359, 3807-3814.

- Liu, J., Zheng, W., Shi, S., Tan, C., Chen, J., Zheng, K. and Ji, L. 2008. Synthesis, Antitumor Activity and Structure-activity Relationships of a Series of Ru(II) Complexes. *J. Inorg. Biochem.* 102, 193-202.
- Luedtke, N.W., Hwang, J.S., Nava, E., Gut, D., Kol, M. and Tor, Y. 2003. The DNA and RNA Specificity of Eilatin Ru(II) Complexes As Compared to Eilatin and Ethidium Bromide. *Nucleic acid Res.* 31(19), 5732-5740.
- Mahadevan, S. and Palaniandavar, M. 1998. Spectroscopic and Voltammetric Studies on Copper Complexes of 2,9-Dimethyl-1,10-Phenanthrolines Bound to Calf Thymus DNA. *Inorg. Chem.* 37, 693-700.
- Maheswari, P.U., and Palaniandavar, M. 2004. DNA Binding and Cleavage Properties of Certain Tetraammine Ruthenium(II) Complexes of Modified 1,10-Phenanthrolines - Effect of Hydrogen-bonding on DNA-binding Affinity. *J. Inorg. Biochem.* 98, 219-230.
- Mahiswari, P.U. and Palaniandavar, M. 2004. DNA Binding and Cleavage Activity of  $[\text{Ru}(\text{NH}_3)_4(\text{diimine})\text{Cl}_2]$  Complex. *Inorg. Chim. Acta.* 357, 901-912.
- Mathews, C.K. and Holde, K.E.V. 1996. *Biochemistry*. 2<sup>nd</sup> ed. The Benjamin/Cummings Publishing Company.: Canada.
- Mathur, T., Dinda, J., Datta, P., Mostafa, G., Lu, T.-H. and Sinha, C. 2006. Ru(0)-Azoimine-carbonyl and Ru(II)-pyridyl-azo-imidazole Complexes. *Polyhedron* 25, 2503-2512.
- Mei, W.-J., Liu, J., Chao, H. and Ji, L.-N. 2003. DNA-binding and Cleavage Studies of a Novel Porphyrin Ruthenium Mixed Complex  $[\text{MPyTPP-Ru}(\text{pip})_2\text{Cl}]^+$ . *Trans. Met. Chem.* 28, 852-857.

- Meyer, T.J. 1997. Efficient Light-to-Electrical Energy Conversion: Nanocrystalline TiO<sub>2</sub> Films Modified with Inorganic Sensitizers. *J. Chem. Ed.* 74, 652-656.
- Misra, T.K., Das, D., Sinha, C., Ghosh, P. and Pal, C.K. 1998. Chemistry of Azoimidazoles: Synthesis, Spectral Characterization, Electrochemical Studies, and X-ray Crystal Structures of Isomeric Dichloro bis[1-alkyl-2-(arylo)imidazole]complexes of Ruthenium(II). *Inorg. Chem.* 37, 1672-1678.
- Mudasir, Wijaya, K., Yoshioka, N. and Inoue, H. 2003. DNA Binding of Iron(II) Complexes with 1,10-Phenanthroline and 4,7-Diphenyl-1,10-phenanthroline: Salt Effect, Ligand Substituent Effect, Base Pair Specificity and Binding Strength. *J. Inorg. Biochem.* 94, 263-271.
- Munshi, P., Samanta, R. and Lahiri, G.K. 1998. A Facile and Preferential Synthesis of the Complexes, *cis-trans-cis*-Ru<sup>II</sup>[NC<sub>5</sub>H<sub>4</sub>-N=N-C<sub>6</sub>H<sub>4</sub>(R)]<sub>2</sub> (R = H, *o*-Me/Cl, *m*-Me/Cl, *p*-Me/Cl. Synthesis, Spectroscopic Characterization and Electron-Transfer Properties. *Polyhedron.* 17(11-12), 1913-1922.
- Murali, S., Sastri, C.V. and Maiya, B. 2002. New Mixed Ligand Complexes of Ruthenium(II) that Incorporate a Modified Phenanthroline Ligand; Synthesis, Spectral Characterization and DNA Binding. *Proc. Indian. Acad. Sci. (Chem. Sci.)*. 114 (4), 403-415.
- Naing, K., Takahashi, M., Taniguchi, M. and Yamagishi, A. 1995. Interaction of Enantiomeric Ruthenium(II) Complexes with Polynucleotides As Studied by Circular Dichroism, Electric Dichroism Measurement, and Phytolysis. *Inorg. Chem.* 34, 350-356.
- Nair, R.B., Teng, E.S., Kirkland, S.L. and Murphy, C.J. 1998. Synthesis and DNA-Binding Properties of [Ru(NH<sub>3</sub>)<sub>4</sub>dppz]<sup>2+</sup>. *Inorg. Chem.* 37, 139-141.

- Nakabayashi, Y., Watanabe, Y., Nakao, T. and Yamauchi, O. 2004. Interactions of Mixed Ligand Ruthenium(II) Complexes Containing an Amino Acid and 1,10-Phenanthroline with DNA. *Inorg. Chim. Acta.* 357, 2553-2560.
- Nakabayashi, Y., Iwamoto, N., Inada, H. and Yamauchi, O. 2006. DNA-binding Properties of Flexible Diamine Bridge Dinuclear Ruthenium(II)-2,2'-bipyridine Complexes. *Inorg. Chem. Commun.* 9, 1033-1036.
- Nakamoto, K. 1992. *Infrared and Raman Spectra of Inorganic and Coordination Compounds.* 4<sup>th</sup> ed. John Wiley & Sons.: New York.
- Pal, S., Das, D., Chattopadhyay, P. and Sinha, C. 2000. Synthesis, Spectral and Electrochemical Properties of 1-Alkyl-2-(naphthyl- $\beta$ -azo)imidazole Complexes of Platinum(II) and the Reaction with Pyridine Bases. Single-Crystal X-ray Structure of Dichloro-[1-ethyl-2-(naphthyl- $\beta$ -azo)imidazole] platinum(II). *Polyhedron.* 19, 1263-1270.
- Pal, S., Misra, T.K., Sinha, C., Slawin, A.M.Z. and Woollins, J.D. 2002. Ruthenium(II) Complexes of  $\alpha$ -Diimines: Synthesis, Spectral Characterization, Electrochemical Properties and Single-crystal X-ray Structure of Bis(2,2'-bipyridine){1-benzyl-2-(p-tolylazo)imidazole}-ruthenium(II) Perchlorate. *Polyhedron.* 19, 1925-1933.
- Panneerselvam, K., Hansongnorn, K., Rattanawit, N., Liao, F-L. and Lu, T-H. 2000. Crystal Structure of the [Protonated 2-(phenylazo)pyridine and Protonated 2-(4-Hydroxyphenylazo)pyridine (3:1)]tetrafluoroborate. *Anal. Sci.* 16, 1107-1108.
- Patra, A.K., Nethaji, M. and Chakravarty, A.R. 2006. Synthesis, Crystal Structure, DNA Binding and Photo-induced DNA Cleavage Activity of (S-methyl-L-cysteine)copper(II) Complexes of Heterocyclic Bases. *J. Inorg. Biochem.* 16, 11-12.

- Perrin, D.D. and Dempsey, B. 1997. Buffer for pH and Metal Ion Control. Chapman and Hall.: New York.
- Purdue University. 2007. Ethidium bromide.  
<http://www.purdue.edu/REM/nmm/ethidbr.htm> (11/4/08).
- Pyle, A.M., Rehmann, J.P., Meshoyrer, R., Kumar, C.V., Turro, N.J. and Barton, J.K. 1989. Mixed-ligand Complexes of Ruthenium(II): Factors Governing Binding to DNA. *J. Am. Chem. Soc.* 111, 3051-3058.
- Rattanawit, N. 2002. Chemistry of Ruthenium with 1,10-Phenanthroline, 2-(Phenylazo)pyridine and Derivatives of 2-(Phenylazo)pyridine. Master of Science Thesis, Prince of Songkla University, Songkhla, Thailand.
- Reedijk, J. 2003. New Clue for Platinum Antitumor Chemistry: Kinetically Controlled Metal Binding to DNA. *Proc. Natl. Acad. Sci. USA.* 100, 3611-3616.
- Santra, P.K., Misra, T.K., Das, D., Sinha, C., Slawin, A.M.Z. and Woollins, J.D. 1999b. Chemistry of Azopyrimidines. Part II. Synthesis, Spectra, Electrochemistry and X-ray Crystal Structures of Isomeric Dichlorobis[2-(aryloxy)pyrimidine] Complexes of Ruthenium(II). *Polyhedron.* 18, 2869-2878.
- Scholz, F. 2002. *Electroanalytical Methods Guide to Experiments and Applications.* Springer-Verlag.: Berlin.
- Seal, A. and Ray, S. 1984. Structures of Two Isomers of Dichlorobis(2-phenylazopyridine)ruthenium(II),  $[\text{RuCl}_2(\text{C}_{11}\text{H}_9\text{N}_3)_2]$ . *Acta. Cryst.* C40, 929-932.

- Selvi, P.T., Stoeckli-Evan, H. and Palaniandavar, M. 2005. Synthesis, Structure and DNA Interaction of Cobalt(III) Bis-complexes of 1,3-Bis(2-pyridylimino) isoindazole and 1,4,7-Triazacyclononane. *J. Inorg. Biochem.* 99, 2110-2118.
- Settle, F. 1997. *Handbook of Instrument Techniques for Analytical Chemistry*. Upper Saddle River, N.J.: Prentice Hall.
- Sullivan, B.P., Salmom, D.J. and Meyer, T.J. 1978. Mixed Phosphine 2,2'-Bipyridine Complexes of Ruthenium. *Inorg. Chem.* 17(12), 3334-3341.
- Tan, L.-F., Chao, H., Liu, Y.-J., Li, H., Sun, B. and Ji, L.-N. 2005. DNA-binding and Photocleavage Studies of  $[\text{Ru}(\text{phen})_2(\text{NMIP})]^{2+}$ . *Inorg. Chim. Acta.* 358, 2191-2198.
- Tan, L.-F., Liu, X.-H., Chao, H. and Ji, L.-N. 2007. Synthesis, DNA-binding and Photocleavage Studies of Ruthenium(II) Complex with 2-(3'-Phenoxyphenyl)imidazo[4,5-f][1,10]phenanthroline. *J. Inorg. Biochem.* 101, 56-63.
- Tan, L.-F., Wang, F., Chao, H., Zhou, Y.-F. and Weng, C. 2007. Ruthenium(II) Mixed-ligand Complex Containing 2-(4'-Benzyloxy-phenyl)imidazo[4,5-f][1,10]phenanthroline: Synthesis, DNA-binding and Photocleavage Studies. *J. Inorg. Biochem.* 101, 700-708.
- Tan, L.-F. and Chao, H. 2007. DNA-binding and Photocleavage Studies of Mixed Polypyridyl Ruthenium(II) Complexes with Calf Thymus DNA. *Inorg. Chim. Acta.* 360, 2016-2022.
- Tan, L.-F., Chao, H., Zhou, Y.-F. and Ji, L.-N. 2007. Synthesis, Characterization, DNA-binding and DNA-photocleavage Studies of  $[\text{Ru}(\text{bpy})_2(\text{BPIP})]^{2+}$  and  $[\text{Ru}(\text{phen})_2(\text{BPIP})]^{2+}$  (BPIP = 2-(4'-Biphenyl)imidazo[4,5-f][1,10]phenanthroline). *Polyhedron.* 26, 3029-3036.

- Tan, L.-F., Chao, H., Zhen, K.-C., Fei, J.-J., Wang, F., Zhou, Y.-F. and Ji, L.-N. 2007. Effects of the Ancillary Ligands of Polypyridyl Ruthenium(II) Complexes on the DNA-binding and Photocleavage Behaviors. *Polyhedron*. 26, 5458-5468.
- Tempiam, S. 2002. Synthesis and Characterization of Ruthenium with 2,2'-Bipyridine, 2-(4-N,N-dimethylaminophenylazo)pyridine and 2-(4-N,N-dimethylaminophenylazo)pyridine Ligands. Master of Science Thesis, Prince of Songkla university, Songkhla, Thailand.
- Vaidyanathan, V.G. and Nair, B.U. 2002. Synthesis, Characterization and DNA Binding Studies of a Ruthenium(II) Complex. *J. Inorg. Biochem.* 91, 405-412.
- Vaidyanathan, V.G. and Nair, B.U. 2003. Oxidative Cleavage of DNA by Tridentate Copper (II) Complex. *J. Inorg. Biochem.* 93, 271-276.
- Vaidyanathan, V.G. and Nair, B.U. 2003. Photooxidation of DNA by a Cobalt(II) Tridentate Complex. *J. Inorg. Biochem.* 94, 121-126.
- Velders, A.H., Kooijman, H., Spek, A.L., Haasnoot, J.G., de Vos, D. and Reedijk, J. 2000. Strong Differences in the in Vitro Cytotoxicity of Three Isomeric Dichlorobis(2-phenylazopyridine)ruthenium(II) Complexes. *Inorg. Chem.* 39 (14), 2966-2967.
- Velder, A.H., Schilden, K.V.D., Hotze, A.C.G., Reedijk, J., Kooijman, H. and Spek, A.L. 2004. Dichlorobis(2-phenylazopyridine)ruthenium(II) Complexes: Characterization, Spectroscopic and Structural Properties of Four Isomers. *J. Chem. Soc. Dalton Trans.* 448-455.

- Vilaplana, R.A., Delmani, F., Manteca, C., Torreblanca, J., Moreno, J., García-Herdugo, G. and González-Vílchez, F. 2006. Synthesis, Interaction with Double-helical DNA and Biological Activity of the Water Soluble Complex *cis*-Dichloro-1,2-propylenediamine-*N,N,N',N'*-tetraacetatoruthenium(III) (PAR). *J. Inorg. Biochem.* 100, 1834-1841.
- Vliet, P.M.V., Haasnoot, J.G. and Reedijk, J. 1994. Binding of 9-Methylhypoxanthine and 9-Ethylguanine to  $[\text{cis-Ru}(2,2'\text{-bipyridine})_2]^{2+}$ . NMR and X-ray Structure of *cis*-Dichlorobis(2,2'-bipyridine)<sub>2</sub>(9-ethylguanine- $\kappa\text{N}^7$ )ruthenium(II) Chloride. *Inorg. Chem.* 33, 1934-1939.
- Wang, X.-L., Chao, H., Li, H., Hong, X.-L., Liu, Y.-J., Tan, L.-F. and Ji, L.-N. 2004. DNA Interactions of Cobalt(III) Mixed-polypyridyl Complexes Containing Asymmetric Ligands. *J. Inorg. Biochem.* 98, 1143-1150.
- Wikipedia, the free encyclopedia. 2008. Ethidium bromide.  
[http://en.wikipedia.org/wiki/Ethidium\\_bromide](http://en.wikipedia.org/wiki/Ethidium_bromide) (11/4/08).
- Wong, E. and Giandomenico, C.M. 1999. Current Status of Platinum-based Antitumor Drugs. *Chem. Rev.* 99, 2451-2466.
- Yang, G., Wu, J.Z., Wang, L., Ji, L.N. and Tian, X. 1997. Study of the Interaction Between Novel Ruthenium(II)polypyridyl Complexes and Calf Thymus DNA. *J. Inorg. Biochem.* 66, 141-144.
- Yau, H.C.M., Chan, H.L. and Yang, M. 2002. Determination of Mode of Interactions Between Novel Drugs and Calf Thymus DNA by Using Quartz Crystal Resonator. *Sensors and Actuators B: Chem.* 81, 283-288.
- Ye, B-H., Chen, X-M., Zeng, T-X. and Ji, L-N. 1995. Syntheses, Spectra and Crystal Structures of Ruthenium(II) Complexes with Polypyridyl:  $[\text{Ru}(\text{bipy})_2(\text{phen})](\text{ClO}_4)_2 \cdot \text{H}_2\text{O}$  and  $[\text{Ru}(\text{bipy})_2(\text{Me-phen})](\text{ClO}_4)_2$ . *Inorg. Chim. Acta.* 240, 5-11.

Zhang, C.X. and Lippard, S.J. 2003. New Metal Complexes as Potential Therapeutics. *Curr. Opin. Chem. Biol.* 7, 481-489.

Zhen, Q.-X., Ye, B.-H., Liu, J.-G., Zhang, G.-L., Ji, L.-N. and Wang, L. 2000. Synthesis, Characterization and DNA Binding Properties of  $[\text{Ru}(\text{phen})_2\text{taptp}]^{2+}$  and  $[\text{Ru}(\text{phen})_2\text{dptatp}]^{2+}$ . *Inorg. Chim. Acta.* 303, 141-147.

**Appendix A** Cut off solvents**Table A.1** Solvent for UV-Visible spectrum and the minimum values for measurement in 1 mm of quartz cell

Solvents	Cut off
Hexane	210
Benzene	280
Dichloromethane (CH <sub>2</sub> Cl <sub>2</sub> )	235
Chloroform (CHCl <sub>3</sub> )	245
Acetonitrile (CH <sub>3</sub> CN)	190
Acetone (CH <sub>3</sub> OCH <sub>3</sub> )	330
Methanol (MeOH)	210
Ethanol (EtOH)	210
<i>N,N</i> -dimethylformamide (DMF)	270
<i>N,N</i> -dimethylsulphoxide (DMSO)	265
Water (H <sub>2</sub> O)	191

(Source: Gordon and Ford, 1972)

**Appendix B** Bond length (Å) and bond angle (°)

**Table B.1** Bond length (Å) and bond angle (°) of *tcc*-[Ru(Clazpy)<sub>2</sub>Cl<sub>2</sub>]

<u>Bond length (Å)</u>			
Ru(1)-N(3)	1.9906(18)	C(7)-C(8)	1.389(4)
Ru(1)-N(6)	1.9963(18)	C(7)-H(7)	0.88(3)
Ru(1)-N(4)	2.0879(18)	C(8)-C(9)	1.377(5)
Ru(1)-N(1)	2.1000(18)	C(8)-H(8)	0.92(3)
Ru(1)-Cl(1)	2.3648(6)	C(9)-C(10)	1.368(5)
Ru(1)-Cl(2)	2.3808(6)	C(9)-H(9)	0.91(3)
N(1)-C(1)	1.331(3)	C(10)-C(11)	1.384(4)
N(1)-C(5)	1.350(3)	C(10)-H(10)	0.93(3)
N(2)-N(3)	1.292(3)	C(11)-H(11)	0.88(3)
N(2)-C(5)	1.378(3)	C(12)-C(13)	1.376(3)
N(3)-C(6)	1.439(3)	C(12)-H(12)	0.88(3)
N(4)-C(12)	1.330(3)	C(13)-C(14)	1.372(4)
N(4)-C(16)	1.351(3)	C(14)-C(15)	1.371(4)
N(5)-N(6)	1.284(3)	C(14)-H(14)	0.91(3)
N(5)-C(16)	1.377(3)	C(15)-C(16)	1.395(3)
N(6)-C(17)	1.438(3)	C(15)-H(15)	0.93(3)
Cl(3)-C(2)	1.725(2)	C(17)-C(18)	1.378(4)
Cl(4)-C(13)	1.732(3)	C(17)-C(22)	1.384(4)
C(1)-C(2)	1.383(3)	C(18)-C(19)	1.371(4)
C(1)-H(3)	0.91(2)	C(18)-H(18)	0.89(3)
C(2)-C(3)	1.375(4)	C(19)-C(20)	1.363(5)
C(3)-C(4)	1.372(4)	C(19)-H(19)	0.95(3)
C(3)-H(4)	0.96(3)	C(20)-C(21)	1.376(6)
C(4)-C(5)	1.387(3)	C(20)-H(20)	0.98(5)
C(4)-H(5)	0.88(3)	C(21)-C(22)	1.389(5)
C(6)-C(7)	1.377(4)	C(21)-H(21)	0.89(3)
C(6)-C(11)	1.385(4)	C(22)-H(22)	0.87(3)

**Table B.1** (Continued)

<u>Bond angle (°)</u>			
N(3)-Ru(1)-N(6)	105.14(8)	C(17)-N(6)-Ru(1)	129.30(15)
N(3)-Ru(1)-N(4)	177.73(7)	N(1)-C(1)-C(2)	122.5(2)
N(6)-Ru(1)-N(4)	75.22(8)	N(1)-C(1)-H(3)	119.1(16)
N(3)-Ru(1)-N(1)	75.70(7)	C(2)-C(1)-H(3)	118.5(16)
N(6)-Ru(1)-N(1)	179.14(7)	C(3)-C(2)-C(1)	120.1(2)
N(4)-Ru(1)-N(1)	103.95(7)	C(3)-C(2)-Cl(3)	120.82(19)
N(3)-Ru(1)-Cl(1)	89.85(6)	C(1)-C(2)-Cl(3)	119.1(2)
N(6)-Ru(1)-Cl(1)	94.91(5)	C(4)-C(3)-C(2)	117.7(2)
N(4)-Ru(1)-Cl(1)	87.89(5)	C(4)-C(3)-H(4)	124.4(17)
N(1)-Ru(1)-Cl(1)	85.25(5)	C(2)-C(3)-H(4)	117.9(17)
N(3)-Ru(1)-Cl(2)	96.03(6)	C(3)-C(4)-C(5)	119.9(2)
N(6)-Ru(1)-Cl(2)	89.73(5)	C(3)-C(4)-H(5)	124.5(17)
N(4)-Ru(1)-Cl(2)	86.20(5)	C(5)-C(4)-H(5)	115.5(17)
N(1)-Ru(1)-Cl(2)	90.01(5)	N(1)-C(5)-N(2)	117.8(2)
Cl(1)-Ru(1)-Cl(2)	171.32(2)	N(1)-C(5)-C(4)	122.1(2)
C(1)-N(1)-C(5)	117.67(19)	N(2)-C(5)-C(4)	119.9(2)
C(1)-N(1)-Ru(1)	131.12(15)	C(7)-C(6)-C(11)	121.1(2)
C(5)-N(1)-Ru(1)	110.75(15)	C(7)-C(6)-N(3)	119.0(2)
N(3)-N(2)-C(5)	112.83(18)	C(11)-C(6)-N(3)	119.9(2)
N(2)-N(3)-C(6)	110.23(18)	C(6)-C(7)-C(8)	118.7(3)
N(2)-N(3)-Ru(1)	120.12(15)	C(6)-C(7)-H(7)	117.6(17)
C(6)-N(3)-Ru(1)	129.51(14)	C(8)-C(7)-H(7)	123.6(17)
C(12)-N(4)-C(16)	118.1(2)	C(9)-C(8)-C(7)	120.4(3)
C(12)-N(4)-Ru(1)	130.18(16)	C(9)-C(8)-H(8)	121.0(18)
C(16)-N(4)-Ru(1)	111.66(16)	C(7)-C(8)-H(8)	118.5(18)
N(6)-N(5)-C(16)	112.32(19)	C(10)-C(9)-C(8)	120.3(3)
N(5)-N(6)-C(17)	110.05(18)	C(10)-C(9)-H(9)	122(2)
N(5)-N(6)-Ru(1)	120.64(15)	C(8)-C(9)-H(9)	118(2)

**Table B.1** (Continued)

<u>Bond angle (°)</u>		N(4)-C(16)-C(15)	122.0(2)
C(9)-C(10)-C(11)	120.3(3)	N(5)-C(16)-C(15)	119.8(2)
C(9)-C(10)-H(10)	121.4(19)	C(18)-C(17)-C(22)	121.3(3)
C(11)-C(10)-H(10)	118.2(19)	C(18)-C(17)-N(6)	118.6(2)
C(10)-C(11)-C(6)	119.1(3)	C(22)-C(17)-N(6)	119.9(2)
C(10)-C(11)-H(11)	122.3(17)	C(19)-C(18)-C(17)	119.3(3)
C(6)-C(11)-H(11)	118.6(17)	C(19)-C(18)-H(18)	124(2)
N(4)-C(12)-C(13)	122.1(2)	C(17)-C(18)-H(18)	116.7(19)
N(4)-C(12)-H(12)	119.7(17)	C(20)-C(19)-C(18)	120.7(3)
C(13)-C(12)-H(12)	118.2(17)	C(20)-C(19)-H(19)	121.8(19)
C(14)-C(13)-C(12)	120.3(3)	C(18)-C(19)-H(19)	117.5(19)
C(14)-C(13)-Cl(4)	121.9(2)	C(19)-C(20)-C(21)	120.1(3)
C(12)-C(13)-Cl(4)	117.8(2)	C(19)-C(20)-H(20)	123(3)
C(15)-C(14)-C(13)	118.3(2)	C(21)-C(20)-H(20)	117(3)
C(15)-C(14)-H(14)	122(2)	C(20)-C(21)-C(22)	120.7(3)
C(13)-C(14)-H(14)	120(2)	C(20)-C(21)-H(21)	123(2)
C(14)-C(15)-C(16)	119.0(3)	C(22)-C(21)-H(21)	116(2)
C(14)-C(15)-H(15)	124.5(18)	C(17)-C(22)-C(21)	117.9(3)
C(16)-C(15)-H(15)	116.5(18)	C(17)-C(22)-H(22)	117.8(18)
N(4)-C(16)-N(5)	117.8(2)	C(21)-C(22)-H(22)	124.3(18)

Symmetry transformations used to generate equivalent atoms:

**Table B.2** Bond length (Å) and bond angle (°) of *ctc*-[Ru(Clazpy)<sub>2</sub>Cl<sub>2</sub>]

<u>Bond length (Å)</u>			
Ru(1)-N(3)	1.9729(17)	C(11)-H(11)	0.9300
Ru(1)-N(3)#1	1.9729(17)		
Ru(1)-N(1)	2.0369(17)	<u>Bond angle (°)</u>	
Ru(1)-N(1)#1	2.0369(17)	N(3)-Ru(1)-N(3)#1	99.82(10)
Ru(1)-Cl(1)	2.4029(6)	N(3)-Ru(1)-N(1)	76.73(7)
Ru(1)-Cl(1)#1	2.4030(6)	N(3)#1-Ru(1)-N(1)	99.70(7)
Cl(2)-C(2)	1.723(2)	N(3)-Ru(1)-N(1)#1	99.70(7)
N(1)-C(1)	1.342(3)	N(3)#1-Ru(1)-N(1)#1	76.73(7)
N(1)-C(5)	1.360(3)	N(1)-Ru(1)-N(1)#1	174.56(9)
N(2)-N(3)	1.283(2)	N(3)-Ru(1)-Cl(1)	85.27(5)
N(2)-C(5)	1.387(3)	N(3)#1-Ru(1)-Cl(1)	171.05(5)
N(3)-C(6)	1.441(3)	N(1)-Ru(1)-Cl(1)	88.61(5)
C(1)-C(2)	1.380(3)	N(1)#1-Ru(1)-Cl(1)	95.22(5)
C(1)-H(1)	0.9300	N(3)-Ru(1)-Cl(1)#1	171.05(5)
C(2)-C(3)	1.382(3)	N(3)#1-Ru(1)-Cl(1)#1	85.27(5)
C(3)-C(4)	1.374(3)	N(1)-Ru(1)-Cl(1)#1	95.22(5)
C(3)-H(3)	0.9300	N(1)#1-Ru(1)-Cl(1)#1	88.60(5)
C(4)-C(5)	1.383(3)	Cl(1)-Ru(1)-Cl(1)#1	90.69(3)
C(4)-H(4)	0.9300	C(1)-N(1)-C(5)	118.03(18)
C(6)-C(7)	1.377(3)	C(1)-N(1)-Ru(1)	129.50(14)
C(6)-C(11)	1.380(3)	C(5)-N(1)-Ru(1)	112.41(13)
C(7)-C(8)	1.398(4)	N(3)-N(2)-C(5)	111.53(17)
C(7)-H(7)	0.9300	N(2)-N(3)-C(6)	113.38(17)
C(8)-C(9)	1.358(4)	N(2)-N(3)-Ru(1)	121.15(14)
C(8)-H(8)	0.9300	C(6)-N(3)-Ru(1)	124.41(13)
C(9)-C(10)	1.369(4)	N(1)-C(1)-C(2)	120.9(2)
C(9)-H(9)	0.9300	N(1)-C(1)-H(1)	119.5
C(10)-C(11)	1.382(3)	C(2)-C(1)-H(1)	119.5
C(10)-H(10)	0.9300	C(1)-C(2)-C(3)	121.3(2)

**Table B.2** (continued)

---

<u>Bond angle (<math>^{\circ}</math>)</u>			
C(1)-C(2)-Cl(2)	119.17(19)	C(6)-C(7)-C(8)	118.6(2)
C(3)-C(2)-Cl(2)	119.51(18)	C(6)-C(7)-H(7)	120.7
C(4)-C(3)-C(2)	117.9(2)	C(8)-C(7)-H(7)	120.7
C(4)-C(3)-H(3)	121.0	C(9)-C(8)-C(7)	120.2(2)
C(2)-C(3)-H(3)	121.0	C(9)-C(8)-H(8)	119.9
C(3)-C(4)-C(5)	118.9(2)	C(7)-C(8)-H(8)	119.9
C(3)-C(4)-H(4)	120.5	C(8)-C(9)-C(10)	120.9(3)
C(5)-C(4)-H(4)	120.5	C(8)-C(9)-H(9)	119.5
N(1)-C(5)-C(4)	122.9(2)	C(10)-C(9)-H(9)	119.5
N(1)-C(5)-N(2)	117.64(17)	C(9)-C(10)-C(11)	119.9(3)
C(4)-C(5)-N(2)	119.46(19)	C(9)-C(10)-H(10)	120.0
C(7)-C(6)-C(11)	121.0(2)	C(11)-C(10)-H(10)	120.0
C(7)-C(6)-N(3)	120.1(2)	C(6)-C(11)-C(10)	119.3(2)
C(11)-C(6)-N(3)	118.81(19)	C(6)-C(11)-H(11)	120.4
		C(10)-C(11)-H(11)	120.4

---

Symmetry transformations used to generate equivalent atoms:

#1  $-x+1, y, -z+1/2$

**Table B.3** Bond length (Å) and bond angle (°) of *ccc*-[Ru(Clazpy)<sub>2</sub>Cl<sub>2</sub>]

<u>Bond length (Å)</u>			
Ru(1)-N(3)	1.967(6)	N(10)-C(38)	1.393(10)
Ru(1)-N(6)	1.977(7)	N(11)-N(12)	1.271(10)
Ru(1)-N(4)	2.026(8)	N(11)-C(38)	1.320(12)
Ru(1)-N(1)	2.075(6)	N(12)-C(39)	1.449(10)
Ru(1)-Cl(2)	2.376(2)	Cl(3)-C(2)	1.736(9)
Ru(1)-Cl(1)	2.395(2)	Cl(4)-C(13)	1.736(9)
Ru(2)-N(9)	1.924(7)	Cl(7)-C(24)	1.725(7)
Ru(2)-N(12)	2.010(6)	Cl(8)-C(35)	1.727(10)
Ru(2)-N(10)	2.053(8)	C(1)-C(2)	1.299(11)
Ru(2)-N(7)	2.063(7)	C(1)-H(1)	0.9300
Ru(2)-Cl(6)	2.390(2)	C(2)-C(3)	1.342(13)
Ru(2)-Cl(5)	2.392(2)	C(3)-C(4)	1.433(12)
N(1)-C(5)	1.361(10)	C(3)-H(3)	0.9300
N(1)-C(1)	1.391(9)	C(4)-C(5)	1.298(11)
N(2)-N(3)	1.236(9)	C(4)-H(4)	0.9300
N(2)-C(5)	1.413(11)	C(6)-C(11)	1.342(14)
N(3)-C(6)	1.467(9)	C(6)-C(7)	1.409(12)
N(4)-C(12)	1.297(11)	C(7)-C(8)	1.399(12)
N(4)-C(16)	1.319(10)	C(7)-H(7)	0.9300
N(5)-N(6)	1.304(10)	C(8)-C(9)	1.441(17)
N(5)-C(16)	1.453(10)	C(8)-H(8)	0.9300
N(6)-C(17)	1.447(11)	C(9)-C(10)	1.212(16)
N(7)-C(23)	1.299(10)	C(9)-H(9)	0.9300
N(7)-C(27)	1.324(11)	C(10)-C(11)	1.550(13)
N(8)-N(9)	1.344(9)	C(10)-H(10)	0.9300
N(8)-C(27)	1.366(11)	C(11)-H(11)	0.9300
N(9)-C(28)	1.419(11)	C(12)-C(13)	1.389(12)
N(10)-C(34)	1.360(9)	C(12)-H(12)	0.9300

**Table B.3** (continued)

<u>Bond length (Å)</u>			
C(13)-C(14)	1.317(14)	C(30)-H(30)	0.9300
C(14)-C(15)	1.393(13)	C(31)-C(32)	1.20(2)
C(14)-H(14)	0.9300	C(31)-H(31)	0.9300
C(15)-C(16)	1.381(12)	C(32)-C(33)	1.368(14)
C(15)-H(15)	0.9300	C(32)-H(32)	0.9300
C(17)-C(18)	1.342(14)	C(33)-H(33)	0.9300
C(17)-C(22)	1.368(12)	C(34)-C(35)	1.388(12)
C(18)-C(19)	1.348(14)	C(34)-H(34)	0.9300
C(18)-H(18)	0.9300	C(35)-C(36)	1.406(13)
C(19)-C(20)	1.408(14)	C(36)-C(37)	1.355(13)
C(19)-H(19)	0.9300	C(36)-H(36)	0.9300
C(20)-C(21)	1.318(15)	C(37)-C(38)	1.401(12)
C(20)-H(20)	0.9300	C(37)-H(37)	0.9300
C(21)-C(22)	1.419(14)	C(39)-C(40)	1.387(11)
C(21)-H(21)	0.9300	C(39)-C(44)	1.413(14)
C(22)-H(22)	0.9300	C(40)-C(41)	1.336(14)
C(23)-C(24)	1.435(10)	C(40)-H(40)	0.9300
C(23)-H(23)	0.9300	C(41)-C(42)	1.411(15)
C(24)-C(25)	1.374(12)	C(41)-H(41)	0.9300
C(25)-C(26)	1.318(12)	C(42)-C(43)	1.341(14)
C(25)-H(25)	0.9300	C(42)-H(42)	0.9300
C(26)-C(27)	1.457(11)	C(43)-C(44)	1.410(13)
C(26)-H(26)	0.9300	C(43)-H(43)	0.9300
C(28)-C(33)	1.315(13)	C(44)-H(44)	0.9300
C(28)-C(29)	1.365(14)	C(45)-C(46)	1.456(15)
C(29)-C(30)	1.271(13)	C(45)-H(45A)	0.9600
C(29)-H(29)	0.9300	C(45)-H(45B)	0.9600
C(30)-C(31)	1.51(2)	C(45)-H(45C)	0.9600
		C(46)-C(47)	1.314(13)

**Table B.3** (continued)

<u>Bond length (Å)</u>			
C(46)-C(51)	1.345(16)	N(9)-Ru(2)-N(10)	93.1(3)
C(47)-C(48)	1.460(14)	N(12)-Ru(2)-N(10)	76.9(3)
C(47)-H(47)	0.9300	N(9)-Ru(2)-N(7)	76.7(3)
C(48)-C(49)	1.449(12)	N(12)-Ru(2)-N(7)	172.8(3)
C(48)-H(48)	0.9300	N(10)-Ru(2)-N(7)	98.6(3)
C(49)-C(50)	1.268(11)	N(9)-Ru(2)-Cl(6)	88.5(2)
C(49)-H(49)	0.9300	N(12)-Ru(2)-Cl(6)	97.9(2)
C(50)-C(51)	1.422(17)	N(10)-Ru(2)-Cl(6)	174.7(2)
C(50)-H(50)	0.9300	N(7)-Ru(2)-Cl(6)	86.7(2)
C(51)-H(51)	0.9300	N(9)-Ru(2)-Cl(5)	170.1(2)
		N(12)-Ru(2)-Cl(5)	92.0(2)
		N(10)-Ru(2)-Cl(5)	88.6(2)
<u>Bond angle (°)</u>			
N(3)-Ru(1)-N(6)	96.5(3)	N(7)-Ru(2)-Cl(5)	93.5(2)
N(3)-Ru(1)-N(4)	92.9(3)	Cl(6)-Ru(2)-Cl(5)	90.62(9)
N(6)-Ru(1)-N(4)	76.1(3)	C(5)-N(1)-C(1)	116.8(7)
N(3)-Ru(1)-N(1)	76.2(3)	C(5)-N(1)-Ru(1)	111.9(5)
N(6)-Ru(1)-N(1)	171.2(3)	C(1)-N(1)-Ru(1)	131.2(6)
N(4)-Ru(1)-N(1)	99.3(3)	N(3)-N(2)-C(5)	113.2(6)
N(3)-Ru(1)-Cl(2)	88.6(2)	N(2)-N(3)-C(6)	112.7(6)
N(6)-Ru(1)-Cl(2)	99.2(2)	N(2)-N(3)-Ru(1)	122.5(5)
N(4)-Ru(1)-Cl(2)	175.1(2)	C(6)-N(3)-Ru(1)	124.7(5)
N(1)-Ru(1)-Cl(2)	85.5(2)	C(12)-N(4)-C(16)	114.3(7)
N(3)-Ru(1)-Cl(1)	169.9(2)	C(12)-N(4)-Ru(1)	130.7(6)
N(6)-Ru(1)-Cl(1)	93.6(2)	C(16)-N(4)-Ru(1)	114.9(6)
N(4)-Ru(1)-Cl(1)	88.5(2)	N(6)-N(5)-C(16)	107.7(6)
N(1)-Ru(1)-Cl(1)	93.7(2)	N(5)-N(6)-C(17)	109.8(6)
Cl(2)-Ru(1)-Cl(1)	90.91(9)	N(5)-N(6)-Ru(1)	123.3(6)
N(9)-Ru(2)-N(12)	97.8(3)	C(17)-N(6)-Ru(1)	126.8(6)

**Table B.3** (continued)

<u>Bond angle (°)</u>			
C(23)-N(7)-C(27)	118.4(7)	C(11)-C(6)-C(7)	127.6(8)
C(23)-N(7)-Ru(2)	129.3(6)	C(11)-C(6)-N(3)	117.7(9)
C(27)-N(7)-Ru(2)	112.3(5)	C(7)-C(6)-N(3)	114.4(8)
N(9)-N(8)-C(27)	109.9(7)	C(6)-C(7)-C(8)	117.4(9)
N(8)-N(9)-C(28)	111.7(7)	C(6)-C(7)-H(7)	121.3
N(8)-N(9)-Ru(2)	121.6(6)	C(8)-C(7)-H(7)	121.4
C(28)-N(9)-Ru(2)	126.7(6)	C(7)-C(8)-C(9)	119.1(9)
C(34)-N(10)-C(38)	121.9(7)	C(7)-C(8)-H(8)	120.4
C(34)-N(10)-Ru(2)	127.1(6)	C(9)-C(8)-H(8)	120.6
C(38)-N(10)-Ru(2)	111.0(6)	C(10)-C(9)-C(8)	118.7(10)
N(12)-N(11)-C(38)	116.0(6)	C(10)-C(9)-H(9)	120.8
N(11)-N(12)-C(39)	112.1(6)	C(8)-C(9)-H(9)	120.5
N(11)-N(12)-Ru(2)	118.3(5)	C(9)-C(10)-C(11)	129.0(11)
C(39)-N(12)-Ru(2)	129.4(5)	C(9)-C(10)-H(10)	115.4
C(2)-C(1)-N(1)	122.3(8)	C(11)-C(10)-H(10)	115.6
C(2)-C(1)-H(1)	119.0	C(6)-C(11)-C(10)	107.8(10)
N(1)-C(1)-H(1)	118.8	C(6)-C(11)-H(11)	126.1
C(1)-C(2)-C(3)	121.3(9)	C(10)-C(11)-H(11)	126.1
C(1)-C(2)-Cl(3)	118.9(7)	N(4)-C(12)-C(13)	126.2(8)
C(3)-C(2)-Cl(3)	119.8(6)	N(4)-C(12)-H(12)	116.9
C(2)-C(3)-C(4)	117.4(8)	C(13)-C(12)-H(12)	116.9
C(2)-C(3)-H(3)	121.4	C(14)-C(13)-C(12)	118.3(9)
C(4)-C(3)-H(3)	121.2	C(14)-C(13)-Cl(4)	121.0(7)
C(5)-C(4)-C(3)	119.9(9)	C(12)-C(13)-Cl(4)	120.6(7)
C(5)-C(4)-H(4)	120.1	C(13)-C(14)-C(15)	118.9(8)
C(3)-C(4)-H(4)	120.0	C(13)-C(14)-H(14)	120.6
C(4)-C(5)-N(1)	122.1(8)	C(15)-C(14)-H(14)	120.5
C(4)-C(5)-N(2)	121.9(8)	C(16)-C(15)-C(14)	117.2(8)
N(1)-C(5)-N(2)	115.8(7)	C(16)-C(15)-H(15)	121.4

**Table B.3** (continued)

<u>Bond angle (°)</u>		C(26)-C(25)-H(25)	120.6
C(14)-C(15)-H(15)	121.5	C(24)-C(25)-H(25)	120.5
N(4)-C(16)-C(15)	125.1(8)	C(25)-C(26)-C(27)	117.3(9)
N(4)-C(16)-N(5)	117.8(7)	C(25)-C(26)-H(26)	121.4
C(15)-C(16)-N(5)	117.0(7)	C(27)-C(26)-H(26)	121.3
C(18)-C(17)-C(22)	120.7(9)	N(7)-C(27)-N(8)	119.3(7)
C(18)-C(17)-N(6)	121.9(8)	N(7)-C(27)-C(26)	123.6(8)
C(22)-C(17)-N(6)	117.4(9)	N(8)-C(27)-C(26)	116.9(8)
C(19)-C(18)-C(17)	119.1(9)	C(33)-C(28)-C(29)	112.7(9)
C(19)-C(18)-H(18)	120.6	C(33)-C(28)-N(9)	126.2(9)
C(17)-C(18)-H(18)	120.3	C(29)-C(28)-N(9)	121.0(9)
C(18)-C(19)-C(20)	122.4(11)	C(30)-C(29)-C(28)	131.9(12)
C(18)-C(19)-H(19)	118.7	C(30)-C(29)-H(29)	114.1
C(20)-C(19)-H(19)	119.0	C(28)-C(29)-H(29)	114.0
C(21)-C(20)-C(19)	118.1(9)	C(29)-C(30)-C(31)	109.1(12)
C(21)-C(20)-H(20)	120.9	C(29)-C(30)-H(30)	125.3
C(19)-C(20)-H(20)	121.0	C(31)-C(30)-H(30)	125.6
C(20)-C(21)-C(22)	120.2(9)	C(32)-C(31)-C(30)	120.9(11)
C(20)-C(21)-H(21)	119.9	C(32)-C(31)-H(31)	119.8
C(22)-C(21)-H(21)	119.8	C(30)-C(31)-H(31)	119.3
C(17)-C(22)-C(21)	119.4(9)	C(31)-C(32)-C(33)	123.6(13)
C(17)-C(22)-H(22)	120.3	C(31)-C(32)-H(32)	118.0
C(21)-C(22)-H(22)	120.3	C(33)-C(32)-H(32)	118.4
N(7)-C(23)-C(24)	120.4(8)	C(28)-C(33)-C(32)	121.1(11)
N(7)-C(23)-H(23)	119.9	C(28)-C(33)-H(33)	119.5
C(24)-C(23)-H(23)	119.7	C(32)-C(33)-H(33)	119.4
C(25)-C(24)-C(23)	121.0(7)	N(10)-C(34)-C(35)	116.6(7)
C(25)-C(24)-Cl(7)	120.1(6)	N(10)-C(34)-H(34)	121.7
C(23)-C(24)-Cl(7)	119.0(7)	C(35)-C(34)-H(34)	121.7
C(26)-C(25)-C(24)	119.0(7)	C(34)-C(35)-C(36)	123.6(9)

**Table B.3** (continued)

<u>Bond angle (°)</u>			
C(34)-C(35)-Cl(8)	116.7(7)	C(43)-C(44)-H(44)	121.1
C(36)-C(35)-Cl(8)	119.7(7)	C(39)-C(44)-H(44)	121.3
C(37)-C(36)-C(35)	117.6(8)	C(46)-C(45)-H(45A)	109.6
C(37)-C(36)-H(36)	121.3	C(46)-C(45)-H(45B)	109.4
C(35)-C(36)-H(36)	121.1	H(45A)-C(45)-H(45B)	109.5
C(36)-C(37)-C(38)	120.6(8)	C(46)-C(45)-H(45C)	109.5
C(36)-C(37)-H(37)	119.6	H(45A)-C(45)-H(45C)	109.5
C(38)-C(37)-H(37)	119.7	H(45B)-C(45)-H(45C)	109.5
N(11)-C(38)-N(10)	117.7(7)	C(47)-C(46)-C(51)	127.0(11)
N(11)-C(38)-C(37)	122.9(7)	C(47)-C(46)-C(45)	127.8(12)
N(10)-C(38)-C(37)	119.4(8)	C(51)-C(46)-C(45)	105.2(13)
C(40)-C(39)-C(44)	122.1(9)	C(46)-C(47)-C(48)	118.0(9)
C(40)-C(39)-N(12)	121.9(8)	C(46)-C(47)-H(47)	121.0
C(44)-C(39)-N(12)	116.0(8)	C(48)-C(47)-H(47)	121.0
C(41)-C(40)-C(39)	119.2(9)	C(49)-C(48)-C(47)	115.3(7)
C(41)-C(40)-H(40)	120.4	C(49)-C(48)-H(48)	122.3
C(39)-C(40)-H(40)	120.4	C(47)-C(48)-H(48)	122.3
C(40)-C(41)-C(42)	119.2(8)	C(50)-C(49)-C(48)	120.8(8)
C(40)-C(41)-H(41)	120.4	C(50)-C(49)-H(49)	119.6
C(42)-C(41)-H(41)	120.4	C(48)-C(49)-H(49)	119.6
C(43)-C(42)-C(41)	123.6(8)	C(49)-C(50)-C(51)	124.5(8)
C(43)-C(42)-H(42)	118.2	C(49)-C(50)-H(50)	117.8
C(41)-C(42)-H(42)	118.3	C(51)-C(50)-H(50)	117.8
C(42)-C(43)-C(44)	118.3(9)	C(46)-C(51)-C(50)	114.4(14)
C(42)-C(43)-H(43)	120.7	C(46)-C(51)-H(51)	122.8
C(44)-C(43)-H(43)	121.0	C(50)-C(51)-H(51)	122.8
C(43)-C(44)-C(39)	117.6(9)		

---

Symmetry transformations used to generate equivalent atoms:

**Table B.4** Bond length (Å) and bond angle (°) of [Ru(Clazpy)(5dmazpy)Cl<sub>2</sub>]

<u>Bond length (Å)</u>			
Ru(1)-N(3)	1.9420(18)	C(8)-C(9)	1.374(4)
Ru(1)-N(6)	2.0050(18)	C(8)-H(8)	0.90(3)
Ru(1)-N(4)	2.0298(17)	C(9)-C(10)	1.370(5)
Ru(1)-N(1)	2.0390(18)	C(9)-H(9)	0.91(3)
Ru(1)-Cl(1)	2.4002(6)	C(10)-C(11)	1.357(6)
Ru(1)-Cl(2)	2.4208(6)	C(10)-H(10)	0.95(4)
N(1)-C(1)	1.341(3)	C(11)-C(12)	1.383(5)
N(1)-C(5)	1.353(3)	C(11)-H(11)	0.84(4)
N(2)-N(3)	1.299(3)	C(12)-H(12)	0.86(3)
N(2)-C(5)	1.379(3)	C(13)-C(14)	1.416(3)
N(3)-C(7)	1.439(3)	C(13)-H(13)	0.94(2)
N(4)-C(13)	1.329(3)	C(14)-C(15)	1.411(3)
N(4)-C(17)	1.364(3)	C(15)-C(16)	1.364(4)
N(5)-N(6)	1.289(2)	C(15)-H(15)	0.97(3)
N(5)-C(17)	1.366(3)	C(16)-C(17)	1.397(3)
N(6)-C(19)	1.432(3)	C(16)-H(16)	0.88(3)
N(7)-C(14)	1.356(3)	C(19)-C(20)	1.374(4)
N(7)-C(26)	1.440(4)	C(19)-C(24)	1.382(3)
N(7)-C(25)	1.450(4)	C(20)-C(21)	1.391(4)
C(1)-C(2)	1.374(3)	C(20)-H(20)	0.92(3)
C(1)-H(1)	0.86(2)	C(21)-C(22)	1.360(6)
C(2)-C(3)	1.381(5)	C(21)-H(21)	0.95(3)
C(2)-Cl(3)	1.722(3)	C(22)-C(23)	1.362(6)
C(3)-C(4)	1.347(6)	C(22)-H(22)	0.94(5)
C(3)-H(3)	0.77(4)	C(23)-C(24)	1.375(4)
C(4)-C(5)	1.393(4)	C(23)-H(23)	0.74(4)
C(4)-H(4)	0.83(3)	C(24)-H(24)	0.92(3)
C(7)-C(8)	1.369(4)	C(25)-H(251)	1.06(6)
C(7)-C(12)	1.377(4)	C(25)-H(252)	1.00(4)

**Table B.4** (Continued)

<u>Bond length (Å)</u>			
C(25)-H(253)	0.95(4)	C(13)-N(4)-Ru(1)	127.54(14)
C(26)-H(261)	1.06(6)	C(17)-N(4)-Ru(1)	112.54(14)
C(26)-H(262)	0.79(5)	N(6)-N(5)-C(17)	112.81(18)
C(26)-H(263)	0.90(5)	N(5)-N(6)-C(19)	113.86(18)
		N(5)-N(6)-Ru(1)	119.03(14)
		C(19)-N(6)-Ru(1)	125.86(14)
<u>Bond angle (°)</u>			
N(3)-Ru(1)-N(6)	100.03(7)	C(14)-N(7)-C(26)	122.0(3)
N(3)-Ru(1)-N(4)	96.00(7)	C(14)-N(7)-C(25)	121.2(2)
N(6)-Ru(1)-N(4)	76.82(7)	C(26)-N(7)-C(25)	116.8(3)
N(3)-Ru(1)-N(1)	76.85(8)	N(1)-C(1)-C(2)	121.2(3)
N(6)-Ru(1)-N(1)	101.61(7)	N(1)-C(1)-H(1)	118.0(16)
N(4)-Ru(1)-N(1)	172.39(7)	C(2)-C(1)-H(1)	120.7(16)
N(3)-Ru(1)-Cl(1)	87.50(6)	C(1)-C(2)-C(3)	120.4(3)
N(6)-Ru(1)-Cl(1)	169.35(5)	C(1)-C(2)-Cl(3)	119.2(3)
N(4)-Ru(1)-Cl(1)	95.01(5)	C(3)-C(2)-Cl(3)	120.4(2)
N(1)-Ru(1)-Cl(1)	87.36(6)	C(4)-C(3)-C(2)	118.4(3)
N(3)-Ru(1)-Cl(2)	172.90(6)	C(4)-C(3)-H(3)	123(3)
N(6)-Ru(1)-Cl(2)	83.51(5)	C(2)-C(3)-H(3)	118(3)
N(4)-Ru(1)-Cl(2)	90.78(5)	C(3)-C(4)-C(5)	120.1(3)
N(1)-Ru(1)-Cl(2)	96.46(6)	C(3)-C(4)-H(4)	128(2)
Cl(1)-Ru(1)-Cl(2)	89.85(2)	C(5)-C(4)-H(4)	112(2)
C(1)-N(1)-C(5)	118.7(2)	N(1)-C(5)-N(2)	117.8(2)
C(1)-N(1)-Ru(1)	129.45(17)	N(1)-C(5)-C(4)	121.2(3)
C(5)-N(1)-Ru(1)	111.84(17)	N(2)-C(5)-C(4)	121.0(3)
N(3)-N(2)-C(5)	111.00(19)	C(8)-C(7)-C(12)	120.5(3)
N(2)-N(3)-C(7)	115.10(19)	C(8)-C(7)-N(3)	119.3(2)
N(2)-N(3)-Ru(1)	121.28(17)	C(12)-C(7)-N(3)	119.9(2)
C(7)-N(3)-Ru(1)	123.15(14)	C(7)-C(8)-C(9)	119.8(3)
C(13)-N(4)-C(17)	119.67(18)	C(7)-C(8)-H(8)	117.8(19)

**Table B.4** (Continued)

---

<u>Bond angle (°)</u>			
C(9)-C(8)-H(8)	122.3(19)	C(20)-C(19)-N(6)	119.4(2)
C(10)-C(9)-C(8)	120.2(3)	C(24)-C(19)-N(6)	120.1(2)
C(10)-C(9)-H(9)	116(2)	C(19)-C(20)-C(21)	119.2(3)
C(8)-C(9)-H(9)	124(2)	C(19)-C(20)-H(20)	117.7(18)
C(11)-C(10)-C(9)	119.5(3)	C(21)-C(20)-H(20)	122.9(19)
C(11)-C(10)-H(10)	118(2)	C(22)-C(21)-C(20)	120.0(4)
C(9)-C(10)-H(10)	122(2)	C(22)-C(21)-H(21)	120(2)
C(10)-C(11)-C(12)	121.4(3)	C(20)-C(21)-H(21)	120(2)
C(10)-C(11)-H(11)	124(3)	C(21)-C(22)-C(23)	120.5(3)
C(12)-C(11)-H(11)	115(3)	C(21)-C(22)-H(22)	109(3)
C(7)-C(12)-C(11)	118.4(3)	C(23)-C(22)-H(22)	131(3)
C(7)-C(12)-H(12)	122(2)	C(22)-C(23)-C(24)	120.6(3)
C(11)-C(12)-H(12)	120(2)	C(22)-C(23)-H(23)	120(3)
N(4)-C(13)-C(14)	122.9(2)	C(24)-C(23)-H(23)	119(3)
N(4)-C(13)-H(13)	116.1(14)	C(23)-C(24)-C(19)	119.2(3)
C(14)-C(13)-H(13)	121.0(14)	C(23)-C(24)-H(24)	124.2(17)
N(7)-C(14)-C(15)	122.8(2)	C(19)-C(24)-H(24)	116.6(17)
N(7)-C(14)-C(13)	120.7(2)	N(7)-C(25)-H(251)	107(3)
C(15)-C(14)-C(13)	116.5(2)	N(7)-C(25)-H(252)	108(3)
C(16)-C(15)-C(14)	120.2(2)	H(251)-C(25)-H(252)	103(3)
C(16)-C(15)-H(15)	120.7(16)	N(7)-C(25)-H(253)	112(2)
C(14)-C(15)-H(15)	119.1(16)	H(251)-C(25)-H(253)	111(4)
C(15)-C(16)-C(17)	120.1(2)	H(252)-C(25)-H(253)	116(3)
C(15)-C(16)-H(16)	122.5(18)	N(7)-C(26)-H(261)	101(3)
C(17)-C(16)-H(16)	117.2(18)	N(7)-C(26)-H(262)	110(4)
N(4)-C(17)-N(5)	117.94(18)	H(261)-C(26)-H(262)	98(5)
N(4)-C(17)-C(16)	120.4(2)	N(7)-C(26)-H(263)	115(3)
N(5)-C(17)-C(16)	121.5(2)		
C(20)-C(19)-C(24)	120.5(2)		

---

**Table B.4** (Continued)

---

Bond angle (°)

H(261)-C(26)-H(263) 101(4)

H(262)-C(26)-H(263) 126(4)

---

Symmetry transformations used to generate equivalent atoms:

**Table B.5** Bond length (Å) and bond angle (°) of [Ru(Clazpy)<sub>2</sub>(phen)](PF<sub>6</sub>)<sub>2</sub>

<u>Bond length (Å)</u>			
Ru(1)-N(6)	1.993(4)	C(6)-C(11)	1.374(7)
Ru(1)-N(3)	2.003(4)	C(6)-C(7)	1.376(7)
Ru(1)-N(1)	2.051(4)	C(7)-C(8)	1.374(8)
Ru(1)-N(4)	2.071(4)	C(7)-H(4)	0.88(5)
Ru(1)-N(8)	2.092(4)	C(8)-C(9)	1.365(9)
Ru(1)-N(7)	2.100(4)	C(8)-H(5)	0.99(6)
Cl(1)-C(2)	1.710(6)	C(9)-C(10)	1.369(9)
Cl(2)-C(13)	1.716(5)	C(9)-H(6)	0.81(6)
N(1)-C(1)	1.352(6)	C(10)-C(11)	1.380(9)
N(1)-C(5)	1.356(6)	C(10)-H(7)	1.12(6)
N(2)-N(3)	1.286(5)	C(11)-H(8)	0.93(5)
N(2)-C(5)	1.390(6)	C(12)-C(13)	1.367(7)
N(3)-C(6)	1.449(6)	C(12)-H(9)	0.98(5)
N(4)-C(12)	1.358(6)	C(13)-C(14)	1.367(8)
N(4)-C(16)	1.362(6)	C(14)-C(15)	1.397(8)
N(5)-N(6)	1.287(5)	C(14)-H(10)	0.95(7)
N(5)-C(16)	1.383(6)	C(15)-C(16)	1.367(7)
N(6)-C(17)	1.450(6)	C(15)-H(11)	0.92(6)
N(7)-C(23)	1.330(7)	C(17)-C(18)	1.375(8)
N(7)-C(34)	1.372(6)	C(17)-C(22)	1.387(7)
N(8)-C(32)	1.338(7)	C(18)-C(19)	1.369(8)
N(8)-C(33)	1.352(6)	C(18)-H(12)	0.79(5)
C(1)-C(2)	1.380(7)	C(19)-C(20)	1.377(9)
C(1)-H(1)	0.93(5)	C(19)-H(13)	1.02(6)
C(2)-C(3)	1.372(8)	C(20)-C(21)	1.363(10)
C(3)-C(4)	1.374(9)	C(20)-H(14)	0.95(6)
C(3)-H(2)	1.06(6)	C(21)-C(22)	1.388(8)
C(4)-C(5)	1.377(7)	C(21)-H(15)	0.97(6)
C(4)-H(3)	0.88(5)	C(22)-H(16)	0.95(5)

**Table B.5** (continued)

<u>Bond length (Å)</u>			
C(23)-C(24)	1.397(9)	P(2)-F(12)	1.576(4)
C(23)-H(17)	0.89(5)	P(2)-F(7)	1.581(4)
C(24)-C(25)	1.348(10)	P(2)-F(10)	1.598(4)
C(24)-H(18)	0.85(6)		
C(25)-C(26)	1.393(9)	<u>Bond angle (°)</u>	
C(25)-H(19)	0.94(6)	N(6)-Ru(1)-N(3)	101.85(16)
C(26)-C(34)	1.395(7)	N(6)-Ru(1)-N(1)	96.48(16)
C(26)-C(27)	1.438(9)	N(3)-Ru(1)-N(1)	76.37(16)
C(27)-C(28)	1.337(10)	N(6)-Ru(1)-N(4)	76.27(16)
C(27)-H(20)	0.89(6)	N(3)-Ru(1)-N(4)	176.94(16)
C(28)-C(29)	1.415(9)	N(1)-Ru(1)-N(4)	101.34(15)
C(28)-H(21)	0.85(6)	N(6)-Ru(1)-N(8)	93.29(16)
C(29)-C(30)	1.407(9)	N(3)-Ru(1)-N(8)	96.96(16)
C(29)-C(33)	1.413(7)	N(1)-Ru(1)-N(8)	169.12(15)
C(30)-C(31)	1.352(9)	N(4)-Ru(1)-N(8)	85.61(15)
C(30)-H(22)	0.93(6)	N(6)-Ru(1)-N(7)	169.23(15)
C(31)-C(32)	1.390(8)	N(3)-Ru(1)-N(7)	86.42(15)
C(31)-H(23)	0.94(7)	N(1)-Ru(1)-N(7)	92.14(15)
C(32)-H(24)	0.84(5)	N(4)-Ru(1)-N(7)	95.74(15)
C(33)-C(34)	1.411(7)	N(8)-Ru(1)-N(7)	78.74(16)
P(1)-F(2)	1.516(6)	C(1)-N(1)-C(5)	118.2(4)
P(1)-F(5)	1.518(6)	C(1)-N(1)-Ru(1)	129.3(4)
P(1)-F(6)	1.522(6)	C(5)-N(1)-Ru(1)	112.3(3)
P(1)-F(3)	1.534(7)	N(3)-N(2)-C(5)	111.8(4)
P(1)-F(4)	1.562(5)	N(2)-N(3)-C(6)	113.4(4)
P(1)-F(1)	1.574(5)	N(2)-N(3)-Ru(1)	120.4(3)
P(2)-F(8)	1.567(4)	C(6)-N(3)-Ru(1)	125.4(3)
P(2)-F(11)	1.571(5)	C(12)-N(4)-C(16)	117.6(4)
P(2)-F(9)	1.575(4)	C(12)-N(4)-Ru(1)	130.4(3)

**Table B.5** (continued)

<u>Bond angle (°)</u>			
C(16)-N(4)-Ru(1)	111.8(3)	C(8)-C(7)-C(6)	119.7(6)
N(6)-N(5)-C(16)	112.7(4)	C(8)-C(7)-H(4)	123(4)
N(5)-N(6)-C(17)	111.4(4)	C(6)-C(7)-H(4)	117(4)
N(5)-N(6)-Ru(1)	120.4(3)	C(9)-C(8)-C(7)	119.0(6)
C(17)-N(6)-Ru(1)	127.7(3)	C(9)-C(8)-H(5)	113(4)
C(23)-N(7)-C(34)	117.6(5)	C(7)-C(8)-H(5)	128(4)
C(23)-N(7)-Ru(1)	129.3(4)	C(8)-C(9)-C(10)	121.8(6)
C(34)-N(7)-Ru(1)	113.0(3)	C(8)-C(9)-H(6)	118(4)
C(32)-N(8)-C(33)	118.4(5)	C(10)-C(9)-H(6)	120(4)
C(32)-N(8)-Ru(1)	127.9(4)	C(9)-C(10)-C(11)	119.5(6)
C(33)-N(8)-Ru(1)	113.7(3)	C(9)-C(10)-H(7)	123(3)
N(1)-C(1)-C(2)	120.5(5)	C(11)-C(10)-H(7)	117(3)
N(1)-C(1)-H(1)	121(3)	C(6)-C(11)-C(10)	118.8(6)
C(2)-C(1)-H(1)	118(3)	C(6)-C(11)-H(8)	114(3)
C(3)-C(2)-C(1)	121.4(5)	C(10)-C(11)-H(8)	127(3)
C(3)-C(2)-Cl(1)	120.3(4)	N(4)-C(12)-C(13)	121.0(5)
C(1)-C(2)-Cl(1)	118.4(5)	N(4)-C(12)-H(9)	112(3)
C(2)-C(3)-C(4)	118.0(5)	C(13)-C(12)-H(9)	127(3)
C(2)-C(3)-H(2)	123(3)	C(12)-C(13)-C(14)	121.7(5)
C(4)-C(3)-H(2)	119(3)	C(12)-C(13)-Cl(2)	119.2(4)
C(3)-C(4)-C(5)	119.3(6)	C(14)-C(13)-Cl(2)	119.0(4)
C(3)-C(4)-H(3)	124(3)	C(13)-C(14)-C(15)	117.7(5)
C(5)-C(4)-H(3)	116(3)	C(13)-C(14)-H(10)	121(4)
N(1)-C(5)-C(4)	122.6(5)	C(15)-C(14)-H(10)	121(4)
N(1)-C(5)-N(2)	118.1(4)	C(16)-C(15)-C(14)	118.8(5)
C(4)-C(5)-N(2)	119.3(5)	C(16)-C(15)-H(11)	122(4)
C(11)-C(6)-C(7)	121.2(5)	C(14)-C(15)-H(11)	119(4)
C(11)-C(6)-N(3)	119.1(5)	N(4)-C(16)-C(15)	123.1(5)
C(7)-C(6)-N(3)	119.6(5)	N(4)-C(16)-N(5)	117.5(4)

**Table B.5** (continued)

<u>Bond angle (°)</u>			
C(15)-C(16)-N(5)	119.3(5)	C(25)-C(26)-C(27)	123.5(6)
C(18)-C(17)-C(22)	120.6(5)	C(34)-C(26)-C(27)	118.4(6)
C(18)-C(17)-N(6)	120.5(5)	C(28)-C(27)-C(26)	120.7(7)
C(22)-C(17)-N(6)	118.9(5)	C(28)-C(27)-H(20)	124(4)
C(19)-C(18)-C(17)	119.9(6)	C(26)-C(27)-H(20)	115(4)
C(19)-C(18)-H(12)	119(4)	C(27)-C(28)-C(29)	122.1(7)
C(17)-C(18)-H(12)	120(4)	C(27)-C(28)-H(21)	121(4)
C(18)-C(19)-C(20)	119.7(7)	C(29)-C(28)-H(21)	116(4)
C(18)-C(19)-H(13)	119(4)	C(30)-C(29)-C(33)	116.4(6)
C(20)-C(19)-H(13)	121(4)	C(30)-C(29)-C(28)	125.2(6)
C(21)-C(20)-C(19)	120.9(6)	C(33)-C(29)-C(28)	118.5(6)
C(21)-C(20)-H(14)	122(4)	C(31)-C(30)-C(29)	120.6(6)
C(19)-C(20)-H(14)	117(4)	C(31)-C(30)-H(22)	127(4)
C(20)-C(21)-C(22)	120.1(6)	C(29)-C(30)-H(22)	112(4)
C(20)-C(21)-H(15)	121(4)	C(30)-C(31)-C(32)	119.5(6)
C(22)-C(21)-H(15)	119(4)	C(30)-C(31)-H(23)	121(4)
C(17)-C(22)-C(21)	118.7(6)	C(32)-C(31)-H(23)	119(4)
C(17)-C(22)-H(16)	118(3)	N(8)-C(32)-C(31)	122.3(6)
C(21)-C(22)-H(16)	123(3)	N(8)-C(32)-H(24)	118(4)
N(7)-C(23)-C(24)	122.2(6)	C(31)-C(32)-H(24)	120(4)
N(7)-C(23)-H(17)	114(4)	N(8)-C(33)-C(34)	117.6(5)
C(24)-C(23)-H(17)	124(4)	N(8)-C(33)-C(29)	122.7(5)
C(25)-C(24)-C(23)	120.4(7)	C(34)-C(33)-C(29)	119.7(5)
C(25)-C(24)-H(18)	129(4)	N(7)-C(34)-C(26)	122.4(5)
C(23)-C(24)-H(18)	111(4)	N(7)-C(34)-C(33)	116.9(4)
C(24)-C(25)-C(26)	119.3(6)	C(26)-C(34)-C(33)	120.7(5)
C(24)-C(25)-H(19)	121(3)	F(2)-P(1)-F(5)	176.3(6)
C(26)-C(25)-H(19)	120(3)	F(2)-P(1)-F(6)	92.8(6)
C(25)-C(26)-C(34)	118.1(6)	F(5)-P(1)-F(6)	90.8(5)

**Table B.5** (continued)

---

<u>Bond angle (°)</u>	
F(2)-P(1)-F(3)	89.0(5)
F(5)-P(1)-F(3)	87.3(5)
F(6)-P(1)-F(3)	178.1(6)
F(2)-P(1)-F(4)	93.1(4)
F(5)-P(1)-F(4)	86.6(4)
F(6)-P(1)-F(4)	88.5(4)
F(3)-P(1)-F(4)	91.6(4)
F(2)-P(1)-F(1)	89.5(4)
F(5)-P(1)-F(1)	91.0(4)
F(6)-P(1)-F(1)	89.8(3)
F(3)-P(1)-F(1)	90.0(4)
F(4)-P(1)-F(1)	177.0(4)
F(8)-P(2)-F(11)	179.5(3)
F(8)-P(2)-F(9)	89.2(3)
F(11)-P(2)-F(9)	91.0(3)
F(8)-P(2)-F(12)	89.9(3)
F(11)-P(2)-F(12)	89.8(3)
F(9)-P(2)-F(12)	179.1(3)
F(8)-P(2)-F(7)	90.3(3)
F(11)-P(2)-F(7)	90.2(3)
F(9)-P(2)-F(7)	89.9(3)
F(12)-P(2)-F(7)	90.2(2)
F(8)-P(2)-F(10)	89.6(3)
F(11)-P(2)-F(10)	89.9(3)
F(9)-P(2)-F(10)	90.2(3)
F(12)-P(2)-F(10)	89.8(2)
F(7)-P(2)-F(10)	179.9(3)

---

Symmetry transformations used to generate equivalent atoms:

**Table B.6** Bond length (Å) and bond angle (°) of [Ru(Clazpy)<sub>2</sub>(azpy)](PF<sub>6</sub>)<sub>2</sub>

<u>Bond length (Å)</u>			
Ru(1)-N(3)	2.0381(19)	C(6)-C(7)	1.383(4)
Ru(1)-N(7)	2.0541(19)	C(6)-C(11)	1.385(4)
Ru(1)-N(4)	2.0588(18)	C(7)-C(8)	1.375(4)
Ru(1)-N(1)	2.0598(19)	C(7)-H(7)	0.87(3)
Ru(1)-N(9)	2.0697(19)	C(8)-C(9)	1.378(4)
Ru(1)-N(6)	2.0741(19)	C(8)-H(8)	0.95(3)
N(1)-C(1)	1.335(3)	C(9)-C(10)	1.373(5)
N(1)-C(5)	1.358(3)	C(9)-H(9)	0.84(4)
N(2)-N(3)	1.274(3)	C(10)-C(11)	1.383(4)
N(2)-C(5)	1.394(3)	C(10)-H(10)	0.92(3)
N(3)-C(6)	1.440(3)	C(11)-H(11)	0.91(3)
N(4)-C(12)	1.335(3)	C(12)-C(13)	1.388(3)
N(4)-C(16)	1.357(3)	C(12)-H(12)	0.92(2)
N(5)-N(6)	1.280(3)	C(13)-C(14)	1.374(4)
N(5)-C(16)	1.392(3)	C(13)-Cl(2)	1.720(2)
N(6)-C(17)	1.440(3)	C(14)-C(15)	1.374(4)
N(7)-C(23)	1.337(3)	C(14)-H(14)	0.90(3)
N(7)-C(27)	1.354(3)	C(15)-C(16)	1.381(3)
N(8)-N(9)	1.280(3)	C(15)-H(15)	0.90(3)
N(8)-C(27)	1.392(3)	C(17)-C(18)	1.385(4)
N(9)-C(28)	1.437(3)	C(17)-C(22)	1.390(4)
C(1)-C(2)	1.382(4)	C(18)-C(19)	1.386(4)
C(1)-H(1)	0.93(3)	C(18)-H(18)	0.91(3)
C(2)-C(3)	1.374(5)	C(19)-C(20)	1.374(5)
C(2)-Cl(1)	1.723(3)	C(19)-H(19)	0.86(4)
C(3)-C(4)	1.365(5)	C(20)-C(21)	1.373(5)
C(3)-H(3)	0.86(3)	C(20)-H(20)	0.88(4)
C(4)-C(5)	1.388(4)	C(21)-C(22)	1.379(4)
C(4)-H(4)	0.95(3)	C(21)-H(21)	0.92(3)

**Table B.6** (continued)

<u>Bond length (Å)</u>			
C(22)-H(22)	0.89(3)	P(2)-F(10)	1.583(2)
C(23)-C(24)	1.379(4)	P(2)-F(9)	1.583(2)
C(23)-H(23)	0.91(3)	P(2)-F(8)	1.586(2)
C(24)-C(25)	1.368(5)	P(2)-F(7)	1.5890(19)
C(24)-H(24)	0.89(3)	P(2)-F(11B)	1.625(12)
C(25)-C(26)	1.370(5)		
C(25)-H(25)	0.88(4)	<u>Bond angle (°)</u>	
C(26)-C(27)	1.380(4)	N(3)-Ru(1)-N(7)	99.28(8)
C(26)-H(26)	0.88(4)	N(3)-Ru(1)-N(4)	95.78(8)
C(28)-C(29)	1.379(4)	N(7)-Ru(1)-N(4)	96.94(7)
C(28)-C(33)	1.391(4)	N(3)-Ru(1)-N(1)	75.85(8)
C(29)-C(30)	1.379(4)	N(7)-Ru(1)-N(1)	86.35(7)
C(29)-H(29)	0.88(3)	N(4)-Ru(1)-N(1)	171.44(7)
C(30)-C(31)	1.371(5)	N(3)-Ru(1)-N(9)	170.66(8)
C(30)-H(30)	0.89(4)	N(7)-Ru(1)-N(9)	76.31(8)
C(31)-C(32)	1.366(5)	N(4)-Ru(1)-N(9)	92.95(7)
C(31)-H(31)	0.89(4)	N(1)-Ru(1)-N(9)	95.51(8)
C(32)-C(33)	1.372(5)	N(3)-Ru(1)-N(6)	80.78(8)
C(32)-H(32)	0.92(4)	N(7)-Ru(1)-N(6)	172.97(7)
C(33)-H(33)	0.84(3)	N(4)-Ru(1)-N(6)	76.09(7)
P(1)-F(4)	1.535(2)	N(1)-Ru(1)-N(6)	100.43(8)
P(1)-F(1A)	1.551(10)	N(9)-Ru(1)-N(6)	104.63(8)
P(1)-F(2)	1.575(2)	C(1)-N(1)-C(5)	118.2(2)
P(1)-F(3)	1.575(3)	C(1)-N(1)-Ru(1)	128.97(17)
P(1)-F(6)	1.578(2)	C(5)-N(1)-Ru(1)	112.85(16)
P(1)-F(5)	1.590(2)	N(3)-N(2)-C(5)	112.2(2)
P(1)-F(1B)	1.596(13)	N(2)-N(3)-C(6)	115.19(19)
P(2)-F(11A)	1.560(8)	N(2)-N(3)-Ru(1)	120.13(16)
P(2)-F(12)	1.5826(19)	C(6)-N(3)-Ru(1)	123.35(15)

**Table B.6** (continued)

<u>Bond angle (°)</u>			
C(12)-N(4)-C(16)	118.08(19)	C(7)-C(6)-C(11)	121.1(2)
C(12)-N(4)-Ru(1)	128.64(16)	C(7)-C(6)-N(3)	119.0(2)
C(16)-N(4)-Ru(1)	112.82(15)	C(11)-C(6)-N(3)	119.6(2)
N(6)-N(5)-C(16)	113.50(19)	C(8)-C(7)-C(6)	119.2(2)
N(5)-N(6)-C(17)	113.06(19)	C(8)-C(7)-H(7)	119.9(19)
N(5)-N(6)-Ru(1)	118.07(15)	C(6)-C(7)-H(7)	120.9(19)
C(17)-N(6)-Ru(1)	127.61(15)	C(7)-C(8)-C(9)	120.2(3)
C(23)-N(7)-C(27)	117.6(2)	C(7)-C(8)-H(8)	121(2)
C(23)-N(7)-Ru(1)	128.71(17)	C(9)-C(8)-H(8)	119(2)
C(27)-N(7)-Ru(1)	113.59(16)	C(10)-C(9)-C(8)	120.4(3)
N(9)-N(8)-C(27)	114.1(2)	C(10)-C(9)-H(9)	119(3)
N(8)-N(9)-C(28)	112.5(2)	C(8)-C(9)-H(9)	121(3)
N(8)-N(9)-Ru(1)	118.12(16)	C(9)-C(10)-C(11)	120.4(3)
C(28)-N(9)-Ru(1)	128.89(16)	C(9)-C(10)-H(10)	120(2)
N(1)-C(1)-C(2)	121.6(3)	C(11)-C(10)-H(10)	119(2)
N(1)-C(1)-H(1)	119.1(17)	C(10)-C(11)-C(6)	118.7(3)
C(2)-C(1)-H(1)	119.2(17)	C(10)-C(11)-H(11)	122.9(18)
C(3)-C(2)-C(1)	120.5(3)	C(6)-C(11)-H(11)	118.4(18)
C(3)-C(2)-Cl(1)	120.5(2)	N(4)-C(12)-C(13)	121.2(2)
C(1)-C(2)-Cl(1)	119.0(2)	N(4)-C(12)-H(12)	118.1(16)
C(4)-C(3)-C(2)	118.3(3)	C(13)-C(12)-H(12)	120.6(16)
C(4)-C(3)-H(3)	124(2)	C(14)-C(13)-C(12)	120.7(2)
C(2)-C(3)-H(3)	117(2)	C(14)-C(13)-Cl(2)	120.15(19)
C(3)-C(4)-C(5)	119.5(3)	C(12)-C(13)-Cl(2)	119.2(2)
C(3)-C(4)-H(4)	125(2)	C(13)-C(14)-C(15)	118.2(2)
C(5)-C(4)-H(4)	115(2)	C(13)-C(14)-H(14)	121.0(18)
N(1)-C(5)-C(4)	121.9(3)	C(15)-C(14)-H(14)	120.8(18)
N(1)-C(5)-N(2)	118.2(2)	C(14)-C(15)-C(16)	119.0(3)
C(4)-C(5)-N(2)	119.9(2)	C(14)-C(15)-H(15)	122.6(17)

Table B.6 (continued)

<u>Bond angle (°)</u>			
C(16)-C(15)-H(15)	118.4(17)	C(24)-C(25)-H(25)	119(2)
N(4)-C(16)-C(15)	122.7(2)	C(26)-C(25)-H(25)	122(2)
N(4)-C(16)-N(5)	118.4(2)	C(25)-C(26)-C(27)	119.1(3)
C(15)-C(16)-N(5)	118.9(2)	C(25)-C(26)-H(26)	123(2)
C(18)-C(17)-C(22)	120.6(2)	C(27)-C(26)-H(26)	118(2)
C(18)-C(17)-N(6)	118.8(2)	N(7)-C(27)-C(26)	122.1(3)
C(22)-C(17)-N(6)	120.6(2)	N(7)-C(27)-N(8)	117.9(2)
C(17)-C(18)-C(19)	119.4(3)	C(26)-C(27)-N(8)	119.9(3)
C(17)-C(18)-H(18)	119.9(19)	C(29)-C(28)-C(33)	119.4(3)
C(19)-C(18)-H(18)	120.6(19)	C(29)-C(28)-N(9)	120.0(2)
C(20)-C(19)-C(18)	119.8(3)	C(33)-C(28)-N(9)	120.6(2)
C(20)-C(19)-H(19)	125(3)	C(28)-C(29)-C(30)	119.8(3)
C(18)-C(19)-H(19)	116(3)	C(28)-C(29)-H(29)	118(2)
C(21)-C(20)-C(19)	120.7(3)	C(30)-C(29)-H(29)	122(2)
C(21)-C(20)-H(20)	119(3)	C(31)-C(30)-C(29)	120.7(3)
C(19)-C(20)-H(20)	120(3)	C(31)-C(30)-H(30)	119(2)
C(20)-C(21)-C(22)	120.4(3)	C(29)-C(30)-H(30)	120(2)
C(20)-C(21)-H(21)	117.6(19)	C(32)-C(31)-C(30)	119.4(3)
C(22)-C(21)-H(21)	121.9(19)	C(32)-C(31)-H(31)	120(2)
C(21)-C(22)-C(17)	119.0(3)	C(30)-C(31)-H(31)	120(2)
C(21)-C(22)-H(22)	119.9(17)	C(31)-C(32)-C(33)	121.1(3)
C(17)-C(22)-H(22)	120.7(17)	C(31)-C(32)-H(32)	118(2)
N(7)-C(23)-C(24)	122.8(3)	C(33)-C(32)-H(32)	121(2)
N(7)-C(23)-H(23)	116.9(17)	C(32)-C(33)-C(28)	119.6(3)
C(24)-C(23)-H(23)	120.4(17)	C(32)-C(33)-H(33)	124(2)
C(25)-C(24)-C(23)	119.1(3)	C(28)-C(33)-H(33)	117(2)
C(25)-C(24)-H(24)	119(2)	F(4)-P(1)-F(1A)	99.2(7)
C(23)-C(24)-H(24)	121(2)	F(4)-P(1)-F(2)	178.1(2)
C(24)-C(25)-C(26)	119.3(3)	F(1A)-P(1)-F(2)	82.7(7)

**Table B.6** (continued)

<u>Bond angle (°)</u>		F(11A)-P(2)-F(10)	99.4(10)
F(4)-P(1)-F(3)	91.6(2)	F(12)-P(2)-F(10)	90.00(13)
F(1A)-P(1)-F(3)	168.7(7)	F(11A)-P(2)-F(9)	96.6(5)
F(2)-P(1)-F(3)	86.55(19)	F(12)-P(2)-F(9)	88.32(13)
F(4)-P(1)-F(6)	89.88(17)	F(10)-P(2)-F(9)	91.37(15)
F(1A)-P(1)-F(6)	85.8(5)	F(11A)-P(2)-F(8)	83.2(10)
F(2)-P(1)-F(6)	90.37(15)	F(12)-P(2)-F(8)	87.28(13)
F(3)-P(1)-F(6)	90.92(15)	F(10)-P(2)-F(8)	176.97(15)
F(4)-P(1)-F(5)	91.15(16)	F(9)-P(2)-F(8)	89.91(15)
F(1A)-P(1)-F(5)	94.0(5)	F(11A)-P(2)-F(7)	84.5(5)
F(2)-P(1)-F(5)	88.60(14)	F(12)-P(2)-F(7)	90.55(12)
F(3)-P(1)-F(5)	89.02(15)	F(10)-P(2)-F(7)	88.81(12)
F(6)-P(1)-F(5)	178.97(15)	F(9)-P(2)-F(7)	178.85(14)
F(4)-P(1)-F(1B)	76.9(17)	F(8)-P(2)-F(7)	89.86(13)
F(1A)-P(1)-F(1B)	24.3(12)	F(11A)-P(2)-F(11B)	24.9(5)
F(2)-P(1)-F(1B)	104.9(17)	F(12)-P(2)-F(11B)	165.8(12)
F(3)-P(1)-F(1B)	166.8(17)	F(10)-P(2)-F(11B)	79.0(9)
F(6)-P(1)-F(1B)	95.4(7)	F(9)-P(2)-F(11B)	83.1(10)
F(5)-P(1)-F(1B)	84.8(7)	F(8)-P(2)-F(11B)	103.9(9)
F(11A)-P(2)-F(12)	169.2(11)	F(7)-P(2)-F(11B)	98.1(10)

Symmetry transformations used to generate equivalent atoms:

**Table B.7** Bond length (Å) and bond angle (°) of [Ru(Clazpy)<sub>2</sub>(phen)](NO<sub>3</sub>)<sub>2</sub>·3.5H<sub>2</sub>O

<u>Bond length (Å)</u>			
Ru1-N22	2.004(4)	C126-H126	0.95
Ru1-N12	2.020(4)	N211-C216	1.341(6)
Ru1-N211	2.043(4)	N211-C212	1.364(6)
Ru1-N111	2.052(4)	C212-N21	1.384(7)
Ru1-N311	2.065(4)	C212-C213	1.401(6)
Ru1-N321	2.074(4)	C213-C214	1.394(8)
N111-C116	1.338(6)	C213-H213	0.95
N111-C112	1.364(6)	C214-C215	1.336(7)
C112-C113	1.385(7)	C214-H214	0.95
C112-N11	1.385(7)	C215-C216	1.408(6)
C113-C114	1.404(8)	C215-C125	1.723(5)
C113-H113	0.95	C216-H216	0.95
C114-C115	1.358(8)	N21-N22	1.284(5)
C114-H114	0.95	N22-C221	1.426(6)
C115-C116	1.406(7)	C221-C226	1.390(7)
C115-C115	1.730(6)	C221-C222	1.416(7)
C116-H116	0.95	C222-C223	1.393(7)
N11-N12	1.279(6)	C222-H222	0.95
N12-C121	1.428(7)	C223-C224	1.375(7)
C121-C122	1.378(7)	C223-H223	0.95
C121-C126	1.396(8)	C224-C225	1.401(8)
C122-C123	1.384(8)	C224-H224	0.95
C122-H122	0.95	C225-C226	1.375(7)
C123-C124	1.369(9)	C225-H225	0.95
C123-H123	0.95	C226-H226	0.95
C124-C125	1.412(9)	N311-C316	1.338(6)
C124-H124	0.95	N311-C312	1.361(6)
C125-C126	1.357(8)	C312-C322	1.400(7)
C125-H125	0.95	C312-C313	1.412(7)

**Table B.7** (continued)

<u>Bond length (Å)</u>		<u>Bond angle (°)</u>	
C314 -H314	0.95	N22-Ru1-N12	84.20(16)
C315-C316	1.415(8)	N22-Ru1-N211	76.30(16)
C315-H315	0.95	N12-Ru1-N211	100.36(16)
C316-H316	0.95	N22-Ru1-N111	97.84(16)
C317-C327	1.330(9)	N12-Ru1-N111	75.92(17)
C317-H317	0.95	N211-Ru1-N111	173.47(16)
N321-C326	1.349(7)	N22-Ru1-N311	99.09(16)
N321-C322	1.390(7)	N12-Ru1-N311	173.54(15)
C322-C323	1.419(7)	N211-Ru1-N311	85.86(15)
C323-C324	1.404(8)	N111-Ru1-N311	98.05(16)
C323-C327	1.412(8)	N22-Ru1-N321	174.36(15)
C324-C325	1.412(8)	N12-Ru1-N321	98.05(17)
C324-H324	0.95	N211-Ru1-N321	98.17(15)
C325-C326	1.402(7)	N111-Ru1-N321	87.73(15)
C325-H325	0.95	N311-Ru1-N321	79.20(16)
C326-H326	0.95	C116-N111-C112	117.7(4)
C327-H327	0.95	C116-N111-Ru1	128.9(3)
N1-O13	1.229(6)	C112-N111-Ru1	113.3(4)
N1-O12	1.237(6)	N111-C112-C113	122.5(5)
N1-O11	1.247(7)	N111-C112-N11	117.2(4)
N2-O23	1.171(10)	C113-C112-N11	120.3(5)
N2-O22	1.213(10)	C112-C113-C114	119.2(5)
N2-O21	1.227(10)	C112-C113-H113	120.4
N3-O33	1.100(15)	C114-C113-H113	120.4
N3-O32	1.331(17)	C115-C114-C113	118.0(5)
N3-O31	1.457(16)	C115-C114-H114	121
C314-C315	1.355(7)	C113-C114-H114	121
C313-C314	1.408(8)	C114-C115-C116	120.6(6)
C313-C317	1.431(8)	C114-C115-C115	120.8(4)

**Table B.7** (continued)

<u>Bond angle (°)</u>			
C116-C115-C115	118.6(5)	N211-C212-N21	118.5(4)
N111-C116-C115	121.9(5)	N211-C212-C213	121.1(5)
N111-C116-H116	119	N21-C212-C213	120.4(5)
C115-C116-H116	119	C214-C213-C212	119.1(5)
N12-N11-C112	112.8(4)	C214-C213-H213	120.4
N11-N12-C121	113.5(4)	C212-C213-H213	120.4
N11-N12-Ru1	120.3(4)	C215-C214-C213	119.1(5)
C121-N12-Ru1	125.2(3)	C215-C214-H214	120.5
C122-C121-C126	120.4(5)	C213-C214-H214	120.5
C122-C121-N12	119.3(5)	C214-C215-C216	120.8(5)
C126-C121-N12	120.3(5)	C214-C215-C125	121.1(4)
C121-C122-C123	119.6(6)	C216-C215-C125	118.1(4)
C121-C122-H122	120.2	N211-C216-C215	121.0(5)
C123-C122-H122	120.2	N211-C216-H216	119.5
C124-C123-C122	120.3(6)	C215-C216-H216	119.5
C124-C123-H123	119.9	N22-N21-C212	111.2(4)
C122-C123-H123	119.9	N21-N22-C221	113.6(4)
C123-C124-C125	120.0(6)	N21-N22-Ru1	121.1(3)
C123-C124-H124	120	C221-N22-Ru1	124.3(3)
C125-C124-H124	120	C226-C221-C222	121.1(5)
C126-C125-C124	119.6(6)	C226-C221-N22	120.3(5)
C126-C125-H125	120.2	C222-C221-N22	118.5(4)
C124-C125-H125	120.2	C223-C222-C221	117.8(5)
C125-C126-C121	120.1(6)	C223-C222-H222	121.1
C125-C126-H126	119.9	C221-C222-H222	121.1
C121-C126-H126	119.9	C224-C223-C222	121.0(5)
C216-N211-C212	118.8(4)	C224-C223-H223	119.5
C216-N211-Ru1	128.6(3)	C222-C223-H223	119.5
C212-N211-Ru1	112.5(3)	C223-C224-C225	120.2(5)

**Table B.7** (continued)

<u>Bond angle (°)</u>			
C223-C224-H224	119.9	C326-N321-C322	118.3(4)
C225-C224-H224	119.9	C326-N321-Ru1	128.5(4)
C226-C225-C224	120.2(5)	C322-N321-Ru1	113.1(3)
C226-C225-H225	119.9	N321-C322-C312	116.2(4)
C224-C225-H225	119.9	N321-C322-C323	122.3(5)
C225-C226-C221	119.5(5)	C312-C322-C323	121.4(5)
C225-C226-H226	120.3	C324-C323-C327	124.7(5)
C221-C226-H226	120.3	C324-C323-C322	118.2(5)
C316-N311-C312	117.9(4)	C327-C323-C322	117.1(5)
C316-N311-Ru1	128.1(4)	C323-C324-C325	119.1(5)
C312-N311-Ru1	114.0(3)	C323-C324-H324	120.4
N311-C312-C322	117.3(5)	C325-C324-H324	120.4
N311-C312-C313	123.6(5)	C326-C325-C324	119.6(5)
C322-C312-C313	119.1(5)	C326-C325-H325	120.2
C314-C313-C312	116.6(5)	C324-C325-H325	120.2
C314-C313-C317	124.6(5)	N321-C326-C325	122.5(5)
C312-C313-C317	118.8(5)	N321-C326-H326	118.8
C315-C314-C313	119.9(5)	C325-C326-H326	118.8
C315-C314-H314	120.1	C317-C327-C323	122.8(5)
C313-C314-H314	120.1	C317-C327-H327	118.6
C314-C315-C316	120.2(5)	C323-C327-H327	118.6
C314-C315-H315	119.9	O13-N1-O12	119.4(7)
C316-C315-H315	119.9	O13-N1O11	120.8(6)
N311-C316-C315	121.7(5)	O12-N1-O11	119.8(6)
N311-C316-H316	119.1	O23-N2-O22	113.4(9)
C315-C316-H316	119.1	O23-N2-O21	128.3(9)
C327-C317-C313	120.7(6)	O22-N2-O21	118.1(9)
C327-C317-H317	119.6	O33-N3-O32	99.7(15)
C313-C317-H317	119.6	O33-N3-O31	147.0(18)

**Table B.7** (Continued)

---

<u>Bond angle (°)</u>	
O32-N3-O31	109.1(15)

---

## Appendix C Cyclic voltammograms

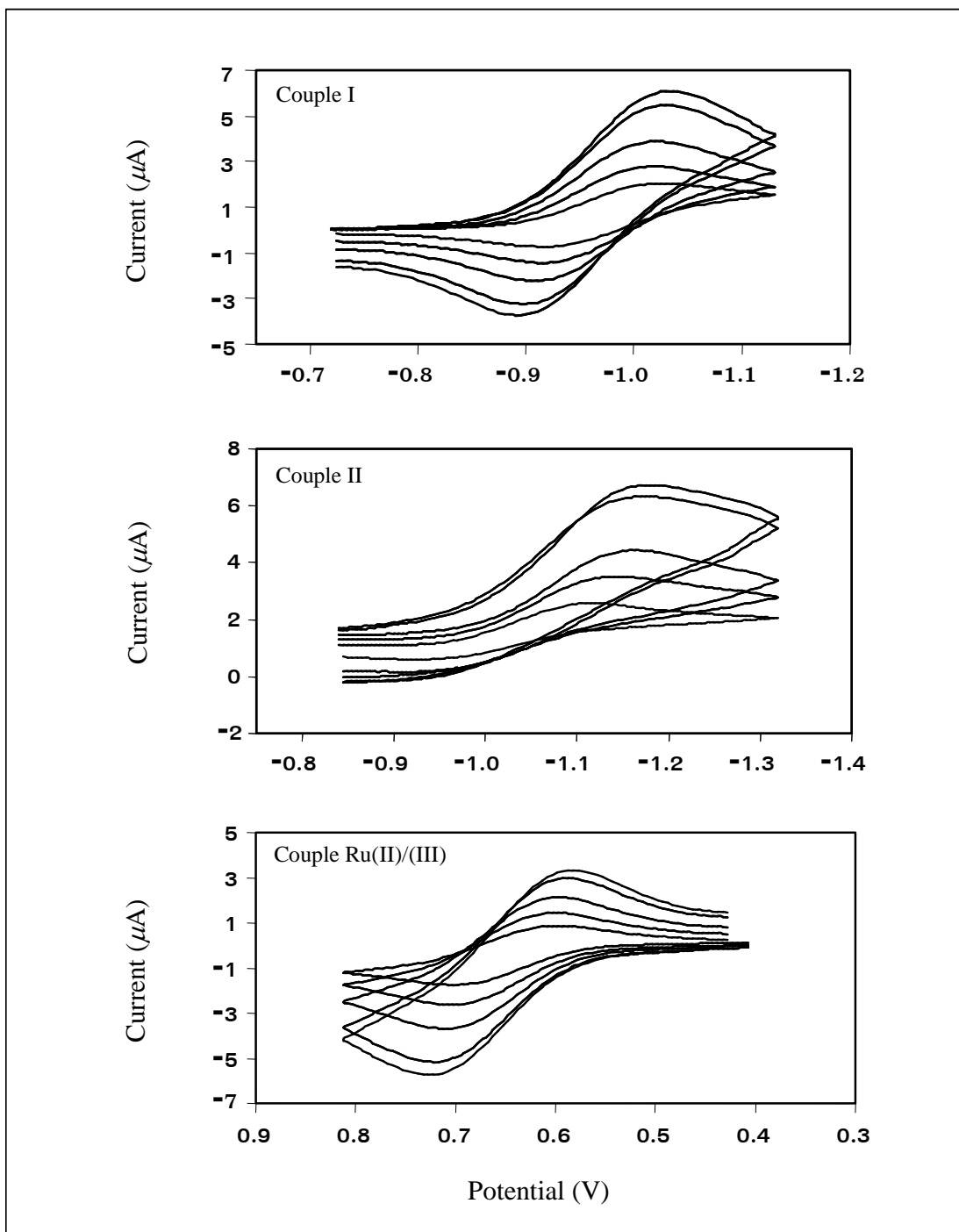


**Figure C.1** Cyclic voltammograms of couple I, II and Ru(II)/(III) in  $tcc\text{-}[\text{Ru}(\text{Clazpy}_2)\text{Cl}_2]$  by varying scan rate  $50\text{-}500\text{ mV}\cdot\text{s}^{-1}$

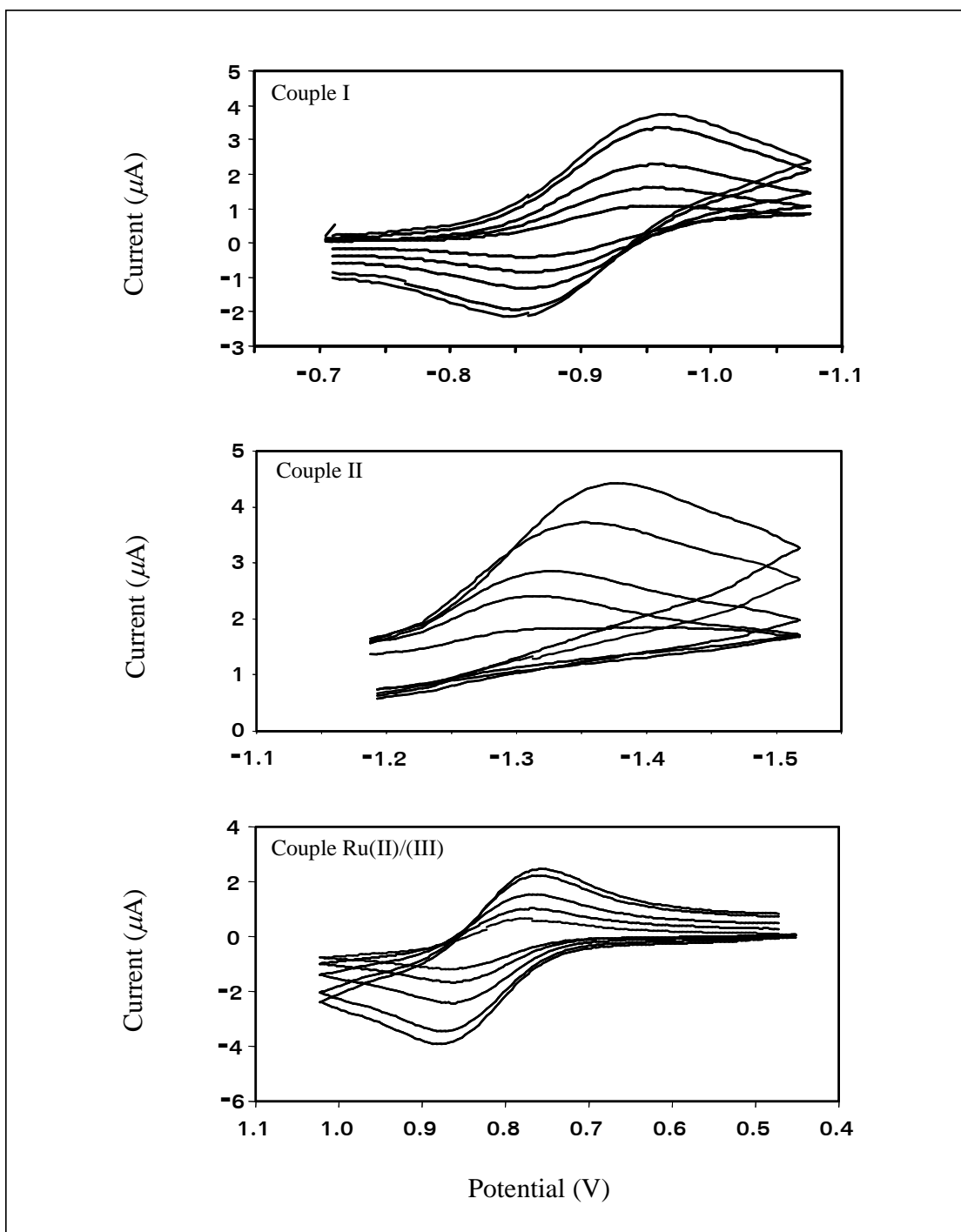


**Figure C.2** Cyclic voltammograms of couple I, II and Ru(II)/(III) in *ctc*-[Ru(Clazpy)<sub>2</sub>Cl<sub>2</sub>] by varying scan rate 50-500  $\text{mV}\cdot\text{s}^{-1}$

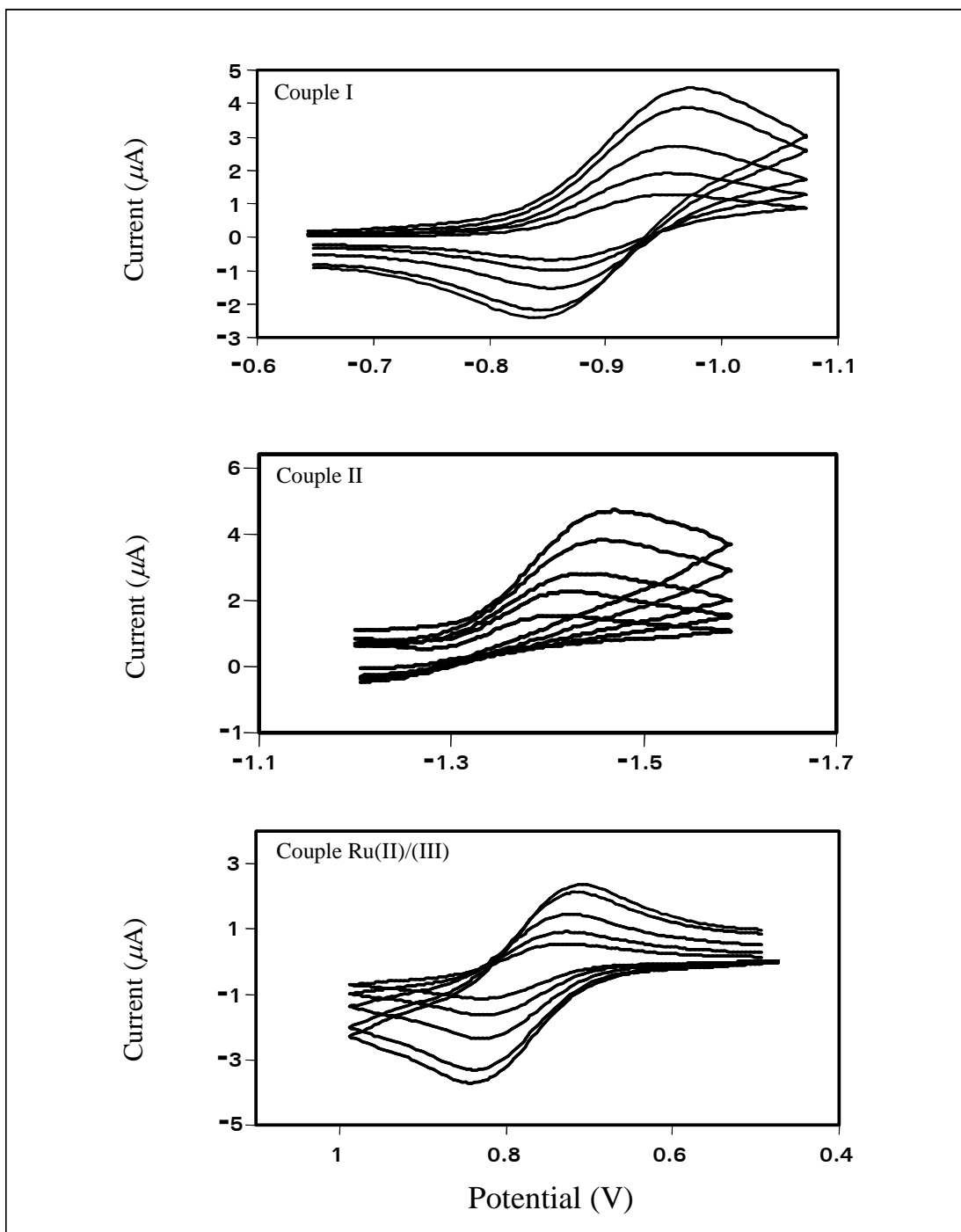


**Figure C.3** Cyclic voltammograms of couple I, II and Ru(II)/(III) in  $ccc\text{-}[\text{Ru}(\text{Clazpy})_2\text{Cl}_2]$  by varying scan rate  $50\text{-}500\text{ mV}\cdot\text{s}^{-1}$

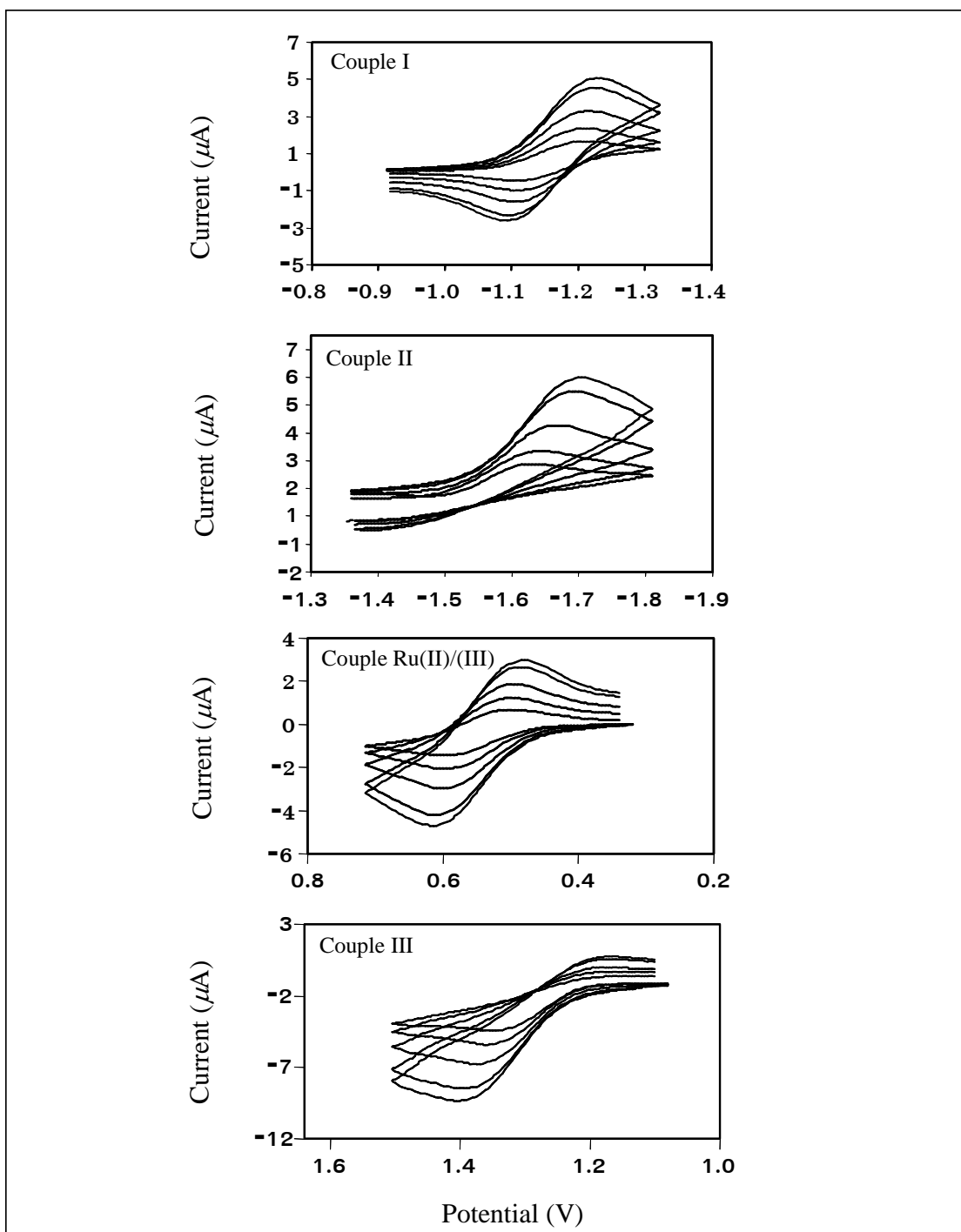


**Figure C.4** Cyclic voltammograms of couple I, II, III and Ru(II)/(III) in  $[\text{Ru}(\text{Clazpy})(5\text{dmazpy})\text{Cl}_2]$  by varying scan rate  $50\text{-}500\text{ mV}\cdot\text{s}^{-1}$

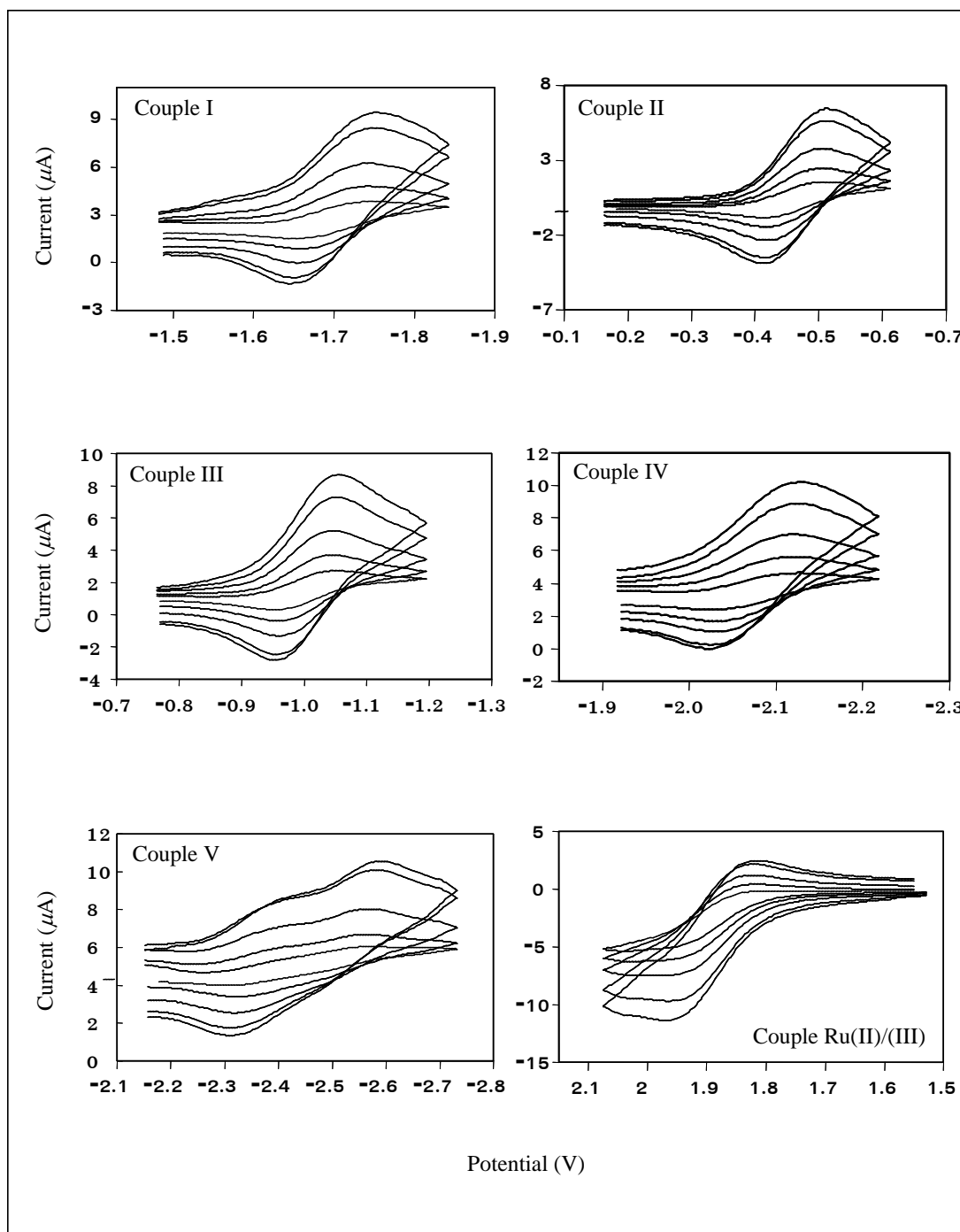


**Figure C.5** Cyclic voltammograms of couple I, II, III, IV, V and Ru(II)/(III) in  $[\text{Ru}(\text{Clazpy})_2(\text{bpy})](\text{PF}_6)_2$  by varying scan rate  $50\text{-}500 \text{ mV}\cdot\text{s}^{-1}$

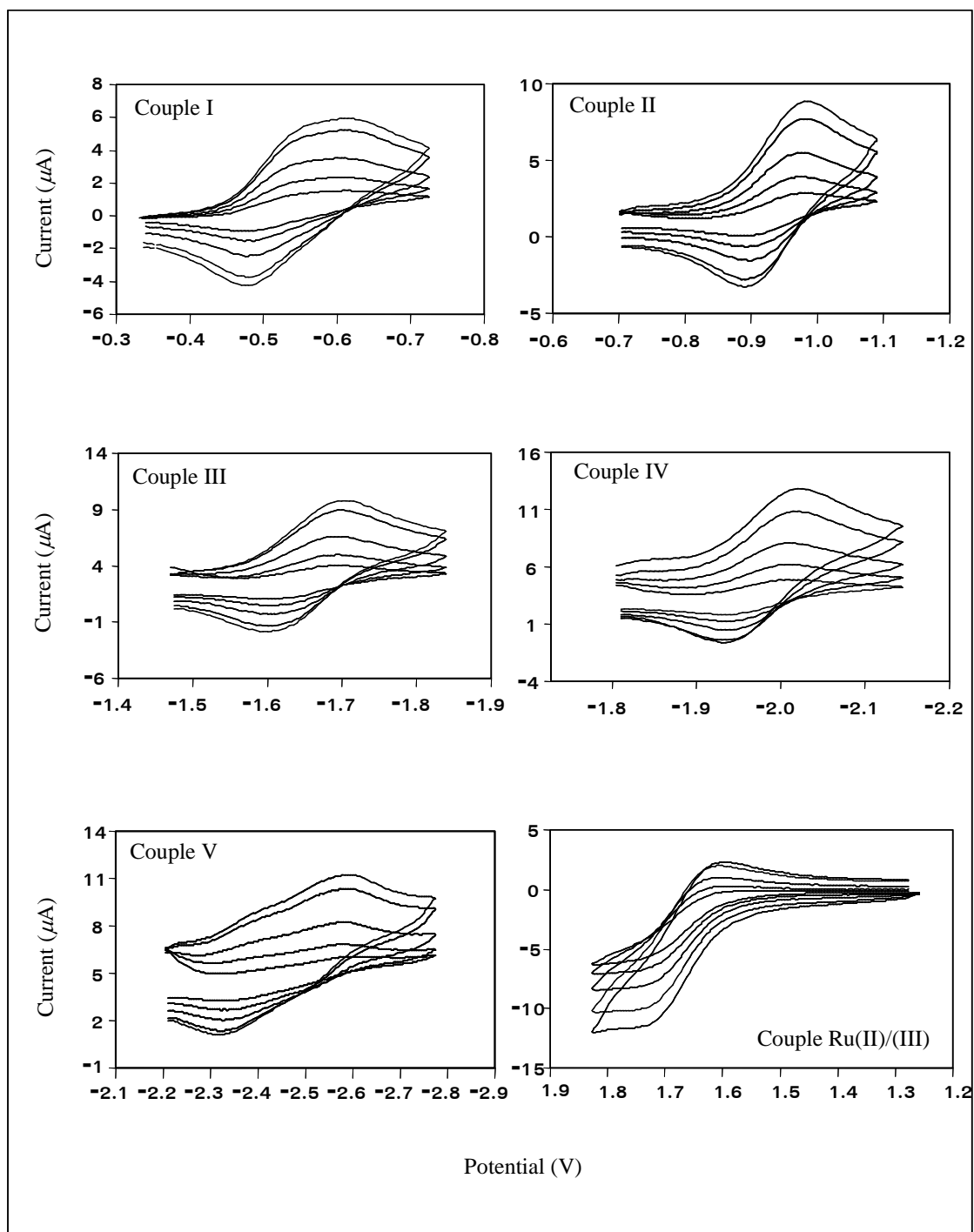


**Figure C.6** Cyclic voltammograms of couple I, II, III, IV, V and Ru(II)/(III) in  $[\text{Ru}(\text{Clazpy})_2(\text{phen})](\text{PF}_6)_2$  by varying scan rate 50-500  $\text{mV}\cdot\text{s}^{-1}$

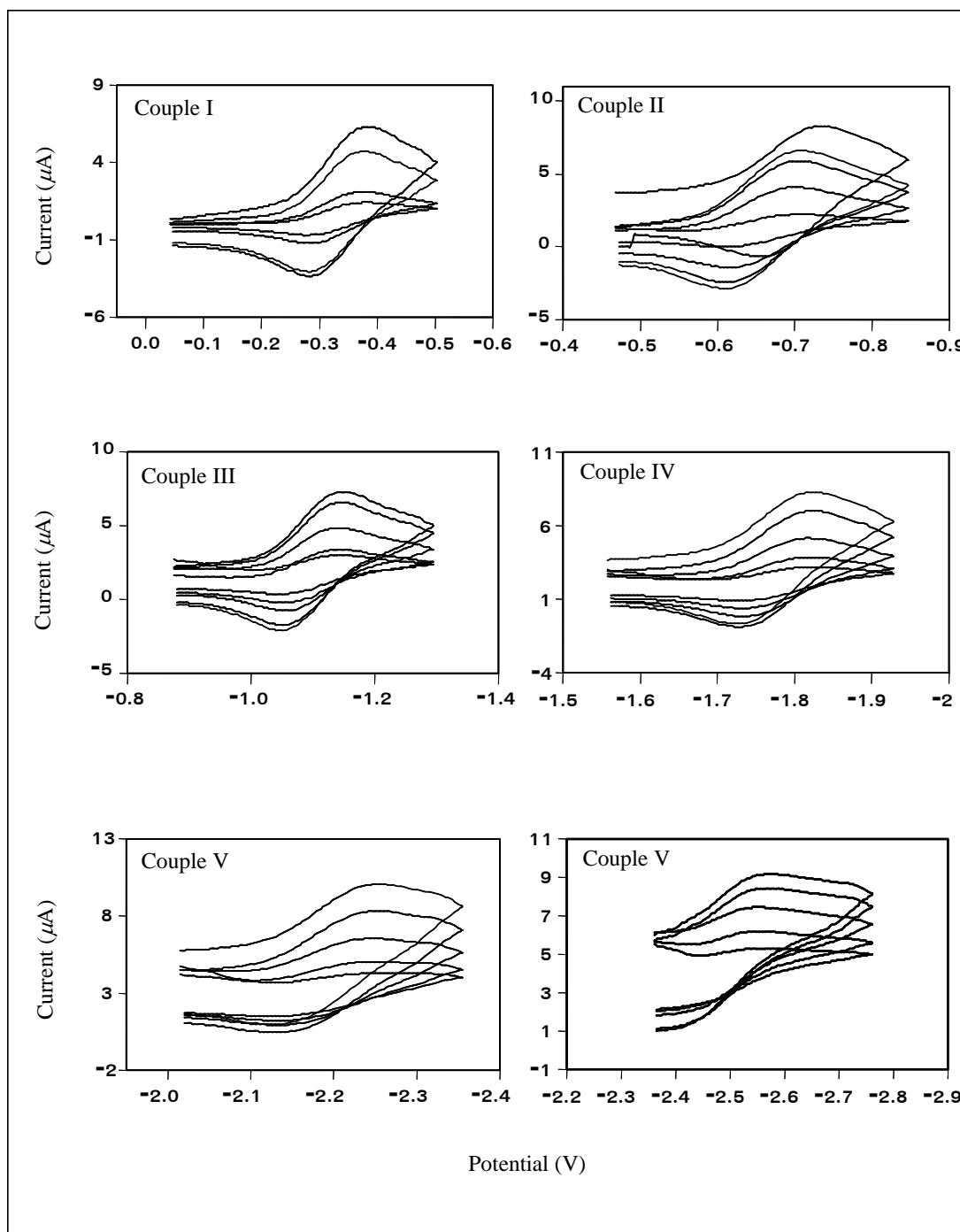


**Figure C.7** Cyclic voltammograms of couple I, II, III, IV, V and VI in  $[\text{Ru}(\text{Clazpy})_2(\text{azpy})](\text{PF}_6)_2$  by varying scan rate 50-500  $\text{mV}\cdot\text{s}^{-1}$

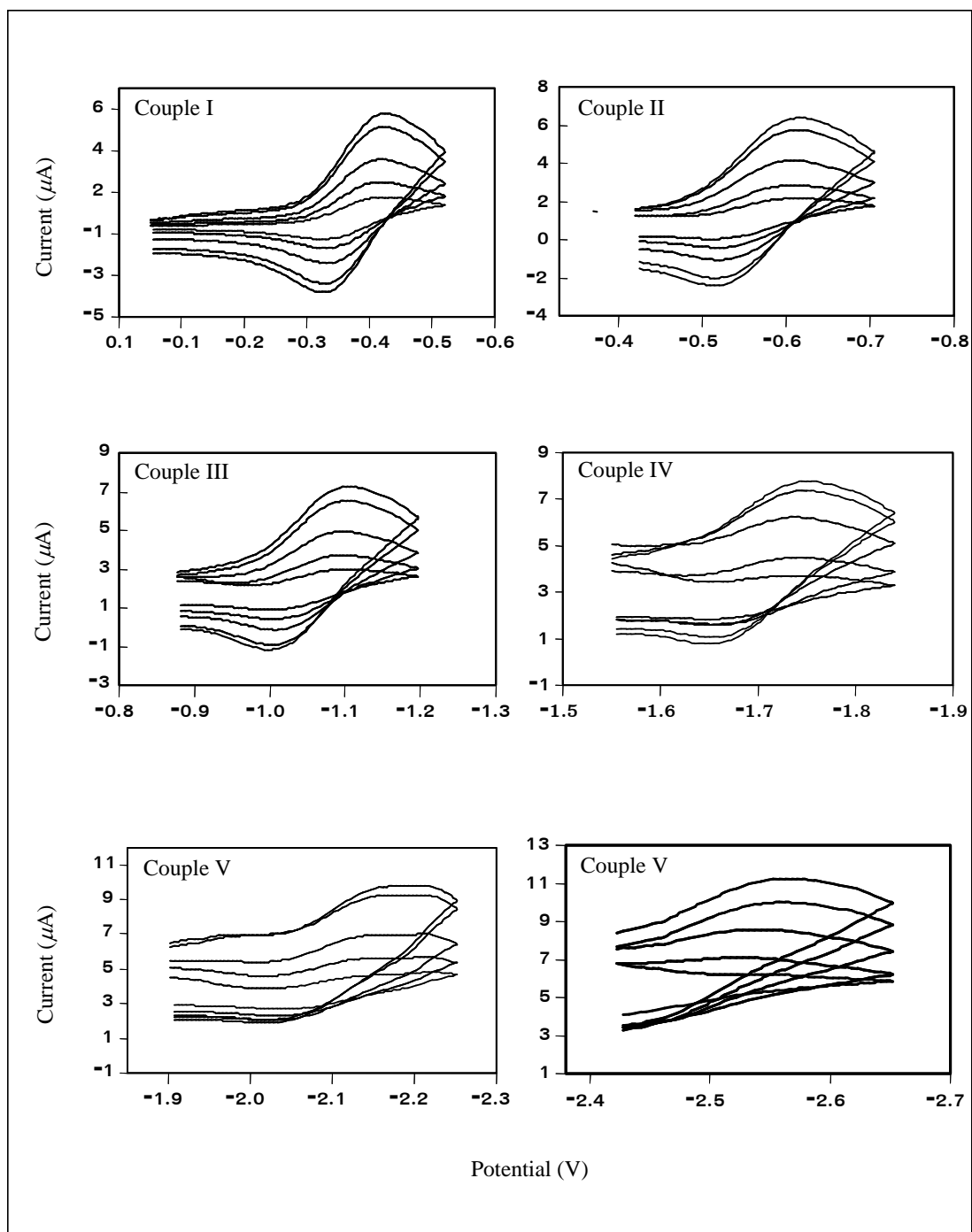


**Figure C.8** Cyclic voltammograms of couple I, II, III, IV, V and Ru(II)/(III) in  $[\text{Ru}(\text{Clazpy})_3](\text{PF}_6)_2$  by varying scan rate 50-500  $\text{mV}\cdot\text{s}^{-1}$

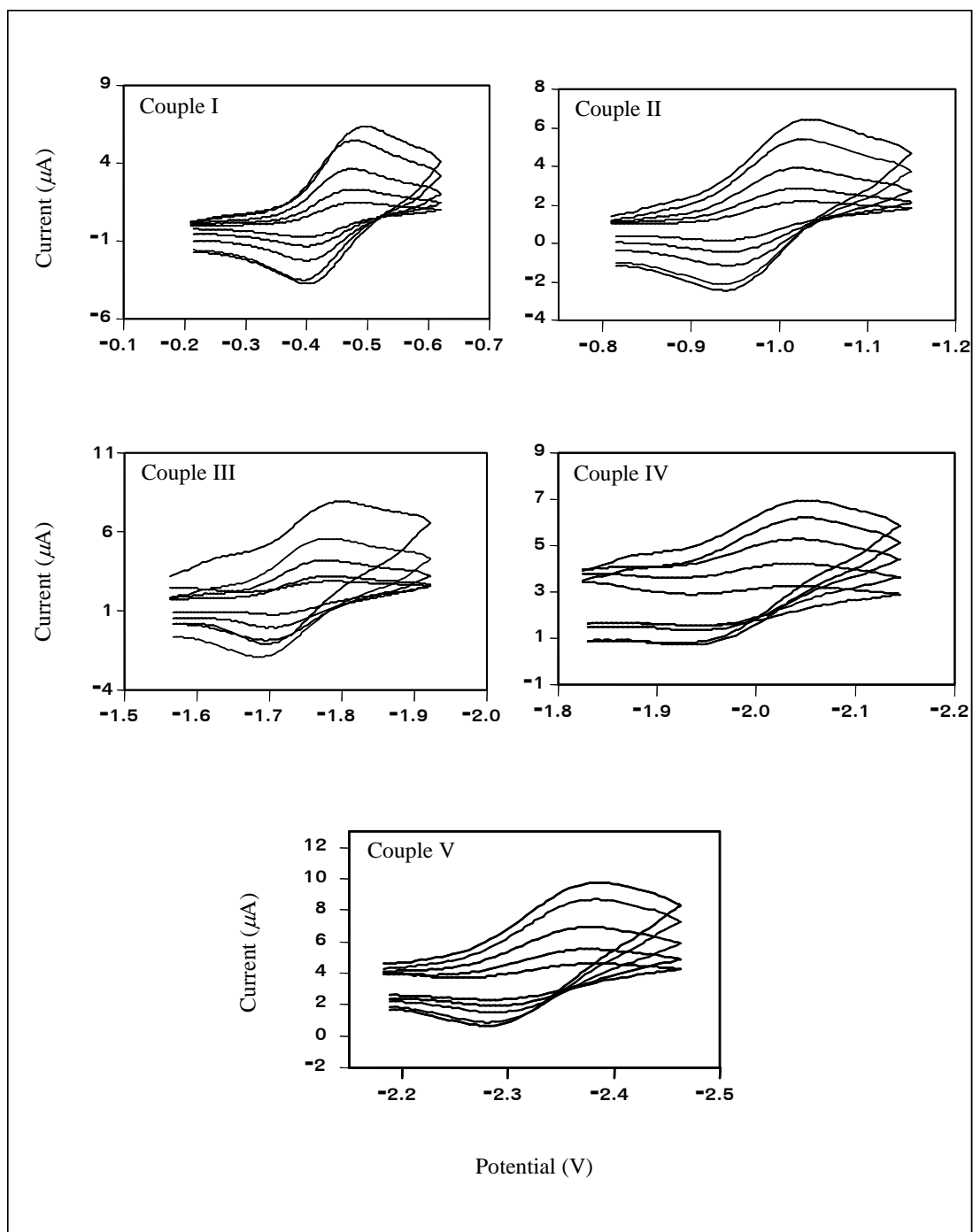


**Figure C.9** Cyclic voltammograms of couple I, II, III, IV and V in  $[\text{Ru}(\text{Clazpy})_2(\text{bpy})](\text{NO}_3)_2 \cdot 5\text{H}_2\text{O}$  by varying scan rate 50-500  $\text{mV} \cdot \text{s}^{-1}$

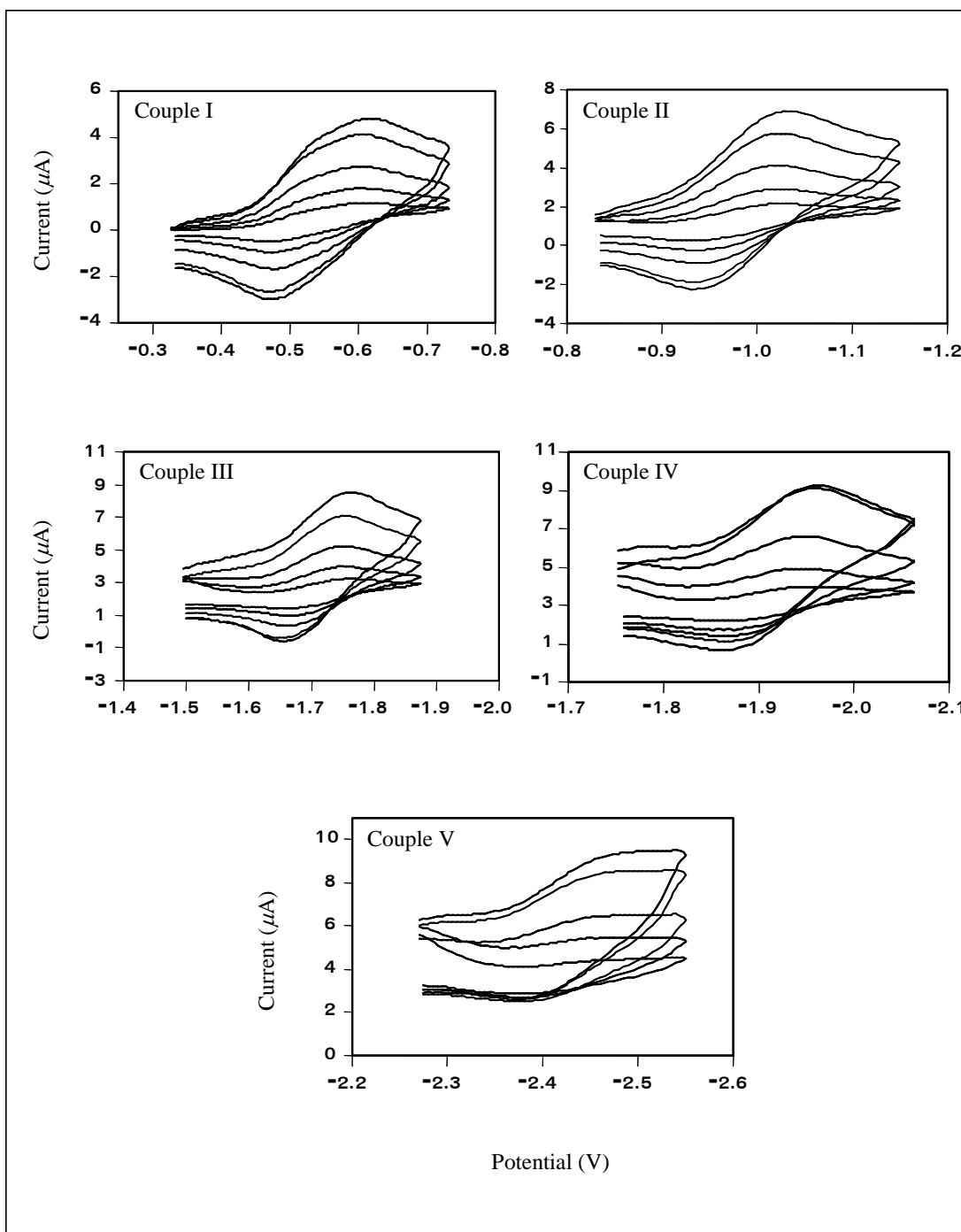


**Figure C.10** Cyclic voltammograms of couple I, II, III, IV and V in  $[\text{Ru}(\text{Clazpy})_2(\text{phen})](\text{NO}_3)_2 \cdot 3\text{H}_2\text{O}$  by varying scan rate  $50\text{-}500 \text{ mV}\cdot\text{s}^{-1}$

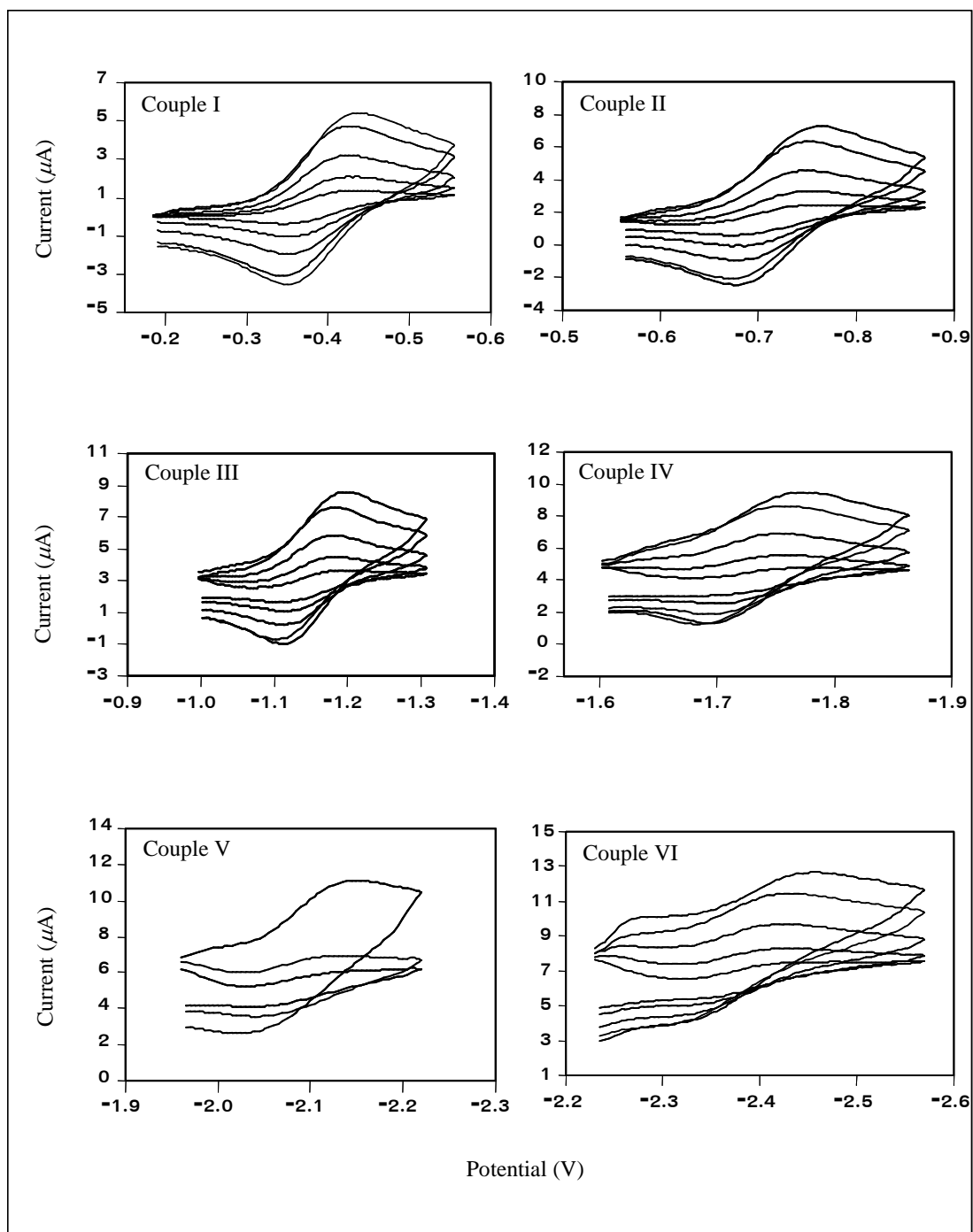


**Figure C.11** Cyclic voltammograms of couple I, II, III, IV and V in  $[\text{Ru}(\text{Clazpy})_2(\text{azpy})](\text{NO}_3)_2\cdot\text{H}_2\text{O}$  by varying scan rate 50-500  $\text{mV}\cdot\text{s}^{-1}$

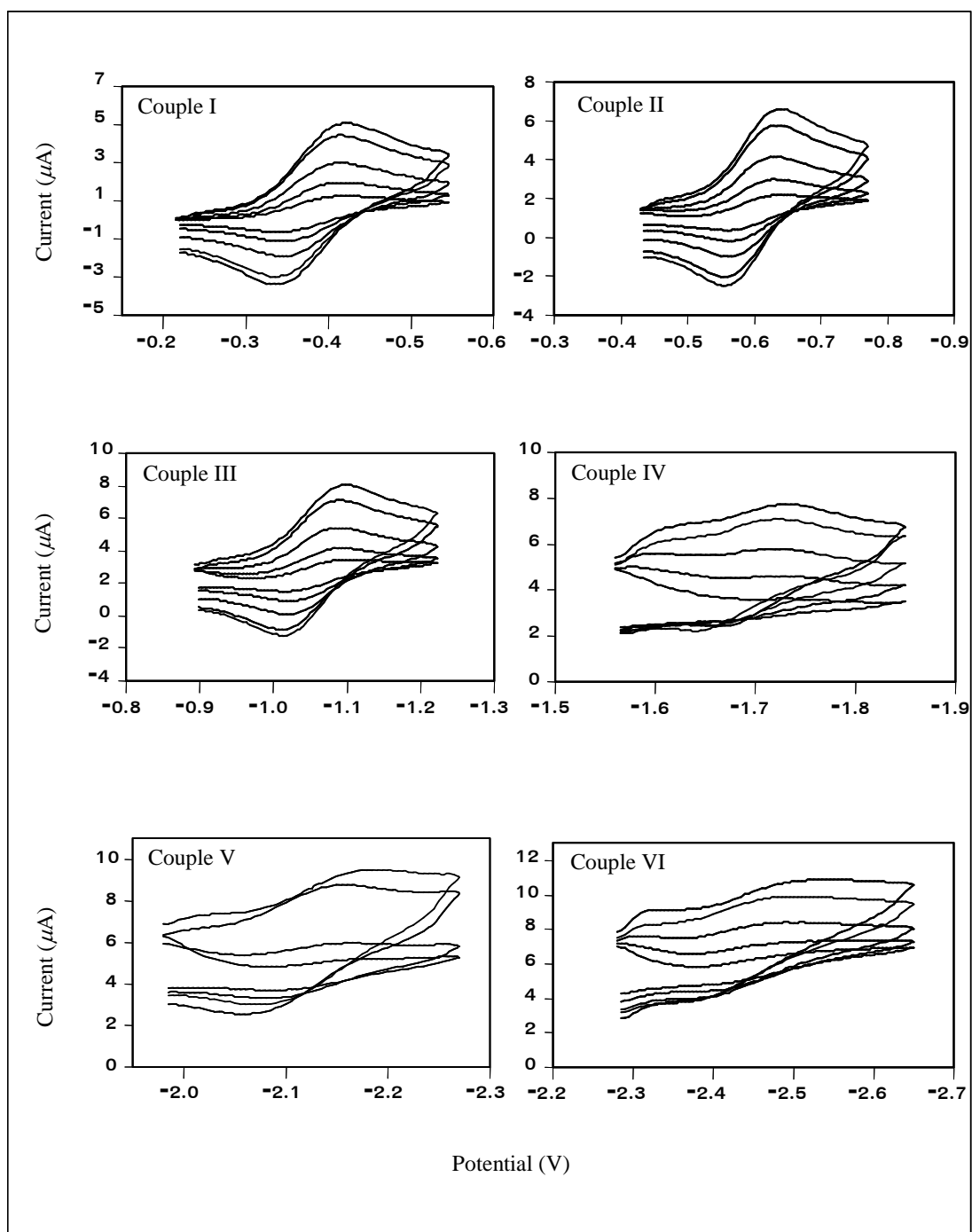


**Figure C.12** Cyclic voltammograms of couple I, II, III, IV and V in  $[\text{Ru}(\text{Clazpy})_3](\text{NO}_3)_2 \cdot 3\text{H}_2\text{O}$  by varying scan rate 50-500  $\text{mV}\cdot\text{s}^{-1}$

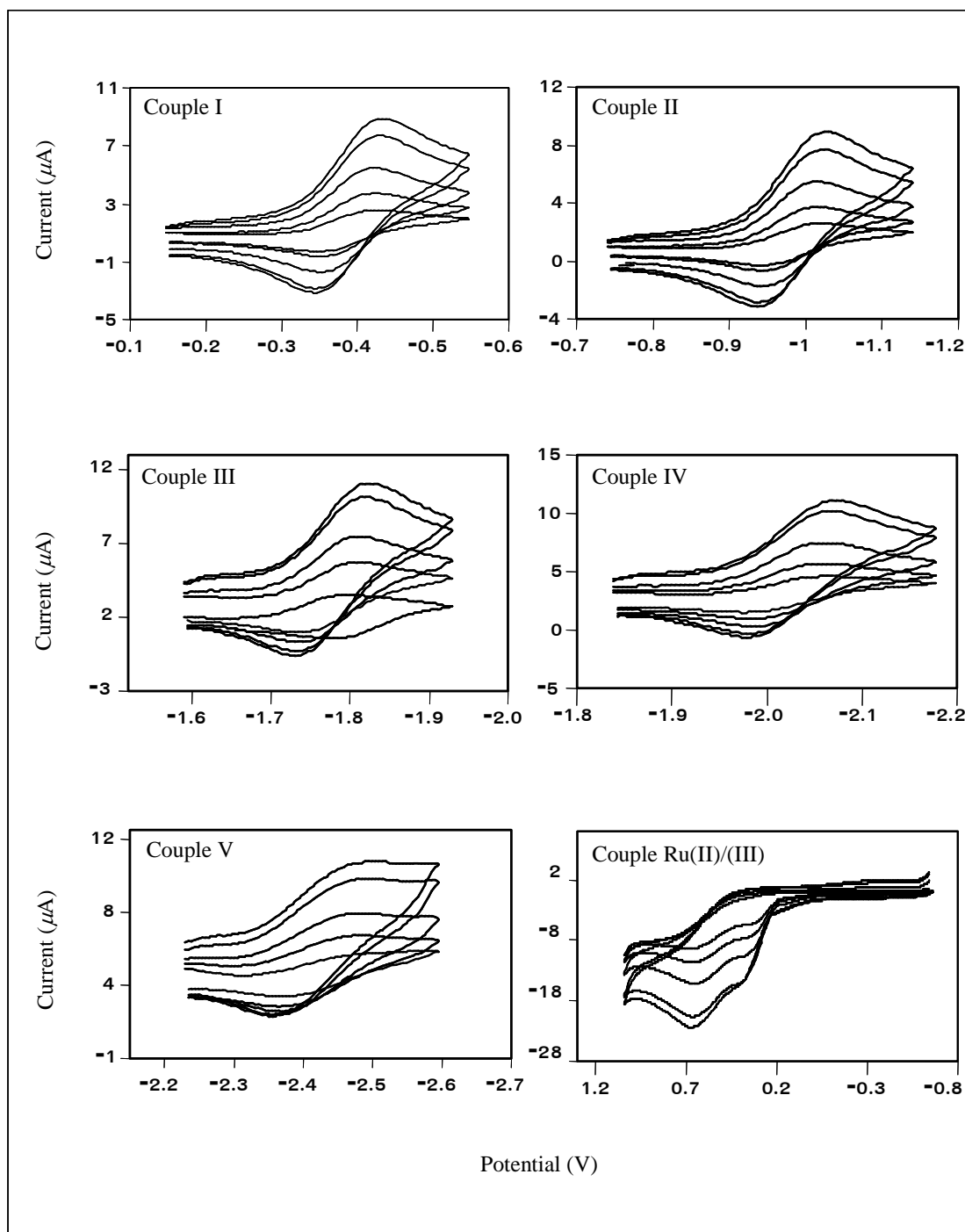


**Figure C.13** Cyclic voltammograms of couple I, II, III, IV, V and Ru(II)/(III) in  $[\text{Ru}(\text{Clazpy})_2(\text{bpy})]\text{Cl}_2\cdot 7\text{H}_2\text{O}$  by varying scan rate 50-500  $\text{mV}\cdot\text{s}^{-1}$

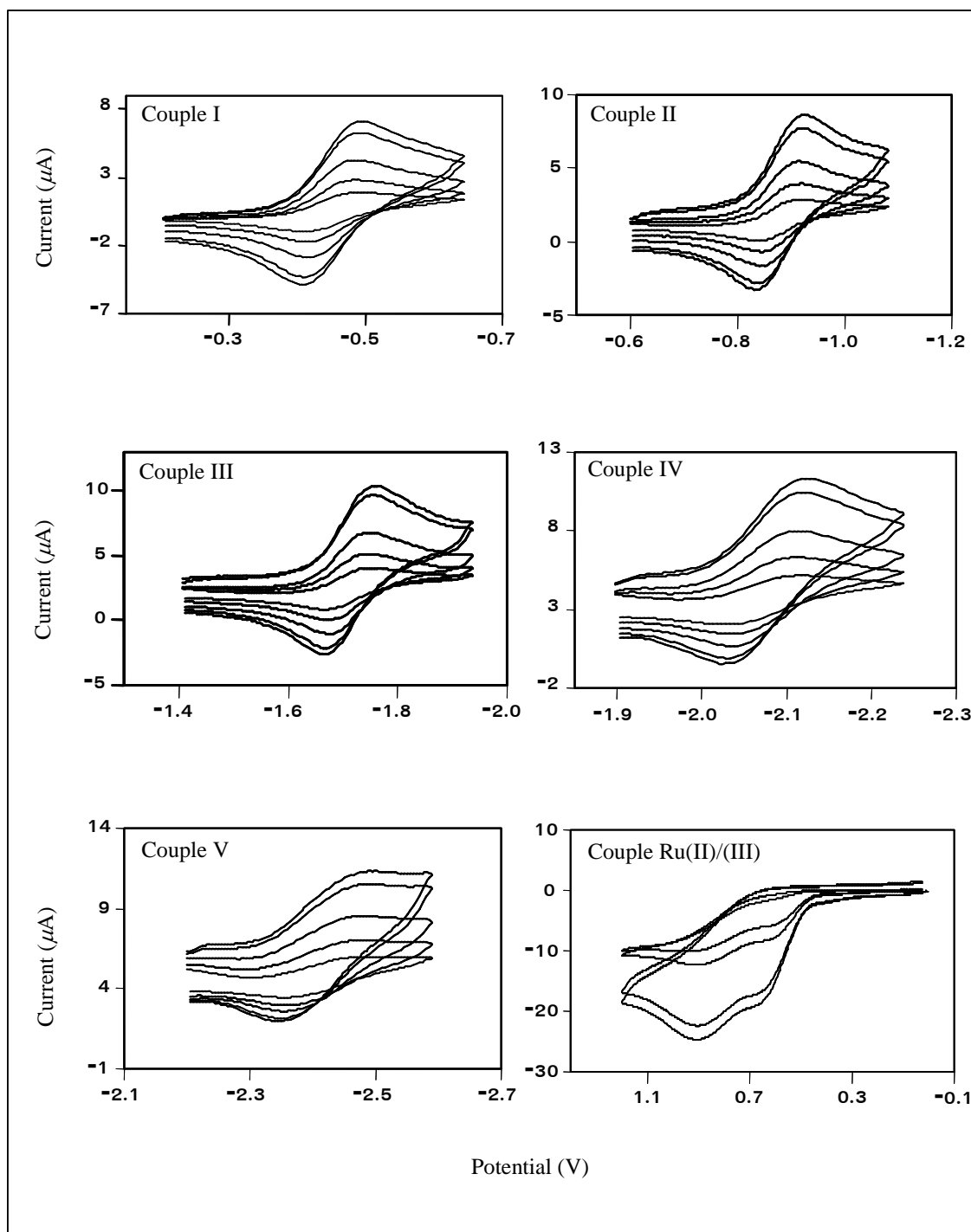


**Figure C.14** Cyclic voltammograms of couple I, II, III, IV, V and Ru(II)/(III) in  $[\text{Ru}(\text{Clazpy})_2(\text{phen})]\text{Cl}_2\cdot 8\text{H}_2\text{O}$  by varying scan rate 50-500  $\text{mV}\cdot\text{s}^{-1}$

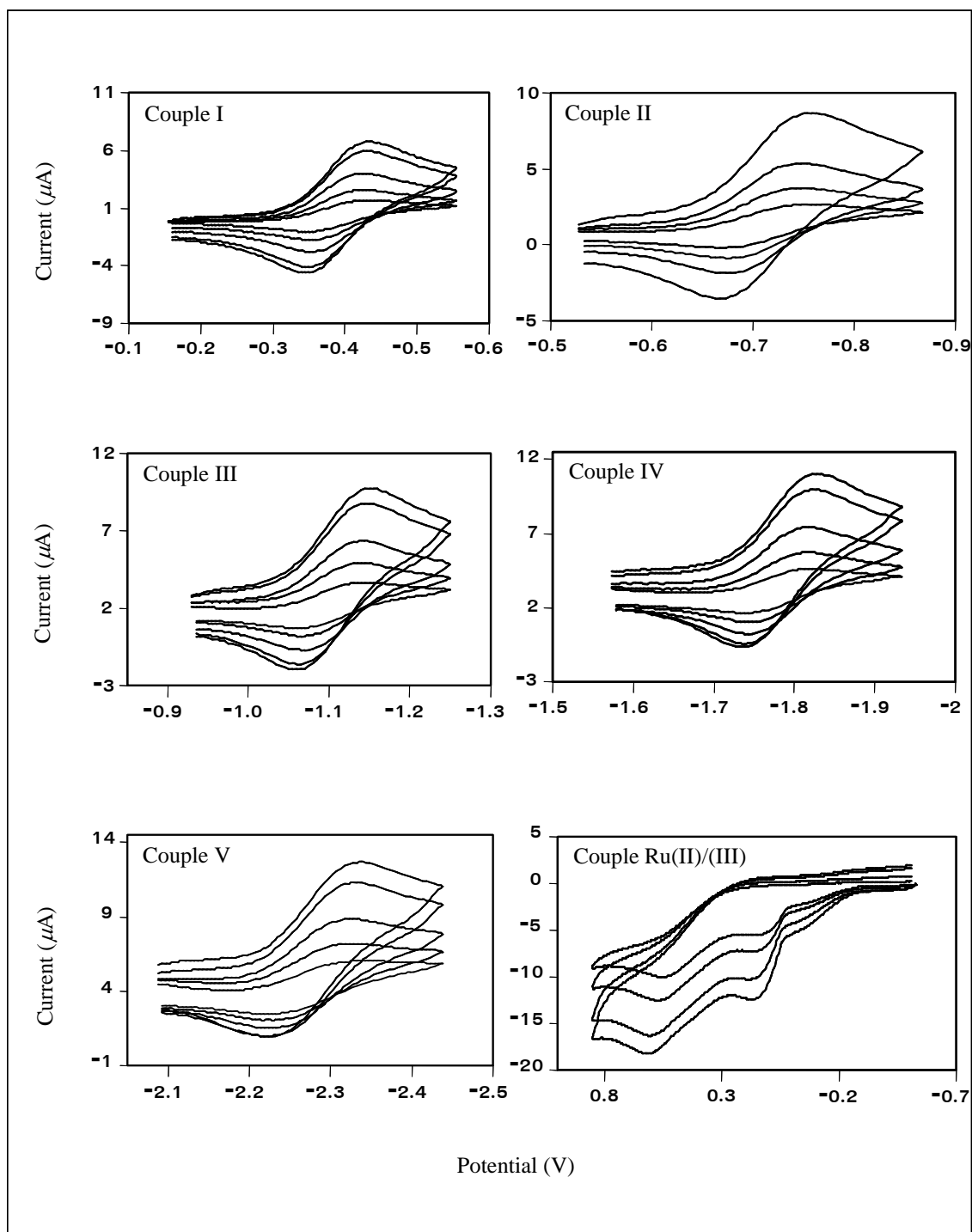


**Figure C.15** Cyclic voltammograms of couple I, II, III, IV, V and Ru(II)/(III) in  $[\text{Ru}(\text{Clazpy})_2(\text{azpy})]\text{Cl}_2\cdot 4\text{H}_2\text{O}$  by varying scan rate 50-500  $\text{mV}\cdot\text{s}^{-1}$

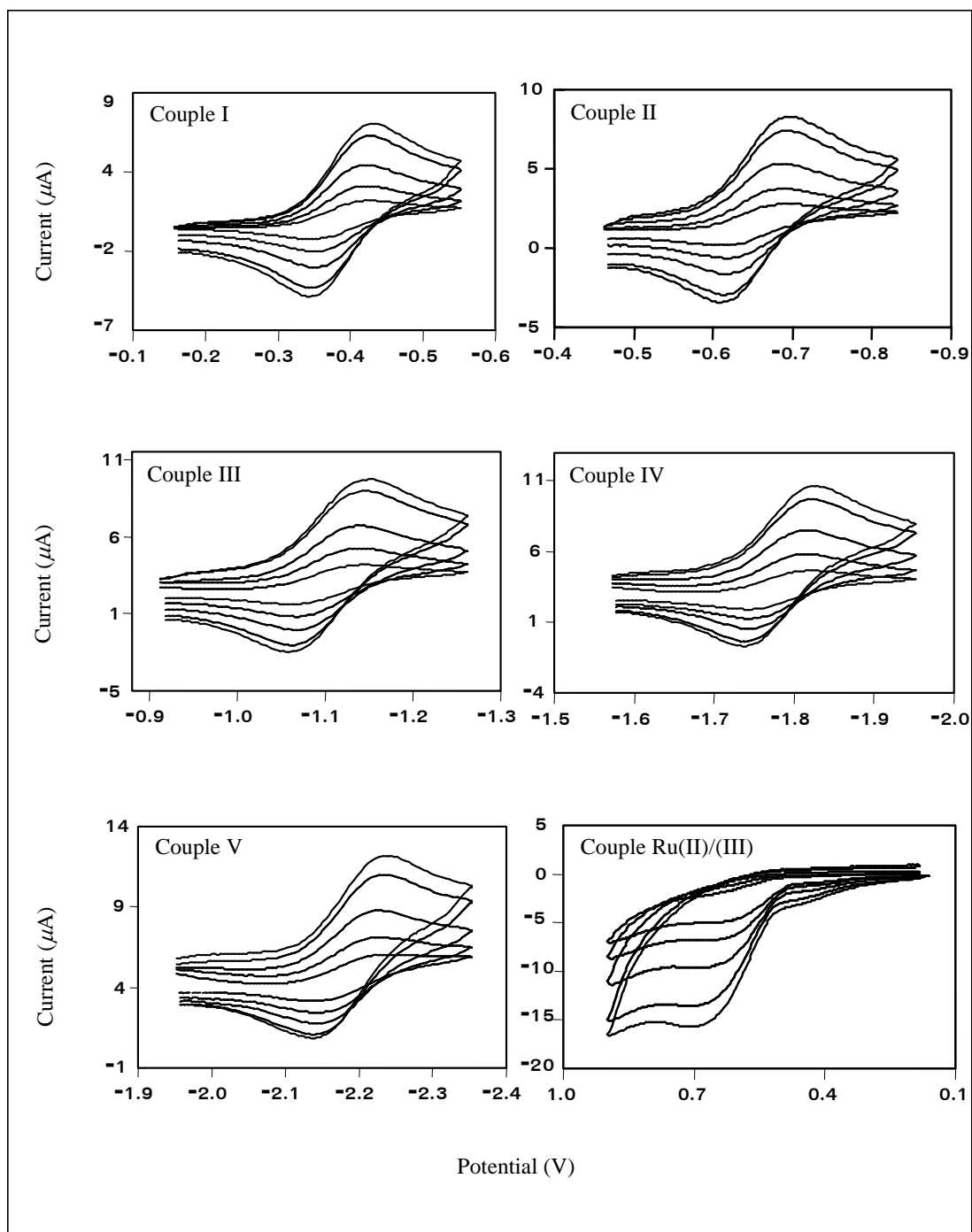


**Figure C.16** Cyclic voltammograms of couple I, II, III, IV, V and Ru(II)/(III) in  $[\text{Ru}(\text{Clazpy})_3]\text{Cl}_2 \cdot 3\text{H}_2\text{O}$  by varying scan rate  $50\text{-}500 \text{ mV}\cdot\text{s}^{-1}$

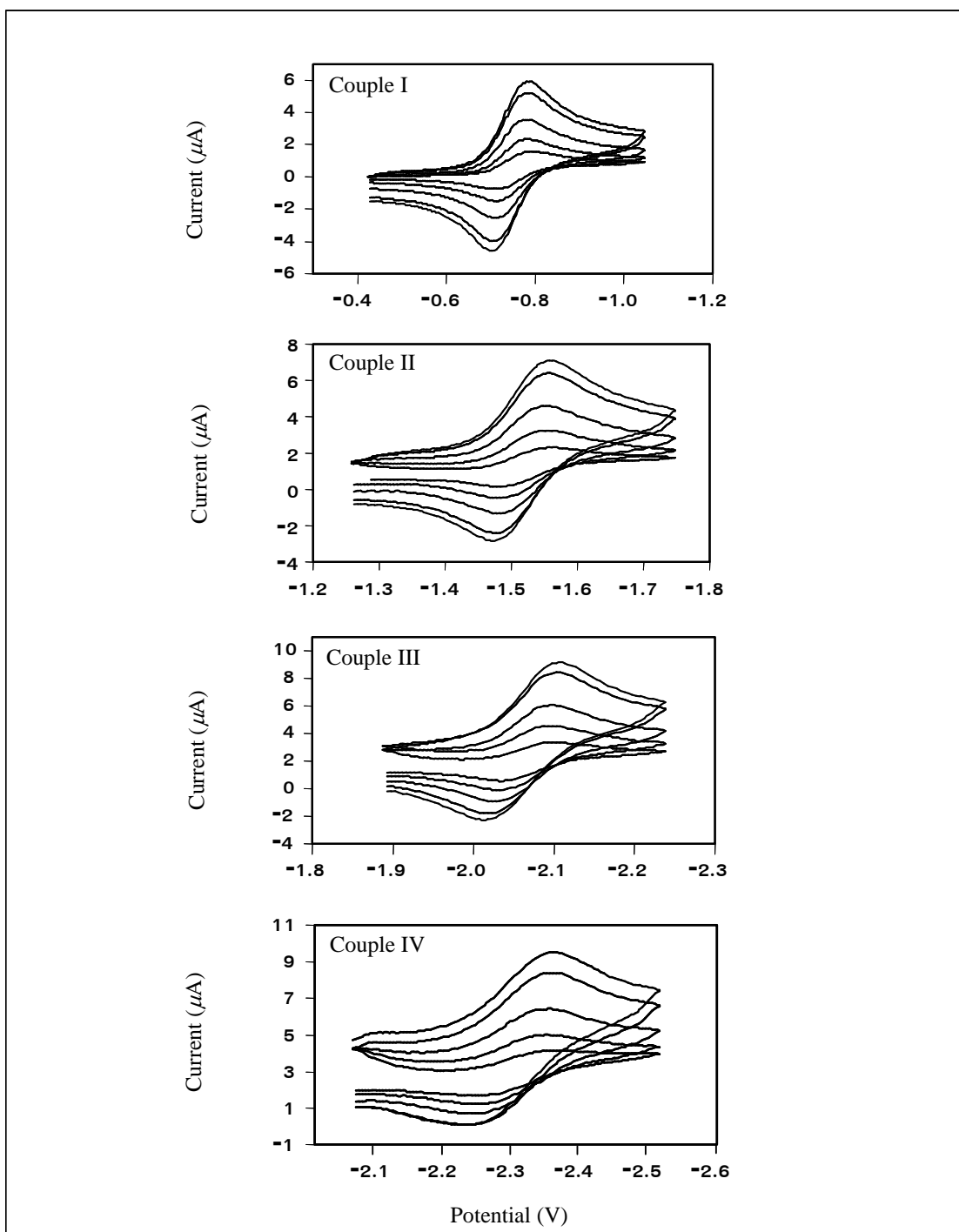


**Figure C.17** Cyclic voltammograms of couple I, II, III and IV in  $[\text{Ru}(\text{bpy})_2(\text{Clazpy})](\text{PF}_6)_2$  by varying scan rate  $50\text{-}500 \text{ mV}\cdot\text{s}^{-1}$

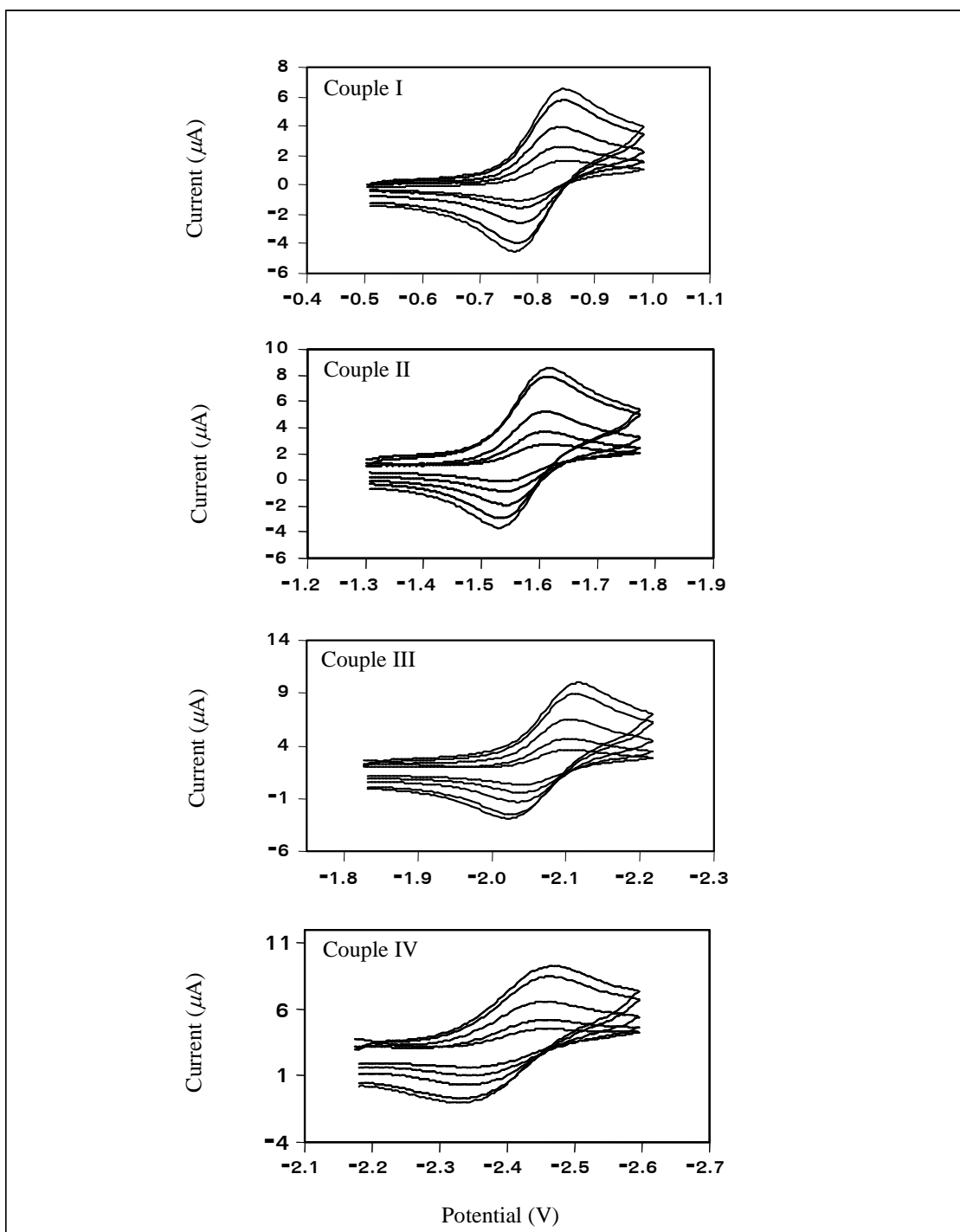


**Figure C.18** Cyclic voltammograms of couple I, II, III IV and V in  $[\text{Ru}(\text{phen})_2(\text{Clazpy})](\text{PF}_6)_2$  by varying scan rate  $50\text{-}500 \text{ mV}\cdot\text{s}^{-1}$

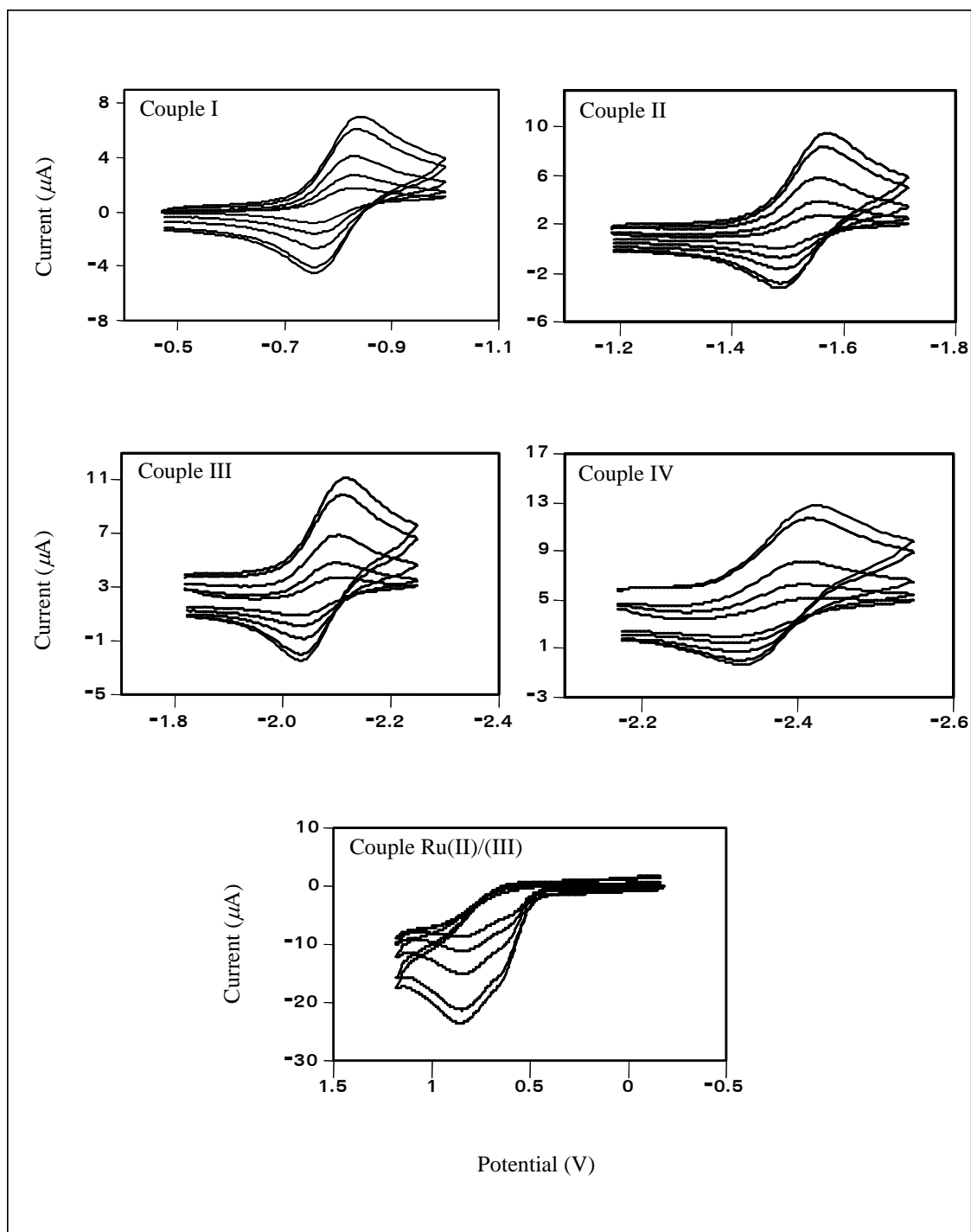


**Figure C.19** Cyclic voltammograms of couple I, II, III, IV and Ru(II)/(III) in  $[\text{Ru}(\text{bpy})_2(\text{Clazpy})]\text{Cl}_2 \cdot 7\text{H}_2\text{O}$  by varying scan rate 50-500  $\text{mV} \cdot \text{s}^{-1}$

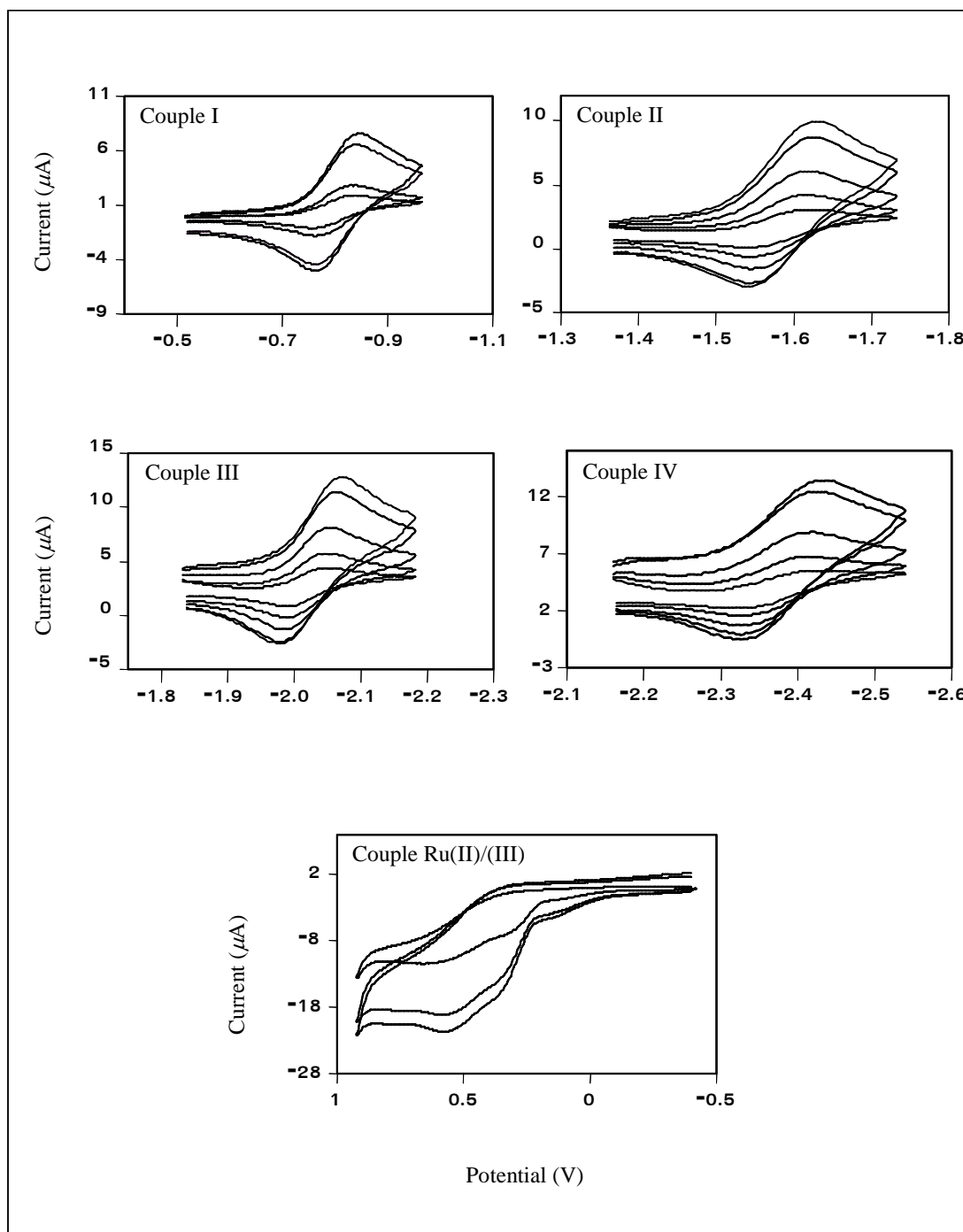


**Figure C.18** Cyclic voltammograms of couple I, II, III, IV and Ru(II)/(III) in  $[\text{Ru}(\text{phen})_2(\text{Clazpy})]\text{Cl}_2 \cdot 8\text{H}_2\text{O}$  by varying scan rate 50-500  $\text{mV} \cdot \text{s}^{-1}$

## VITAE

**Name** Miss Luksamee Sahavisit

**Student ID** 4523018

### Education Attainment

Degree	Name of Institution	Year of Graduation
B. Sc. (Chemistry)	Prince of Songkla University	1999
M.Sc. (Inorganic Chemistry)	Prince of Songkla University	2002

### Scholarship Awards during Enrolment

1. Center for Innovation in Chemistry: Postgraduate Education and Research Program in Chemistry (PERCH-CIC), Commission on Higher Education, Ministry of Education
2. Teaching assistance (TA)

### List of Publication and Proceeding

#### Publications

1. Sahavisit, L. and Hansongnern, K. 2005. Synthesis, Spectral Studies and Electrochemical Properties of Ruthenium(II) Complex with the New Bidentate Ligand 5-Chloro-2-(phenylazo)pyridine. *Songklanakarin J. Sci. Technol.* 27, 751-759.
2. Hansongnern, K., Sahavisit, L. and Pakawatchai, C. 2008. Crystal Structure of *cis*-Bis(5-Chloro-2-(phenylazo)pyridine)dichlororuthenium (II). *Anal. Sci.* 24, x57-x58.

## Proceedings

1. Hansongnern, K. and Sahavisit, L. 2003. Synthesis and Characterization of Ruthenium(II) Complexes with 5-Chloro-2-(phenylazo)pyridine Ligand. The 29<sup>th</sup> Congress on Science and Technology of Thailand. Golden Jubilee Convention Hall: Khon Kean University, October 20-22, 2003. pp. 116. (Poster presentation)
2. Hansongnern, K. and Sahavisit, L. 2004. NMR Study of Ruthenium(II) Complexes with 5-Chloro-(2-phenylazo)pyridine. The third PERCH Annual Scientific Congress (PERCH Congress III). Jomtien Palm Beach Resort: Pattaya Chonburi, May 9-12, 2004. pp. 205. (Poster presentation)
3. Sahavisit, L. and Hansongnern, K. 2004. Synthesis and Characterization of [Ru(Clazpy)<sub>2</sub>Cl<sub>2</sub>]. The 30<sup>th</sup> Congress on Science and Technology of Thailand. Impact Exhibition, and Convention Center, Muang Thong Thani, October 19-21, 2004. pp. 85. (Poster presentation)
4. Hansongnern, K. and Sahavisit, L. 2005. Synthesis and Characterization of *cis*-[Ru(Clazpy)<sub>2</sub>Cl<sub>2</sub>]. The fourth PERCH Annual Scientific Congress (PERCH Congress IV). Jomtien Palm Beach Resort, Pattaya Chonburi, May 8-11, 2005. pp. 86. (Oral presentation)
5. Hansongnern, K. and Sahavisit, L. 2005. Chemistry of Isomeric Complexes of Ruthenium(II) with a New Bidentate Ligand. Connect 2005 Chemical Challenges for the 21<sup>st</sup> Century. The 12<sup>th</sup> Royal Australian Chemical Institute(RACI) Convention, Sydney Convention and Exhibition Centre, Darling Harbour, Australia, July 3-7, 2005. (Poster presentation)

6. Sahavisit, L. and Hansongnern, K. 2005. Synthesis, Characterization and DNA-Binding of  $[\text{Ru}(\text{Clazpy})_2\text{bpy}]^{2+}$ . The 31<sup>th</sup> Congress on Science and Technology of Thailand. Technopolis, Suranaree University of Technology, Nakhon Ratchasima, October 18-20, 2005. pp. 160. (Poster presentation)
7. Sahavisit, L. and Hansongnern, K. 2006. Chemistry of ruthenium(II) Complex with 5-Chloro-2-(phenylazo)pyridine. The 1<sup>st</sup> Penang International Conference for Young Chemists. Universiti Sains Malaysia, May 24-27, 2006. pp. 79. (Oral presentation)
8. Sahavisit, L., Hansongnern, K. and Pakawatchai, C. 2006. Synthesis and Molecular Structure of  $[\text{Ru}(\text{Clazpy})_2\text{phen}](\text{PF}_6)_2$ . The 32<sup>th</sup> Congress on Science and Technology of Thailand. Queen Sirikit Convention Center(QSNCC), October 10-12, 2006. pp. 170. (Poster presentation)